The CHD4 NuRD complex links epigenetics to glycolytic flux and proliferation of melanoma and a variety of cancer cells

Sébastien Coassolo

UNIVERSITÉ DE STRASBOURG

ÉCOLE DOCTORALE DES SCIENCES DE LA VIE ET DE LA SANTE

Institut de Génétique et de Biologie Moléculaire et Cellulaire

THÈSE présentée par :

Sébastien COASSOLO

Soutenue le 30 Septembre 2019

Pour obtenir le grade de : **Docteur de l'Université de Strasbourg**

Discipline : Science de la Vie et de la Santé
Spécialité : Aspects moléculaires et cellulaires de la biologie

The CHD4 NuRD complex links epigenetics to glycolytic flux and proliferation of melanoma and a variety of cancer cells

THÈSE dirigée par :

Dr. DAVIDSON Irwin	Directeur de Recherche CNRS, IGBMC, Illkirch

RAPPORTEURS :

Dr. BERTOLOTTO Corine	Directeur de Recherche INSERM, C3M, Nice
Dr. GODING Colin	Professor, Ludwig Cancer Research, Oxford

AUTRES MEMBRES DU JURY :

Dr. LANFRANCONE Luisa	Directeur de Recherche, IEO, Milan
Dr. KEYES Bill	Directeur de Recherche INSERM, IGBMC, Illkirch

“Learn from yesterday, live for today, hope for tomorrow. The important thing is not to stop questioning.”

Albert Einstein

This thesis is dedicated to my parents, Christine and Philippe, my endless source of inspiration and unconditional support.

Table of contents

Acknowledgement in English……..2

Acknowledgement in French – Remerciements……..….3

List of abbreviations……....5

List of figures……7

French summary – Résumé en Français……..8

Introduction

CHAPTER 1 Melanocytes: from origins to melanoma……..18

A. Localization……19

1) Anatomy of the skin

2) The epidermis

B. Cellular origins of melanocytes……24

C. Function……...26

D. Melanoma skin cancer……28

1) Epidemiology

2) Melanoma classifications

3) Melanomagenesis

E. Therapy strategies……36

F. MITF is the “master” transcriptional regulator of melanocytes and melanoma……39

1) Genomic organization and protein structure

2) Biological functions

3) Heterogeneous expression of MITF in melanoma

CHAPTER 2 Epigenetic regulation and the NuRD complex……44

A. Chromatin: structure, organization, modifications and transcriptional dynamics……45

1) Post-Translational Modifications on DNA bases

2) Post-Translational Modifications on histone proteins

3) Epigenetic tools and biological relevance

B. Citrullination is an emerging post-translational modification..49

C. ATP-dependent chromatin remodeling……..51

1) The SWI/SNF subfamily

2) The ISWI subfamily

3) The CHD subfamily

CHAPTER 3 An overview of central carbon metabolic pathways and cancer……61

A. Glucose metabolism……62

1) Glycolysis

2) Oxidative metabolism

B. Glutamine metabolism and cancer cell addiction……80

C. Metabolic states and adaptive strategies of melanoma cells…….82

D. Crosstalk between metabolism and epigenetic regulation of chromatin……84

1) Metabolite-mediated modulation of chromatin

2) Metabolic enzyme-mediated modulation of chromatin

Results

Article 1 - CHD3 and CHD4-containing NuRD complexes are essential in melanoma cells and act as co-factors for SOX10 and RREB1-regulated transcription……..92

Article 2 - CHD4 regulates PADI1 and PADI3 expression linking pyruvate kinase M2 citrullination to glycolysis and proliferation……115

Discussion and conclusions……..……136

Annexes

Annexe 1 - Dynamic Evolution of Clonal Composition and Neoantigen Landscape in Recurrent Metastatic Melanoma with a Rare Combination of Driver Mutations……145

Annexe 2 - Chromatin remodellers Brg1 and Bptf are required for normal gene expression and progression of oncogenic Braf-driven mouse melanoma…….158

Annexe 3 - CHD4 regulates PADI1 and PADI3 expression linking pyruvate kinase M2 citrullination to glycolysis and proliferation……...174

Publications & conferences……..……..202

Bibliography……..……203

Ce travail a été rendu possible grâce aux financements accordés par la Ligue contre le Cancer qui m'ont permis d'effectuer ces 4 années de thèse dans les meilleures conditions possibles.
Je leur suis extrêmement reconnaissant de m'avoir accordé leur confiance et pour leur intérêt porté à mon projet.

Ce travail a pu être réalisé dans les meilleures conditions également grâce à l'accueil de l'Institut de Génétique et de Biologie Moléculaire et Cellulaire (IGBMC) ainsi que l'ensemble de ses plateformes à la pointe de la recherche biomédicale.

Je remercie les membres actuels et passés de ces nombreuses plateformes pour leur implication et leurs conseils dans le développement et l'amélioration de mon projet.

ACKNOWLEDGEMENT in English

I would like to thank Dr. Colin Goding, Dr. Corine Bertolotto, Dr. Bill Keyes and Dr. Luisa Lanfrancone for their critical assessment of the present manuscript. I feel deeply honored that those high quality researchers kindly accepted to participate the thesis committee. The pioneering research activities in their respective fields have definitely inspired my own work and imprinted my current and future research interests.

This thesis would not have been possible without the guidance and advice of my supervisor Dr. Irwin Davidson. Irwin, joining your laboratory almost 5 years ago was for me the start of an incredibly enriching adventure. You did guide and inspire me all along these past several years with all the kindness, patience and above all the scientific passion that characterizes you. I do want to warmly thank you not only for your continuous support and confidence but also the great opportunity you offered me as a PhD student to present my work at several international conferences at incredible locations around the world.

I would like to thank Dr. Christophe Romier for his kindness and endless patience to upgrade my project through sharing his expertise on Structural Biology.

I would like to thank Pr. Gabriel Malouf for his numerous questions and suggestions along my research project.

I would like to thank Dr. Sylvain Daujat for having kindly shared his knowledge and experience that greatly help to move my project forward.

ACKNOWLEDGEMENT in French – REMERCIEMENTS

Je souhaiterais remercier un grand nombre de personnes, du milieu professionnel et/ou personnel, sans qui ce travail n'aurait pas été possible.

Tout d'abord un grand merci aux membres de mon équipe, passés et présents.

A Isabelle et Gabrielle, pour leur soutien technique et moral dans la vie de laboratoire de tous les jours.

A Bujamin, mon voisin de paillasse, merci d'avoir supporté mes nombreuses pauses déjeuners au bureau et surtout mon caractère de cochon, toujours neutralisé par l'attitude calme et posée qui te caractérise.

A Giovanni et Pietro, mes deux bruyants voisins italiens sans qui cette thèse aurait été un peu trop calme.

Un grand merci à Guillaume, bioinformaticien de l'équipe, devenu au fil du temps un ami. Merci pour ton professionnalisme, ta réactivité et ton calme face à toute demande d'analyse aussi saugrenue soit-elle.

Merci à Anas et Igor pour leur bonne humeur et leur expertise technique qui m'ont bien souvent aidé dans mon projet.

Merci à Alice, Alexandra, Véronique et Marc pour leur bonne humeur. Je leur souhaite autant de chance que moi dans leurs futures expériences de chercheurs.

Ensuite je souhaiterais remercier les personnes rencontrées dans mon entourage professionnel et qui font maintenant partie intégrante de mon entourage personnel.

Merci à mes deux Thomas favoris, nos soirées et notre « team Get Together » resteront des souvenirs mémorables.

Merci à Marine, Elise et Coralie pour avoir embelli mes années d'études.

Merci à Maryssa, ton départ du labo a laissé un grand vide (ou calme ? difficile à définir…). Merci pour ta bonne humeur sans failles.

Merci à mon grand ami Jérémy. Tu es rempli de défauts, et pourtant il y a aucune autre personne au monde avec qui je peux passer autant de temps à rigoler et commérer sans jamais arriver à saturation. A croire finalement qu'on a autant de

défauts l'un que l'autre. J'espère sincèrement que cette amitié traversera les frontières et les années.

Pour finir je souhaiterais remercier mon entourage personnel, famille et amis, même si à mes yeux la différence entre les deux est infime.

Un grand merci à mes amis d'enfance, Laetitia, Bastien, Romain et les deux Marie. On a traversé tellement d'années ensemble. On a grandi, muri, évolué ensemble, aucune épreuve de la vie ne pourra nous séparer.

Laetitia, ma plus belle rencontre de ces dernières années, ma plus belle rencontre du reste de ma vie. Il n'y a pas de mots pour décrire ce qui a changé depuis ton arrivée dans ma vie. Nos plus grandes aventures restent à vivre, et je suis impatient de les vivre à tes cotés.

Un grand merci à ma famille, ma grand-mère Jacqueline et mon oncle Jean-Yves, les fondations de tout ce que j'entreprends. Papa, marcher dans tes pas est ma plus grande fierté. Maman, tu as tellement tout donné pour nous, aucun merci n'est à la hauteur de ce que tu as fait. Patrice, il n'y a personne de plus différent de moi que toi, et pourtant il n'y a personne au monde qui compte plus pour moi. Vous rendre fiers est la plus grande des récompenses de mon travail.

List of abbreviations

ADP	**Adenosine DiPhosphate**
AKT	**Protein kinase B**
ALDO	**ALDOlase**
AMPK	**AMPactivated protein Kinase**
APC	**Antigen-Presenting Cell**
ATP	**Adenosine TriPhosphate**
BAF	**BRG1 Associated Factor**
BRAF	**v-RAF murine sarcoma viral oncogene homolog B**
BRG1	**Brahma-Related Gene-1**
BRM	**BRahMa**
CHD	**Chromodomain Helicase DNA-binding**
CSD	**Chronically Sun Damaged**
CTLA-4	**Cytotoxic T-Lymphocyte-Associated protein-4**
Cyt C	**Cytochrome C**
DCT	**L-DopaChrome Tautomerase**
DHAP	**DiHydroxyAcetone Phosphate**
EGF	**Epidermal Growth Factor**
EGFR	**Epidermal Growth Factor Receptor**
ENO	**ENOlase**
EPU	**Epidermal Proliferating Unit**
ERK	**Extracellular signal-Regulated Kinase**
ETC	**Electron Transport Chain**
F1,6BP	**Fructose 1,6-BisPhosphate**
F2,6BP	**Fructose-2,6-BisPhosphate**
FBPase1	**Fructose 1,6-BisPhosphatase**
G-6P	**Glucose-6-Phosphate**
GAPDH	**GlycerAldehyde 3 Phosphate DeHydrogenase**
GLS	**GLutaminaSe**
GLUT	**GLUcose Transporter**
GLUD	**GLUtamate Dehydrogenase**
GPI	**Glucose-6-Phosphate Isomerase**
H	**Histone**
HAP	**Hair follicle-Associated-Pluripotent**
HF	**Hair Follicle**
HIF1α	**Hypoxia- Inducible Factor 1α**
HK	**HexoKinase**
IFE	**InterFollicular Epidermis**
K	**Lysine**
KDM2	**α-KG-Dependent Lysine-specific Demethylase 2**
LDH	**Lactate DeHydrogenase**

MAP	**Mitogen-Activated Protein**
MEK	**Mitogen-activated protein kinase**
MITF	**MIcrophthalmia-associated Transcription Factor**
MYC	**avian MYeloCytomatosis viral oncogene homolog**
NAD+	**oxidized Nicotinamide Adenine Dinucleotide**
NADH	**reduced Nicotinamide Adenine Dinucleotide**
NCCs	**Neural Crest Cells**
NRAS	**Neuroblastoma RAS viral oncogene**
NuRD	**Nucleosome Remodelling Deacetylase**
OXPHOS	**OXydative PHOSphorylation**
PBAF	**Polybromo-associated BAF**
PD-1	**Programmed cell Death protein-1**
PDHc	**Pyruvate DeHydrogenase complex**
PDKs	**Pyruvate Dehydrogenase Kinases**
PDPs	**Pyruvate Dehydrogenase Phosphatases**
PFKFB	**6-PhosphoFructo-2-Kinase/Fructose2,6-Bisphosphatase**
PGK	**PhosphoGlycerate Kinase**
PGM1	**PhosphoGlycerate Mutase 1**
PHGDH	**PHosphoGlycerate DeHydrogenase**
PI3K	**PhosphoInositide-3-Kinase**
PKM	**Pyruvate Kinase Muscle isozyme**
PPP	**Pentose Phosphate Pathway**
PRC2	**Polycomb Repressive Complex 2**
PTMs	**Post-translational Modifications**
RGP	**Radial Growth Phase**
ROS	**Reactive Oxygen Species**
SCFR	**Mast/Stem Cell growth Factor Receptor**
SCs	**Stem Cells**
SDH	**Succinate DeHydrogenase**
SKPs	**SKin-derived Precursors**
SOX10	**SRY-BOX 10**
TACs	**Transit Amplifying Cells**
TCA	**Tri-Carboxylic Acid**
TCR	**T-Cell Receptor**
TOR	**Target Of Rapamycin**
TPI	**TriosePhosphate Isomerase**
Tregs	**regulatory T-cells**
UV	**UltraViolet**
VGP	**Vertical Growth Phase**
Wnt	**Wingless-iNT**

List of figures

Figure 1. **The integumentary system.**

Figure 2. **Epidermal layers.**

Figure 3. **The pilosebaceous unit.**

Figure 4. **Melanocytes migration and specification from NCCs.**

Figure 5. **Melanin synthesis pathway.**

Figure 6. **Diagnosis and classification of melanoma.**

Figure 7. **Morphological, histological and molecular properties of melanoma progression.**

Figure 8. **Available therapies and potential mechanisms of resistance to BRAF inhibitors.**

Figure 9. **Activation and modulation of T-cell response.**

Figure 10. **MIcrophthalmia-associated Transcription Factor (MITF).**

Figure 11. **Post-translational modifications of histone tails.**

Figure 12. **Structural and functional classification of remodellers.**

Figure 13. **Structure of the CHD superfamily and mammalian Nucleosome Remodelling and Deacetylase complex (NuRD) architecture.**

Figure 14. **Chemical reactions and related enzymes involved in glycolytic metabolism.**

Figure 15. **Pyruvate kinase, from gene and protein structure to allosteric regulation.**

Figure 16. **Dynamic regulation of PKM2 activity and functions.**

Figure 17. **General overview of oxidative metabolism.**

Figure 18. **Glutamine metabolism.**

French Summary
Résumé en Français

Contexte

Le mélanome malin est un cancer très agressif capable de générer des métastases à des stades précoces de son développement. La transformation oncogénique des mélanocytes résulte principalement de mutations dans les gènes BRAF, NRAS ou NF1 qui activent de façon constitutive la voie de signalisation des MAP kinases et la prolifération cellulaire (Hayward et al., 2017). Les cellules issues de mélanome, lorsqu'elles sont cultivées *in vitro*, adoptent au moins deux phénotypes dits 'prolifératif' et 'invasif'. Ces phénotypes sont régulés par des processus épigénétiques et transcriptionnels, eux-mêmes régis par la variation du niveau fonctionnel de MITF (MIcrophthalmia-associated Transcription Factor) en coopération avec un second facteur de transcription, SOX10 (SRY (Sex-determining Region Y-bOX 10) (Verfaillie et al., 2015).

L'étude par spectrométrie de masse des interactomes de MITF, réalisée au sein de notre groupe, a démontré que MITF interagit physiquement et fonctionnellement avec les complexes de remodelage de la chromatine NURF (NUcleosome Remodelling Factor) et PBAF (PolyBromo BRG1-Associated Factor) (Laurette et al., 2015). Notre groupe a également démontré que NURF et PBAF ont chacun un rôle spécifique et distinct dans les cellules de mélanome *in vitro* et dans la lignée mélanocytaire *in vivo* (Koludrovic et al., 2015; Laurette et al., 2019, 2015). NURF et PBAF apparaissent ainsi comme des régulateurs épigénétiques majeurs dans le contrôle de l'expression des gènes de la lignée mélanocytaire.

L'étude de l'interactome de MITF dans les cellules de mélanome a permis de mettre en évidence son interaction avec un troisième complexe de remodelage de la chromatine appelé NuRD (Nucleosome Remodelling and histone Deacetylation complex). NuRD comporte plusieurs sous-unités dont les ATPases CHD3, CHD4 ou CHD5 (Chromodomain Helicase DNA-binding protein), les Histones DéACétylases HDAC1 ou HDAC2, MBD2 ou MBD3 (Methyl cytosine-guanosine (CpG) Binding

Domain) ainsi que MTA1, MTA2 ou MTA3 (MeTastasis Associated gene protein). La composition exacte de NuRD dans un tissu donné dépend donc de l'expression relative de chacune de ces sous-unités. Ce complexe est unique, puisqu'il est le seul à posséder deux types de sous-unités catalytiques, CHD3, CHD4 ou CHD5 dont l'activité ATPase est responsable du remodelage de la chromatine, et HDAC1/2 qui catalyse la désacétylation de protéines dont les histones. Comme les autres complexes de remodelage de la chromatine, NuRD est impliqué dans la régulation de nombreux processus essentiels tels que la transcription et l'assemblage de la chromatine, la progression du cycle cellulaire et la stabilité génomique (Torchy, Hamiche, & Klaholz, 2015).

Les objectifs de mon projet de thèse ont porté tout d'abord sur la caractérisation de l'interaction physique et fonctionnelle du complexe NuRD avec des facteurs de transcription essentiels tels que MITF et SOX10 ou d'autres facteurs de transcription. Puis, sur la détermination des différentes fonctions du complexe NuRD au sein des cellules de mélanome. Et enfin, sur l'extrapolation des fonctions régulatrices de NuRD dans d'autres cancers que le mélanome.

MITF et SOX10 interagissent avec le complexe NuRD.

Au vu de la présence de sous-unités de NuRD dans l'interactome de MITF, nous avons réalisé une analyse similaire de l'interactome de SOX10 au sein des cellules de mélanome. Tout comme pour MITF, les données de spectrométrie de masse ont permis de détecter que SOX10 interagit avec une multitude de sous-unités des complexes BAF, PBAF et NuRF associées à SOX10 telles que les sous-unités catalytiques BRG1, BRM et BPTF. Ces interactions ont ensuite été confirmées par immunoblots après immunoprécipitations indépendantes en tandem. L'interactome de SOX10 montre également la présence de plusieurs sous-unités du complexe NuRD.

Plus particulièrement, l'analyse des interactomes de MITF et SOX10 a montré la présence de CHD4 mais pas de CHD3 dans l'interactome de MITF, ainsi que la présence de CHD4 et de CHD3 dans l'interactome de SOX10. D'autres sous-unités telles que HDAC1, HDAC2, MTA1 et MTA2 sont présentes dans les deux interactomes. Les interactions sélectives de MITF avec CHD4 et de SOX10 avec CHD3 et CHD4 ont été confirmées par co-immunoprécipitation et immunoblots.

Afin de caractériser la composition du complexe NuRD dans les cellules de mélanome, nous avons démontré que les sous-unités de NuRD sont bien exprimées au sein des lignées prolifératives, et ce contrairement aux lignées dites invasives où le niveau d'expression des sous-unités catalytiques CHD3 et CHD4 est fortement réduit au niveau protéique. De plus, la répression de CHD4 entraine une surexpression de CHD3 suggérant que ces deux isoformes sont en compétition dans l'assemblage du complexe NuRD. D'autre part, CHD4 ne co-précipite pas avec CHD3, mettant ainsi en évidence la présence dans les cellules de mélanome de deux complexes NuRD composés soit de CHD3 soit de CHD4. Il semble donc que MITF interagisse sélectivement avec le complexe CHD4/NuRD, alors que SOX10 interagit avec les complexes CHD3/NuRD et CHD4/NuRD.

NuRD est un cofacteur de SOX10 dans la régulation de l'expression d'un sous-ensemble de gènes.

Des expériences de ChIP-seq ont permis d'identifier dans l'ensemble du génome plus de 60'000 sites de fixation de CHD4. Plus de 4000 de ces sites sont communs entre CHD4, MITF et SOX10. CHD4 occupe les nucléosomes bordant ces sites dont la plupart sont également occupés par BRG1, la sous-unité catalytique de PBAF. Cette observation n'implique cependant pas que ces nucléosomes soient fixés par les deux complexes en même temps. Il est plus raisonnable d'imaginer que la fixation par NuRD ou PBAF définisse deux états alternatifs de ces nucléosomes.

L'analyse comparative des RNA-seq après la répression de CHD4 et MITF ne révèle qu'un petit nombre de gènes régulés de façon positive ou négative par les deux facteurs CHD4 et MITF. Néanmoins, la comparaison des gènes dérégulés par CHD4, CHD3 ou SOX10 met en évidence environ 300 gènes co-régulés par ces facteurs. L'ensemble des données montre donc que, malgré leur association et leur co-localisation dans le génome, CHD4 ne semble pas agir en tant que cofacteur de MITF mais agit en fait en tant que cofacteur de SOX10 dans la régulation d'un sous-ensemble de gènes cibles au sein des cellules de mélanome.

CHD3 and CHD4 s'associent avec RREB1 et co-régulent un sous-ensemble de gènes cibles.

Par ailleurs, CHD3 et CHD4 régulent l'expression de nombreux autres gènes. Afin d'identifier d'autres facteurs impliqués dans la régulation de ces gènes, nous avons analysé les séquences des 800 sites de fixation génomique de CHD4 les plus forts. Cette analyse a démontré un très fort enrichissement de motifs fixés par RREB1 (Ras Responsive Element Binding protein 1), un facteur de transcription fréquemment amplifié dans le mélanome et situé en aval de la voie RAS. Ce facteur est connu pour fixer les sites RREs (Ras Responsive Elements) et réprimer l'expression génique. En effet, plus de 30% des gènes dérégulés par la répression de CHD4 présentent un site de fixation de CHD4 associé à un motif RRE à moins de 30kb du site d'initiation de la transcription. Par des expériences d'immunoprécipitation, nous avons pu mettre en évidence une interaction spécifique et stable entre NuRD et RREB1. Des expériences de siARN ont montré l'importance de RREB1 dans la prolifération et la survie des cellules de mélanome. Une analyse RNA-seq après siRREB1 a montré qu'un nombre important de gènes régulés par CHD3 et CHD4 le sont aussi par RREB1. Ces résultats montrent que NuRD s'associe avec RREB1 et agit comme un co-répresseur dans la régulation d'un sous-ensemble de ses gènes cibles dans les cellules de mélanome.

CHD3 et CHD4 sont nécessaires à la prolifération des cellules de mélanome.

La répression de CHD4 dans plusieurs lignées prolifératives de cellules de mélanome ainsi que dans des mélanocytes entraîne un changement important de leur morphologie, un ralentissement de leur prolifération ainsi qu'une activation de la réponse aux dommages de l'ADN. La répression de CHD3 provoque également un changement de morphologie de ces cellules, différent de celui observé après répression de CHD4, ainsi qu'un arrêt de la prolifération cellulaire.

De plus, la répression de CHD4 dans la lignée proliférative 501mel entraîne la dérégulation de plus de 1300 gènes, la plupart étant induits, parmi lesquels des gènes impliqués dans l'adhésion, la migration et la prolifération cellulaire. CHD3 régule plus de 900 gènes, parmi lesquels des gènes impliqués dans le cycle cellulaire, le métabolisme des lipides et la réponse inflammatoire. La comparaison

des données RNA-seq indique cependant que très peu de gènes sont dérégulés en commun par CHD3 ou CHD4, mettant ainsi en évidence le rôle spécifique et distinct des complexes NuRD comprenant soit CHD3 soit CHD4.

CHD4 régule l'activité de la voie de signalisation MAP-kinase et la glycolyse.

La répression de CHD4 dans différentes lignées de cellules de mélanome a pour conséquence une activation de la voie MAP-kinase qui se traduit par une augmentation de la phosphorylation d'ERK1/2. La voie MAP-kinase régule en particulier la voie de signalisation mTOR impliquée dans la régulation de la prolifération et du métabolisme cellulaire. La répression de CHD4 augmente la phosphorylation de mTOR (S2448) et stimule la glycolyse dans les cellules de mélanome. Une telle augmentation de la glycolyse ainsi qu'une diminution de la phosphorylation oxydative ont pu être confirmées par mesure de l'ECAR (Extracellular Acidification Rate) et de l'OCR (Oxygen Consumption Rate). Ainsi, nous avons montré que le ralentissement de la prolifération observée suite à la répression de CHD4 est dû au moins en partie à une hyperactivation de la glycolyse qui résulte de la stimulation des voies MAP-kinase et mTOR provoquant une déplétion du niveau de l'ATP total des cellules de mélanome.

CHD4 régule l'expression des PADs et la citrullination de PKM2 dans les cellules de mélanomes et d'autres cancers.

Nous avons par ailleurs pu mettre en évidence une seconde voie importante de régulation de la glycolyse. Parmi les gènes les plus fortement dé-réprimés par la répression de CHD4 se trouvent PADI1 (Protein Arginine DeIminase 1) et PADI3, deux enzymes responsables de la conversion des arginines en citrulline. Nous avons montré que dans plusieurs lignées de mélanomes l'expression de ces deux enzymes, qui sont pratiquement indétectables dans les conditions controles, est activée au niveau ARN et protéique après répression par CHD4.

L'augmentation de la glycolyse induite par la répression de CHD4 est fortement réduite à la suite de la répression de PADI1 et PADI3. De plus, l'expression exogène des protéines PADI1 ou PADI3, ou des deux à la fois, montre une forte

stimulation de la glycolyse. Nous avons ainsi pu démontrer que PADI1 et PADI3 étaient à la fois nécessaires et suffisants à l'augmentation de la glycolyse.

Afin d'identifier les potentiels substrats de ces enzymes, nous avons réalisé des immunoprécipations d'extraits protéiques de cellules en conditions contrôle ou siCHD4 en utilisant un anticorps pan-citrulline, suivies d'analyses par spectrométrie de masse. Nous avons ainsi pu mettre en évidence une citrullination de multiples enzymes de la glycolyse dont PKM2 (Pyruvate Kinase Muscle isozyme M2). Des immunoblots dans différentes lignées ont permis de valider l'augmentation de la citrullination de PKM2 suite à la répression de CHD4 ou après expression ectopique de PADI1 et PADI3.

PKM2 est une enzyme hautement régulée qui joue un rôle central dans la régulation de la glycolyse. En effet, son activité est positivement régulée par la sérine, le Fructose 1.6-BisPhosphate (FBP) ainsi que le Succinyl Amino Imidazole-CarboxAmide Riboside (SAICAR) et négativement régulée par le Tryptophane (Trp), la Phénylalanine (Phe) et l'Alanine (Ala), couplant ainsi le flux glycolytique aux niveaux cellulaires des métabolites intermédiaires (Chaneton et al., 2012; Christofk, Vander Heiden, Wu, Asara, & Cantley, 2008a; Keller, Doctor, Dwyer, & Lee, 2014a; Macpherson et al., 2019; O'Neill et al., 2013). Ainsi, en cas d'excès de glycolyse, la balance activateurs/inhibiteurs penche en faveur d'une inhibition de l'activité de l'enzyme par la fixation de Trp, Phe ou Ala (P. Wang, Sun, Zhu, & Xu, 2015; Yuan et al., 2018).

Des données de spectrométrie de masse ont permis d'identifier 3 arginines de PKM2 enrichies en citrullination dans la condition siCHD4. Parmi lesquelles R106, R246 et R489, chacune d'entre elles placées à des sites critiques aux processus de régulation de l'activité de l'enzyme.

R489 est directement impliquée dans la fixation du FBP. Il a été montré que muter spécifiquement R489 prévient la fixation du FBP et atténue son effet activateur (Macpherson et al., 2019; Morgan et al., 2013). La perte de charge de R489 par la citrullination diminuerait ou préviendrait alors la fixation du FBP, augmentant ainsi l'effet de la régulation allostérique de PKM2 par les acides aminés libres.

R246 forme des interactions à un point central du mouvement des domaines structuraux de l'enzyme impliqués dans les variations entre les formes actives et

inactives. La citrullination de R246 pourrait fortement affaiblir ces interactions et faciliter ainsi le maintien de la forme active de l'enzyme.

R106 est en contact direct soit avec la sérine qui agit comme un activateur allostérique, soit avec le Trp, la Phe ou l'Ala, qui agissent comme répresseurs allostériques. Ces régulateurs se fixent de façon compétitive dans la même poche, et l'activité de l'enzyme dépend alors de leur concentration relative dans la cellule. La fixation de la sérine stabilise la conformation active de l'enzyme, alors que la fixation du Trp, de la Phe ou de l'Ala, de par leur pôle hydrophobe, repousse le domaine N-terminal, menant ainsi à la conformation inactive de l'enzyme. La citrullination de R106 entraine une perte de charge et d'interaction avec les acides aminées libres. La fixation de la sérine est alors peu affectée puisque elle est à l'origine de nombreuses liaisons hydrogènes impliquées dans sa stabilisation au sein de la poche et ainsi ne modifie pas la conformation active de l'enzyme. Par contre, les acides aminés hydrophobes, qui induisent un changement structural important pour passer en forme inactive, pourraient être affectés par une interaction plus faible ou absente avec R106. Par voie de conséquence, la citrullination de R106 affaiblirait la répression allostérique augmentant ainsi l'activation de l'enzyme par la sérine.

Par expérimentations au sein des cellules de mélanomes, nous avons pu en effet montrer que la présence de sérine était nécessaire à la stimulation de la glycolyse par citrullination. Par contre, la citrullination provoque une stimulation de la glycolyse même en présence de concentrations élevées de Trp, Phe ou Ala, les inhibiteurs allostériques de PKM2. Ces résultats montrent donc que la citrullination de PKM2 par PADI1 et PADI3 diminue l'inhibition allostérique par Trp, Phe, et Ala favorisant ainsi l'activation par la sérine.

CHD4 régule l'expression de PADI1 et PAD3 et la glycolyse dans d'autres cancers.

La capacité de CHD4 à réguler l'expression de PADI1/PADI3 et la glycolyse n'est pas spécifique aux cellules de mélanome. En effet, la répression de CHD4 dans des lignées cellulaires de carcinome du col de l'utérus ou du carcinome du rein entraîne un ralentissement de la prolifération ainsi qu'une diminution de la capacité clonogénique des cellules. Ce ralentissement de la prolifération est accompagné

d'une induction de PADI1 et de PADI3 ou parfois de PADI3 seul, ainsi que d'une augmentation de la glycolyse. PADI1 et PADI3, qu'ils soient induits par répression de CHD4 ou exprimés de façon exogène, sont à la fois nécessaires et suffisants pour stimuler la glycolyse.

Ces résultats ont ainsi pu démontrer que la répression de CHD4 ou l'expression ectopique de PADI1 et PADI3 est responsable d'une augmentation de la glycolyse entraînant un ralentissement de la prolifération cellulaire qui résulte de la déplétion de la cellule en ATP dans les lignées cellulaires de carcinome du col de l'utérus ou du carcinome du rein.

Conclusions

L'ensemble de ce travail a permis de mettre en évidence le rôle déterminant du complexe NuRD dans les cellules de mélanome. Ce travail a en effet montré que MITF et SOX10 interagissent avec NuRD. CHD4 co-localise sur le génome avec MITF et SOX10. Mais seuls SOX10 et NuRD répriment ensemble un programme d'expression génique. De plus, ce travail a mis en évidence l'interaction de NuRD avec un autre répresseur, RREB1, avec lequel il régule l'expression d'un ensemble de gènes liés à la voie de signalisation RAS-MAP-kinase.

Cependant, le résultat le plus important de ce travail de recherche concerne le rôle de CHD4 dans la régulation de l'expression de PADI1 et PADI3, deux enzymes responsables de la citrullination de l'enzyme glycolytique PKM2. PADI1 et PADI3 sont nécessaires et suffisants pour stimuler la glycolyse des cellules de mélanome ainsi que d'autres cellules cancéreuses. La citrullination des arginines de PKM2, localisées à des sites critiques de la régulation allostérique, diminue la sensibilité de l'enzyme à l'effet inhibiteur du tryptophane, de la phénylalanine et de l'alanine, et ainsi module la régulation dynamique de PKM2 en maintenant son activité, même lorsque le niveau de sérine activatrice dans la cellule est diminué.

L'ensemble de ce travail de thèse a ainsi permis de mettre en évidence le lien entre la régulation épigénétique par NuRD notamment de l'expression de PADI1 et PADI3, la citrullination de PKM2 et la régulation du métabolisme et de la prolifération des cellules cancéreuses.

INTRODUCTION

CHAPTER 1

Melanocytes: from origins to melanoma

CHAPTER 1. Melanocytes: from origins to melanoma

A. Localization

1) Anatomy of the skin

The skin is the largest organ of the human body that ensures a number of critical functions necessary for survival. The skin is involved in the regulation of several functions including protection against external physical, chemical, and biological assailants, as well as hydration regulation and thermoregulation. The skin has also many roles in health maintenance, but conversely has many potential problems, with a large number of skin disorders identified.

The skin is composed of three main layers: the epidermis, the dermis and the hypodermis (Fig.1) (K.L. Moore and T.V.N. Persaud, 1998):

- The **epidermis** mainly consists of a specific constellation of cells known as keratinocytes which synthesize keratin, filament-forming proteins with specific physicochemical properties. The epidermis is associated with the different epidermal appendages but relies solely on the blood supply from the dermis for nutrients and oxygen delivery. The basement membrane, also called the dermo-epidermal junction, is located at the junction between the dermis and the epidermis and has a role in the spatial organization and architecture of the epidermis as it controls the anchoring and the polarity of basal proliferating keratinocytes and other epidermal cell types.

- The **dermis** is the layer of connective tissue underneath the epidermis. It houses capillaries, lymphatic vessels, immune cells (Langerhans cells, macrophages and mast cells), a variety of nerve fibers and sensory receptors (Meissner, Pacini, Ruffini corpuscles) and epidermal appendages structures, such as nails, hair follicles, sebaceous glands and sweat glands.

  The dermis is made of two layers of connective tissue that result in an interconnected mesh of elastin and collagenous fibers produced by fibroblasts.

  - The superficial layer of the dermis so-called papillary layer is made of loose, areolar connective tissue. This layer contains fibroblasts, a small

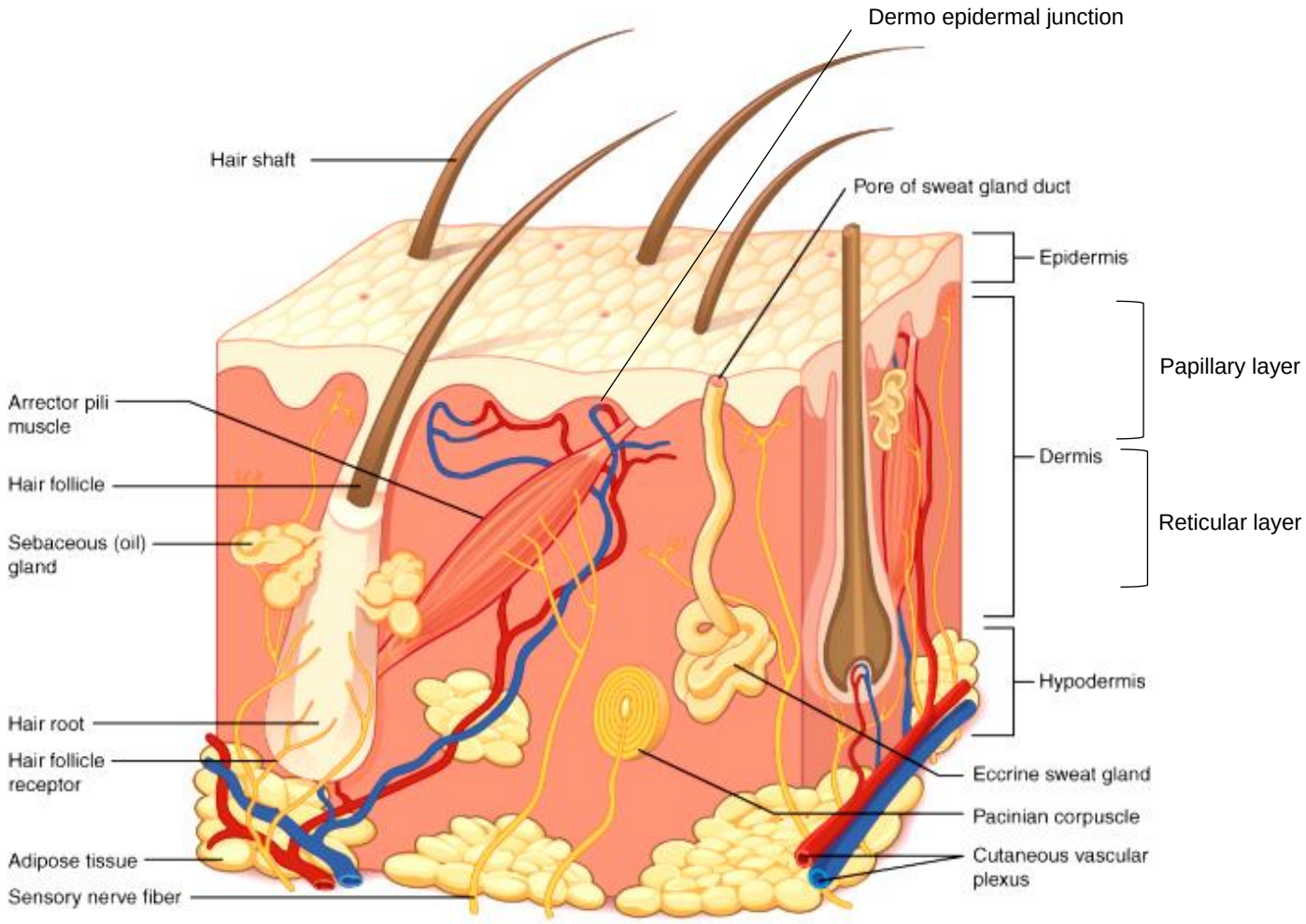

Figure 1. The integumentary system.

The skin and its accessory structures form the integumentary system. The skin is composed of three major layers: the epidermis, the dermis (itself divided into the papillary and reticular layers) and the hypodermis. Accessory structures are also illustrated such as e.g. hair follicles, sebaceous glands and sweat glands (Adapted from courses.lumenlearning.com).

number of adipocytes and an abundance of small blood vessels, lymphatic capillaries, nerve fibers and touch receptors.

- The reticular layer represents the deeper region and is composed of dense and irregular connective tissue well vascularized, giving the skin his overall strength and elasticity, and rich of sensory and sympathetic nerve supply.

- The **hypodermis** is the innermost layer that anchors the skin to underlying fascia of the bones and muscles. This layer consists of well-vascularized, loose and areolar connective tissues which function as a mode of fat storage and acts as energy reserve and heat insulators.

The thickness of these different layers varies considerably depending on the body location. The eyelid, for example, has the thinnest layer of the epidermis (less than 0.1 mm), whereas the palms and soles of the feet have the thickest epidermal layer (approximately 1.5 mm) (L.P.Gartner and J.L. Hiatt, 2007).

2) The epidermis

The epidermis is a stratified and squamous epithelium layer that ensures most protective functions of the skin.

i) Anatomy

The epidermis is commonly divided into four to five layers (Fig.2) according to keratinocyte morphology and position and includes the basal cell layer (stratum basale), the squamous cell layer (stratum spinosum), the granular cell layer (stratum granulosum), the thin clear cell layer (stratum lucidum) and the cornified or horny cell layer (stratum corneum). Most of the skin is classified as “thin skin” but “thick skin” (that as said above is found on the palms of the hands and the soles of the feet) only includes the thin clear cell layer, called the stratum lucidum, located between the stratum corneum and the stratum granulosum (K.L. Moore and T.V.N. Persaud, 1998).

- The **stratum basale** is the deepest epidermal layer that attaches the epidermis to the basal lamina, below which the layers of the dermis lie. The stratum basale is a single layer of basal cells. These cuboidal-shaped stem

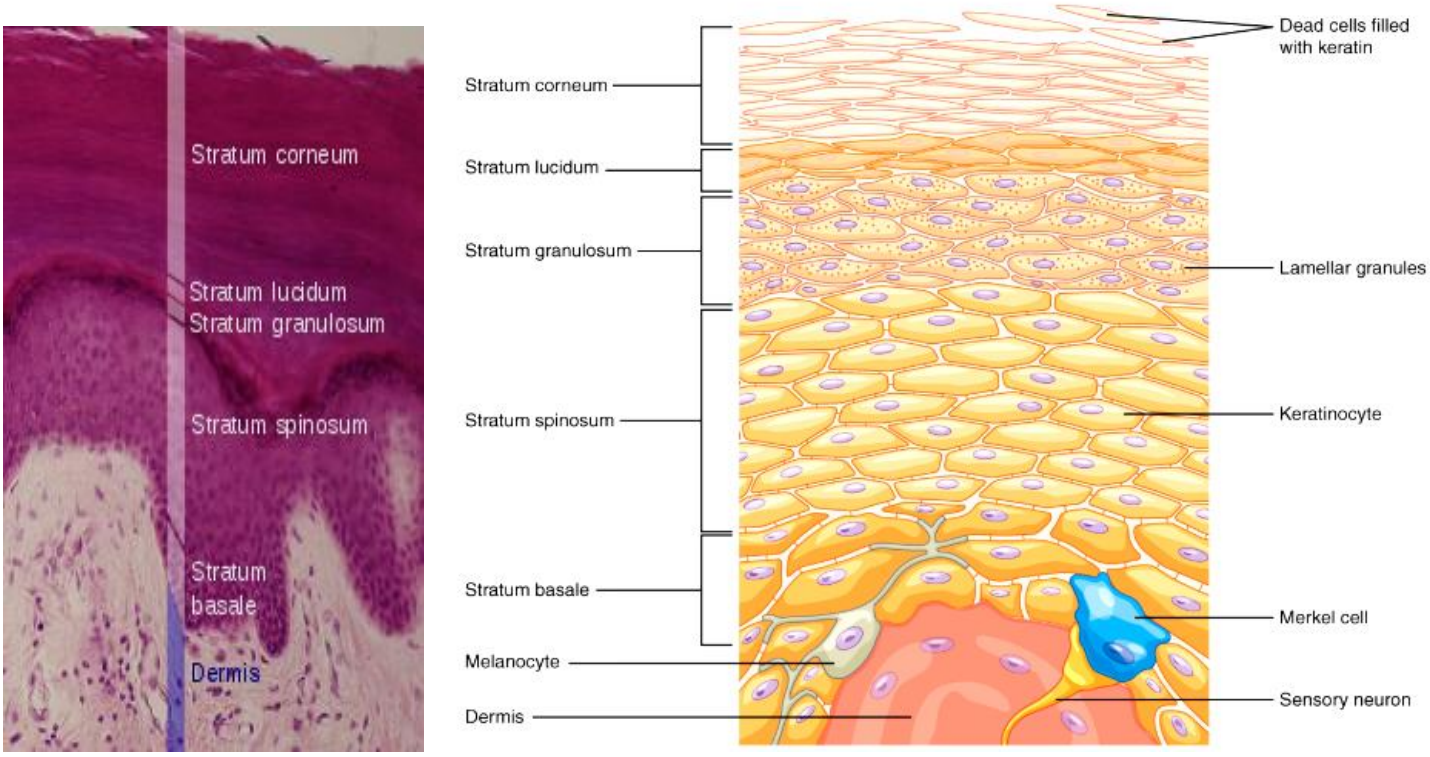

Figure 2. Epidermal layers.

The epidermis is composed of multiple cell layers (histological features on the left panel and schematic representation on the right panel): the basal cell layer (stratum basale), the squamous cell layer (stratum spinosum), the granular cell layer (stratum granulosum), the thin clear cell layer (stratum lucidum) and the cornified or horny cell layer (stratum corneum). (Adapted from https://opentextbc.ca/anatomyandphysiology).

cells are the precursors of the epidermal cells. As new cells are formed, the existing cells are pushed superficially away from the stratum basale.

- The **stratum spinosum** is composed of eight to ten layers of keratinocytes, formed as the result of cell division in the stratum basale. Such keratinocytes control the synthesis of keratin and release a water-repelling glycolipid that helps preventing water loss from the body, making the skin relatively waterproof.
- The **stratum granulosum** is composed of three to five layers of keratinocytes becoming flatter, with thicker membranes. These cells generate large amounts of keratin and keratohyalin, which accumulate as lamellar granules within the cells.
- The **stratum lucidium** is composed of dead and flattened keratinocytes, densely packed with Eleiden, a keratohyalin derived protein rich in lipids, which gives these cells a transparent appearance and provides a waterproof barrier.
- The **stratum corneum** is composed of 15 to 30 layers of cells with increased keratinization (cornification) physiology. This dry and dead layer of cells form an efficient mechanical protection against the environment. Cells in this layer are shed periodically (desquamation) and are naturally compensated by renewal of the epidermis. The entire layer is replaced within a period of approximately 4 weeks.

The epidermis can be subdivided into the Inter Follicular Epidermis (IFE) unit and the associated adnexal structures called the pilosebaceous unit. The pilosebaceous unit is attached to the IFE and has important functions within the tissue that are mediated through its components: infundibulum, isthmus, sebaceous glands and hair follicles (Fig.3).

ii) Epidermal cell lineages

The epidermis is composed of a diverse organized array of cells from different embryonic origins. The epidermis is mainly composed of keratinocytes (90%) but

harbors as well a number of other cell populations, such as Langerhans cells (3-5%), Merkel cells (2-5%) and melanocytes (2-4%) (Fig.2).

- **Keratinocytes** represent the most abundant cell type of the epidermis and derive from embryonic ectoderm. Keratinocytes proliferate from the stratum basale and undergo multiple stages of cell differentiation as illustrated while moving up through the strata (I.Brody, 1960).
- **Langerhans cells** are mobile dendritic cells derived from hematopoietic stem cells of the bone marrow. They reside in the epidermis as a dense network of immune system sentinels (P.Langerhans, 1868).
- **Merkel cells** are neuroendocrine epidermal resident cells that originally emerged from the embryonic epidermis. These cells are present in the basal layer of the epidermis, transmitting sensory signals through synaptic contacts with somatosensory neurons (F.S. Merkel, 1875).
- **Melanocytes** represent a minority cell population within the basal epidermis that divide infrequently. Their function is mainly to provide melanin pigment to their neighboring keratinocytes to protect them from UV radiation–induced DNA damages (K.L. Moore and T.V.N. Persaud, 1998).

iii)Epidermal stem cells

Stem Cells (SCs) carry the remarkable capacity to both self-renew for an extended period of time and give rise to the differentiating cells that constitute one or more tissues. In cancers, SCs have been demonstrated to be essential cells at origin of tumor formation, so that SC characteristics and markers are detectable in many types of cancers (da Silva-Diz et al., 2013; Lapouge et al., 2011; White et al., 2011).

The mammalian epidermis contains several self-renewing compartments including many different types of SCs that ensure the maintenance of skin homeostasis and hair regeneration but also participate in the repair of the epidermis after injuries (reviewed in Y. Li et al. 2017). Indeed, skin contains separate SCs compartments located in niches. Major niches are located on the basement membrane of the IFE, in the bulge region of the hair follicle and in the sebaceous gland (Fig.3) (Ghazizadeh & Taichman, 2001). Each compartment maintains its own

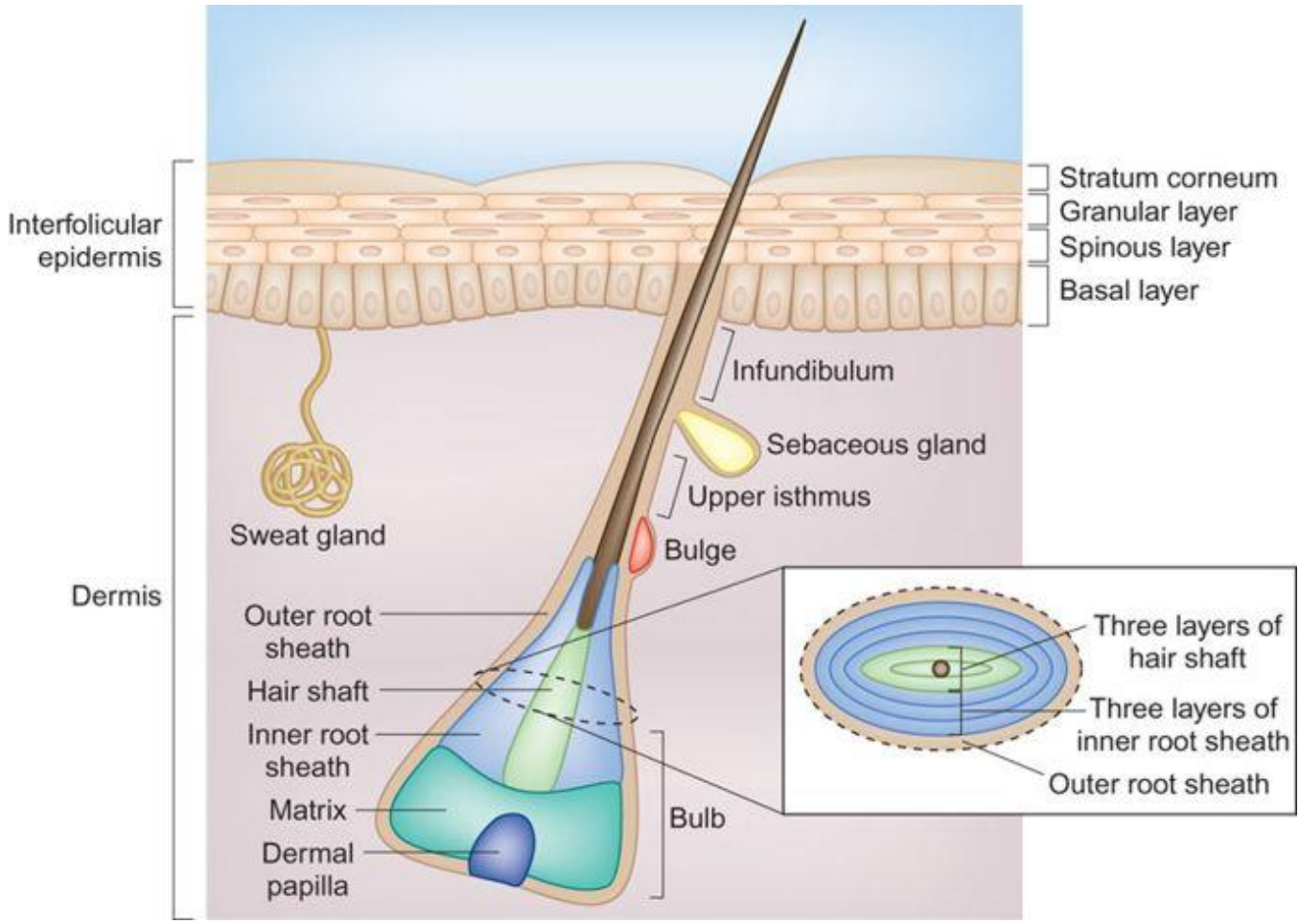

Figure 3. The pilosebaceous unit.

The pilosebaceous unit is composed of the hair follicle, the hair shaft and the sebaceous gland. The hair follicle can be divided in three segments including Infundibulum, Isthmus and Bulb. The bulb is composed of seven concentric cell layers: the outer root sheath, three layers of inner root sheath (Henley's, Huxley's and cuticle) and three layers of hair shaft (hair cuticle, hair cortex and medulla) (David M. Owens et al. 2009).

discreet cell number however it can supplement each other's cell population under particular conditions such as wound repair (M. Ito et al., 2005a).

Over the years a number of models have been proposed to explain epidermal maintenance (reviewed in Schepeler, Page, and Jensen 2014). The classical hierarchical model proposes that slow cycling stem cells divide in the basal layer thus giving rise to progeny with limited proliferative potential so called Transit Amplifying Cells (TACs), amplify the number of cells and participate in epidermis replenishment. TACs undergo a finite number of cell divisions before becoming terminally differentiated as they transit upwards through the suprabasal layers. According to this model, SCs were described in the basal layer of adult epidermis and architecturally defined as Epidermal Proliferative Units (EPUs). Each EPU is made of one self-renewing stem cell with 10 tightly packed basal cells yielding a stack of increasingly larger and flatter cells, the aforementioned TACs (Ghazizadeh & Taichman, 2001; Mackenzie, 1997; Paterson & Christie, 1974). More recent studies suggest that basal epidermal cells can divide asymmetrically, affording a different view of how one basal stem cell and one committed cell might arise (Clayton et al., 2007; Lechler & Fuchs, 2005).

The hair follicle (HF) is an epidermal mini-organ endowed with a unique structure and cyclic behaviour. HFs cycle throughout life between growth (anagen), regression (catagen) and resting (telogen) phases. The best-characterized stem cell population of HFs is located in the upper permanent region below the sebaceous glands commonly referred as the bulge or the niche (Fig.3). These cells have been thoroughly investigated because of their prominent location, highly quiescent nature (Cotsarelis, Sun, & Lavker, 1990), extensive clonogenic capacity *in vitro* (Oshima, Rochat, Kedzia, Kobayashi, & Barrandon, 2001) and their expression of a set of distinct markers (reviewed in Fuchs and Horsley 2008). Indeed, stem cells of the bulge area were shown to differentiate into hair-follicle matrix cells, sebaceous-gland basal cells, and epidermis.

In addition to the bulge SCs other SC populations were identified in the HFs that differ on their expression markers. These include the isthmus region (Nijhof et al., 2006; Snippert et al., 2010), the junctional zone (K. B. Jensen et al., 2009; U. B. Jensen et al., 2008), the lower bulge and hair germ (Jaks et al., 2008) and the sebaceous gland (Horsley et al., 2006) containing melanocytes with SC characteristics (Grichnik et al., 1996; Okamoto et al., 2014). However, the

interconnection among these cell populations as well as their contribution to skin homoeostasis are not yet fully understood.

Under homeostatic conditions each stem cell population generally contributes only to the differentiation program that exists within its location. However, following injury, when the systemic and local environments change dramatically, these stem cell populations display remarkable plasticity. Even if their own niche is not perturbed, nearby stem cells respond to wound-induced stimuli by exiting their niche thus participating in re-epithelialization or protection of the damaged tissues (M. Ito & Cotsarelis, 2008; M. Ito et al., 2005b; P. J. Jensen, Taylor, Lavker, Lehrer, & Sun, 2000). Interestingly, it has been demonstrated that after wounding or ultraviolet type B irradiation, Melanocyte Stem Cells (MSCs) in the HFs exit the stem cell niche before their initial cell division and migrate to the epidermis to differentiate into functional epidermal melanocytes, thus providing a pigmented protective barrier against ultraviolet irradiation over the damaged skin (Wei Chin Chou et al. 2013).

Hence, HFs and sweat glands are recognized as reservoirs of MSCs. Whether these observations reflect the normal homoeostatic mechanism of melanocyte renewal, or unperturbed IFE can maintain a melanocyte population independently of the skin's appendages is yet poorly understood. Nevertheless, regions of skin in patients with vitiligo that lack HFs can occasionally become repopulated by melanocytes thus suggesting that IFE is capable of long-term maintenance of melanocytes. Indeed, James D. Glover et al. showed that mouse tail skin lacking appendages maintains a stable melanocyte number throughout adult life via actively cycling differentiated and amelanotic melanocytes (Glover et al., 2015; Seleit, Bakry, Abdou, & Dawoud, 2014).

B. Cellular origins of melanocytes

Melanocytes arise from a group of migratory embryonic cells referred as the Neural Crest Cells (NCCs). NCCs derive from the embryonic germ layer named ectoderm at the interface between the neural plate and the adjacent non-neural ectoderm (Dupin, Creuzet, & Le Douarin, 2006) with the exception of retinal pigment epithelium melanocytes that arise from the neuroectoderm.

NCCs are induced during gastrulation and initially reside in the neural plate border territory. During neurulation the neural plate invaginates so that the elevating neural

folds containing neural crest precursors form the leading edges of the closing neural tube (Bronner, 2012). Then, NCCs undergo an Epithelial-Mesenchymal Transition (EMT) which enables them to acquire the motility and migratory properties required to detach from the dorsal neural tube and then colonize their different target sites in the organism. NCCs form a transient population of pluripotent progenitor cells that progressively give rise to several different lineages (Betters, Liu, Kjaeldgaard, Sundström, & García-Castro, 2010; Ernfors, 2010). Their migratory trajectory takes place along two major paths, dorsoventrally or dorsolaterally. Most NCCs migrate dorsoventrally to give rise to multiple cell types like Schwann cells, smooth muscle cells, peripheral neurons or adipocytes. While cells taking the dorsolateral path are thought to give rise to melanocytes precursors, the melanoblasts (Ernfors, 2010). However, there is strong evidence that a fraction of melanocytes arise from cells migrating first ventrally and then along the nerves (Adameyko et al., 2009; Cramer, 1984), suggesting the double origin of melanocytes in the skin. Thus, melanocytes either derive directly from NCCs populating the skin via a dorsolateral migratory pathway or arise from ventrally migrating precursors (Sommer, 2011).

Induction of the neural crest formation is dependent upon Bone-Morphogenetic Proteins (BMPs) (Bond, Bhalala, & Kessler, 2012) and induction of many signaling pathways including the Wnt (Wingless-type), FGF (Fibroblast Growth Factor) and Notch pathways (Ikeya, Lee, Johnson, McMahon, & Takada, 1997; LaBonne & Bronner-Fraser, 1998; Steventon, Araya, Linker, Kuriyama, & Mayor, 2009). In mammals, melanoblasts are specified from NCCs via expression of essential transcription factors (Fig.4A) such as SRY-BOX 10 (SOX10), MIcrophthalmia-associated Transcription Factor (MITF), L-DopaChrome Tautomerase (DCT) and Mast/Stem Cell growth Factor Receptor (SCFR or KIT). SOX10 expression remains switched on in both melanocytes and glia lineage. Melanoblasts acquire MITF, DCT and KIT expression only when specified (Fig.4A). After colonizing the developing embryonic HFs some melanoblasts differentiate into melanocytes and produce melanin that pigments the first hair cycle. A subset of melanoblasts dedifferentiate (losing MITF and KIT expression but not DCT) to form melanocyte SCs in the HF bulge (Fig.4A-B) (Mort, Jackson, & Patton, 2015).

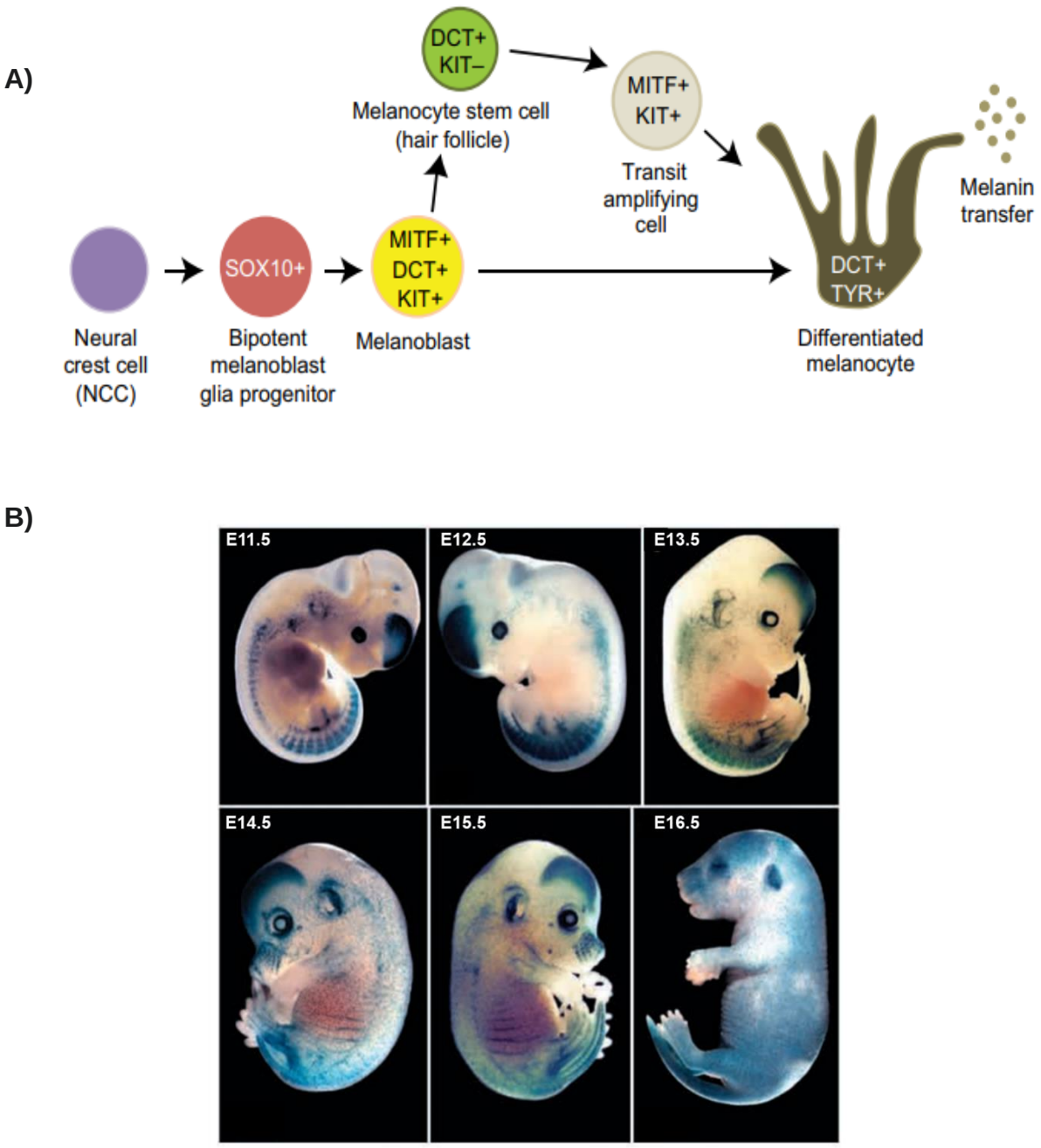

Figure 4. Melanocytes migration and specification from NCCs.

(A) Melanoblasts are specified via a SOX10-positive melanoblast/glial bipotent progenitor and subsequently acquire MITF, DCT and KIT expression. Then, melanoblasts either differentiate into melanocytes to produce melanin or dedifferentiate (loosing MITF and KIT expression but not DCT) to form melanocyte stem cells in the hair follicle bulge (Mort, Jackson and Patton 2015).

(B) The transgenic mouse embryo expressing lacZ under the control of the melanoblast promoter Dct reveals X-GAL blue-stained melanoblasts. By E13.5, melanoblasts begin to disperse ventrally and a significant proportion of the body and face is populated. By E14.5, melanoblasts are more numerous and colonize almost the entire embryo including the ventrum and the crown of the head. Finally, melanoblasts continue to increase in number and start to colonize hair follicles (E15.5-E16.5). Also, the telencephalon, the dorsal root ganglia (DRG) and the retinal pigmented epithelium of the eye are stained (Adapted from Wilkie et al. 2002).

C. Function

Melanocytes are dendritic cells capable of producing melanin. Melanin is the main contributor to pigmentation of skin and hair providing protection from damage by ultraviolet radiation (Bush & Simon, 2007; Costin & Hearing, 2007). Melanin containing granules are known as melanosomes, a lysosome-like structure where melanin is synthetized and exported from melanocytes to adjacent keratinocytes (Dell'Angelica, 2003; Schiaffino, 2010; Wasmeier, Hume, Bolasco, & Seabra, 2008). Melanosomes undergo a multistage maturation from immature endoplasmic vesicles to fully structured and pigmented organelles (Wasmeier et al., 2008).

Skin color and ease of tanning determine the skin 'phototype' (Fitzpatrick, 1988), one of the most useful predictor of skin cancer risk within the population. Differences in skin phototypes arise mainly from variations in the number, size, shape, melanin content and distribution of melanosomes, while the number and spacing of melanocytes remain relatively constant. The melanin content can vary considering that two main types of melanin are synthesized during melanogenesis namely red/yellow pheomelanin or brown/black eumelanin (Kondo & Hearing, 2011). The observed phototype is the result of the ratio of the two, balanced by variables including pigment enzyme expression or availability of tyrosine and sulphydryl-containing reducing agents in the cell (Land & Riley, 2000).

Hence, several enzymes are involved into melanin synthesis such as TYRosinase (TYR), TYRosinase-related Protein 1 (TYRP1) and DCT (Fig.5). Both types of melanin derive from a tyrosinase-dependent biochemical pathway in which L-tyrosine is first hydroxylated to L-3,4-DihydrOxyPhenylAlanine (DOPA) and then oxidized to DOPAquinone in a process catalyzed by TYR. Thus, TYR is the crucial rate-limiting enzyme for the entire melanogenic process (Hearing and Jiménez 1987; Edward J. Land, Christopher A. Ramsden, and Riley. 2003).

The eumelanin and pheomelanin pathways diverge from DOPAquinone (Hearing, 2011). In the eumelanin synthesis pathway DOPAquinone undergoes a redox reaction with another DOPAquinone molecule to generate DOPAchrome. Then, DOPAchrome undergoes tautomerisation resulting in 5,6-DiHydroxyIndole-2-Carboxylic Acid (DHICA) in a process catalyzed by DCT or in 5,6-DiHydroxylIndole (DHI) in absence of DCT. Finally both compounds are further oxidized (DHI by TYR and DHICA by TYRP-1) and polymerized to produce brown to dark eumelanin. In the

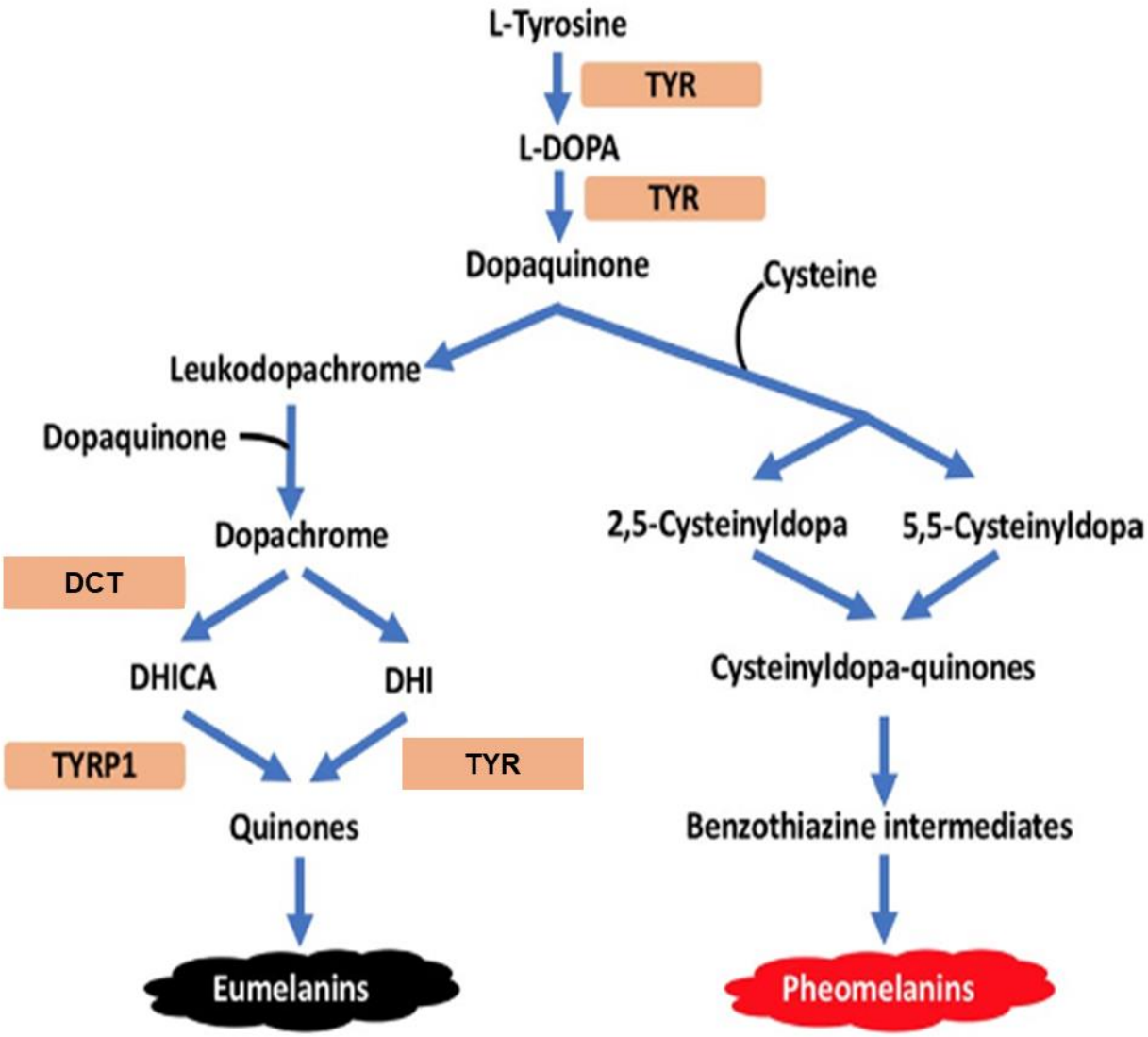

Figure 5. Melanin synthesis pathway.

Melanin is a large bioaggregate derived from the amino acid tyrosine. Epidermal melanins are present in two major forms: eumelanins and pheomelanins differing from their synthesis pathway being eumelanogenesis or pheomelanogenesis, respectively (Adapted from Nguyen and Fusher 2017).

pheomelanin synthesis pathway, a cysteine, freely available or derived from glutathione is spontaneously conjugated to DOPAquinone to form cysteinylDOPA isomers (2S- and 5S-) that are further oxidized and polymerized into pheomelanin (Kondo & Hearing, 2011) (Fig.5).Pheomelanin and eumelanin differ not only in colour but also in size, shape and packaging of their granules (Slominski, Tobin, Shibahara, & Wortsman, 2004).

Finally, melanin is packed into melanosomes transported through the melanocytic dendrites using the actin and tubulin fibers (Xufeng Wu, Bowers, Rao, Wei, & Hammer, 1998) and then delivered to the contacting keratinocytes. The formation, maturation and trafficking of melanosomes is crucial to pigmentation. Defects in this process lead to depigmented and dilutionary disorders (Wei, 2006).

Thus, while melanocytes produce pigments, keratinocytes are the actual pigmented cells in the skin. Melanosome transfer is not completely understood yet and different models have been proposed, including melanin released by exocytosis prior to uptake by the keratinocyte, melanosome export over molecular bridges between the cells, or cytophagocytosis of whole dendritic extremities by the keratinocytes (Yamaguchi & Hearing, 2009). Recent research provides evidence for a shedding vesicle system whereby pigment globules containing melanosomes are transferred (Ando et al., 2012, 2011). Once in keratinocytes, melanosomes are distributed and in response to UVR, positioned strategically over the ‘sun-exposed’ side of nuclei to form cap-like structures resembling umbrellas (J. Y. Lin & Fisher, 2007).

Indeed, UVB exposure triggered melanogenesis by a variety of paracrine cytokines secreted by keratinocytes such as a-Melanocyte-Stimulating Hormone (a-MSH) (Hachiya, Kobayashi, Ohuchi, Takema, & Imokawa, 2001; Hachiya et al., 2004), Stem Cell Factor (SCF) (Abdel-Malek et al., 1995; I. Suzuki, Cone, Im, Nordlund, & Abdel-Malek, 1996), EndoThelin1 (ET-1) (Imokawa, Miyagishi, & Yada, 1995), Nitric Oxide (NO), AdrenoCorTicotropic Hormone (ACTH) (Schauer et al., 1994; THODY & GRAHAM, 1998), prostaglandins (Nordlund, Collins, & Rheins, 1986), thymidine dinucleotide (Eller, Yaar, & Gilchrest, 1994) and histamine (Yoshida, Takahashi, & Inoue, 2000). These factors induce melanogenesis in neighboring melanocytes through activation of diverse signaling pathways including the Mitogen-Activated Protein Kinases (MAPK), the PhosphoInositide-3-Kinase–

protein kinase B/Akt (PI3K/Akt) and the Wingless-int (Wnt)/B-catenin signaling pathway (reviewed in Pillaiyar, Manickam, and Jung 2017). Triggered melanogenesis through this factors enhances DNA repair and melanin production by activating pigment-related proteins such as MITF that induces the expression of the melanogenesis enzymes TYR, TRP-1 and TRP-2 (Vachtenheim & Borovanský, 2010a).

D. Melanoma skin cancer

Melanoma is a malignant tumor that results from uncontrolled proliferation of melanocytes. It is the most lethal form of skin cancer. In the past 50 years its incidence rose faster than that of any other cancer. While melanoma represents less than 5% of all cutaneous malignancies it accounts for the majority of skin cancer deaths. If melanoma is diagnosed in its early stages, resection of the lesion is associated with favorable survival rates. However, melanoma is an aggressive malignancy that tends to metastasize beyond its primary site. Once melanoma is advanced surgery is no longer sufficient and the disease becomes difficult to treat and thus is associated with poor long-term prognosis (W. H. Ward & Farma, 2017).

1) Epidemiology

Worldwide incidence of melanoma steadily increased over the past decades (Erdmann et al., 2013; Whiteman, Green, & Olsen, 2016). Annual incidence rose as rapidly as 4–6% in many fair-skinned populations predominately in regions like North America, Northern Europe, Australia, and New Zealand (Shen, Sakamoto, & Yang, 2016). Increases in incidence rates vary considerably across populations of different ethnicity and geographical location and even within same population across age and gender.

- **Ethnicity:** The variability of the incidence rates of melanoma across various ethnic groups is higher than for most other cancers (“Global Cancer Observatory,” 2017). Melanoma is disproportionally reported among fair-skinned Caucasian populations (Chao et al., 2017; Padovese et al., 2018). This is partly attributable to decreased photoprotection from reduced melanin content in melanocytes (Brenner & Hearing, 2008). Indeed, compared to fairer-skinned people, UVB

radiation through the epidermis is diminished by approximately 50% in darker-skinned people (Brenner & Hearing, 2008; Everett, Yeargers, Sayre, & Olson, 1966).

- **Geography:** Incidence differences as a function of geographical location originate from variables that influence incident UV radiation including atmospheric absorption, latitude, altitude, cloud cover and season. In 1956, Lancaster proposed the “latitude gradient” theory postulating that the increased melanoma mortality rates correlate with the increased proximity to equator (Lancaster 1956; Oliveria et al. 2006; Elwood et al. 1974). Similar trends were reported since then (Crombie et al., 1979; Moan et al., 2015). Australia e.g. reported a higher incidence of melanoma in relation to a higher degree of sun exposure (Baade, Meng, Youlden, Aitken, & Youl, 2012). However, an inverse latitude gradient was observed in Europe (Armstrong, 1988) with a 3 to 6 fold higher incidence in northern countries like Scandinavia than in southern countries like Spain and Italy (Global Cancer Observatory, 2017). This paradox could partly be attributed to different pigmentation characteristics of the populations of those regions. Indeed, the fairer-skinned populations in Scandinavia and darker skinned populations in southern Europe reflect patterns of melanoma incidence related to ethnicity as discussed above (W. H. Ward & Farma, 2017).
- **Age:** Melanoma incidence ASRs (Age Standardized Rates) climbs steadily and peaks in the seventh and eighth decades of life (http://globocan.iarc.fr). However, while melanoma incidence is lower among people below 40, it is one of the most commonly diagnosed cancers among adolescents and young adults (Ballantine et al., 2017; Garbe & Leiter, 2009; Watson, Geller, Tucker, Guy, & Weinstock, 2016).
- **Sex:** Adolescent and young adult women are more susceptible to melanoma than men in the same age range (Garbe & Leiter, 2009). This may be partly due to the widespread use of indoor tanning by women that is associated with an increased melanoma risk (Colantonio, Bracken, & Beecker, 2014; Guy, Zhang, Ekwueme, Rim, & Watson, 2017; M. Zhang et al., 2012). However, beyond 40, melanoma

incidence is higher in men than women (Garbe & Leiter, 2009; Watson et al., 2016), making men overall more susceptible than women to melanoma.

- **Anatomic distribution:** Among Caucasian populations melanoma is more frequently reported in men on backs and shoulders and in women on the lower limbs (Østerlind, Hou-Jensen, and Møller Jensen 1988; Magnus 1981; Popescu et al. 1990; Cho, Rosner, and Colditz 2005). Considering that these body sites are associated with lower sunlight exposure, these findings were used as a supportive evidence for the intermittent UV exposure theory, suggesting that intermittent and intense sun exposure increased risk for melanoma (Elder, 1989; Stierner, Augustsson, Rosdahl, & Suurküla, 1992). When considering age, melanomas that develop on the trunk occur more often in the fifth and sixth decades of life, whereas melanomas that develop in high UV-exposed body regions like head and neck occur more frequently in the eighth decade (Lachiewicz, Berwick, Wiggins, & Thomas, 2008; Pérez-Gómez et al., 2008; Stang, Stabenow, Eisinger, & Jöckel, 2003).

2) Melanoma classifications

Classification schemes for melanoma help clinicians to identify those patients who are at high risk of developing an advanced disease, to compare treatment results, to recommend the best therapy, and to offer prognostic information to patients and their family.

Typically, melanoma lesions are incidentally discovered during routine skin examination using the “ABCDE” mnemonic that stands for Asymmetry, Border, Color, Diameter and Evolution or Elevation of the suspected lesion (Fig.6.1-2A). Primary tumors can have diverse anatomic distribution, histopathological features, biological and clinical behaviour. Additionally, melanoma primary tumors have a higher propensity to metastasize at an early stage in body locations such as lymph nodes, liver, lungs, bones and central nervous system (Hombuckle et al., 2003; Belhocine et al., 2006). Clark’s classification established in 1970s classified histologic subtypes of melanoma based on the tissues in which the primary tumour arises and included

1)

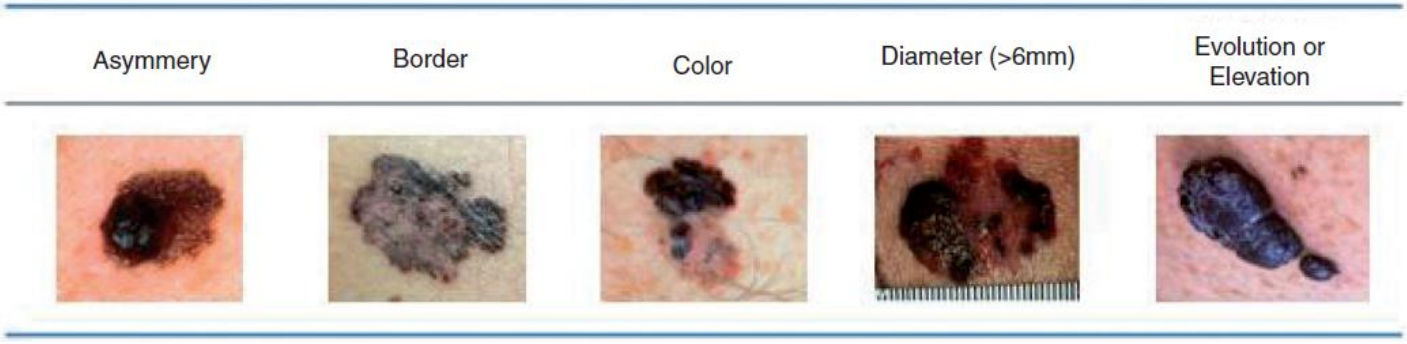

2)

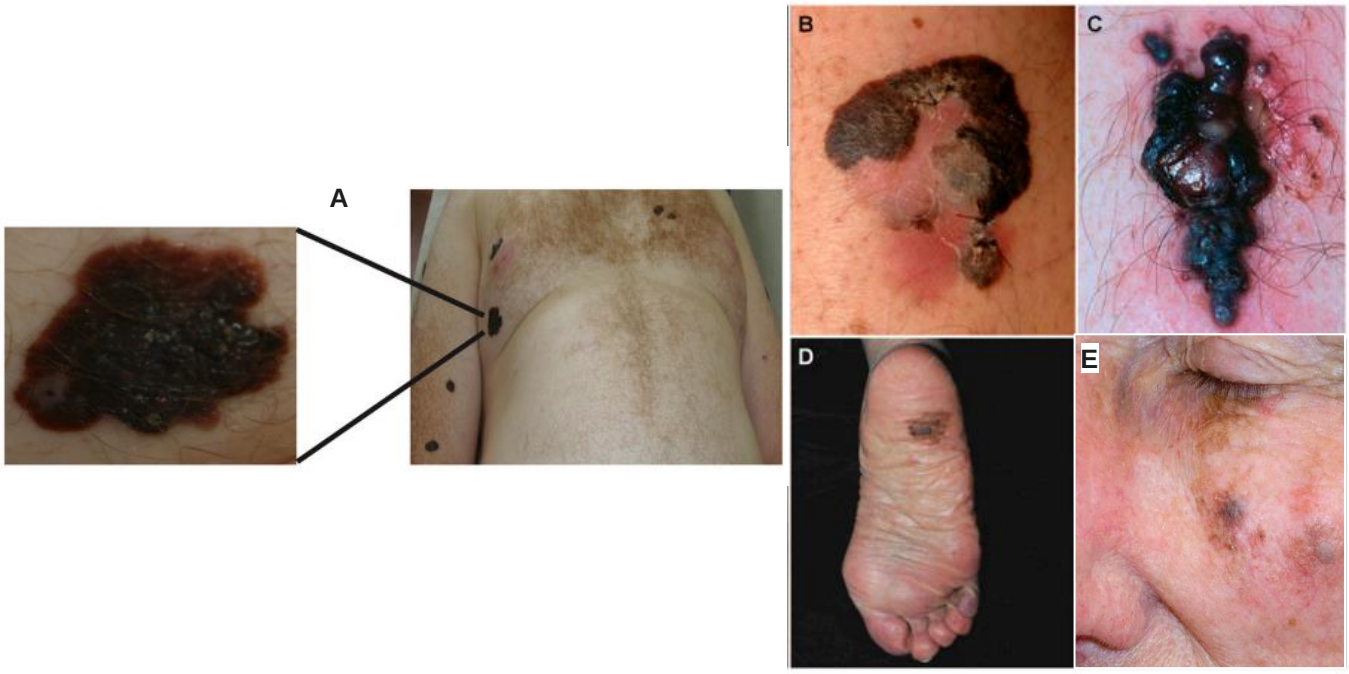

Figure 6. Diagnosis and classification of melanoma

1. ABCDE system for melanoma diagnosis*. Dermatologists and clinicians use during routine skin examination the "ABCDE" mnemonic method that stands for Asymmetry, Borders, Colors, Diameter and Evolution or Elevation of a suspected lesion (Ward and Farma 2017).*

2. Major melanoma subtypes. *(A) Patient with multiple and recurrent cutaneous atypical lesions (Adapted from Davidson et al. 2019). The primary histologic subtypes of cutaneous melanoma include (B) superficial spreading melanoma, (C) nodular melanoma, (D) acral lentiginous and (E) lentigo maligna melanoma (Adapted from Tsao et al. 2012).*

superficial spreading, lentigo maligna, nodular and acral lentiginous subtypes (Clark et al., 1969) (Fig.6.2).

The **superficial spreading** subtype (70%) is the most common type and looks like a slowly growing flat patch of discolored skin (brown or black) and occasionally arise from existing nevus (Fig.6.2B). The **lentigo maligna** subtype (4-15%) frequently appears in sun-exposed areas of fair-skinned older individuals and grows slowly over 5-20 years (Fig.6.2E). The **nodular melanoma** subtype (15%) appears mostly *de novo*, grows rapidly over weeks to months and shows fast and high vertical growth (Fig.6.2C). The **acral lentiginous melanoma subtype** (5%) has a higher incidence in patients with darker skin pigmentation and frequently occurs on the palms, soles, and subungual spaces (Fig.6.2D) (W. H. Ward & Farma, 2017).

Melanoma staging is then completed by a clinical and histological assessment using one of the following scaling approaches:

- The **Clark** scale (I–IV) that categorizes the tumor by the invasion level of the dermal skin layers and subcutaneous fat (Clark, From, Bernardino, & Mihm, 1969b).
- The **Breslow** scale that measures the thickness of the primary tumor in millimeters from top to bottom.
- The **TNM** staging system (**T**umour, **N**ode, **M**etastases), that takes into account the tumor thickness and ulceration (T), the lymph nodes status including in-transit metastasis (N) and distant and systemic metastasis (M) (C. J. Kim et al.2002). TNM was first introduced in 1992 by the American Joint Committee on Cancer (AJCC) and is the most widely accepted staging system for cutaneous melanoma.

Additionally, cutaneous melanomas could be subcategorized from their anatomic origin being or not Chronically Sun Damaged (CSD and non-CSD melanomas). CSD and non-CSD melanomas differ from their anatomical site of origin, degree of cumulative exposure to UV radiations, host age, mutation burden and type of oncogenic alterations (Curtin et al., 2005; Shain & Bastian, 2016). Indeed, melanomas in chronically sun-exposed skin usually appear in older individuals (>55), on chronically sun-exposed areas such as head and neck, as well as the dorsal

region of the upper extremities. Conversely, melanoma associated with intermittent sun-exposed skin cases arises in younger individuals, on intermittent sun-exposed area such as the trunk and proximal extremities. Thus, in their effort to integrate clinicopathological features with somatic genetic alterations, Boris Bastian *et al.* proposed a classification system that takes into account the multiple pathogenic mutations that affect genes in key signaling pathways governing proliferation (BRAF, NRAS and NF1), growth and metabolism (PTEN and KIT), cell identity (ARID2), resistance to apoptosis (TP53), cell cycle control (CDKN2A) and replicative lifespan (TERT) (Curtin et al., 2005).

3) Melanomagenesis

i) Molecular genetic abnormalities associated with melanoma

Over the past decades, the knowledge of somatic genetic events related to melanoma pathogenesis made clear that genetic and epigenetic alterations are critical. Melanomas are thus associated with one of the highest burdens of somatic genetic alterations of all human tumors. The most frequent somatic mutations considered as driver alterations in melanoma development affect BRAF (45-50%, predominantly V600E), NRAS (30%, predominantly affecting codons G12 or Q61), NF1 (5-10%) and KIT (2-8%). Therefore, CSD melanomas have a high mutation burden and are associated with NF1, NRAS and $BRAF^{nonV600E}$ while non-CSD melanomas are associated with a moderate mutation burden and a predominance of $BRAF^{V600E}$ mutations (Birkeland et al., 2018; Curtin et al., 2005). These genomic alterations typically lead to the aberrant activation of the MAPK and the PI3K/AKT pathways (Chappell et al., 2011).

Indeed, up to 90% of melanomas exhibit an aberrant MAPK pathway activation (Wellbrock, Karasarides, & Marais, 2004) mostly due to BRAF mutations, the most frequent genetic abnormalities. BRAF protein is a serine/threonine protein kinase organized in three domains: two domains with regulatory function and one catalytic domain responsible for MEK phosphorylation. The catalytic domain is also responsible for maintaining the protein in its inactive conformation through an hydrophobic interaction between the ‘so-called’ glycine-rich loop and the activation segment, making it non accessible to ATP binding (H. Davies et al., 2002). With

$BRAF^{V600E}$ mutation, the hydrophobic valine is replaced by polar hydrophilic glutamic acid resulting in an abnormal flip of the catalytic domain that generates a constitutive active conformation with a kinase activity 500-fold higher than that of the wild-type BRAF kinase (Richtig et al., 2017; Wan et al., 2004).

The second most common cause of aberrant signaling through the MAPK pathway is represented by NRAS activating mutations. Mutations of codon Q61 lead to the prolongation of the NRAS-active GTP-bound state, thus abnormally maintaining NRAS signaling through both the MAPK and the PI3K pathways. Importantly, NRAS and BRAF mutations are considered mutually exclusive (Fedorenko, Gibney, & Smalley, 2013; Giehl, 2005; Hodis et al., 2012a).

The NF1 (NeuroFibromin 1) is a GTPase-activating protein that regulates the RAS family by converting the active RAS-Guanosine TriPhosphate (RAS-GTP) into the inactive RAS-Guanosine DiPhosphate (RAS-GDP), thereby inhibiting downstream RAS signaling. Therefore, NF1 loss-of-function determines the hyperactivation of NRAS protein and subsequently an increased MAPK and PI3K pathways signaling (Krauthammer et al., 2015; Nissan et al., 2014).

Additionally, the somatic activation of the receptor tyrosine kinase KIT by KIT amplification or mutation in the locus (most frequently in exons 11 (L576P) and 13 (K642E)), is involved in melanoma proliferation and survival through these two pathways (Beadling et al., 2008; Handolias et al., 2010; Slipicevic & Herlyn, 2015).

ii) Progress in the understanding of melanoma progression (Fig.7)

From both clinical and histopathological observations of non-CSD melanomas, Clark et al. (1984) proposed a multi-step progression model. Subsequently, several models of the genetic basis of melanoma development and progression were based on such Clark's model, which was universally recognized by the melanoma research community (Bennett, 2003; Michaloglou, Vredeveld, Mooi, & Peeper, 2008; A. J. Miller & Mihm, 2006). According to such models, the first phenotypic change in normal melanocytes is the development of a benign melanocytic nevus that frequently harbors activating BRAF mutations (Pollock et al., 2003) being thought to be the initial step in melanocytic neoplasia. However, the initial growth of melanocytic nevus is followed by stabilization of the size and loss of most proliferative activity due to oncogene-induced senescence (Michaloglou et al., 2008). The next step of melanoma evolution is dysplastic nevus that may arise from a preexisting

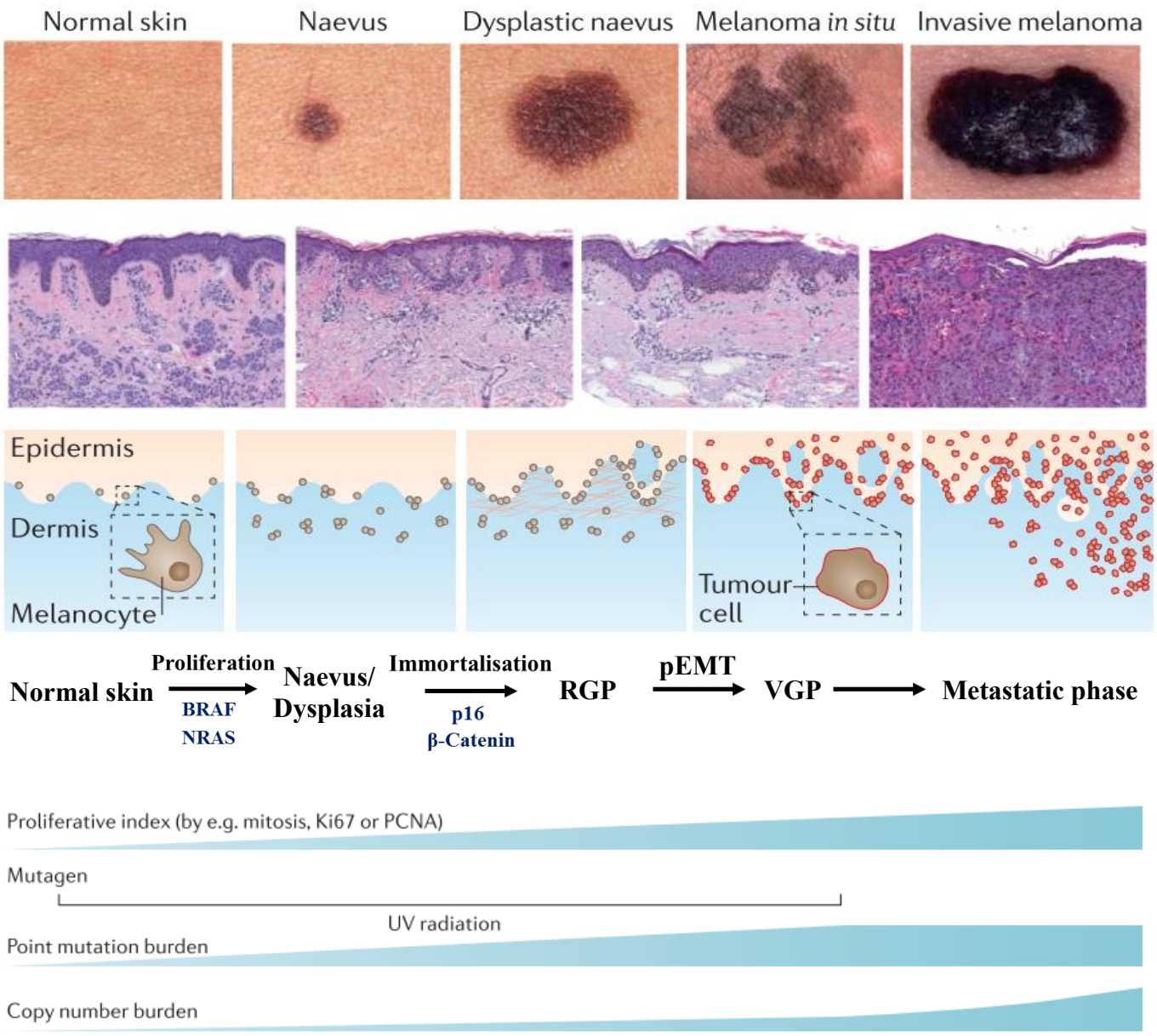

Figure 7. Morphological, histological and molecular properties of melanoma progression.

Top row: clinical images of melanoma progression from normal skin to in situ melanoma and invasive melanoma.

Second row: photomicrographs illustrating the representative histopathological features of each type of lesion.

Third row: schematics illustrating the architectural features of each type of lesion.

Fourth row: adaptation of Clark's model across melanoma progression.

Bottom row: melanocytic neoplasms become more proliferative and accumulate point mutations caused by UV radiations. Copy number alterations increases once melanoma becomes invasive.

(Adapted from Boris C. Bastian et al. 2016)

melanocytic nevus or as a new lesion. The molecular abnormality at this stage of progression may be the disruption of the p16INK4a-Retinoblastoma (Rb) pathway, mostly by the inactivation of CDKN2A (cyclin-dependent kinase Inhibitor 2A, p16), a gene encoding p16INK4a and p19ARF. The third step in progression is the Radial Growth Phase (RGP) of melanoma, which spreads progressively within or just beneath the epidermis. In this phase of progression, neoplastic melanocytes are immortal due to deficiency in the p16INK4a-Rb pathway as well as hTERT activation (Sviderskaya et al., 2003). The final stage in melanoma progression is the Vertical Growth Phase (VGP) in which the tumor grows deeply into the dermis and is metastasis competent. For progression to the vertical growth phase, mutations repressing apoptosis would be required including PTEN loss, over-expression of a number of protein kinases or RAS activation, and β-catenin activation, which allow cells to survive in the absence of keratinocytes. Progression from RGP to VGP required a pseudo-Epithelial-Mesenchymal Transition (pEMT) marked by the loss of E-cadherin as well as the aberrant expression of N-cadherin and aVb3 integrin (Fig.7) (A. J. Miller & Mihm, 2006).

However, many questions and studies challenge the Clark's model suggesting that alternative models are conceivable. Indeed, if the melanocytic nevus is a senescent clone of melanocytes that acquire a BRAF mutation, all cells within the lesions should be BRAF mutants, that is not what is observed (Ichii-Nakato et al., 2006; J. Lin et al., 2009). Additionally, most primary melanomas arise *de novo* from normal skin and thus are not associated with melanocytic nevus. This suggests therefore that melanoma development is not represented by a single evolutionary pattern, but from divergent precursor lesions, gene mutations and pathways, as well as stages of transformation (Rivers, 2004).

Alternative models are thus necessary. Michaloglou et al. speculated that the first event in *de novo* melanoma development would be a yet unidentified hit which may enable melanocytes to escape from oncogene-induced senescence. When a melanocyte already suffering from this hit acquires a proliferative mutation such as $BRAF^{V600E}$, it may fail to undergo oncogene induced senescence and thus clonally proliferates. It is therefore possible that the order of somatic genetic changes determines whether a melanoma originates from a nevus or *de novo* (Michaloglou et al., 2008).

More recently, the use of Whole-Exome Sequencing (WES) coupled with transcriptomic analysis notably single-cell RNA-seq technology led to a more comprehensive identification of the genomic events driving tumor progression. These studies offered insights on the chronological sequence of genomic alterations and their transcriptional consequences on pathways deregulation in tumor progression, from benign nevi and primary tumors to metastatic lesions (Birkeland et al., 2018; Sanborn et al., 2015; Shain et al., 2018a; Tirosh et al., 2016a).

Importantly, these analysis revealed significant differential gene expression in the comparison of benign nevus to melanoma (Badal, Solovyov, Cecilia, et al., 2017) and varying degrees of inter- and intratumor heterogeneity conferred by the variable expression of distinct sets of genes in different primary tumors (Marie Ennen et al., 2017; Tirosh et al., 2016a).

These analyses also highlighted the genomic heterogeneity across metastasis and permitted assessment of ancestral relationships between primary tumors and metastases in order to build models of metastatic dissemination (Birkeland et al., 2018; Sanborn et al., 2015; Shain et al., 2018a). Indeed, analysis demonstrated that genetic diversity among multiple metastasis is a late event and arises naturally while no mutations were specifically associated with metastatic progression (Shain et al., 2018a, 2015). Birkeland et al. demonstrated little intermetastatic heterogeneity with low branch/trunk mutations ratio and driver mutations almost completely shared between lesions while branch mutations were consistent with UV damage suggesting that metastases may arise from different subclones of the primary tumor (Birkeland et al., 2018). Additionally, by analyzing primary melanomas and multiple matched metastases, Sanborn et al. highlighted that metastasis can arise from distinct cell populations or from a common parental subpopulation within the primary tumors. Thus, this study suggested that distinct primary tumor cell populations metastasized in parallel to different anatomic sites and not sequentially from one site to another (Sanborn et al., 2015).

Finally, Boris Bastian’s group, by combination of genomic alterations identification with transcriptomic analysis, delineated the sequential order in which signaling pathways become perturbed by genetic alterations along melanoma progression. Interestingly, this study highlighted the sequential MAPK pathway activation, telomerase upregulation, chromatin landscape modulation, G1/S

checkpoint override, MAPK signaling ramp-up, p53 pathway disruption, and PI3K pathway activation during melanoma progression (Shain et al., 2018, 2015).

E. Therapy strategies

Cutaneous malignant melanomas represent the most aggressive and deadliest forms of skin cancers due to their ability to rapidly become metastatic. Therefore, early identification of this cancer is crucial for the success of patient treatment. Over the past years, several therapeutic options have been approved by the US Food and Drug Administration (FDA) taking in account the location, stage, and genetic profile of the tumor.

Local surgical excision represents the treatment of choice that is indeed curative for the majority of patients with newly-diagnosed melanomas at early stages (Ross & Gershenwald, 2011). Furthermore, for patients with a solitary melanoma metastasis, metastasectomy is part of the standard of care while in some metastatic melanoma cases chemotherapy may also be considered (Batus et al., 2013) even if it is usually not as effective for melanoma as it is for some other types of cancer. Also, despite being rarely indicated for primary tumor treatment, radiotherapy has been considered for the treatment of skin, bone, and brain metastases (Garbe et al., 2016).

In the past few years, with the development and the approval of highly effective targeted therapies and immunotherapy, a revolution for patients facing advanced-stage melanomas occurred. Thus, both immunotherapy and targeted therapies are considered to be the backbone of systemic therapy while both chemotherapy and radiotherapy are now considered as second-line or even further treatment options (Domingues, Lopes, Soares, & Pópulo, 2018).

1) Targeted Therapies

As described above, the major melanoma driver alteration constitutively activates BRAF resulting in the activation of the MAPK pathway. This discovery led to the development of targeted inhibitors of the BRAF protein namely vemurafenib and dabrafenib (Fig.8A). The initial publication of the clinical trials in 2011 and 2012 comparing the targeted inhibitors with standard chemotherapy agents demonstrated consistent results with single-agent BRAF inhibitors showing an excellent response rate of approx. 50%. However, such response was short lived with a median duration

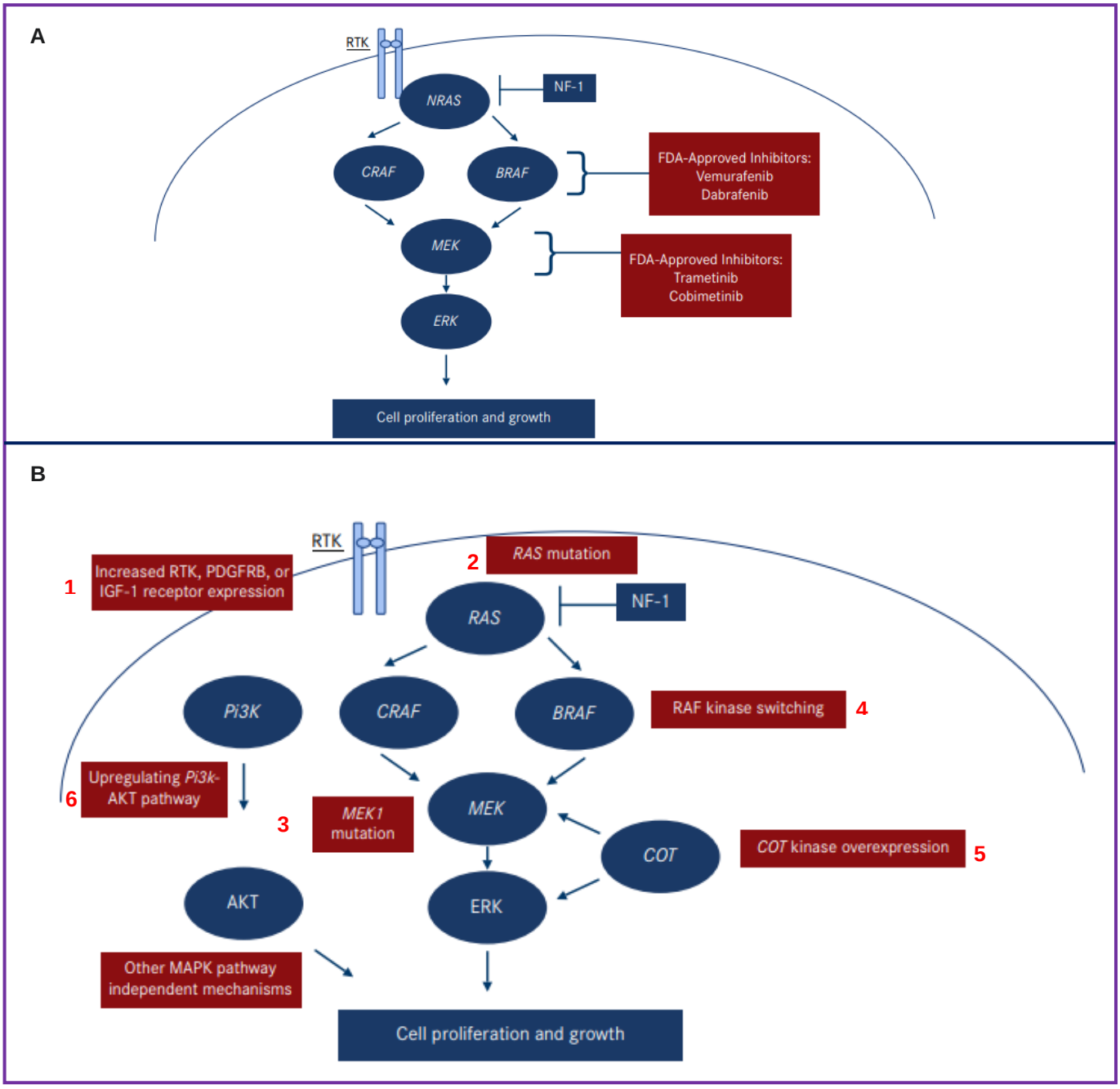

Figure 8. Available therapies and potential mechanisms of resistance to BRAF inhibitors.

(A) *Therapies targeting either BRAF or MEK within the MAP kinase pathway (the critical driver pathway in melanoma)* ***(B)*** *Resistance mechanisms to BRAF inhibitors (shown in red) include upregulation or bypass of the MAPK pathway: (1) Upstream overexpression of receptor tyrosine kinases (RTKs), (2) RAS mutation, (3) MEK1 downstream mutation, (4) RAF kinase switching and (5) COT kinase overexpression capable of MEK-dependent MAP-kinase activation, (6) Upregulation of Pi3k-AKT pathway (Adapted from Wood and Luke 2017).*

of disease control of 6 to 7 months (Chapman et al., 2011; Hauschild et al., 2012). The lack of durability of response is due to the development of resistance partly explained by the reactivation or bypassing of the MAPK pathway (Fig.8B). Identified resistance mechanisms to BRAF inhibitor therapy are summarized in figure 8.B (Wood & Luke, 2017) and are still extensively explored.

However, the response rates and the duration of disease control have been shown to be largely improved by the addition of inhibitors of the downstream kinase MEK (trametinib or cobimetinib) to dabrafenib blocking then the reactivation of the MAPK pathway induced by a single-agent (Fig.8A) (King et al., 2013; Su et al., 2012; Wood & Luke, 2017). Subsequently, several combination therapies with BRAF and MEK inhibitors became a worldwide standard of care for BRAF mutation-positive advanced or unresectable melanomas (Flaherty et al., 2012; Pavlick et al., 2015; Sullivan et al., 2015).

Additionally, since cKIT mutations or amplifications in melanoma led to the constitutive ligand-independent activation and upregulation of the MAPK and PI3K/AKT pathways, this receptor was also considered for targeted therapies. However, only Imatinib as cKIT inhibitor revealed significant activity in patients with metastatic melanoma harboring cKIT aberrations. Other multikinase inhibitors such as sunitinib, dasatinib and nilotinib, potentially efficient in patients with melanoma harboring cKIT mutations, are in clinical trials in combination with chemo- and immunotherapies (Hsueh & Gorantla, 2016).

2) Immunotherapies

The concept that cancer and immune system are closely related is not new and was based on the frequent appearance of tumors at the sites of chronic inflammation and the presence of immune cells in tumor tissues (reviewed in Balkwill & Mantovani, 2001).

In antitumoral responses, T-cells recognize tumor-specific antigens and then become activated, proliferate and differentiate to finally acquire the capacity to destroy targeted cells. T-cell activation begins with the binding of a specific T-Cell Receptor (TCR) to its cognate peptide-Major Histocompatibility Complex (MHC) presented on the surface of an Antigen-Presenting Cell (APC). Then, to reach a full T-cell activation co-stimulatory signals are required such as CD28 which interacts with the B7 family ligands CD80 and CD86 on APCs, promoting enhanced

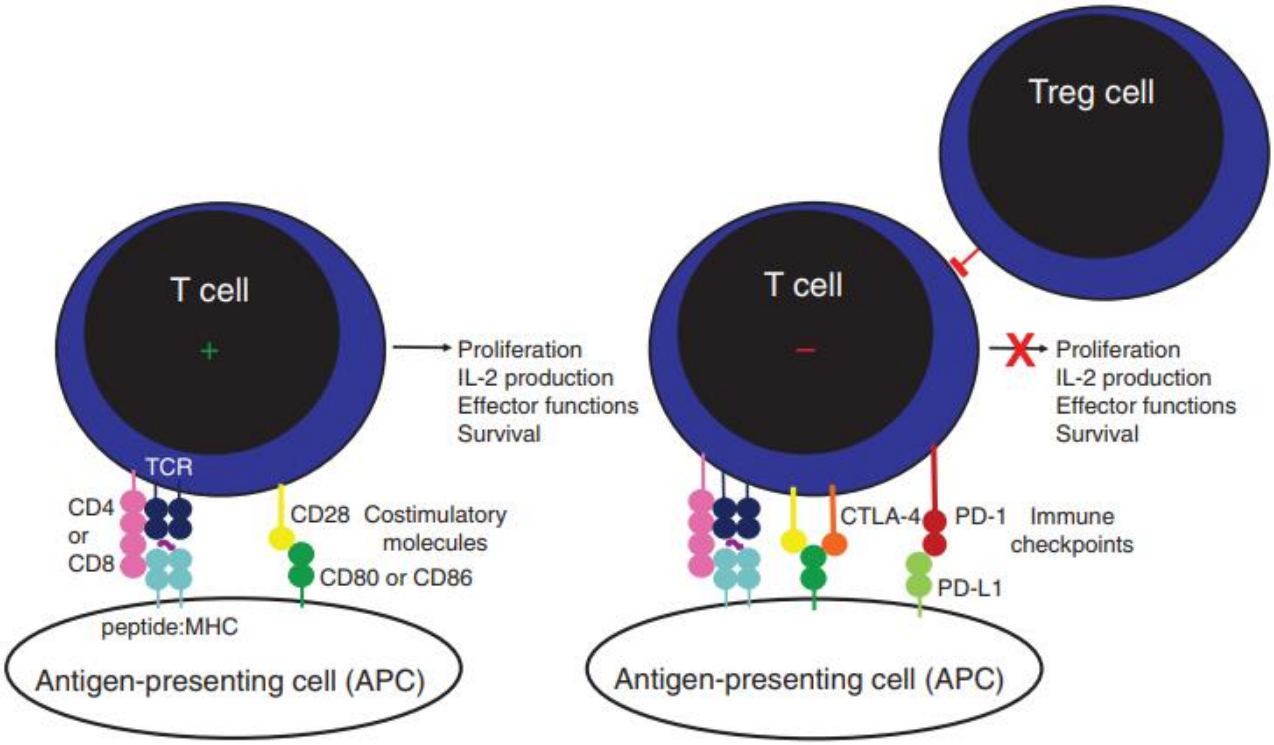

Figure 9. Activation and modulation of T-cell response.

Schematic representation of the T-cell receptor and accessory molecule. T-cell activation results from their interaction with peptide-MHC on the APC together with co-stimulatory molecule CD28 with CD80 or CD86. Immune checkpoints CTLA-4 and PD-1 are expressed on T-cell surface after activation and serve to dampen T-cell response as well as Treg cells. CTLA-4 and PD-1 are considered as immunotherapeutic targets in melanoma therapy, their blockade thus increasing the antitumor T-cell response (Raush and Hastings, 2017).

proliferation, IL-2 production, and T-cell survival (Fife & Bluestone, 2008). However, T-cell activation involves the integration of a number of co-inhibitory signals delivered by immune checkpoint receptors to turn off T-cell response and modulate inflammation. Some of the most studied immune checkpoint receptors are the Cytotoxic T-Lymphocyte-Associated protein-4 (CTLA-4) and the Programmed cell Death protein-1 (PD-1) (Fig.9).

CTLA-4 inhibits T-cell activation via binding to the B7 ligands CD80 and CD86 on APCs with a much higher affinity than its homologue and does not deliver a positive signal leading to attenuation of co-stimulatory signaling, inhibition of IL-2 production and blockade of T-cells cycle progression (Fig.9) (Krummel & Allison, 1995; Linsley et al., 1994; Walunas et al., 1994). Thus, blockade of CTLA-4 would enhance T-cell mediated antitumor immunity by removing the inhibitory feedback mechanism signal.

The research undertaken to target the immune system did not revolutionize the treatment approaches of melanoma until 2010 when Hodi et al. (2010) reported on the survival benefit using a fully human monoclonal IgG1 antibody that blocks CTLA-4, named ipilimumab, as a second line therapy. Since then several clinical trials support the use of ipilimumab or other CTLA-4 blocking antibodies in both first- and second-line therapies for advanced melanoma (Domingues et al., 2018; Widakowich, de Castro, de Azambuja, Dinh, & Awada, 2007).

PD-1, another “immune checkpoint”, inhibits T-cell activity but instead of competitively inhibiting co-stimulation by interfering with CD28/B7 ligand interaction, PD-1 negatively regulates TCR-signaling events at a later stage in peripheral tissues. PD-1 has two ligands namely PD-L1 and PD-L2 (Fig.9). Elevated PD-L1 expression was observed on both tumor cells and immune cell infiltrates in many different cancers including melanoma (Kaunitz et al., 2017). Such observation suggests that PD-1/PD-L1 functions as an adaptive tumor immune escape mechanism, thus infiltrating T-cells may induce their own suppression through the production of pro-inflammatory cytokines (Freeman et al., 2000; Noguchi et al., 2017).

Subsequently, the field of immune therapy moved quickly with the development of PD-1-based therapies. PD-1 therapies consist of a high-affinity anti-PD-1 monoclonal antibody such as nivolumab that blocks the interaction between PD-1 and PD-L1

leading to the release of the cytotoxic function of tumour-specific T cells and thus inducing immune antitumor activity that reduces tumor progression (Melero, Grimaldi, Perez-Gracia, & Ascierto, 2013; Specenier, 2016). In addition, pembrolizumab, another anti-PD-1 antibody, was approved for the treatment of advanced melanomas and may turn into a new standard for the treatment of ipilimumab refractory melanomas (Ribas et al., 2015; Robert et al., 2015). Finally, several clinical trials are ongoing using anti-PD-1 antibodies in monotherapy or in combination with other checkpoint inhibitors, chemotherapy, radiotherapy, immunotherapies, and targeted therapies (Domingues et al., 2018).

Unfortunately, only a subset of melanoma patients respond to immune checkpoint inhibitors for reasons still to be elucidated. In addition, severe immune-related Adverse Events (irAEs) appear in some patients, highlighting the necessity to identify predictive markers for treatment efficacy/safety and develop strategies to overcome such resistance.

F. MITF is the “master” transcriptional regulator of melanocytes and melanoma

1) Genomic organization and protein structure

In humans, the MIcrophthalmia-associated Transcription Factor (*MITF*) gene is located on the short arm of chromosome 3 and encodes a b-HLH-Zip (basic HelixLoop-Helix leucine zipper) transcription factor that belongs to the MYC superfamily. The locus contains at least nine alternative promoters each driving a specific 5’ exons that is spliced to the common remaining exons 2 to 9 encoding the major functional domains (Fig.10A) (Hershey & Fisher, 2005; Steingrmsson, 2008; Udono et al., 2000). While expression patterns of the different isoforms range from widely expressed to tissue specific, the M-isoform is expressed almost exclusively in melanocytes and melanoma (Hershey & Fisher, 2005).

The largest functional domain of MITF consists of two α-helices separated by a loop (Fig.10B). The N-terminal part of the first helix is a basic domain that provides most of the specific DNA major groove contacts (Pogenberg et al., 2012). The following HLH domain is composed of the C-terminal part of the first helix and the N-

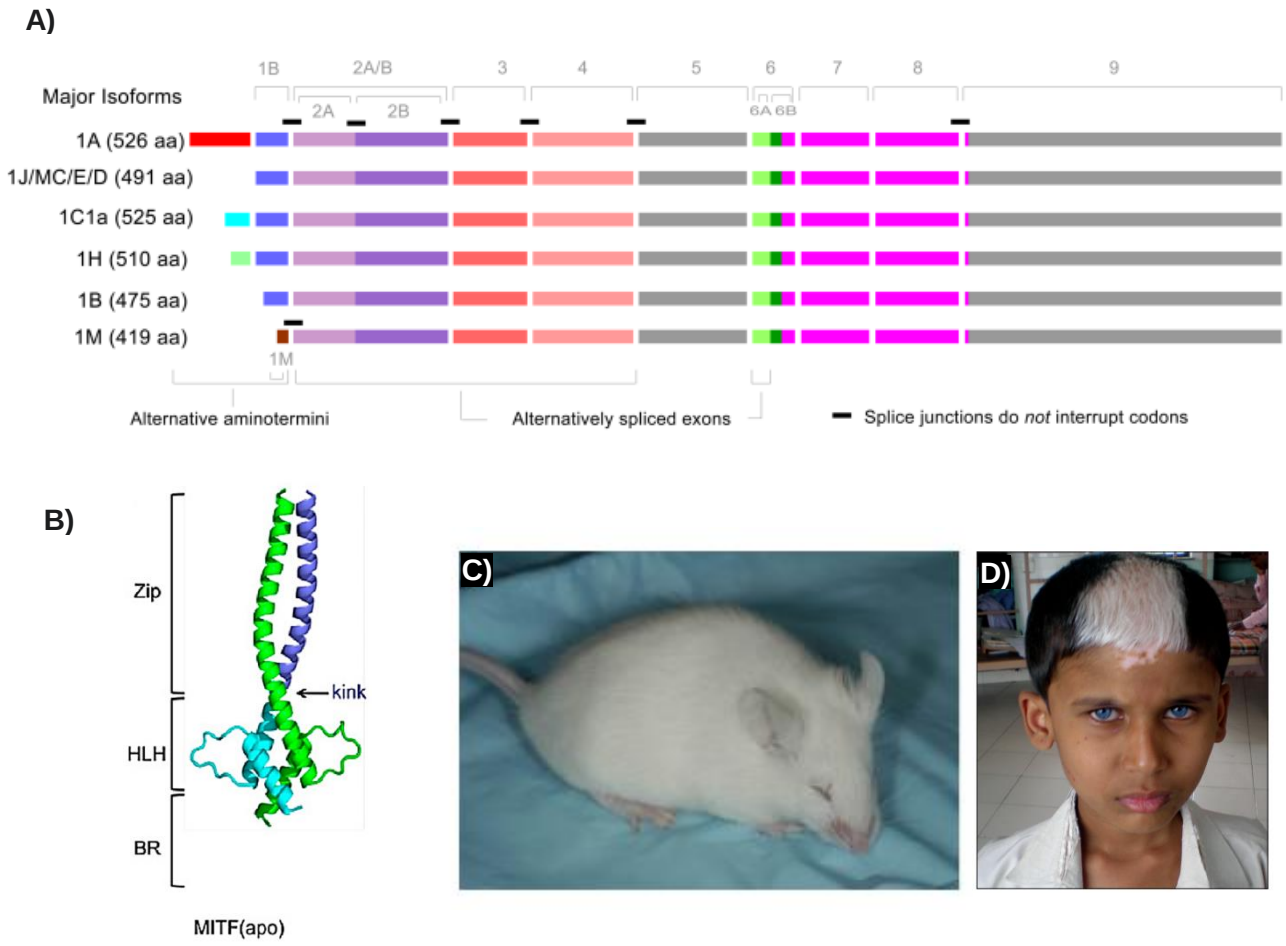

Figure 10. MIcrophthalmia-associated Transcription Factor (MITF).

(A) *Schematic representation of the human MITF gene and protein isoforms containing the bhlh-zip domain. The MITF M-isoform is expressed in melanocytes and melanoma (Colin R. Goding and Heinz Arnheiter, 2019)* ***(B)*** *Crystal structure of MITF in the absence of DNA (adapted from Pogenberg et al.2012).* ***(C)*** *Microphthalmia and white coat seen with Mitfmi-vga-9 homozygous mice (Colin R. Goding and Heinz Arnheiter, 2019)* ***(D)*** *Phenotypes associated with human MITF mutations, e.g. the Waardenburg syndrome type II in a 10 year old child with light colored eyes, a patch of white hair, patched skin at the frontal area and congenitally deaf with sensorineural hearing loss (Gaikwad et al. 2019).*

terminal part of the second helix separated by a loop and is the core part of the protein dimerization interface in MITF followed by a leucine-zipper, also involved in protein interactions (C Murre et al., 1989; Cornelis Murre et al., 1994; Pogenberg et al., 2012). MITF and other related family members such as the transcription factor E3 (TFE3), the transcription factor EB (TFEB) and TFEC, form the 'MiT' transcription factor family that regulates gene transcription through homo- or heterodimerization. MITF, TFE3, TFEB and TFEC bind to E-box and M-box motifs and dictate tissue-specific gene expression of critical pigmentation enzymes (Bertolotto et al., 1998; Hemesath et al., 1994; Pogenberg et al., 2012). Of note, MITF does not form heterodimers with other bHLHZip proteins due the insertion of three residues in the N-terminal part of the zipper (Pogenberg et al., 2012).

Also, MITF interacts with various cofactors to regulate gene expression. Thus, MITF was shown to associate with chromatin modifiers and remodellers such as CBP/p300 (Sato-Jin et al., 2008), NURF and SWI/SNF complexes containing BRG1 (Laurette et al., 2015), and with essential transcription factors including β-catenin (A. Schepsky et al., 2006).

The microphthalmia phenotype was first observed some 70 years ago in mice having significantly reduced eye size and a depigmentation phenotype due to the mutant locus mi (Hertwig, 1942). Nowadays, a variety of additional forward mutations at this locus, with more or less subtle effects on pigmentation, have been generated in mice (http://www.informatics.jax.org; Steingrímsson, Copeland, and Jenkins 2004b; Hou and Pavan 2008). For instance, the Mitfmi-vga-9 mutant mice, harboring an insertion in the sequence of the MITF-M promoter gives rise to microphthalmic, deaf and completely white mice (Fig.10C) (Hodgkinson et al., 1993) reflecting the lack of melanocytes and demonstrating the key role of MITF-M in the development of the melanocyte lineage. As in mice, human germline mutations in bHLH-LZ domain are largely associated with pigmentary disturbances and deafness such as the Waardenburg syndrome IIa (Fig.10D), the Tietz syndrome and more recently the COMMAD syndrome (https://databases.lovd.nl/shared/genes/MITF,George et al., 2016).

The expression of MITF is finely regulated at a transcriptional level by the factor itself in a negative feedback loop (Louphrasitthiphol et al., 2019) or by various

activators and repressors, while the activity of MITF is regulated by diverse posttranslational modifications (reviewed in Colin R Goding & Arnheiter, 2019).

2) Biological functions

MITF plays a pivotal role in many aspects of melanocyte biology including melanocyte survival, proliferation and differentiation (Yann Cheli, Ohanna, Ballotti, & Bertolotto, 2010; Colin R Goding & Arnheiter, 2019; Hou & Pavan, 2008; Vachtenheim & Borovanský, 2010b). MITF controls survival of melanoblasts, skin and hair follicles melanocytes and MSCs through the anti-apoptotic proteins B Cell Leukemia/lymphoma 2 (BCL2) (McGill et al., 2002), Baculoviral IAP Repeat-Containing protein 7 (BIRC7) (Dynek et al., 2008), Hypoxia-Inducible Factor 1-alpha (HIF1α) (Buscà et al., 2005) and MET proto-oncogene (Beuret et al., 2007). MITF is also an important regulator of proliferation in these cells as it activates the expression of cell cycle regulators such as Cyclin Dependent Kinase 2 (CDK2) (J. Du et al., 2004), the cyclins CCNB1 and CCND1 (Strub et al., 2011) and T-BoX factor 2 (TBX2) (Prince, Carreira, Vance, Abrahams, & Goding, 2004). Genes implicated in mitosis are also regulated by MITF including Polo-Like Kinase 1 (PLK1) encoding a key regulator of M-phase progression, and components of the complexes connecting mitotic spindle microtubules to kinetochores (Strub et al., 2011). As described above MITF is also known to stimulate melanin synthesis by regulating transcription of pigmentation genes including TYR, TYRP1, DCT, PMEL, and MLANA and contributes to melanocytes differentiation (Yann Cheli et al., 2010). Results from our group and others have shown that MITF also regulates many other genes involved in melanin or melanosome biosynthesis and trafficking in both melanocytes and melanoma cells (J. Du et al., 2003; Laurette et al., 2015).

In malignant melanoma, MITF was termed a lineage survival oncogene (Garraway et al., 2005). Indeed, immortalized primary melanocytes infected with viral constructs expressing $BRAF^{V600E}$ cannot form colonies without ectopic expression of MITF thus illustrating how MITF can function as a oncogene (Garraway et al., 2005).

Genomic amplifications of the MITF locus were described in about 5–20% of human melanomas and correlated with decreased overall patient survival (Akbani et al., 2015; Garraway et al., 2005) while mutations of MITF are rather rare since they

were recorded in only 8 % of the melanoma samples analyzed (Bertolotto et al., 2011; Julia C. Cronin et al., 2009; Garraway & Sellers, 2006; Garraway et al., 2005; Gast et al., 2010; Levy, Khaled, & Fisher, 2006; Newton Bishop et al., 2000). Additionally, the germline missense substitution $MITF^{E318K}$ was demonstrated to encode for a familial melanoma gene increasing the risk for both melanoma and renal cell carcinoma (Bertolotto et al., 2011; Bonet et al., 2017; Yokoyama et al., 2011) by affecting an MITF sumoylation normally suppressing MITF transcriptional functions (Ballotti & Bertolotto, 2017; A. J. Miller, Levy, Davis, Razin, & Fisher, 2005).

In addition to functioning as a melanoma oncogene, MITF also regulates the metabolic landscape of melanoma cells. Indeed, BRAF inhibition induces oxidative phosphorylation and increased the expression of PGC1α (PPRGC1A) the master regulator of mitochondrial biogenesis. PGC1α was shown among the MITF regulated target genes suggesting the impact of MAPK-mediated MITF regulation on metabolic state in melanoma and permitted Haq et al. group (2013) to better understand the adaptive program limiting the efficiency of BRAF inhibitors. Also, MITF controls melanoma metabolism by regulation of the SIRT1 gene encoding a key NAD-dependent deacetylase, important in promoting proliferation and suppression of melanoma cells senescence (Ohanna et al., 2014). Recently, MITF was shown to control the TCA cycle by regulating the expression of the Succinate DeHydrogenase (SDH) complex that catalyzes the conversion of succinate to fumarate (Louphrasitthiphol et al., 2019).

Finally, MITF regulates a broad range of cellular functions, acting both as an activator and a repressor in a promoter-specific manner (Yann Cheli et al., 2010; Giuliano et al., 2010; Colin R Goding & Arnheiter, 2019; Strub et al., 2011), thus suggesting a complex role of MITF in melanoma tumorigenesis.

3) Heterogeneous expression of MITF in melanoma

Bioinformatic analyses of melanoma gene expression datasets revealed that a subset of melanomas expresses a low level of MITF while another subset expresses a high level of MITF. MITF-low melanomas are associated with invasiveness properties while MITF-high melanomas are described more proliferative (less invasive) with distinct gene expression programs. The “proliferative” or “melanocytic”

state displays not only high levels of MITF but also SOX10, and functional pathways associated with the lineage such as pigmentation. Conversely, the “invasive” or “mesenchymal” state shows both SOX9 expression and AP-1 activity (Hoek et al., 2006; Verfaillie et al., 2015).

Thus, the level of functional MITF determines many biological properties of melanoma cells and can be represented by a so called ‘rheostat model’ (Carreira et al., 2006; Goding, 2011; Hoek & Goding, 2010). The ‘rheostat model’ postulates that high MITF levels lead to terminal differentiation and cell cycle exit, intermediate levels to proliferation while lower levels result in slow cycling, invasive (Carreira et al., 2006), tumor-initiating (Y Cheli et al., 2011), and drug- and immunotherapy-resistant phenotypes (Müller et al., 2014; Tirosh et al., 2016; Wellbrock & Arozarena, 2015). In contrast, very low levels of MITF or its rapid and sustained depletion as achieved in siRNA experiments trigger cellular senescence and eventually cell death (Giuliano et al., 2010; Strub et al., 2011).

However, Hoek et al (2008) showed that when MITF-high or MITF-low cells are used to make xenografts the resulting tumors comprise heterogeneous type of cells with both high and low MITF expression levels. Additionally, single-cell analysis revealed that the MITF expression level is heterogeneous in human melanoma cells, with high-, intermediate-, and low-MITF subpopulations of melanoma cells (Marie Ennen et al., 2015; Marie Ennen et al., 2017). Increasing evidence also suggests the existence of additional intermediate state(s) (Rambow et al., 2018; Tsoi et al., 2018). These observations support the so-called ‘phenotype switching’ model predicting that the two melanoma cell subpopulations are only temporarily distinct and that these cells can reversibly and dynamically switch transcriptional programs between the proliferative/melanocytic and invasive/mesenchymal states regulated by local microenvironmental conditions (Y. Cheli et al., 2011; Hoek & Goding, 2010; Quintana et al., 2010; Roesch et al., 2010).

CHAPTER 2

Epigenetic regulation and the NuRD complex

CHAPTER 2 Epigenetic regulation and the NuRD complex

The term ‘epigenetics’, originally defined as changes in phenotype without changes in genotype, already emerged some 80 years ago (Waddington, 1942). We know nowadays that epigenetics relates to the mechanisms of inheritance of gene expression patterns without alteration of the underlying DNA sequence through adapting chromatin. Genome wide technological and analysis advances such as chromatin immunoprecipitation or ATAC (Assay for Transposase-Accessible Chromatin) assays followed by next-generation sequencing and variations have enabled the analysis of the epigenome in cells and tissues.

These recent technological advances identified various epigenetics alterations leading to the disruption of gene functions contributing to cancer initiation and progression. Importantly, epigenome deregulation in combination with genetic alterations are described in high-risk melanomas with poor survival characteristics (Badal et al., 2017; Sarkar et al., 2015).

A. Chromatin: structure, organization, modifications and transcriptional dynamics

In eukaryotic cells, the genetic material is organized into a complex structure composed of DNA and proteins called chromatin, localized in a specialized compartment, the nucleus. The repeating structural unit of chromatin is the nucleosome which consists of a histone octamer comprising two copies of each core histone H2A, H2B, H3 or H4 wrapped with 147 base pairs of DNA (Hayes & Wolffe, 1995; Luger, Mäder, Richmond, Sargent, & Richmond, 1997). A subset of nucleosomes associates with the linker histone H1 (Suganuma & Workman, 2011). Each histone forms a structure consisting of a three-helix domain termed the histone fold that form a “handshake” structure connecting the histone heterodimers H2A-H2B and H3-H4 (Arents et al., 1991; Harp et al., 2000; Khorasanizadeh, 2004; Zlatanova et al., 2009).

In proliferative cells, the DNA replication process requires the temporary removal and subsequent reassembly of the parental nucleosomal histones along with a full complement of newly synthesized histones (Smith & Stillman, 1991). To enable

propagation of chromatin, cells developed efficient nucleosome assembly machineries including components of the replication machinery, nucleosome remodellers and a diverse class of proteins known as histone chaperones (Gurard-Levin, Quivy, & Almouzni, 2014; Hammond, Strømme, Huang, Patel, & Groth, 2017; T. C. Miller & Costa, 2017; Yadav & Whitehouse, 2016). Histone chaperones are negatively charged proteins that mostly associate either with H3-H4 dimers or tetramers, or with H2A-H2B dimers for histones and DNA assembly into the nucleosome structure (Das, Tyler, & Churchill, 2010).

Aside from the so-called 'canonical' histones, evolution drove the emergence of histone variants. With respect to the core histones, eight variants of H2A (H2A.X, H2A.Z.1, H2A.Z.2.1, H2A.Z.2.2, H2A Barr body deficient (H2A.Bbd), macroH2A1.1, macroH2A1.2 and macroH2A2) and six variants of H3 (H3.3, histone H3-like centromeric protein A (CENP-A), H3.1T, H3.5, H3.X and H3.Y) have been identified in human somatic cells while two testis-specific variants of H2B (histone H2B type WT (H2BFWT) and testis-specific histone H2B (TSH2B)) have been found. Each histone variant has a unique temporal expression accounting for specific cellular functions regulating essential processes such as cell fate decisions and development (Buschbeck & Hake, 2017).

1) Post-Translational Modifications on DNA bases

Epigenetic diversity in regulating gene expression is accomplished in part by DNA modifications such as the methylation of the fifth carbon of Cytosine in CpG dinucleotides (5mC). 5mC is the most common modified bases in the genome and hence is considered as the fifth base of DNA (Breiling and Lyko, 2015). This modification represses gene expression by altering nucleosome positioning and stability and by recruiting chromatin-modifying complexes with subunits capable of binding methylated DNA (Bartke et al., 2010). While mammalian genomes are globally CpG-depleted, 60–80% of the remaining CpGs are generally methylated and less than 10% of CpGs occur in CG dense regions termed CpG islands, prevalent at transcription start sites of housekeeping and developmental regulator genes, and resistant to DNA methylation (Deaton & Bird, 2011). Interestingly, Genome-wide single-base-resolution maps of methylated cytosines in mammalian genome revealed

how enhancer and promoter regions are differentially methylated in a cell-type-specific manner (Lister et al., 2009) underscoring the critical function of DNA methylation in development and diseases.

For note, other DNA modifications such as oxidation of 5mC to 5-hydroxymethylcytosine (5-hmC), 5-formylcytosine (5-fC), 5-carboxylcytosine (5-caC), and methylation of adenine (A) to N6-methyladenine (6-mA) were also identified as important epigenetic regulators (Klungland & Robertson, 2017).

2) Post-Translational Modifications on histone proteins

Each core histone contains an N-terminal extension that projects from the nucleosome called the histone tail subject to Post-Translational Modifications (PTMs) (Fig.11A). Those histone tails PTMs constitute the main features of the so-called “histone code” (Fig.11A) (Jenuwein & Allis, 2001) and provide a mechanism to modulate chromatin structure affecting the accessibility of transcription factors and chromatin modifiers to their binding sites (Clapier & Cairns, 2009; Juan, Utley, Adams, Vettese-Dadey, & Workman, 1994; Swinstead, Paakinaho, Presman, & Hager, 2016; Vettese-Dadey et al., 1996). Indeed, this code influences all DNA-based processes including chromatin compaction, nucleosome dynamics and transcription. PTMs may affect higher-order chromatin structures by altering the contact between different histones in adjacent nucleosomes or the interaction of histones with DNA (Bannister & Kouzarides, 2011). Such PTMs include acetylation, methylation, phosphorylation, ubiquitylation, sumoylation and GlcNAcylation. More recently, emerging modifications were described such as propionylation, butyrylation or deimination (also called citrullination) (Kebede, Schneider, & Daujat, 2015; Kouzarides, 2007) (Fig.11A).

As well as the tails, also the central globular domains of the histones contains a large number of modification sites including acetylation, methylation, phosphorylation and ubiquitination (Cosgrove, Boeke, & Wolberger, 2004; Tropberger & Schneider, 2013). Overall, recent work showed that histone core modifications not only can directly regulate transcription but also influence processes such as DNA repair, replication, stemness and changes in cell state (reviewed in Lawrence, Daujat, and Schneider 2016).

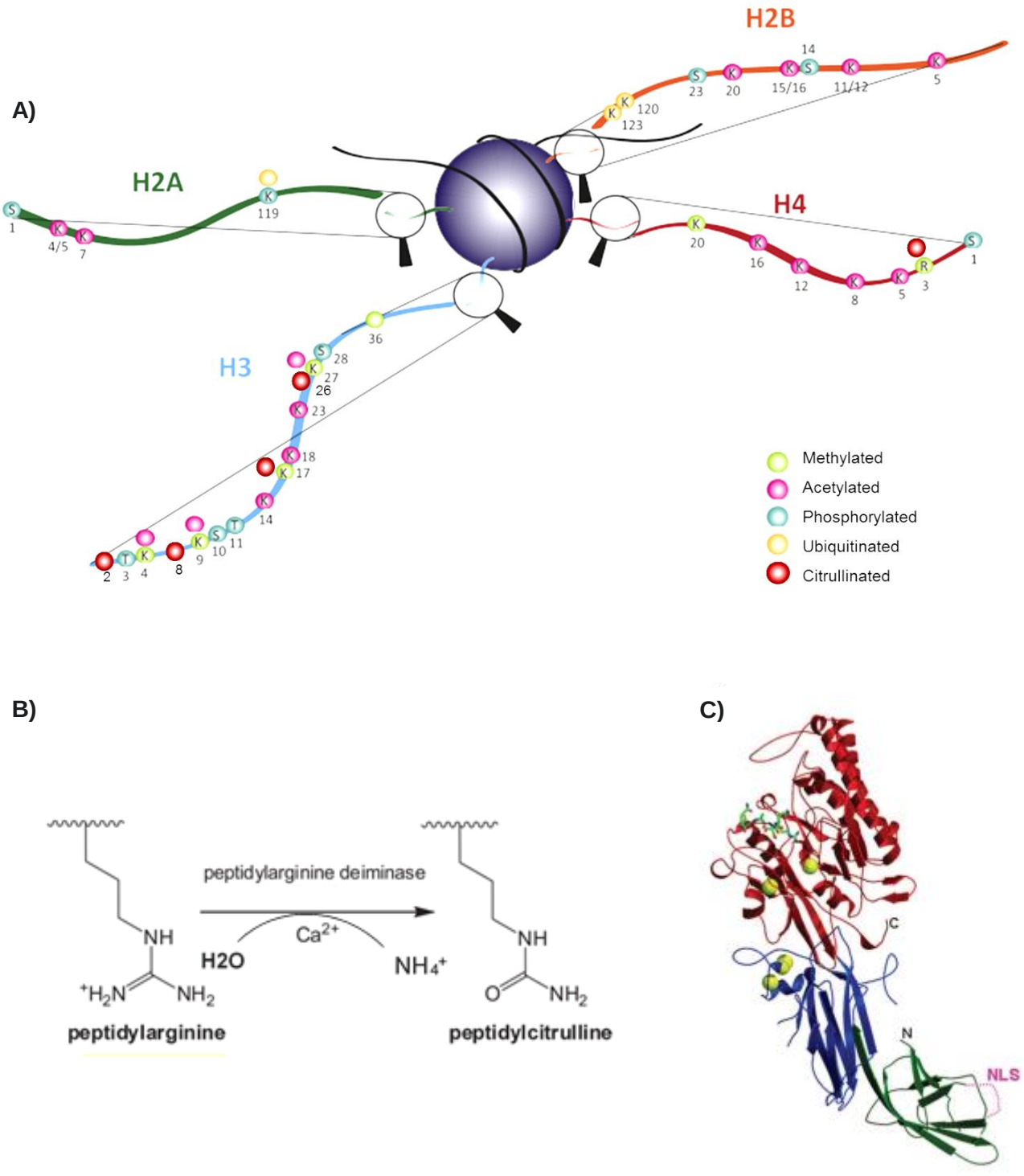

Figure 11. Post-translational modifications of histone tails.

(A) Schematic representation of post-translational modifications of histone tails including citrullination (Adapted from Schneider et al.2016) (B) Citrulline is generated from the side-chain conversion of peptidylarginine into peptidylcitrulline in a calcium-dependent process known as citrullination (or deimination) catalyzed by PADI enzymes. (C) 3D structure of Ca2+-bound PADI4 (C645A) with Ca2+ ions and the histone peptide illustrated as yellow and green sticks, respectively. The N-terminal subdomains 1 (residues 1–118) and 2 (residues 119–300) and the C-terminal domain (residues 301–663) are reported in green, blue and red, respectively. The Nuclear Localization Signal (NLS) region is shown as a dotted line (Arita et al. 2005).

3) Epigenetic tools and biological relevance

Modifications of DNA and histone proteins occur through the addition of various chemical groups utilizing numerous enzymes. The protein machinery that adds, removes, or recognizes these PTMs are categorized as “writers”, “erasers”, and “readers” respectively (Gillette & Hill, 2015). They are divided into classes on the basis of the specific PTM and residue they affect.

Thus, the two most widely studied PTMs, methylation and acetylation are accomplished by “writers” including DNA MethylTransferases (DNMTs), Histone Lysine MethylTransferases (KMTs), Protein arginine methyltransferases (PRMTs) and Histone AcetylTransferases (HATs). Methylation and acetylation are removed by “erasers” including Lysine Specific DeMethylases (LSDs/KDMs) and Histone DeACetylases (HDACs) (Biswas & Rao, 2018). PTMs govern DNA transcription by the mediation of “readers” containing domains with a high affinity for PTMs. These domains are located within the chromatin modifying proteins themselves but are also found in chromatin remodellers, as detailed further.

While most of PTMs are catalyzed or removed by large groups of clearly identified enzymes, demethylating and “decitrullinating” (citrulline eraser) activities for arginine methylation and citrullination, thought to be dynamic (Cuthbert et al., 2004), have not yet been described.

Interestingly, the process of deimination was demonstrated to correlate with the disappearance of methylarginine suggesting that deimination has the potential to antagonize arginine methylation (Cuthbert et al., 2004). However, further studies report that methylation of the guanidinium group may prevent and inhibit PADs capabilities of generating peptidyl citrulline or peptidyl methylcitrulline from either mono- or dimethylated peptidyl arginine (Hidaka, Hagiwara, & Yamada, 2005; Raijmakers et al., 2007). Finally, while the dynamic nature of citrulline marks could be caused by histone tail clipping, epitope occlusion, or nucleosome displacement, the existence of a decitrullinase remains a possibility unresolved so far (Fuhrmann, Clancy, & Thompson, 2015).

Therefore, the dynamics of the chromatin organization and the diverse combinatorial alterations of chromatin structures and DNA lead to fine regulation of

gene expression and other chromatin functions. These epigenetic processes play an essential role in many biological activities including development. Thus, epigenetic reprograming in mammalian development allows establishment of tissue- and temporal-specific transcriptional programs from a single genome sequence. Pluripotent stem cells express genes that encode a set of core transcription factors, while genes that are required later in development are repressed by histone marks and DNA methylation conferring flexible epigenetic silencing (Reik, 2007).

Thus, epigenetics processes are part of an intense field of research especially since aberrant regulation of DNA modifications and histone PTMs were linked to a number of diseases including cancers (Dawson & Kouzarides, 2012).

B. Citrullination is an emerging post-translational modification

The nonessential amino acid Citrulline (Cit, $C_6H_{13}N_3O_3$) was isolated from the juice of the watermelon Citrullus vulgaris by Koga and Ohtake (1914). The structure of citrulline was established in 1930 and first evidence that this amino acid can be found in proteins was provided (Wada M. et al.1930; Wada M. et al. 1933). Further studies demonstrated that citrulline is enzymatically generated by side-chain conversion of peptidylarginine to peptidylcitrulline in a calcium-dependent process known as deimination or citrullination (Fig.11B) (Rogers and Simmonds 1958; Rogers Ge 1962; Rogers, Harding, and Llewellyn-Smith 1977). The discovery of citrullination generated interest in different areas of research notably since citrullinated proteins were shown to play an essential role in the progression of Rheumatoid Arthritis (RA) through generation of autoantibodies and exacerbation of the inflammatory response (Schellekens, de Jong, van den Hoogen, van de Putte, & van Venrooij, 1998).

The enzyme responsible for this reaction named PeptidylArginine DeIminase (PADI) was partially purified by Fujisaki and Sugawara (1981). Since then, 5 PADIs were identified in humans (PADI1–4 and 6) sharing 70% to 95% sequence homology and being expressed in a wide range of tissues and organs (Chavanas et al., 2004; Guerrin et al., 2003; Ishigami et al., 2002; Kanno et al., 2000; Nakashima et al., 1999; Jiayi Zhang et al., 2004). PADIs typically exist as homodimeric proteins (in a head-to-tail fashion) that contain a catalytic α/β propeller domain located on the C-terminal

half (Fig.11C) (Arita et al., 2004; Shirai, Mokrab, & Mizuguchi, 2006). The N-terminal domain can be subdivided into two Immunoglobulin-like (Ig) subdomains that were suggested to be important for protein−protein interactions and to facilitate substrate selection (Arita et al., 2004).

PADIs hydrolyze a guanidino group of arginine into urea group, resulting in 1 Da change in molecular mass and converting a positively charged arginine into the electrically neutral citrulline (Fig.11B). Such modification affects hydrogen bond formation and protein folding ultimately resulting in altered hydrophobicity, altered protein–protein interactions or even causing protein denaturation. The most frequent PADI substrates identified are keratin, filaggrin, vimentin, actin, collagen, myelin basic protein and histones (Lee et al., 2018a; Tilvawala et al., 2018; Witalison, Thompson, & Hofseth, 2015), all having a high arginine content clearly essential to their function. Recently, citrullinated proteins and sites mapped in human (Lee et al., 2018a) and mice (Fert-Bober et al., 2019) revealed a tissue dependent subcellular distribution and citrullinated targets involved in various fundamental physiological processes.

PADI proteins and/or activity are/is detected in various cellular compartments including cytoplasm and mitochondria. Only PADI4 was shown to translocate to the nucleus thanks to a canonical nuclear localization sequence (Fig.11C) (Nakashima, Hagiwara, & Yamada, 2002; Vossenaar, Zendman, van Venrooij, & Pruijn, 2003). Nevertheless, emerging evidence indicates that other PADI isozymes such as PADI1 (Xiaoqian Zhang et al., 2016) or PADI2 (Cherrington, Morency, Struble, Coonrod, & Wakshlag, 2010) could localize to the nucleus as well.

Citrullinated histones account for approximately 10% of all histones emphasizing the significance of this posttranslational modification in many nucleus-associated processes. Thus, similar to acetylation and methylation histone citrullination either activates or represses gene expression thus contributing to the increasingly complex histone code. Indeed, it was shown that citrullination of a single arginine residue within the DNA-binding site of H1 results to its displacement from chromatin and global chromatin decondensation (Christophorou et al., 2014). Moreover, PADI4 was shown to mediate gene expression by regulating H3 and H4 arginine methylation and citrullination. PADI1 was shown to citrullinate H4R3 and H3R2/8/17 during embryonic development in mouse embryo (Xiaoqian Zhang et al., 2016) while PADI2 was shown

to citrullinate H3R2/8/17 and H3R26 specifically leading to local chromatin decondensation and transcriptional activation (Fig.11A) (Christophorou et al., 2014; Yanming Wang; Joanna Wysocka, 2004).

In addition to direct histone citrullination PADIs can also affect gene expression by regulating the activity of transcription factors. Indeed, PADI4 was shown to associate with several transcriptionally active promoters functioning as an activator of c-Fos (Xuesen Zhang et al., 2011).

Finally, in addition to the citrullination of histones, transcription factors, and a large number of other proteins, PADIs are also capable of auto-citrullination. For example, PADI4 is known to autocitrullinate at numerous sites *in vitro* and *in vivo* (Andrade et al., 2010; Fuhrmann et al., 2015) while the function of such process still remains elusive.

C. ATP-dependent chromatin remodelling

Chromatin remodelling is a process established by both ATP-dependent and ATP-independent mechanisms that modify the position, occupancy or the histone composition of nucleosomes within the chromatin (Aalfs & Kingston, 2000). ATP-independent mechanisms can occur by the action of some histone chaperones dedicated to the deposition of specific histone variants (De Koning et al. 2007; Workman and Kingston 1992). In contrast, ATP-dependent mechanisms are of enzymatic nature and represent the majority of the remodelling activities in the cell (Z. Zhang et al., 2011).

ATP-dependent remodellers are multisubunit complexes containing an ATPase subunit involved in chromatin binding and ATP hydrolysis. Based on the nature of additional functional domains the catalytic ATPase subunits are organized in SWI/SNF (SWIching/Sucrose Non-Fermenting), ISWI (Imitation SWItch), CHD (Chromodomain Helicase DNA binding) and INO80 (INOsitol requiring 80) families (Fig.12A) (Boyer, Latek, and Peterson 2004; Eberharter and Becker 2004; Marfella and Imbalzano 2007; Sif 2004).

Moreover, chromatin remodellers can also be classified by their identified functions. Indeed, ISWI and CHD subfamily remodellers participate in nucleosome assembly by histones deposition, nucleosomes maturation and spacing. SWI/SNF, ISWI and CHD subfamily remodellers alter chromatin access by repositioning

nucleosomes. Only SWI/SNF subfamily remodellers were shown to alter chromatin access by evicting histone dimers while INO80 subfamily remodelers change nucleosome composition by exchanging canonical and variant histones (Fig.12B) (Clapier, Iwasa, Cairns, & Peterson, 2017).

1) The SWI/SNF subfamily

The SWI/SNF family was the first chromatin remodelling complex identified. It is conserved from yeast to humans. Founding members were identified in yeast screens for mutants affecting mating-type SWItching (SWI) and sucrose fermentation ("Sucrose Non-Fermenting", SNF) (Breeden L 1987; Neigeborn and Carlson 1984; Stern, Jensen, and Herskowitz 1984). The ATPase subunit of the SWI/SNF family of proteins contains a bromodomain which preferentially binds acetylated histones (Muchardt & Yaniv, 1993). The SWI/SNF family is composed of large multisubunit complexes including BAF, PBAF and WINAC complexes which function as coregulators of transcription and are also implicated in the repair of DNA damages (W. Wang et al., 1996). Remodelling reactions catalyzed by SWI/SNF family members include simple nucleosome sliding reactions but also more dramatic reactions such as creating DNA loops on the surface of nucleosomes or evicting histones such H2A/H2B dimers from chromatin (Bowman, 2010).

The mammalian BRG1/BRM Associated Factor/ Polybromo-associated BAF (BAF/PBAF) complexes consist of the two paralogue ATPase subunits namely Brahma-Related Gene-1 (BRG1) and BRahMa (BRM) and a collection of BAFs (Muchardt & Yaniv, 1993). BRG1 and BRM share over 70% sequence identity and display similar biochemical activities *in vitro* (Khavari, Peterson, Tamkun, Mendel, & Crabtree, 1993; Phelan, Sif, Narlikar, & Kingston, 1999; Randazzo, Khavari, Crabtree, Tamkun, & Rossant, 1994). The functional contribution of each BAF to the overall complex activity has not yet been clearly determined. It is clear however that combinatorial assembly mechanisms result in specific interactions with various transcriptional activators and repressors and thus specific targeting (Belandia, Orford, Hurst, & Parker, 2002; Hsiao, Fryer, Trotter, Wang, & Archer, 2003; T. Ito et al., 2001; Pal et al., 2003; Phelan et al., 1999). SWI-SNF-family complexes consist of several related complexes with many shared and specific subunits. Human SWI/SNF can be subdivided into the BAF complex which uniquely contains BAF250A (ARID1A) or BAF250B (ARID1B) and the PBAF complex which specifically contains BAF200

A)

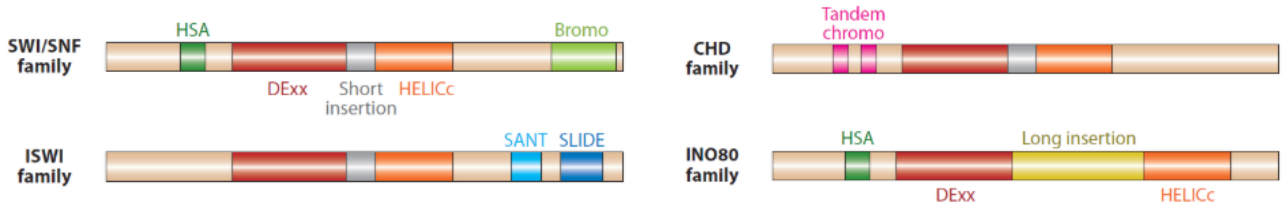

B)

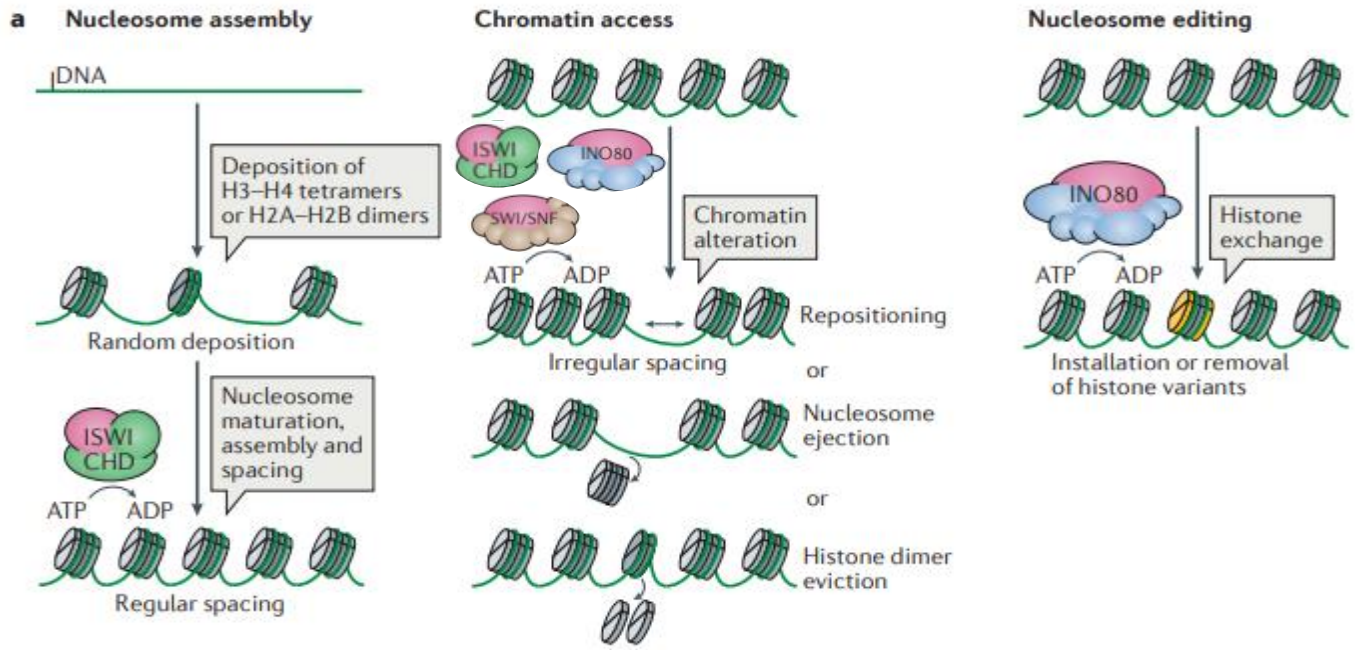

Figure 12. Structural and functional classification of remodellers.

(A) Schematic representation showing the domain organization of remodeller subfamilies. (B) Schematic representation of remodellers functions in chromatin landscape remodelling. ISWI and CHD subfamily remodellers participate in nucleosome assembly by histones deposition, nucleosomes maturation and spacing. SWI/SNF, ISWI and CHD subfamilies remodellers alter chromatin access by repositioning nucleosomes. Only SWI/SNF subfamily remodellers alter chromatin access by evicting histone dimers. INO80 subfamily remodellers change nucleosome composition by exchanging canonical and variant histones, and, for example, installing H2A.Z variants (yellow). (Adapted from Clapier et al.2017).

(ARID2) and BAF180 (PBRM1) (Laurette et al., 2015; Lemon, Inouye, King, & Tjian, 2001; Nie et al., 2000; Yan et al., 2005).

Interestingly, the PBAF complex was shown to play an essential role in melanocyte specific gene expression and melanocyte differentiation notably through BRG1. BRG1 is recruited by both MITF and SOX10 to establish the epigenetic landscape of melanocytes and proliferative melanoma cells (de la Serna et al., 2006; Keenen, Qi, et al., 2010; Laurette et al., 2019, 2015). Furthermore, PBAF remodelling is required for SOX10 expression (Keenen et al., 2010; Laurette et al., 2015; Ondrušová, Vachtenheim et al., 2013) and SOX10 target genes expression during schwann cell differentiation (Limpert et al., 2013; Marathe et al., 2013, 2017).

Similarly, the expression of MITF is completely dependent on the functional SWI/SNF complex (Laurette et al., 2015; Vachtenheim, Ondrušová, & Borovanský, 2010). However, the role of BAF/PBAF complexes in SOX10/MITF low “mesenchymal” melanoma cells state still remains unclear.

Generally, BAF subunits are highly expressed in melanoma cell lines while there is increasing evidence suggesting that some SWI/SNF subunits are deregulated or mutated in melanoma and cooperate with MITF to promote melanoma tumorigenicity (T. M. Becker et al., 2009; Hodis et al., 2012b; Keenen et al., 2010; Krauthammer et al., 2012; H. Lin, Wong, Martinka, & Li, 2010; Nikolaev et al., 2012). BRG1 levels were shown to be elevated in the later stages of melanoma metastasis while BRM levels decreased suggesting the critical role of the BAF/PBAF complexes in melanoma tumorigenesis (T. M. Becker et al., 2009; Saladi et al., 2010). In addition, the SWI/SNF complex is known to antagonize Polycomb Repressive Complex 2 (PRC2) which silences gene expression by tri-methylation of H3K27 and modulates the expression of target genes (Wilson et al., 2010). Interestingly, it has been recently shown that the balance of chromatin-remodelling activity shifts in favor of PRC2 over SWI/SNF complex when pre-malignant lesions progress to melanoma (Shain et al., 2018).

2) The ISWI subfamily

The ISWI subfamily of chromatin remodellers includes NURF (NUcleosome Remodelling Factor), CHRAC, RSF and ACF complexes. They are characterized by the presence of the SLIDE and SANT domains which help in the preferential interaction with nucleosomes containing linker DNA over core nucleosomes (Längst, Bonte, Corona, & Becker, 1999). Mammals contain two isoforms of the ISWI ATPase encoded by two related genes Snf2L/SMARCA1 and Snf2H/SMARCA5. These ATPases show intrinsic chromatin remodelling activity. They were purified from cells as complexes that contain at least one additional accessory subunit (Clapier & Cairns, 2009b). Those complexes are recruited to chromatin through a variety of mechanisms including modified histones, DNA binding proteins or specific DNA sequences. Once recruited they modulate accessibility to DNA by sliding or exchanging histone octamer subunits to ultimately regulate DNA dependent processes (P. B. Becker & Workman, 2013). Additionally, the ISWI family has recently emerged as one of the major ATP-dependent chromatin remodelling complex families that functions in the response to DNA damage since implicated in homologous recombination, non-homologous end-joining and nucleotide excision repair (Aydin, Vermeulen, and Lans 2014).

In mammals, the NURF complex is the major ISWI chromatin remodelling complex involved in the regulation of gene expression. NURF was first identified in Drosophila Melanogaster (Tsukiyama, Daniel, Tamkun, & Wu, 1995; Tsukiyama & Wu, 1995) and comprises NURF301 (in mammals, BPTF, Bromodomain, PHD-finger Transcription Factor), the ISWI-related SNF2L (SMARCA1) ATPase subunit, NURF55 (RbAp46, RBBP7) and NURF38 (Alkhatib & Landry, 2011; Koludrovic et al., 2015; Wysocka et al., 2006; Hua Xiao et al., 2001). BPTF contains multiple highly conserved domains essential for NURF interactions with a variety of transcription factors, thus promoting NURF recruitment to specific DNA sequences (Jones, Hamana, & Shimane, 2000; H Xiao et al., 2001). BPTF can also interact with H3K4me3 and H4K16ac modified histones through the C-terminal PHD finger and the bromodomain, respectively (Ruthenburg et al., 2011; Wysocka et al., 2006). It was recently shown that BPTF preferentially localizes to gene bodies but is also found in promoters, enhancers and terminators. However, its chromatin remodelling activity is constrained to the promoters while BPTF is required for exon splicing and

intron removal suggesting thus additional and functional roles within the gene bodies in mRNA processing (Alhazmi et al., 2018).

Compared to BRG1, BPTF is not required for melanoblast development in mice but for the generation of melanocytes from the adult melanocyte stem cell population (Koludrovic et al., 2015).

In human melanoma, the gene encoding BPTF is amplified in around 5–7% (Akbani et al., 2015) and BPTF expression can be upregulated during tumor progression, an event associated with poor prognosis and resistance to BRAF inhibitors (Dar et al., 2015). Additionally, BPTF/NURF was shown to associate physically and functionally with MITF to co-regulate genes involved in the proliferation of melanoma cells (Koludrovic et al., 2015).

3) The CHD subfamily

The CHD family contains nine different ATPases (CHD1–9). CHD family members share CHROMatin Organizing (CHROMO) domains (Fig12A) that bind specifically modified histones and a SNF2-like ATP-dependent helicase domain that facilitates nucleosome mobilization (Marfella & Imbalzano, 2007). CHD family members are classified into 3 subfamilies based on structural features and sequence homology. Subfamily I includes human CHD1 and CHD2 and is based on members having a DNA-binding motif domain (Delmas, Stokes, & Perry, 1993). Subfamily II includes CHD3, CHD4 and CHD5 and contains additional PHD (Plant HomeoDomain), zinc finger domains and DUFs (Domains of Unknown Function). Subfamily III includes CHD6, CHD7, CHD8 and CHD9 and contains a SANT (for switching-defective protein 3 (Swi3), Adaptor 2 (Ada2), Nuclear receptor Co-Repressor (N-CoR), transcription factor (TF)IIIB')) and a BRK (BRahma and Kismet) domain (Fig.13A) (Kolla, Zhuang, Higashi, Naraparaju, & Brodeur, 2014).

CHD proteins affect chromatin compaction and therefore the cellular machinery’s access to DNA. Thus, these enzymes control fundamental biological processes including transcription, cellular proliferation and DNA damage repair.

The Nucleosome Remodelling and Deacetylase (NuRD) multicomponent complex is the best characterized chromatin remodelling complex of the CHD family.

i) The mammalian NuRD complex

The NuRD complex, a 1 MDa multi-subunit protein complex, is one of the 4 major ATP-dependent chromatin remodelling complexes (Clapier & Cairns, 2009). The NuRD complex was first purified in cells from different species (Tong, Hassig, Schnitzler, Kingston, & Schreiber, 1998; Wade, Jones, Vermaak, & Wolffe, 1998; Xue et al., 1998; Y Zhang, LeRoy, Seelig, Lane, & Reinberg, 1998). This complex is unique as it contains at least two subunits with enzymatic functions. Indeed, the CHD3 (also known as Mi-2α) or CHD4 (Mi-2β) subunits show ATP-dependent chromatin remodelling activity with HDAC1 or HDAC2 catalyzing protein deacetylation. Thus NuRD is, along with Tip60/p400, one of the two known complexes coupling two independent chromatin-regulating activities (Bowen, Fujita, Kajita, & Wade, 2004; Torchy et al., 2015). A potential reason is that ATP-remodelling activity is necessary for the HDACs subunits to access their target (Pegoraro & Misteli, 2009). More recently, it has been shown that the lysine specific histone demethylase 1A (LSD1/KDM1A) can also be associated with the NuRD complex in some cell types (Yan Wang et al., 2009) suggesting an additional catalytic activity within a particular context.

NuRD comprises many other subunits among which the specific DNA-binding MTA1/2/3 (MeTastasis Associated), the CpG-binding proteins MBD2/3 (Methylated CpG-Binding Domain), the histone chaperones RbAp46/48 (Retinoblastoma Associated protein), the GATAD2a (p66a) and/or GATAD2b (p66b) proteins and DOC-1 (Deleted in Oral Cancer, also named CDK2AP1 (Cyclin-Dependent Kinase 2 Associated Protein 1)) protein (Fig.13B) (Kloet et al., 2015; Mohd-Sarip et al., 2017a). With the exception of the HDAC proteins and RbAp46/48, these proteins were only found within the NuRD complex. For note, the CHD4 remodelling subunit is capable of functioning independently of intact NuRD (O'Shaughnessy-Kirwan, Signolet, Costello, Gharbi, & Hendrich, 2015; O'Shaughnessy & Hendrich, 2013; Ostapcuk et al., 2018). Interestingly, a complex lacking CHDs with an HDAC activity but without remodelling capacity was identified as a stable species and named the NuDe (Nucleosome Deacetylase) complex (Low et al., 2016).

The NuRD complex, highly conserved among higher eukaryotes, is expressed in a large variety of tissues. It forms a large macromolecular assembly with a

stoichiometry of the different subunits that still remains elusive. Different studies suggested that NuRD complexes may be composed of one CHD3, CHD4 or CHD5 (Hoffmeister et al., 2017; Quan & Yusufzai, 2014), one HDAC1 or HDAC2, 3 MTA1/2/3, 1 MBD2 or MBD3, 6 RbAp46/48, 2 GATAD2b (p66a) or GATAD2a (p66b) and 2 DOC-1 (Fig.13B) (Smits, Jansen, Poser, Hyman, & Vermeulen, 2013). These data are nevertheless in contradiction with another structural analysis of the HDAC1/MTA1 complex that shows a dimerization of MTA1 thus suggesting a NuRD model with two MTA1/2/3 and two HDAC1 or HDAC2 (Millard et al., 2013). Recently, an additional model of the NuRD complex based on all the interaction maps available and the structures of NuRD subcomplexes was proposed (Torrado et al., 2017) and reported in Fig.13C.

Different homologs and isoforms were described for each of the NuRD subunits among which some were found to be mutually exclusive. This is particularly the case for the CHD, MBD and MTA proteins thus leading to a variety of coexisting NuRD complexes (N. Fujita et al., 2003; Hoffmeister et al., 2017; Le Guezennec et al., 2006) involved in various biological processes (Hoffmeister et al., 2017; Nitarska et al., 2016) depending on the cellular, physiological or pathological context. Illustrating this, a surprisingly sequential functional switch of CHDs within the complex resulting in combinatorial assembly of NuRD complexes was recently shown to regulate the transcription of genes involved in cortical development (Nitarska et al., 2016). Additionally, NuRD containing either CHD3 or CHD4 ATPase was shown to exhibit distinct nuclear localization patterns in unperturbed cells and distinct nucleosome remodelling and positioning behavior *in vitro* (Hoffmeister et al., 2017).

Since several of the core subunits are associated with transcriptional repression, the NuRD complex was mainly defined as a transcriptional repressor (Tong et al., 1998; Xue et al., 1998). NuRD may create a chromatin environment that facilitates subsequent Polycomb repression since its activity results in loss of H3K27 acetylation thus providing a substrate for PRC2-mediated trimethylation (Bracken, Brien, & Verrijzer, 2019b; Morey et al., 2008; Reynolds et al., 2012). Moreover, the nucleosome remodelling activity of CHD4 was shown to increase nucleosome density at target sites thus facilitating lineage commitment through control of gene expression

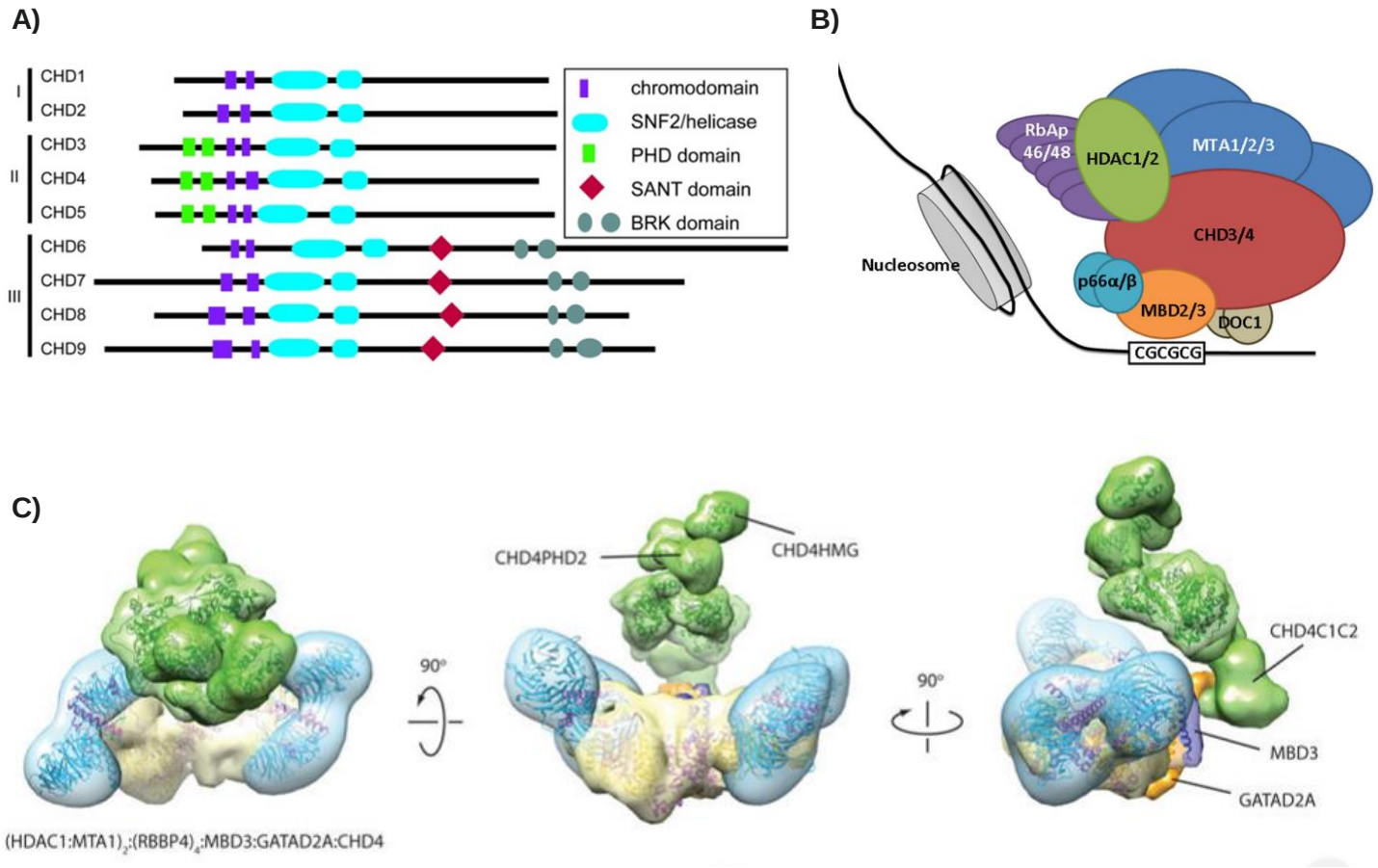

Figure 13. Structure of the CHD superfamily and mammalian Nucleosome Remodelling and Deacetylase complex (NuRD) architecture.

(A) *CHD families are defined based upon structural features and sequence homology. All CHD proteins contain two tandem CHRomatin Organization MOdifier (CHROMO) domains and two Sucrose NonFermentable2 (SNF2)-like ATP-dependent helicase domains. CHD3, CHD4, and CHD5 lack DNA-binding domains and contain two tandem Plant HomeoDomains (PHDs). In addition to the chromodomain and helicase domains, CHD6–9 proteins also contain tandem BRahma Kismet (BRK) and SANT domains (for switching-defective protein 3 (Swi3), Adaptor 2 (Ada2), Nuclear receptor Co-Repressor (N-CoR), transcription factor (TF)IIIB')) (Kolla et al. 2014).* ***(B)*** *Schematic representation of the NuRD multisubunit complex (Morgan P.Torchy et al. 2015) (**C**) Hypothetical recent model of the NuRD complex generated using the previously resolved subcomplex and positioning MBD3, GATAD2A and CHD4 in agreement with the observed protein–protein interactions. MBD3 (blue) bridges MTA1 and GATAD2A (orange) while GATAD2A is in contact with the C-terminal third part of CHD4 (green). MBD3 is represented by the MBD2:GATAD2A structure and a MBD domain. A density envelope derived from a disordered polypeptide chain was used to depict GATAD2A (Torrado et al. 2017).*

(de Dieuleveult et al., 2016; Z. Liang et al., 2017; Morris et al., 2014a; Moshkin et al., 2012; O'Shaughnessy & Hendrich, 2013).

Genome-wide mapping of chromatin binding patterns of NuRD components showed, in a variety of cell types, occupancy at active enhancers and promoters (de Dieuleveult et al., 2016; Günther et al., 2013; A. Miller et al., 2016; Shimbo et al., 2013; Stevens et al., 2017). Such global localization suggests that NuRD may have a general affinity for open chromatin or possibly for the transcription machinery rather than being recruited to every active enhancer or promoter by individual sequence-specific transcription factors. These transcription factors might then act to locally increase NuRD concentrations at individual target loci (Bornelö et al., 2018). Affinity for open chromatin was recently confirmed in prostate cancer cells and led to the classification of CHD3 and CHD4/NuRD in a functional group of remodellers with a clear preference for binding at 'actively marked' chromatin along with BRG1 and SNF2H/SMARCA5 (Giles et al., 2019).

Additionally, NuRD activity was recently shown to influence the association of RNA polymerase II at transcription start sites and subsequent nascent transcript production by restricting access to regulatory sequences thereby guiding the establishment of lineage-appropriate transcriptional programs in embryonic stem cells and in B-cell progenitors (Bornelö et al., 2018; Z. Liang et al., 2017).

ii) Biological functions of CHD3, CHD4 or CHD5 NuRD subunits

ATP-dependent chromatin-remodelling functions are ensured by CHD3, CHD4 or CHD5 proteins. These enzymes utilize the energy from ATP hydrolysis to destabilize interactions between DNA and histones. The chromatin structure is thus altered by displacement of nucleosomes along the DNA (Torchy et al., 2015). CHD3, CHD4 and CHD5, highly preserved among all eukaryotes, contain two PHD domains able to bind two distinct H3 tails within a single nucleosome or on adjacent nucleosomes. Thus, H3K9 trimethylation promotes enzyme binding while H3K4 methylation abolishes it (C. A. Musselman et al., 2012; Catherine A. Musselman et al., 2009).

CHD3 and CHD4 were initially identified as autoantigens in dermatopolymyositis (Ge, Nilasena, O'Brien, Frank, & Targoff, 1995; Seelig et al., 1995). Additionally to its role in transcriptional regulation CHD4 was shown to be implicated in DNA damage

response (McKenzie et al., 2019a; W. Qi et al., 2016; Stanley, Moore, & Goodarzi, 2013a), cell cycle progression (O'Shaughnessy & Hendrich, 2013), cell stemness (Nio et al., 2015), organogenesis and postnatal organ/tissue differentiation (Gómez-del Arco et al., 2016; Wilczewski et al., 2018). CHD3 is also implicated in DNA damage repair response by regulating heterochromatin formation and stimulating ATM-induced double-strand break repair (Klement et al., 2014; McKenzie et al., 2019b; Stanley, Moore, & Goodarzi, 2013b).

In cancer, *in vivo* genetic screens of patient-derived metastatic melanomas highlighted CHD4 as a critical factor in tumor growth (Bossi et al., 2016). CHD4 was identified as an essential regulator of breast cancer growth in murine and Patient Derived Xenograft (PDX) breast cancers. Indeed, CHD4 depletion impairs cell proliferation and migration of a triple negative breast cancer cell line and decreases the tumor mass *in vivo* (D'Alesio et al., 2016). CHD4 depletion in ERBB2+ cell lines (an oncogenic driver in 20-30% of breast cancer) also strongly inhibits proliferation and prevents *in vitro* cancer cell resistance to the anti-ERBB2 antibody Trastuzumab (D'alesio et al., 2019). In addition, CHD4 was shown to couple HDAC activity to promoter hypermethylation in colorectal cancer (Cai et al., 2014). CHD4 inhibits E-cadherin thereby inhibiting EMT and metastasis *in vitro* in lung cancer cells (J. Fu et al., 2011). Also CHD4 maintains tumor-initiating cells in glioblastoma (Chudnovsky et al., 2014).

Finally, aberrations in expression levels or mutations of NuRD components including CHD3 or CHD4 were associated in humans with cancer progression (Lai & Wade, 2011; Mohd-Sarip et al., 2017b), chemoresistance, EMT, metastasis (J. Wang et al., 2011; Xiao Wu et al., 2012) and overall poor patient survival (X. Du et al., 2013; Garcia et al., 2010a; Hall et al., 2014; Nio et al., 2015; Wong et al., 2011; Xiao Wu et al., 2012; C.-R. Xie et al., 2015a).

CHD5 differs from CHD3 and CHD4 at the carboxyl terminus. CHD5 showed a unique capability of nucleosome "unwrapping" *in vitro* that is not seen with CHD3 or CHD4 suggesting a specific role for CHD5. In addition, CHD5 was demonstrated to play a dynamic role in the remodelling of the genome during maturation of the male germline (W. Li & Mills, 2014; Zhuang et al., 2014) that is another specificity of CHD5.

In diverse human cancer, CHD5 is considered as a tumor suppressor that is frequently lost or inactivated by different mechanisms such as compromised expression, promoter hypermethylation, deletion, and/or mutation in many types of human cancers among them glioma (Bagchi et al., 2007; Mulero-Navarro & Esteller, n.d.; L. Wang et al., 2013a), neuroblastoma (T. Fujita et al., 2008; Garcia et al., 2010b; Koyama et al., 2012; LI et al., 2012), lung cancer (R. Zhao et al., 2012), prostate cancer (Robbins et al., 2011), breast cancer (Mulero-Navarro & Esteller, 2008; Xiao Wu et al., 2012) and melanoma (Lang, Tobias, & MacKie, 2011). In addition, CHD5 expression directly correlates with overall patient survival for several cancers such as glioma (L. Wang et al., 2013b), neuroblastoma (Garcia et al., 2010b), liver (C.-R. Xie et al., 2015b) and breast cancer (Xiao Wu et al., 2012).

Therefore, a growing body of evidence implicates CHD remodelling proteins in human cancer, notably CHD3, CHD4 and CHD5, underscoring the importance of this class of enzymes.

CHAPTER 3

An overview of central carbon metabolic pathways and cancer

CHAPTER 3

An overview of central carbon metabolic pathways and cancer

A. Glucose metabolism

The metabolism of glucose, the essential macronutrient, allows for energy to be generated in the form of ATP through the oxidation of its carbon bonds. In mammals, the end product is either lactate or CO_2 upon full oxidation of glucose via respiration in the mitochondria. The aerobic glycolysis process is carried out in the cytoplasm and only generates 2 ATP molecules per molecule of glucose. While the much more efficient mitochondrial OXidative PHOSphorylation (OXPHOS) pathway theoretically generates 36 ATP molecules per molecule of glucose. In mammals, energy production is a response to energy demand in the cell and relies primarily on both processes but the ratio of glycolysis versus OXPHOS for the total ATP yield varies in different type of cells depending on growth state and microenvironment (J. Zheng, 2012).

The first observations that cancer cells rewire their metabolism to promote growth, survival, proliferation and long-term maintenance were made nearly a century ago by Otto Warburg, a German physiologist. He indeed first described the unique metabolic features of cancer cells namely the dramatic increase in glucose uptake/consumption resulting in increased lactate production even in the presence of oxygen and fully functioning mitochondria (O Warburg, Wind, & Negelein, 1927; Otto Warburg, 1924). These features were confirmed in a number of tumor contexts and shown to correlate with poor tumor prognosis (Som et al., 1980). Thus, the Positron Emission Tomography (PET) scan of radiolabeled glucose analogs, technique currently used in clinics for tumor imaging and detection as well as monitoring responsiveness to treatment, was derived from such biological observations (Almuhaideb, Papathanasiou, & Bomanji, 2011). Those peculiar characteristics of tumor and other proliferative cells relate to the so-called “Warburg effect”. A major axis of research is still ongoing to understand

how such metabolic shift benefits to cell growth and survival particularly for cancer cells, and its potential exploitation in the clinic.

1) Glycolysis

Glycolysis is the initial step of glucose metabolism and is divided in ten steps of chemical reactions, converting glucose into pyruvate to ultimately produce ATP. Each reaction is catalyzed by a specific enzyme including HexoKinase (HK), Glucose-6-Phosphate Isomerase (GPI), PhosphoFructokinase 1 (PFK1), ALDOlase (ALDO), Triose-Phosphate Isomerase (TPI), GlycerAldehyde 3 Phosphate DeHydrogenase (GAPDH), PhosphoGlycerate Kinase 1 (PGK1), PhosphoGlycerate Mutase 1 (PGM1), ENOlase (ENO) and Pyruvate Kinase (PK) (Fig.14).

i) Steps of glycolysis (Figure 14)

- **Glucose uptake** is regulated and facilitated by the GLUcose Transporter (GLUT) family proteins of which 14 tissue dependent members were identified. GLUTs enable the entry of glucose into the cell and are increasingly found to be deregulated in numerous cancer types as a result of modified gene expression, protein relocalization or stabilization.

  In hepatocellular carcinomas GLUT2 is overexpressed with respect to other GLUTs and correlates with poor survival (Y. H. Kim et al., 2017). In bladder cancers, GLUT3 is overexpressed in muscle-invasive compared to noninvasive tumors (Han et al., 2017). In glioblastomas, GLUT3 expression is elevated in aggressive compared to lower grade lesions and is associated with poorer survival (Flavahan et al., 2013). Overall, considering all publicly available gene expression datasets high expression of GLUT1 and/or GLUT3 is associated with poor survival in most cancer types including colorectal carcinoma, breast carcinoma, lung adenocarcinoma, squamous cell carcinoma, ovarian carcinoma and glioblastoma (Chai et al., 2017). Interestingly, the expression of GLUT-1 while very rare in benign melanocytic nevi was shown to be a common feature of malignant melanoma and correlates with decreased survival (Důra et al., 2019).

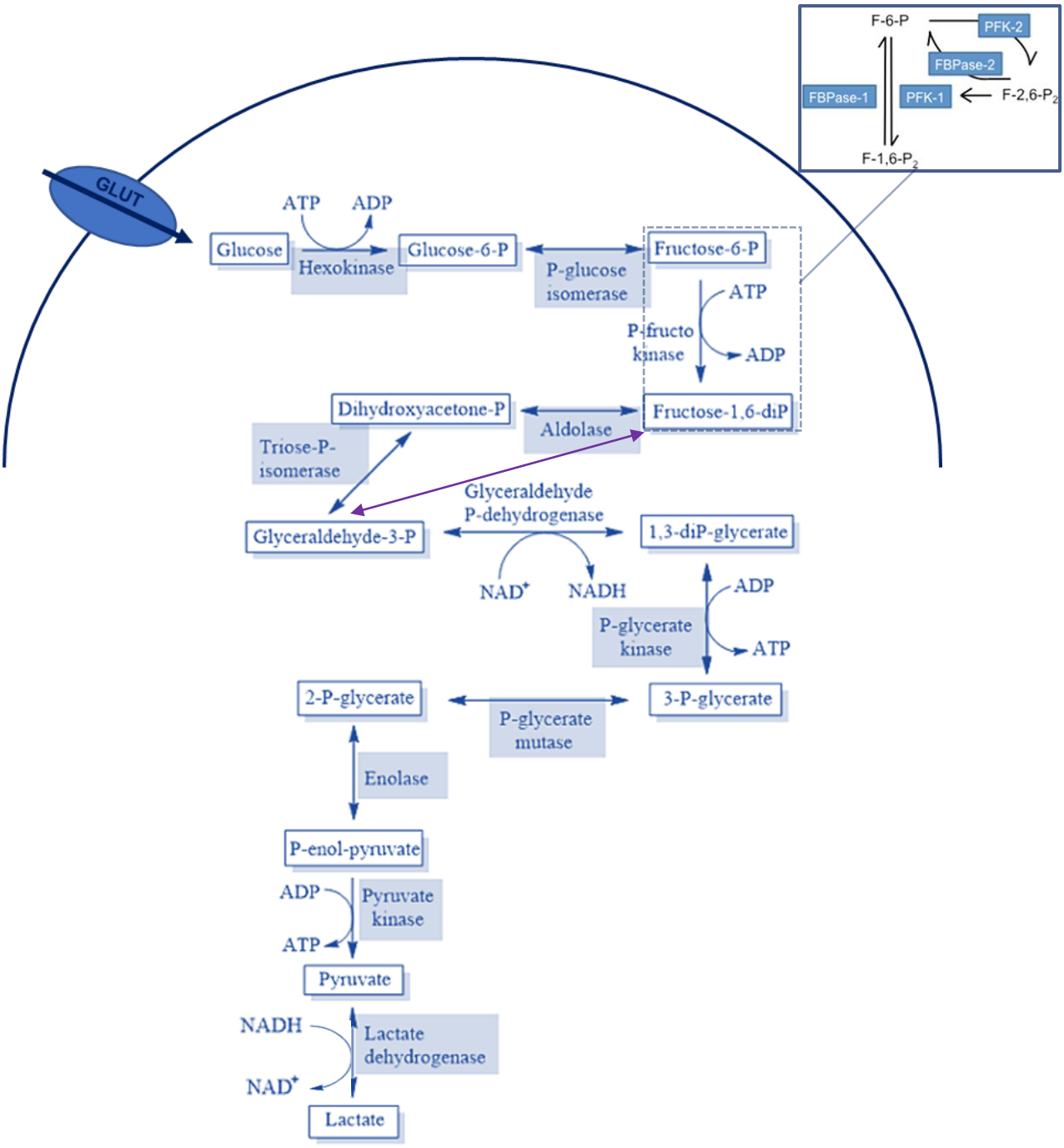

Figure 14. Chemical reactions and related enzymes involved in glycolytic metabolism.

Glycolysis, the initial step in glucose metabolism, involves 10 subsequent chemical reactions that convert in the cytoplasm glucose into pyruvate to finally produce ATP. The enzymes that catalyze those reactions include HexoKinase (HK), Glucose-6-Phosphate Isomerase (GPI), PhosphoFructoKinase 1 (PFK1), ALDOlase (ALDO), Triose-Phosphate Isomerase (TPI), GlycerAldehyde 3 Phosphate DeHydrogenase (GAPDH), PhosphoGlycerate Kinase 1 (PGK1), PhosphoGlycerate Mutase 1 (PGM1), ENOlase (ENO) and Pyruvate Kinase (PK) (Adapted from Tilvawal et al. 2018).

- **HexoKinases (HKs)** catalyze the first committed step of glucose metabolism that is phosphorylation of glucose to glucose-6-phosphate (G-6P) using ATP.

  There are four isoforms of HK (I-IV) in mammals with different tissues and organ distribution. The G-6P produced can serve as precursor for one or more of subsequent alternative pathways or for inhibition of HKs activity providing thus a feedback inhibition mechanism (John E. Wilson, 2003).

  Interestingly, Rose and Warms (1967) described significant quantities of HK-I and HK-II binding to the outer mitochondrial membrane via a mitochondrial binding motif located at the N-terminal domain (Sui & Wilson, 1997). With a direct access to ATP derived from OXPHOS bound HKs can thus efficiently phosphorylate glucose. The ADP generated by mitochondrial HK catalytic activity is then shuttled back into mitochondria for rephosphorylation conferring a metabolic advantage (Dean Nelson et al. 1986).

  HK-I or HK-II overexpression in tumors is thought to provide both a metabolic benefit and an anti-apoptotic capacity that give the cancer cells a growth advantage. Indeed, HK-II expression levels were shown to closely associate with tumor grade and mortality in hepatocellular carcinomas (Kwee, Hernandez, Chan, & Wong, 2012). Although in normal brain and low-grade gliomas HK-I is the predominant form while HK-II is highly upregulated in human multiform glioblastomas (Wolf et al., 2011). Poor prognosis is associated with upregulation of HK-II in human brain metastases of breast cancer (Palmieri et al., 2009). However, the functional role of both HK-I and HK-II in the malignant progression of cancers is not yet fully understood, especially considering that for decreased or low expression HK levels, an inverse correlation was shown e.g. in human cervical carcinoma cells. In these cells HK-I but not HK-II knockdown alters energy metabolism and induces an EMT phenotype which enhances tumor malignancy both *in vitro* and *in vivo* (Tseng et al., 2018).

  For note, 2-Deoxyglucose (2-DG), a glucose derivative without the 2-hydroxyl group that is taken up into cells and phosphorylated by HK, acts as a competitive glucose inhibitor that cannot follow the glycolytic pathway. Because of its glycolytic blocking ability 2-DG was considered as a potential clinical candidate but showed poor efficacy when administered alone in solid

tumors (L. Sun, Liu, Fu, Zhou, & Zhong, 2016). In addition, the clinical use of 2-DG is greatly limited by toxicity as the dual metabolic flux of glycolysis and oxidative Pentose Phosphate Pathway (PPP) is inhibited.

- **Glucose-6-Phosphate Isomerase (GPI)** also known as phosphohexose isomerase is the second enzyme in the glycolytic pathway that catalyzes the interconversion of glucose-6-phosphate into fructose-6-phosphate.

  *G*enetic disruption of GPI in both human colon adenocarcinoma and mouse B16 melanoma cells suppresses the aerobic glycolytic flux. However, cell growth is minimally affected due to a reprogrammed metabolic oxidative phenotype. Thus, the growth of those GPI-KO mutant cancer cells become oxygen-dependent and therefore is extremely sensitive to respiratory chain inhibitors (Cunha De Padua et al., 2017). In addition, GPI was linked to the proliferation and motility of cancer cells via its control on glucose-6-phosphate levels. Moreover, GPI was shown to induce the expression of a matrix metalloproteinase-3 protein in some cancer cells that subsequently increases tumor invasiveness (Cairns, Harris, & Mak, 2011).

  - **PhosphoFructokinase 1 (PFK1)** is one of the most prominent rate-limiting enzymes as it catalyzes the first glycolysis committed step. This enzyme converts the fructose-6-phosphate into fructose-1,6-bisphosphate by catalyzing the transfer of a phosphate from ATP, adenosine diphosphate (ADP) or PyroPhosphate (PPi) to the 1 position of the fructose-6-phosphate. For note, Fructose 1,6-BisPhosphatase (FBPase1), a rate-limiting enzyme, catalyzes the opposite reaction to that of PFK1 (Mcgilvery R, 1956).

    In mammalian cells, PFK1 has 3 isoforms: platelet (PFKP), muscle (PFKM), and liver (PFKL). PFKL is the most abundant in liver and kidney, whereas PFKM and PFKP are the only forms present in adult muscle and platelet, respectively. In contrast, all 3 isoforms are present in the brain and other tissues (Dunaway & Kasten, 1987; Dunaway et al., 1979; Moreno-Sánchez et al., 2007a).

    The protein is synthesized as unstable inactive monomers (Zancan, Almeida, Faber-Barata, Dellias, & Sola-Penna, 2007b) that rapidly associate to form minimally active dimers while full enzymatic activity is only reached by

formation of tetramers (Moreno-Sánchez, Rodríguez-Enríquez, Marín-Hernández, & Saavedra, 2007b). Higher oligomeric complexes could also be functional (Ferreras, Hernández, Martínez-Costa, & Aragón, 2009). Thus, the equilibrium between active tetramers and inactive dimers appears to be highly relevant for enzyme regulation.

The regulation of PFK1 activity is important not only for glycolytic flux and cellular energy production but also affects carbon distribution, redox balance, cell cycle, tumor formation and adaption of cells to oxidative stress (Katherine R. Mattaini and Matthew G. Vander Heiden, 2012). Several mechanisms of regulation of PFK1 activity were proposed including regulation of its expression by oncogenes, allosteric regulation and posttranslational modifications. PFK1 activity that can be inhibited by its own substrate is also regulated by intracellular concentrations of ATP thus being activated at 1 mM ATP and inhibited at higher ATP concentrations (Zancan, Marinho-Carvalho, Faber-Barata, Dellias, & Sola-Penna, 2008). PFK1 activity is also modulated by AMP, ADP, cAMP and Fructose-2,6-Biphosphate (F2,6B) that stabilize tetramers whereas ATP, citrate and lactate favor dimer formation (Costa Leite et al., 2007; Marinho-Carvalho, Costa-Mattos et al., 2009; Zancan et al., 2007a; Zancan et al., 2008) thus coordinating PFK1 activity to the energy status of the cell. F2,6B is catalyzed by dual kinase/phosphatase family of enzymes: 6-PhosphoFructo-2-Kinase (PFK2) /Fructose2,6-BisPhosphatase (FBPase2) (PFKFB1-4) (Bartrons et al., 2018; Okar & Lange, 1999; Pilkis, Claus, Kurland, & Lange, 1995). The balance between the activity of PFK-2 and FBPase-2 determines the concentration of F2,6B and therefore modulates PFK1 activity.

In human lymphomas and gliomas, PFK1 is less sensitive to inhibition by ATP and citrate, and more sensitive to activation by F2,6B and AMP (Colomer, Vives-Corrons, Pujades, & Bartrons, 1987; Staal, Kalff, Heesbeen, van Veelen, & Rijksen, 1987). F2,6B concentration was shown to be significantly higher in tumor than in normal cells (Colomer et al., 1987; Rider et al., 2004; Riera, Manzano, Navarro-Sabaté, Perales, & Bartrons, 2002) while FBPase1 overexpression suppresses cancer cell growth (B. Li et al., 2014) and its loss correlates with advanced tumor stage and poor prognosis (Juan Zhang et al., 2016). Additionally, FBPase1 that catalyzes the opposite reaction

of PFK1 has been reported to be lost in several human cancers (Dai et al., 2017).

- **ALDOlase (ALDO)** is involved in the conversion of the Fructose 1,6-BisPhosphate (F1,6BP) into Glyceraldehyde 3-Phosphate (G3P) and DiHydroxyAcetone Phosphate (DHAP). Considering the 3 ALDO isoforms: ALDOA is expressed in embryos and is abundantly available in adult muscle tissues (Mamczur & Dzugaj, 2008; D. C. Yao et al., 2004); ALDOB is expressed in liver and kidneys (Mukai, Joh, Arai, Yatsuki, & Hori, 1986) while ALDOC is abundant in the central nervous system (Mukai et al., 1986; Xu et al., 2017). Aldolases are differentially expressed in normal human tissues but aberrant expression or translocation was observed in several cancer types including oral squamous cell carcinoma, osteosarcoma, hepatocellular cell carcinoma, and lung cancer (Chang et al., 2017; Ji et al., 2016; Yamamoto et al., 2016). Moreover, ALDOA expression levels are associated with poor overall survival in lung adenocarcinoma, pancreatic ductal adenocarcinoma, clear cell renal carcinoma, breast cancer and gastric cancer. ALDOB was reported to correlate with the hazard ratio of liver and gastrointestinal tract related cancer types (He et al., 2016; Peng, Lai, Pan, Hsiao, & Hsu, 2008). Recent studies confirmed the overexpression of aldolase family members in tumorigenesis that was shown to promote several phenotypes in cancer cells through transcriptomic and proteomic models (X. Chen et al., 2014; Yamamoto et al., 2016; F. Ye, Chen, Xia, Lian, & Yang, 2018).

- **TriosePhosphate Isomerase (TPI)** is a homodimeric enzyme that operates in a non-linear step of glycolysis by catalyzing the fast interconversion of DiHydroxyAcetone Phosphate (DHAP) into Glyceraldehyde 3-Phosphate (G3P) both DHAP and G3P resulting from F1,6B catabolism by aldolase (Wierenga, Kapetaniou, and Venkatesan 2010). However, only G3P can be utilized in the remaining glycolysis steps. TPI was reported as upregulated in many types of cancers including esophageal (Y.-J. Qi et al., 2008), lung (J. E. Kim, Koo, Kim, Sohn, & Park, 2008) and prostate cancers (W.-Z. Chen, Pang, Yang, Zhou, & Sun, 2011). In addition, Linge et al.(2012) found that TPI expression in uveal melanoma tissues was higher in patients who have

subsequently developed metastasis than those who have not, while TPI silencing was associated with a decreased invasion and metastasis suggesting thus the important role of TPI in tumor development and progression. Moreover, TPI was shown to play an oncogenic role in gastric cancer cells (T. Chen, Huang, Tian, Lin, et al., 2017; T. Chen, Huang, Tian, Wang, et al., 2017) while TPI might function as a tumor suppressor in hepatocellular carcinoma cells (H. Jiang et al., 2017).

- **GlycerAldehyde 3 Phosphate DeHydrogenase (GAPDH)** catalyzes the conversion of G3P into 1,3-biphosphoglycerate in the presence of NAD+ and inorganic phosphate thus mediating the formation of NADH. In addition to glycolysis GAPDH is involved in cellular processes such as DNA repair (Kosova, Khodyreva, & Lavrik, 2017; Meyer-Siegler et al., 1991), tRNA export (Singh & Green, 1993), membrane fusion and transport (Glaser & Gross, 1995; Tisdale, 2001), cytoskeletal dynamics (Kumagai & Sakai, 1983), cell death (Hara et al., 2005) and apoptosis (Tarze et al., 2007). The multifunctional properties of GAPDH are likely to be regulated by its oligomerization, posttranslational modification and subcellular localization (J.-Y. Zhang et al., 2015).

  GAPDH is frequently upregulated in cancer cells to meet their energy requirements such as in breast cancer cells (Révillion, Pawlowski, Hornez, & Peyrat, 2000), lung cancer cells (Tokunaga et al., 1987), colorectal cancer cells (Tarrado-Castellarnau et al., 2017) and pancreatic adenocarcinomas (Schek, Hall, & Finn, 1988). Clearly, these cells expressing elevated GAPDH persist and profusely proliferate despite the established role of GAPDH as a potent apoptosis inducer. Therefore, GAPDH can both positively and negatively regulate cell survival and proliferation (J.-Y. Zhang et al., 2015).

- **PhosphoGlycerate Kinase 1 (PGK1)** is the first ATP-generating enzyme that catalyzes the transfer of high-energy phosphate from the 1 position of 1,3-DiPhospho-Glycerate (1,3-DPG) to ADP thus leading to 3-PhosphoGlycerate (3-PG) and ATP. PGK1 expression is upregulated in human breast cancer (Zhanget al., 2005), pancreatic ductal adenocarcinoma (Hwang et al.,2006), radioresistant astrocytoma (Yan et al., 2012) and multi-drug-resistant ovarian

cancer cells (Duan et al., 2002) as well as in metastatic gastric cancer, colon cancer and hepatocellular carcinoma cells (Ahmad et al., 2013; Ai et al., 2011; Ziekeret al., 2010). However, the mechanisms underlying the PGK1-promoted tumor development remain largely unclear.

Surprisingly, in addition to its glycolytic role PGK1 can act as a protein kinase to coordinate glycolysis and the TriCarboxylic Acid (TCA) cycle. Indeed, Li et al. (2016) showed that conditions such as hypoxia and oncogenic mutations that activate ERK signaling can induce the mitochondrial translocation of PGK1. Mitochondrial PGK1 then acting as a protein kinase phosphorylates and activates Pyruvate DeHydrogenase Kinase 1 (PDHK1) that inhibits mitochondrial pyruvate metabolism and ROS production and enhances lactate production, thereby promoting the Warburg effect and thus tumor development (X. Li et al., 2016).

- **PhosphoGlycerate Mutase 1 (PGM1)** catalyzes the conversion of 3-PhosphoGlycerate (3-PG) into 2-PhosphoGlycerate (2-PG). Several studies showed that PGM1 is upregulated in a variety of human cancers such as hepatocellular carcinoma, lung cancer, breast cancer, colorectal cancer, prostate cancer and renal clear cell carcinoma and that its enzymatic activity was increased in cancerous tissues compared to adjacent normal tissues (Bührens, Amelung, Reymond, & Beshay, 2009; Cortesi et al., 2009; C. Li et al., 2015; Ren et al., 2010; Wen et al., 2018). Conversely, silencing of PGM1 reduces lung and breast cancer cell growth in nude mouse xenograft models (Cortesi et al., 2009; Hitosugi et al., 2012; Ren et al., 2010). More recently, PGM1 silencing was shown to inhibit prostate cancer cell proliferation, migration and invasion as well as to enhance cancer cell apoptosis *in vitro* and to suppress xenograft tumor growth *in vivo* (Wen et al., 2018).

- **ENOlase (ENO)** is a metalloenzyme that requires Mg^{2+} to catalyze the dehydration of 2-phosphoglycerate into phosphoenolpyruvate in the last steps of the glycolytic pathway. Three isoforms were described and include α-ENOlase (ENO1) found in almost all human tissues, β-ENOlase (ENO3) predominantly found in muscles and γ-ENOlase (ENO2) only found in neurons and neuroendocrine tissues (Marangos, Parma, & Goodwin, 1978). Those

ENO isoforms share high-sequence identity and kinetic properties (Feo et al., 1990; Fletcher L, Rider CC, 1976; Giallongo et al., 1986). The enzymatically active enolase exists as homodimer or heterodimer and is composed of two subunits facing each other in an antiparallel fashion (Fletcher L, Rider CC, 1976; Kato et al., 1983).

ENO1 was shown to be upregulated in several tumors and correlates with shorter overall survival in cancer patients (Capello, Ferri-Borgogno, Cappello, & Novelli, 2011; Ceruti, Principe, Capello, Cappello, & Novelli, 2013). ENO1-silenced cells from breast, lung and pancreatic cancers display increased glucose uptake that consequently leads to an excess of intracellular glucose which is then forced towards alternative pathways such as the PPP and the polyol pathway thus resulting in decreased lactate levels (Capello et al., 2016). Similar results in terms of glycolysis inhibition are obtained after ENO1 silencing in endometrial carcinoma cells (M. Zhao et al., 2015). Finally, overexpression of ENO1 has been correlated with size, disease stage, metastasis and prognosis for many tumors (Ceruti et al., 2013).

ENO1 mainly acts as an enzyme but can also act as a plasminogen receptor at the surface of cancer cells thus promoting cancer cell proliferation, metastasis and spreading (Capello et al., 2011; Pancholi, 2001). Indeed, ENO1 induces the activation of plasminogen into plasmin (a serine protease involved in extracellular matrix degradation) thus favoring cell invasion and metastasis (Ceruti et al., 2013; Pancholi, 2001). Thus ENO1 silencing in tumor cells reduces not only glycolysis but also migration and invasion *in vitro* and tumorigenesis and metastasis *in vivo* (Capello et al., 2016; Q.-F. Fu et al., 2015; M. Zhao et al., 2015) that may be partly explained by ENO1 association with the cytoskeleton system (K.-J. Liu et al., 2007; Walsh, Keith, & Knull, 1989).

- **Pyruvate Kinase (PK)** is the final rate-limiting glycolytic enzyme that catalyzes the irreversible transphosphorylation between PhosphoEnolPyruvate (PEP) and ADP which results in pyruvate and ATP. In mammals, the PK family consists of four isoforms: Liver-type PK (PKL), Red blood cell PK (PKR) and PK Muscle isozymes M1 and M2 (PKM1 and PKM2). The two latter are produced via a splicing mechanism including exons 9 and 10 into PKM1 and

PKM2 mRNA, respectively (Fig.15A) (Takenaka et al. 1991). The non-allosteric isoform PKM1 is constitutively active and expressed in terminally differentiated tissues including muscles and brain that require a large supply of ATP. By contrast, PKM2 is expressed in tissues with anabolic functions. Indeed, PKM2 is highly expressed during development but reduced in a number of adult tissues while being reactivated in tumors (Christofk, Vander Heiden, Harris, et al., 2008; Mazurek, 2011).

Both PKM1 and PKM2 are tetrameric proteins formed by four identical subunits. Each subunit (or monomer) contains 4 structural domains namely A, B, C and a N-terminal domain (Fig.15B). The monomer first dimerizes then two dimers interact via the dimer-dimer interface orchestrated by the C domains of the monomers to form a tetramer. Because PKM1 and PKM2 include different exons in their mRNAs the encoded amino acids differ in the C domain and alter tetramer stability. Under physiological conditions PKM1 constitutively organizes as a tetramer while PKM2 alternates between high-activity tetramer and low-activity dimer forms (Yuan et al., 2018).

A switch from the PKM1 to the PKM2 isoform was shown in various types of cancers (Hacker, Steinberg, & Bannasch, 1998; Iqbal, Gupta, Gopinath, Mazurek, & Bamezai, 2014). Thus, PKM2 expression is increased in lung, breast, prostate, blood, cervix, kidney, bladder, papillary thyroid and colon cancer cells (Bluemlein et al., 2011; C. Feng et al., 2013). Interestingly, the change of mRNA splicing from PKM1 to PKM2 was shown to be enhanced by the c-Myc oncogene suggesting that cancer cells actively engage in such switch to fit their requirements for proliferation and metabolism (David, Chen, Assanah, Canoll, & Manley, 2010). These findings partly explain why PKM2 caught more researchers' attention than PKM1 thus leading to extensive studies on the potential role of PKM2 in tumorigenesis.

PKM2 activity is regulated by post-translational modifications, such as phosphorylation, acetylation, succinylation and oxidation which favor the low activity of dimeric PKM2 (Anastasiou et al., 2011; Lv et al., 2013; Park et al., 2016; Xiangyun et al., 2017) (Fig.16).

In addition to post-translational modifications, PKM2 but not PKM1 activity is tightly regulated by various allosteric modulators that affect tumor growth *in vitro* (Fig15C, Fig.16) (Anastasiou et al., 2012; Porporato, Dhup,

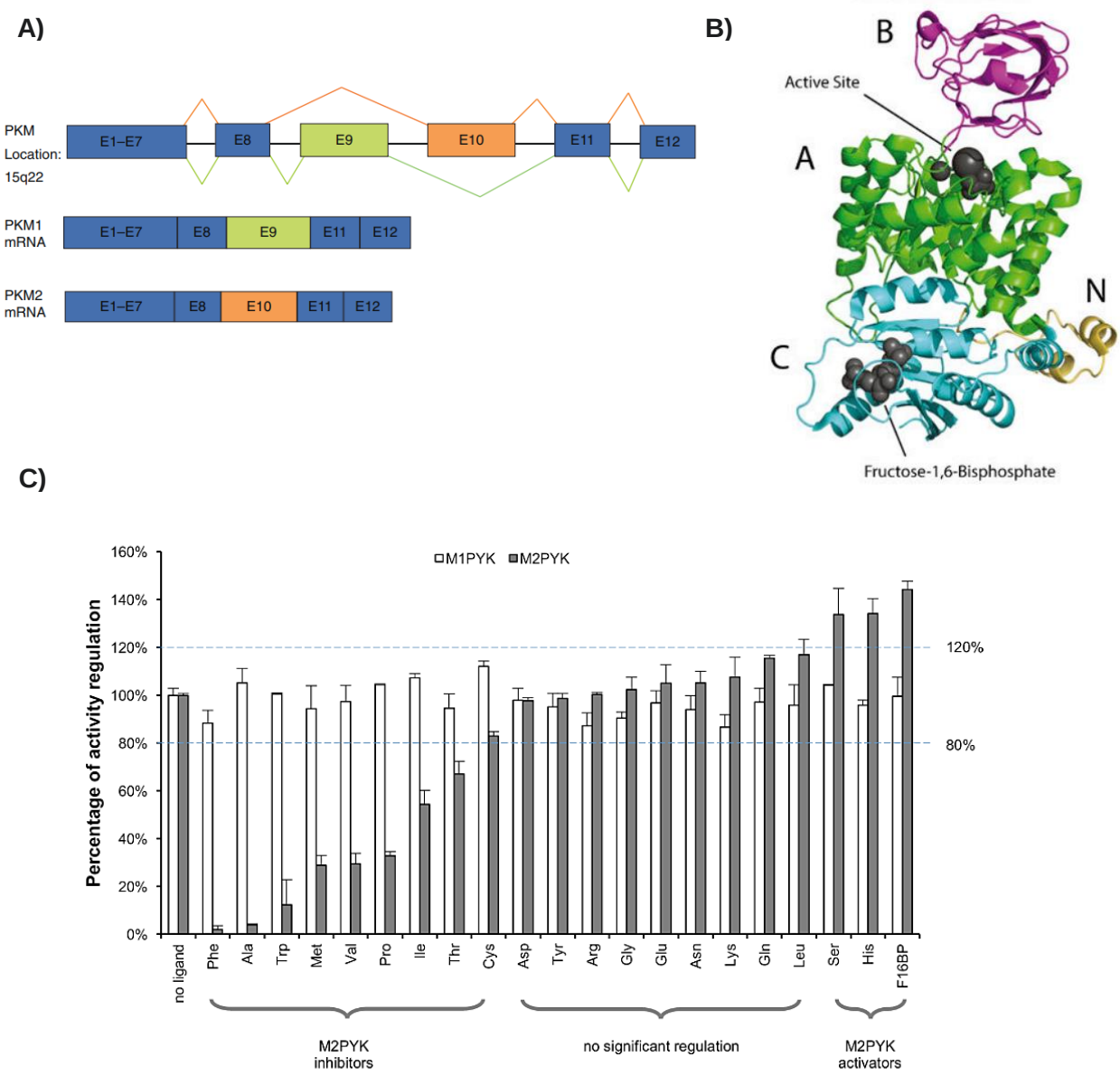

Figure 15. Pyruvate kinase, from gene and protein structure to allosteric regulation.

(A) *PKM1 and PKM2 are alternatively spliced forms of the PKM gene. They differ by the presence of either exon 9 (in green) in PKM1 or exon 10 (in orange) in PKM2 (Barbara Chaneton and Eyal Gottlieb, 2012).* ***(B)*** *Structure of monomeric PKM2 shown with the A, B, C and N-terminal domains depicted in green, magenta, cyan and yellow, respectively. Bound ligands are shown as black spheres: the catalytic active site is occupied by K+, Mg2+ and oxalate (a PEP mimetic), and FBP is bound at its allosteric pocket (Israelsen et al. 2015). (C) Effect of amino acids and FBP on PKM1 (in white) and PKM2 activity (in grey). Phenylalanine, alanine, tryptophan, methionine, valine and proline are strong inhibitors of PKM2 activity (99–65%) whereas the inhibition by isoleucine, threonine and cysteine is more modest (50–20%). Serine and histidine were identified as activators (higher than 120%) of PKM2 activity (Yuan et al. 2018).*

Dadhich, Copetti, & Sonveaux, 2011; Yuan et al., 2018). Indeed, PKM2 is allosterically activated by the upstream glycolytic metabolite F1,6BP (FBP) in a feed-forward regulatory loop to promote its tetramerization (Fig.15C, Fig.16) (J. Yang et al., 2016). This glycolytic intermediate directly binds to PKM2 that increases the PKM2 affinity for its substrate PEP (Jurica et al., 1998). Also, tyrosine-phosphorylated peptides bind directly to PKM2 which results in the release of the allosteric activator FBP leading to the inhibition of the PKM2 enzymatic activity (Fig.15C, Fig.16) (Anastasiou et al., 2011; Christofk, Vander Heiden, Wu, Asara, & Cantley, 2008b). Succinyl-5-AminoImidazole-4-CarboxAmide-1-Ribose-5'-phosphate (SAICAR), an intermediate of the *de novo* purine nucleotide synthesis pathway, specifically stimulates PKM2 (Fig.16). Upon glucose starvation cellular SAICAR concentration increases in an oscillatory manner and stimulates PKM2 activity in cancer cells for more energy production (Keller, Doctor, Dwyer, & Lee, 2014b; Kirstie E. Keller, 2012). Among the allosteric activators serine is a natural ligand that highly activates PKM2 in the absence of FBP (Chaneton et al., 2012; Labuschagne, van den Broek, Mackay, Vousden, & Maddocks, 2014; Vousden et al., 2012; Yuan et al., 2018). Several amino acids regulate PKM2 activity by stabilizing the tetrameric form (Fig.15C, Fig.16). Thus, such competition between allosteric activatory and inhibitory amino acids at a single allosteric site provides a finely tuned regulatory mechanism of PKM2 activity.

Also on top of its role as a pyruvate kinase, PKM2 functions as a protein kinase and transcriptional coactivator of genes involved in cell proliferation migration and apoptosis. Indeed, studies showed PKM2 tetramer as an active pyruvate kinase but PKM2 dimer as an active protein kinase (X. Gao, Wang, Yang, Liu, & Liu, 2012). Thus, PKM2 is translocated to the nucleus and transactivates β-catenin upon Epidermal Growth Factor Receptor (EGFR) activation promoting thus cell proliferation and tumorigenesis (X. Gao et al., 2012; W. Yang et al., 2011). Also, nuclear PKM2 translocation was shown to activate transcription of the Mitogen-activated protein Kinase 5 (MEK5) by phosphorylation of Signal Transducer and Activator of Transcription 3 (STAT3) enhancing cell proliferation (X. Gao et al., 2012). Additionally, PKM2 binds and forms a complex with the Octamer-binding transcription factor 4 (Oct4) leading

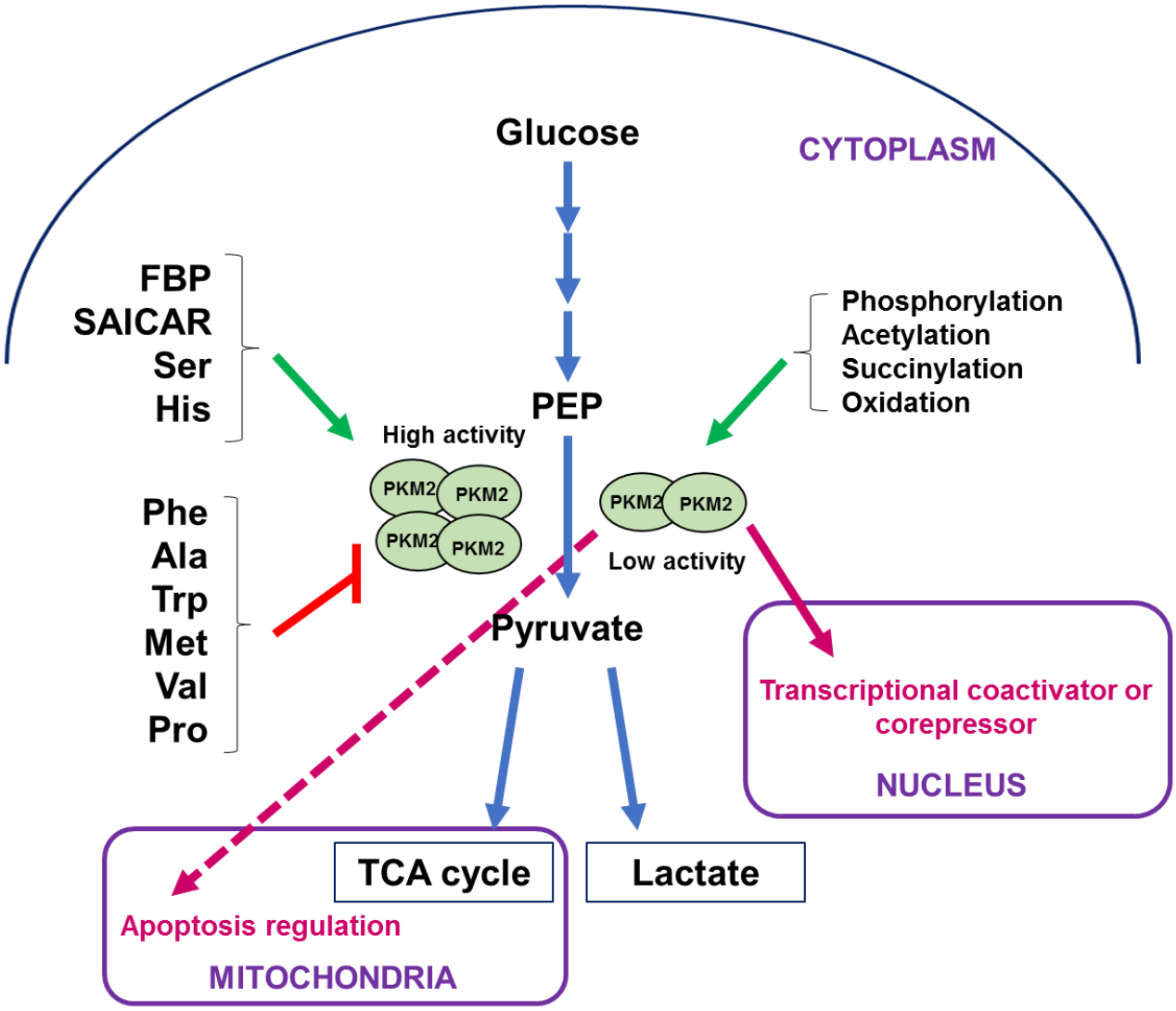

Figure 16. Dynamic regulation of PKM2 activity and functions.

The activity of the critical glycolytic enzyme PKM2 is regulated by both allosteric modulators and post-translational modifications. The potential roles of PKM2 in transcriptional regulation (in the nucleus) and apoptosis regulation (in the mitochondria) are shown in pink.

to Oct4-mediated transcription inhibition and promoting differentiation of glioma stem cells (Morfouace et al., 2014).

Besides transcription factors, PKM2 was shown to phosphorylate Myosin Light Chain 2 (MLC2), enhanced by EGF stimulation or oncogenic EGFR, K-Ras and B-Raf ($EGFR^{vIII}$, $K\text{-}Ras^{G12V}$ and $B\text{-}Raf^{V600E}$ respectively), playing a pivotal role in cytokinesis, cell proliferation and brain tumor development (Y. Jiang, Wang, et al., 2014). PKM2 binds and phosphorylates the spindle checkpoint protein Bub3 (Budding uninhibited by benzimidazole 3) regulating the fidelity of chromosome segregation, cell-cycle progression and tumorigenesis (Y. Jiang, Li, et al., 2014). Importantly, EGFR-activated ERK2 binds and phosphorylates PKM2 leading to PKM2 translocation, co-activation of β-catenin inducing c-MYC expression and upregulation of GLUT1 and LDHA (W. Yang, Zheng, et al., 2012). Also, PKM2 was shown to bind the abundant metabolite in cancer cells SAICAR, leading to phosphorylation of 100 human proteins, mostly protein kinases. PKM2-SAICAR phosphorylates and activates ERK1/2 inducing MAPK signaling activation and cell proliferation (Keller et al., 2014b). Additionally, PKM2 regulates transcription through histone modifications. Indeed, PKM2 was shown to bind and phosphorylate specifically Histone 3 at Threonine 11 (H3T11) upon EGFR activation, thus regulating gene expression and tumorigenesis through epigenetic modifications (W. Yang, Xia, et al., 2012).

Also, PKM2 translocates to mitochondria (Fig.16) and phosphorylates the regulator of apoptosis B-cell lymphoma 2 (Bcl2) correlating with both grades and prognosis of glioma malignancy. Bcl2 phosphorylation prevents its degradation and leads to inhibition of glioma cells apoptosis under oxidative stress (J. Liang et al., 2017).

ii) Lactate metabolism

During the last step of glycolysis pyruvate is reversibly reduced in the cytoplasm into lactate by Lactate DeHydrogenase (LDH) while NADH is oxidized to NAD+ (Fig.14). Cytosolic regeneration of NAD+ by LDH is mandatory for glycolysis to continue since NAD+ is required by the glycolytic reaction that converts glyceraldehyde-3-phosphate into 1,3-bisphosphoglycerate (Lemire, Mailloux, & Appanna, 2008).

Active LDH is a homo- or a heterotetramer which is made of two major subunits LDH-A and LDH-B that can assemble into five different isoenzymes (LDH1-5). LDH-A is the predominant form in skeletal muscle and has a higher affinity for pyruvate. Thus, the LDH5 tetramer that only contains LDH-A subunits favors the conversion of pyruvate to lactate with production of NAD+. In contrast, LDHB is mainly found in heart and muscle and converts lactate into pyruvate that can be further oxidized in mitochondria (Dawson, Goodfriend, and Kaplan 1964).

Lactate (2-hydroxypropanoate) is a hydroxycarboxylic acid that may exist in the human body as two stereoisomers L- and D-lactate, the L-form being the predominant physiological enantiomer (Connor, Woods, & Ledingham, 1983; Talasniemi, Pennanen, Savolainen, Niskanen, & Liesivuori, 2008). In humans, the main sources of intracellular L-lactate are glucose (approx. 65%) and alanine (approx. 20%) through their conversion into pyruvate and to a lesser extent serine, threonine, and cysteine (Perriello et al., 1995).

High concentrations of lactate act as a poison to the cell. Lactate production is also a contributor to tumor acidity alongside CO2 production (Marchiq & Pouysségur, 2016). As cancer cells take in more glucose more lactate is secreted (Y.-J. Chen et al., 2014). Additionally, lactate inhibits PFK1 activity (Costa Leite, Da Silva, Guimarães Coelho, Zancan, & Sola-Penna, 2007). Hence, to allow for the second committed step of glycolysis, lactate intracellular accumulation is prevented by MonoCarboxylate Transporters 1−4 (MCT1−4) that efficiently secreted lactate out of the cell.

For a long period of time lactate was considered as an inert end-product of glycolysis. However, accumulating evidence suggests that lactate governs multiple regulatory functions in cellular processes including energy regulation, immune tolerance, wound healing or cancer growth (S. Sun et al., 2017).

Elevated LDH is a well-established negative prognostic biomarker in many cancer types that directly correlates with tumor growth, proliferation, maintenance, metastasis and tumor survival. Indeed, LDH-A silencing in human hepatocellular carcinoma cells results in a significant reduction of tumor growth and metastasis (Sheng et al., 2012). In breast cancer cells LDH-A silencing results in an inhibited cancer cell proliferation, elevated intracellular oxidative stress and induction of mitochondrial pathway apoptosis (Z.-Y. Wang et al., 2012). Interestingly, it was shown that loss of LDH-B expression is an early frequent event in human breast and

prostate cancer due to promoter methylation and is likely to contribute to enhanced glycolysis in cancer cells under hypoxia (Brown et al., 2013; Leiblich et al., 2006). Triple negative breast tumor LDH-A expression and plasma LDH levels are two metabolic predictors for brain metastasis (Dong et al., 2017). Inactivation of LDH-A in mouse model of non-small cell lung cancer results in reprogramming of pyruvate metabolism and reactivation of mitochondrial function thus inhibiting tumorigenesis and tumor progression (H. Xie et al., 2014). Moreover, LDH-A is overexpressed in pancreatic cancer and is required for tumorigenicity of esophageal squamous cell carcinoma and pancreatic cancer cells (Rong et al., 2013; F. Yao, Zhao, Zhong, Zhu, & Zhao, 2013). In addition to the effect of LDH on tumorigenicity it was recently shown that LDH-A also regulates the tumor microenvironment via HIF-signaling and modulates the immune response (Serganova et al., 2018).

2) Oxidative metabolism

The oxidation of pyruvate into carbon dioxide to generate energy requires the collaboration of the Pyruvate DeHydrogenase complex (PDHc), the tri-carboxylic acid (TCA) cycle and the mitochondrial respiratory chain to ultimately produce ATP in an oxygen consuming reaction named OXidative PHOSphorylation (OXPHOS) of ADP (Fig.17).

i) Pyruvate DeHydrogenase complex (PDHc)

The role of the multi-subunit PDHc located in the mitochondrial matrix is to insert pyruvate into the TCA cycle by catalyzing the rate-limiting oxidative decarboxylation of pyruvate into acetyl-CoA. Since this step interconnects both the glycolysis and the TCA cycle it represents a key regulatory step in glucose metabolism. Thus, PDHc activity is highly regulated by reversible phosphorylations through Pyruvate Dehydrogenase Kinases (PDKs) and Pyruvate Dehydrogenase Phosphatases (PDPs) (Fig.17A).

- **PDKs** form a family of mitochondrial protein kinases responsible for phosphorylation of PDHc leading to its inhibition. These are serine-specific protein kinases which consist of a catalytically active α-subunit and a regulatory β-subunit. Four PDK isoenzymes (PDK1-4) were identified in mammalian tissues whose activity was shown to be efficiently regulated by

pyruvate and ATP/ADP, NADH/NAD+ and acetyl-SCoA/CoA-SH ratios. However, individual recombinant PDK isoforms differently respond to each of these factors (Fig.17A) (Bowker-Kinley, Davis, Wu, Harris, & Popov, 1998).

- **PDPs**, a mammalian family of phosphatases, are responsible for dephosphorylation and thus reactivation of PDHc. PDPs are dimeric enzymes consisting of catalytic and regulatory subunits (G. Chen, Wang, Liu, Chuang, & Roche, 1996). There are two isoforms of PDP (PDP1 and PDP2) capable of dephosphorylating all the 3 phosphorylation sites of PDHc (Fig.17A).

Accumulating evidence suggests that the metabolic changes observed in cancer cells may partly relate to a reduced mitochondrial function as a result from PDHc inhibition via an increased PDK1, PDK2 and PDK4 expression (McFate et al., 2008; Vander Heiden, Cantley, & Thompson, 2009).

In cutaneous melanoma both PDK1 and 2 isoforms are overexpressed compared to nevi. Their expression is associated with that of the mammalian Target Of Rapamycin (mTOR) pathway effectors and is independent of the BRAF mutational status. Indeed, the treatment of melanoma cells with a pan-PDK inhibitor shows a shift in metabolism, downregulation of proliferation, increase of apoptosis and reduced mTOR pathway activation (Pópulo et al., 2015). Interestingly, it was shown that PDHc is a crucial mediator of senescence induced by $BRAF^{V600E}$, the commonly mutated oncogene in melanoma and other cancers. Indeed, $BRAF^{V600E}$-induced senescence is accompanied by simultaneous PDK1 depletion and PDP2 induction thus enhancing the use of pyruvate in the TCA cycle with increased respiration and redox stress. Therefore, PDK1 depletion was shown to eradicate melanoma subpopulations resistant to targeted BRAF inhibition that results in regression of established melanomas (Kaplon et al., 2013). In a similar way, a recent study showed that the increased production of ROS upon inhibition of the MAP kinase pathway is responsible for activation of PDKs which in turn phosphorylates and inactivates PDHc reducing OXPHOS and ROS. Thus, small molecule PDK inhibitors might represent promising drugs for combination therapy in melanoma patients with activating MAP kinase pathway mutations (Cesi, Walbrecq, Zimmer, Kreis, & Haan, 2017).

For sake of completeness, it is worth mentioning a PHDc independent pathway involving Pyruvate Carboxylase (PC) that catalyzes the $HCO3^{-}$- and Mg-

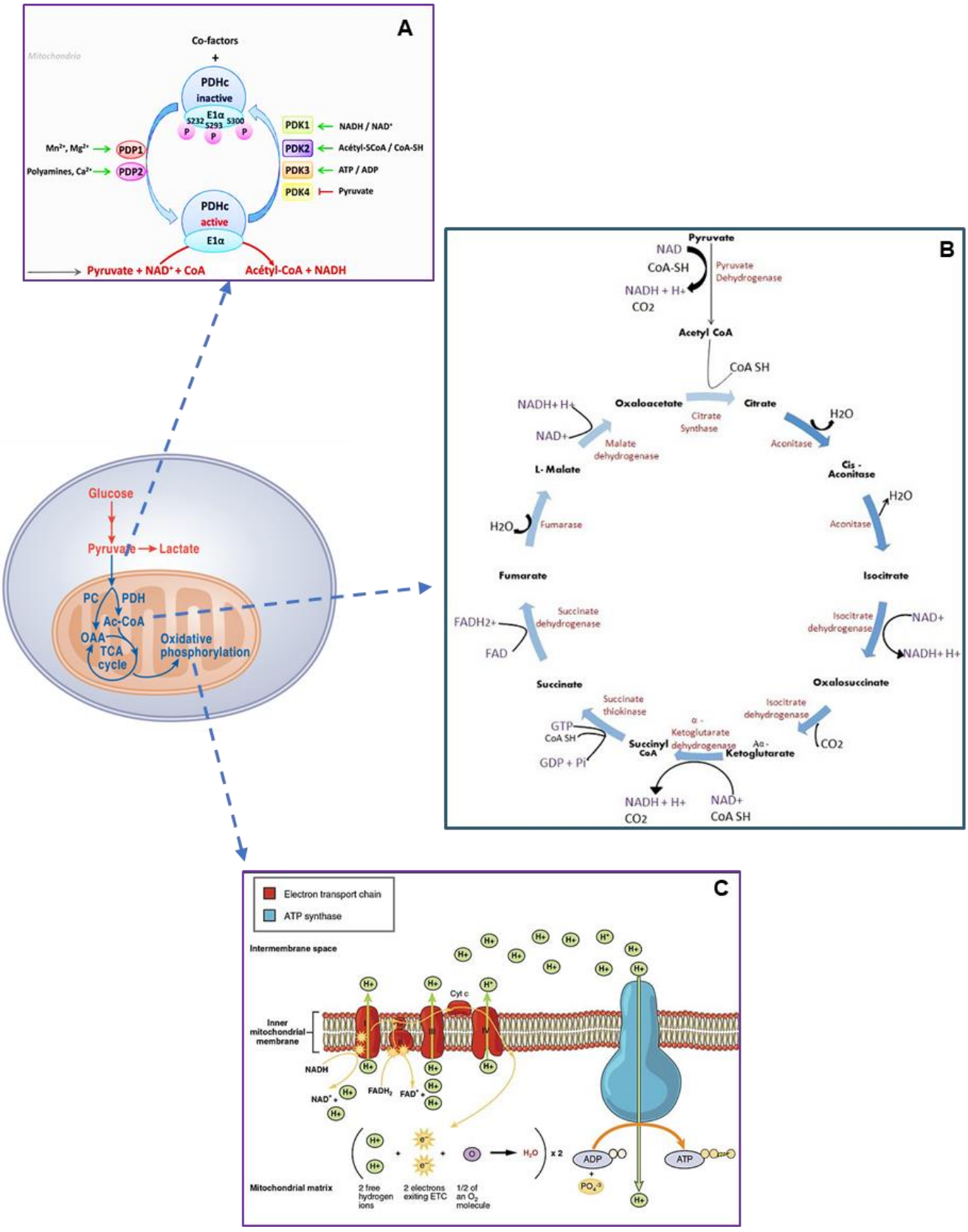

Figure 17. General overview of oxidative metabolism.

(A) *PDHc catalyzes the decarboxylation of pyruvate into acetyl-CoA in mitochondria. This reaction is tightly regulated by PDHc phosphorylation modulated by PDKs and PDPs.* ***(B)*** *TCA cycle occurs in the mitochondrial matrix and provides electron acceptors that are needed downstream in the ETC reactions.* ***(C)*** *ETC is composed of four protein complexes coupling the energy-yielding reactions of electron transport to ATP synthesis.*

ATP-dependent carboxylation of pyruvate into oxaloacetate thus replenishing the TCA cycle (Fig.17B) (reviewed in Jitrapakdee et al. 2008).

ii) Tri-Carboxylic Acid (TCA) Cycle

The TCA cycle that occurs in the mitochondrial matrix is a central hub for energy metabolism, macromolecule synthesis and redox balance. The TCA cycle allows aerobic organisms to oxidize cell fuel sources thus providing energy, macromolecules and electron acceptors that are utilized in downstream cellular processes such as the Electron Transport Chain (ETC) reactions. The TCA cycle is composed of a series of biochemical reactions briefly described below (Fig.17B).

1. In a 1st step acetyl CoA reacts with oxaloacetate (a 4-carbon molecule) to form citrate (a 6-carbon molecule) catalyzed by citrate synthase with release of a CoA group.
2. In a 2nd step citrate is converted by aconitase into its isomer isocitrate. This is a two-step process involving sequentially the removal and the addition of a water molecule.
3. In a 3rd step isocitrate is oxidized into α-ketoglutarate (a 5-carbon molecule) with release of a carbon dioxide molecule. In parallel NAD+ is reduced into NADH. The enzyme that catalyzes this step namely isocitrate dehydrogenase plays a crucial role in regulating the speed of the TCA cycle.
4. In the 4th step, similarly to the 3rd step, α-ketoglutarate is further oxidized by α-ketoglutarate dehydrogenase into a 4-carbon molecule that picks up Coenzyme A to form succinyl CoA. Also NAD+ is reduced into NADH and carbon dioxide is released.
5. In the 5th step the CoA moiety within the unstable succinyl CoA is replaced by a phosphate group (catalyzed by succinyl-CoA synthetase or succinate thiokinase) to form succinate (a 4-carbon molecule). CoA is then transferred to ADP to form ATP. In cells in which Guanosine DiPhosphate (GDP) is used instead of ADP, Guanosine TriPhosphate (GTP) is formed instead of ATP.
6. In the 6th step succinate is oxidized into fumarate (another 4-carbon molecule). In parallel two hydrogen atoms are transferred to FAD to produce $FADH_2$. Succinate DeHydrogenase (SDH) that carries out this step is embedded in the inner membrane of the mitochondrion so that $FADH_2$ can transfer its electrons directly into the Electron Transport Chain (ETC). Indeed, the electron carriers NADH and $FADH_2$

connect with the last portion of cellular respiration depositing their electrons into ETC to drive synthesis of ATP through OXPHOS.

7. In the 7th step, catalyzed by fumarase, water is added to convert fumarate into malate (another 4-carbon molecule).

8. In the 8th and last step of the TCA cycle, oxaloacetate (the initial 4-carbon compound) is regenerated with oxidation of malate by Malate DeHydrogenase (MDH). Another molecule of NAD+ is reduced into NADH in the process.

Overall, each round of the TCA cycle produces 3 NADH, one $FADH_2$ and one ATP or GTP, with the release of 2 carbon dioxide molecules. The TCA cycle runs around twice for each molecule of glucose that enters cellular respiration as glycolysis produces 2 pyruvates per glucose molecule.

While glucose represents the main source of pyruvate entering the TCA cycle in normal cells, cancer cells often shunt the TCA cycle for catabolism through anaerobic glycolysis being thus more dependent on other strategies to replenish TCA cycle intermediates. To feed the TCA cycle glucose can also be provided through gluconeogenesis, an essential process that leads to the synthesis of glucose from pyruvate and other non-carbohydrate precursors reciprocally regulated compared to glycolysis in order to maintain cell metabolism efficient (Berg, Tymoczko, Stryer, & Stryer, 2002). Amino acids can also fuel the TCA cycle but they enter after being converted into either acetyl-CoA or intermediates like pyruvate, oxaloacetate or succinyl-CoA (Berg et al., 2002).

The third type of fuel source for cancer cells is fatty acids which enter the TCA cycle after undergoing β-oxidation to generate acetyl-CoA. Acetyl-CoA is the substrate for both the fatty acid synthesis pathway and the TCA cycle thus making lipogenesis an important convergence point for TCA cycle flux and cellular biosynthesis. This process generates more acetyl-CoA per molecule than from either glucose or glutamine (Berg et al., 2002). While enzymes regulating lipid synthesis are often expressed at low levels in most normal tissues (Clarke, 1993) they are overexpressed in multiple types of cancers such as among others non-small cell lung cancer, breast cancer and cervical cancer (Migita et al., 2008; D. Wang, Yin, Wei, Yang, & Jiang, 2017; Xin et al., 2016) to meet tumor cell needs. Such enzyme activation or overexpression in tumors correlates with disease progression, poor prognosis and is being investigated as a potential biomarker of metastasis (Xin et al., 2016).

iii) Electron Transport Chain (ETC)

OXPHOS is the process that leads to ATP as the result of electron transfer from NADH or $FADH_2$ to O_2 by a series of electron carriers. These carriers are organized in the inner mitochondrial membrane into 4 complexes (complex I-IV). An additional protein complex then serves to couple the energy-yielding reactions of electron transport to ATP synthesis (Fig.17C).

Briefly, NADH and $FADH_2$ shuttle high energy molecules to the ETC. NADH transfers electrons to protein complex I while $FADH_2$ transfers electrons to protein complex II. The shuttling of high energy molecules induce oxidation of NADH and FADH2. NADH oxidation leads to the pumping of protons through protein complex I from the matrix to the intermembrane space. The electrons received by protein complex I or protein complex II are given to another membrane-bound electron carrier called ubiquinone or coenzyme Q. Coenzyme Q is a small lipid-soluble molecule that carries electrons through the membrane to complex III. The transfer of electrons from $FADH_2$ to coenzyme Q is not associated with a significant decrease in free energy and, therefore, is not coupled to ATP synthesis. Consequently, the passage of electrons derived from $FADH_2$ through the ETC yields free energy only at complexes III and IV and donates protons to the intermembrane space. Electrons reaching the protein complex III are picked up by cytochrome C (cyt C) a peripheral membrane protein bound to the outer face of the inner membrane, then carries electrons to complex IV where they are finally transferred to the final electron acceptor O_2 that causes again protons to be pumped into the intermembrane space. Thus, the oxidation of NADH and $FADH_2$ leads to a high concentration of protons on the outside part of the mitochondrial membrane creating an electrochemical gradient. This gradient causes movement of ATP synthase that binds ADP and Pi then producing the final ATP (Fig.17C).

Alterations in respiratory activity and mitochondrial DNA (mtDNA) appear to be common features of malignant cells. Indeed, the complex I polymorphism correlates with breast cancer incidence (Czarnecka, Klemba, et al. 2010a; Czarnecka, Krawczyk, et al. 2010b). Complexes III−IV were also implicated in cancer pathogenicity. The UbiQuinol-Cytochrome C Reductase Hinge protein (UQCRH), a protein within complex III, was shown to be downregulated in clear cell renal cell

carcinomas as compared to other renal cell carcinomas raising its potential as a biomarker (W.-S. Liu et al., 2016). Also, recent studies revealed that cancerous cells inhibit cyt C mediated apoptosis through supplying sufficient glutathione to keep cyt C in a reduced inactive state. In addition, it was shown that silencing of complex IV increases cancer aggressiveness and has specifically been implicated in esophageal tumor progression (Srinivasan et al., 2016).

Additional metabolic pathways essential for proliferation and maintenance of normal and cancer cells connected with glycolysis and OXPHOS are well described and include amino acid metabolism, one-carbon metabolism, PPP metabolism and fatty acid metabolism. They participate in protein and nucleotide synthesis, cell membrane structure and function maintenance, energy storage and signaling mediation (Counihan, Grossman, & Nomura, 2018; DeBerardinis & Chandel, 2016).

B. Glutamine metabolism and cancer cell addiction

Amino acids are essential nutrients for proliferation and maintenance of all living cells. In humans, some essential amino acids including histidine, isoleucine, leucine, lysine, methionine, phenylalanine, threonine, tryptophan and valine cannot be synthesized *de novo* and thus must be supplied exogenously. Conversely, non-essential amino acids including arginine, glutamine, tyrosine, cysteine, glycine, proline, serine, ornithine, alanine, asparagine and aspartate are generated within the body. Obviously, tumor cells have higher amino acid demand than normal cells since they proliferate more rapidly. Thus, additional supply is needed to meet such demand even for non-essential amino acids (Bhutia, Babu, Ramachandran, & Ganapathy, 2015a). Although the primary function of amino acids is to serve as building blocks for protein synthesis some amino acids such as glutamine play specific biologic functions in energetic and cellular homeostasis pathways.

H. Eagle (1955) observed that the development of mammalian cell lines in culture depends on an abundant exogenous supply of the non-essential amino acid glutamine. He showed that the optimal growth of cultured HeLa cells requires a 10- to 100-fold molar excess of glutamine in culture medium relative to other amino acids. Glutamine is the second (after glucose) most rapidly consumed nutrient by many

human cancer cell lines grown in culture (Hosios et al., 2016; Mohit Jain, 2012). However, glutamine requirements are very heterogeneous among different cancer cell lines ranging from those that are glutamine auxotroph to those that can survive and proliferate in the absence of an exogenous glutamine supply (Son et al., 2013; Timmerman et al., 2013).

In mammals, glutamine is synthesized in a number of tissues and transported into cells through various amino acid transporters described in the literature (Bhutia, Babu, Ramachandran, & Ganapathy, 2015b). Glutamine can then be used for biosynthesis of proteins or exported back out of the cell by antiporters in exchange for other amino acids (Wise & Thompson, 2010).

In addition, cancer cells can acquire glutamine through the breakdown of macromolecules under nutrient-deprived conditions. Macropinocytosis e.g. that plays a role in supplying proteins to most non-cancerous cells (Kerr & Teasdale, 2009) can be stimulated by oncogenic RAS (Bar-Sagi & Feramisco, 1986) thus enabling cancer cells to scavenge extracellular proteins. Proteins are then degraded into amino acids including glutamine essential for cell survival (Commisso et al., 2013; Kamphorst et al., 2015).

Upon entry into the cell, glutamine can serve as an important source of reduced nitrogen for the biosynthesis of purine and pyrimidine nucleotides as well as Uridine DiPhosphate N-Acetylglucosamine (UDP-GlcNAc) to support protein folding and trafficking (Wellen et al., 2010). Alternatively, glutamine can be converted into glutamate by glutaminase (GLS1 or GLS2) (Curthoys & Watford, 1995). Glutamate is subsequently converted into α-ketoglutarate (α-KG) through GLUtamate Dehydrogenase (GLUD1 or GLUD2) or aminotransferases (Moreadith & Lehninger, 1984) then enters the TCA cycle to provide energy for the cell. For note, α-KG can proceed backwards through the TCA cycle in a process called Reductive Carboxylation (RC) to produce citrate which supports the synthesis of acetyl-CoA and lipids (Fig.18) (P. S. Ward et al., 2010).

The expression of the enzymes involved in glutamine metabolism is highly variable in cancer cells and depends on tissue of origin and oncogenotypes. Indeed, GLS1 is broadly expressed in normal tissues and is thought to play a crucial role in many cancers whereas GLS2 expression is restricted primarily to the liver, brain, pituitary gland and pancreas (Ardlie et al., 2015). GLS1 and GLS2 are controlled through post-translational modifications and allosteric regulation. GLS1 but not GLS2

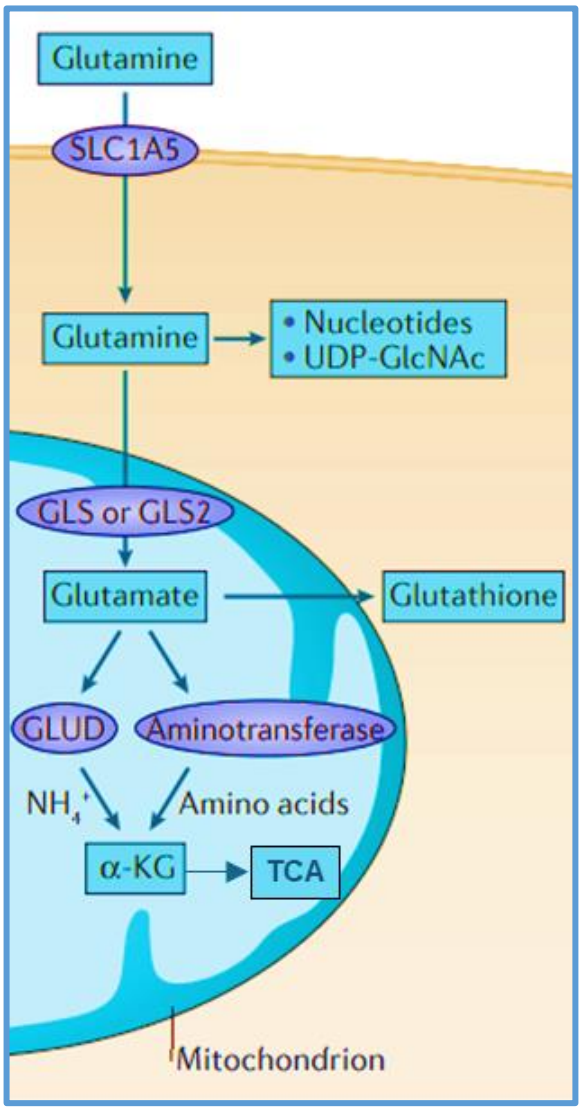

Figure 18. Glutamine metabolism.

Upon entry into the cell glutamine serves as an important source of reduced nitrogen for biosynthesis of nucleotides and UDP-GlcNAc synthesis or is converted to glutamate by GLS or GLS2. Glutamate is converted to α-KG through GLUD1/GLUD2 or aminotransferases and then enters the TCA cycle to provide cellular energy (Adapted from Altman et al. 2016).

is inhibited by its product glutamate whereas GLS2 but not GLS1 is activated by its final product ammonia *in vitro* (Curthoys & Watford, 1995; Krebs, 1935). Additionally, it was shown that GLS1 is regulated through transcription (L. Zhao, Huang, & Zheng, 2013), RNA-binding protein regulation of alternative splicing (Ince-Dunn et al., 2012; Masamha et al., 2014; Redis et al., 2016; Xia et al., 2014), post-transcriptional regulation by microRNAs (miRNAs), pH stabilization of the GLS mRNA (P. Gao et al., 2009; Hansen, Barsic-Tress, Taylor, & Curthoys, 1996) and protein degradation (Colombo et al., 2011, 2010). By contrast, the role of GLS2 in cancer seems to be more complex. Silenced by promoter methylation in liver cancer, colorectal cancer and glioblastoma, reexpression of GLS2 was shown to exhibit tumor suppressor activities in colony formation assays (J. Liu et al., 2014; S. Suzuki et al., 2010; Szeliga, Bogacińska-Karaś, Kuźmicz, Rola, & Albrecht, 2016).

As aforementioned, once produced via glutaminase, glutamate is deaminated to α-KG by GLUD, tightly regulated through post-translational modifications, allosteric regulators, ADP, GTP, palmitoyl-CoA and SIRT4-dependent ADP ribosylation (Csibi et al., 2013; Erecińska & Nelson, 1990; Fahien & Kmiotek, 1981; Haigis et al., 2006; M. Li, Li, Allen, Stanley, & Smith, 2012).

C. Metabolic states and adaptive strategies of melanoma cells

Similar to the majority of cancer cells, melanoma cells display high glycolytic phenotypes independently of their oncogenic background. However, their metabolism is not strictly glycolytic since the TCA cycle is still functional even under hypoxia (Scott et al., 2011).

Glycolysis in melanoma cells is partly driven by the activation of the MAPK pathway that induces the transcription and stabilization of the Hypoxia-Inducible Factor 1α (HIF1α) (Kumar et al., 2007) thus promoting glycolysis via transcription of LDH, aldolase and ENO1 (Semenza et al., 1996). Furthermore, HIF1α activates PDK that prevents pyruvate synthesis and thus OXPHOS (J. Kim, Tchernyshyov, Semenza, & Dang, 2006). Besides HIF1α, MAPK pathway activation also induces the transcription of MYC (Parmenter et al., 2014) which promotes glucose uptake and

increases glycolytic activity by activating glucose and glutamine transporters as well as LDH and HKs (Stine et al., 2015). Additionally, MAPK pathway activation also promotes glycolysis through negative regulation of MITF expression and activity (Wellbrock & Marais, 2005; Wellbrock et al., 2008) which is involved (as detailed earlier) in the regulation of PGC1α expression and mitochondrial respiration (Haq et al., 2013a).

In addition to the MAPK pathway, the PI3K/AKT/mTOR signaling pathway is also activated in melanoma cells (M. A. Davies et al., 2008; Kwong & Davies, 2013; Omholt, Kröckel, Ringborg, & Hansson, 2006). Activation of this pathway also promotes glycolysis by phosphorylation and activation of AKT that drives mTOR signaling, which can promote transcription and activity of HIF1α and MYC, thereby driving the metabolic regulation described above (Hudson et al., 2002; Land & Tee, 2007).

In melanoma, MAPK and PI3AKT pathways also regulate the expression of the Fatty Acid Synthase (FASN) that catalyzes the rate-limiting step of the endogenous synthesis of fatty acids. Thus FASN was shown to be strongly expressed in melanomas and associated with Breslow thickness (Innocenzi et al., 2003). Increased FASN ensures an adequate concentration of phospholipids that represent the structural foundation of cell and organelle membranes thus providing a survival benefit to proliferative cells (Menendez & Lupu, 2007). Indeed, FASN expression levels correlate with tumor invasion and poor prognosis in cutaneous melanoma (Innocenzi et al., 2003; Zecchin et al., 2011). For note, experimental evidence suggests that not only fatty acid synthesis but also Fatty Acid Oxidation (FAO) plays a role in melanoma. However, how exactly FAO promotes melanoma progression still remains unresolved (Fischer et al., 2018).

Moreover, melanoma cells exhibit an altered serine biosynthetic pathway. Indeed, the first enzyme involved in this pathway namely the PHosphoGlycerate DeHydrogenase (PHGDH) is frequently amplified in melanoma (Beroukhim et al., 2010; Mullarky, Mattaini, Vander Heiden, Cantley, & Locasale, 2011). Therefore, considering that the serine biosynthetic pathway is involved in glycine, purine and pyrimidine synthesis and also modulates the activity of the critical glycolytic enzyme PKM2 (as previously described) any alteration of this pathway affects cancer cell

proliferation (Amelio, Cutruzzolá, Antonov, Agostini, & Melino, 2014; Labuschagne et al., 2014; Locasale, 2013; J. Ye et al., 2014)

Besides the Warburg phenotype OXPHOS plays a crucial role in melanoma. OXPHOS is indeed much more efficient at generating ATP than glycolysis as previously detailed. While only 7% of the available pyruvate accesses the TCA cycle in hypoxic cells, OXPHOS still contributes to a significant extent to provide ATP to tumor cells (Scott et al., 2011). It is a matter of fact that a significant proportion of cell lines (BRAF mutant or wildtype) and patient samples can be characterized as “High-OXPHOS” a phenotype predominantly driven by the highly expressed PGC1α (Vazquez, Markert, & Oltvai, 2011) that regulates multiple mitochondrial genes (Gopal et al., 2014; Haq et al., 2013a; G. Zhang et al., 2016).

The treatment of $BRAF^{V600E}$ melanoma cells with a BRAF inhibitor results in an increased expression of several genes associated with the TCA cycle and OXPHOS thus increasing mitochondrial density, ROS production and decreasing glucose conversion to lactate. This is partly explained by the activation of MAPK pathway in melanoma cells downregulating PGC1a expression thus reducing mitochondrial biogenesis and oxidative phosphorylation (Haq et al., 2013a; Puigserver & Spiegelman, 2003). Indeed, mutations in PGC1a have been detected in whole-genome melanoma analysis and elevated MITF and PGC1α levels were observed in patients treated with BRAF/MEK inhibitors highlighting thus the dynamic energetic adaptation of melanoma cells (Haq et al., 2013b; Prickett et al., 2009; Stark et al., 2012).

D. Crosstalk between metabolism and epigenetic regulation of chromatin

Alterations in cellular metabolism and transcriptional programs are hallmarks of cancer cells. Both processes support cell growth, proliferation, migration, differentiation and apoptosis. The interconnection between epigenetic regulation and metabolism is crucial to adapt the cell metabolic needs at the gene expression level.

How cell metabolism influences chromatin modifications and gene expression is briefly described below.

1) Metabolite-mediated modulation of chromatin

Metabolites serve as important cofactors and regulators of various enzymes implicated in DNA and histones modifications influencing thus gene expression (X. Li, Egervari, Wang, Berger, & Lu, 2018).

One of the key chromatin modifications that is strongly interconnected with metabolism is methylation. A number of methyltransferases are involved in epigenetic gene regulation (Berger, 2007; Cheng, 2014). Methylation is regulated by the abundance of S-AdenosylMethionine (SAM) whereby SAM serves as a universal methyl donor that is synthesized from methionine and ATP (Grillo & Colombatto, 2008). Methylation produces S-AdenosylHomocysteine (SAH) a potent inhibitor of all methyltransferases. Thus, the intracellular SAM:SAH ratio that is itself tightly regulated by the metabolism of methionine, threonine and serine regulates in turn the methyltransferase activity (Etchegaray & Mostoslavsky, 2016; Mentch et al., 2015).

Histone and DNA methylation can be removed by demethylases LSD1 or LSD2 that require α-KG. Indeed, high levels of α-KG maintained through glucose and glutamine catabolism promote demethylation of target histones (Carey, Finley, Cross, Allis, & Thompson, 2015; Hwang et al., 2016).

In addition, histone acetylation is also regulated by the activity of enzymes (still strongly correlated with metabolites) including Histone AcetylTransferases (HATs) and HDACs that are inhibited by products of the fatty acid hydrolysis (Shimazu et al., 2013). Nuclear enzymes that deacetylate histones including SIRT1 and SIRT2 require NAD+ for their activity. Such enzymes are activated by high NAD+ levels and inhibited by NicotinAMide (NAM) a precursor of NAD+ (Cantó, Menzies, & Auwerx, 2015).

2) Metabolic enzyme-mediated modulation of chromatin

As described before for PKM2, various metabolic enzymes which typically localize to the cytoplasm or mitochondria can also translocate into the nucleus.

Indeed, PFK1 migrates to the nucleus in response to aerobic glycolysis where it binds to the TEAD transcription factor thus regulating YAP-TAZ signaling (Enzo et al., 2015).

Additionally, PFKFB4 that catalyzes both the synthesis and the degradation of F2,6B and is required for the activation of the Steroid Receptor Co-activator protein 3 (SRC3), a transcription co-activator that contains several nuclear receptor interacting domains and intrinsic HAT activity. PFKFB4 phosphorylates SRC3 leading to increased interaction between SRC3 and Activating Transcription Factor 4 (ATF4) at gene promoters, thus inducing gene expression of metabolic enzymes (Dasgupta et al., 2018).

In addition, GAPDH is selectively recruited to the H2B promoter in S phase and is essential for S phase-specific H2B gene transcription *in vivo* and *in vitro* underscoring the nuclear role of GAPDH in coupling histone gene expression and DNA replication (L. Zheng, Roeder, & Luo, 2003).

Moreover, not only glycolytic enzymes are found in the nucleus but also TCA enzymes such as α-KG dehydrogenase and fumarase (X. Li et al., 2018).

In glioblastoma cells, a fraction of α- KGDH is distributed in the nucleus and interacts with the histone acetyltransferase KAT2A at gene promoters and locally supplies succinyl-CoA, which is then bound by KAT2A with high affinity. The high binding affinity of succinyl-CoA as well as its high local concentration facilitate histone succinylation on K79 in the promoter regions of more than 7’000 genes. Inhibition of nuclear entrance of the α- KGDH complex or expression of the KAT2A mutant with low binding affinity for succinyl-CoA reduces gene expression and inhibits tumor cell proliferation and glioma growth in mice (Yugang Wang et al., 2017).

Also, fumarase was shown to translocate from the cytosol into the nucleus upon ionizing radiation-induced DNA damage (Yogev et al., 2010). In the nucleus, DNA-dependent Protein Kinase (DNA-PK) phosphorylates fumarase thus promoting its binding to histone H2A.Z leading to the enrichment of fumarase at irradiation-induced double-strand break regions and subsequent localized fumarate production. Such locally accumulated fumarate inhibits α-KG-Dependent lysine-specific DeMethylase 2B (KDM2B) activity and increases dimethylation of histone H3K36 and accumulation of the DNA-PK complex at DNA damaged regions for subsequent Non Homologous End Joining (NHEJ), DNA repair and cell survival (Y. Jiang et al., 2015). Chromatin-

associated fumarase also directly participates in gene transcription. Under glucose deprivation conditions, fumarase is phosphorylated by the ATP sensor AMPactivated Protein Kinase (AMPK) leading to its binding to the transcription factor ATF2 and translocation to ATF2-regulated gene promoter regions. There, Fumarase catalyzed fumarate inhibits KDM2A thereby promoting histone H3K36 methylation and expression of genes mediating cell growth arrest (T. Wang et al., 2017).

Therefore, in response to nutrient availability and physiological or pathological stimuli, the altered activity and localization of metabolic enzymes or metabolites regulate many essential biological functions by reprogramming gene expression.

RESULTS

Context and aims of research

Cutaneous malignant melanoma is an aggressive form of skin cancer resulting from oncogenic transformation of melanocytes. Several recurrent somatic mutations were described in epidermal melanoma, the most frequent of which being $BRAF^{V600E}$, an activating mutation found in 50-60% of tumors (Hodis et al., 2012a). Two other frequent alterations are activating mutations in NRAS (≈20%) and loss of function mutations in NF1 (≈10%). All these mutations lead to constitutive activation of the MAP kinase signaling pathway and melanocyte proliferation. Current models propose that founder $BRAF^{V600E}$ or NRAS mutations are first detected in benign precursor lesions that give rise to melanoma by accumulation of additional mutations that allow bypass of oncogene-induced senescence (Shain et al., 2015). Such stepwise model for tumor development is derived from the analyses of lesions at different stages in separate individuals or different regions within the same lesions. This approach was supported by the analyses of larger numbers of matched primary and metastatic lesions (Birkeland et al., 2018; Shain et al., 2018). Whole exome sequencing approaches allowed us to follow the dynamic clonal evolution composition and to identify a rare combination of driver mutations in an atypical case of epidermotropic metastatic melanoma.

The results of this study are described in **Annexe 1** related to the following manuscript:

Guillaume DAVIDSON, Sebastien COASSOLO *et al.* (2019) **Dynamic evolution of clonal composition and neoantigen landscape in recurrent metastatic melanoma with a rare combination of driver mutations.** Journal of Investigative Dermatology.

Transcription factors MITF and SOX10 play important roles in melanoma by driving cell proliferation (J. C. Cronin et al., 2013; Giuliano et al., 2010; Shakhova et al., 2012; Strub et al., 2011). MITF and SOX10 bind together at a large number of cis-regulatory elements, enhancers and promoters, to regulate not only genes involved in pigmentation, but also genes involved in DNA replication and repair as well as mitosis (Laurette et al., 2015). Consequently, silencing of either factor leads to arrested proliferation and senescence (Giuliano et al., 2010; Strub et al., 2011).

We show that MITF associates and coregulates a gene expression program with the NURF chromatin-remodelling factor whose catalytic ATPase subunit BPTF is essential for differentiation of adult melanocyte stem cells. ShRNA-mediated BPTF silencing suppresses the proliferative capacity and metastatic potential of melanoma cells (Dar et al., 2016; 2015; Koludrovic et al., 2015) while BPTF overexpression predicts poor survival in melanoma patients and promotes resistance to BRAF inhibitors in melanoma cell lines (Dar et al., 2015).

Also, MITF and SOX10 interact with the PBAF chromatin remodelling complex whose catalytic ATPase subunit BRG1 is recruited to the nucleosomes surrounding the MITF and SOX10 bound cis-regulatory elements. BRG1 is essential for melanoma cell proliferation, and somatic Brg1 inactivation of the melanocyte lineage in mouse leads to loss of developing melanoblasts and the resulting animals lack pigmentation (Laurette et al., 2015; Marathe et al., 2017). Given the essential but differing roles of BRG1/PBAF and BPTF/NuRF in human melanoma cells *in vitro* and in the normal physiology of mouse melanocytes *in vivo*, we addressed their implication in melanoma *in vivo* using a genetically modified mouse model.

The results of this study are described in **Annexe 2** related to the following manuscript:

Patrick Laurette*, Sebastien COASSOLO* *et al.* (2019) **Chromatin remodellers Brg1 and Bptf are required for normal gene expression and progression of oncogenic Braf-driven mouse melanoma.** Cell Death & Differentiation.

Further evidence for the importance of BRG1 in melanoma comes from an shRNA dropout screen performed by Bossi *et al.* where BRG1 was shown to be essential for the growth of Patient Derived melanoma Xenograft (PDX) (Bossi et al., 2016). Interestingly, this screen also identified CHD3 and CHD4, the catalytic ATPase subunits of the NuRD complex, as essential genes for PDX growth. Our previous analysis of the MITF interactome in 501Mel melanoma cells also identified peptides for the CHD4, MTA1, MTA2 and HDAC1/2 subunits of the transcriptional repressor NuRD. NuRD is an epigenetic regulator of gene expression acting in many contexts as a co-repressor that remodels chromatin through its ATPase subunits and deacetylates nucleosomes through its HDAC1 and HDAC2 subunits (Bracken, Brien, & Verrijzer, 2019a; Laugesen & Helin, 2014; McDonel, Costello, & Hendrich, 2009).

Thus we investigated how CHD3 and CHD4 define chromatin organization of melanoma cells.

The results of this study are described in **Article 1** related to the following manuscript:

Sebastien COASSOLO, Patrick LAURETTE *et al.* (Unpublished) **CHD3 and CHD4-containing NuRD complexes are essential in melanoma cells and act as co-factors for SOX10 and RREB1-regulated transcription.**

The dramatic effect of CHD4 silencing on the clonogenic capacity, the proliferation and the morphology of melanoma cells prompted us to investigate how CHD4 regulates such essential functions in cancer cells.

The results of this study are described in **Article 2** related to the following manuscript:

Sebastien COASSOLO, Guillaume DAVIDSON *et al.* (Submitted) **CHD4 regulates PADI1 and PADI3 expression linking pyruvate kinase M2 citrullination to glycolysis and proliferation.**

The original submitted version is available in **Annexe 3**

ARTICLE 1

Unpublished

CHD3 and CHD4-containing NuRD complexes are essential in melanoma cells and act as co-factors for SOX10 and RREB1-regulated transcription.

Sebastien Coassolo, Patrick Laurette, Guillaume Davidson and Irwin Davidson.

Results

Defining the SOX10 interactome.

We had previously noted the presence of CHD4 and other NuRD subunits in the MITF interactome (Laurette et al., 2015). Considering that much of the essential role of BRG1 in melanoma can be ascribed to its activity as a cofactor for MITF and SOX10, we further investigated the SOX10 interactome. To identify proteins interacting with SOX10 we performed tandem affinity purification and mass-spectrometry as previously described for the MITF interactome (Strub et al., 2011) using a 501Mel cell line stably expressing Flag-HA-tagged (F-H-)SOX10. Tandem immunopurification of the cytoplasmic, soluble nuclear and chromatin associated fractions was performed along with the equivalent fractions from native 501Mel cells. The immunoprecipitates (IP) from the F-H-SOX10 cells comprised a complex mix of proteins (Fig. S1A). Mass-spectrometry identified sets of proteins specifically present in these fractions (Dataset S1).

Multiple subunits of the BAF and PBAF complexes associated with SOX10 in the soluble nuclear and chromatin-associated fractions (Fig. S1B) including both the BRG1 and BRM catalytic subunits, PBAF-specific subunits, PBRM1 and ARID2, as well as BAF-specific subunits, ARID1A and ARID1B. Mass-spectrometry also identified the BPTF, SMARCA1, SMARCA5, RBBP7 and RBBP4 subunits of the NURF complex (Fig. S1B). The interaction of SOX10 with the BAF, PBAF and NURF complexes was confirmed by immunoblot of an independent tandem IP where co-precipitation of BRM, BRG1, ARID1A, ARID2, SMARCB1, SMARCD2, SMARCE1 and SMARCA5 with F-H-SOX10 was seen in the soluble nuclear and chromatin fractions (Fig. S1C).

Many of the additional proteins interacting with SOX10 were also previously shown to interact with MITF (Strub et al., 2011). For example, SOX10 associated with CTNNB1 both in the cytoplasm and on chromatin suggesting that like MITF (Alexander Schepsky et al., 2006), SOX10 may use β-catenin as a cofactor as described in hepatocellular carcinoma (Zhou et al., 2014). Similarly, multiple proteins involved in DNA repair and the ubiquitin cycle such as USP7, the Pol III, the transcription factor TFIIIC, cohesion complex subunits or the Mini-Chromosome Maintenance (MCM) complex also associated with SOX10. In contrast, several

potential cofactors were shown to selectively associate with SOX10 such as the NONO-SFPQ complex (Chaoui et al., 2015), subunits of the Five Friends of Methylated Chtop (5FMC) complex (Fanis et al., 2012), the ILF2-ILF3 complex, and SON (J.-H. Kim et al., 2016). We therefore defined a SOX10 interactome in melanoma cells comprising a variety of chromatin remodelling complexes and potential co-factors.

MITF and SOX10 interact with the NuRD complex.

In addition to the above, multiple subunits of the NuRD chromatin remodelling and co-repressor complex were also detected in the F-H-SOX10 fractions. The ATPase subunits CHD3 and CHD4 were detected along with MTA1/2, RBBP4/7, HDAC1/2, MBD2/3 and GATAD2A/B (Fig. 1A). In our previous analysis of the MITF-interactome (Laurette et al., 2015), we noted the presence of peptides for CHD4, MTA1/2 and HDAC1/2, while no peptides for CHD3 or the MBD subunits were observed and only a single peptide for GATAD2B was seen (Fig. 1A). Nevertheless, we examined more closely the potential interactions of MITF and SOX10 with NuRD.

IP of CHD4 from 501Mel cell extracts precipitated CHD4, MTA1, MBD2 and MITF, but not CHD3 (Fig. 1B). IP of CHD3 precipitated CHD3, but not CHD4 or MITF (Fig. 1B and C). However, SOX10 was precipitated in both CHD3 and CHD4 IPs, but not in control IP (Fig. 1C). CHD3 and CHD4 were not co-precipitated and therefore are mutually exclusive in distinct NuRD complexes. Both complexes associate with SOX10 whereas MITF associates only with CHD4/NuRD complex in agreement with the mass-spectrometry datasets (Fig. 1A).

To confirm the MITF-CHD4 interaction, 501Mel cells were transfected with vectors encoding GST-tagged MITF or GST. Cell extracts were prepared and captured on glutathione agarose. Using this approach, endogenous CHD4 but not CHD3 were captured by GST-MITF (Fig. 1D). The association was optimal at 300 mM KCL but remained stable at higher ionic strength (Fig. 1E). These experiments confirmed a selective interaction of MITF with CHD4.

Further evidence for the implication of NuRD and in particular the CHD4 subunit came from mining of public data sets. Examination of the TCGA melanoma datasets showed that both CHD3 and CHD4 are expressed at comparable levels in melanomas with different mutation status with a lower expression of CHD3 only seen in oncogenic NRAS melanomas (Fig. S2A). In the Badal dataset (Badal, Solovyov,

Di Cecilia, et al., 2017) CHD4 but not CHD3 is up-regulated upon the transition from benign nevi to metastatic melanoma (Fig. S2B). Analyses of single cell data from Tirosh (Tirosh et al., 2016) showed that while CHD3 expression was weaker in melanoma tumour cells compared to the infiltrating B and T lymphocytes, CHD4 expression was higher in melanoma tumours (Fig. S2C). Those data show that both CHD3 and CHD4 are expressed in melanoma with CHD4 showing the highest expression and up-regulation during tumour progression. Surprisingly *in vitro*, both CHD3 and CHD4 expressions are strongly downregulated in melanoma cells bearing a so called “mesenchymal” gene signature while both ATPases are normally expressed in “melanocytic” cells (Fig S2D).

Genomic co-localisation of CHD4 with MITF and SOX10.

Given the physical association of SOX10 and MITF with CHD3 and/or CHD4, we performed CHD3 and CHD4 ChIP-seq to define where they localize on the 501Mel cell genome and whether they co-localize with MITF and SOX10. We were unable to ChIP CHD3, but CHD4 ChIP-seq allowed us to identify more than 60’000 binding sites distributed over the genome with enrichment at the proximal promoter and transcription start sites (TSS) (Fig. 2A). A large proportion of CHD4 binding sites also overlapped with those bound by BRG1 (Fig. 2B, Laurette et al., 2015). Extensive SOX10, MITF and BRG1 genomic co-localization was previously shown (Laurette et al., 2015). Read density heat maps aligned on the 16’000 MITF-occupied sites indicated that CHD4 flanked the subset of MITF binding sites that co-localized with SOX10 but not the other MITF sites (Fig. 2C). Read density heat maps aligned on the 6’000 SOX10 sites as reference indicated that the vast majority of SOX10 binding sites were flanked by CHD4 either strongly (clusters A-C), less strongly (cluster D) or with only trace signal (cluster E) (Fig. 2D). Clusters A and C also showed strong H3K27 acetylation indicating they were active SOX10/MITF bound regulatory elements as previously described (Laurette et al., 2019). It is also striking to note that a majority of CHD4 bound nucleosomes were also bound by BRG1. We therefore identified a set of SOX10 binding sites with or without strong MITF occupancy that were flanked by nucleosomes bound by BRG1 or CHD4, a subset of which were also strongly labelled by H3K27ac. As CHD4 localized only at sites with SOX10 and not at sites where only MITF was bound we could conclude that SOX10 is determinant in CHD4 recruitment.

CHD3 and CHD4 are required for normal melanoma cell proliferation, but regulate distinct gene expression programs.

To address CHD3 and CHD4 functions we performed RNA silencing in a collection of melanoma cell lines. Silencing was specific for each subunit as measured by RT-qPCR and confirmed by immunoblot (Fig. 3A-B). CHD4 silencing led to an upregulation of CHD3 protein levels suggesting that both subunits compete for assembly in NuRD. Loss of CHD3 also mildly reduced MITF expression whereas SOX10 expression remained unchanged (Fig. 3B). Either of the CHD3 and CHD4 silencing led to a strong reduction of the clonogenic capacity of 501Mel and MM117 cells (Fig. 3C). Similar effect was observed in 3 different melanoma cells lines with a marked increase in the number of slow or non-proliferating cells. Although the effects were less dramatic than seen upon MITF silencing that induces cell cycle arrest and senescence (Fig. 3D). Silenced cells displayed a pronounced change in morphology with CHD3 silencing leading to a rounder and more flattened shape in 501Mel and MM117 cells (Fig. 3E and Fig. S3) and a more bipolar shape with cytoplasmic projections in Sk-Mel-28 cells (Fig. S3). CHD4 silencing led to cytoskeleton reorganisation with multiple cytoplasmic projections in 501Mel cells and to frequent bi-nucleate cells indicative of defective mitosis together with morphological changes in MM117 and Sk-Mel-28 cells. Nevertheless, CHD3 and CHD4 silencing did not induce apoptosis nor senescence (Fig. 3F). These data showed that both CHD3 and CHD4 are required for normal melanoma cell proliferation with their silencing leading to reorganised cell morphology and appearance of defective mitoses.

To identify the CHD3 and CHD4 regulated genes, we performed RNA-seq following their silencing in 501Mel cells. Consistent with the idea that CHD4/NuRD is a transcriptional repressor, CHD4 silencing up-regulated more than 1’000 genes with down-regulation of 364 genes (Fig. 4A-B and Dataset S2). In contrast, a similar number of genes were up or down-regulated by CHD3 silencing (Fig. 4A-B). Importantly, no statistically significant overlap of the two genes sets was observed. Ontology analyses (GSEA and David functional annotation and KEGG pathway, Dataset S2) of the genes de-regulated following CHD3 silencing revealed down-regulation of genes involved in cytokine signaling, PI3K/AKT signaling as well as a set of glycoproteins involved in cell adhesion (Fig. 4D). Up-regulated genes were

involved in Notch signaling, fatty acid metabolism, cell junction and pathways in cancer involving protein kinase signaling (Fig.4D). In contrast, the genes up-regulated by siCHD4 silencing revealed several highly enriched pathways. Indeed, a large set of cell membrane and extracellular proteins grouped under the terms apical surface, transmembrane and glycoprotein, and a collection of genes involved in RAS/MAP kinase signaling and genes regulated by STAT3 signaling are up-regulated after siCHD4 (Fig. 4C). In addition, CHD4 silencing up-regulated several cytokines and receptor tyrosine kinases (cytokine/cytokine receptor, adrenergic signaling), also under the later term a group of genes involved in calcium signaling and several ATPases including ATPases 1A3 and 1A4 (Fig. 4E). However, the down-regulated genes did not led to any significant enrichment in functional annotation of KEGG pathway, with only the term MYC targets, involved in cell cycle control, enriched in GSEA. The de-regulated expression of several genes was confirmed by RT-qPCR on independent RNA samples in both 501Mel and MM117 cells (Fig. 4F-G).

CHD3/4 co-regulate a subset of SOX10 repressed genes.

As CHD3/4 associate with MITF and/or SOX10 and at least CHD4 co-localizes with both on the genome, we investigated whether CHD3/4 act as co-repressors by comparing the genes de-regulated by the silencing of CHD3 and CHD4 with those regulated by MITF and SOX10. The genes regulated by MITF silencing in 501Mel cells were reported previously (Laurette et al., 2015; Strub et al., 2011). We did not find any significant overlap neither between genes regulated by MITF and those regulated by CHD4 with which it interacts, nor between genes regulated by both CHD3 and CHD4 (Fig. 5A). CHD3 and CHD4 do not therefore appear to act as co-repressors for MITF.

To make analogous comparisons with SOX10 regulated genes, we first performed RNA-seq following SOX10 silencing in 501Mel cells. As previously reported (J. C. Cronin et al., 2013; Shakhova et al., 2012) SOX10 silencing dramatically reduced cell proliferation, clonogenic capacity and strongly induced senescence in melanoma cells (Fig. 5B). RNA-seq data showed that SOX10 regulates positively or negatively more than 2’000 genes (Fig. 5D and Dataset S3). Ontology analyses showed that the down-regulated genes were strongly enriched in terms reflecting control of cell cycle and mitosis, whereas the upregulated genes

comprised many membrane-associated genes as well as multiple signaling pathways such as Wnt and Hippo (Fig. 5C). Many MITF regulated genes were similarly up- or downregulated by SOX10 silencing (Fig. 5D) reflecting the fact that MITF and SOX10 bind together to a large number of regulatory elements, and that SOX10 silencing also leads to loss of MITF expression (Laurette et al., 2015). In contrast, a large number of genes were only regulated by SOX10 and not by MITF. Further comparison of the SOX10 and the CHD3/4 up-regulated genes allowed to identify 274 co-regulated genes indicating that they act as co-repressors for a subset of SOX10-regulated genes, in particular genes that are not co-regulated by MITF (Fig. 5E). All together, these data indicate that despite their association CHD4 does not act as a cofactor for MITF. Moreover, CHD3/4 only co-regulate a small subset of SOX10 regulated genes.

CHD3 and CHD4 associate with the transcriptional repressor RREB1 and co-regulate a subset of its target genes.

The above data suggested that the major functions of CHD3/4 could not be ascribed to their function as co-factors for MITF or SOX10. To identify other transcription factors that may use CHD3/4 as cofactors, we analyzed the DNA-sequence motifs at the top 800 CHD4 bound sites. *De novo* motif discovery with MEME identified a sequence motif for transcription factor RREB1 (Ras Responsive Element Binding factor 1) enriched at these sites (Fig. 6A). We analyzed the same 800 sites with a previously described motif enrichment tool (S. Joshi et al., 2017) that allowed to identify more than 1’000 occurrences of the RREB1 binding motif, by far the most enriched motif at the 800 CHD4 bound sites (Fig. 6A). Further analyses of all CHD4 bound sites with FIMO identified around 75’000 occurrences of the RREB1 motif. RREB1 is a Kruppel-like zinc-finger transcription factor that positively or negatively regulates gene expression downstream of RAS and other signaling pathways (Flajollet, Poras, Carosella, & Moreau, 2009; Kent, Fox-Talbot, & Halushka, 2013; H. Liu et al., 2009; Melani, Simpson, Brugge, & Montell, 2008; Thiagalingam et al., 1996). The RREB1 locus is frequently amplified in melanoma and Fluorescence In Situ Hybridization (FISH) for this locus is used as part of a diagnostic tool for melanoma (Ferrara & De Vanna, 2016). Moreover, RREB1 was identified in a proteomics screen for HDAC interactors as a protein interacting with the NuRD subunits HDAC1 and HDAC2 (P. Joshi et al., 2014). Indeed, we co-precipitated

RREB1 with both CHD3 and CHD4 from melanoma cell extracts (Fig. 6B). The data we obtained indicate that RREB1 associates with CHD3 and CHD4 and likely recruits them to its binding sites in the genome although we could not fully confirm it, as the RREB1 antibodies were not ChIP-grade.

RREB1 silencing in melanoma cells resulted into strongly reduced cell proliferation with a consequent increase of senescent cells (Fig. 6C). In addition, this silencing led to altered flattened and spread cell morphology characteristic of senescence with multiple bi-nucleate cells (Fig. 6D). RREB1 looks therefore essential for normal melanoma cell proliferation. RNA-seq following RREB1 silencing identified 995 de-regulated genes a majority of which were up-regulated (Fig. 6F and Dataset S4). Up-regulated genes were enriched in several signaling pathways and in the apical junction category seen above in the CHD4 up-regulated genes (Fig. 6E and Dataset S4). Consistent with their association, a consequent subset of CHD3/4 regulated genes were also regulated by RREB1 particularly the CHD3 regulated genes (Fig. 6F).

All together, these data showed that CHD3/4 physically associates with RREB1 and co-regulates a subset of RREB1 target genes.

Methods

Cell culture, siRNA silencing and expression vector transfection.

Melanoma cell lines 501Mel and SK-Mel-28 were grown in RPMI 1640 medium supplemented with 10% foetal calf serum (FCS). MM074 and MM117 were grown in HAM-F10 medium supplemented with 10% FCS, 5.2 mM glutamax and 25 mM Hepes. Hermes-3A cell line was grown in RPMI 1640 medium (Sigma) supplemented with 10% FCS, 200 nM TPA, 200 pM cholera toxin, 10 ng/ml human stem cell factor (Invitrogen) and 10 nM endothelin-1 (Bachem).

SiRNA knockdown experiments were performed with the corresponding ON-TARGET-plus SMARTpools purchased from Dharmacon Inc. (Chicago, Il., USA). SiRNAs were transfected using Lipofectamine RNAiMax (Invitrogen, La Jolla, CA, USA) and cells were harvested after 72 hours. PADI1 and PADI3 expression vectors were transfected using X-tremeGENE™ 9 DNA Transfection Reagent (Sigma) for 48 hours. To assess clonogenic capacity cells were counted and seeded in 6 well plates for 7 to 15 days.

Generation of 501Mel cells stably expressing F-H-SOX10.

501Mel melanoma cells cultured in RPMI 1640 medium (Sigma, St Louis, MO, USA) supplemented with 10% FCS were transfected with a pCDH vector expressing Flag-HA-tagged human SOX10 and selected with puromycin (3 µg/ml) for several passages.

Proliferation, viability and senescence analyses by flow cytometry.

To assess proliferation after siRNA treatment cells were stained with Cell Trace Violet (Invitrogen) on the day of transfection. To assess cell viability cells were harvested 72 hours after siRNA transfection and stained with Annexin-V (Biolegend) following manufacturer instructions. To assess senescence cells were treated with Bafilomycin A (Sigma) for 1 hour and then with C_{12}FDG (Invitrogen) for 2 hours. Cells were analyzed on a LSRII Fortessa (BD Biosciences) and data were analyzed using Flowjo software.

Tandem immunoaffinity purification and mass-spectrometry.

For tandem immunoaffinity purification cells were lysed in hypotonic buffer (10 mM Tris-HCl at pH 7.65, 1.5 mM MgCl2, 10 mM KCl) and disrupted by dounce homogenisation. The cytosolic fraction was separated from the nuclei pellet by centrifugation at 4°C. The nuclear soluble fraction was obtained by incubation of the pellet in high salt buffer (final NaCl concentration of 300 mM) and then separated by centrifugation at 4°C. To obtain the chromatin fraction, the remaining pellet was digested with micrococcal nuclease and sonicated. Tagged-SOX10 was immunoprecipitated with anti-Flag M2-agarose (Sigma), washed and eluted with Flag peptide (0.5 mg/mL), further purified with anti-HA antibody-conjugated agarose (Sigma), washed and eluted with HA peptide (1 mg/mL). Samples were concentrated on Amicon Ultra 0.5 mL columns (cutoff: 10 kDa, Millipore), resolved by SDS-PAGE and stained using the Silver 7 Quest kit (Invitrogen). Mass-spectrometry was performed at the Taplin Biological Mass Spectrometry Facility (Harvard Medical School, Boston, MA, USA).

Protein extraction and Western blotting.

Whole cell extracts were prepared by the standard freeze-thaw technique using LSDB 500 buffer (500 mM KCl, 25 mM Tris at pH 7.9, 10% glycerol (v/v), 0.05% NP-40 (v/v), 16 mM DTT, and protease inhibitor cocktail). Cell lysates were subjected to SDS–polyacrylamide gel electrophoresis (SDS-PAGE) and proteins were transferred onto a nitrocellulose membrane. Membranes were incubated with primary antibodies in 5% dry fat milk and 0.01% Tween-20 overnight at 4 °C. Membranes were then incubated with HRP-conjugated secondary antibody (Jackson Immuno Research) for 1 hour at room temperature and visualized using the ECL detection system (GE Healthcare).

Immunofluorescence.

Staining was performed following a standard IF protocol. Briefly, cells were washed with PBS, fixed in freshly prepared 4% paraformaldehyde (PFA) for 10 min at RT and permeabilized with PBS 0.1% Triton X-100 at RT. Blocking (RT for 20 min) and incubations with antibodies (RT for 1 hour) were performed with 10% heat-inactivated FCS in PBS/0.1%Triton X-100 and washes were done with PBS/0.1% Triton X-100 at RT. Nuclei were counterstained with freshly prepared 1 µg/mL DAPI in PBS for 2 min at RT and cells were mounted using the ProLong Gold antifade reagent of Molecular Probes.

Chromatin immunoprecipitation and sequencing.

CHD4 ChIP experiments were performed on 0.4% paraformaldehyde fixed and sonicated chromatin isolated from 501Mel cells according to standard protocols as previously described (Strub et al., 2011). MicroPlex Library Preparation kit v2 was used for ChIP-seq library preparation. The libraries were sequenced on Illumina Hiseq 4000 sequencer as Single-Read 50 base reads following Illumina's instructions. Sequenced reads were mapped to the Homo Sapiens genome assembly hg19 using Bowtie with the following arguments: -m 1 --strata --best -y -S -l 40 -p 2. After sequencing peak detection was performed using the MACS software ((Yong Zhang et al., 2008), http:// liulab.dfci.harvard.edu/MACS/). Peaks were annotated with Homer using the GTF from ENSEMBL v75. Peak intersections were computed using bedtools and Global Clustering was done using seqMINER (http://homer.salk.edu/homer/ngs/annotation.html). *De novo* motif discovery was

performed using the MEME suite (meme-suite.org). Motif enrichment analyses were performed using in house algorithms based on FIMO as previously described (S. Joshi et al., 2017).

RNA preparation, quantitative PCR and RNA-seq analysis.

RNA isolation was performed according to standard procedure (Qiagen kit). qRT-PCR was carried out with SYBR Green I (Qiagen) and Multiscribe Reverse Transcriptase (Invitrogen) and monitored using a LightCycler 480 (Roche). RPLP0 gene expression was used to normalize the results. Primer sequences for each cDNA were designed using Primer3 software and are available upon request. RNA-seq was essentially performed as previously described (Laurette et al., 2019). Gene ontology analyses were performed with the Gene Set Enrichment Analysis software GSEA v3.0 using the hallmark gene sets of the Molecular Signatures Database v6.2 and the functional annotation clustering function of DAVID.

Figure legends

Figure 1. Association of MITF and SOX10 with NuRD. A. Number of PSMs for the different NuRD subunits found in the MITF and SOX10 interactomes. **B**. Immunoblots showing results of immunoprecipitations against CHD3 or CHD4 from 501Mel cell extracts. The detected proteins are indicated. **C**. Co-precipitation of SOX10 with CHD3 and CHD4. **D** and **E**. Extracts from cells transfected with GST-MITF expression and captured on GST-agarose. The eluted proteins were detected with antibodies against GST, CHD3 or CHD4. Agarose beads were washed with the indicated KCl concentrations (mM) before elution and detection on immunoblot.

Figure 2. Genomics colocalization of CHD4 with MITF and SOX10. A. Genomic distribution of CHD4 bound sites. **B.** Venn diagrams showing overlap between CHD4 and BRG1. **C**. Read density maps of the indicated factors at the 16763 MITF occupied sites in 501Mel cells. **D.** Read density maps of the indicated factors at the 5997 SOX10 occupied sites in 501Mel cells. Lower panel schematizes binding of BRG1 and CHD4 on nucleosomes surrounding the MITF and SOX10 bound regulatory elements.

Figure 3. CHD3 and CHD4 are required for normal melanoma cell proliferation. A-B. 501Mel cells were transfected with the indicated siRNAs. The CHD3 and CHD4 expression was evaluated by RT-qPCR or immunoblot along with that of MITF and SOX10. **C**. The indicated cell lines were transfected with siRNA. After reseeding the number of colonies was counted after 15 days. **D**. The indicated cell lines were transfected with siRNAs. Cell proliferation was evaluated by cell trace violet assay. **E**. Cells transfected with siRNAs were immunostained with antibody against β-tubulin and nuclei counterstained with DAPI (magnification x200). **F**. The indicated cell lines were transfected with siRNA. Apoptosis was detected by FACs after labelling with Annexin-V. For all experiments: n=3, statistical unpaired t-tests analyses were performed by Prism 5 with a confidence interval of 95%.
*P-values: *= p<0.05; **= p<0.01; ***= p<0.001.*

Figure 4. CHD3 and CHD4 regulate distinct gene expression programs. A-B. RNA-seq was performed on triplicate samples of 501Mel cells after siRNA transfection. Genes up or down-regulated based on Log2 fold-change >1/<-1 with an adjusted p-value <0.05 were identified. Venn diagrams show an overlap between the CHD3 and CHD4 regulated genes along with the hypergeometric probability Representation Factor (RF) in this case non-significant. **C-D**. Ontology analyses of CHD3 and CHD4 regulated genes. The enrichment scores for GSEA are shown as well as the David functional enrichment and KEGG pathway categories. **E**. Examples of CHD4 up-regulated genes of the indicated categories. **F-G**. Verification of deregulated expression of the selected indicated genes in independent RNA samples from 501Mel or MM117 cells.

Figure 5. CHD3 and CHD4 do not appear to act as cofactors for MITF. A. Venn diagrams showing the overlap between MITF regulated genes and those regulated collectively by CHD3 and CHD4 with a non-significant hypergeometric Representation Factor (RF). **B.** Number of slow proliferating and senescent cells following SOX10 silencing. **C**. Ontology of SOX10 regulated genes analyzed by GSEA, David functional enrichment and KEGG pathway. **D.** Venn diagrams showing overlap between MITF and SOX10 regulated genes with a significant hypergeometric Representation Factor (RF). **E**. Venn diagrams showing overlap between SOX10 and

CHD3/4 regulated genes with a weakly significant hypergeometric Representation Factor (RF).

Figure 6. CHD4 acts as a cofactor for RREB1. A. The RREB1 binding motif defined by JASPAR is strongly enriched at the top 800 CHD4 binding sites as detected by MEME and a motif enrichment algorithm. **B**. Immunoblot showing co-precipitation of endogenous RREB1 with CHD3 and CHD4 under the indicated KCl concentrations (mM). **C**. SiRNA mediated RREB1 silencing induces slowed cell growth and senescence. In all experiments: n=3, statistical unpaired t-tests analyses were performed by Prism 5 with a confidence interval of 95%. *P-values:* ***= *p<0.001.* **D.** SiRNA mediated RREB1 silencing leads to altered cell morphology showed by staining with antibody to β-tubulin and counterstaining of nuclei with DAPI (magnification x200). **E.** Ontology analyses of RREB1 regulated genes. The enrichment scores for GSEA are shown as well as the David functional enrichment and KEGG pathway categories. **F.** Venn diagrams show overlap between RREB1 and CHD3 and between RREB1 and CHD4 regulated genes along with the significant hypergeometric probability Representation Factor (RF).

Legends to Supplementary Figures and Tables.

Supplementary Figure 1. The SOX10 interactome. A. Silver nitrate staining of an SDS PAGE gel showing the proteins precipitated from the chromatin-associated (Ch) soluble nuclear (Sn) and cytoplasmic (Cy) fraction of Flag-HA-SOX10 (FH) or native 501Mel (C) cells. **B**. Heatmap showing the number of peptides found in IPs from the indicated fractions of F-H-SOX10 cells. The identified proteins are grouped into known complexes and functions. **C**. Immunoblots verifying the specificity of the interactions of the indicated proteins in an independent series of tandem IPs from the indicated cells and fractions.

Supplementary Figure 2. CHD3 and CHD4 expression in melanoma. A. CHD3 and CHD4 expression in melanoma from the TCGA database carrying the indicated mutations. **B**. CHD3 and CHD4 expression in nevi and melanoma from the Badal *et al.* dataset. **C**. CHD3 and CHD4 expression in melanoma cells and infiltrating immune cells in three analyzed tumors of the Tirosh *et al*. dataset. D. Immunoblot

showing CHD3 and CHD4 expression in “melanocytic” versus “mesenchymal” melanoma cell lines.

Supplementary Figure 3. CHD3 and CHD4 silencing impacts melanoma cell morphology. Each panel shows phase contrast microscopy of the indicated cells lines after CHD3 or CHD4 silencing (magnification x200).

Supplementary Dataset 1. The number of peptides detected for each protein in each fraction after tandem affinity immunoprecipitation from F-H-SOX10 cells is indicated.

Supplementary Dataset 2. Summary of RNA-seq results following CHD3 or CHD4 silencing in 501Mel cells. Gene names, description fold change, p-values and adjusted p-values are shown. As indicated other pages on the spreadsheet show the ontology analyses of each gene set.

Supplementary Dataset 3. Summary of RNA-seq results following SOX10 silencing. In 501Mel cells. Gene names, description, fold change, p-values and adjusted p-values are shown. As indicated other pages on the spreadsheet show the ontology analyses of each gene set.

Supplementary Dataset 4. Summary of RNA-seq results following RREB1 silencing. In 501Mel cells. Gene names, description, fold change, p-values and adjusted p-values are shown. As indicated other pages on the spreadsheet show the ontology analyses of each gene set.

A

Subunit	Peptides MITF	Peptides SOX10
CHD3	0	19
CHD4	16	30
MTA1	3	12
MTA2	6	4
HDAC1	3	4
HDAC2	4	5
GATAD2A	0	1
GATAD2B	1	3
MBD2	0	2
MBD3	0	4

B

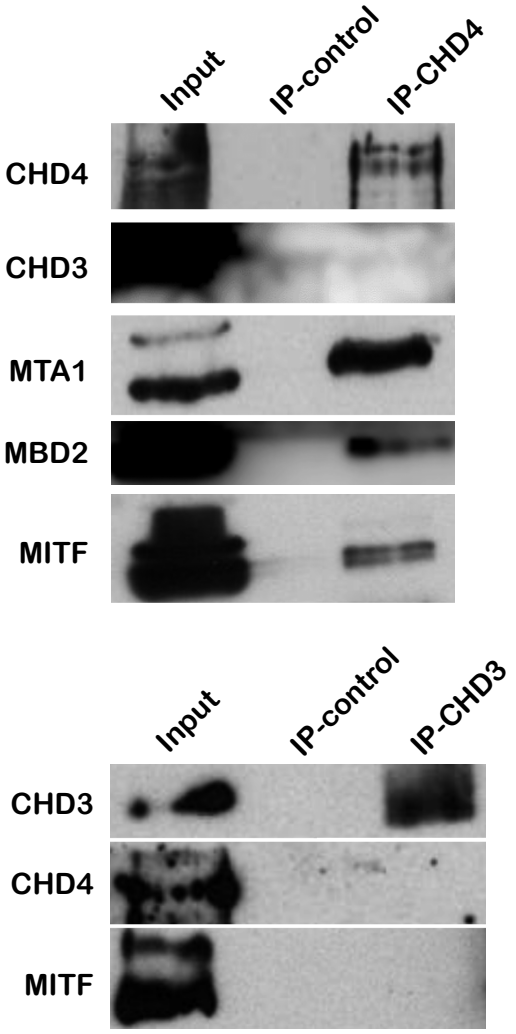

C

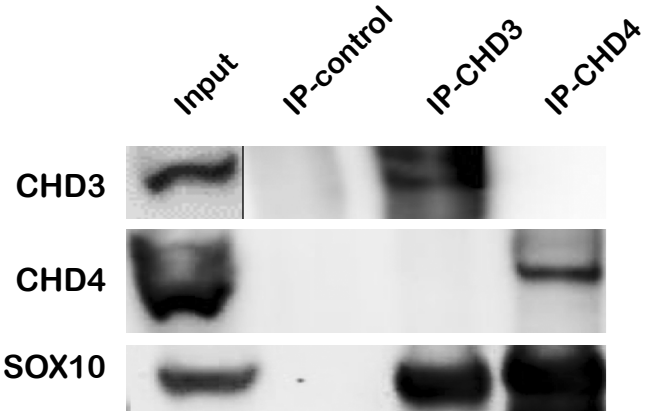

D

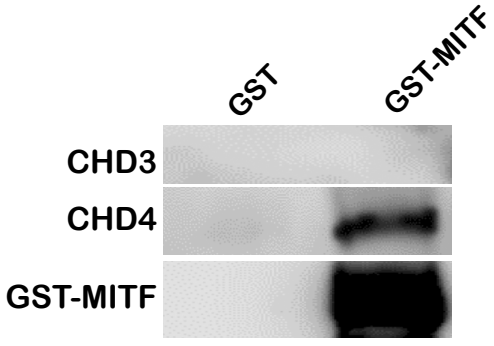

E

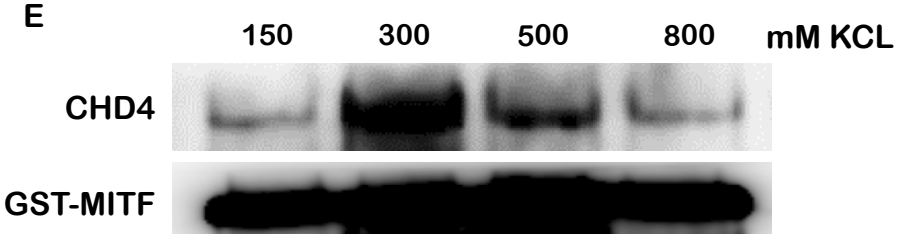

Coassolo et al., Figure 1

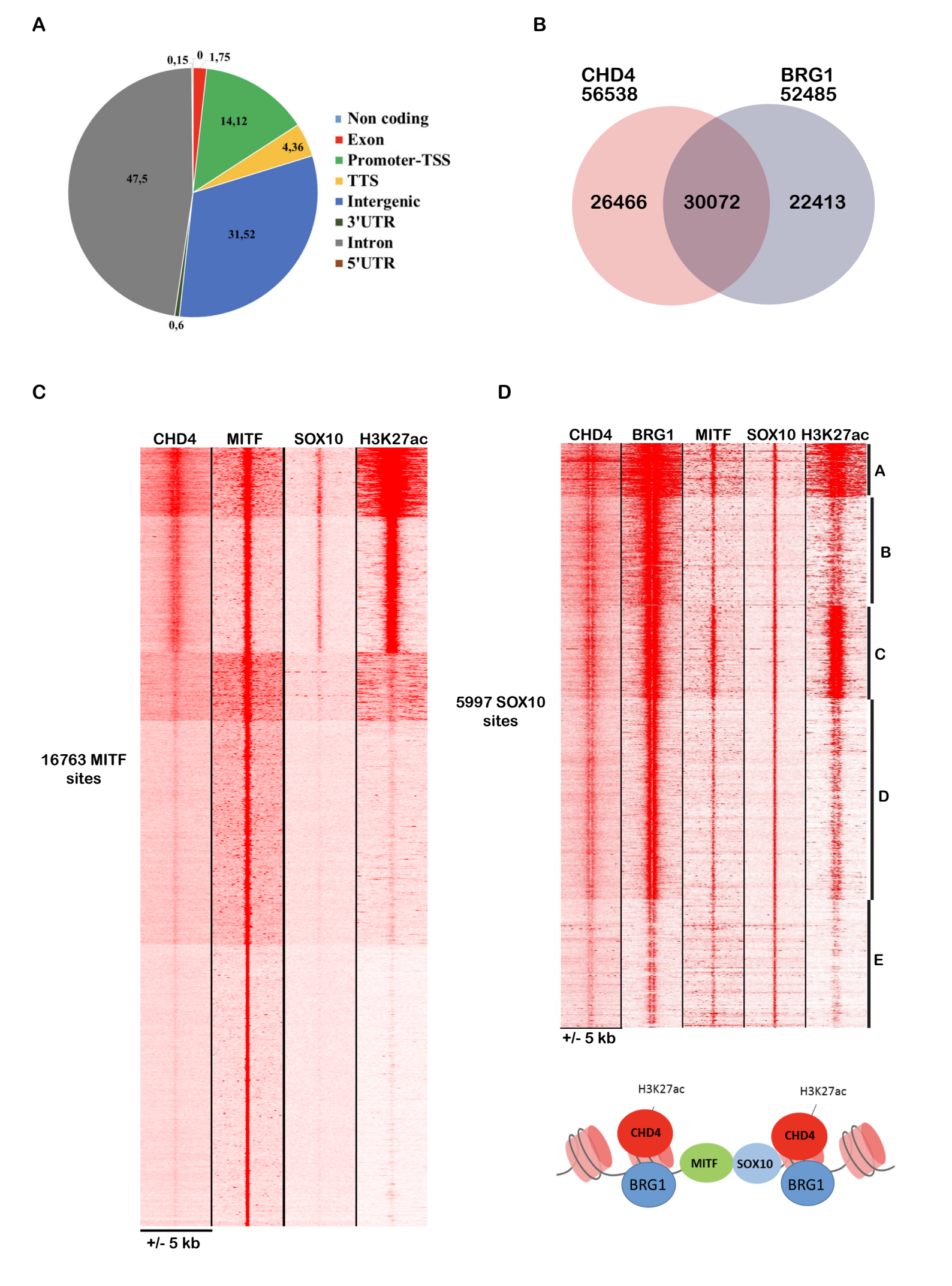

Coassolo et al., Figure 2

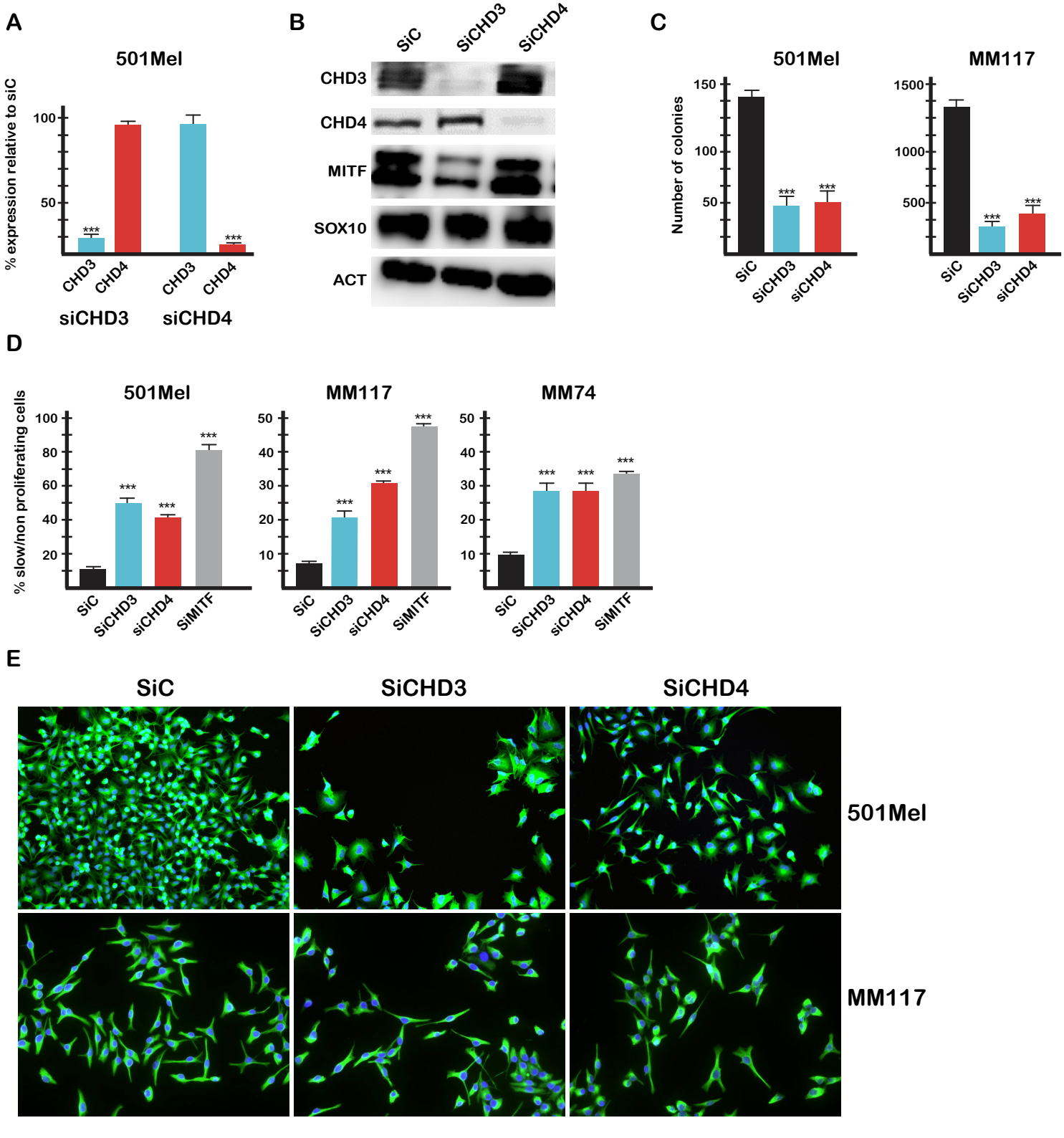

Coassolo et al., Figure 3

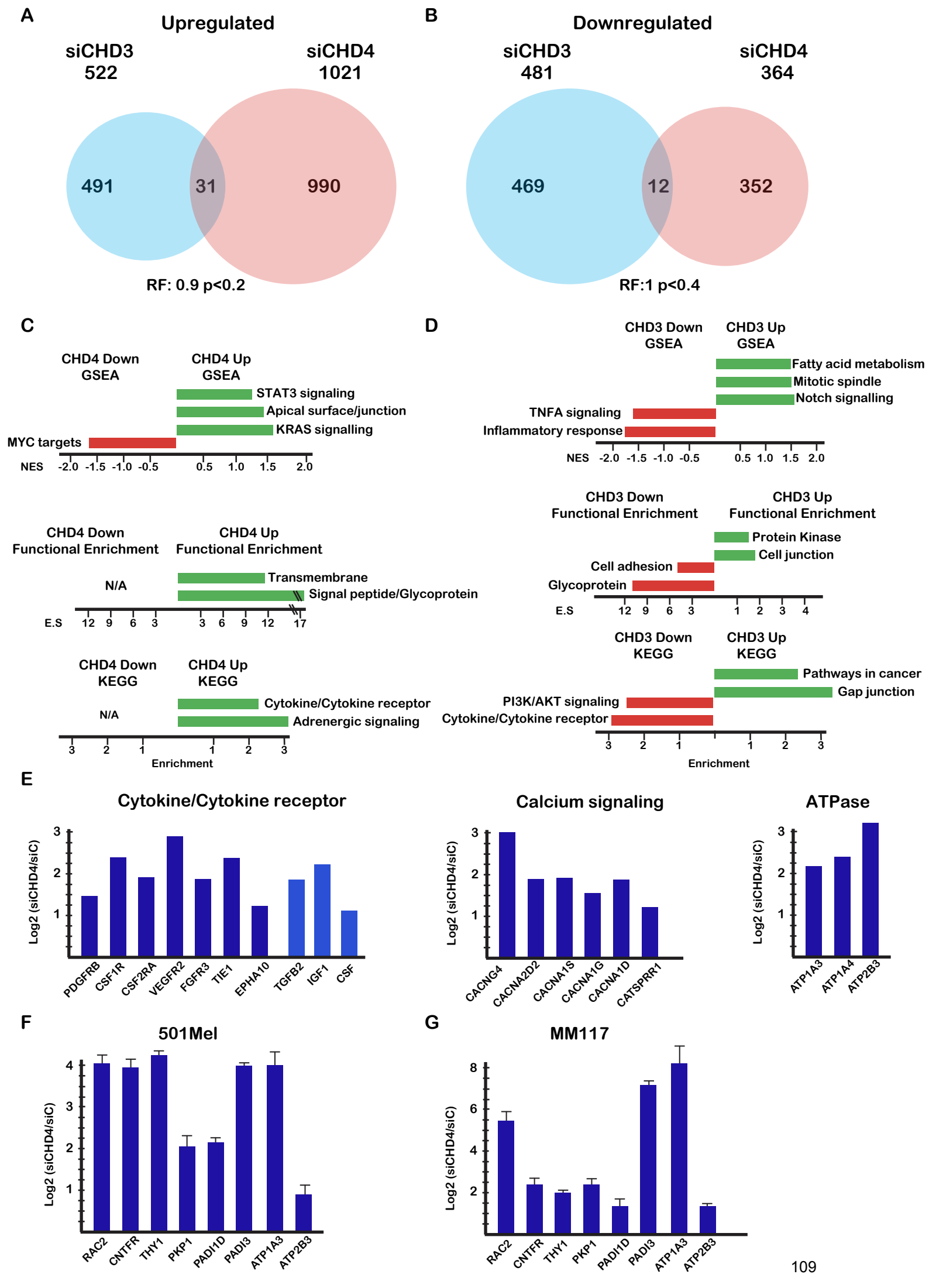

Coassolo et al., Figure 4

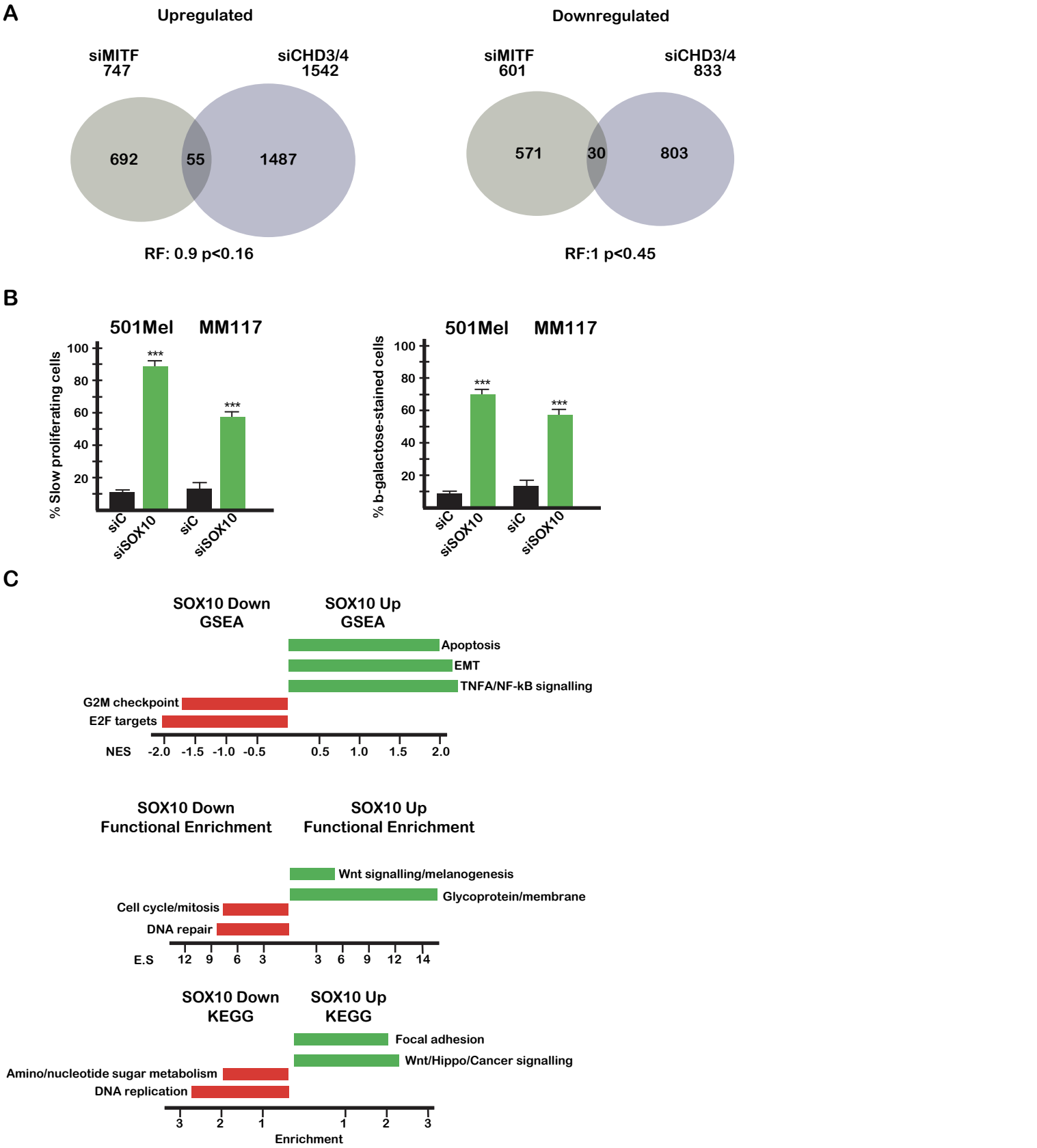

Coassolo et al., Figure 5

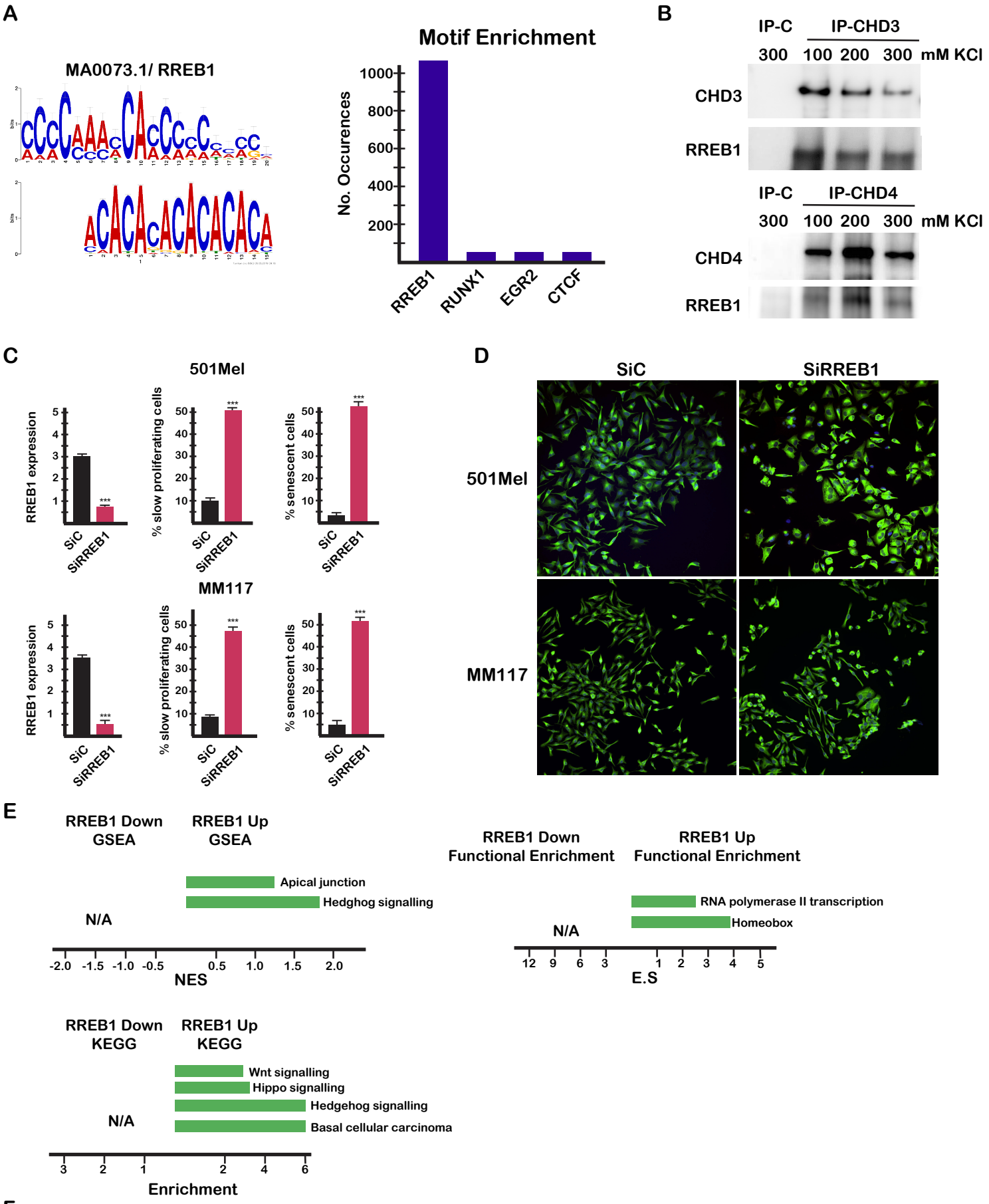

Coassolo et al., Figure 6

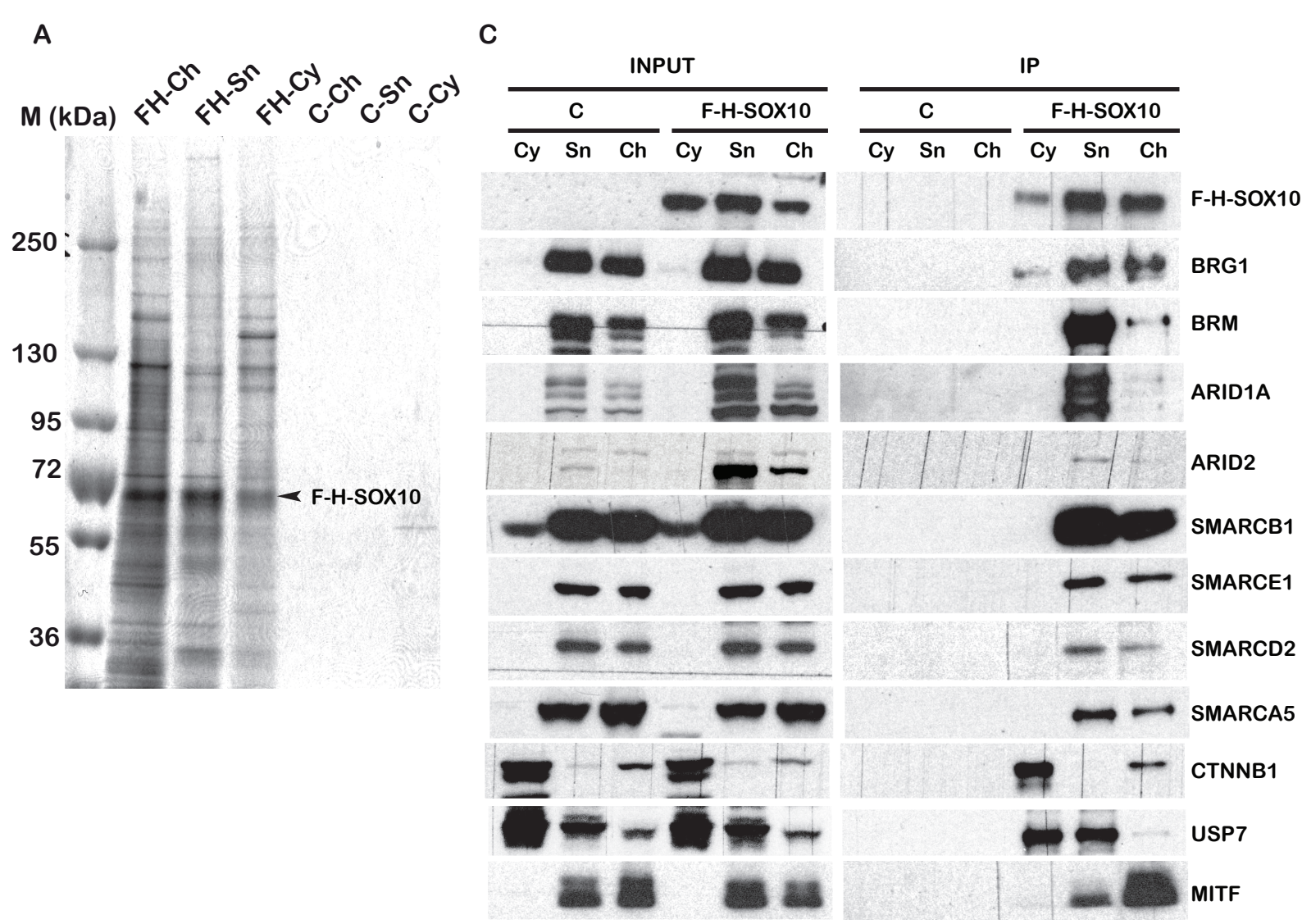

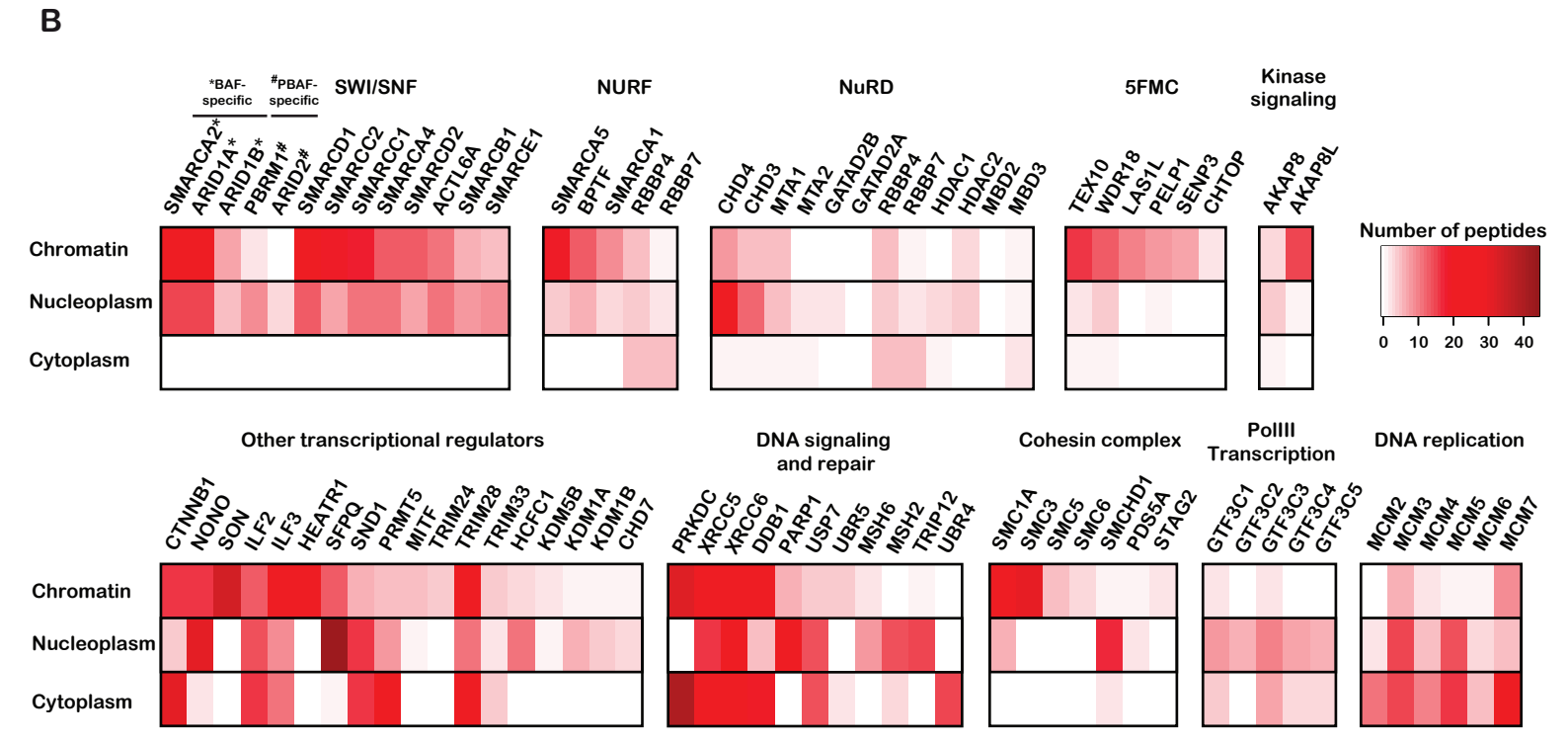

Coassolo et al., Figure S1

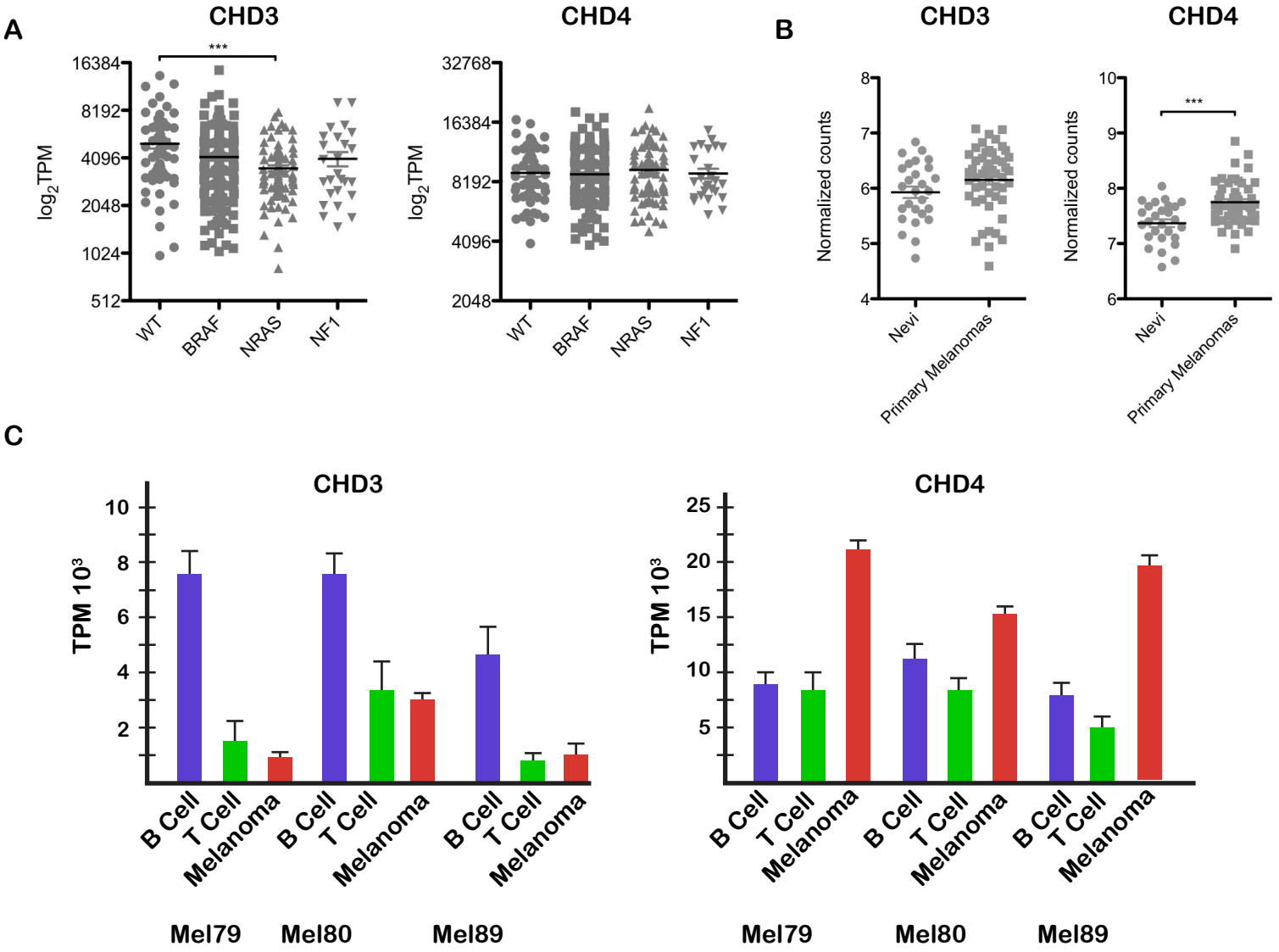

Coassolo et al., Figure S2

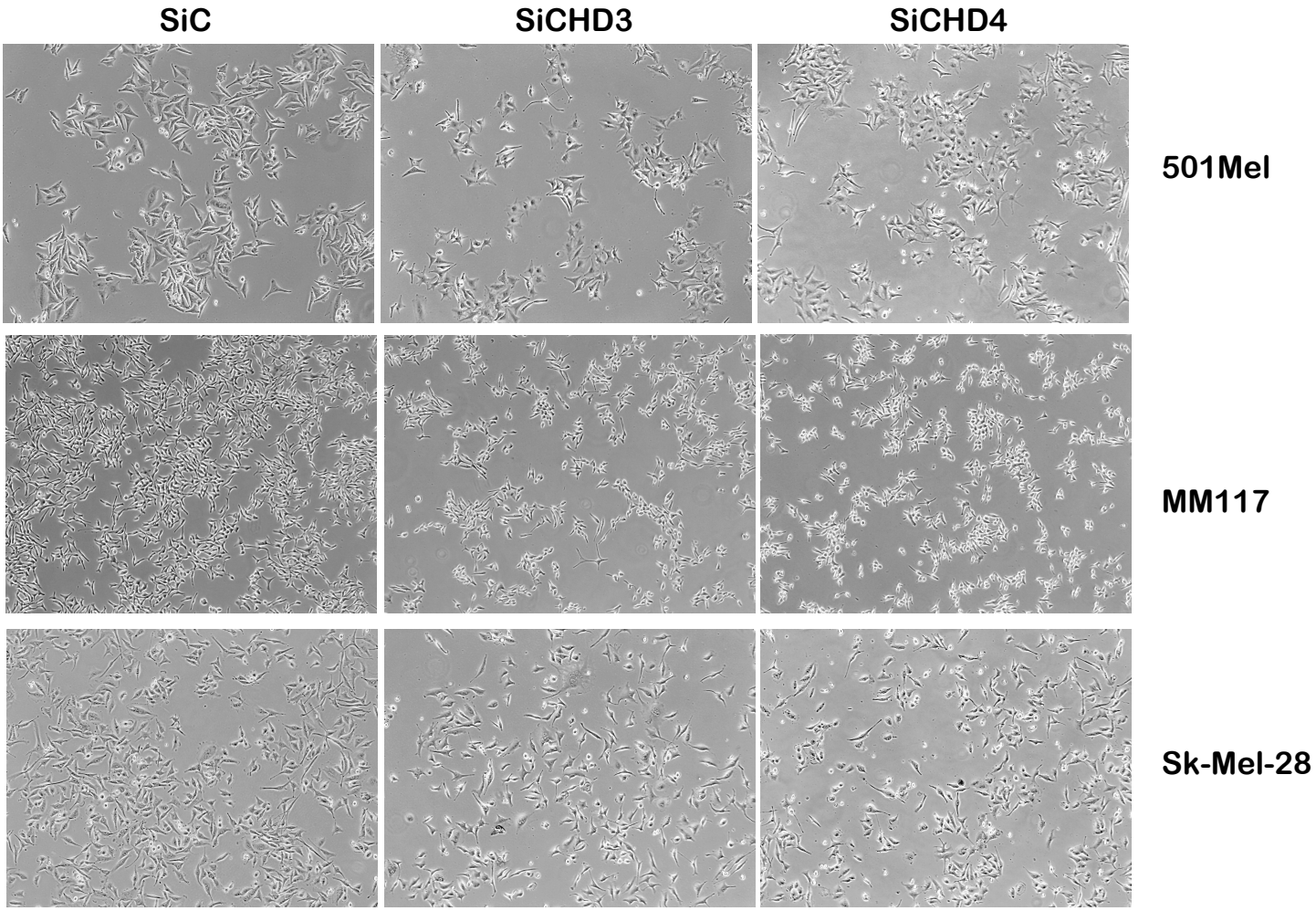

Coassolo et al., Figure S3

ARTICLE 2

Submitted

Original submitted version available in **Annexe 3**

CHD4 regulates PADI1 and PADI3 expression linking pyruvate kinase M2 citrullination to glycolysis and proliferation.

Sebastien Coassolo, Guillaume Davidson, Luc Negroni, Giovanni Gambi, Sylvian Daujat, Christophe Romier and Irwin Davidson.

Results

CHD4 regulates MAP kinase signaling and glycolysis.

The observations that CHD4 silencing regulates genes associated with RAS signaling and up-regulates a set of growth factors and receptor tyrosine kinases (Article 1,Fig. 4C-D), some of which being co-regulated by RREB1 (Article 1,Fig. 6F), led us to investigate whether CHD4 silencing modulates the MAP-kinase signaling.

CHD4 silencing in 3 melanoma cell lines resulted in a strong increase in phospho-ERK1/2 while no activation of the AKT signaling was seen (Fig. 1A). MAP-kinase signaling can activate several downstream pathways amongst which mTOR. We observed that mTOR S2448 phosphorylation concomitantly increased with that of phospho-ERK1/2 after siCHD4 (Fig. 1A). mTOR activation can stimulate glycolysis, a critical source of energy in cancer cells. To elucidate whether CHD4 silencing alters glycolysis we profiled melanoma cell metabolism in real time using the Seahorse instrument. The measured metabolic parameters of several melanoma cell lines showed that CHD4 silencing increases the basal OCR (Oxygen Consumption Rate) and ECAR (Extracellular Acidification Rate) and also markedly increased maximum OCR and ECAR (Fig. 1B-D). The Increased ECAR was blocked using 2-deoxy-D-glucose (2-DG) confirming that the higher acidification was due to increased glycolysis (Fig. 1D). CHD4 silencing decreased the OCR/ECAR ratio due to the increased ECAR values. However, the mitochondrial metabolism might be affected as observed by the increase of basal OCR and the ROS lipid peroxidation product 4-hydroxy-2-nonenal (HNE) after siCHD4 (Fig.1E) (Breitzig, Bhimineni, Lockey, & Kolliputi, 2016).

Increased glycolysis and lactic acid production diverts pyruvate from oxidative metabolism that generates more ATP per glucose molecule. In agreement with this, CHD4 silencing led to decreased intracellular ATP levels and increased phosphorylation of the ATP/ADP sensor AMPK (Fig. 1A). Hence, the decreased cell proliferation seen upon CHD4 silencing can be at least partially accounted for by hyper-activation of the glycolytic pathway leading to reduced overall ATP production. Such increased glycolysis can also deplete cells from metabolite intermediates produced during this process that are necessary for synthesis of amino acids, lipids

and nucleotides further accounting for diminished proliferation (Icard, Fournel, Wu, Alifano, & Lincet, 2019).

CHD4 regulates expression of the PADI1 and PADI3 enzymes that citrullinate PKM2.

While activation of MAP-kinase and mTOR may contribute to increased glycolysis, we identified an additional pathway that strongly regulates glycolysis. Amongst the genes potently up-regulated by CHD4 silencing are *PADI1* (Protein Arginine Deiminase 1) and *PADI3* encoding enzymes that convert arginine to citrulline (Bicker & Thompson, 2013) (Fig S1A). In all tested melanoma lines, the expression of PADI3 was almost undetectable and potently activated by CHD4 silencing, whereas PADI1 had a low basal level that were also strongly increased by CHD4 silencing (Fig. S1B). Increased PADI1 and PADI3 protein levels were also seen following CHD4 silencing (Fig. S1C).

The genes encoding the PADI enzymes cluster together with *PADI1* and *PADI3* located next to each other (Fig. S1D). ChIP-seq in melanoma cells revealed that CHD4 binds together with transcription factors CTCF and FOSL2 (AP1) to an intronic regulatory element in *PADI1* that is predicted to regulate both the *PADI1* and *PADI3* genes (Fig. S1D). This element is marked by H2AZ, H3K4me1, BRG1 and ATAC-seq for open chromatin, but not by the lineage specific transcription factors MITF and SOX10.

To identify potential substrates of these enzymes in melanoma cells, we prepared protein extracts from siC and siCHD4 cells, performed IP with a pan-citrulline antibody and analyzed the precipitated proteins by mass-spectrometry (Fig. 2A). Following CHD4 silencing, an increased total number of Peptide Spectral Matches (PSMs) and PSMs for citrullinated peptides were detected for a set of predominantly cytoplasmic proteins including tubulins, multiple 14-3-3 proteins and enzymes of the glycolytic pathway PFKP, HK1/2, GAPDH, ALDOA/C, ENO1/2 and PKM2 (Fig. 2B-D and Dataset S1).

We focused our attention on PKM2, a highly regulated enzyme playing a central role in the control of glycolysis. PKM2 converts Phospho-Enol-Pyruvate (PEP) into pyruvate that can then be converted to lactic acid.

To confirm the increased PKM2 citrullination, melanoma cells were transfected with siC, siCHD4 or PADI1 and PADI3 expression vectors to ectopically express the

enzymes (Fig. 2E). The resulting cell extracts were precipitated with pan-citrulline antibody and the precipitated PKM2 assessed by immunoblot. CHD4 silencing or PADI1 and PADI3 expression did not affect overall PKM2 levels compared to cells transfected with siC or empty expression vector (EV, Fig. 2F). However, after pan-citrulline IP, strongly increased amounts of PKM2 were observed following siCHD4 compared to siC in both 501Mel and MM117 cells (Fig. 2G). Furthermore, increased amounts of PKM2 were also recovered after expression of PADI1 and PADI3 and particularly upon expression of both enzymes (Fig. 2H). These data show that PADI1 and PADI3 strongly stimulate PKM2 citrullination.

PADI1 and PADI3 are necessary and sufficient for increased glycolytic flux.

We next investigated if PADI1 and PADI3 expression alters glycolysis. The increased glycolysis seen upon CHD4 silencing was strongly reduced when PADI1 and PADI3 were additionally silenced (Fig. 3A). Moreover, exogenous expression of PADI1, PADI3 or both also stimulated glycolysis (Fig. 3B). PADI1 and PADI3 are therefore necessary and sufficient for increased glycolysis. Consistent with this observation, PADI1/3 expression led to reduced intracellular ATP levels, increased levels of phosphorylated AMPK and decreased cell proliferation (Fig. 3C). Analogous results were seen in a second melanoma cell line (Fig. 3D-F). These data showed that CHD4 silencing de-repressed PADI1 and PADI3 expression leading to increased citrullination of several enzymes of the glycolytic pathway in particular PKM2 one of the rate limiting enzymes thus leading to increased glycolytic flux.

Interestingly, ectopic PADI1/3 expression also induced activation of the MAPkinase pathway through ERK phosphorylation, suggesting that PADs induction by CHD4 silencing could partially regulates glycolysis via MAPkinase and mTOR pathway regulation (Fig.3 G).

It was previously shown that the treatment of melanoma cells with BRAF inhibitors involves metabolic reprogramming with strongly reduced glycolysis (Parmenter et al., 2014). Moreover, their dependence on glycolysis sensitizes melanoma cells to the effects of BRAF inhibition (Hardeman et al., 2017). Consistently, CHD4 silencing or ectopic PADI1/3 expression sensitized Sk-Mel-28 cells to the effects of the BRAF inhibitor Verumafenib (Fig.3H). Hence, by regulating

PADI1/3 expression and glycolysis, CHD4 modulates melanoma cell sensitivity to BRAF inhibition.

CHD4 regulates PADI1 and PADI3 expression and glycolysis in a variety of cancer cells.

As aforementioned, CHD4 may regulate PADI1/3 expression not via melanoma-specific factors but via the more ubiquitous CTCF and therefore, may also regulate PADI1/3 expression in non-melanoma cancer cells. CHD4 silencing in SiHa cervical carcinoma cells led to a strong reduction of their clonogenic capacity (Fig. S2A) as well as a potent increase of PADI3 expression, but did not affect basal PADI1 expression (Fig. S2B) and stimulated glycolysis (Fig. S2C-D). Moreover, glycolysis was increased by ectopic PADI1/3 expression that led to reduce the OCR/ECAR ratio and ATP levels (Fig. S2E-G).

In HeLa cells, CHD4 silencing also reduced their clonogenic capacity and both PADI1 and PADI3 expression were potently induced while glycolysis was stimulated by both CHD4 silencing and ectopic PADI1/3 expression (Fig. S2H-J).

Analogous results were observed in two renal carcinoma cell lines (Fig. S2K-R). CHD4 silencing potently induced both PADI1 and PADI3 expression and glycolysis was stimulated by both CHD4 silencing and ectopic PADI1/3 expression decreasing the clonogenic capacity and proliferation of those carcinoma cell lines (Fig. S2K-R).

Therefore, in all tested cell lines CHD4 silencing induced PADI1 and/or PADI3 expression and increased glycolysis that was also stimulated by ectopic PADI1/3 expression. CHD4 repression of PADI1/3 expression and citrullination represent therefore a more general mechanism for regulation of glycolysis and cell physiology in cancer cells.

Citrullination of arginines reprograms PKM2 allosteric regulation at a structural level.

In contrast to PKM1, PKM2 activity is positively regulated by serine (Ser), Fructose 1, 6-BiPhosphate (FBP) and SuccinylAminoImidazole-CarboxAmide Riboside (SAICAR) and negatively regulated by Tryptophan (Trp), Phenylalanine (Phe) and Alanine (Ala), thus coupling the glycolytic flux to the level of critical

intermediate metabolites (Chaneton et al., 2012; Christofk, Vander Heiden, Wu, et al., 2008; Kirstie E. Keller, 2012; O'Neill et al., 2013).

Allosteric regulation involves three distinct enzyme conformations (Fig. S3A). In the apo (resting) state and in the absence of any small molecules and ions, the PKM2 N-terminal and A domains adopt an active conformation, but the B domain remains in an inactive conformation. In the activated R-state, binding of FBP or Ser and magnesium stabilizes the N and A domains in their active conformation and rotates the B domain towards the A domain that together form the active site. In the inactive T-state, upon binding of inhibitors (Trp, Ala and Phe), the B domain retains an active conformation but the N and A domains undergo structural changes that prevent FBP binding and disorganize the active site. The structural changes observed between the different PKM2 states are reinforced allosterically by organisation into a tetramer that is essential for enzyme function.

In siCHD4 extracts, enhanced citrullination of 3 arginine residues, R106, R246 and R489 that play important roles in allosteric regulation of PKM2 was identified by mass-spectrometry due to their altered mass/charge ratio (Fig. 2C).

R489 is directly involved in FBP binding with bidentate interactions between its guanidino group and the FBP 1' phosphate group (Fig. S3B). Mutation of R489 was shown to prevent FBP binding and attenuate activation of PKM2 by FBP (Macpherson et al., 2019; Morgan et al., 2013). Therefore, loss of R489 side chain charge upon citrullination diminishes or potentially prevents FBP binding, reinforcing PKM2 allosteric regulation by the free amino acids.

In the apo state, R246 forms salt bridges between its guanidino group and the main chain carboxyl groups of V216 and L217 at the pivotal point where the B domain moves between its active and inactive conformations (Dombrauckas, Santarsiero, & Mesecar, 2005) (Fig. S3C). This interaction is not observed in the R- and T-states and hence contributes to maintaining the inactive B domain conformation in the apo state. R246 citrullination may strongly weaken or abolish the interaction with V216 and L217 facilitating the release of the B domain from its inactive conformation to form the active site.

R106 participates in the free amino acid binding pocket. In the apo state R106 mostly faces the solvent but upon free amino acid binding R106 rotates towards the pocket and its guanidino group interacts with the carboxylate group of the bound

amino acid and the main chain carbonyl of A domain P471 [(Chaneton et al., 2012; Morgan et al., 2013; Yuan et al., 2018)and Fig. 4A]. Ser binding increases the hydrogen bond network formed between the N and A domains thus stabilizing their active conformations, whereas upon Trp, Phe, or Ala binding their hydrophobic side chain causes displacement of the N-domain outwards, away from the A domain, leading to the allosteric changes that characterize the inactive T-state.

Transition between the R- and T-states is finely regulated by changes in the relative concentrations of Ser versus Trp, Ala and Phe that compete for binding to the pocket (Yuan et al., 2018). Loss of R106 positive side chain charge upon citrullination weakens its interaction with the free amino acids. We postulate that Ser binding is weakly affected due to its extended network of hydrogen bonds within the pocket and since it does not modify the active conformations of the N and A domains. In contrast, hydrophobic amino acids induce important structural changes within the N and A domains and hence their binding may be more affected by the weaker interaction with citrullinated R106. Consequently, R106 citrullination may lead to a change in the relatively affinity for Ser compared to Trp, Ala and Phe thereby weakening their inhibitory effect and reinforcing activation by Ser.

To verify the above hypothesis, we elucidated whether citrullination could bypass the requirement for Ser as an allosteric activator. On one hand, when cells were grown in the absence of Ser, basal glycolysis was reduced and no longer stimulated upon siCHD4 or PADI1/3 expression (Fig. 4B). On the other hand, exogenous Ser stimulated basal glycolysis was not further increased by siCHD4 (Fig. 4C). In contrast, in the presence of exogenous Trp, basal glycolysis was reduced but remained stimulated by siCHD4 and PADI1/3 expression (Fig. 4D). Similarly, glycolysis was stimulated by siCHD4 in the presence of increased Phe concentrations (Fig. 4E), an effect that was particularly visible in MM117 cells where basal glycolysis was strongly inhibited by Phe but still stimulated upon siCHD4 (Fig. 4F). PADI1/3 expression also stimulated glycolysis in presence of exogenous Ala (Fig. 4G).

PKM2 citrullination did not therefore bypass the requirement for Ser, but strongly diminished inhibition by Trp, Phe or Ala, consistent with the postulate that R106 citrullination more strongly affected Trp/Phe/Ala than Ser hence modifying the equilibrium between the allosteric activator and inhibitors in favor of the activator Ser.

Methods

Cell culture, siRNA silencing and expression vector transfection.

Melanoma cell lines 501Mel and SK-Mel-28 were grown in RPMI 1640 medium supplemented with 10% foetal calf serum (FCS). MM074 and MM117 were grown in HAM-F10 medium supplemented with 10% FCS, 5.2 mM glutamax and 25 mM Hepes. Hermes-3A cell line was grown in RPMI 1640 medium (Sigma) supplemented with 10% FCS, 200 nM TPA, 200 pM cholera toxin, 10 ng/ml human stem cell factor (Invitrogen) and 10 nM endothelin-1 (Bachem). HeLa cells were grown in Dulbecco's modified Eagle's medium supplemented with 10% FCS. SiHA cells were grown in EAGLE medium supplemented with 10% FCS, 0.1 mM non-essential amino acids and 1mM sodium pyruvate. UOK cell lines were cultured in DMEM medium (4.5 g/L glucose) supplemented with 10% heat-inactivated FCS and 0.1 mM AANE.

SiRNA knockdown experiments were performed with the corresponding ON-TARGET-plus SMARTpools purchased from Dharmacon Inc. (Chicago, Il., USA). SiRNAs were transfected using Lipofectamine RNAiMax (Invitrogen, La Jolla, CA, USA) and cells were harvested after 72 hours. PADI1 and PADI3 expression vectors were transfected using X-tremeGENE™ 9 DNA Transfection Reagent (Sigma) for 48 hours. To assess clonogenic capacity cells were counted and seeded in 6 well plates for 7 to 15 days.

Proliferation, viability and senescence analyses by flow cytometry.

To assess proliferation after siRNA treatment cells were stained with Cell Trace Violet (Invitrogen) on the day of transfection. To assess cell viability cells were harvested 72 hours after siRNA transfection and stained with Annexin-V (Biolegend) following manufacturer instructions. To assess senescence cells were treated with Bafilomycin A (Sigma) for 1 hour and then with C_{12}FDG (Invitrogen) for 2 hours. Cells were analyzed on a LSRII Fortessa (BD Biosciences) and data were analyzed using Flowjo software.

ATP measurement.

ATP concentrations were determined 72 hours after siRNA transfection using a method based on the luminescent ATP detection system (Abcam, ab113849) following the manufacturer's instructions.

Protein extraction and Western blotting.

Whole cell extracts were prepared by the standard freeze-thaw technique using LSDB 500 buffer (500 mM KCl, 25 mM Tris at pH 7.9, 10% glycerol (v/v), 0.05% NP-40 (v/v), 16 mM DTT, and protease inhibitor cocktail). Cell lysates were subjected to SDS–polyacrylamide gel electrophoresis (SDS-PAGE) and proteins were transferred onto a nitrocellulose membrane. Membranes were incubated with primary antibodies in 5% dry fat milk and 0.01% Tween-20 overnight at 4 °C. Membranes were then incubated with HRP-conjugated secondary antibody (Jackson Immuno Research) for 1 hour at room temperature and visualized using the ECL detection system (GE Healthcare).

Mass spectrometry and analysis.

Mass-spectrometry was performed at the IGBMC proteomics platform (Strasbourg, France). Samples were reduced, alkylated and digested with LysC and trypsin at 37°C overnight. Peptides were then analyzed with a nanoLC- MS/MS system (Ultimate nano-LC and LTQ Velos ion trap, Thermo Scientific, San Jose, CA, USA). Briefly, peptides were separated on a C18 nano-column with a 1 to 30 % linear gradient of acetonitrile and analyzed in a TOP20 CID data-dependent MS method. Peptides were identified with SequestHT algorithm in Proteome Discoverer 2.2 (Thermo Fisher Scientific) using Human Swissprot database (20'347 sequences). Precursor and fragment mass tolerance were set at 0.9 Da and 0.6 Da respectively. Trypsin was set as enzyme and up to 2 missed cleavages were allowed. Oxidation (M) and Citrullination (R) were set as variable modifications and Carbamido methylation (C) as fixed modification. Peptides were filtered with a 1 % FDR (false discovery rate) on peptides and proteins. For statistical analyses data were re-analyzed using Perseus (Tyanova et al., 2016).

Immunofluorescence.

Staining was performed following a standard IF protocol. Briefly, cells were washed with PBS, fixed in freshly prepared 4% paraformaldehyde (PFA) for 10 min at RT and permeabilized with PBS 0.1% Triton X-100 at RT. Blocking (RT for 20 min) and incubations with antibodies (RT for 1 hour) were performed with 10% heat-inactivated FCS in PBS/0.1%Triton X-100 and washes were done with PBS/0.1% Triton X-100 at RT. Nuclei were counterstained with freshly prepared 1 µg/mL DAPI in PBS for 2 min at RT and cells were mounted using the ProLong Gold antifade reagent of Molecular Probes.

RNA preparation, quantitative PCR and RNA-seq analysis.

RNA isolation was performed according to standard procedure (Qiagen kit). qRT-PCR was carried out with SYBR Green I (Qiagen) and Multiscribe Reverse Transcriptase (Invitrogen) and monitored using a LightCycler 480 (Roche). RPLP0 gene expression was used to normalize the results. Primer sequences for each cDNA were designed using Primer3 Software and are available upon request. RNA-seq was essentially performed as previously described (Laurette et al., 2019). Gene ontology analyses were performed with the Gene Set Enrichment Analysis software GSEA v3.0 using the hallmark gene sets of the Molecular Signatures Database v6.2 and the functional annotation clustering function of DAVID.

Analysis of oxygen consumption rate (OCR) and glycolytic rate (ECAR) in living cells.

The ECAR and OCR were measured in an XF96 extracellular analyzer (Seahorse Bioscience). A total of 20’000 cells per well were seeded and transfected by siRNA or expression vector for 72 and 24h hours prior the experiment, respectively. Cells were incubated in a CO2-free incubator at 37°C and the medium was changed to XF base medium supplemented with 1 mM pyruvate, 2 mM glutamine and 10 mM glucose for 1 hour before measurement. For OCR profiling cells were sequentially exposed to 2 µM oligomycin, 1 µM carbonyl cyanide-4-(trifluorome- thoxy) phenylhydrazone (FCCP) and 0.5 µM rotenone and antimycin A. For ECAR profiling cells were sequentially exposed to 2 µM oligomycin and 150 mM 2-deoxyglucose (2-DG). After measurement cells were washed with PBS, fixed with 3% PFA, permeabilized with 0.2% triton. Nuclei were counterstained with Dapi

(1:500) and number of cells per well calculated by the IGBMC High Throughput Cell-based Screening Facility (HTSF, Strasbourg, France). L-Phe (Sigma, P2126), L-Trp (Sigma T0254), L-Ala (Sigma A7627) or L-Ser (Sigma S4500) were added to the complete medium and the refreshed XF base medium prior the experiment.

Figure legends

Figure 1. CHD4 silencing stimulated MAP kinase signaling and glycolysis. A. Immunoblots showing stimulation of ERK1/2, MTOR and AMPK phosphorylation, but not AKT phosphorylation following CHD4 silencing. Right panel shows the intracellular ATP levels measured under the same conditions. In all experiments: n=3, statistical unpaired t-tests analyses were performed by Prism 5 with a confidence interval of 95%. *P-values: ***= p<0,001.* **B.** Effect of CHD4 silencing on the basal and maximal OCR values in 501Mel cells. **C**. Effect of CHD4 silencing on the basal OCR/ECAR ratio in the indicated cell types. **D**. Effect of CHD4 silencing on the basal and maximal ECAR values in 501Mel cells and the basal ECAR values in the indicated cell types. In all experiments: n=6 with 6 technical replicates for each experiment. Statistical unpaired t-tests analyses were performed by Prism 5 with a confidence interval of 95%. *P-values: *= p<0.05; **= p<0.01; ***= p<0.001.* **E.** Cells transfected with siRNAs were immunostained with antibody against HNE and nuclei counterstained with DAPI (magnification x200). Right panels show quantifications of stained cells for each condition in two melanoma cell lines.

Figure 2. CHD4 silencing increases citrullination in 501Mel cells. A. Silver nitrate staining of an SDS PAGE gel shows the proteins precipitated from SiC and SiCHD4 following immunoprecipitation with a pan-citrulline antibody **B.** Increases in number of total and citrullinated PSMs upon CHD4 silencing following immunoprecipitation with a pan-citrulline antibody. **C**. Volcano plot showing proteins with increased or decreased total PSMs after CHD4 silencing and immunoprecipitation with a pan-citrulline antibody. Lower table shows PKM2 peptides with increased citrullination after CHD4 silencing and immunoprecipitation with a pan-citrulline antibody. **D**. Increased recovery of glycolytic enzymes following CHD4 silencing and immunoprecipitation with a pan-citrulline antibody. **E.** Immunoblot showing expression of recombinant PADI1 and PADI3 in cells transfected with the corresponding expression vectors or the Empty Vector (EV). **F.** Immunoblot showing

expression of PKM2 in cells after CHD4 silencing or transfection with the PADI1 and PADI3 vectors in the cell extracts used for immunoprecipitation with a pan-citrulline antibody. **G.** Immunoblots of PKM2 in the pan-citrulline immunoprecipitates from 501Mel or MM117 cells. **H.** Immunoblot showing PKM2 in the pan-citrulline immunoprecipitates after transfection with the PADI1 and PADI3 expression vectors.

Figure 3. PADI1 and PADI3 are necessary and sufficient for increased ECAR (glycolysis). A-B. ECAR values in 501Mel cells following transfection with the indicated siRNAs or expression vectors. **C.** Intracellular ATP levels following CHD4 silencing or PADI1/3 expression and cell proliferation evaluated by cell trace violet assay. The lower panel shows AMPK phosphorylation in extracts from the same cells. **D-F**. ECAR values and intracellular ATP levels in MM117 cells following transfection with the indicated siRNAs or expression vectors. **G.** Immunoblots showing phosphorylation of ERK from 501Mel cell extracts transfected with PADI1/3 or the Empty Vector (EV). **H.** Percentages of viable Sk-mel-28 cells after a 72 hours of transfection with the indicated siRNAs or after 24 hours of transfection with expression vectors in the presence of the indicated concentrations of BRAFi Vemurafinib for 72 hours. In all experiments: n=3, statistical unpaired t-tests analyses were performed by Prism 5 with a confidence interval of 95%. *P-values: P-values: *= p<0.05; **= p<0.01; ***= p<0.001.*

Figure 4. PKM2 citrullination diminishes allosteric inhibition by Phe/Ala/Trp. **A.** Close up view of free Ser and Phe interactions within the free amino acid binding pocket in the Apo, R-active and T-inactive states with a superposition of the three structures. All residues displayed are shown as sticks. In the superposition, the peptide bearing R43 is represented as ribbon to show the allosteric changes created upon Phe binding. Colour coding is as in Fig. S3. Salt bridges and hydrogen bonds are shown as dashed lines. For clarity, the side chain of Phe 470, which stacks on R106 side chain, is not displayed. **B.** ECAR values in presence of exogenous Ser or absence of Ser after CHD4 silencing or PADI1/3 expression in 501Mel or MM117 cells; NM = normal medium. **C.** ECAR values in presence of increased exogenous Ser with or without CHD4 silencing in 501Mel cells. **D-E.** ECAR values in presence of exogenous Trp or Phe with or without CHD4 silencing or PADI1/3 expression in 501Mel cells. **F.** ECAR values in presence of exogenous Phe with or without CHD4

silencing in MM117 cells. **G.** ECAR values in presence of exogenous Ala with or without PADI1/3 expression in 501Mel cells. In all experiments ECAR values were determined from N=6 with 6 technical replicates for each N. Unpaired t-test analysis were performed by Prism 5. P-values: *= p<0,05; **= p<0,01; ***= p<0,001.

Legends to Supplementary Figures and Tables.

Supplementary Figure 1. CHD4 represses PADI1 and PADI3 expression. A-B. Changes in PADI1 and PADI3 expression in the indicated cells lines following CHD4 silencing shown by RNA-seq and RT-qPCR. In all experiments: n=3, statistical unpaired t-tests analyses were performed by Prism 5 with a confidence interval of 95%. *P-values: *= p<0.05; **= p<0.01; ***= p<0.001.***C.** Immunoblot showing increased PADI1 and PADI3 protein expression following CHD4 silencing. **D.** CHD4 CTCF and FOSL2 co-occupy a regulatory element at the PADI1-PADI3 locus. Screenshot of UCSC genome browser at the PADI1-PADI3 locus showing the indicated ChIP-seq data. Arrows highlight the putative cis-regulatory elements occupied by CTCF, FOSL1 and CHD4 and marked by ATAC-seq, H3K4me1, BRG1 and H2AZ. The following data sets were used: H3K4me1 GSM2476344; ATAC GSM2476338; FOSL2 GSM2842801; TEAD4 GSM2842802 (27). Other data are from CHD4 Chip-seq (Article 1) or Laurette et al., 2015.

Supplementary Figure 2. Citrullination regulates glycolysis and proliferation in multiple types of cancer cells. A. Diminished clonogenicity of SiHA cells following CHD4 silencing. **B**. PADI1 and PADI3 expression in SiHA cells following CHD4 silencing. **C-D**. Basal and maximal glycolysis in SiHA cells following CHD4 silencing. **E.** Glycolysis in SiHA cells following PADI1/3 expression. **F.** OCR/ECAR ratio in SiHA cells following CHD4 silencing or PADI1/3 expression. **G.** Intracellular ATP levels in SiHA cells following CHD4 silencing. **H-J**. Clonogenicity, PADI1, PADI3 expression and glycolysis in HeLa cells following CHD4 silencing or PADI1/3 expression as indicated. **K-N**. Clonogenicity, cell trace assay, PADI1, PADI3 expression and glycolysis in UOK-109 translocation renal cell carcinoma cells following CHD4 silencing or PADI1/3 expression as indicated. **O-R**. Clonogenicity, cell trace assay, PADI1, PADI3 expression and glycolysis in A498 clear cell renal carcinoma cells (ccRCC) following CHD4 silencing or PADI1/3 expression as indicated. For

A,B,G,H,I,K,L,N,O,P,R, n=3, statistical unpaired t-tests analyses were performed by Prism 5 with a confidence interval of 95%. *P-values: *= p<0.05; **= p<0.01; ***= p<0.001.* In C,D,E,F,J,M,Q, n=3 with 6 technical replicates for each experiment. Statistical unpaired t-tests analyses were performed by Prism 5 with a confidence interval of 95%. *P-values: *= p<0.05; **= p<0.01; ***= p<0.001.*

Supplementary Figure 3. Locations and interactions of citrullinated arginines in PKM2 activity. Locations and interactions of citrullinated arginines in PKM2. **A.** Ribbon representation of a PKM2 monomer in the apo resting state (grey; PDB 3SRH), the active R state (yellow; PDB 6GG6 with FBP and oxalate molecules from 3SRD) and the inactive T state (cyan; PDB 6GG4). The three citrullinated arginines (R106, R246 and R489), the free amino acids Serine and Phenylalanine, FBP and oxalate (surrogate of pyruvate to occupy the active site) are shown as sticks (carbon, grey; nitrogen, blue; oxygen, red; phosphorus, orange). AS, active site. AP, free amino acid binding pocket. The regions of PKM2 undergoing allosteric structural transitions between the three states are boxed. **B.** Close up view of FBP interactions within the R-active state. Salt bridges and hydrogen bonds are shown as dashed lines. Colour coding as panel A. For clarity, the side chain of K433 is not displayed. **C.** Closeup view of R246 interactions with the B domain in the Apo, R-active and T-inactive states along with a superposition of the three 10 structures. Color coding and representation of salt bridges/hydrogen bonds is as in panels A and B.

Supplementary Dataset 1. Proteins enriched after pan-citrulline immunoprecipitation from CHD4 silenced cells. Are shown: accessions, gene names, gene descriptions, Log P-values, differences (siCHD4-siCTRL), sum peptides scores, percentage of coverages, peptides number, PSMs number, NSAF values (PSMs/protein length), unique peptides number, amino acids number and molecular weights.

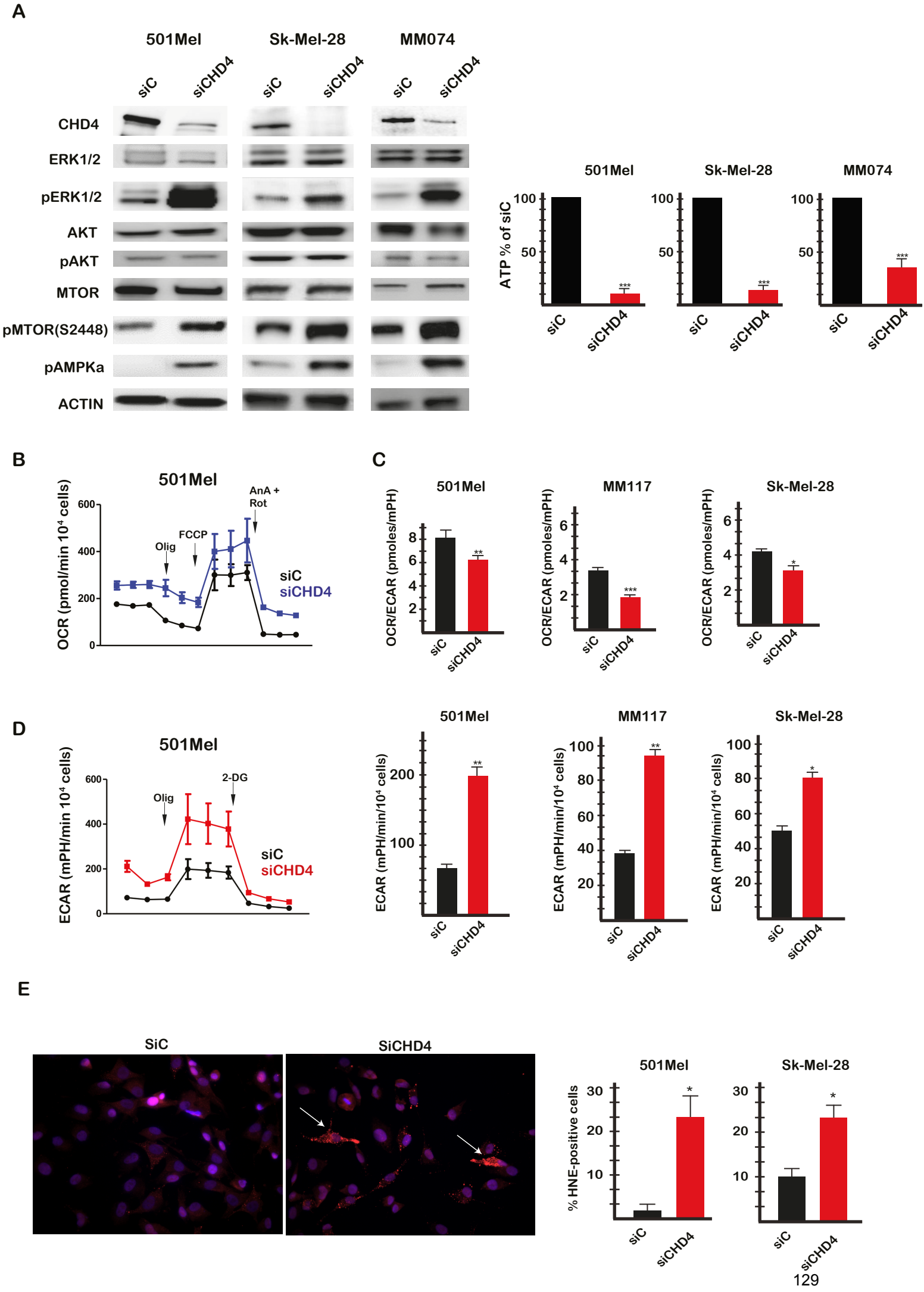
A
501Mel
Sk-Mel-28
MM074
siC
siCHD4
CHD4
ERK1/2
pERK1/2
AKT
pAKT
MTOR
pMTOR(S2448)
pAMPKa
ACTIN
ATP % of siC
B
OCR (pmol/min 10⁴ cells)
Olig
FCCP
AnA + Rot
C
OCR/ECAR (pmoles/mPH)
MM117
D
ECAR (mPH/min 10⁴ cells)
2-DG
E
SiC
SiCHD4
% HNE-positive cells
Coassolo et al., Figure 1
129

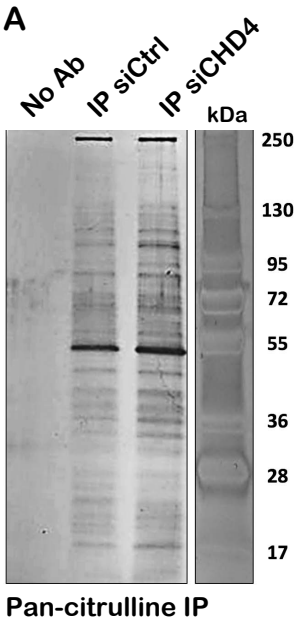

B

	all PSMs	Cit PSMs
SiCTRL	22058	2561
SiCHD4	34365	4311

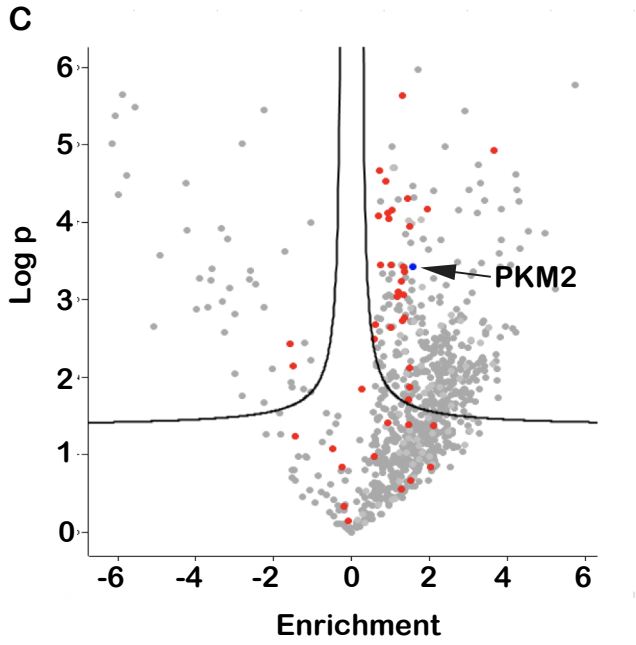

PKM2 Cit peptides	Position	PSMs SiCTRL	PSMs SiCHD4
TATESFASDPILYRPVAVALDTK	R106	2	7
FGVEQDVDMVFASFIR	R246	0	5
DPVQEAWAEDVDLR	R489	2	10

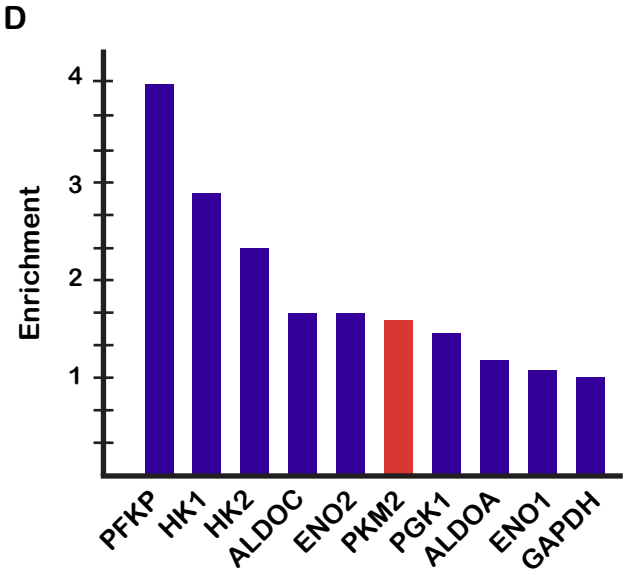

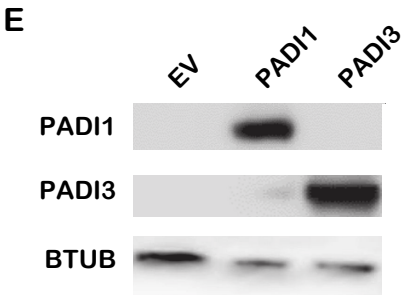

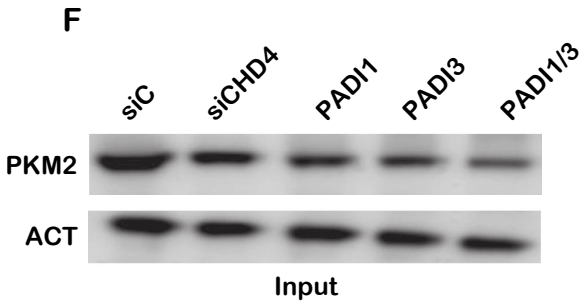

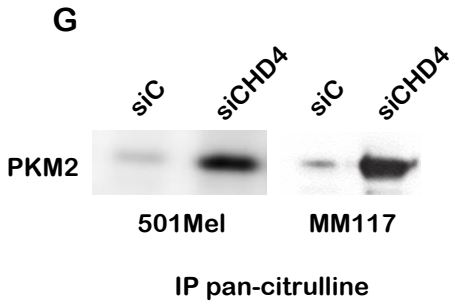

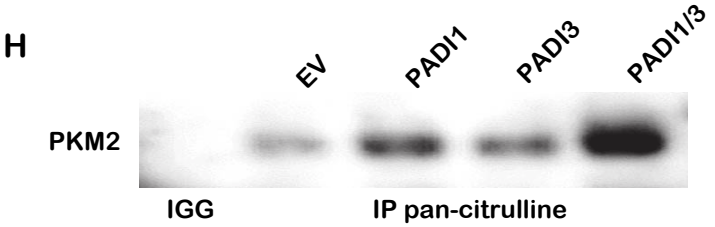

Coassolo et al., Figure 2

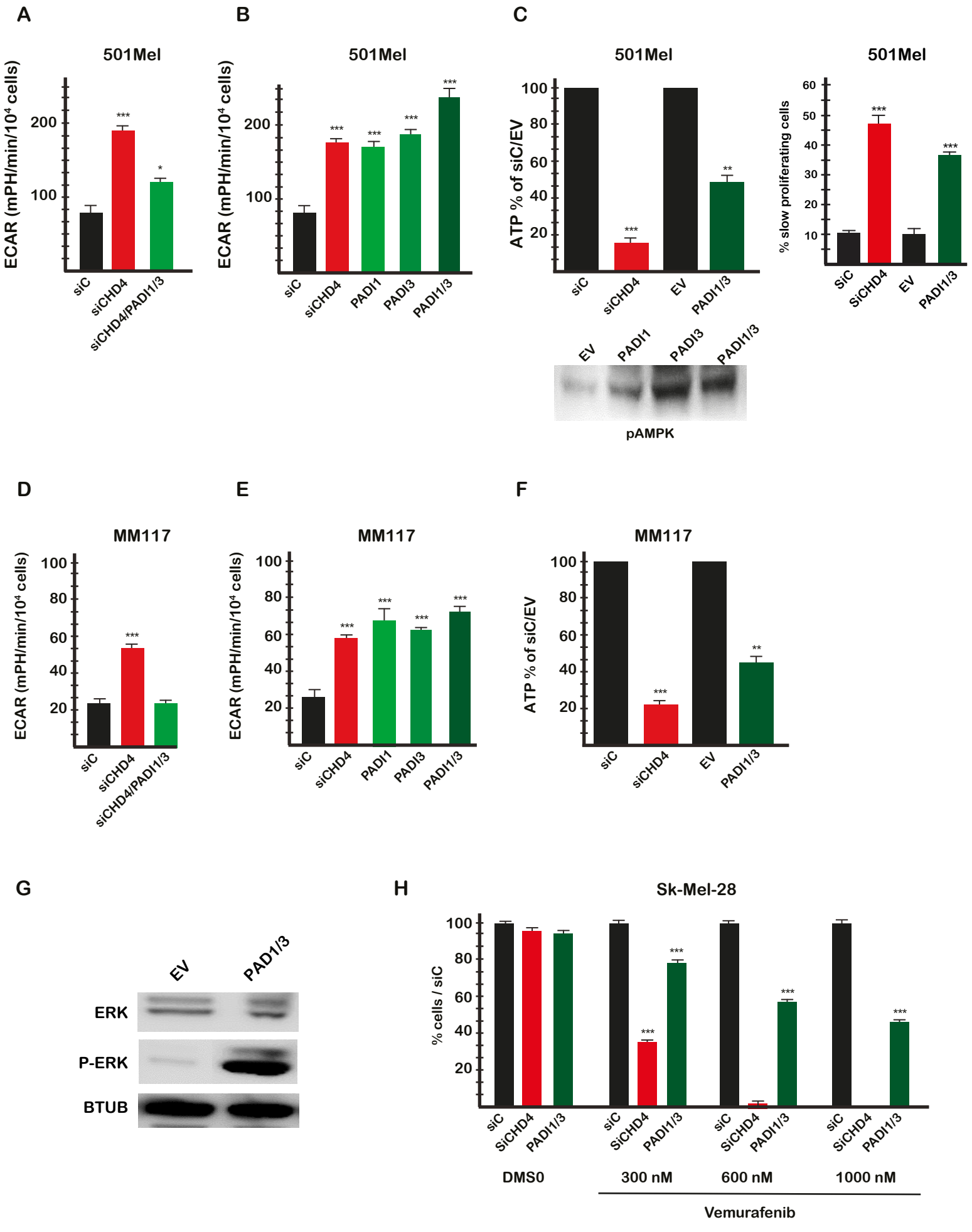

Coassolo et al., Figure 3

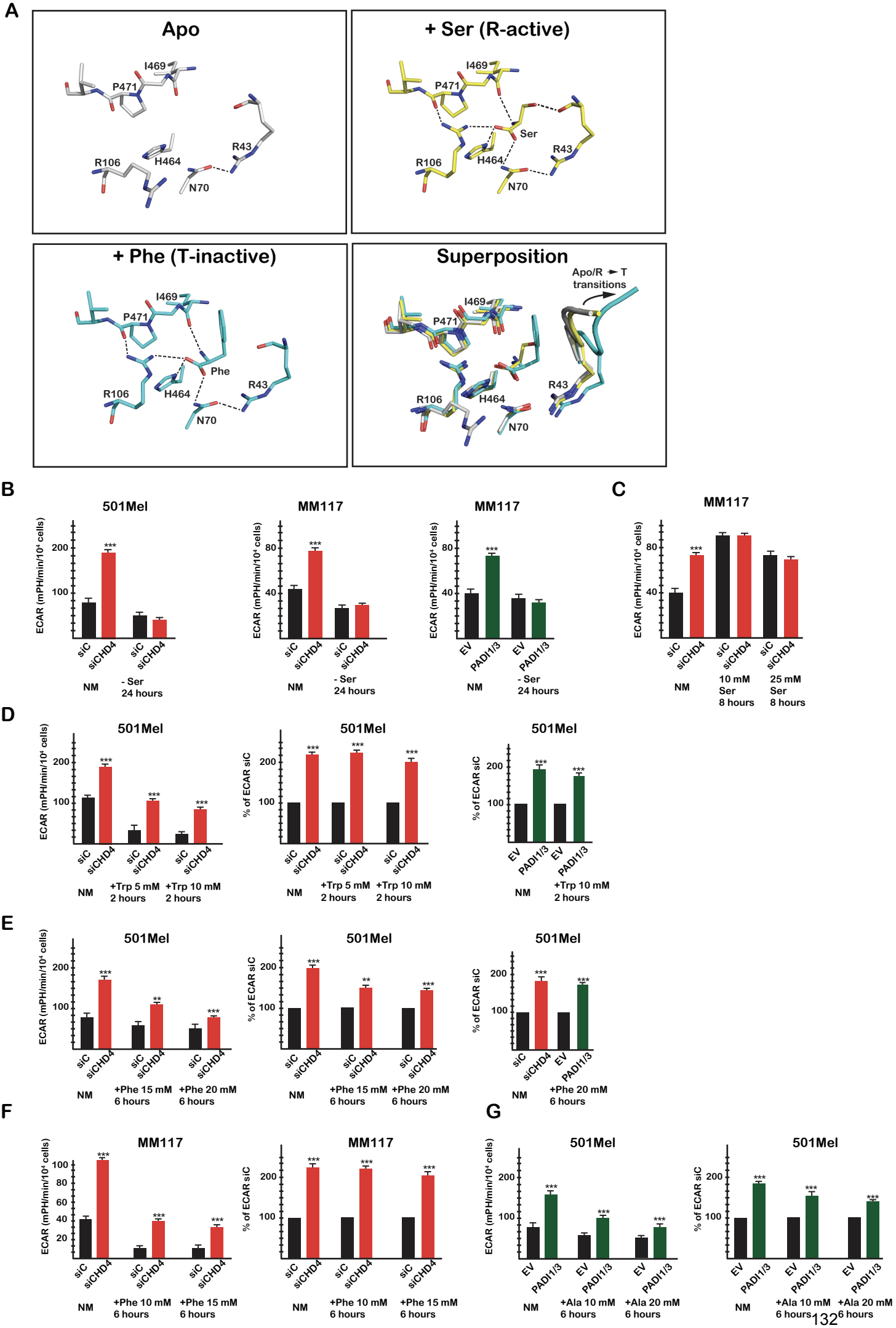

Coassolo et al., Figure 4

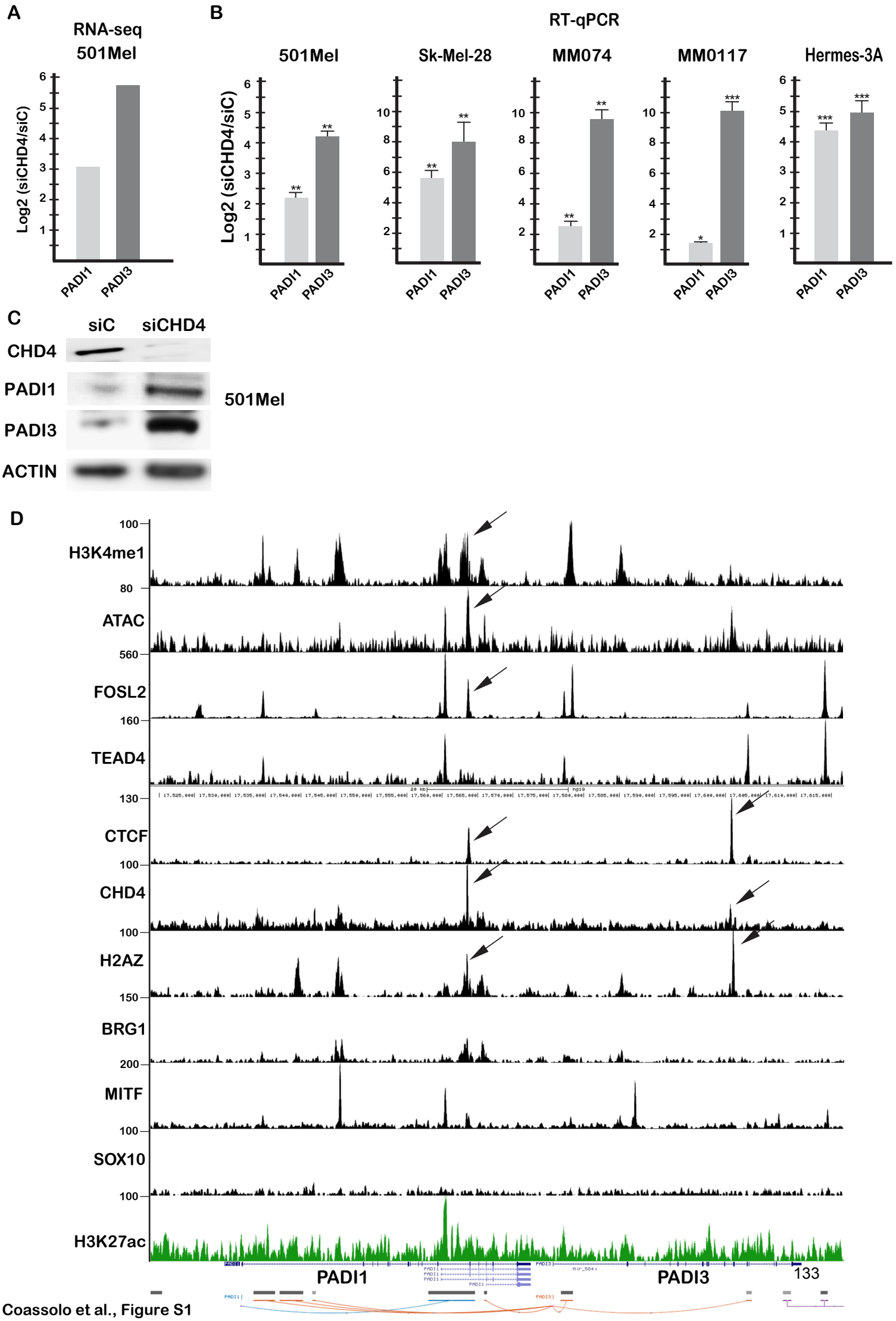

Coassolo et al., Figure S1

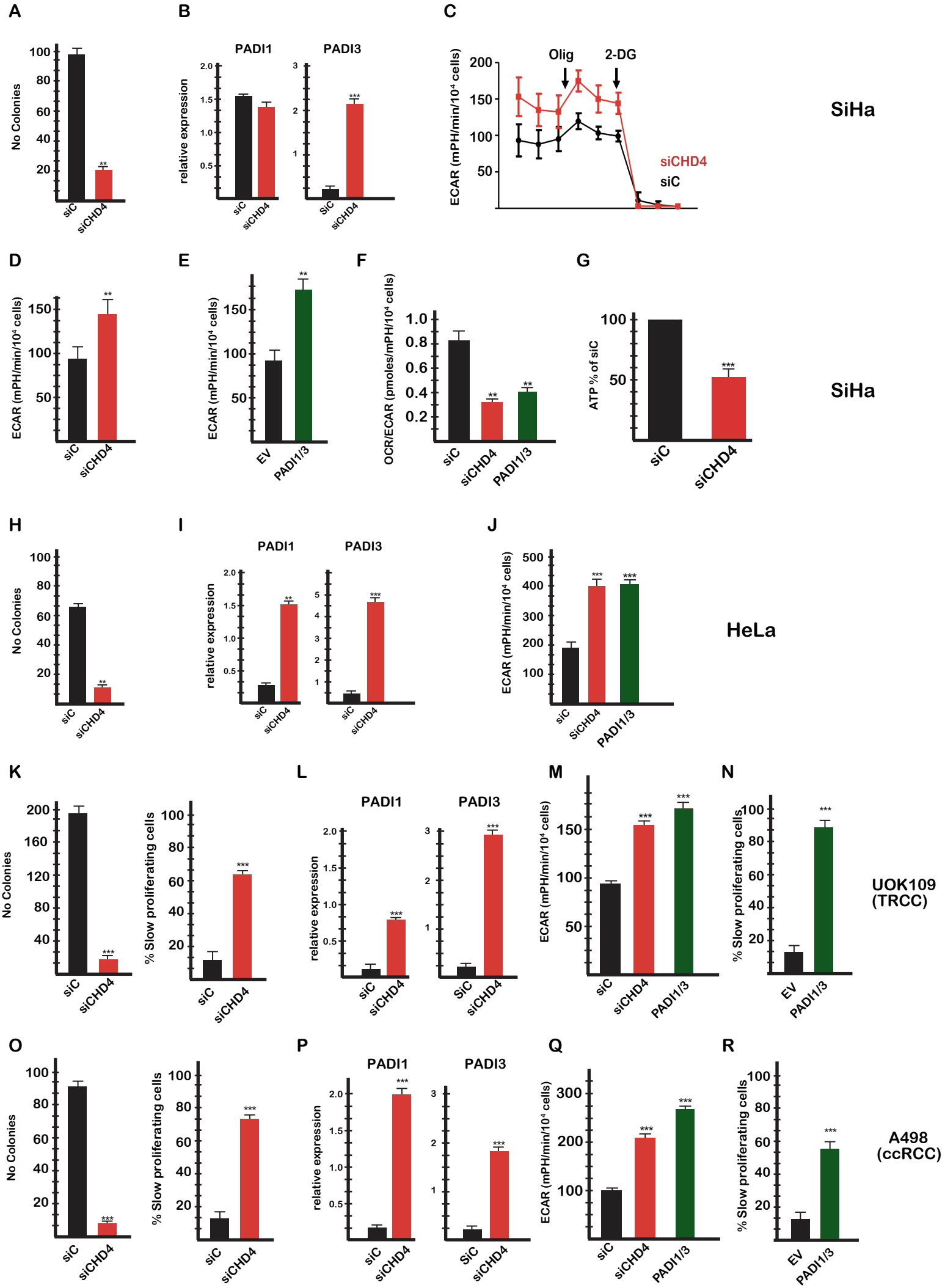

Coassolo et al., Figure S2

A

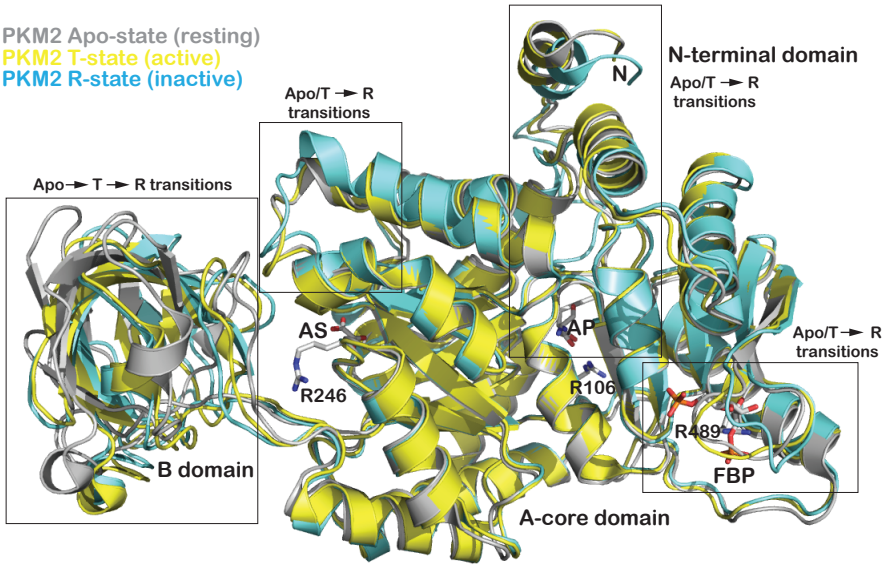

B

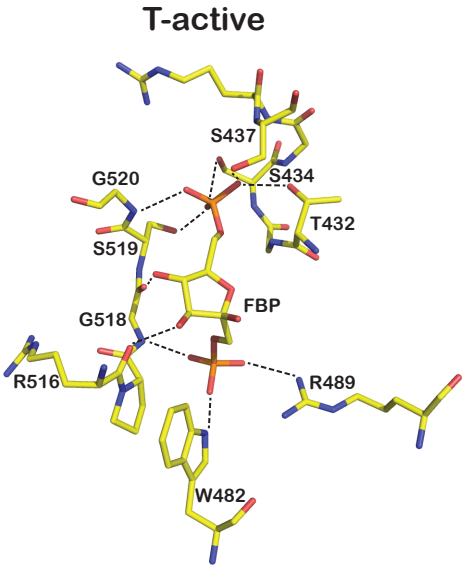

C

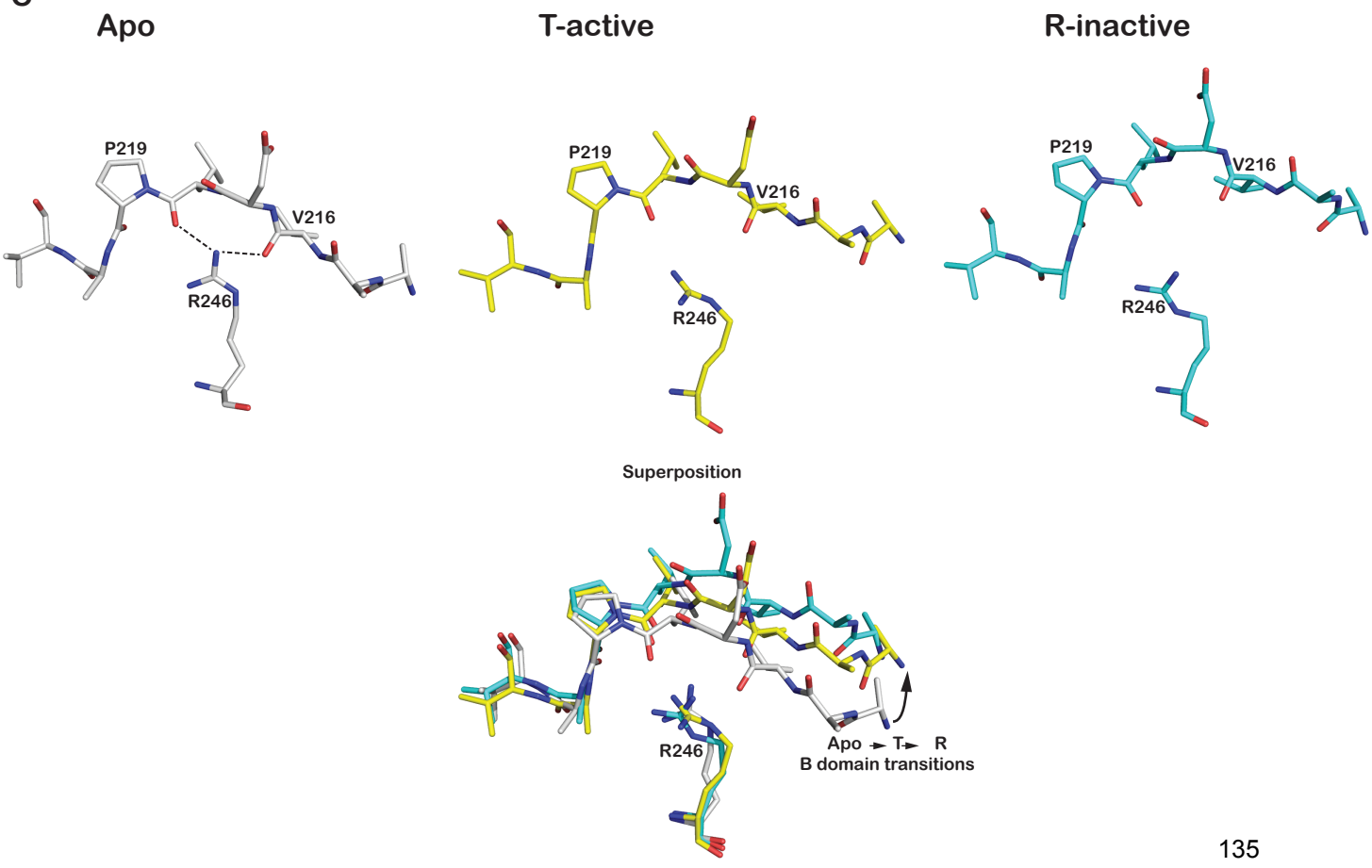

Coassolo et al., Figure S3

DISCUSSION AND CONCLUSIONS

Discussion and Conclusions

Multiple functions of CHD4 in melanoma cells.

We showed in the present work that CHD4 is involved in multiple functional pathways in melanoma cells, as a cofactor for SOX10 and REBB1, a regulator of cytokine and cytokine receptor expression and a regulator of glycolysis via PADI1/3-mediated PKM2 citrullination.

Tandem immunopurification of tagged SOX10 combined with mass-spectrometry revealed that both MITF and SOX10 interact with a common set of cofactors. Thus, both factors interact with the PBAF complex. However, while MITF is selective for BRG1/PBAF, SOX10 also associates with the BAF complex as attested by peptides for BRM and ARID1A/B, not seen with MITF. How these differential interactions with the BAF and PBAF complexes are specified remains to be determined. Moreover, both SOX10 and MITF associate with NuRF, Cohesin subunits, TFIIIC, the MCM replication complex as well as with proteins involved in DNA repair and the ubiquitin cycle such as MSH2/6, XRCC5/6, USP7 and CTNNB1. Nevertheless, SOX10 selectively interacts with the 5FMC complex and other potential cofactors such as ILF2/3 and NONO/SFPQ, NONO being a multifunctional protein involved in both splicing and transcription that was previously shown to act as a co-factor for SOX10 (Chaoui et al., 2015).

In addition, we also identified subunits of the NuRD complex that associate with both MITF and SOX10. However, while SOX10 associates with both CHD3 and CHD4, MITF selectively associates with CHD4, a result confirmed by independent immunoprecipitation experiments.

In agreement with previously reported data, CHD3 and CHD4 did not co-precipitate indicating that they form two distinct NuRD complexes (Hoffmeister et al., 2017). In support of this CHD3 and CHD4 regulate distinct gene expression programs. CHD4 predominantly acts as a repressor with a majority of up-regulated genes whereas comparable numbers of genes are up- or down-regulated upon CHD3 silencing.

CHD isoforms were shown to have both distinct and redundant functions within the cell (Hoffmeister et al., 2017; Nitarska et al., 2016). Thus, the small number of genes co-regulated by both CHD3 and CHD4 that was observed in our own RNA-seq dataset could be explained by a functional switch in CHD subunits triggered by RNA silencing, in line with previously published data (Nitarska et al., 2016). In support of this, CHD4 silencing induced CHD5 expression in RNA-seq dataset and increased CHD3 expression in immunoblots. Unfortunately, the high apoptotic effect induced by the silencing of multiple CHD subunits made difficult to discriminate the redundant and the specific functions for each CHD. Additionally, even if CHD3 ChIP-seq in melanoma cells was not possible, ChIP-seq data mining of CHD3 and CHD4 in human cancer prostate cells (LnCAP) revealed that more than 40% of the binding sites are common to CHD3 and CHD4 (Tencer et al., 2017). Such co-localization supports both the distinct and the redundant functions of CHD3 and CHD4.

We further showed that CHD4 co-localizes on the genome with composite MITF and SOX10 bound sites where it was bound to the nucleosomes flanking the transcription factors in a manner analogous to BRG1. Such binding of multiple remodelling complexes to the same nucleosomes is in line with previously published data (De Dieuleveult et al., 2016; Morris et al., 2014b) and with observations along which NuRD binds to active enhancers and promoters possibly via H3.3 to fine tune transcription (Bornelö et al., 2018; Giles et al., 2019; Kraushaar et al., 2018). However, despite their association and genomic co-localization there does not seem to be any significant overlap between the MITF and the CHD4-driven gene expression programs, and only a limited overlap with the SOX10 expression program. Therefore, acting as co-repressors for both MITF and SOX10 cannot be considered as a major function of the CHD3 and CHD4 NuRD complexes in melanoma cells.

The analysis of DNA-sequence motifs at CHD4 bound sites revealed a strong enrichment of motifs for the RREB1 transcriptional repressor, a protein known to interact with the HDAC1 and HDAC2 subunits of NuRD (P. Joshi et al., 2014). In contrast to MITF and SOX10, a significant fraction of the RREB1 regulated genes including several cytokines and cytokine receptors was shown to be co-regulated by CHD3 or CHD4 indicating that NuRD activity accounts in part for the repressive function of RREB1. Additionally, analysis of DNA-sequence motifs at CHD4 bound

sites also revealed a significant enrichment for other factors. Among them, CTCF binding motif showed a significant enrichment score therefore supporting that CHD4/NuRD might regulate gene expression including PADI1/3 locus through modulation of CTCF activity.

Connecting epigenetics to citrullination and glycolysis defines a novel pathway regulating proliferation of melanoma and other cancer cells.

The aforementioned observations, however, do not account for the majority of the CHD4 regulated genes. Two major pathways were identified from the analysis of the CHD4 up-regulated gene expression programs. Multiple cytokines and cytokine receptors were up-regulated and increased levels of phosphorylated ERK1/2 indicative of increased MAP kinase signaling were observed. Such increase in MAP kinase signaling was associated with increased mTOR phosphorylation on serine 2448 and increased glycolysis. Thus, increased cytokine and cytokine receptor expression, MAP-kinase and mTOR activation can be one of the mechanisms that contributes to increased glycolysis, ATP depletion and slower melanoma cell proliferation. However, the mechanism by which mTOR pathway activation participates in the increased glycolysis after CHD4 silencing still remains unclear. mTOR is known to regulate glycolysis through effectors such as the proto-oncogene Myc and Hypoxia-Inducible Factors (HIFs) (Dang, Kim, Gao, & Yustein, 2008) leading to a transcriptional regulation of glycolytic enzymes (Y. Feng & Wu, 2017; Poulain et al., 2017; Q. Sun et al., 2011; Xiaoyu et al., 2018). RNA-seq analysis after CHD4 silencing did not show any significant enrichment in any metabolic pathway. Hence, the regulation of glycolysis by mTOR does not rely on transcriptional regulation but on direct or indirect regulation mechanisms that still remain to be determined.

Interestingly, ectopic PADI1/3 expression in melanoma cells also induced the activation of the MAP kinase signaling as observed by ERK phosphorylation. Citrullination of chemokine and chemokine receptors modifying ERK phosphorylation was previously observed both *in vitro* and *in vivo* (Proost et al., 2008) suggesting that

ectopic PADI1/3 expression could induce the specific citrullination of MAP kinase signaling effectors and modulate their activity, thus regulating ERK phosphorylation and activating signaling pathways. In support of this, the Receptor of Activated protein C Kinase 1 (RACK1) known for its role in rewiring ERK and JNK signaling pathways in melanoma (Campagne et al., 2017; Vomastek et al., 2007), showed increased citrullination upon CHD4 silencing and might be a candidate of choice to explain PADI1 and PADI3-dependent MAP kinase activation.

In addition, it cannot be excluded that the multiple ATPases that are upregulated after CHD4 silencing participate in the cellular ATP depletion and the slow cell proliferation as well as control glycolysis fluctuations through increasing the cellular ATP demand (Epstein, Xu, Gillies, & Gatenby, 2014).

Nevertheless, our observations rather support the hypothesis that the increased glycolysis results from the PADI1 and PADI3-mediated citrullination of glycolytic enzymes. The PADI1 and/or PADI3 expression was shown to be induced in all tested melanoma and non-melanoma cell lines. Some cell lines showed basal PADI1 expression, however, PADI3 was almost completely silenced in all cell lines. De-repressed enzymes expression led to increased citrullination of multiple target proteins including glycolytic enzymes. Interestingly, citrullination is a calcium-dependent process and CHD4 silencing increases the expression of a series of genes regulating calcium signaling.

Immunoblot experiments confirmed that the citrullination of PKM2, a rate limiting enzyme in glycolysis, was increased upon CHD4 silencing and ectopic PADI1 and PADI3 expression. PKM2 was recently shown as a citrullinated protein by mass-spectrometry-based deep proteomic profiling of mice and human tissues (Fert-Bober et al., 2019; Lee et al., 2018b). Thus, PKM2 was detected with a basal level of citrullination in control melanoma cells. In addition, citrullination of glycolytic enzymes by PADs was previously observed in rheumatoid arthritis (Tilvawala et al., 2018). Tilvawala et al. showed that PADI1 but not PADI3 could citrullinate PKM2 *in vitro*. In melanoma cells, we showed that both PADI1 and PADI3 increased PKM2 citrullination, however, a much stronger effect was observed upon both enzymes expression. Tilvawala et al. also reported that the enzymatic activity of PKM2 against PEP in the presence of FBP was stimulated *in vitro* by PADI1 or PADI3. Our experimental data expand these observations by showing that PADI1 and PADI3

citrullinate PKM2 thus stimulating glycolysis in living cells and regulating their proliferation.

Glycolysis is allosterically regulated by both Ser and SAICAR products of metabolic intermediates of the glycolytic pathway (Chaneton et al., 2012; Christofk, Vander Heiden, Wu, et al., 2008a; Keller et al., 2014a; Morgan et al., 2013). Thus, whenever the Ser levels decline through excessive glycolysis, the recognition pocket of PKM2 becomes more readily occupied by Phe, Trp or Ala inducing allosteric changes that inhibit the enzyme hence reducing glycolysis and leading to the accumulation of metabolic intermediates and increased Ser synthesis.

Here, enhanced citrullination of the arginine residues R106, R246 and R489 was identified by mass-spectrometry. Data indicate that citrullination of R489, an arginine directly involved in FBP binding, may diminish FBP binding reinforcing thus PKM2 allosteric regulation by the free amino acids. The citrullination of R246 may facilitate the active conformation of the enzyme while R106 citrullination may lead to a change in the relative affinity for Ser compared to Trp, Ala and Phe, thereby weakening their inhibitory effect and reinforcing activation by Ser.

Consequently, glycolysis may be maintained at lower Ser concentrations that would normally result in increased Phe, Ala or Trp binding and PKM2 inhibition. Through bypassing the physiological regulatory feedback loop, citrullination of PKM2 thus leads to excessive glycolysis and inhibition of cell growth. This hypothesis is supported by the observation that small molecules that increase PKM2 activity stimulate glycolysis and inhibit cell proliferation (Anastasiou et al., 2012; Chaneton et al., 2012; Dayton, Jacks, & Vander Heiden, 2016). Excessive glycolysis upon small molecule activation of PKM2 also results in serine auxotrophy and reduced cell proliferation (Kung et al., 2012). Bypassing the normal Ser-regulated PKM2 activity by small molecules or citrullination therefore results in excessive glycolysis that represents a major cause of reduced cell proliferation rate.

In addition, CHD4 silencing may affect the mitochondrial metabolism as evidenced by an increased basal OCR and ROS lipid peroxidation product 4-Hydroxy-2-NonEnal (HNE). As recently described, PKM2 promotes mitochondrial fusion and OXPHOS in human liver and lung cancer cells (T. Li et al., 2019)

suggesting that the enhanced PKM2 activity by citrullination might not only stimulate glycolysis but also OXPHOS by a mechanism that still remains to be elucidated.

It is worth to mention that PKM2 is not the only glycolytic enzyme that can be subject to increased citrullination. Thus, although our data are consistent with the key role of PKM2, it cannot be excluded that the altered activity of other enzymes may as well contribute to the observed increased glycolysis. For instance, PhosphoFructoKinase (PFK), a rate-limiting enzyme that catalyzes the first glycolysis-committed step is subject to citrullination after CHD4 silencing. Indeed, PFK is 4-fold enriched for citrullination following CHD4 silencing. However, unlike PKM2, PFK did not show any basal level of citrullination under control conditions. PFK activity is finely modulated by the cellular ATP concentrations and several allosteric regulators including its own substrate (Webb et al., 2015; C. Wu, Khan, Peng, & Lange, 2006) suggesting that, as we described for PKM2, PFK activity may be modulated through PADI-mediated citrullination.

HexoKinases (HKs) 1 and 2, glucokinase isoforms with highest affinity for glucose, display more than a 2-fold enrichment for citrullination following CHD4 silencing. HKs catalyze the first committed step of glucose metabolism to produce G-6P, a precursor for the Pentose Phosphate Pathway (PPP), glycogenesis and the hexosamine pathways (Robey & Hay, 2006). Thus, it cannot be excluded that citrullination may modulate HKs activity and participate the increased glycolysis, or impact alternative metabolic pathways leading to cancer cell proliferation defects.

In addition to glycolytic enzymes, CHD4 silencing leads to increased citrullination of a number of cellular proteins. In particular, we noted the presence of multiple 14-3-3 proteins, a class of proteins that bind phosphorylated serine and threonine and thus regulate their intracellular transport. For instance, 14-3-3 proteins bind phosphorylated YAP1 to export it from the nucleus thus regulating the TEAD-driven cell proliferation via the Hippo signaling pathway. It remains to be determined if and how 14-3-3 citrullination affects the activity of these enzymes and consequently the signaling pathways they regulate.

Interestingly, a majority of melanomas were reported to be auxotrophic for arginine because of the lack of Argininosuccinate Synthetase (AS) (Dillon et al., 2004), the first of the two enzymes involved in arginine biosynthesis that converts

citrulline into arginine. Therefore, it cannot be excluded that the induction of PADI1 and PADI3 following CHD4 silencing, leading to increased citrullination and hence arginine depletion in cells unable to synthetize this amino acid, slowed down cellular proliferation and increased sensitivity to BRAF inhibitors. In support of this, arginine deiminase, that degrades extracellular arginine leading to arginine cell deprivation, showed positive results in clinical trials in the treatment of several arginine-auxotrophic tumors including melanomas (Feun et al., 2012; Ott et al., 2013).

In conclusion, the present PhD research activities allowed to identify a novel pathway regulating melanoma cell proliferation. Mechanistically, we showed that CHD4 regulates the expression of PADI1 and PADI3 and consequently their potential to citrullinate the key arginines of PKM2 involved in the allosteric regulation of this enzyme. We could thus establish the essential link between epigenetics, the glycolytic flux and melanoma cell proliferation. This regulatory pathway that is shared in other cancer types, does therefore represent a more general mechanism for regulating cancer cell proliferation potentially leading to the identification of novel therapeutic targets.

ANNEXES

ANNEXE 1

Journal of Investigative Dermatology (2019)

Dynamic Evolution of Clonal Composition and Neoantigen Landscape in Recurrent Metastatic Melanoma with a Rare Combination of Driver Mutations

Davidson, G., Coassolo, S., Kieny, A., Ennen, M., Pencreach, E., Malouf, G. Lipsker D. and Davidson, I.

Dynamic Evolution of Clonal Composition and Neoantigen Landscape in Recurrent Metastatic Melanoma with a Rare Combination of Driver Mutations

Guillaume Davidson[1], Sébastien Coassolo[1], Alice Kieny[1,2], Marie Ennen[1], Erwan Pencreach[3], Gabriel G. Malouf[1], Dan Lipsker[2] and Irwin Davidson[1]

In melanoma, initiating oncogenic mutations in *BRAF* or *NRAS* are detected in premalignant lesions that accumulate additional mutations and genomic instability as the tumor evolves to the metastatic state. Here we investigate evolution of clonal composition and neoantigen landscape in an atypical melanoma displaying recurrent cutaneous lesions over a 6-year period without development of extracutaneous metastases. Whole exome sequencing of four cutaneous lesions taken during the 6-year period identified a collection of single nucleotide variants and small insertions and deletions shared among all tumors, along with progressive selection of subclones displaying fewer single nucleotide variants. Later tumors also displayed lower neoantigen burden compared to early tumors, suggesting that clonal evolution was driven, at least in part, by counter selection of subclones with high neoantigen burdens. Among the selected mutations are a missense mutation in *MAP2K1* (F53Y) and an inversion on chromosome 7 generating a *AKAP9-BRAF* fusion. The mutant proteins cooperatively activate the MAPK signaling pathway confirming they are potential driver mutations of this tumor. We therefore describe the long-term genetic evolution of cutaneous metastatic melanoma characterized by an unexpected phenotypic stability and neoantigen-driven clonal selection.

Journal of Investigative Dermatology (2019) ■, ■–■; doi:10.1016/j.jid.2019.01.027

INTRODUCTION

Cutaneous melanoma is linked to environmental factors, in particular, UV light and polymorphisms in a variety of genes (Goldstein and Tucker, 2001; Hawkes et al., 2016; Hayward, 2003). Melanocyte transformation involves somatic mutations activating the MAPK pathway, most frequently $BRAF^{V600E}$ and $NRAS^{Q16L/R/H}$ and $NRAS^{Q61K}$ (Hodis et al., 2012; The Cancer Genome Atlas Network, 2015).

The principal hazard of cutaneous melanoma is its potential to metastasize rapidly. Current models propose that founder $BRAF^{V600E}$ or *NRAS* mutations are first detected in benign precursor lesions that give rise to melanoma by accumulation of additional mutations, such as gain of function in *TERT* and/or inactivation of *CDKN2A* or *PTEN* that allow bypass of oncogene-induced senescence (Shain et al., 2015b; The Cancer Genome Atlas Network, 2015). Subsequent genomic instability gives rise to insertions and deletions (indels) and large-scale rearrangements as the tumor acquires metastatic potential (Birkeland et al., 2018; Shain et al., 2018). This stepwise model for tumor development was derived from analyses of lesions at different stages in separate individuals or of different regions within the same lesions and has been supported by analyses of larger numbers of matched primary and metastatic lesions (Birkeland et al., 2018; Sanborn et al., 2015; Shain et al., 2018).

Here we describe whole exome sequencing (WES) in an atypical case of recurrent epidermotropic metastatic melanoma (Lestre et al., 2011; White and Hitchcock, 1998) showing that tumor evolution over a prolonged period was associated with selection of subclones with fewer mutations and reduced neoantigen load. No $BRAF^{V600E}$ or *NRAS* mutations or other mutations commonly found in melanoma were detected. Instead, two potential driver mutations, $MAP2K1^{F53Y}$ and an inversion on chromosome 7 generating an *AKAP9-BRAF* fusion, were identified.

RESULTS AND DISCUSSION

An atypical case of recurrent metastatic epidermotropic melanoma

The affected individual was referred to Strasbourg University Hospital dermatology clinic in 2010 when he was 43 years old. He had no remarkable personal or family history, had red hair and multiple freckles and lentigines on photo-exposed

[1]*Department of Functional Genomics and Cancer, Institut de Génétique et de Biologie Moléculaire et Cellulaire, Unité Mixte de Recherche 7104, Le Centre National de la Recherche Scientifique, U1258 Institut National de la Santé et de la Recherche Médicale, Université de Strasbourg, Illkirch Cédex, France;* [2]*Faculté de Médecine and Service de Dermatologie, Hôpital Civil, Hôpitaux Universitaires de Strasbourg, Strasbourg, France; and* [3]*Pôle de Biologie, Hôpitaux Universitaires de Strasbourg, Hôpital de Hautepierre, Strasbourg, France*

Correspondence: Irwin Davidson, Institut de Génétique et de Biologie Moléculaire et Cellulaire, Unité Mixte de Recherche 7104, Le Centre National de la Recherche Scientifique, U1258 Institut National de la Santé et de la Recherche Médicale, Université de Strasbourg, 1 Rue Laurent Fries, 67404 Illkirch Cédex, France. E-mail: irwin@igbmc.fr

Abbreviations: indel, insertion and deletion; SNV, single nucleotide variant; WES, whole exome sequencing

Received 30 August 2018; revised 11 January 2019; accepted 17 January 2019; accepted manuscript published online 15 February 2019; corrected proof published online XXX

areas. A month earlier at the individual's request, his dermatologist excised two pigmented lesions that had recently grown in size. A few days later, four other pigmented lesions were excised and histopathological examination suggested one superficial spreading melanoma and three in situ epidermotropic melanomas. Two years earlier, a pigmented lesion had been excised on his left shoulder that biopsy concluded was a melanoma.

During the next 6 years (Figure 1a), the individual developed once or twice per year in an eruptive manner, multiple asymmetric, pigmented, large (1−2 cm), irregular, often lobulated or spicular melanocytic lesions, randomly located on the trunk and the limbs (Figure 1b), the histological characteristics, discrete nature, and random location of which distinguished them from "in transit" cutaneous metastases. Subsequent lesions, of which 82 were surgically removed, had clear malignant histopathology highly suggestive of primary superficial spreading melanoma. Nevertheless, the synchronous appearance of multiple large lesions within less than 1 month was not compatible with this diagnosis. The excised lesions revealed a remarkable consistency in their histological features (Figure 1c, 1d) suggestive of primary melanomas with pagetoid melanocytic proliferation in the epidermis, and involvement of the upper part of the reticular and papillar dermis together with strong S100 staining. Multiple cell nests of varying size were seen in the basal and suprabasal layers of the epidermis, with substantial scattering of isolated cells or small nests up to the granular layer. Nests comprised mainly monomorphous ovoid cells, of which only a few were pigmented. Staining with CD8 antibody showed immune infiltrate in tumors from 2010 to 2016, illustrated in particular by presence of $CD8^+$ cells in the epidermal tumor nests (Supplementary Figure S1a online). Nevertheless, the number of infiltrating $CD8^+$ cells was strongly reduced in the 2015 and 2016 tumors (Supplementary Figure S1b).

During the 6-year period, no extracutaneous metastases developed and the individual received 3 million units of IFN-α every other day. In 2016, he developed metastasis in the left supraclavicular lymph nodes (Figure 1e) and the gallbladder. He received 15 perfusions of nivolumab without substantial response and then four perfusions of ipilimumab with an incomplete regression of lymph node metastasis. He was then shifted back to nivolumab, displaying a partial response with overall stability for about 1 year. In late 2018, the patient had recurrent episodes of headache, nausea, and vomiting with intense fatigue. Malignant melanocytes were eventually found in cerebrospinal fluid, though no meningeal thickening or cerebral metastases were found on repeated imaging studies. He died in November 2018. No autopsy was performed.

This case history describes what appeared as recurrent epidermotropic metastatic melanoma with stable phenotypic characteristics during a period of 6 years before the appearance of the first extracutaneous metastases.

Tumors share a set of trunk single nucleotide variants and indels

As no $BRAF^{V600E}$ or common oncogenic *NRAS* mutations were detected in the epidermal lesions and, given the exceptional clinical characteristics, we performed WES to investigate the genetic alterations in these tumors.

Analyses of the constitutive exome revealed the individual to be homozygous for several known melanoma risk polymorphisms: *MC1R*c.451C>T (p.Arg151Cys) in the *MC1R* gene, associated with red hair and in accordance with his phenotype, rs11515 in the 3′-untranslated region of *CDKN2A* and two polymorphisms rs10533201 and rs11282266 in *CDKN2AIP*. The *MC1R* and *CDKN2A* variants have been previously associated with increased melanoma risk (Aitken et al., 1999; Cust et al., 2012), while the risk associated with the other two variants is so far unknown (Kim et al., 2012). Although these polymorphisms may predispose to melanoma, they do not account for the exceptional clinical profile of this individual. Neither the affected individual's parents nor children (15 and 21 years old) have reported melanoma, arguing for a sporadic rather than a familial nature of the disease.

WES was performed on DNA extracted from frozen cutaneous tumor samples excised in 2015 and 2016, and from formalin-fixed, paraffin-embedded samples of lesions removed in 2010 and in 2012. Somatic single nucleotide variants (SNVs), indels, gene fusions, and rearrangements were identified. Sequencing statistics for each WES are listed in Supplementary Dataset S1 online, along with the location of each tumor, its cellularity, and ploidy.

SNVs predicted to affect coding potential were detected in each tumor using stringent filtering criteria (Figure 2a). Strikingly, a comparable number of SNVs were detected in each tumor, showing no major accumulation during this prolonged period, despite the higher read coverage in tumors 3 and 4 than in 1 and 2 (Supplementary Dataset S1). Comparison of SNVs present in the four tumors revealed branch SNVs shared between two or three tumors, private mutations found in only a single tumor and trunk SNVs present in all four tumors. The number of branch SNVs was highest between the chronologically closest tumors, with very few uniquely shared between tumors 1 and 4 or 2 and 4. The shared trunk SNVs indicated that the cutaneous lesions were not independent primary melanomas, but recurrent cutaneous metastases.

We asked whether SNVs detected in the 2015 and 2016 tumors were present in the 2010 and 2012 tumors, but at a lower frequency and not called using the stringent criteria mentioned. By lowering the detection threshold, the number of SNVs in tumor 1 increased to 741 and to 476 in tumor 2 (Figure 2b). In contrast, lowering the threshold did not lead to a comparable strong increase in the number of SNVs in tumors 3 and 4, confirming the absence of their accumulation even at low frequency over time. After this reanalysis, 73 trunk SNVs were detected (Supplementary Dataset S2 online). The high proportion of private and branch SNVs compared to trunk SNVs contrasts with previously reported low mutational diversity among metastases (Birkeland et al., 2018), and likely reflects the long period during which the metastases occurred in this individual. As with SNVs affecting coding potential, the number of "silent," mainly intronic SNVs was also reduced in the later tumors (Supplementary Figure S2a online).

We identified SNVs present in tumor 1, lost already in tumor 2 (*HYDIN*, Supplementary Figure S2c) or whose frequency

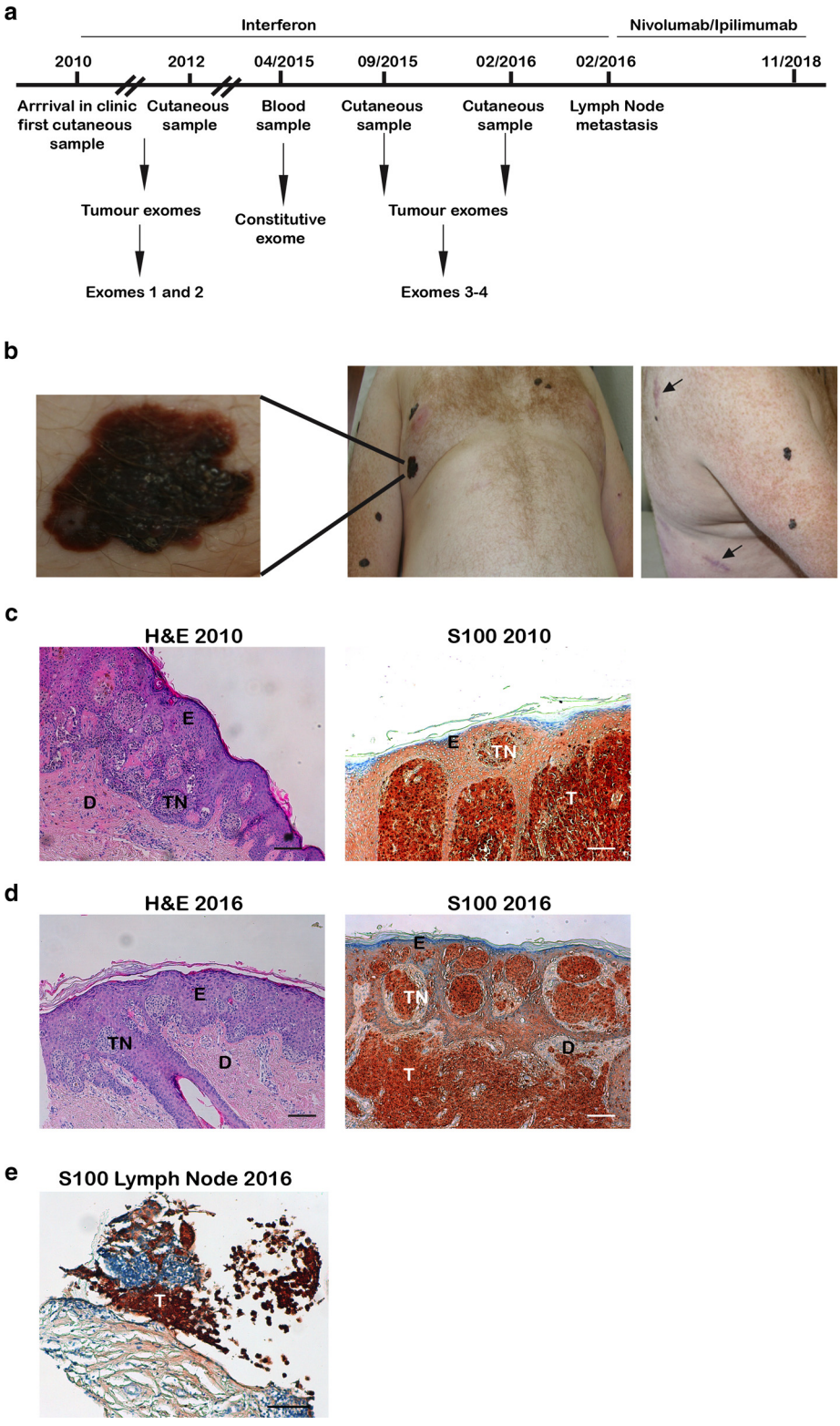

Figure 1. Atypical cutaneous melanoma. (**a**) Timeline summarizing case history, sample collection, and treatments. (**b**) Cutaneous lesions on the affected individual. Note scar tissue resulting from previous removal of lesions indicated by arrows in the right-hand panel. The left-hand panel shows a closeup of a typical lesion. (**c**) H&E- or S100A4-stained sections from lesions removed in 2010 and 2016 as indicated. (**d**) S100 staining of a section from the lymph node metastasis of 2016. Permission to publish and reproduce photographs was obtained with written informed consent from the affected individual. Scale bar = 100 μm. D, dermis; E, epidermis; H&E, hematoxylin and eosin; T, S100-labeled tumor cells; TN, tumor nest.

decreased more gradually (*CD55*), present in tumors 1 and 2, or *OSTC* present at very low frequency also in tumor 3. Other SNVs like, *SYVN1*, were present only in tumor 3 or, like *PDE1C*, were present at very low frequency in tumor 3 and much higher frequency in tumor 4. These analyses described SNVs initially present then lost, SNVs whose frequency increased over time and a set of more constant trunk SNVs over the prolonged period (Supplementary Figure S2d).

Interrogation of The Cancer Genome Atlas melanoma database showed that *RP1* is altered in 38% of melanomas (Supplementary Figure S2e) where 196 SNVs have been described. The G>A inducing amino acid substitution G962E

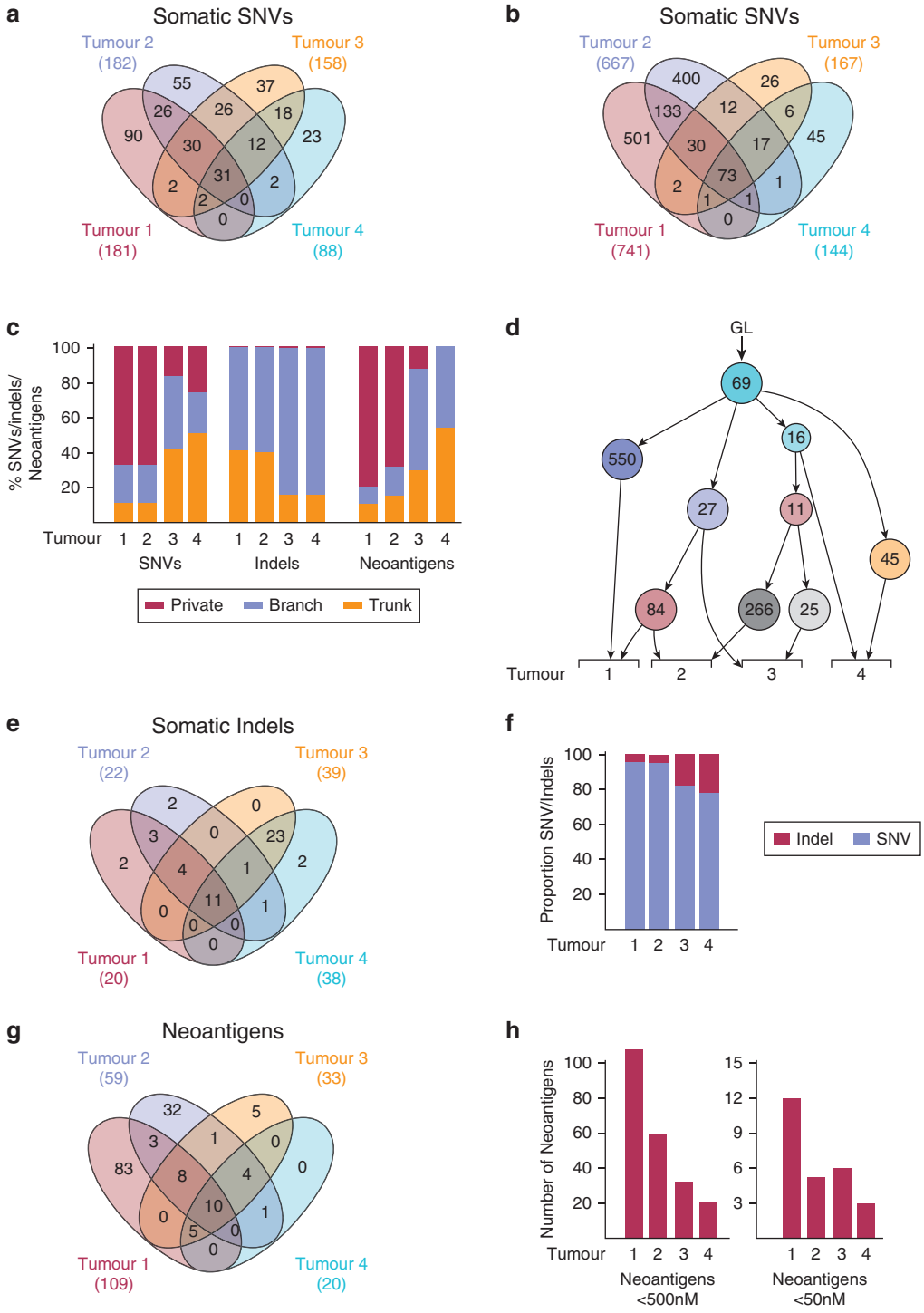

Figure 2. Genetics of melanoma metastases. Venn diagrams showing overlap of somatic SNVs in each tumor using stringent (**a**) or relaxed criteria (**b**). (**c**) Percentage of trunk, branch, and private SNVs, indels, or neoantigens in each tumor. (**d**) Subclonal compositions and phylogenetic tree illustrating relationships between tumors. The number of private, branch and trunk mutations defined by LICHeE differ from those defined by our filtering criteria. (**e**) Venn diagram showing somatic indels in each tumor. (**f**) Ratio between SNVs and indels during tumor evolution. (**g**) Venn diagram showing predicted neoantigens. (**h**) Neoantigens in each tumor using binding affinity criteria of <500 nM or <50 nM. indels, insertions and deletions; SNV, single nucleotide variant.

detected here was present in four other cases. Interrogation of the COSMIC database revealed eight instances of the G962E mutation, five in melanoma (four overlapping with The Cancer Genome Atlas), two basal cell carcinomas, and one squamous cell carcinoma. *RP1* (retinitis pigmentosa 1, axonemal microtubule associated) encodes a member of the doublecortin family. Germ line *RP1* mutations cause autosomal dominant, or autosomal recessive retinitis pigmentosa (Pierce et al., 1999; Sullivan et al., 1999). Its potential role in cancer, however, is not characterized. Six additional genes (not counting *MAP2K1*) mutated in the trunk were also frequently affected in melanoma, but with SNVs distinct from those in this study.

Counter selection of subclones with high neoantigen burden

These observations are consistent with persistent reseeding by cells comprising the trunk mutations in the form of branched subclones showing a progressive reduction in the number of SNVs. Trunk SNVs represented almost 50% of the SNVs in tumor 4 compared to only around 10% in tumor 1

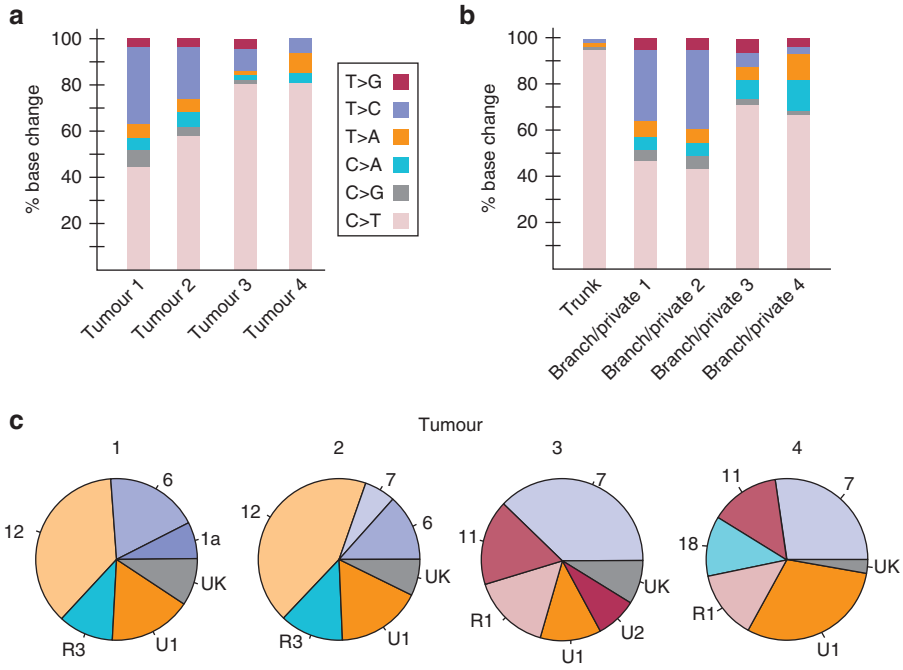

Figure 3. Mutational signatures. (**a**) The percentages of base changes of SNVs in each tumor are indicated. (**b**) The frequency of the base changes of trunk SNVs and the private and branch SNVs in each tumor are indicated. (**c**) The proportion of defined mutation signatures in each tumor are indicated as pie charts. SNV, single nucleotide variant.

(Figure 2c). Data analyses using Sequenza further indicated higher ploidy in the 2010–2012 tumors than in the later tumors (Supplementary Dataset S1). The progressive enrichment of the trunk SNVs through reductions in private and branch SNVs and ploidy suggested negative selection of highly mutated and genetically unstable clones in favor of cell populations with reduced SNV burden and close to normal ploidy. A phylogenetic tree showed that each tumor comprised at least two subclones derived from the trunk, with the most related subclones contributing to the chronologically closest tumors and the later tumors comprising subclones with fewer private and branch SNVs (Figure 2d).

We further identified private, branch, and trunk indels predicted to affect coding potential (Figure 2e, Supplementary Figure S2f, and Supplementary Dataset S3 online) and silent indels (Supplementary Figure 2b), but strikingly, while the number of SNVs decreased over time, indels accumulated. Consequently, the proportion of indels to SNVs increased in the later tumors (Figure 2f). To better understand this paradoxical evolution of the genetic makeup, we analyzed potential neoantigen load in each tumor. We inferred HLA alleles in each tumor and identified peptides where the mutated, but not wild-type, versions had predicted affinities of either <500 nM or <50 nM for the corresponding HLA types as high affinity neoantigens (Supplementary Dataset S4 online). SNVs strongly contributed to neoantigen burden, whereas indels made only a minor contribution. As a result, neoantigen load was much reduced in later tumors (Figures 2g, 2h). This observation showed that subclones with high neoantigen burden were counter selected, favoring emergence of later subclones with lower neoantigen burden. As SNVs, but not indels, strongly contributed to neoantigen burden, the SNVs were counter selected, whereas indels could accumulate with time. A close examination of the coding effect indels indicated that a majority were intronic and predicted to affect splicing with only a minority located in exons and directly affecting the coding sequence (Supplementary Dataset S3), accounting for their low contribution to neoantigens.

Alexandrov et al. (2013a, 2013b) have defined mutational signatures specific to different types of tumors with cutaneous melanoma normally dominated by C>T transitions (Hayward et al., 2017). SNV analyses showed that tumors 1 and 2 displayed a higher proportion of T>C than typical of cutaneous melanoma (Figure 3a). As a consequence, tumor signature 12, enriched in T>C, was highly represented in tumors 1 and 2 (Figure 3c). This signature is not typical of melanoma, but of liver or uterine cancer (Alexandrov et al., 2013a). However, between tumor 2 and tumors 3 and 4, the majority of newly acquired branch and private SNVs were C>T transitions such that they constituted >80% of the overall SNVs (Figure 3b). Trunk mutations were dominated by C>T transitions and their higher proportion in tumors 3 and 4 also contributed to the enriched C>T signature (Figure 3b) and the consequent strong representation of the typical melanoma signatures 7 and 11 (Figure 3c).

These analyses describe a unique view of the long-term evolution of the genetic landscape in recurrent cutaneous melanoma metastases. The shared trunk alterations indicated the lesions corresponded to metastases formed by persistent reseeding of subclones from a population of cells that gave rise to the earliest analyzed tumor in 2010, itself a likely metastasis derived from a primary tumor excised 2 years prior. Metastases do not necessarily accumulate mutations compared to the primary tumor (Shain et al., 2018), but individual metastases can be initiated by different cells from the primary tumor and, as observed here, metastases can comprise more than one population of cells (Sanborn et al., 2015). Here, a persistent cell population, identified by the trunk alterations, gave rise to multiple subclones that formed

the successive metastases. The case described here is analogous to MM61 (Birkeland et al., 2018), where the affected individual showed more than 100 cutaneous metastases covering multiple body regions as a result of persistent reseeding.

The melanoma analyzed here displayed several unique features, its recurrent nature, long-term absence of extracutaneous metastases, absence of common melanoma driver mutations, and absence of SNV accumulation. The reasons underlying these atypical features remain to be determined. Nevertheless, our analysis indicated that the disease course may be explained, in large part, by elimination of subclones with high SNV and neoantigen burden favoring the emergence of subclones with low SNV and neoantigen burden. Negative selection of subclones with high neoantigen burden is further consistent with the reduction in tumor infiltrating immune cells in the latter lesions. Neoantigen-mediated clonal selection can be a mechanism of resistance to immune checkpoint therapy (Anagnostou et al., 2017). In this individual, it appeared to occur as part of the natural disease history and may explain why the individual poorly responded to immune checkpoint therapy when subclones with low neoantigen burden eventually gave rise to lymph node and visceral metastases.

Identification of potential driver mutations activating the MAPK pathway

WES confirmed the absence of common melanoma driver mutations. Moreover, copy number variation analyses did not reveal alterations of *PTEN* or *CDKN2A* frequently deleted in melanoma (Supplementary Dataset S5 online). Instead, we identified a mutation in *MAP2K1* (MEK1) changing phenylalanine 53 into tyrosine (Figure 4a) among the trunk SNVs. F53 is located in a regulatory α-helix of MAP2K1, where its mutation in leucine, valine, or isoleucine have been described in lung adenocarcinoma associated with smoking. The F53L mutation was shown to activate ERK phosphorylation (Arcila et al., 2015). *MAP2K1* is affected in 7% of melanomas of The Cancer Genome Atlas database (Figure 4b) and only one mutation affecting F53 is registered (F53L, see Nikolaev et al., 2011). In all but one case, the *MAP2K1* mutations co-occurred with *BRAF* or *NRAS* mutations (Figure 4b). The F53Y mutation is, however, registered in the COSMIC database and was previously reported as a rare melanoma mutation (Shain et al., 2015a; Van Allen et al., 2014), or in pediatric-type nodal follicular lymphoma (Louissaint et al., 2016).

We identified translocations or inversions among which an inversion on chromosome 7 resulted in a fusion protein of 2,253 amino acids comprising exons 1−22 of *AKAP9* and exons 9−18 of *BRAF* containing the catalytic domain (Figures 4c, 4d). The breakpoints could be accurately mapped from multiple chimeric reads in tumor 3 (Figure 4c), but lower numbers of chimeric/discordant reads were detected in tumors 1, 2, and 4, showing that it was present from 2010 to 2016. The fusion protein resulted from a different breakpoint than previously described AKAP9-BRAF fusions (Ciampi et al., 2005; Fusco et al., 2005; Ross et al., 2016). Such fusion proteins conserve the catalytic BRAF domain, but lack the corresponding N-terminal regulatory domain and are hence constitutively active.

To assess the capacity of $MAP2K1^{F53Y}$ and the AKAP9-BRAF fusion protein to activate the MAPK pathway, we designed vectors expressing wild-type or mutated MAP2K1 with an N-terminal FLAG-tag and a vector expressing AKAP9-BRAF. As controls, we expressed wild-type or V600E-mutated BRAF. All recombinant proteins were detected in extracts from transfected serum-starved HEK293T cells (Figures 5a, 5b). ERK phosphorylation was mildly stimulated by $MAP2K1^{F53Y}$, but not by wild-type and more strongly by AKAP9-BRAF (Figure 5a, 5b). More importantly, co-expression of $MAP2K1^{F53Y}$ with either AKAP9-BRAF or $BRAF^{V600E}$ (Figure 5a) potently stimulated ERK phosphorylation to levels much higher than that seen with either of the proteins alone (Figure 5a, 5b). In both experiments, the synergistic ERK phosphorylation by the $BRAF^{V600E}$ or AKAP9-BRAF combination with $MAP2K1^{F53Y}$ was much stronger than that seen by the $BRAF^{V600E}$ and AKAP9-BRAF combination.

To test the ability of wild-type MAP2K1 and $MAP2K1^{F53Y}$ to stimulate ERK phosphorylation together with oncogenic NRAS, we expressed them in MM047 melanoma cells that harbor endogenous oncogenic *NRAS* (Verfaillie et al., 2015). In MM047 cells, ERK phosphorylation was stimulated by expression of $MAP2K1^{F53Y}$ or by AKAP9-BRAF, but not wild-type MAP2K1 (Figure 5c).

We verified ERK phosphorylation by immunohistochemistry in sections of tumors 3 and 4 and in the lymph node metastasis. In all samples, strong phosphorylated ERK staining could be seen in the tumor cells, but not in the surrounding keratinocytes or lymph node cells (Figure 5d).

These results show that $MAP2K1^{F53Y}$ was able to activate ERK phosphorylation, but less strongly than AKAP9-BRAF. Nevertheless, the combination of the two had a strong synergistic effect and $MAP2K1^{F53Y}$ could also cooperate with oncogenic NRAS. We have therefore identified two potential and synergistically acting driver mutations in this individual.

As described here, all but one of The Cancer Genome Atlas data set melanomas carrying *MAP2K1* mutations also showed either *BRAF* or *NRAS* mutations (Figure 4b). Interestingly, cases with *MAP2K1* and *BRAF* double mutations had a longer median survival (297 months) compared to cases that did not carry these mutations (78.9 months) (Figure 4c) and a longer median survival than *BRAF* alone (103 months, $P = 0.05$; The Cancer Genome Atlas data set, not shown). Therefore, melanomas with two mutations affecting the MAPK pathway may be less aggressive than *BRAF* alone, perhaps contributing to the long extracutaneous metastasis-free period seen with this individual.

MATERIAL AND METHODS

Affected individual and tumors

This study was conducted following approval by the University of Strasbourg Medical faculty ethics board and conducted according to good clinical practice. Biopsies from epidermal melanomas and permission to publish and reproduce photographs were obtained with written informed consent from the affected individual.

WES and data analyses

WES was performed by standard procedures on the Illumina HiSeq4000 platform of GenomEast (Illumina, San Diego, CA).

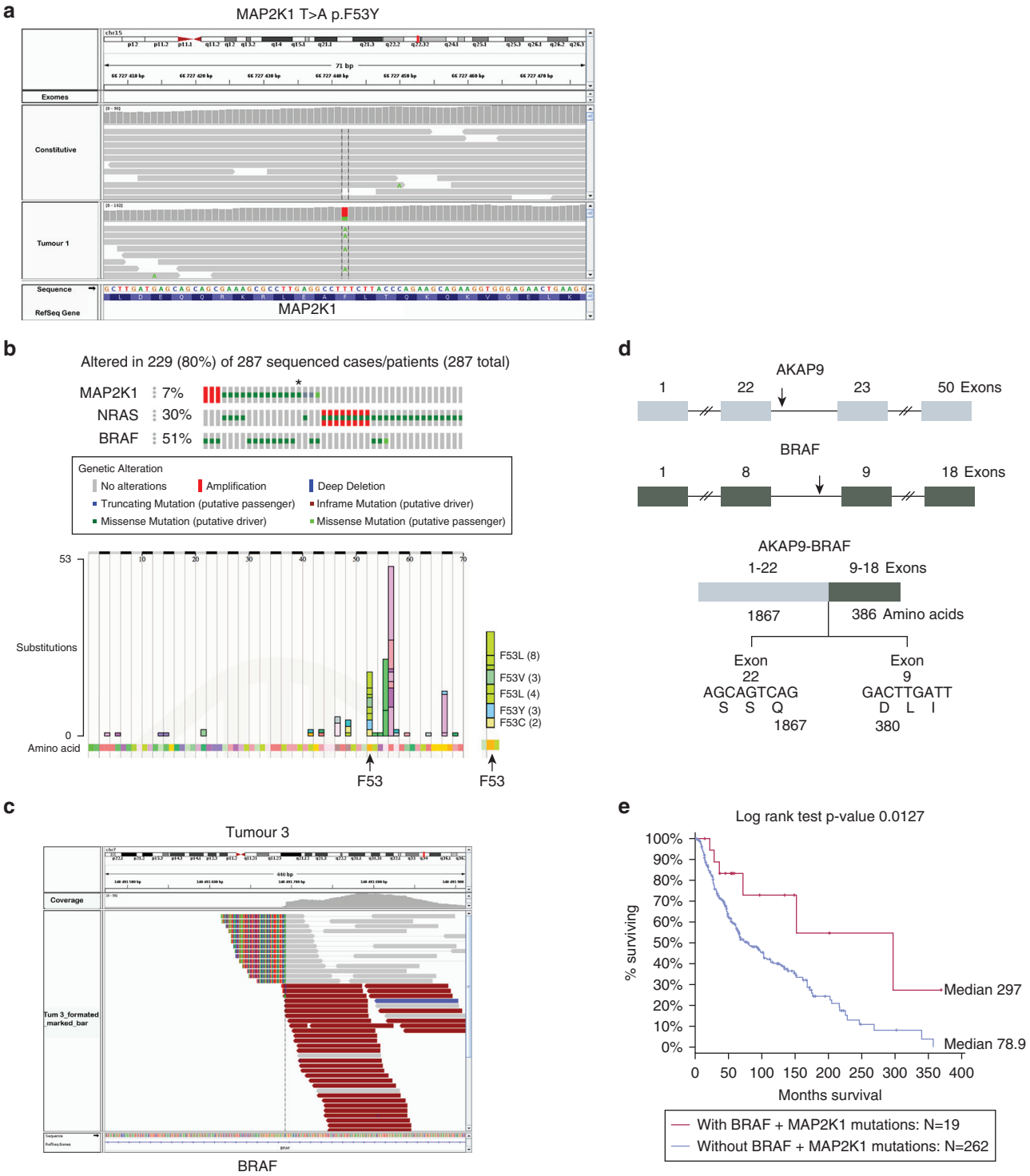

Figure 4. A rare combination of melanoma driver mutations. (**a**) Integrated Genomics Viewer screenshot illustrating the T>A single nucleotide variant changing the TTT (F) codon to TAT (Y) at amino acid position 53. (**b**) Screenshot of The Cancer Genome Atlas melanoma oncoprint showing MAP2K1, BRAF, and NRAS mutations. The asterisk shows the single case of an MAP2K1^{K57N} mutation in absence of BRAF or NRAS mutations. Lower panel shows a screenshot from the COSMIC database with MAP2K1 mutations at position F53. The adjacent K57 residue represents a hotspot in MAP2K1. (**c**) Integrated Genomics Viewer screenshot illustrating discordant and chimeric reads from tumor 3 at the *BRAF* locus. The breakpoint is indicated by the dotted vertical lines. (**d**) Schematic representation of the predicted AKAP9-BRAF fusion protein showing, introns, exons, number of amino acids and the last nucleotides and amino acids of AKAP9 exon 22, and the first of BRAF exon 9. (**e**) Kaplan-Meier survival curves for The Cancer Genome Atlas melanomas with or without combinations of BRAF and MAP2K1 mutations.

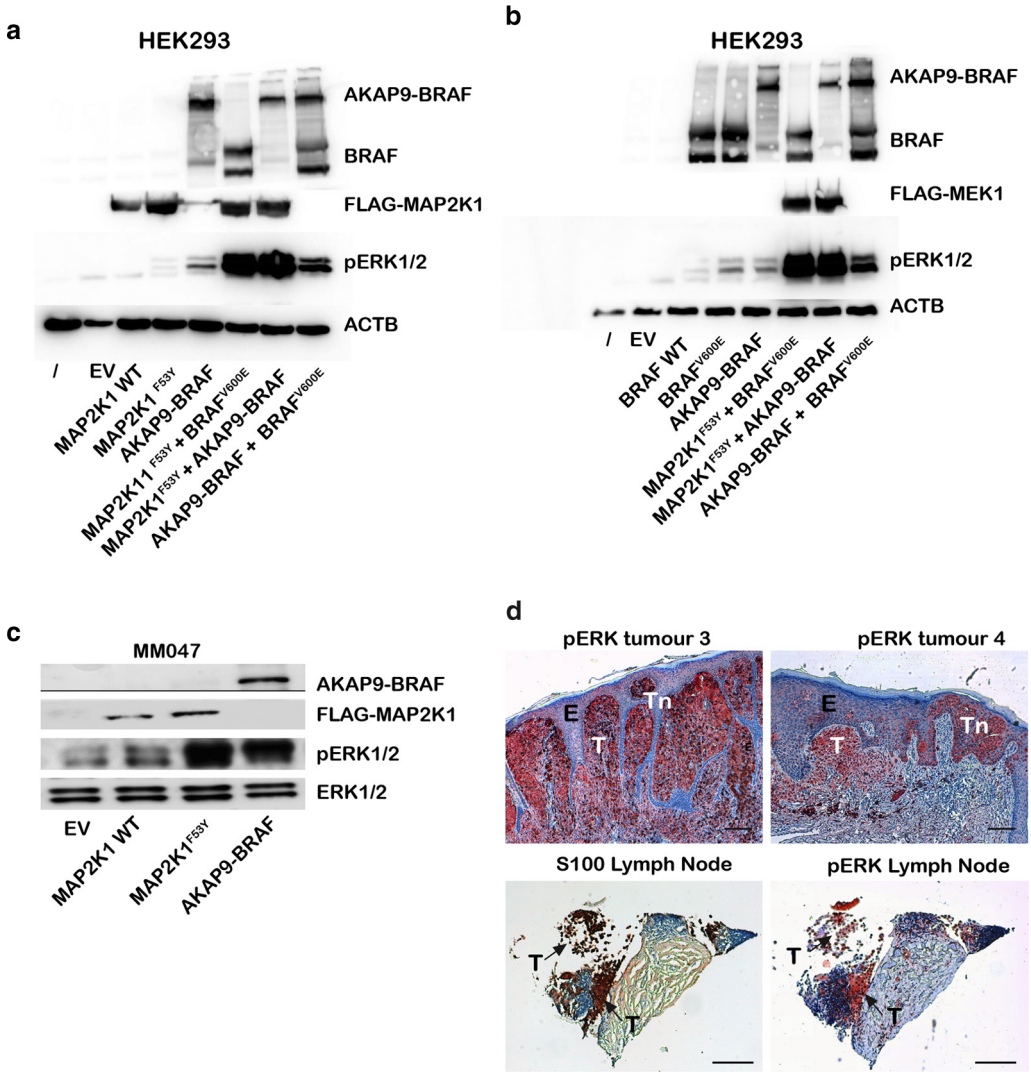

Figure 5. Driver mutations synergistically activate the AMPK signaling pathway. (**a**, **b**) Duplicate transfection experiments in serum starved HEK293T cells. Recombinant proteins are detected by Western blot. (**c**) Transfection of MM047 cells were transfected with the indicated expression vectors. (**d**) Phosphorylated ERK immunostaining of tumors 3 and 4. Lower panel: staining of lymph node metastasis, showing strong phosphorylated ERK staining of S100-labeled melanoma cells (T indicated by arrows). Scale bar = 100 μm. E, epidermis; EV, empty vector; T, melanoma tumor; TN, melanoma tumor nest.

Variant calling, indel realignment, and base quality score recalibration were performed with the GATK Toolkit, version 3.8-0, using hard-filtering parameters and the "newQual" option. Variants were annotated using SnpEff, version 2.0.5, and SnpSift, version 4.4l, with functional annotation and external databases (dbSNP, Hapmap, EVS, and 1000 Genomes). Variants were scored and ranked using VaRank. Somatic genome rearrangements were called by Meerkat.

Somatic variants were filtered with the following criteria: (i) stringent; (ii) a minimum of 30× coverage; (iii) a minimum of 10 instances of the variant; (iv) at least 10% of reads must carry the variation; and (v) variants must have a FisherStrand score <15 and a StrandOddsRatio <1.5 and Phred quality score of >10. Data were visualized with the Integrated Genomics Viewer. Variants were also filtered with (i) lower stringency; (ii) a minimum of 10× coverage; (iii) a minimum of three instances of the variant; (iv) at least 5% of reads must carry the variation; and (v) variants must have a FisherStrand score <15. For indels, a minimum coverage of two was required with a Phred quality score of >10. However, >97% of indels had a coverage >10. Ploidy and cellularity were estimated using R package Sequenza, version 2.1.2 (Favero et al., 2015). Mutational signatures were analyzed with R package deconstructSigs, version 1.8.0 (Rosenthal et al., 2016). HLA alleles present in each tumor were inferred with Polysolver, version 1.0 (Shukla et al., 2015). Neoantigens were determined using an in-house python script based on the TIminer API and NetMHCpan (Nielsen and Andreatta, 2016; Tappeiner et al., 2017). Mutant protein sequences of around 20 amino acids centered on the mutation site were retrieved and the binding affinities of 9mer peptides to HLA types inferred by Polysolver were assessed by NetMHCpan for both wild-type and mutant peptides. High-affinity neoantigens were defined as peptides where the mutated, but not the wild-type, version had affinities of <500 nM or <50 nM. Subclonal composition inference of each tumor and cell lineage tree construction were done with LICHeE (Popic et al., 2015). Copy number variations were called using CONTRA (Li et al., 2012).

Plasmid construction

Wild-type and F53Y MAP2K1 carrying an N-terminal Flag-tag were synthesized by GeneCopoeia and cloned into the M11 vector. AKAP9-BRAF carrying an N-terminal Flag-tag was synthesized by

Proteogenix and cloned into the pLent-N-Flag vector. The wild-type and V600E BRAF expression vectors were a gift from Colin Goding. All plasmids were resequenced before use.

Transfections and immunoblots

HEK293T cells were cultured in DMEM with 10% fetal calf serum, glucose (1 g/l), and penicillin/streptomycin (50 μg/μl). MM047 was grown in Ham's F10 nutrient mix (Invitrogen, Carlsbad, CA) supplemented with 10% fetal calf serum, 25 mM HEPES (Sigma, St Louis, MO), 5.2 mM Glutamax-1, and penicillin/streptomycin (50 μg/μl). Transfections, protein extraction, SDS-PAGE, and immunoblots were performed as described previously (Mengus et al., 2005). The following antibodies were used; Flag M2 (Sigma, F1804); BRAF (Santa Cruz Biotechnology, Santa Cruz, CA, sc-166), phosphorylated ERK1/2 (Santa Cruz Biotechnology, sc-7383), and total ERK1/2 (Cell Signaling, Danvers, MA, #9102).

Immunohistochemistry

Hematoxylin and eosin staining and immunohistochemistry were performed by standard procedures on 5-μm sections from the indicated tumors. Total ERK1/2 and phosphorylated ERK1/2 were detected using the antibodies described above.

Data availability statement

The data reported are available at the Sequence Read Archive database with access number PRJNA508873.

ORCID

Irwin Davidson: http://orcid.org/0000-0001-5533-1171

CONFLICT OF INTEREST

GM declares consulting for BMS, Pfizer, Ipsen, Astellas, and Novartis. The remaining authors state no conflict of interest.

ACKNOWLEDGMENTS

We thank all the staff of the Institute of Genetics and Molecular and Cellular Biology common facilities and the staff of the Strasbourg Hospital Dermatology Clinic. This work was supported by institutional grants from the Centre National de la Recherche Scientifique, the Institut National de Santé et de la Recherche Médicale, the Université de Strasbourg, the Association pour la Recherche Contre le Cancer, the Ligue Nationale Contre le Cancer, the Institut National du Cancer, the Agence Nationale de la Recherche-10-LABX-0030-INRT and ANR-10-IDEX-0002-02. The Institute of Genetics and Molecular and Cellular Biology high-throughput sequencing facility is a member of the "France Génomique" consortium (ANR10-INBS-09-08). ID is an *équipe labellisée* of the Ligue Nationale Contre le Cancer.

AUTHOR CONTRIBUTIONS

GD performed all of the bioinformatics analyses, AK and SC generated the expression vectors and performed the cell transfection experiments, ME, AK, and EP, supervised the collection of tumor samples and DNA preparation, DL performed patient management, diagnosis, and histopathology analyses, GD, GM, DL, and ID conceived experiments analyzed the data and wrote the paper.

SUPPLEMENTARY MATERIAL

Supplementary material is linked to the online version of the paper at www.jidonline.org, and at https://doi.org/10.1016/j.jid.2019.01.027.

REFERENCES

Aitken J, Welch J, Duffy D, Milligan A, Green A, Martin N, et al. CDKN2A variants in a population-based sample of Queensland families with melanoma. J Natl Cancer Inst 1999;91:446–52.

Alexandrov LB, Nik-Zainal S, Wedge DC, Aparicio SA, Behjati S, Biankin AV, et al. Signatures of mutational processes in human cancer. Nature 2013a;500(7463):415–21.

Alexandrov LB, Nik-Zainal S, Wedge DC, Campbell PJ, Stratton MR. Deciphering signatures of mutational processes operative in human cancer. Cell Rep 2013b;3:246–59.

Anagnostou V, Smith KN, Forde PM, Niknafs N, Bhattacharya R, White J, et al. Evolution of neoantigen landscape during immune checkpoint blockade in non-small cell lung cancer. Cancer Discov 2017;7:264–76.

Arcila ME, Drilon A, Sylvester BE, Lovly CM, Borsu L, Reva B, et al. MAP2K1 (MEK1) mutations define a distinct subset of lung adenocarcinoma associated with smoking. Clin Cancer Res 2015;21:1935–43.

Birkeland E, Zhang S, Poduval D, Geisler J, Nakken S, Vodak D, et al. Patterns of genomic evolution in advanced melanoma. Nat Commun 2018;9:2665.

Ciampi R, Knauf JA, Kerler R, Gandhi M, Zhu Z, Nikiforova MN, et al. Oncogenic AKAP9-BRAF fusion is a novel mechanism of MAPK pathway activation in thyroid cancer. J Clin Invest 2005;115:94–101.

Cust AE, Goumas C, Holland EA, Agha-Hamilton C, Aitken JF, Armstrong BK, et al. MC1R genotypes and risk of melanoma before age 40 years: a population-based case-control-family study. Int J Cancer 2012;131:E269–81.

Favero F, Joshi T, Marquard AM, Birkbak NJ, Krzystanek M, Li Q, et al. Sequenza: allele-specific copy number and mutation profiles from tumor sequencing data. Ann Oncol 2015;26:64–70.

Fusco A, Viglietto G, Santoro M. A new mechanism of BRAF activation in human thyroid papillary carcinomas. J Clin Invest 2005;115:20–3.

Goldstein AM, Tucker MA. Genetic epidemiology of cutaneous melanoma: a global perspective. Arch Dermatol 2001;137:1493–6.

Hawkes JE, Truong A, Meyer LJ. Genetic predisposition to melanoma. Semin Oncol 2016;43:591–7.

Hayward NK. Genetics of melanoma predisposition. Oncogene 2003;22:3053–62.

Hayward NK, Wilmott JS, Waddell N, Johansson PA, Field MA, Nones K, et al. Whole-genome landscapes of major melanoma subtypes. Nature 2017;545(7653):175–80.

Hodis E, Watson IR, Kryukov GV, Arold ST, Imielinski M, Theurillat JP, et al. A landscape of driver mutations in melanoma. Cell 2012;150:251–63.

Kim RN, Kim A, Kim DW, Choi SH, Kim DS, Nam SH, et al. Analysis of indel variations in the human disease-associated genes CDKN2AIP, WDR66, USP20 and OR7C2 in a Korean population. J Genet 2012;91:e1–11.

Lestre S, Joao A, Ponte P, Peixoto A, Vieira J, Teixeira MR, et al. Intraepidermal epidermotropic metastatic melanoma: a clinical and histopathological mimicker of melanoma in situ occurring in multiplicity. J Cutan Pathol 2011;38:514–20.

Li J, Lupat R, Amarasinghe KC, Thompson ER, Doyle MA, Ryland GL, et al. CONTRA: copy number analysis for targeted resequencing. Bioinformatics 2012;28:1307–13.

Louissaint A Jr, Schafernak KT, Geyer JT, Kovach AE, Ghandi M, Gratzinger D, et al. Pediatric-type nodal follicular lymphoma: a biologically distinct lymphoma with frequent MAPK pathway mutations. Blood 2016;128:1093–100.

Mengus G, Fadloun A, Kobi D, Thibault C, Perletti L, Michel I, et al. TAF4 inactivation in embryonic fibroblasts activates TGFbeta signalling and autocrine growth. EMBO J 2005;24:2753–67.

Nielsen M, Andreatta M. NetMHCpan-3.0; improved prediction of binding to MHC class I molecules integrating information from multiple receptor and peptide length datasets. Genome Med 2016;8:33.

Nikolaev SI, Rimoldi D, Iseli C, Valsesia A, Robyr D, Gehrig C, et al. Exome sequencing identifies recurrent somatic MAP2K1 and MAP2K2 mutations in melanoma. Nat Genet 2011;44:133–9.

Pierce EA, Quinn T, Meehan T, McGee TL, Berson EL, Dryja TP. Mutations in a gene encoding a new oxygen-regulated photoreceptor protein cause dominant retinitis pigmentosa. Nat Genet 1999;22:248–54.

Popic V, Salari R, Hajirasouliha I, Kashef-Haghighi D, West RB, Batzoglou S. Fast and scalable inference of multi-sample cancer lineages. Genome Biol 2015;16:91.

Rosenthal R, McGranahan N, Herrero J, Taylor BS, Swanton C. DeconstructSigs: delineating mutational processes in single tumors distinguishes DNA repair deficiencies and patterns of carcinoma evolution. Genome Biol 2016;17:31.

Ross JS, Wang K, Chmielecki J, Gay L, Johnson A, Chudnovsky J, et al. The distribution of BRAF gene fusions in solid tumors and response to targeted therapy. Int J Cancer 2016;138:881–90.

Sanborn JZ, Chung J, Purdom E, Wang NJ, Kakavand H, Wilmott JS, et al. Phylogenetic analyses of melanoma reveal complex patterns of metastatic dissemination. Proc Natl Acad Sci USA 2015;112:10995–1000.

Shain AH, Garrido M, Botton T, Talevich E, Yeh I, Sanborn JZ, et al. Exome sequencing of desmoplastic melanoma identifies recurrent NFKBIE promoter mutations and diverse activating mutations in the MAPK pathway. Nat Genet 2015a;47:1194–9.

Shain AH, Joseph NM, Yu R, Benhamida J, Liu S, Prow T, et al. Genomic and transcriptomic analysis reveals incremental disruption of key signaling pathways during melanoma evolution. Cancer Cell 2018;34:45–55 e4.

Shain AH, Yeh I, Kovalyshyn I, Sriharan A, Talevich E, Gagnon A, et al. The genetic evolution of melanoma from precursor lesions. N Engl J Med 2015b;373:1926–36.

Shukla SA, Rooney MS, Rajasagi M, Tiao G, Dixon PM, Lawrence MS, et al. Comprehensive analysis of cancer-associated somatic mutations in class I HLA genes. Nat Biotechnol 2015;33:1152–8.

Sullivan LS, Heckenlively JR, Bowne SJ, Zuo J, Hide WA, Gal A, et al. Mutations in a novel retina-specific gene cause autosomal dominant retinitis pigmentosa. Nat Genet 1999;22:255–9.

Tappeiner E, Finotello F, Charoentong P, Mayer C, Rieder D, Trajanoski Z. TIminer: NGS data mining pipeline for cancer immunology and immunotherapy. Bioinformatics 2017;33:3140–1.

The Cancer Genome Atlas Network. Genomic classification of cutaneous melanoma. Cell 2015;161:1681–96.

Van Allen EM, Wagle N, Sucker A, Treacy DJ, Johannessen CM, Goetz EM, et al. The genetic landscape of clinical resistance to RAF inhibition in metastatic melanoma. Cancer Discov 2014;4:94–109.

Verfaillie A, Imrichova H, Atak ZK, Dewaele M, Rambow F, Hulselmans G, et al. Decoding the regulatory landscape of melanoma reveals TEADS as regulators of the invasive cell state. Nat Commun 2015;6:6683.

White WL, Hitchcock MG. Dying dogma: the pathological diagnosis of epidermotropic metastatic malignant melanoma. Semin Diagn Pathol 1998;15:176–88.

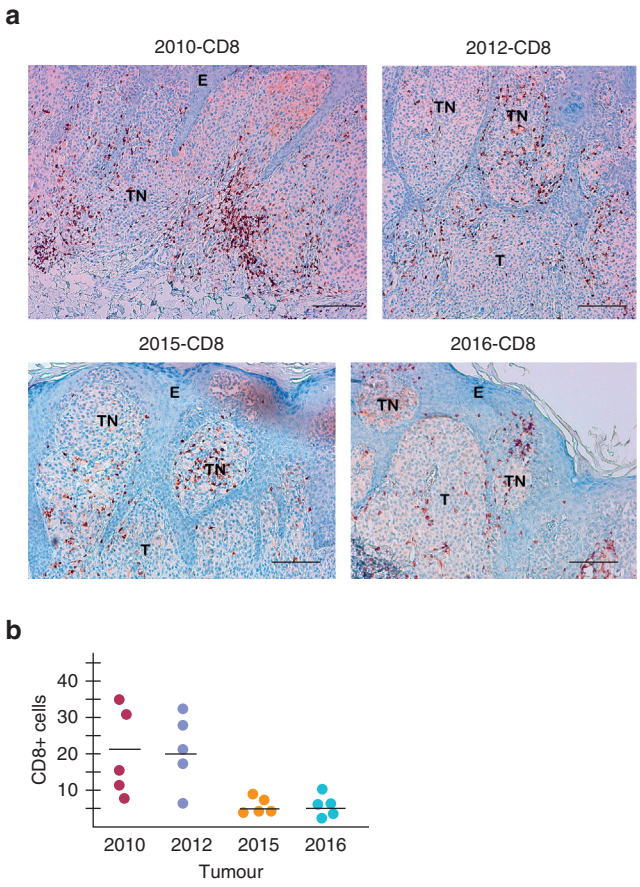

Supplementary Figure S1. Infiltrating immune cells in cutaneous metastases. (**a**) CD8 staining reveals immune infiltrate in tumors from 2010 to 2016. (**b**) Assessment of the number of CD8-positive cells in five random 200 × 200 pixel areas from two independent slides from each tumor. Scale bar = 100 μm. E, epidermis; T, melanoma tumor; TN, melanoma tumor nests within the epidermis.

a

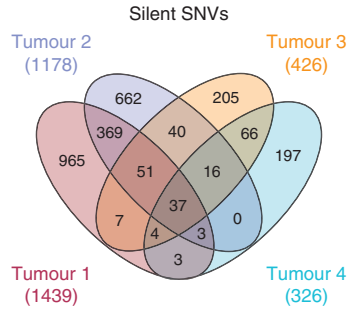

b

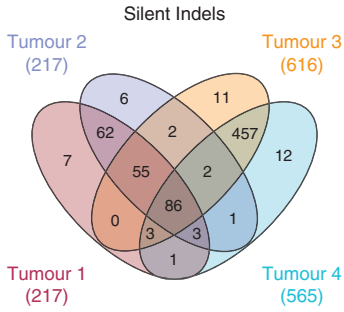

c

Gene	Ref	Mut	AA	Total read depth 1	2	3	4	Var read depth 1	2	3	4	% Var 1	2	3	4	Blood total/variant	
MAP2K1	T	A	F53Y	73	139	426	109	22	60	142	17	30	43	33	16	78/0	
OMA1	G	A	R18*	48	34	459	201	10	13	92	21	21	38	20	10	119/0	
STX11	G	A	D155N	175	194	1128	248	45	53	235	30	26	27	21	12	201/0	Trunk
TRIM56	C	T	S651L	105	159	474	168	17	33	92	19	16	21	19	11	68/0	
SLIT1	C	T	G559E	50	54	927	269	8	14	169	28	16	25	18	10	184/0	
DENR	G	T	A149S	15	11	86	42	0	1	10	2	0	9	12	4	13/0	
PDE1C	G	A	Splice	5	11	323	89	0	0	3	15	0	0	.09	17	78/0	
CD55	G	A	R392H	147	159	147	159	16	5	0	0	10	3	0	0	24/0	Branch and private
OSTC	G	A	A148T	121	193	163	80	15	4	1	0	12	4	0,6	0	46/0	
HYDIN	C	T	Splice	67	78	348	115	10	0	0	0	14	0	0	0	39/0	
SYVN1	C	A	Q351H	93	129	128	42	0	0	23	0	0	0	18	0	19/0	

d

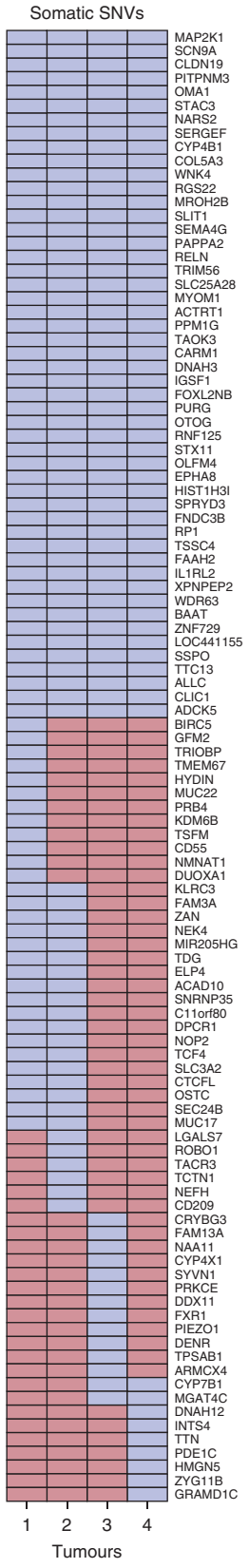

e

Gene	% TCGA
RP1	38
PAPPA2	30
DNAH3	29
HIVEP1	18
SCN9A	17
RGS22	14
CELSR1	13

f

Gene	Reads 1	2	3	4	Effect	
HRNR	31	25	516	107	Deletion; frameshift_variant	
TNRC18	94	98	65	28	Disruptive_inframe_insertion	Trunk
SVEP1	15	13	275	103	Deletion; splice_region_variant	
EZH2	0	0	447	135	Deletion; splice_region_variant	
RAPGEF2	0	0	0	67	Insertion; frameshift_variant	Branch and private
FAT1	42	31	0	0	Insertion; intron_variant	
HERC2	205	0	0	0	Insertion; frameshift_variant	

Supplementary Figure S2. Genetics of melanoma metastases. (**a, b**) Venn diagrams of silent SNVs and insertions and deletions. (**c**) Frequency of selected somatic SNVs in each tumor, together with the control coverage in the constitutive exome. (**d**) Heatmap showing the incidence of a representative set of SNVs in each tumor. Blue indicates presence of the SNV, red its absence. (**e**) Genes affected by the core set of SNVs frequently (>10%) affected in The Cancer Genome Atlas melanoma collection. (**f**) Frequency of selected somatic insertions and deletions in each tumor. SNV, single nucleotide variant.

ANNEXE 2

Cell Death & Differentiation (2019)

Chromatin remodellers Brg1 and Bptf are required for normal gene expression and progression of oncogenic Braf-driven mouse melanoma

Patrick Laurette*, Sébastien Coassolo*, Guillaume Davidson, Isabelle Michel, Giovanni Gambi, Wenjin Yao, Pierre Sohier, Mei Li, Gabrielle Mengus, Lionel Larue, Irwin Davidson.

Cell Death & Differentiation
https://doi.org/10.1038/s41418-019-0333-6

Cell Death & Differentiation

ARTICLE

Chromatin remodellers Brg1 and Bptf are required for normal gene expression and progression of oncogenic Braf-driven mouse melanoma

Patrick Laurette[1] · Sébastien Coassolo[1] · Guillaume Davidson[1] · Isabelle Michel[1] · Giovanni Gambi[1] · Wenjin Yao[1] · Pierre Sohier[2,3,4] · Mei Li[1] · Gabrielle Mengus[1] · Lionel Larue[2,3,4] · Irwin Davidson[1,4]

Received: 1 June 2018 / Revised: 4 March 2019 / Accepted: 28 March 2019

Abstract

Somatic oncogenic mutation of BRAF coupled with inactivation of PTEN constitute a frequent combination of genomic alterations driving the development of human melanoma. Mice genetically engineered to conditionally express oncogenic $Braf^{V600E}$ and inactivate Pten in melanocytes following tamoxifen treatment rapidly develop melanoma. While early-stage melanomas comprised melanin-pigmented Mitf and Dct-expressing cells, expression of these and other melanocyte identity genes was lost in later stage tumours that showed histological and molecular characteristics of de-differentiated neural crest type cells. Melanocyte identity genes displayed loss of active chromatin marks and RNA polymerase II and gain of heterochromatin marks, indicating epigenetic reprogramming during tumour progression. Nevertheless, late-stage tumour cells grown in culture re-expressed Mitf, and melanocyte markers and Mitf together with Sox10 coregulated a large number of genes essential for their growth. In this melanoma model, somatic inactivation that the catalytic Brg1 (Smarca4) subunit of the SWI/SNF complex and the scaffolding Bptf subunit of the NuRF complex delayed tumour formation and deregulated large and overlapping gene expression programs essential for normal tumour cell growth. Moreover, we show that Brg1 and Bptf coregulated many genes together with Mitf and Sox10. Together these transcription factors and chromatin remodelling complexes orchestrate essential gene expression programs in mouse melanoma cells.

Introduction

Melanoma is a highly aggressive skin cancer resulting from oncogenic transformation of melanocytes. Microphthalmia-associated transcription factor (MITF) and SOX10 are two critical transcription factors regulating gene expression programs essential for melanocyte and melanoma cell proliferation. We showed that MITF interacts with the PBAF chromatin remodelling complex, a member of the SWI/SNF family [1] in human melanoma cells [2–4]. Its catalytic subunit BRG1 is essential for the proliferation of MITF-high cells and immortalised Hermes 3A melanocytes. Both MITF and SOX10 [5] actively recruit BRG1 to chromatin to establish the epigenetic landscape of proliferative melanoma cells [4, 6]. In agreement with its potentially important role, BRG1 expression is frequently upregulated in human melanomas [7]. In mouse, somatic Brg1 inactivation in the melanocyte lineage leads to loss of developing melanoblasts and the resulting animals lack pigmentation [4, 8].

MITF also interacts with the NuRF chromatin remodelling complex and together they coregulate genes involved in

These authors contributed equally: Patrick Laurette, Sébastien Coassolo

Edited by S. Fulda

Supplementary information The online version of this article (https://doi.org/10.1038/s41418-019-0333-6) contains supplementary material, which is available to authorized users.

✉ Irwin Davidson
irwin@igbmc.fr

1 Department of Functional Genomics and Cancer, Institut de Génétique et de Biologie Moléculaire et Cellulaire, CNRS/INSERM/UNISTRA, 1 Rue Laurent Fries, 67404 Illkirch Cédex, France

2 INSERM U1021, Normal and Pathological Development of Melanocytes, Institut Curie, PSL Research University, Orsay, France

3 Univ. Paris-Sud, Univ. Paris-Saclay, CNRS UMR3347, Orsay, France

4 Equipes Labellisées Ligue Contre le Cancer, Paris, France

the proliferation of melanoma cells [9]. The gene encoding BPTF, the scaffolding subunit of NuRF, is amplified in around 5–7% of human melanomas [10]. BPTF expression can be upregulated during tumour progression and elevated BPTF expression is associated with poor prognosis and acquisition of resistance to BRAF inhibitors [11]. However, in contrast to Brg1, Bptf is not required for mouse melanoblast development, but is required for generation of melanocytes from the adult melanocyte stem cell population [9]. These two chromatin remodelling complexes therefore play distinct but complementary roles in the establishment and renewal of the melanocyte lineage and in human melanoma.

Given the essential but differing roles of BRG1/PBAF and BPTF/NuRF in human melanoma cells in vitro and in the normal physiology of mouse melanocytes in vivo, we addressed their implication in melanoma in vivo using a genetically modified mouse model.

Results

Initiation and evolution of Braf/Pten melanoma tumours

We established a previously described model [12–15] where treatment with 4-hydroxy-Tamoxifen (4-OHT) induces expression of oncogenic *Braf*^{V600E} and inactivates *Pten* selectively in the melanocyte lineage (*Tyr*:Cre-ER^{T2}::*Braf*$^{LSL\text{-}V600E/+}$::*Pten*$^{lox/lox}$). Adult mice were depilated and treated with a 5 µL drop of 5 mM 4-OHT leading to rapid appearance of small pigmented naevi and around 40 days later of prominent melanoma lesions (Fig. 1a). Fifteen days after 4-OHT treatment, histological examination revealed small naevus-like lesions with proliferating pigmented epithelioid melanocytes in the dermis surrounding the hair follicles (Fig. 1b) expressing Sox10, Mitf and Dct (Fig. 1c). As lesions progressed deeper into the dermis, a transition from pigmented epithelioid cells to a nonpigmented ovoid or spindle-shaped morphology was observed with some pigmented S100A4 or Dct-stained cells remaining close to the epidermis and more rarely deeper in the tumours (Figs. 1d, S1a and S2a). Later stage tumours were composed of bland spindle cells disposed haphazardly in a loose myxoid stroma and numerous regions showed a focal whorling of tumour cells (Fig. S1b, c). The invasive nature of these melanomas was highlighted by the appearance of pigmented and/or Sox10-labelled cells in lymph nodes and partially pigmented lung metastases (Fig. S1d, e). Cells invading the underlying dermal muscle by 26 days expressed invasive markers Zeb1 and Zeb2 (Fig. S2a, b). By 36 days however, Zeb1 and Zeb2 staining was weaker and more irregular with not all cells labelled (Fig. S2c).

At early stages, the majority of tumour cells stained with Mitf, Dct, S100A4, Sox10 (Fig. 1c, e) and Ki67 (Fig. 1f), whereas at later stages Mitf and Dct staining was progressively lost (Fig. 1e, f). Nonpigmented cells deep in larger tumours stained with KI67, whereas Dct staining was limited to the epidermal surface (Fig. S2d). Relative to their expression at day 22, expression of *Mitf*, *Dct* and *Tyr* was strongly diminished at later times, whereas expression of Sox10 increased (Fig. S3). While Mitf, Dct and Sox10 staining was restricted to tumour cells, Brg1 was present in cells of the tumour, the surrounding stroma and epidermis (Fig. 1e).

Hence, early melanoma cells express Mitf, and melanocyte markers, whereas later tumours invading deeper into the underlying dermis lost expression of Mitf and melanocyte genes, but maintained the SOX10 expression.

An epigenetic map of Braf/Pten melanoma tumours

We generated an epigenetic map of later stage tumours by ChIP-seq for acetylated lysine 27 of histone H3 (H3K27ac), marking active enhancers and promoters, trimethylated lysine 27 of histone H3 (H3K27me3), marking repressed heterochromatin, and RNA polymerase II (Pol II) (Fig. S4a, b). Around 2700 H3K27me3-marked genes with the absence of Pol II were identified (Fig. S4c) and strongly enriched in homeobox-containing and developmental genes involved in the differentiation of multiple ectodermal, mesodermal and endodermal tissues (Data set S1). These genes were stably repressed in the neural crest-derived tumour cells.

In contrast, the H3K27ac and Pol II data identified around 1500 highly transcribed genes with a 'super-enhancer' signature consisting of high levels of H3K27ac at wide regulatory elements around and within the coding region and high levels of transcribing Pol II [16–20] (Fig. 2a). Ontology analysis showed enrichment in transcription regulation, nucleosomes, angiogenesis, apoptosis and signalling pathways such as the cAMP response (Fig. 2a and Data set S1). Specifically, several clusters encoding core histones were identified along with transcription factors such as *Mycn*, *Zeb2* and *Snai2* or cyclins *Ccnd1* and *Ccnd3* (Fig. 2b and Data set S1). Core histones genes are short and intron-less and therefore may bias the analysis. Nevertheless, they were not detected in similar analyses of ChIP-seq data for 'super-enhancer' signature genes from mouse skeletal muscle or striatal neurons [21, 22]. Their presence in the signature here may rather reflect the active division of the mouse tumour cells.

The *Sox10* locus displayed a 'super-enhancer' signature, whereas, although extended regions with strong H3K27ac signals were seen throughout the *Mitf* locus, only a low level of Pol II was observed at the Mitf-A promoter with no Pol II signal at the Mitf-M promoter (Fig. 2b, c). No Pol II

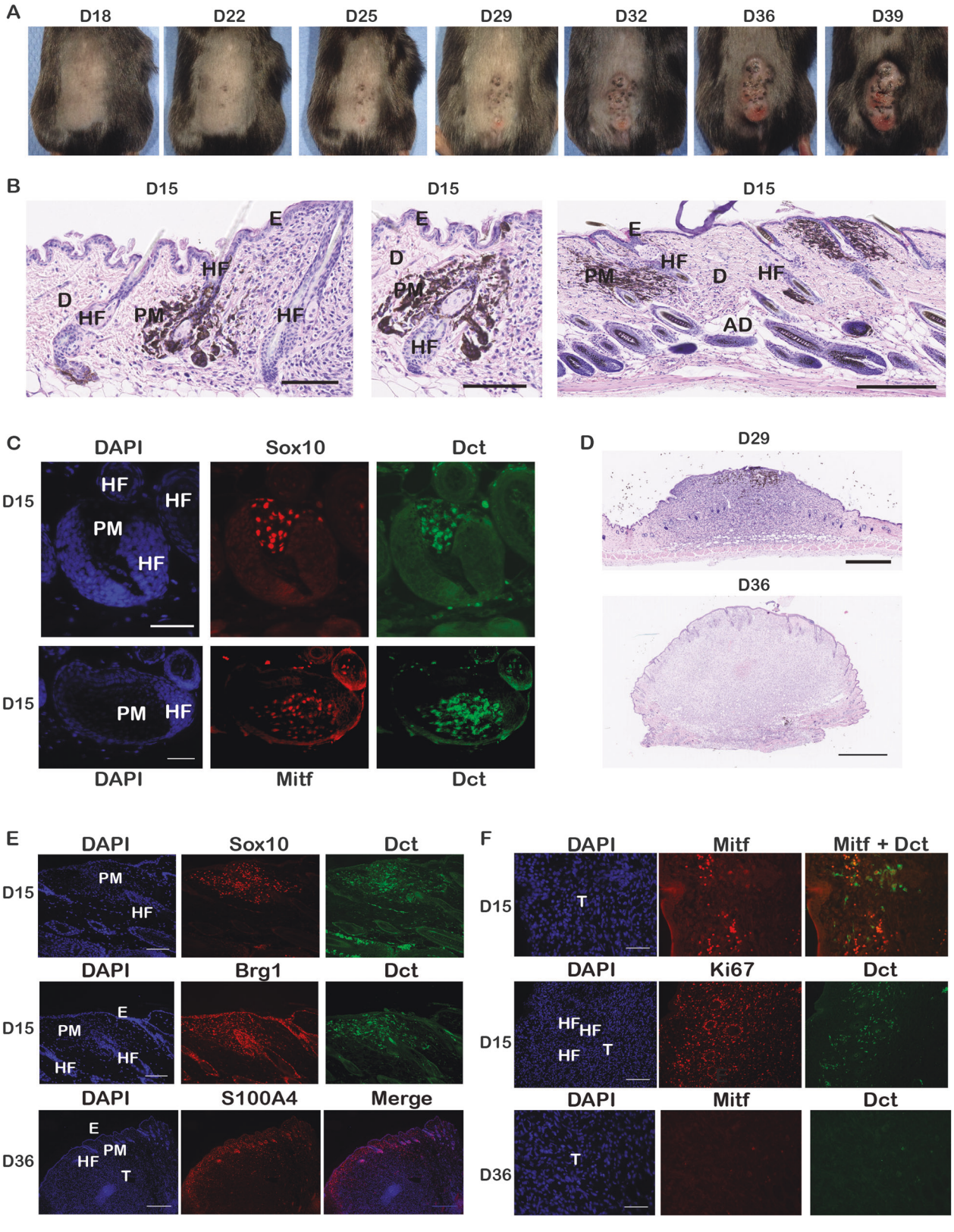

and low or no H3K27ac was seen at the *Dct* and *Tyrp1* promoters (Fig. S5a, b). Moreover, these loci were marked by H3K27me3. At the *Rab27a* locus, Pol II and H3K27ac signals seen around the TSS corresponded to expression of the divergently transcribed *Pigb*, whereas *Rab27a* was selectively marked by H3K27me3 (Fig. S5c). At the *Tyr*

◀ **Fig. 1** Development of oncogenic Braf-driven mouse melanoma. **a** Photographs of the 4-OHT-treated area on the backs of mice at the indicated days after treatment. **b** H&E-stained skin sections 15 days after 4-OHT treatment. HF hair follicle, PM pigmented melanocytes, E epidermis, D dermis, AD adipocytes. Scale bar 100 µm. **c** Immunofluorescence staining of sections from mouse skin 15 days after 4-OHT treatment with the indicated antibodies. DAPI-stained nuclei are also shown. Scale bar 100 µm. **d** H&E-stained sections from tumours 29 days (upper panel) and 36 days (lower panel) after 4-OHT treatment. Scale bar 500 µm. **e**, **f** Immunofluorescence of sections from mouse skin with the indicated antibodies along with DAPI-stained nuclei. In (**e**), the upper, middle and lower panels show sections taken 15, 15 and 36 days after 4-OHT treatment, respectively. In (**f**), the upper and middle panels show sections taken 22 and the lower panel 36 days after 4-OHT treatment, respectively. T tumour. Scale bar 100 µm, S100A4 panel, 400 µm

locus, no Pol II was seen at the TSS, but H3K27ac and H3K27me3 were observed at the TSS and the upstream enhancer, suggesting this locus was in a transcriptionally silent, but 'bivalent' [23] state (Fig. S5d). Alternatively, tumours may comprise two populations of cells, with either H3K27ac or H3K27me3. Irrespective of the explanation, no Pol II was seen in keeping with their lost expression. In contrast, a 'super-enhancer' signature was seen at the *Ngfr* and *Snai2* loci, two neural crest markers (Fig. S5e, f).

A transcriptional signature for human melanoma has been derived [24] comprising MITF and SOX10, but also TFAP2A, LEF1, DLX2, ALX1 PAX3 and GAS7. The *Dlx2, Lef1* and *Alx1* loci showed a striking absence of Pol II and H3K27ac and high levels of H3K27me3, whereas these loci were strongly marked by MITF, BRG1 and H3K27ac in human 501Mel melanoma cells (Fig. S6a, b). Only low levels of Pol II were seen at *Pax3* and for *Tfap2a* a mixed signature of high levels of H3K27ac and H3K27me3 was seen. Only *Gas7* showed high levels of H3K27ac and Pol II, a locus bound by SOX10 in 501Mel cells and in mouse melanocytes [25]. Persistent *Gas7* expression may therefore reflect its activation by Sox10, whereas loss of Mitf expression may account for repression of the other genes.

Hence in this model, tumours initially expressed melanocyte markers, but then progressively adopted a de-differentiated state switching off expression of Mitf, melanocyte marker and human melanoma melanocyte signature target genes.

Brg1 and Bptf are required for normal melanoma development in vivo

As mentioned in the introduction, BRG1 and BPTF are cofactors for MITF in human melanoma. We investigated their expression levels using TCGA datasets and recently published transcriptome data [26]. The *SMARCA4* gene encoding BRG1 was altered in 8% of TCGA melanoma, 8 truncating mutations and 1 deep deletion (Fig. S7a). All cases with loss of function mutations were associated with either *BRAF* or *NRAS* mutations, suggesting that loss of *SMARCA4* by itself is not a driver. *ARID2* was the most affected subunit, altered in 15% of melanoma with frequent truncating mutations, 5 of which occurred in a 'triple negative' background. *ARID1A* and *ARID1B* were altered at a frequency similar to *SMARCA4*, but with numerous truncating mutations and deep deletions, several occurring in the triple-negative background. *BPTF* was altered in 11% of melanoma with no truncating mutations or deep deletions, but frequent amplifications of which 7 of 28 occurred in a triple-negative background.

Consistent with the increased BRG1 protein levels [9], *SMARCA4* mRNA expression was upregulated in primary melanoma compared to benign naevi in the Badal data set (Fig. S7b). In contrast, *BPTF* expression was upregulated in metastatic versus primary melanoma (Fig. S7c). *BPTF* expression was also higher with NRAS mutations than with BRAF, NF1 or triple wild-type, whereas *SMARCA4* was lower expressed with *BRAF*-mutation (Fig. S7d).

We addressed the requirement for Brg1 and Bptf in mouse melanoma in vivo. They and several subunits of their respective complexes were expressed at relatively constant levels throughout tumour development (Fig. S3). We crossed *Tyr*::Cre-ER^{T2}:: *Braf*$^{LSL\text{-}V600E/+}$::*Pten*$^{lox/lox}$ animals with mice where the *Bptf* or Brg1 genes (*Smarca4*) were floxed such that they would be inactivated by the 4-OHT treatment and tumour formation was monitored.

Compared to mice wild-type or heterozygous for *Smarca4* and *Bptf*, inactivation of these genes strongly delayed tumour formation (Fig. 3a, b). Compared to large tumours in wild-type or heterozygous mice, much smaller lesions were observed on homozygous *Smarca4* or *Bptf* mice. The effect was strongest for *Bptf*-floxed animals where only small pigmented foci were seen by day 44, whereas small tumours were seen by this time in the *Smarca4*-floxed mice. Comparison of the number of days required for the tumours to reach a 1 cm^3 volume showed a strong delay in *Bptf*-floxed animals (median of 57 ± 6 days, compared to 34 ± 3 days for wild type) and a less marked delay (median of 46 ± 4 days) for *Smarca4*-floxed mice. Tumour formation was delayed from the earliest stages as the number of pigmented naevi seen at day 26 was dramatically reduced in the *Smarca4*- and *Bptf*-floxed animals (Fig. 3d, e).

Sections were prepared from the back skin or the tail of *Smarca4*-floxed mice 5 days after the 4-OHT application. In the hair follicle and tail epidermis, Dct-labelled melanocytes lacking Brg1 could be identified amongst surrounding Brg1-expressing keratinocytes (Fig. S8a, b). Nevertheless, a Dct-labelled melanocyte expressing Brg1 could be seen in the same follicle. Staining of another animal several days later also revealed a heterogeneous population where most

A

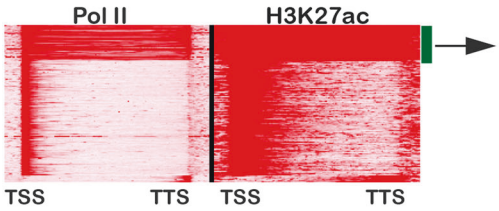

1587 genes

Functional Annotation Clustering

Term	E.S.	No. Genes	p-value
Nucleosome	10.1	42	8.3E-31
Nucleosome assembly	10.1	35	1.2E-22
Transcription regulation	8.2	110	3.2E-7

Go-BP-direct

Term	No. Genes.	p-value
Nucleosome assembly	35	1.2E-22
Transcription	114	2.0E-6
Angiogenesis	26	2.4E-6
cAMP response	12	3.4E-6
cell-cell adhesion	23	4.8E-6
Apoptotic process	46	6.2E-6

B

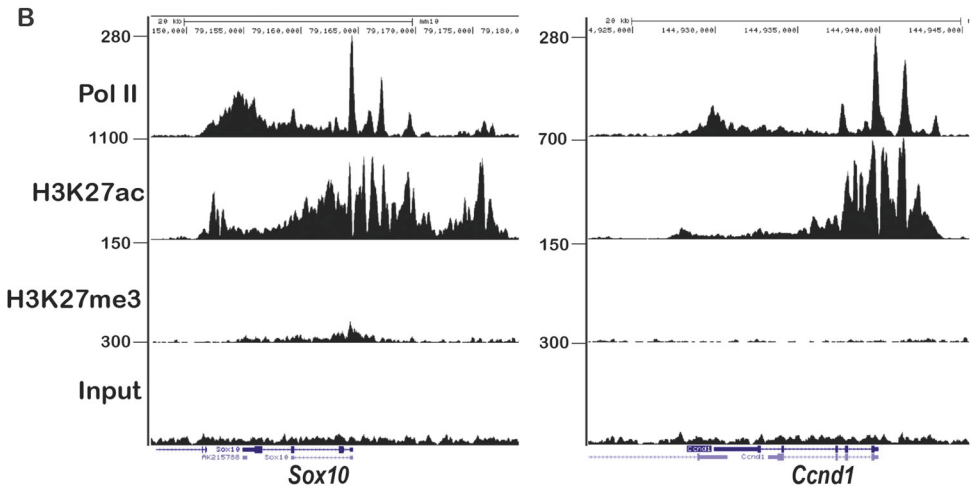

C

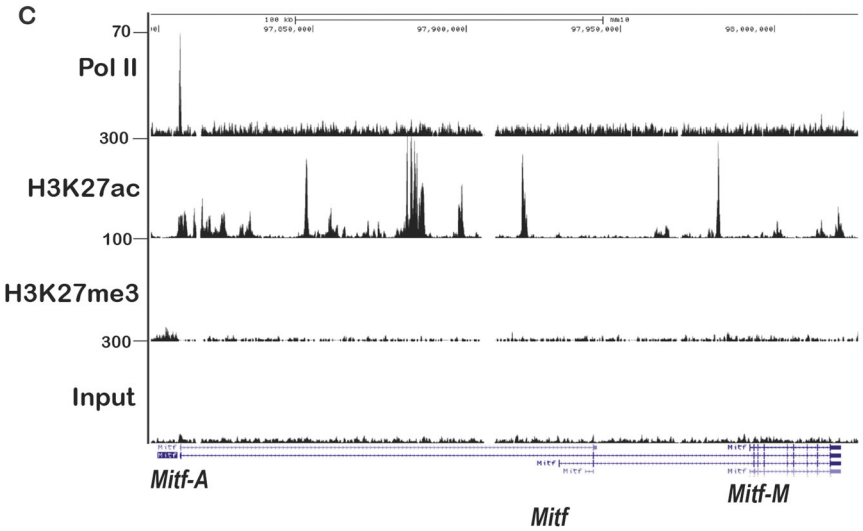

Fig. 2 An epigenetic map of oncogenic Braf-driven mouse melanoma. **a** Read density analyses of Pol II and H3K27ac of Ensembl annotated genes identifying those with a super-enhancer signature of high transcribing Pol II density and extended H3K27ac labelling. TSS transcription start site, TTS transcription termination site. Results of gene-annotation enrichment analysis of super-enhancer signature genes showing the enriched terms, the enrichment score (ES) and the modified Fisher exact *p* values. **b**, **c** UCSC genome browser view showing Pol II, H3K27ac and H3K27me3 profiles at the indicated loci

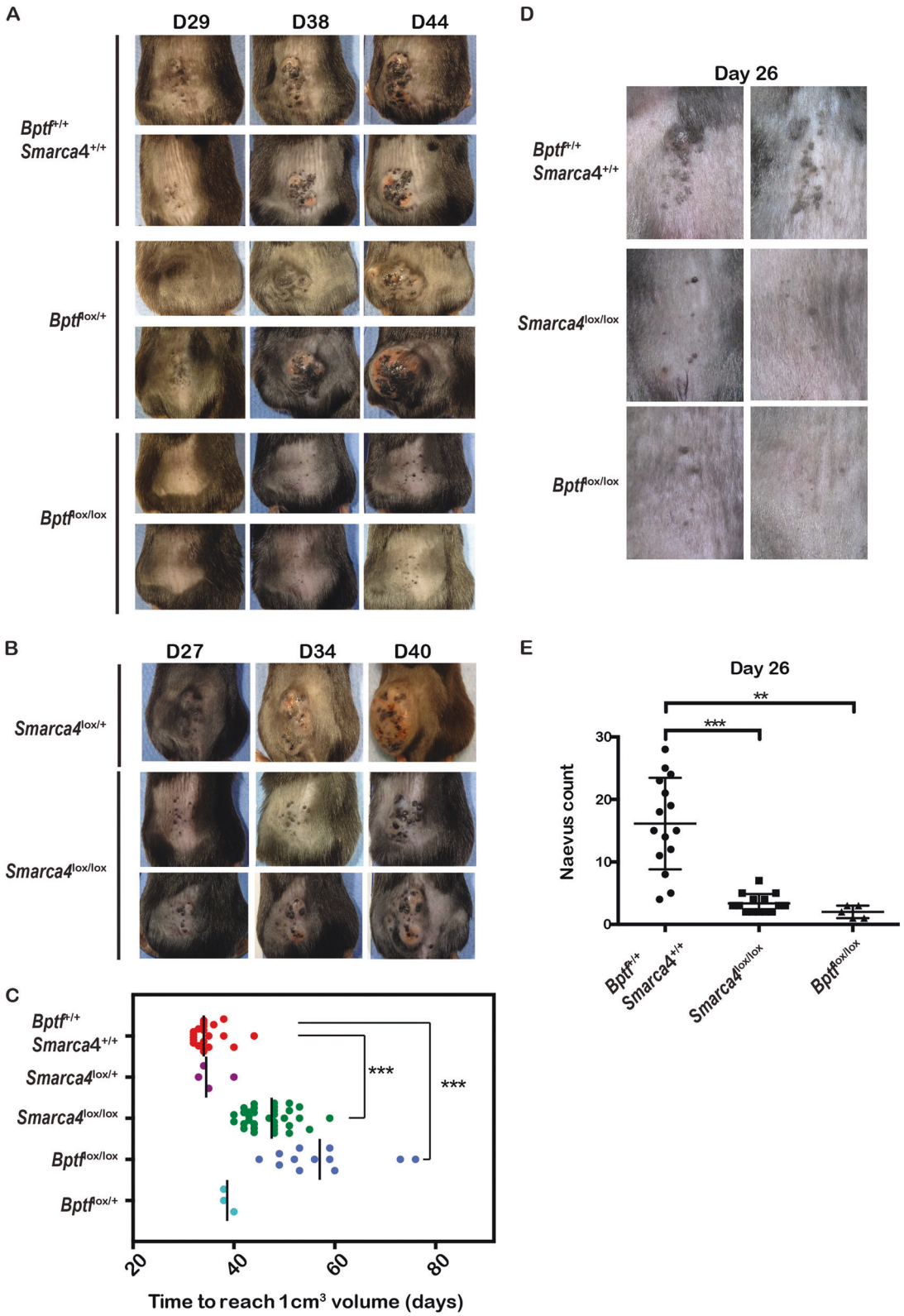

Dct-labelled melanocytes emerging from the hair follicle expressed Brg1, while Brg1-negative cells were still observed (Fig. S8c). In the early-stage dermal tumours, strong and homogeneous Brg1 labelling was observed (Fig. S8d). Immunoblots of later stage tumour extracts revealed expression of Brg1 and other SWI/SNF subunits in tumours from animals with a *Smarca4*$^{lox/lox}$ genotype and expression of Bptf and other NuRF subunits in tumours from animals

◀ **Fig. 3** Brg1 and Bptf are required for normal melanoma growth. **a**, **b** Photographs of the 4-OHT-treated area on the backs of *Tyr*:Cre-ER^{T2}; *Braf*$^{LSL\text{-}V600E/+}$; *Pten*$^{lox/lox}$ mice at the indicated days (29, 38 or 44) after treatment. The genotypes of mice with respect to the *Smarca4* and *Bptf* alleles are indicated to the left. **c** The number of days required for tumours to reach a volume of 1 cm^3 on mice with the indicated genotypes are indicated. ***$p < 0.001$ with unpaired two-tailed Student's *t* test. **d** Photographs of pigmented naevi developing on the Tam-treated areas on the backs of mice at day 26. The genotypes of mice are indicated to the left. **e** The numbers of pigmented naevi for each genotype are indicated. ***$p < 0.001$; **$p < 0.005$

with a *Bptf*$^{lox/lox}$ genotype (Fig. S9). Hence, tumours were formed from cells escaping full recombination of the floxed *Smarca4* and *Bptf* alleles.

These results showed that 4-OHT treatment inactivated Brg1 in a many, but not all, melanocytes. As a result, naevi and tumour formation were both delayed as they arose from a smaller initial pool of cells.

Mitf and Sox10 regulate overlapping gene expression programs in mouse melanoma cells

Later stage tumours with wild-type or homozygous floxed *Smarca4* or *Bptf* genotypes were excised, dissociated and the cells cultured in vitro. These in vitro cultured tumour cells expressed Sox10, and while Mitf was not expressed in later stage tumours from which the cells were isolated, immunostaining, RT-qPCR and RNA-seq showed its expression was reactivated after 24–48 h in vitro (Fig. 4a, b and Fig. 5). Cells from wild-type tumours were transfected with siRNAs directed against *Sox10* or *Mitf* leading to pronounced morphological modifications (Fig. 4c) and a strong reduction in the number of viable cells (Fig. 4d).

We performed RNA-seq from the si*Mitf* and si*Sox10* silenced cells. Using standard criteria on triplicate samples (Log2 fold change >1; <−1 and $p < 0.05$) or more relaxed criteria (Log2 fold change >0.5; <−0.5 and $p < 0.05$), we found a large overlap between the regulatory programs of Mitf and Sox10 (Fig. 5a, b and Data set S2) consistent with the binding of MITF and SOX10 together at regulatory elements in human melanoma cells [4]. Ontology analyses showed pigmentation and UV-response genes were downregulated in both conditions along with cell membrane and extracellular proteins (Fig. 5c, d). Paradoxically, a large collection of cell cycle and mitosis genes positively coregulated by MITF and SOX10 in human melanoma cells [4, 27] appeared negatively regulated in mouse melanoma cells and were upregulated upon si*Mitf* or si*Sox10* silencing (Fig. 5e). These cell cycle genes were observed only when more relaxed criteria were used showing they were not potently upregulated, but they were strongly represented in the 511 Mitf and Sox10 co-upregulated genes (Fig. 5b).

Brg1 and Bptf regulate extensive gene expression programs in mouse melanoma cells

Cultured cells of appropriate genotypes were treated with 4-OHT to recombine residual floxed *Smarca4* or *Bptf* alleles. Treatment of *Smarca4*$^{lox/lox}$ cells led to a loss not only of Brg1, but also of multiple other subunits of the PBAF complex and of Sox10 (Fig. 6a). Treatment of *Bptf*$^{lox/lox}$ cells led to diminished Bptf and Smarca5 expression, but not of Smarca1 (Fig. 6b). 4-OHT treatment of wild-type tumour cells had little effect on their morphology, whereas treatment of cells from *Smarca4*$^{lox/lox}$ or *Bptf*$^{lox/lox}$ tumours led to a major change in cell morphology, cytoskeleton reorganisation and reduced cytoplasmic volume (Fig. 6c). In addition, while 4-OHT treatment had little effect on the viability of wild-type cells, viability of *Smarca4*$^{lox/lox}$ or *Bptf*$^{lox/lox}$ cells was strongly diminished (Fig. 6d) with a concomitant increase in apoptosis 72 h after treatment (Fig. 6e). After 10 days, almost no viable *Smarca4*$^{lox/lox}$ or *Bptf*$^{lox/lox}$ tumour cells persisted.

RNA-seq following 4-OHT-induced Brg1 or Bptf inactivation revealed de-regulation of more than 2000–3000 genes with a notable overlap of the programs controlled by each factor (Fig. 7a and Data set S2). Bptf inactivation deregulated genes involved in cell cycle and mitosis, innate immunity, secreted glycoproteins and oxidative phosphorylation (Fig. 7b). Brg1 inactivation also downregulated innate immunity, secreted glycoprotein genes and upregulated genes of the TP53 pathway (Fig. 7c). These data show that Brg1 and Bptf regulate extensive gene expression programs affecting multiple functional pathways in mouse melanoma cells.

A comparison of the Mitf, Sox10, Brg1 and Bptf regulated genes identified sets of coregulated genes (Fig. 7d, e). Using hypergeometric probability to calculate the representation factor (RF), we found in each case a highly significant overlap. More than 50% of genes downregulated by Mitf or Sox10 silencing were also down following Brg1 inactivation (Fig. 7d, e). This group of genes were enriched in signalling pathways such as Hippo, Wnt and MAP kinase, as well as melanogenesis (Data set S2). Brg1 and Bptf therefore coregulated a notable fraction of Mitf and Sox10 target genes. However, Brg1 and Bptf regulated additional genes and functional pathways, showing they acted as more general cofactors.

Discussion

Similarities and differences between human melanoma and mouse oncogenic BRAF-driven melanoma

The genetically modified mouse model described here was used to study the roles of CTNNB1, PIKC3A, DNMT3B

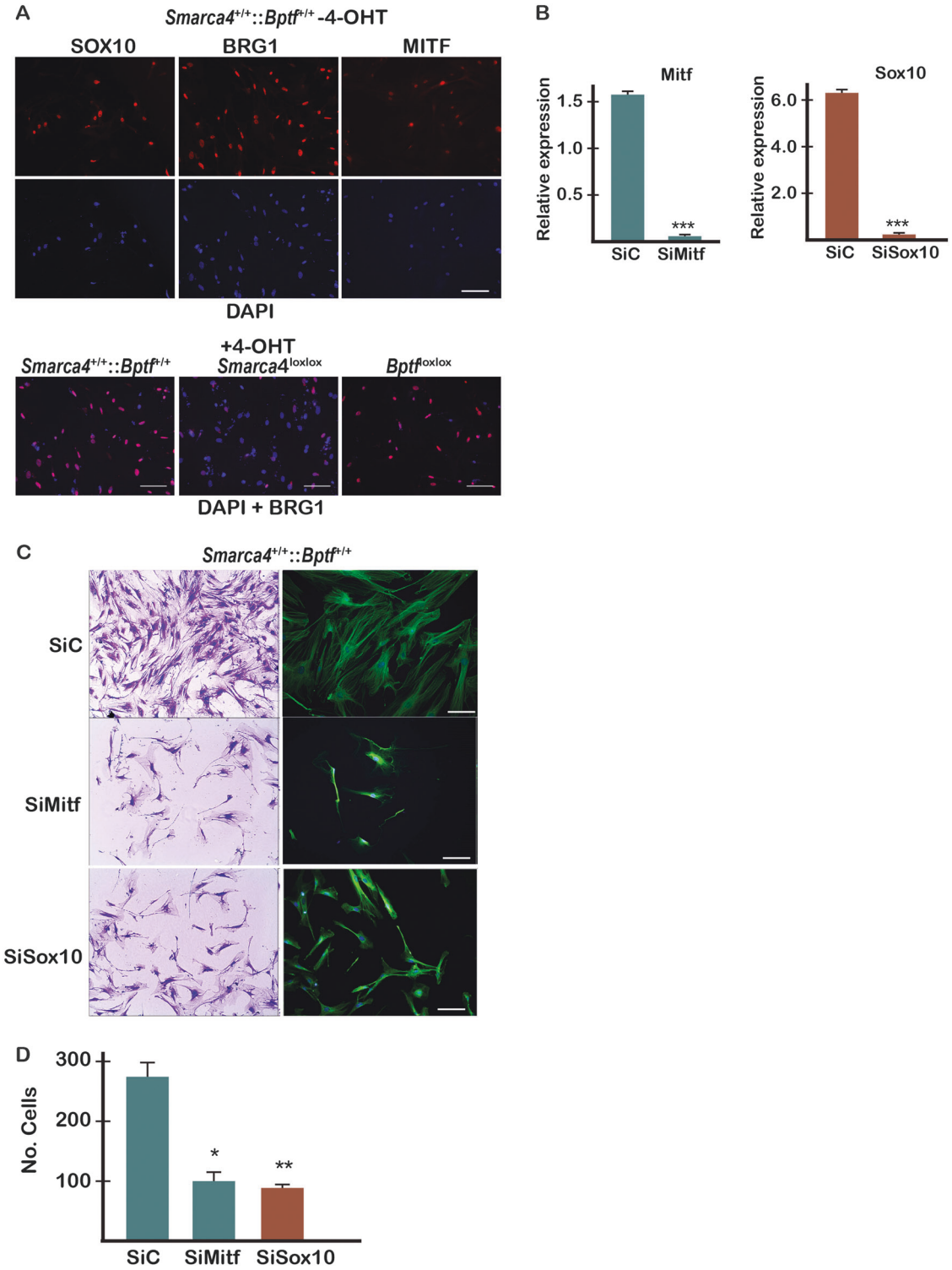

Fig. 4 Sox10 and Mitf are required for tumour cell growth in vitro. **a** Immunofluorescence staining of cultured mouse melanoma cells with the indicated antibodies and DAPI staining of nuclei. Scale bar 100 µm. 4-OHT treatment leads to loss of Brg1 staining in the cells with floxed Smarca4 alleles, but not in the other genetic backgrounds. **b** RT-qPCR of Mitf and Sox10 expression 48 h after transfection the indicated siRNAs. **c** Staining with Crystal Violet and immunolabelling with beta-tubulin and counting of cells 72 h after transfection. $N = 3$. $*p < 0.05$; $**p < 0.01$; $***p < 0.005$

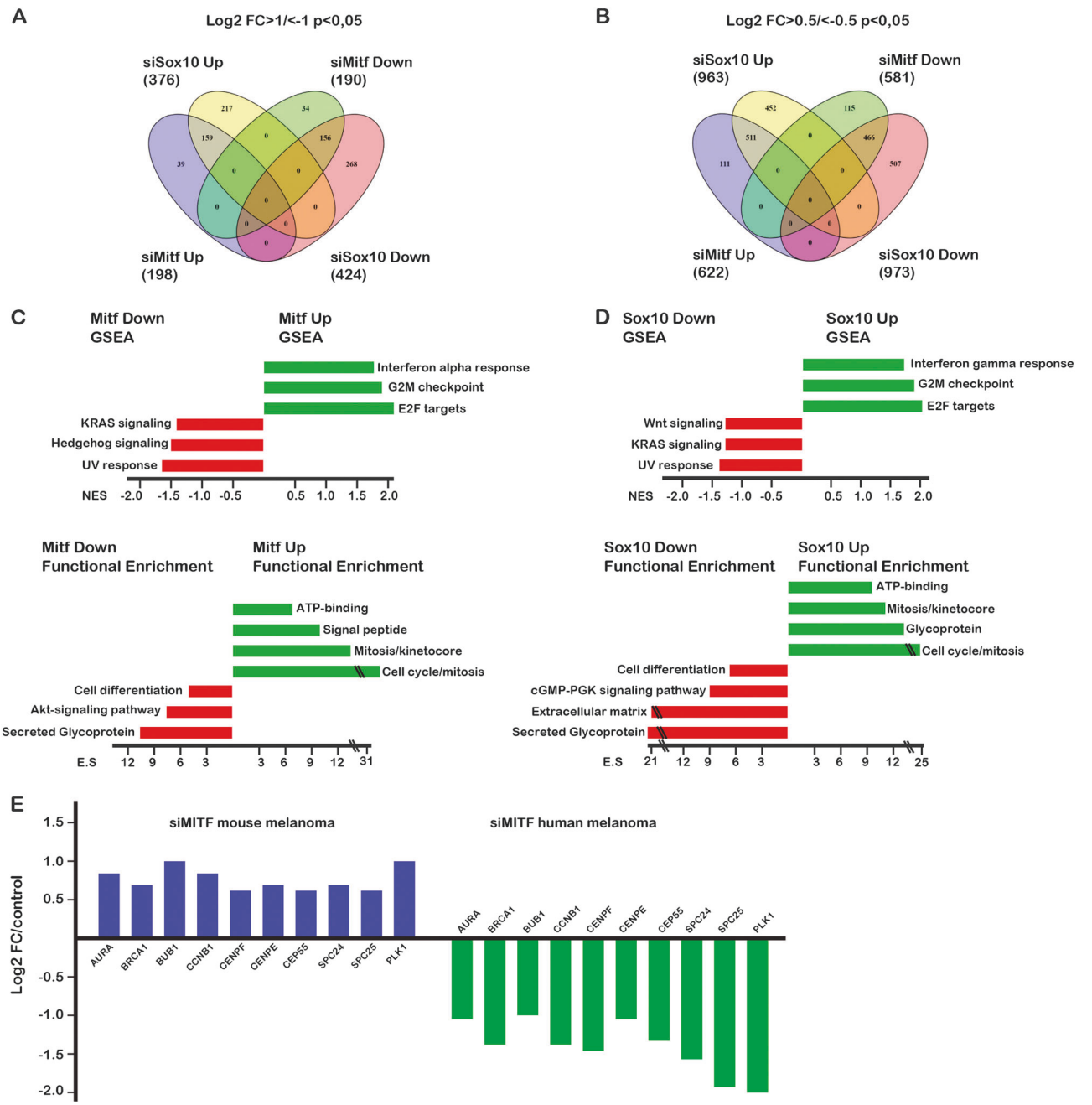

Fig. 5 RNA-seq analyses of Mitf and Sox10-regulated gene expression. **a**, **b** Venn diagrams indicating the number of up- and down-regulated genes after siMitf or siSox10 silencing compared to control siRNA. Each Venn shows the overlap between the two data sets using the indicated cut-off criteria. **c**, **d** Ontology analyses of regulated genes using GSEA or the DAVID Functional Enrichment tool. **e** Expression changes of selected cell cycle and mitosis genes after siMitf in mouse or human 501Mel melanoma cells

and PDK1 in melanoma development [12, 13, 15, 26, 28]. At least two models have been independently developed [12, 14] using Cre-ER^{T2} transgenes with differing expression profiles. Despite this, the resulting tumours have not been fully characterised, particularly at the epigenetic level. At early stages, tumours comprised Sox10, Dct, and Mitf-expressing melanocytes, whereas cells in later tumours reaching deep into the dermis lost expression of melanocyte markers and gained that of invasion markers, such as Zeb1 and Zeb2, but with persistent expression of Sox10.

Primary dermal melanomas are a rare occurrence in humans. The focal whorling patterns and loose myxoid background seen in later stage mouse tumours also differentiate them from what is typically observed in human melanoma. However, using a Braf/Pten genetic model, Kohler et al. [29] performed cell lineage tracing to show

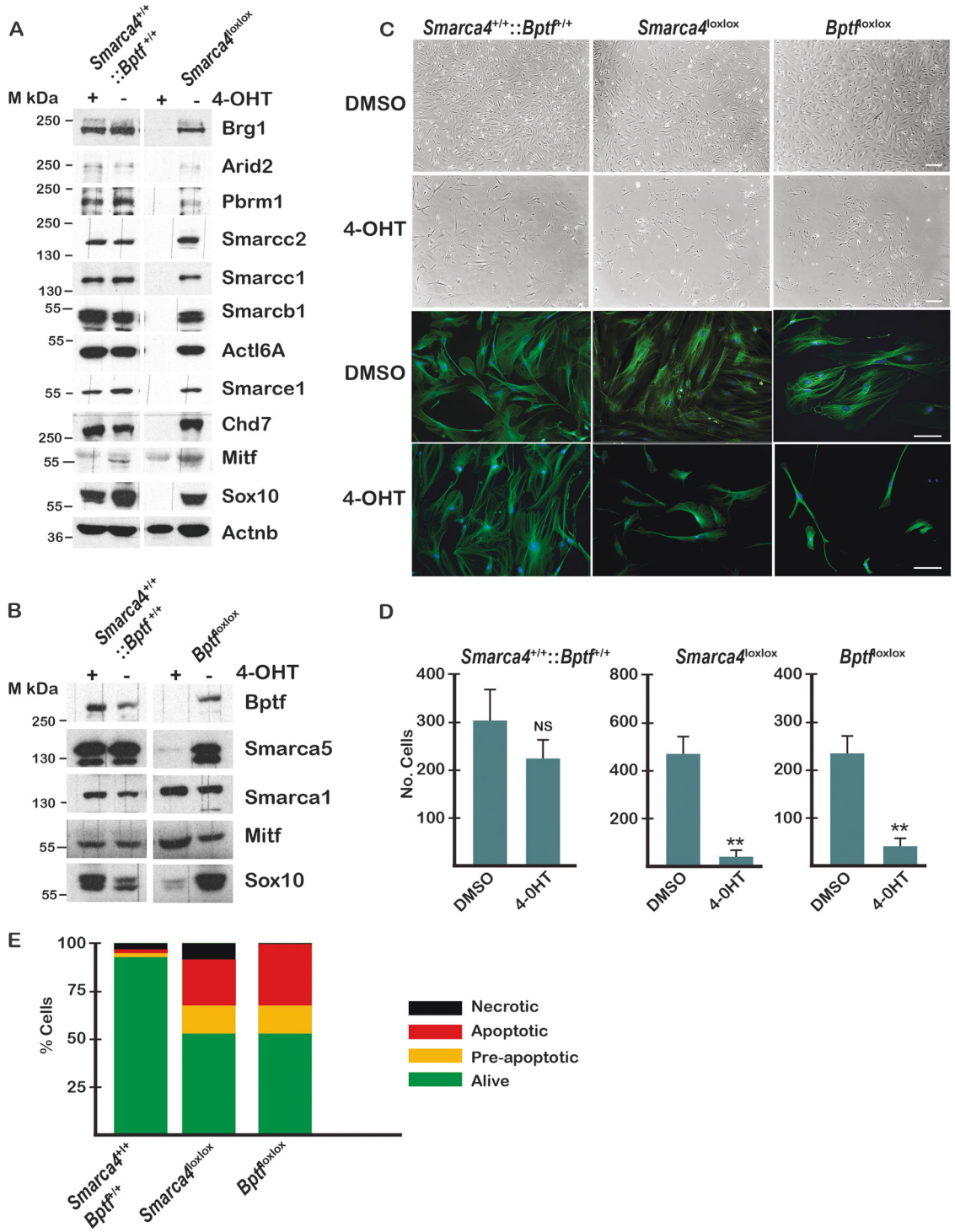

Fig. 6 4-OHT-induced inactivation of Brg1 and Bptf in cultured mouse melanoma cells. **a**, **b** Immunoblots from the indicated cells 48 h after treatment with 4-OHT or DMSO as control. The position of migration of molecular mass markers is indicated. **c** Bright field views and immunolabelling with beta-tubulin of cultured melanoma cells with the indicated genotypes 48 h after treatment with DMSO or 4-OHT. Scale bar 100 µm **d** Number of viable cells counted in each condition 48 h after the indicated treatments. $N = 3$. $^{**}p < 0.01$. **e** FACS analyses to detect Annexin V-stained apoptotic cells 48 h after 4-OHT treatment

that melanoma developed from mature melanocytes in the tail epidermis and pigmented Mitf-expressing bulb melanocytes analogous to what we observed here. Thus, transformed melanocytes originate from the epidermal compartment, but invasion of dermis is rapid occurring a few days after 4-OHT exposure. In the tail, transformed

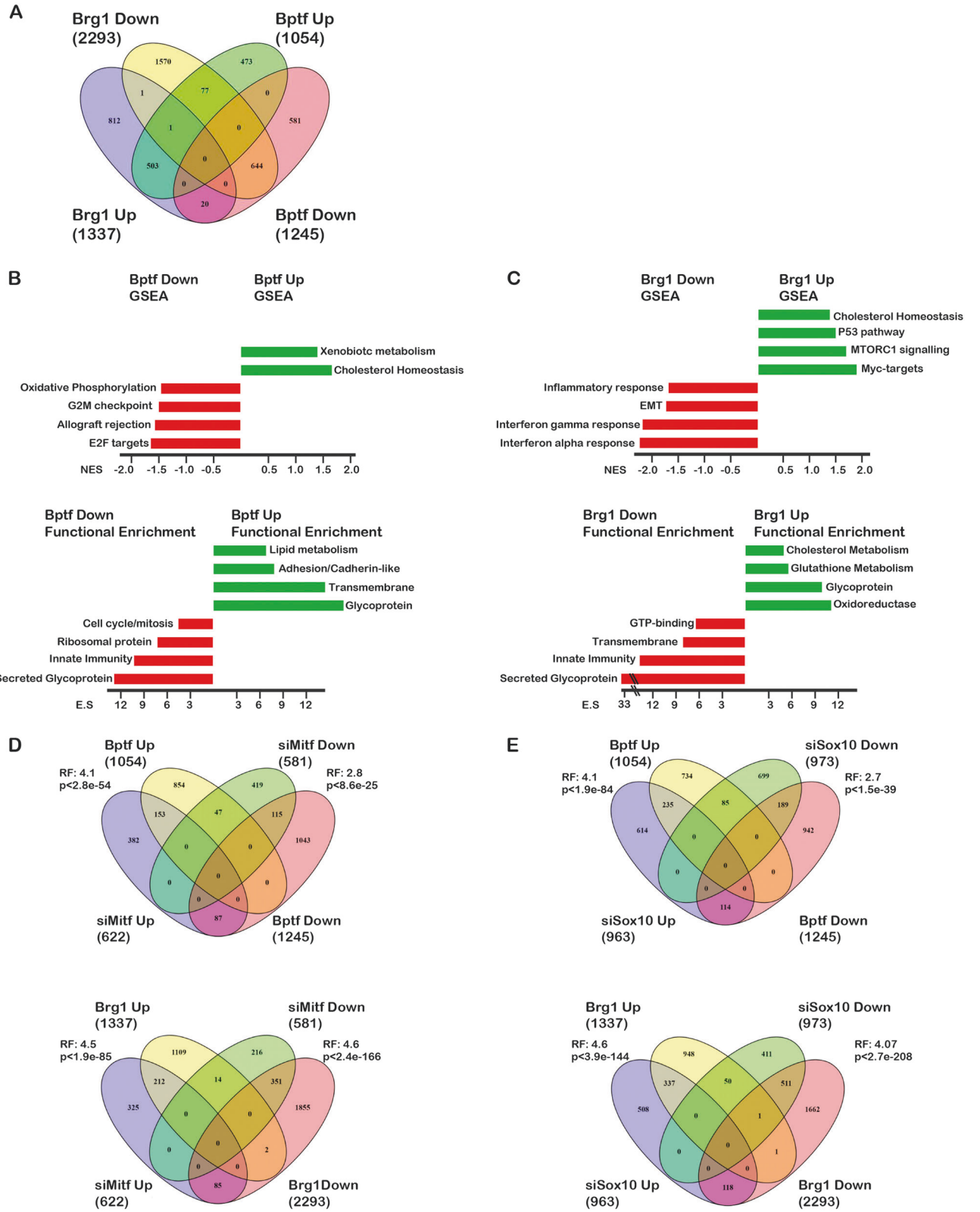

Fig. 7 RNA-seq analyses of Brg1- and Bptf-regulated gene expression. **a** Venn diagram indicating the number of up- and downregulated genes after Brg1 or Bptf inactivation compared to the 4-OHT-treated control cells. The Venn shows the overlap between the two data sets. **b**, **c** Ontology analyses of regulated genes using GSEA or the DAVID Functional Enrichment tool. **d**, **e** Venn diagrams indicating the overlap between the Mitf, Sox10, Brg1 and Bptf regulated genes highlighting the overlap between the data sets. The RF for the common up- and downregulated genes are indicated

melanocytes clonally expanded in the epidermis, but underwent 'de-differentiation' with loss of Mitf and melanocyte markers upon invasion in the dermis [29]. In contrast, we found that transformed melanocytes from the hair follicles continue to express Mitf and melanocyte markers after invasion of the dermis and show 'de-differentiation' only later as they invade more deeply within the dermis.

Consistent with the loss of Mitf expression, no Pol II was detected at the *Mitf*-M isoform promoter. Moreover, Pol II was lost from other melanocyte lineage markers that were often organised into H3K27me3-marked heterochromatin. Thus, our observations are consistent with the idea of an epigenetic switch between early stages with expression of Mitf and melanocyte markers to a later de-differentiated state where these genes loose Pol II and often gain H3K27me3. De-differentiation takes place in tumour cells expressing Sox10 and Brg1, an axis normally required for melanocyte differentiation and activation of melanocyte marker genes [8]. The mechanisms responsible for bypassing this axis remain to be determined.

Transcriptome and epigenetic analyses of human melanomas showed the existence of *MITF*-high and *MITF*-low type cells [30, 31]. More recent classifications based on vulnerability to ferroptosis [32] and single-cell analyses of patient-derived xenografts [33] highlighted additional cell states, in particular neural crest-like cells expressing SOX10, but not MITF and 'mesenchymal' cells expressing neither MITF nor SOX10. The late-stage mouse tumour cells were reminiscent of a neural crest-like phenotype with the absence of melanocyte markers, but strong expression of *Sox10* and *Ngfr1*. However, when cultured in vitro, they rapidly adopted a more differentiated phenotype with re-expression of Mitf and other melanocyte markers, suggesting that their expression was repressed in tumours by signals from the micro-environment. Previous reports showed that a proinflammatory microenvironment can induce a reversible de-differentiation and 'mesenchymal-like' phenotype through a mechanism involving c-JUN-mediated repression of MITF expression [34, 35]. Such dynamic transitions may be explained by the maintenance of the *Mitf* locus in an 'open' state retaining strong H3K27ac labelling even at the region around the *Mitf*-M promoter, facilitating re-recruitment of Pol II when the tumour cells were grown in the absence of repressive microenvironmental signals. In contrast, in human 'mesenchymal' cells exemplified by those profiled by Verfaillie et al. [31], the MITF and SOX10 loci displayed a more stable repressed state with low or no H3K27ac.

Contribution of Brg1 and Bptf to Mitf/Sox10 regulated gene expression in mouse melanoma

Here we show that Brg1 and Bptf are required for normal development of murine melanoma in vivo. Melanoma was strongly delayed by their inactivation, but Brg1 or Bptf-expressing tumours eventually developed from non-recombined cells. This observation is in accordance with a previous dropout shRNA screen that identified BRG1 as an essential actor in human melanoma cells [36]. 4-OHT-induced Brg1 or Bptf inactivation in cultured tumour cells deregulated numerous genes affecting multiple functional pathways and was accompanied by apoptosis and loss of cell viability. These data highlight the essential roles of these chromatin remodelling factors in the regulation of gene expression in mouse melanoma cells.

In mouse melanoma cells, Mitf and Sox10 coregulated overlapping gene sets. A majority of Mitf-regulated genes were also regulated by Sox10, whereas Sox10 regulated an additional set of genes independently of Mitf. We noted a collection of cell cycle and mitosis genes whose expression was mildly induced upon Mitf/Sox10 silencing. Amongst these are numerous genes whose expression is normally activated by MITF and SOX10 in human melanoma cells. The basis for this apparent conversion of MITF/SOX10 from activators of these genes in human melanoma cells to repressors in in vitro cultured mouse melanoma cells remains to be established.

We reported that BRG1 and BPTF acted as cofactors coregulating subsets of MITF and SOX10 target genes in human melanoma [4, 9]. Here, we identified genes coregulated in mouse melanoma. This can in part be explained by reduced Sox10 expression after Brg1 inactivation. This role of Brg1 in activating Sox10 expression and acting as a potential cofactor for Mitf/Sox10 accounts for its essential role not only in melanoma, but more generally for melanocyte biology as previously shown [4, 8, 25, 37]. An essential role for BRG1 in melanocyte and melanoma biology is in line with the observation that it is rarely subject to loss-of-function mutations in melanoma and only in the background of BRAF or NRAS mutations. In contrast, ARID2, ARID1A and ARID1B showed more frequent loss of function even in the triple-negative background suggesting they may be tumour suppressors [38, 39]. SWI/SNF subunits therefore appear to make distinct contributions to melanoma, some acting as putative tumour suppressors and others such as BRG1 essential for tumour growth.

Methods

Mice and genotyping

All animal experiments were performed in accordance with the European and national guidelines and policies (2010/63/UE directive and French decree 2013-118) and with the approval of the National Ethics Committee. Mice bearing the *Tyr:Cre*-ER^{T2} transgene [40], *Braf*$^{LSL\text{-}V600E/+}$

[41], and floxed alleles of *Pten* [38], *Smarca4* [39] or *Bptf* [42] alleles were bred and kept on C57BL/6J background to generate experimental mice with the desired genotypes. Genotyping was carried out by PCR analysis of genomic tail, skin or tumour DNA with primers detailed in the respective publications.

Tumour induction and growth analysis

4-hydroxytamoxifen (4-OHT) was prepared freshly as a 25 mg/mL solution (65 mM) of 4-OHT (70% Z-isomer, Sigma) in dimethylsulfoxide (DMSO) and further diluted with 100% ethanol to a 1.9 mg/mL working solution (5 mM). Localised melanomas were induced by topical application of 5 µL of 4-OHT on the shaved back skin of 6−7-week-old mice for 2 consecutive days. For distal tail or ear inductions, 2 µL of 4-OHT was applied. Tumour growth was monitored twice weekly by digital photography of the skin, including a size reference. Tumour size was then analysed using ImageJ software. For Fig. 3e, only pigmented lesions with a minimal diameter of 1 mm were included for counting.

Primary cell culture and treatment

Primary melanoma cell cultures were derived from resected mouse tumours as described elsewhere [43] and cultured in Ham-F12 supplemented with 5% foetal calf serum. For in vitro Cre-ER^{T2}-induced recombination, cultured melanoma cells were treated with 1 µM 4-OHT or vehicle (DMSO) for 48 h. The siRNA knockdown of MITF (SMARTpool L-047441-00, Dharmacon) and SOX10 (SMARTpool L-049957-01, Dharmacon) was performed with Lipofectamine RNAi max (Invitrogen, La Jolla, CA, USA) for 48 h following the manufacturer's instructions. To assess cell viability, 50,000 cells were seeded into 24-well plates, treated and grown for 3 days, stained with Cristal Violet and counted under the microscope.

Immunofluorescence and histochemistry

Immunofluorescence staining of primary cells and formalin-fixed, paraffin-embedded skin and tumour samples was performed as described previously [4]. The following antibodies were used: goat anti-Dct (Santa Cruz Biotechnology, sc-10451), rabbit anti-Sox10 (Abcam, ab155279), rabbit anti-Brg1 (ab110641), rabbit anti-Mitf (Sigma, St Louis, MO), rabbit anti-ZEB1 (Santa Cruz, sc-25388), rabbit anti-ZEB2, rabbit anti-β-tubulin (Abcam, ab6046), Alexa 488 donkey anti-goat, and Alexa 555 donkey anti-rabbit (Invitrogen, Carlsbad, CA). For histology analysis, sections were stained with haematoxylin and eosin (H&E) following standard procedures. Immunostaining of melanoma cells in vitro was performed on cells after less than three passages and were seeded and grown on glass coverslips for 2 days prior to treatment with 4-OHT, DMSO or siRNAs.

Protein extraction and western blotting

Whole-cell extracts were prepared by the standard freeze-thaw technique using LSDB 500 buffer (500 mM KCl, 25 mM Tris at pH 7.9, 10% glycerol (v/v), 0.05% NP-40 (v/v), 1 mM dithiothreitol (DTT), and protease inhibitor cocktail) except for tumour pieces that were homogenised in RIPA (50 mM Tris pH 8.0, 150 mM sodium chloride, 0.5 mM Ethylenediaminetetraacetic acid (EDTA), 0.1% SDS, 0.5% sodium deoxycholate, 1% NP-40). Cell lysates were subjected to SDS–polyacrylamide gel electrophoresis (SDS-PAGE) and proteins were transferred onto a nitrocellulose membrane. Membranes were incubated with primary antibodies in 5% dry fat milk and 0.01% Tween-20 overnight at 4 °C. The membrane was then incubated with HRP-conjugated secondary antibody (Jackson ImmunoResearch) for 1 h at room temperature, and visualised using the ECL detection system (GE Healthcare).

Apoptosis and FACs analysis

Following treatments, primary cells were harvested and stained for annexin V using Annexin V-FITC Apoptosis Detection Kit (Sigma) and propidium iodide following the manufacturer instructions. Cells were analysed on an LSRII Fortessa (BD Biosciences) and data were analysed with Flowjo software (Tree Star).

Chromatin-immunoprecipitation and sequencing

For in vivo ChIP-seq, freshly resected mouse melanoma tumours were separated from the epidermis, cut into small pieces and homogenised by douncing in hypotonic buffer. Nuclei were isolated by centrifugation on a sucrose cushion (1.2 M sucrose, 60 mM KCl, 15 mM NaCl, 5 mM $MgCl_2$, 0.1 mM EDTA, 15 mM Tris-HCl (pH 7.5), 0.5 mM DTT, 0.1 mM phenylmethylsulfonyl fluoride (PMSF), PIC). For Pol II ChIP, nuclei were further fixed in 0.4% PFA for 10 min and sonicated with a Covaris S220 as described [27]. Alternatively, H3K27ac and H3K27me3 ChIP experiments were performed on native Mnase-digested chromatin as described previously [4]. ChIP-seq libraries were prepared and sequenced as single-end 50-base reads, peak detection was performed using MACS [44] http://liulab.dfci.harvard.edu/MACS/). Datasets were normalised for the number of unique mapped reads for subsequent comparisons. Global clustering analysis and quantitative comparisons were performed using seqMINER [45] and R (http://www.r-project.org/). Gene ontology analyses were performed

using the functional annotation clustering function of DAVID (http://david.abcc.ncifcrf.gov/).

RNA preparation, quantitative PCR and RNA-seq analysis

RNA isolation was performed according to standard procedure (Qiagen kit). qRT-PCR was carried out with SYBR Green I (Qiagen) and Multiscribe Reverse Transcriptase (Invitrogen) and monitored using a LightCycler 480 (Roche). GAPDH gene expression was used to normalise the results. Primer sequences for each cDNA were designed using Primer3 Software and are available upon request. RNA-seq was performed essentially as previously described. Gene ontology analyses were performed with the Gene Set Enrichment Analysis software GSEA v3.0 using the hallmark gene sets of the Molecular Signatures Database v6.2 and the functional annotation clustering and KDEGG pathway functions of DAVID (https://david.ncifcrf.gov/).

Analyses of public datasets

Analyses of mutations in the melanoma TCGA datasets were performed using the cBiopotal website http://www.cbioportal.org/. Melanoma (SKCM) RNAseqV2 data generated by the TCGA Research Network (http://cancergenome.nih.gov/), processed and normalised using RSEM were downloaded together with the patient clinical features (BRAF, NRAS, NF1 mutational status; Clark score of the lesion; primary tumour or metastatic origin) from cBioportal. Expression values of SMARCA4 and BPTF were extracted and compared between the groups indicated in the figures by Kruskal−Wallis test, assuming nonparametric distribution (***$p < 0.001$, **$p < 0.01$, *$p < 0.05$).

Analysis of SMARCA4 and BPTF expression in nevi and primary melanoma lesions was performed by extracting their normalised expression levels from RNA-seq data obtained from Badal et al. [46]. Two-tailed unpaired t test was used for statistical significance (***$p < 0.001$, **$p < 0.01$, *$p < 0.05$).

Data availability

All sequencing data in this paper have been submitted to the Geo database under the accession number. SuperSeries GSE129621.

Acknowledgements We thank R. Marais for the *Braf*$^{LSL\text{-}V600E}$ mice, D. Metzger for floxed *Smarca4* and *Pten* mice, C. Wu for *Bptf* floxed mice, all the staff of the IGBMC high-throughput sequencing facility, a member of "France Génomique" consortium (ANR10-INBS-09-08). This work was supported by grants from the CNRS, the INSERM, Ligue National Contre le Cancer; Institut National du Cancer; ITMO-Cancer, Agence National de la Recherche, ANR10-Labex-0030-INRT. PL was supported by fellowships from the Ministère de l'enseignement supérieur et de la recherche and Fondation ARC pour la recherche sur le cancer. ID and LL are "équipes labellisées" of the Ligue Nationale contre le Cancer.

Author contributions PL and SC performed and analysed all of the wet lab experiments. PL and GM generated and maintained the mouse lines. PL and GD performed the bioinformatics analysis. IM performed the tail and tumour genotyping. PS performed histopathology analysis, LL provided mice, performed histology analysis and analysed the data, ML and WY provided samples from the lymph nodes and skin sections, ID, PL, SC and LL conceived experiments, analysed the data and wrote the paper.

Compliance with ethical standards

Conflict of interest The authors declare that they have no conflict of interest.

Publisher's note: Springer Nature remains neutral with regard to jurisdictional claims in published maps and institutional affiliations.

References

1. Clapier CR, Iwasa J, Cairns BR, Peterson CL. Mechanisms of action and regulation of ATP-dependent chromatin-remodelling complexes. Nat Rev Mol Cell Biol. 2017;18:407–22.
2. Keenen B, Qi H, Saladi SV, Yeung M, de la Serna IL. Heterogeneous SWI/SNF chromatin remodeling complexes promote expression of microphthalmia-associated transcription factor target genes in melanoma. Oncogene. 2010;29:81–92.
3. de la Serna IL, Ohkawa Y, Higashi C, Dutta C, Osias J, Kommajosyula N, et al. The microphthalmia-associated transcription factor requires SWI/SNF enzymes to activate melanocyte-specific genes. J Biol Chem. 2006;281:20233–41.
4. Laurette P, Strub T, Koludrovic D, Keime C, Le Gras S, Seberg H, et al. Transcription factor MITF and remodeller BRG1 define chromatin organisation at regulatory elements in melanoma cells. eLife. 2015. https://doi.org/10.7554/eLife.06857.
5. Weider M, Kuspert M, Bischof M, Vogl MR, Hornig J, Loy K, et al. Chromatin-remodeling factor Brg1 is required for Schwann cell differentiation and myelination. Dev Cell. 2012;23:193–201.
6. Seberg HE, Van Otterloo E, Cornell RA. Beyond MITF: multiple transcription factors directly regulate the cellular phenotype in melanocytes and melanoma. Pigment Cell Melanoma Res. 2017;30:454–66.
7. Lin H, Wong RP, Martinka M, Li G. BRG1 expression is increased in human cutaneous melanoma. Br J Dermatol. 2010;163:502–10.
8. Marathe HG, Watkins-Chow DE, Weider M, Hoffmann A, Mehta G, Trivedi A, et al. BRG1 interacts with SOX10 to establish the melanocyte lineage and to promote differentiation. Nucleic Acids Res. 2017:45:6442–58. https://doi.org/10.1093/nar/gkx259.
9. Koludrovic D, Laurette P, Strub T, Keime C, Le Coz M, Coassolo S, et al. Chromatin-remodelling complex NURF is essential for differentiation of adult melanocyte stem cells. PLoS Genet. 2015;11:e1005555.
10. Cancer Genome Atlas N. Genomic classification of cutaneous melanoma. Cell. 2015;161:1681–96.
11. Dar AA, Nosrati M, Bezrookove V, de Semir D, Majid S, Thummala S, et al. The role of BPTF in melanoma progression and in response to BRAF-targeted therapy. J Natl Cancer Inst. 2015;107: pi: djv034. https://doi.org/10.1093/jnci/djv034.

12. Dankort D, Curley DP, Cartlidge RA, Nelson B, Karnezis AN, Damsky WE Jr., et al. Braf(V600E) cooperates with Pten loss to induce metastatic melanoma. Nat Genet. 2009;41:544–52.
13. Marsh Durban V, Deuker MM, Bosenberg MW, Phillips W, McMahon M. Differential AKT dependency displayed by mouse models of BRAFV600E-initiated melanoma. J Clin Invest. 2013;123:5104–18.
14. Dhomen N, Reis-Filho JS, da Rocha Dias S, Hayward R, Savage K, Delmas V, et al. Oncogenic Braf induces melanocyte senescence and melanoma in mice. Cancer Cell. 2009;15:294–303.
15. Micevic G, Muthusamy V, Damsky W, Theodosakis N, Liu X, Meeth K, et al. DNMT3b modulates melanoma growth by controlling levels of mTORC2 component RICTOR. Cell Rep. 2016;14:2180–92.
16. Whyte WA, Orlando DA, Hnisz D, Abraham BJ, Lin CY, Kagey MH, et al. Master transcription factors and mediator establish super-enhancers at key cell identity genes. Cell. 2013;153:307–19.
17. Hnisz D, Abraham BJ, Lee TI, Lau A, Saint-Andre V, Sigova AA, et al. Super-enhancers in the control of cell identity and disease. Cell. 2013;155:934–47.
18. Pott S, Lieb JD. What are super-enhancers? Nat Genet. 2015;47:8–12.
19. Sengupta S, George RE. Super-enhancer-driven transcriptional dependencies in cancer. Trends Cancer. 2017;3:269–81.
20. Siersbaek R, Madsen JGS, Javierre BM, Nielsen R, Bagge EK, Cairns J, et al. Dynamic rewiring of promoter-anchored chromatin loops during adipocyte differentiation. Mol Cell. 2017;66:420–35 e425.
21. Joshi S, Davidson G, Le Gras S, Watanabe S, Braun T, Mengus G, et al. TEAD transcription factors are required for normal primary myoblast differentiation in vitro and muscle regeneration in vivo. PLoS Genet. 2017;13:e1006600.
22. Achour M, Le Gras S, Keime C, Parmentier F, Lejeune FX, Boutillier AL, et al. Neuronal identity genes regulated by super-enhancers are preferentially down-regulated in the striatum of Huntington's disease mice. Hum Mol Genet. 2015;24:3481–96.
23. Bernstein BE, Mikkelsen TS, Xie X, Kamal M, Huebert DJ, Cuff J, et al. A bivalent chromatin structure marks key developmental genes in embryonic stem cells. Cell. 2006;125:315–26.
24. Rambow F, Job B, Petit V, Gesbert F, Delmas V, Seberg H, et al. New functional signatures for understanding melanoma biology from tumor cell lineage-specific analysis. Cell Rep. 2015;13:840–53.
25. Fufa TD, Harris ML, Watkins-Chow DE, Levy D, Gorkin DU, Gildea DE, et al. Genomic analysis reveals distinct mechanisms and functional classes of SOX10-regulated genes in melanocytes. Hum Mol Genet. 2015;24:5433–50.
26. Damsky WE, Curley DP, Santhanakrishnan M, Rosenbaum LE, Platt JT, Gould Rothberg BE, et al. beta-catenin signaling controls metastasis in Braf-activated Pten-deficient melanomas. Cancer Cell. 2011;20:741–54.
27. Strub T, Giuliano S, Ye T, Bonet C, Keime C, Kobi D, et al. Essential role of microphthalmia transcription factor for DNA replication, mitosis and genomic stability in melanoma. Oncogene. 2011;30:2319–32.
28. Scortegagna M, Ruller C, Feng Y, Lazova R, Kluger H, Li JL, et al. Genetic inactivation or pharmacological inhibition of Pdk1 delays development and inhibits metastasis of Braf(V600E)::Pten (-/-) melanoma. Oncogene. 2014;33:4330–9.
29. Kohler C, Nittner D, Rambow F, Radaelli E, Stanchi F, Vandamme N. et al. Mouse cutaneous melanoma induced by mutant BRaf arises from expansion and dedifferentiation of mature pigmented melanocytes. Cell Stem Cell. 2017;21:679–93 e676.
30. Goodall J, Carreira S, Denat L, Kobi D, Davidson I, Nuciforo P, et al. Brn-2 represses microphthalmia-associated transcription factor expression and marks a distinct subpopulation of microphthalmia-associated transcription factor-negative melanoma cells. Cancer Res. 2008;68:7788–94.
31. Verfaillie A, Imrichova H, Atak ZK, Dewaele M, Rambow F, Hulselmans G, et al. Decoding the regulatory landscape of melanoma reveals TEADS as regulators of the invasive cell state. Nat Commun. 2015;6:6683.
32. Tsoi J, Robert L, Paraiso K, Galvan C, Sheu KM, Lay J. et al. Multi-stage differentiation defines melanoma subtypes with differential vulnerability to drug-induced iron-dependent oxidative stress. Cancer Cell. 2018;33:890–904 e895.
33. Rambow F, Rogiers A, Marin-Bejar O, Aibar S, Femel J, Dewaele M. et al. Toward minimal residual disease-directed therapy in melanoma. Cell. 2018;174:843–55 e819.
34. Landsberg J, Kohlmeyer J, Renn M, Bald T, Rogava M, Cron M, et al. Melanomas resist T-cell therapy through inflammation-induced reversible dedifferentiation. Nature. 2012;490:412–6.
35. Riesenberg S, Groetchen A, Siddaway R, Bald T, Reinhardt J, Smorra D, et al. MITF and c-Jun antagonism interconnects melanoma dedifferentiation with pro-inflammatory cytokine responsiveness and myeloid cell recruitment. Nat Commun. 2015;6:8755.
36. Bossi D, Cicalese A, Dellino GI, Luzi L, Riva L, D'Alesio C, et al. In vivo genetic screens of patient-derived tumors revealed unexpected frailty of the transformed phenotype. Cancer Disco. 2016;6:650–63.
37. Harris ML, Buac K, Shakhova O, Hakami RM, Wegner M, Sommer L, et al. A dual role for SOX10 in the maintenance of the postnatal melanocyte lineage and the differentiation of melanocyte stem cell progenitors. PLoS Genet. 2013;9: e1003644.
38. Suzuki A, Yamaguchi MT, Ohteki T, Sasaki T, Kaisho T, Kimura Y, et al. T cell-specific loss of Pten leads to defects in central and peripheral tolerance. Immunity. 2001;14:523–34.
39. Indra AK, Dupe V, Bornert JM, Messaddeq N, Yaniv M, Mark M, et al. Temporally controlled targeted somatic mutagenesis in embryonic surface ectoderm and fetal epidermal keratinocytes unveils two distinct developmental functions of BRG1 in limb morphogenesis and skin barrier formation. Development. 2005;132:4533–44.
40. Yajima I, Belloir E, Bourgeois Y, Kumasaka M, Delmas V, Larue L. Spatiotemporal gene control by the Cre-ERT2 system in melanocytes. Genesis. 2006;44:34–43.
41. Dhomen N, Dias SD, Hayward R, Ogilvie L, Hedley D, Delmas V, et al. Inducible expression of (V600E)Braf using tyrosinase-driven Cre recombinase results in embryonic lethality. Pigment Cell Melanoma Res. 2009;23:112–20.
42. Landry JW, Banerjee S, Taylor B, Aplan PD, Singer A, Wu C. Chromatin remodeling complex NURF regulates thymocyte maturation. Genes Dev. 2011;25:275–86.
43. Gallagher SJ, Luciani F, Berlin I, Rambow F, Gros G, Champeval D, et al. General strategy to analyse melanoma in mice. Pigment Cell Melanoma Res. 2011;24:987–8.
44. Zhang Y, Liu T, Meyer CA, Eeckhoute J, Johnson DS, Bernstein BE, et al. Model-based analysis of ChIP-Seq (MACS). Genome Biol. 2008;9:R137.
45. Ye T, Krebs AR, Choukrallah MA, Keime C, Plewniak F, Davidson I, et al. seqMINER: an integrated ChIP-seq data interpretation platform. Nucleic Acids Res. 2011;39:e35.
46. Badal B, Solovyov A, Di Cecilia S, Chan JM, Chang LW, Iqbal R, et al. Transcriptional dissection of melanoma identifies a high-risk subtype underlying TP53 family genes and epigenome deregulation. JCI Insight. 2017;2:pii: 92102. https://doi.org/10.1172/jci.insight.92102.

ANNEXE 3

Submitted to Science (August 2019)

Available on bioRχiv: https://www.biorxiv.org/content/10.1101/718486v1

CHD4 regulates PADI1 and PADI3 expression linking pyruvate kinase M2 citrullination to glycolysis and proliferation.

Sebastien Coassolo, Guillaume Davidson, Luc Negroni, Giovanni Gambi, Sylvian Daujat, Christophe Romier and Irwin Davidson.

CHD4 regulates PADI1 and PADI3 expression linking pyruvate kinase M2 citrullination to glycolysis and proliferation.

Sebastien Coassolo[1], Guillaume Davidson[1], Luc Negroni[2], Giovanni Gambi[1], Sylvain Daujat[1], Christophe Romier[3] and Irwin Davidson[1]#.

Institut de Génétique et de Biologie Moléculaire et Cellulaire. CNRS; INSERM; Université de Strasbourg. 1 Rue Laurent Fries, 67404 Illkirch Cedex, France.

1. Department of Functional Genomics and Cancer.

2. Mass-spectrometry platform.

3. Department of Integrated Structural Biology.

FAX: 33 3 88 65 32 01. TEL: 33 3 88 65 34 40 (45)

To whom correspondence should be addressed

E mail : irwin@igbmc.fr

Running Title : Citrullination of PKM2 regulates glycolysis

Key words : NuRD complex, chromatin, melanoma, protein arginine deiminase, allosteric regulation.

The authors declare no potential conflicts of interest.

Abstract.

The CHD4 subunit of the Nucleosome Remodelling and Deacetylation (NuRD) complex regulates expression of PADI1 (Protein Arginine Deiminase 1) and PADI3 in multiple cancer cell types modulating citrullination of three arginines of the allosterically-regulated glycolytic enzyme pyruvate kinase M2 (PKM2). PKM2 citrullination lowers its sensitivity to the inhibitors Tryptophan, Alanine and Phenylalanine shifting the equilibrium towards the activator Serine bypassing normal physiological regulation by low Serine levels and promoting excessive glycolysis, lowered intracellular ATP and slowed proliferation. Our data provide unique insight as to how conversion of arginines to citrulline impacts key interactions within PKM2 adding another layer of complexity to the mechanisms that regulate the activity of this important enzyme.

One Sentence Summary: Citrullination of key arginines in pyruvate kinase M2 modulates its allosteric regulation, glycolysis and cancer cell proliferation.

Main text

CHD3 and CHD4 are mutually exclusive ATPase subunits of the Nucleosome Remodelling and Deacetylation (NuRD) complex that regulates gene expression, acting in many contexts as a co-repressor (*1*) (*2*) (*3*). An shRNA dropout screen previously identified CHD4 as essential for growth of multiple patient derived melanoma xenografts and for breast cancer (*4*) (*5*). Mining public data sets showed up-regulation of CHD4 upon transition from benign nevi to metastatic melanoma (Fig. S1A). In melanomas, CHD4 expression was comparable in the different mutation status, although CHD3 was lowered in NRAS mutated melanomas (Fig. S1B). Single cell RNA-seq (*6*) showed higher CHD4 expression in melanoma tumour cells compared to infiltrating B and T lymphocytes (Fig. S1C). SiRNA-mediated CHD3 or CHD4 silencing in a collection of melanoma cells *in vitro* reduced clonogenic capacity, increased the proportion of slow or non-proliferating cells (Fig. 1A-D), but did not induce apoptosis (Fig. 1E).

RNA-seq following CHD4 silencing in melanoma cells identified more than 1000 up-regulated genes compared to 364 down-regulated genes showing that CHD4 was primarily a transcriptional repressor (Fig. 1F-G, and Dataset S1). In contrast, similar numbers of genes were up or down-regulated by CHD3 silencing (Fig. 1F-G), but no significant overlap of the two genes sets was observed. CHD3 and CHD4 up and down-regulated genes were involved in diverse and distinct sets of pathways (Fig. 1H-I, Dataset S1). De-regulated gene expression was confirmed by RT-qPCR on independent RNA samples in both 501Mel and MM117 melanoma cells (Fig. S2A-B).

Amongst the genes potently up-regulated by CHD4 silencing are *PADI1* (Protein Arginine Deiminase 1) and *PADI3* encoding enzymes that convert arginine to citrulline (*7*)(Fig. S2A-C). In all tested melanoma lines, *PADI3* expression was almost undetectable and potently activated by CHD4 silencing, whereas others had low basal *PADI1* levels that were increased by CHD4 silencing (Fig. S2D). The *PADI1* and *PADI3* genes are located next to each other (Fig. S2E). ChIP-seq in melanoma cells revealed that CHD4 binds together with transcription factors CTCF and FOSL2 (AP1) to an intronic regulatory element in *PADI1* that is predicted to regulate both the *PADI1* and *PADI3* genes (Fig. S3). This element is marked by H2AZ, H3K4me1, BRG1 and ATAC-seq for open chromatin, but not by the lineage-specific transcription factors MITF and SOX10.

To identify potential PADI1/3 substrates in melanoma cells, we made protein extracts from siC and siCHD4 cells, performed immunoprecipitation (IP) with a pan-citrulline antibody and analysed precipitated proteins by mass-spectrometry (Fig. S4A and Dataset S2). An increased number of total peptide spectral matches (PSMs) and PSMs for citrullinated peptides were detected following CHD4 silencing. A set of predominantly cytoplasmic proteins including tubulins, multiple 14-3-3 proteins and glycolytic enzymes PFKP, HK1/2, GAPDH, ALDOA/C, ENO1/2 and PKM2 were enriched in the IP from siCHD4 cells (Fig. S4B-C and Dataset S2).

We focussed on PKM2, a highly regulated enzyme playing a central role in integrating cellular metabolic status and cell cycle with control of glycolysis (*8*). PKM2 converts phosphoenolpyruvate (PEP) to pyruvate that can then be converted to lactic acid. To investigate PKM2 citrullination by immunoblot following pan-citrulline IP, melanoma cells were transfected with siC, siCHD4 or vectors allowing ectopic expression of PADI1 and PADI3 (Fig. S4D-E). Strongly increased amounts of PKM2 were detected in the IP following siCHD4 compared to siC in both 501Mel and MM117 melanoma cells and after ectopic PADI1 and PADI3 expression, particularly upon co-expression of both enzymes (Fig. S4F-G).

To determine if siCHD4 silencing and the enhanced PKM2 citrullination altered glycolysis, we profiled melanoma cell metabolism in real time. CHD4 silencing in all tested melanoma lines increased the basal OCR (oxygen consumption rate) and ECAR (extracellular acidification rate), markedly increased maximum OCR and ECAR and decreased the OCR/ECAR ratio due to the increased ECAR values (Fig. 2A-D). ECAR was blocked using 2-deoxy-D-glucose confirming that it was due to increased glycolysis (Fig. 2C). Increased glycolysis and lactic acid production diverts pyruvate from oxidative metabolism a more efficient ATP source. Consequently, excessive glycolysis

following CHD4 silencing led to decreased intracellular ATP levels (Fig. 2E) at least partially accounting for reduced proliferation.

The increased glycolysis seen upon CHD4 silencing was strongly diminished when *PADI1* and *PADI3* were additionally silenced (Fig. 2F and J). In contrast, exogenous expression of PADI1, PADI3 or both stimulated glycolysis (Fig. 2G and K). Consistent with increased glycolysis, PADI1/3 expression led to reduced intracellular ATP levels (Fig. 2H and L) and reduced cell proliferation (Fig. 2I). PADI1 and PADI3 were therefore necessary and sufficient for increased glycolysis accounting for the effects seen upon CHD4 silencing.

As mentioned above CHD4 may control PADI1/3 expression not via melanoma-specific factors, but through a regulatory element binding more ubiquitous factors and therefore regulate their expression in non-melanoma cancer cells. SiCHD4 silencing in SiHa cervical carcinoma cells strongly diminished clonogenic capacity (Fig. S5A), potently increased *PADI3* expression (Fig. S5B) and stimulated glycolysis (Fig. S5C-D). Moreover, glycolysis was stimulated by ectopic PADI1/3 expression leading to reduced OCR/ECAR ratio and ATP levels (Fig. S5E-G). In HeLa cells, CHD4 silencing reduced clonogenic capacity and activated *PADI1* and *PADI3* expression (Fig. S5H-I). Glycolysis was stimulated by both CHD4 silencing and ectopic PADI1/3 expression (Fig. S5J). Analogous results were observed in two different types of renal cell carcinoma cell lines (Fig. S5K-T). Therefore, in cell lines from four distinct cancer types, CHD4 silencing or ectopic PADI1/3 expression increased glycolysis and negatively impacted cell proliferation.

In contrast to PKM1 isoform that is constitutively active, PKM2 isoform activity is positively regulated by serine (Ser), fructose 1,6-biphosphate (FBP) and succinylaminoimidazole-carboxamide riboside (SAICAR) and negatively regulated by tryptophan (Trp), alanine (Ala) and phenylalanine (Phe), thus coupling glycolytic flux to the level of critical intermediate metabolites (*9-12*). Allosteric regulation involves three distinct enzyme conformations [(*13-15*) and Figure 3A]. In the apo (resting) state, in absence of small molecules and ions, the PKM2 N-terminal and A domains adopt an active conformation, but the B domain is in an inactive conformation. In the activated R-state, binding of FBP or Ser and magnesium, stabilizes the N and A domains in their active conformation, and rotates the B domain towards the A domain that together form the active site. In the inactive T-state, upon binding of inhibitors (Trp, Ala and Phe), the B domain adopts a partially active conformation, but the N and A domains undergo structural changes that prevent FBP binding and disorganize the active site. The structural changes observed between the different PKM2 states are reinforced allosterically by organisation into a tetramer that is essential for enzyme function.

In siCHD4 extracts, only 3 citrullinated arginine residues, R106, R246 and R489 were identified by mass-spectrometry and enriched in the siCHD4 extracts (Fig. S4A). R489 is directly involved in FBP binding with interactions between its guanidino group and the FBP 1' phosphate group (Figure 3B). Importantly, despite its extensive interaction network with PKM2, FBP binding is lost upon mutation of R489 into alanine (*13*) (*16*). R489 therefore plays a critical role in FBP binding. Loss of its side chain charge upon citrullination should therefore diminish FBP binding, reinforcing PKM2 allosteric regulation by the free amino acids.

In the apo state, R246 forms salt bridges between its guanidino group and the main chain carboxyl groups of V215 and L217 at the pivotal point where the B domain moves between its active and inactive conformations [(*14*) and Fig. 3C]. This interaction contributes to maintaining the inactive B domain conformation in the apo state and is lost in the R- and T-states. R246 citrullination should strongly weaken or abolish interaction with V215 and L217 facilitating release of the B domain from its inactive conformation.

R106 participates in the free amino acid binding pocket. In the apo state, R106 mostly faces the solvent, but upon free amino acid binding, it rotates towards the pocket and its guanidino group interacts with the carboxylate group of the bound amino acid and the P471 main chain carbonyl [(*9*) (*15*) (*13*) and Fig. 4A]. Ser forms a hydrogen bond network with the N and A domains stabilizing their active conformations, whereas upon Trp, Ala, or Phe binding, their hydrophobic side chain causes displacement of the N-domain outwards leading to the allosteric changes that characterize the inactive T-state (Fig. 4A).

Transition between the R- and T-states is finely regulated by changes in the relative concentrations of Ser versus Trp, Ala and Phe that compete for binding to the pocket (*15*). Loss of R106 positive side chain charge upon citrullination will weaken its interaction with free amino acids. Due to its extended network of hydrogen bonds within the pocket and as it does not modify the active conformations of the N and A domains, we postulate that Ser binding is less affected, than the hydrophobic amino acids that induce important structural changes within the N and A domains. Consequently, R106 citrullination could weaken the inhibitory effect of Trp, Ala and Phe thereby shifting the equilibrium towards activation by Ser.

To test the above hypotheses, we asked if citrullination modulated glycolysis under different conditions. When cells were grown in absence of Ser, basal glycolysis was reduced and was no longer stimulated upon siCHD4 or PADI1/3 expression (Fig. 4B). On the other hand, exogenous Ser stimulated basal glycolysis that was not further increased by siCHD4 (Fig. 4C). In contrast, basal glycolysis was reduced by exogenous Trp, but remained stimulated

by siCHD4 and by PADI1/3 expression (Fig. 4D). Similarly, glycolysis was stimulated by siCHD4 in presence of increasing Phe concentrations (Fig. 4E), an effect particularly visible in MM117 cells where despite strongly inhibited basal glycolysis, stimulation was seen upon siCHD4 (Fig. 4F). PADI1/3 expression also stimulated glycolysis in presence of exogenous Ala (Fig. 4G). PKM2 citrullination did not therefore bypass the requirement for Ser, but diminished inhibition by Trp/Ala/Phe, consistent with the idea that R106 citrullination preferentially diminished binding of Phe, Ala and Trp hence modifying the equilibrium in favour of the activator Ser.

PKM2 is an allostatic regulator integrating a finely balanced feedback mechanism that modulates its activity over a wide range of absolute and relative amino acid concentrations (*15*). When Ser levels are lowered through glycolysis, PKM2 is more readily occupied by inhibitory amino acids reducing glycolysis and allowing accumulation of metabolic intermediates required for Ser synthesis. R106 citrullination upsets this feedback loop by lowering PKM2 sensitivity to Trp/Ala/Phe shifting the equilibrium towards Ser thereby maintaining glycolysis at low Ser concentrations and inhibiting cell proliferation. Previous reports described small molecules that increase PKM2 activity and stimulate glycolysis resulting in Ser auxotrophy and reduced cell proliferation (*9, 11, 17, 18*). PKM2 citrullination therefore represents a physiological mechanism to regulate glycolysis and cell proliferation adding another layer of complexity to the control of PKM2 activity.

Citrullination of glycolytic enzymes was observed in rheumatoid arthritis (*19*). Tilvawala et al, found that citrullination increased PKM2 enzymatic *in vitro*. We extend these observations to demonstrate that PADI1 and PADI3 citrullinate PKM2 and stimulate glycolysis in cancer cells. Furthermore, our data provide unique insight as to how conversion of arginines to citrulline impacts their key interactions within PKM2 to reprogram its regulation by activating and inhibiting amino acids. While our experiments are consistent with citrullination of PKM2 as the major regulator of glycolysis, PKM2 was not the only glycolytic enzyme that showed increased citrullination and we cannot exclude that their citrullination also contributed to increased glycolysis.

We identify a novel pathway regulating melanoma cell proliferation where CHD4 regulates PADI1 and PADI3 expression and their potential to citrullinate key arginines in PKM2 involved in its allosteric regulation and potentially in other glycolytic enzymes, thereby linking epigenetics to glycolytic flux and cell proliferation. This pathway is shared in other cancer cells indicating a more general mechanism for regulating cell proliferation and a novel potential therapeutic target.

References and notes:

1. A. P. Bracken, G. L. Brien, C. P. Verrijzer, Dangerous liaisons: interplay between SWI/SNF, NuRD, and Polycomb in chromatin regulation and cancer. *Genes Dev*, (2019).
2. A. Laugesen, K. Helin, Chromatin repressive complexes in stem cells, development, and cancer. *Cell Stem Cell* **14**, 735-751 (2014).
3. P. McDonel, I. Costello, B. Hendrich, Keeping things quiet: roles of NuRD and Sin3 co-repressor complexes during mammalian development. *Int J Biochem Cell Biol* **41**, 108-116 (2009).
4. D. Bossi *et al.*, In Vivo Genetic Screens of Patient-Derived Tumors Revealed Unexpected Frailty of the Transformed Phenotype. *Cancer Discov* **6**, 650-663 (2016).
5. C. D'Alesio *et al.*, RNAi screens identify CHD4 as an essential gene in breast cancer growth. *Oncotarget* **7**, 80901-80915 (2016).
6. I. Tirosh *et al.*, Dissecting the multicellular ecosystem of metastatic melanoma by single-cell RNA-seq. *Science* **352**, 189-196 (2016).
7. K. L. Bicker, P. R. Thompson, The protein arginine deiminases: Structure, function, inhibition, and disease. *Biopolymers* **99**, 155-163 (2013).
8. Z. Lu, T. Hunter, Metabolic Kinases Moonlighting as Protein Kinases. *Trends Biochem Sci* **43**, 301-310 (2018).
9. B. Chaneton *et al.*, Serine is a natural ligand and allosteric activator of pyruvate kinase M2. *Nature* **491**, 458-462 (2012).
10. H. R. Christofk *et al.*, The M2 splice isoform of pyruvate kinase is important for cancer metabolism and tumour growth. *Nature* **452**, 230-233 (2008).
11. T. L. Dayton, T. Jacks, M. G. Vander Heiden, PKM2, cancer metabolism, and the road ahead. *EMBO Rep* **17**, 1721-1730 (2016).
12. K. E. Keller, I. S. Tan, Y. S. Lee, SAICAR stimulates pyruvate kinase isoform M2 and promotes cancer cell survival in glucose-limited conditions. *Science* **338**, 1069-1072 (2012).
13. H. P. Morgan *et al.*, M2 pyruvate kinase provides a mechanism for nutrient sensing and regulation of cell proliferation. *Proc Natl Acad Sci U S A* **110**, 5881-5886 (2013).
14. J. D. Dombrauckas, B. D. Santarsiero, A. D. Mesecar, Structural basis for tumor pyruvate kinase M2 allosteric regulation and catalysis. *Biochemistry* **44**, 9417-9429 (2005).
15. M. Yuan *et al.*, An allostatic mechanism for M2 pyruvate kinase as an amino-acid sensor. *Biochem J* **475**, 1821-1837 (2018).
16. J. A. Macpherson *et al.*, Functional cross-talk between allosteric effects of activating and inhibiting ligands underlies PKM2 regulation. *Elife* **8**, (2019).
17. D. Anastasiou *et al.*, Pyruvate kinase M2 activators promote tetramer formation and suppress tumorigenesis. *Nat Chem Biol* **8**, 839-847 (2012).
18. C. Kung *et al.*, Small molecule activation of PKM2 in cancer cells induces serine auxotrophy. *Chem Biol* **19**, 1187-1198 (2012).
19. R. Tilvawala *et al.*, The Rheumatoid Arthritis-Associated Citrullinome. *Cell Chem Biol* **25**, 691-704 e696 (2018).
20. T. Strub *et al.*, Essential role of microphthalmia transcription factor for DNA replication, mitosis and genomic stability in melanoma. *Oncogene* **30**, 2319-2332 (2011).
21. S. Tyanova *et al.*, The Perseus computational platform for comprehensive analysis of (prote)omics data. *Nat Methods* **13**, 731-740 (2016).
22. P. Laurette *et al.*, Transcription factor MITF and remodeller BRG1 define chromatin organisation at regulatory elements in melanoma cells. . *eLife* **10.7554/eLife.06857**, (2015).
23. Y. Zhang *et al.*, Model-based analysis of ChIP-Seq (MACS). *Genome Biol* **9**, R137 (2008).
24. S. Joshi *et al.*, TEAD transcription factors are required for normal primary myoblast differentiation in vitro and muscle regeneration in vivo. *PLoS Genet* **13**, e1006600 (2017).
25. P. Laurette *et al.*, Chromatin remodellers Brg1 and Bptf are required for normal gene expression and progression of oncogenic Braf-driven mouse melanoma. *Cell Death Differ*, (2019).
26. B. Badal *et al.*, Transcriptional dissection of melanoma identifies a high-risk subtype underlying TP53 family genes and epigenome deregulation. *JCI Insight* **2**, (2017).
27. B. Fontanals-Cirera *et al.*, Harnessing BET Inhibitor Sensitivity Reveals AMIGO2 as a Melanoma Survival Gene. *Mol Cell* **68**, 731-744 e739 (2017).

Acknowledgements

We thank, Dr Goncalo Castelo-Branco for the PADI3 expression vector, all the staff of the IGBMC common facilities in particular the IGBMC mass spectrometry platform and the high throughput screening facility. This work was supported by institutional grants from the Centre National de la Recherche Scientifique, the Institut National de la Santé et de la Recherche Médicale, the Université de Strasbourg, the Association pour la Recherche contre le Cancer (CR, contract number PJA 20181208268), the Ligue Nationale contre le Cancer, the Institut National du Cancer, the ANR-10-LABX-0030-INRT French state fund through the Agence Nationale de la Recherche under the frame programme Investissements d'Avenir labelled ANR-10-IDEX-0002-02. The IGBMC high throughput sequencing facility is a member of the "France Génomique" consortium (ANR10-INBS-09-08). The mass spectrometry facility is supported by grants from the ARC foundation and from the Canceropole Grand Est. ID is an 'équipe labellisée' of the Ligue Nationale contre le Cancer. SC was supported by a fellowship from the Ligue Nationale contre le Cancer.

Author Contributions. SC performed ChIP-seq, RNA-seq, transfections and metabolism experiments, GD performed bioinformatics analyses, LN performed and analysed mass-spectrometry experiments, GG analysed public data sets, SD constructed and provided PADI1 expression vector, CR performed structural analyses. SC, SD, CR and ID conceived the experiments, analysed the data and wrote the paper.

Data availability. CHD4 ChIP-seq and RNA-seq data described here have been deposited in GEO with the accession number GSE134850

Supplementary Materials:

Materials and Methods

Figures and legends S1-S5

External Databases S1-S2

References (*21-27*)

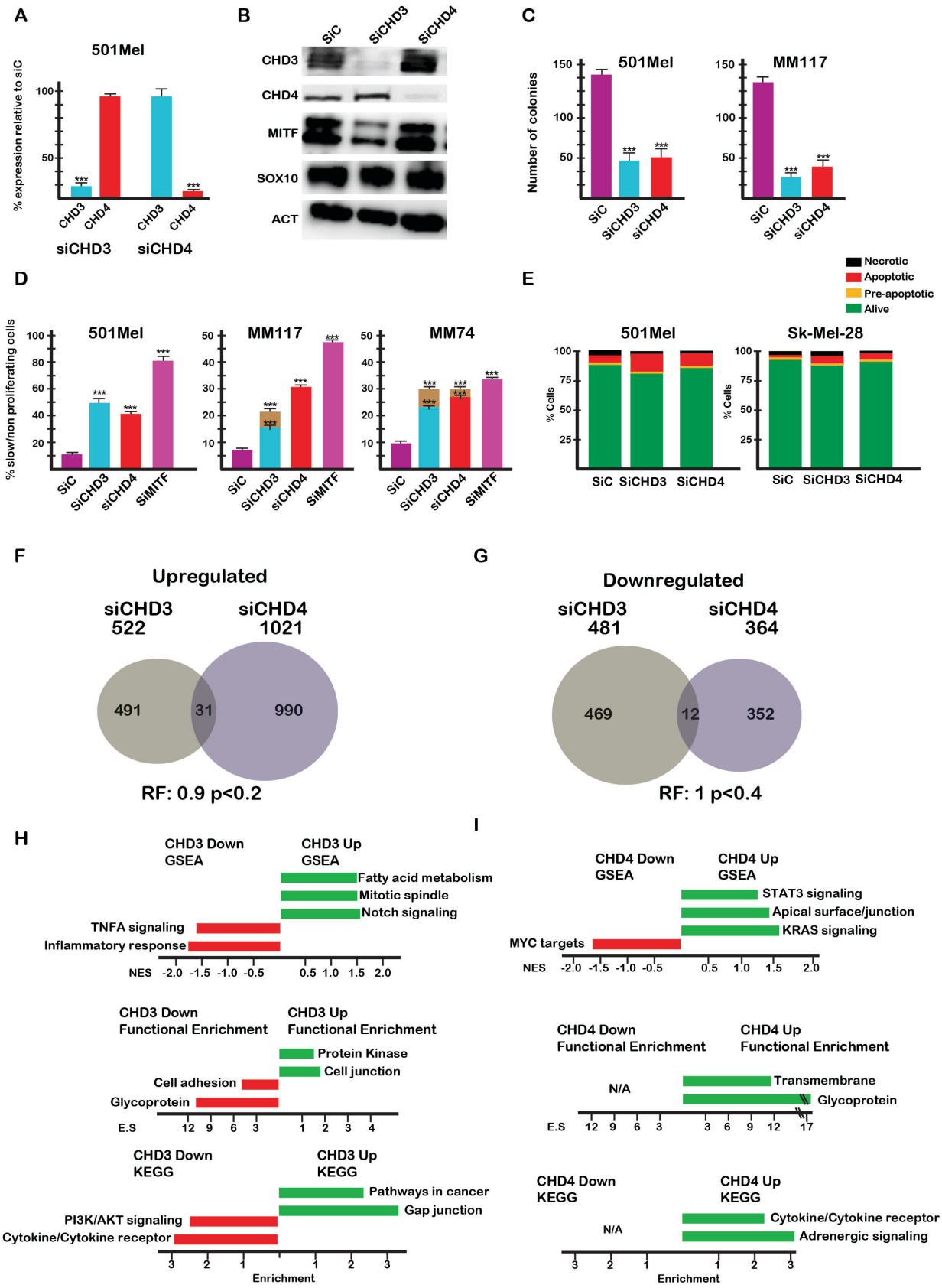

Coassolo et al., Figure 1

Figure 1. CHD3 and CHD4 are required for normal melanoma cell proliferation. **A-B**. 501Mel cells were transfected with the indicated siRNAs and CHD3 and CHD4 expression evaluated by RT-qPCR or by immunoblot along with that of MITF and SOX10. **C**. The indicated cell lines were transfected with siRNA and after reseeding the number of colonies counted after 10 days. **D**. The indicated cell lines were transfected with siRNAs and cell proliferation evaluated by cell trace violet assay. **E**. The indicated cell lines were transfected with siRNA and apoptosis detected by FACs after labelling with Annexin-V. In all experiments N=3 and unpaired t-tests analyses were performed by Prism 5. P-values: *= p<0,05; **= p<0,01; ***= p<0,001. Silencing of MITF known to induce cell cycle arrest and senescence was included as a control (*20*). **F-G** RNA-seq was performed on triplicate samples of 501Mel cells after transfection of siRNA. Genes up or down-regulated based on Log2 fold-change >1/<-1 with an adjusted p-value <0,05 were identified. Venn diagrams show overlap between the CHD3 and CHD4 regulated genes along with the hypergeometric probability representation factor (RF), in this case non-significant. **I-H**. Ontology analyses of CHD3 and CHD4 regulated genes. Shown are the enrichment scores for GSEA, as well as David functional enrichment and KEGG pathway categories.

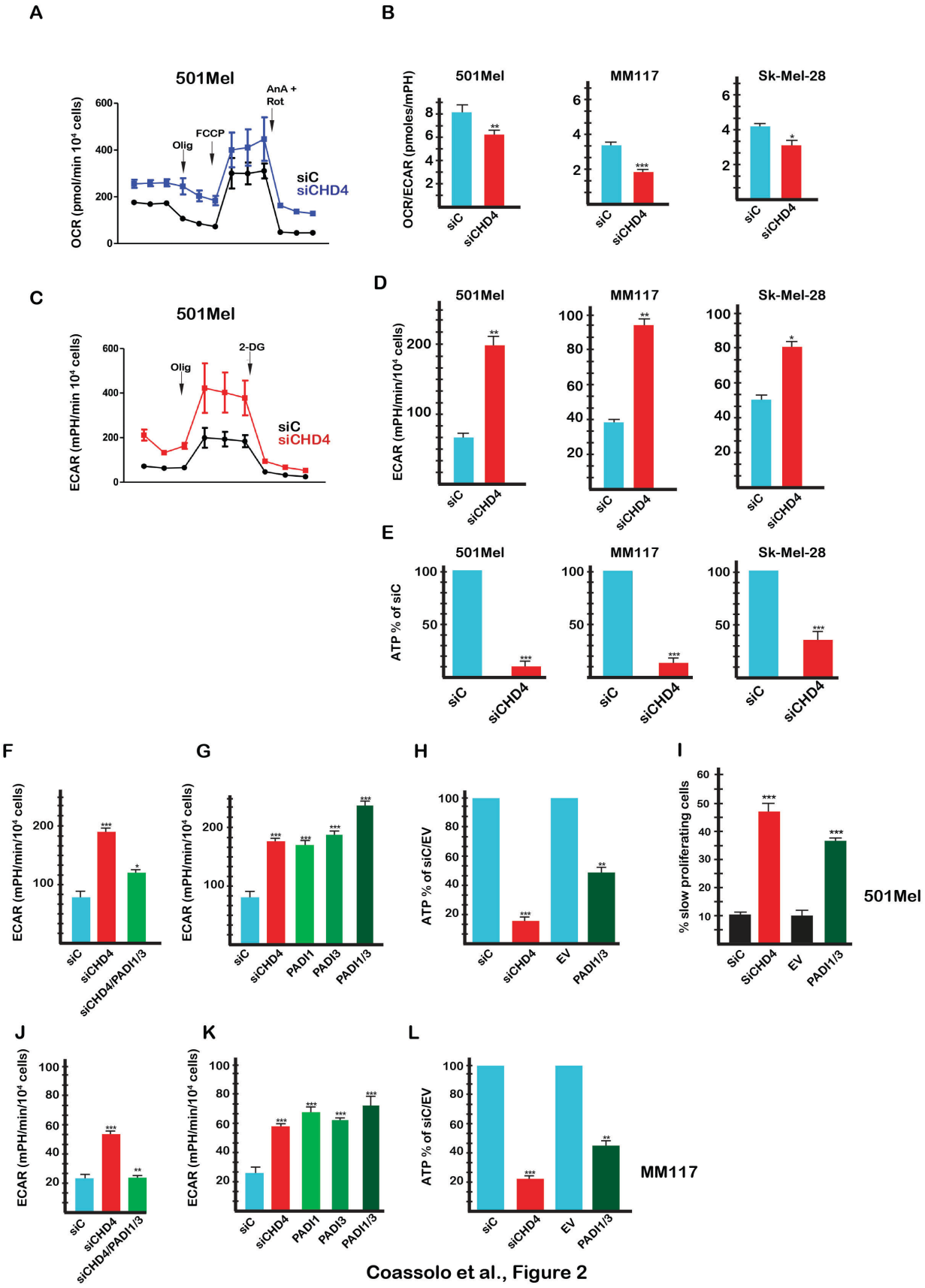

Coassolo et al., Figure 2

Figure 2. CHD4 silencing regulates glycolysis and cell proliferation. **A.** Effect of CHD4 silencing on basal and maximal OCR values in 501Mel cells. **B**. Effect of CHD4 silencing on the basal OCR/ECAR ratio in the indicated cell types. **C-D**. Effect of CHD4 silencing on basal and maximal ECAR values in 501Mel cells and basal ECAR values in the indicated cell types. **E.** CHD4 silencing reduces intracellular ATP levels in the indicated cell lines. **F-G**. ECAR values in 501Mel cells following transfection with indicated siRNAs or expression vectors. **H.** Intracellular ATP levels following CHD4 silencing or PADI1/3 expression. EV = empty expression vector control. **I** Reduced cell proliferation following PAD1/3 expression. **J-L**. ECAR values and intracellular ATP levels in MM117 cells following transfection with indicated siRNAs or expression vectors. In all experiments ECAR values were determined from N=6 with 6 technical replicates for each N. Unpaired t-test analyses were performed by Prism. P-values: *= p<0,05; **= p<0,01; ***= p<0,001.

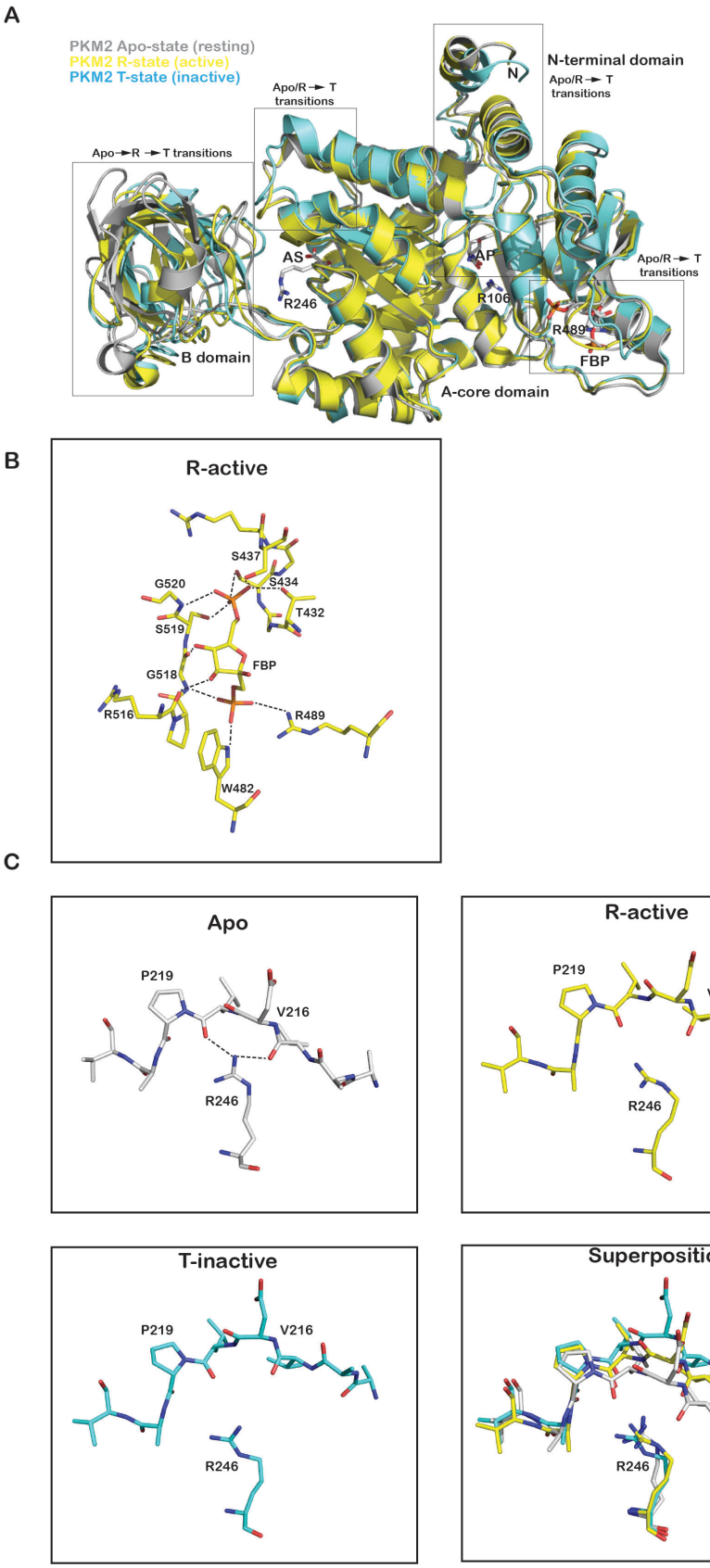

Coassolo et al., Figure 3

Figure 3. Locations and interactions of citrullinated arginines in PKM2. **A.** Ribbon representation of a PKM2 monomer in the apo resting state (grey; PDB 3SRH), the active R state (yellow; PDB 6GG6 with FBP and oxalate molecules from 3SRD) and the inactive T state (cyan; PDB 6GG4). The three citrullinated arginines (R106, R246 and R489), the free amino acids Serine and Phenylalanine, FBP and oxalate (surrogate of pyruvate to occupy the active site) are shown as sticks (carbon, grey; nitrogen, blue; oxygen, red; phosphorus, orange). AS, active site. AP, free amino acid binding pocket. The regions of PKM2 undergoing allosteric structural transitions between the three states are boxed. **B.** Close up view of FBP interactions within the R-active state. Salt bridges and hydrogen bonds are shown as dashed lines. Colour coding as panel A. For clarity, the side chain of K433 is not displayed. **C.** Closeup view of R246 interactions with the B domain in the Apo, R-active and T-inactive states along with a superposition of the three structures. Colour coding and representation of salt bridges/hydrogen bonds is as in panels A and B.

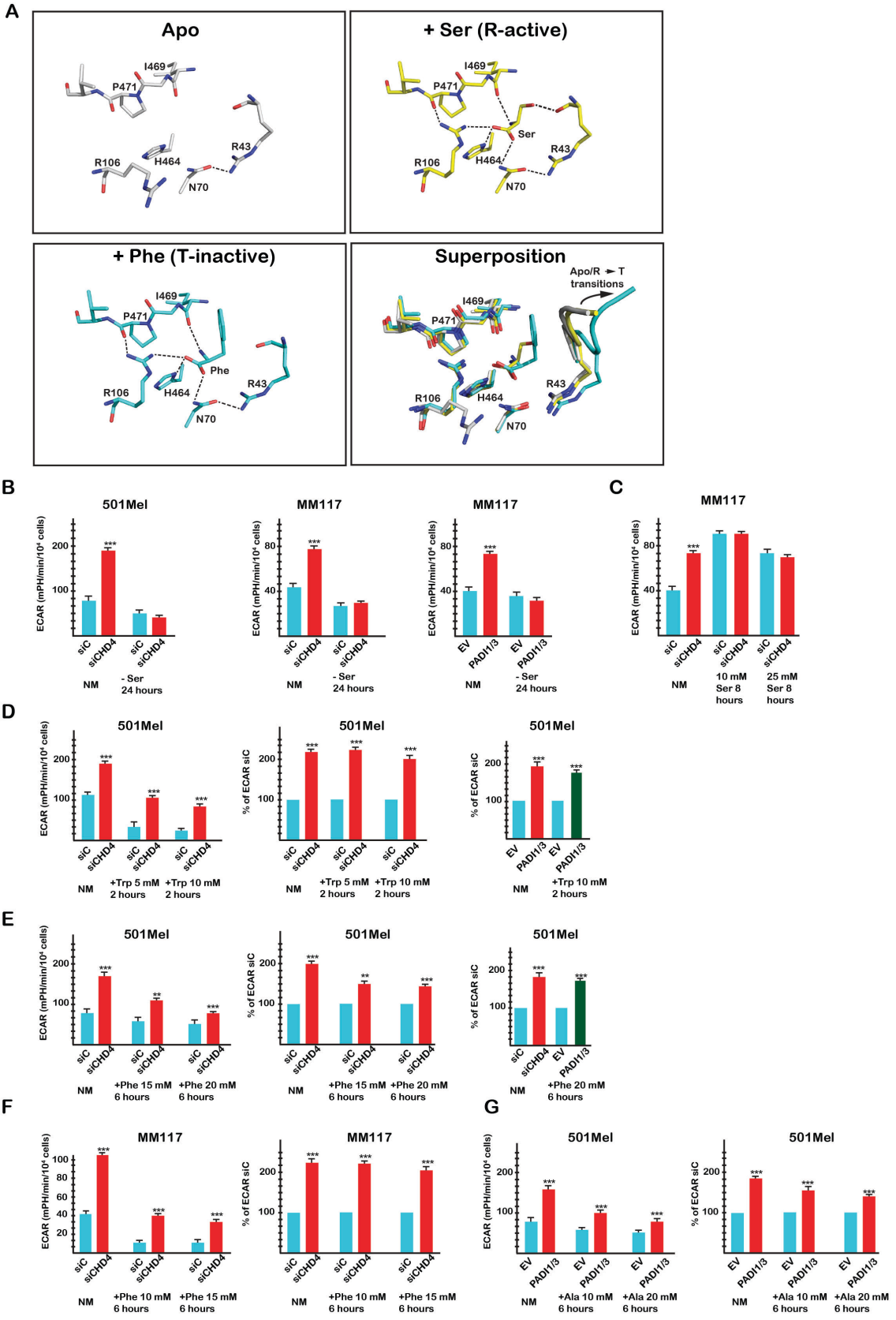

Coassolo et al., Figure 4

Figure 4. PKM2 citrullination diminishes allosteric inhibition by Phe/Ala/Trp. **A.** Close up view of free Ser and Phe interactions within the free amino acid binding pocket in the Apo, R-active and T-inactive states with a superposition of the three structures. All residues displayed are shown as sticks. In the superposition, the peptide bearing R43 is represented as ribbon to show the allosteric changes created upon Phe binding. Colour coding is as in Fig. 3. Salt bridges and hydrogen bonds are shown as dashed lines. For clarity, the side chain of Phe 470, which stacks on R106 side chain, is not displayed. **B**. ECAR values in presence of exogenous Ser or absence of Ser after CHD4 silencing or PADI1/3 expression in 501Mel or MM117 cells; NM = normal medium. **C.** ECAR values in presence of increased exogenous Ser with or without CHD4 silencing in 501Mel cells. **D-E**. ECAR values in presence of exogenous Trp or Phe with or without CHD4 silencing or PADI1/3 expression in 501Mel cells. **F**. ECAR values in presence of exogenous Phe with or without CHD4 silencing in MM117 cells. **G.** ECAR values in presence of exogenous Ala with or without PADI1/3 expression in 501Mel cells. In all experiments ECAR values were determined from N=6 with 6 technical replicates for each N. Unpaired t-test analysis were performed by Prism 5. P-values: *= p<0,05; **= p<0,01; ***= p<0,001.

Methods

Cell culture, siRNA silencing and expression vector transfection

Melanoma cell lines 501Mel and SK-Mel-28 were grown in RPMI 1640 medium supplemented with 10% foetal calf serum (FCS). MM074 and MM117 were grown in HAM-F10 medium supplemented with 10% FCS, 5.2 mM glutamax and 25 mM Hepes. Hermes-3A cell line was grown in RPMI 1640 medium (Sigma) supplemented with 10% FCS, 200nM TPA, 200pM cholera toxin, 10ng/ml human stem cell factor (Invitrogen) and 10 nM endothelin-1 (Bachem). HeLa cells were grown in Dulbecco's modified Eagle's medium supplemented with 10% FCS. SiHA cells were grown in EAGLE medium supplemented with 10% FCS, 0.1mM non-essential amino acids and 1mM sodium pyruvate. UOK cell lines were cultured in DMEM medium (4.5g/L glucose) supplemented with 10% heat-inactivated FCS and 0.1mM AANE.

SiRNA knockdown experiments were performed with the corresponding ON-TARGET-plus SMARTpools purchased from Dharmacon Inc. (Chicago, Il., USA). SiRNAs were transfected using Lipofectamine RNAiMax (Invitrogen, La Jolla, CA, USA) and cells were harvested 72 hours after. PADI1 and PADI3 expression vectors were transfected using X-tremeGENE™ 9 DNA Transfection Reagent (Sigma) for 48h. To assess clonogenic capacity, cells were counted and seeded in 6 well plates for 7 to 15 days.

Proliferation, viability and senescence analyses by flow cytometry

To assess proliferation after siRNA treatment, cells were stained with Cell Trace Violet (Invitrogen) on the day of transfection. To assess cell viability, cells were harvested 72 hours after siRNA transfection and stained with Annexin-V (Biolegend) following manufacturer instructions. To assess senescence, cells were treated with Bafilomycin A (Sigma) for an hour and then with C_{12}FDG (Invitrogen) for two hours. Cells were analysed on a LSRII Fortessa (BD Biosciences) and data were analysed using Flowjo software.

ATP measurement

The concentration of ATP was determined 72h after siRNA transfection using the luminescent ATP detection system (Abcam, ab113849) following the manufacturer's instructions.

Protein extraction and Western blotting

Whole cell extracts were prepared by the standard freeze-thaw technique using LSDB 500 buffer (500 mM KCl, 25 mM Tris at pH 7.9, 10% glycerol (v/v), 0.05% NP-40 (v/v), 16mM DTT, and protease inhibitor cocktail). Cell lysates were subjected to SDS–polyacrylamide gel electrophoresis (SDS-PAGE) and proteins were transferred onto a nitrocellulose membrane. Membranes were incubated with primary antibodies in 5% dry fat milk and 0.01% Tween-20 overnight at 4 °C. The membrane was then incubated with HRP-conjugated secondary antibody (Jackson ImmunoResearch) for 1h at room temperature, and visualized using the ECL detection system (GE Healthcare).

Immunoprecipitation and mass-spectrometry

Citrullinated proteins were immunoprecipitated from whole cell extracts with an anti-pan-citrulline antibody (Abcam, ab6464). Samples were concentrated on Amicon Ultra 0.5 mL columns (cutoff: 10 kDa, Millipore), resolved by SDS-PAGE and stained using the Silver 7 Quest kit (Invitrogen).

Mass spectrometry and analysis

Mass-spectrometry was performed at the IGBMC proteomics platform (Strasbourg, France). Samples were reduced, alkylated and digested with LysC and trypsin at 37°C overnight. Peptides were then analyzed with an nanoLC- MS/MS system (Ultimate nano-LC and LTQ Velos ion trap, Thermo Scientific, San Jose Califronia). Briefly, peptides were separated on a C18 nano-column with a 1 to 30 % linear gradient of acetonitrile and analyzed in a TOP20 CID data-dependent MS method. Peptides were identified with SequestHT algorithm in Proteome Discoverer 2.2 (Thermo Fisher Scientific) *using* Human Swissprot database (20347 sequences). Precursor and fragment mass tolerance were set at 0.9 Da and 0.6 Da respectively. Trypsin was set as enzyme, and up to 2 missed cleavages were

allowed. Oxidation (M) and Citrullination (R) were set as variable modifications, and Carbamidomethylation (C) as fixed modification. Peptides were filtered with a 1 % FDR (false discovery rate) on peptides and proteins. For statistical analyses data was re-analysed using Perseus (*21*).

Chromatin immunoprecipitation and sequencing

CHD4 ChIP experiments were performed on 0.4% Paraformaldehyde fixed and sonicated chromatin isolated from 501Mel cells according to standard protocols as previously described (*22*). MicroPlex Library Preparation kit v2 was used for ChIP-seq library preparation. The libraries were sequenced on Illumina Hiseq 4000 sequencer as Single-Read 50 base reads following Illumina's instructions. Sequenced reads were mapped to the Homo sapiens genome assembly hg19 using Bowtie with the following arguments: -m 1 --strata --best -y -S -l 40 -p 2. After sequencing, peak detection was performed using the MACS software (*23*). Peaks were annotated with Homer (http://homer.salk.edu/homer/ngs/annotation.html) using the GTF from ENSEMBL v75. Peak intersections were computed using bedtools and Global Clustering was done using seqMINER. De novo motif discovery was performed using the MEME suite (meme-suite.org). Motif enrichment analyses were performed using in house algorithms as described in (*24*).

RNA preparation, quantitative PCR and RNA-seq analysis

RNA isolation was performed according to standard procedure (Qiagen kit). qRT-PCR was carried out with SYBR Green I (Qiagen) and Multiscribe Reverse Transcriptase (Invitrogen) and monitored using a LightCycler 480 (Roche). RPLP0 gene expression was used to normalize the results. Primer sequences for each cDNA were designed using Primer3 Software and are available upon request. RNA-seq was performed essentially as previously described (*25*). Gene ontology analyses were performed with the Gene Set Enrichment Analysis software GSEA v3.0 using the hallmark gene sets of the Molecular Signatures Database v6.2 and the functional annotation clustering function of DAVID.

Analysis of oxygen consumption rate (OCR) and glycolytic rate (ECAR) in living cells

The ECAR and OCR were measured in an XF96 extracellular analyzer (Seahorse Bioscience). A total of 20000 cells per well were seeded and transfected by siRNA or expression vector 72h and 24h hours respectively prior the experiment. The cells were incubated in a CO2-free incubator at 37°C and the medium was changed to XF base medium supplemented with 1mM pyruvate, 2 mM glutamine and 10mM glucose for an hour before measurement. For OCR profiling, cells were sequentially exposed to 2 μM oligomycin, 1 μM carbonyl cyanide-4-(trifluorome-

thoxy) phenylhydrazone (FCCP), and 0.5 μM rotenone and antimycin A. For ECAR profiling, cells were sequentially exposed to 2 μM oligomycin and 150 mM 2-deoxyglucose (2-DG). After measurement, cells were washed with PBS, fixed with 3% PFA, permeabilized with 0.2% triton. Nuclei were counterstained with Dapi (1:500) and number of cells per well determined by the IGBMC High Throughput Cell-based Screening Facility (HTSF, Strasbourg). L-Phe (Sigma, P2126), L-Trp (Sigma T0254) or L-Ser (Sigma S4500) were added in the complete medium (24-48h for Serine and 6-8h for Trp/Phe) and in the refreshed XF base medium prior the experiment.

Supplemental Figures:

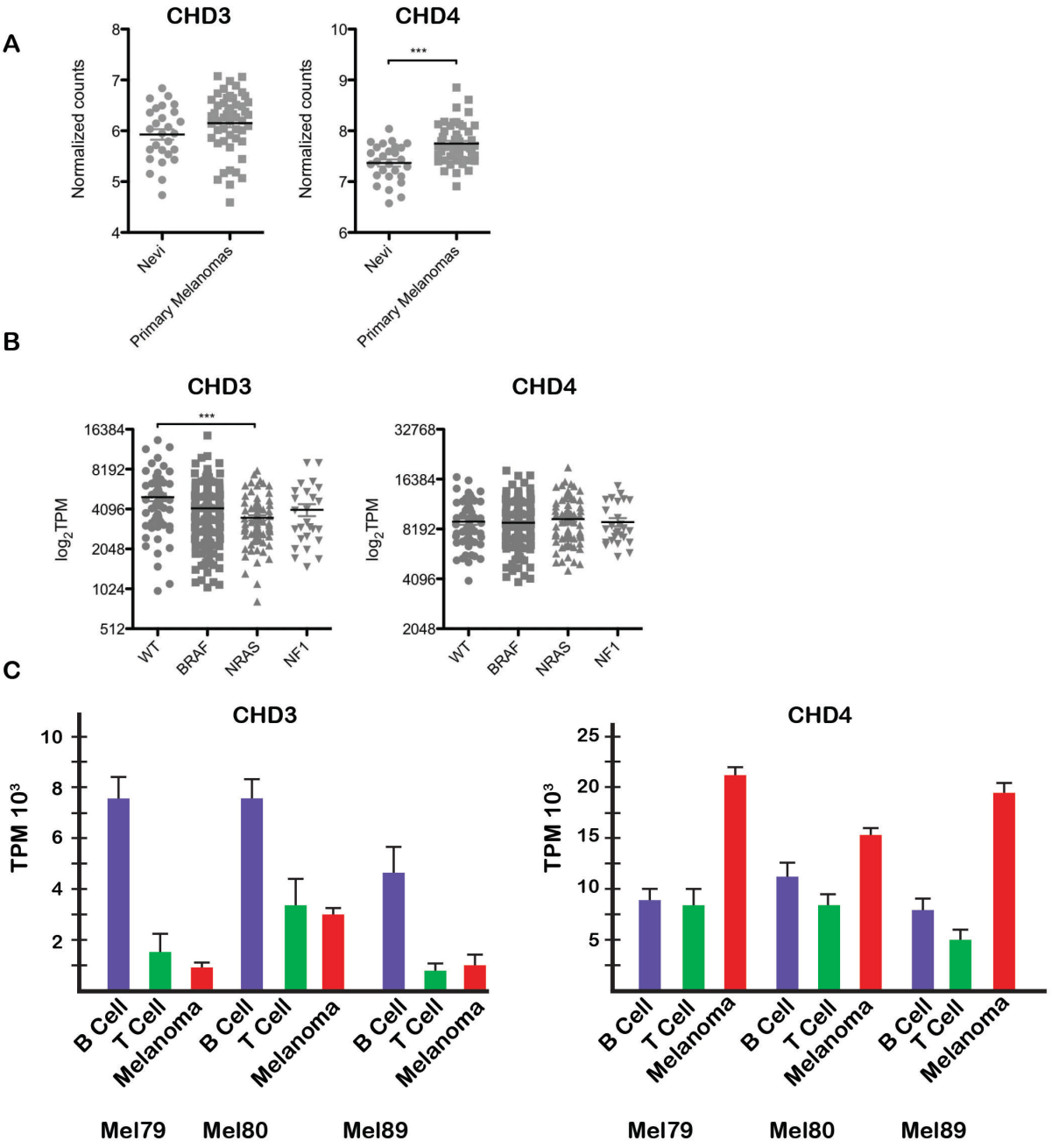

Coassolo et al., Figure S1

Supplementary Figure 1. CHD3 and CHD4 expression in melanoma. **A**. CHD3 and CHD4 expression in nevi and melanoma from the Badal et al dataset (*26*). **B**. CHD3 and CHD4 expression in melanoma from the TCGA database (www.cbioportal.org) carrying the indicated mutations. **C**. CHD3 and CHD4 expression in melanoma cells and infiltrating immune cells in three analyzed tumours of the Tirosh et al., data set (*6*).

5

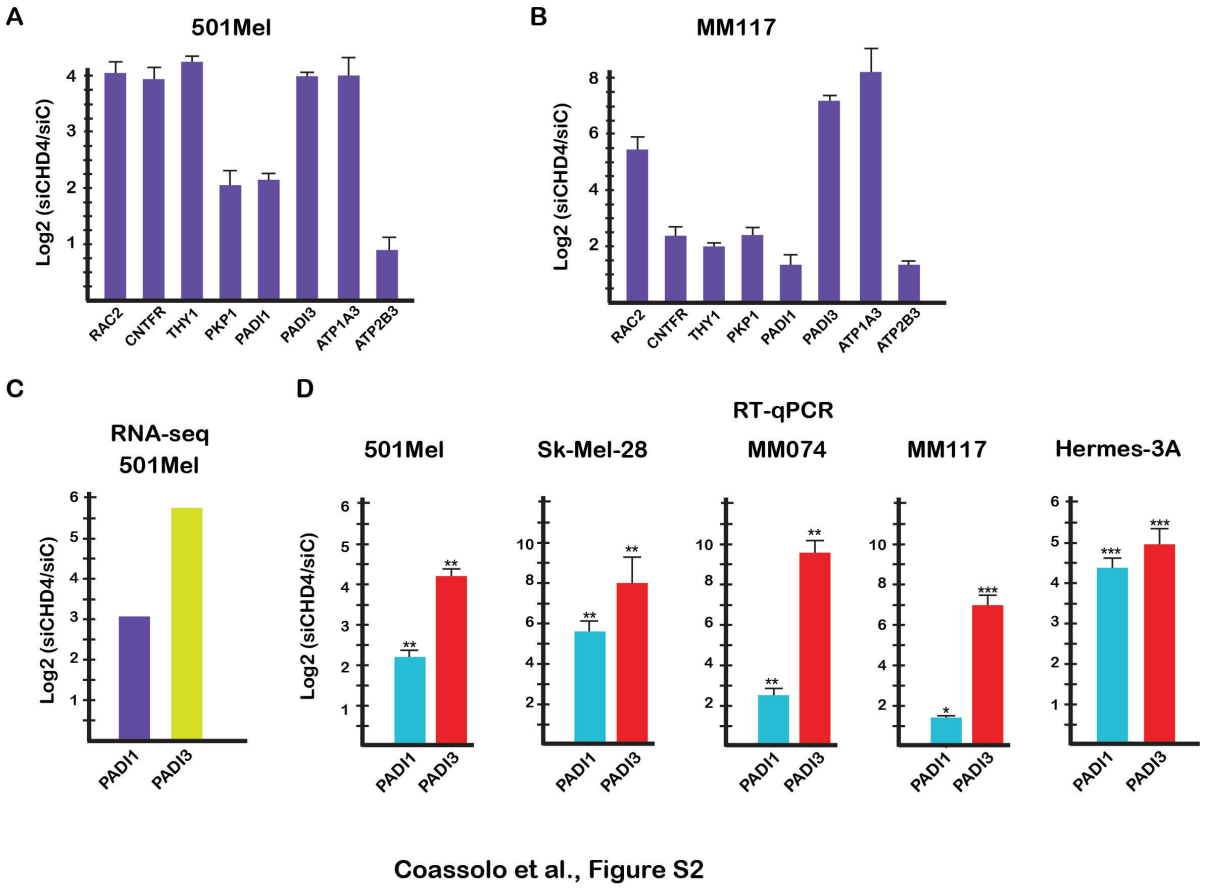

Coassolo et al., Figure S2

Supplementary Figure 2. Genes de-regulated upon CHD4 silencing. **A-B**. Verification of deregulated expression of selected genes in independent RNA samples from 501Mel or MM117 cells. **C-D**. Changes in *PADI1* and *PADI3* expression in the indicated cells lines following CHD4 silencing shown by RNA-seq and RT-qPCR. In all RT-qPCR experiments N=3 and unpaired t-test analyses were performed by Prism 5. P-values: *= p<0,05; **= p<0,01; ***= *p<0,001*.

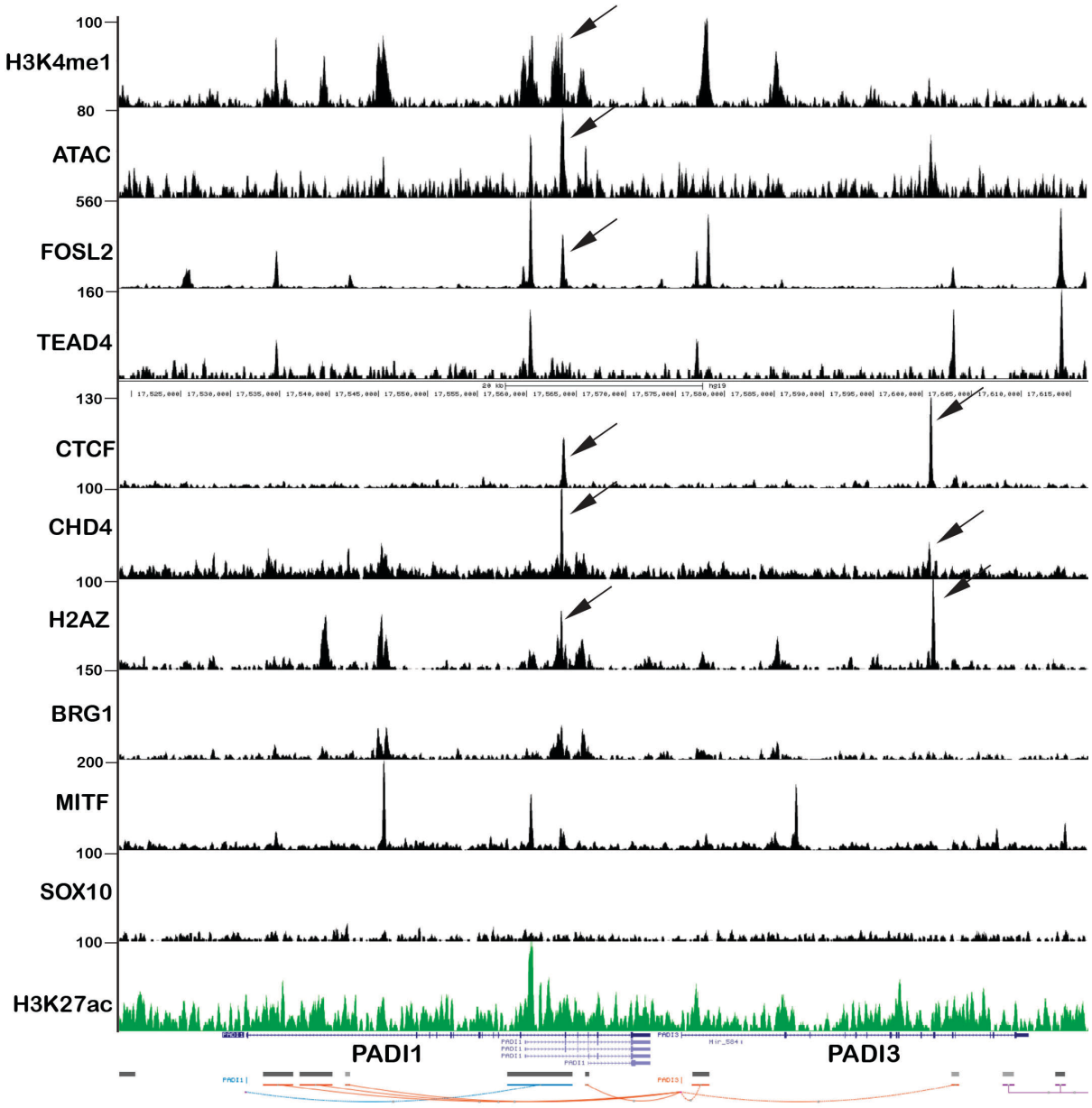

Coassolo et al., Figure S3

Supplementary Figure 3. CHD4 CTCF and FOSL2 co-occupy a regulatory element at the *PADI1-PADI3* locus. Screenshot of UCSC genome browser at the *PADI1-PADI3* locus showing the indicated ChIP-seq data. Arrows highlight the putative cis-regulatory elements occupied by CTCF, FOSL1 and CHD4 and marked by ATAC-seq, H3K4me1, BRG1 and H2AZ. The following data sets were used: H3K4me1 GSM2476344; ATAC GSM2476338; FOSL2 GSM2842801; TEAD4 GSM2842802 (*27*); CHD4 XX this study. Other data are from Laurette et al., 2015 (*22*).

A

Total PSM		Citrullinated PSM	
siC	siCHD4	siC	siCHD4
22058	34365	2561	4311

PKM2 Peptide	C>R	Citrullinated PSM siC	siCHD4
TATESFASDPILYRPVAVALDTK*	R106	2	7
FGVEQDVDMVFASFIR*	R246	0	5
DPVQEAWAEDVDLR*	R489	2	10

B

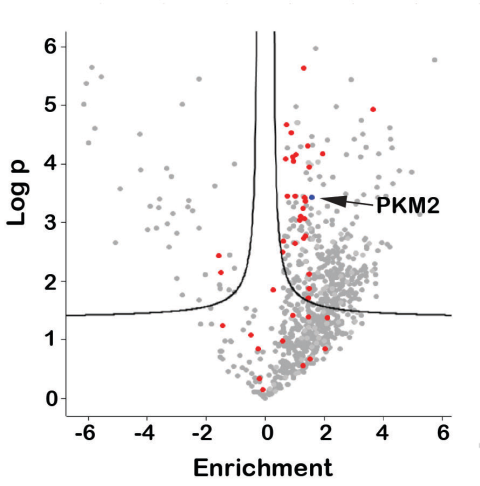

C

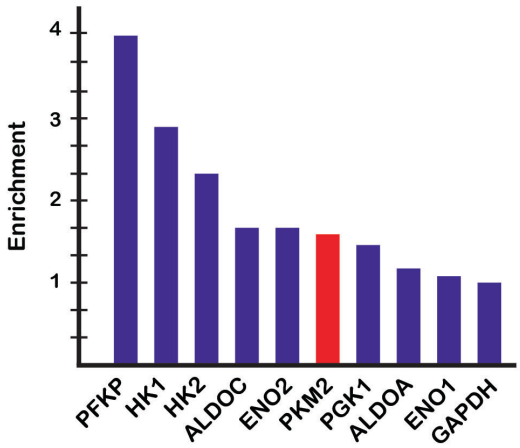

D

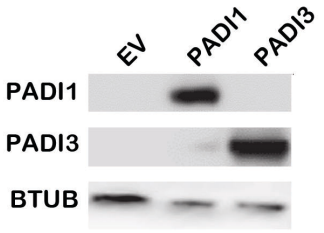

E

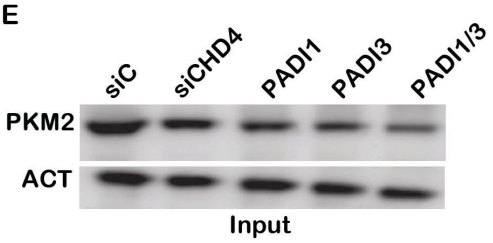

F

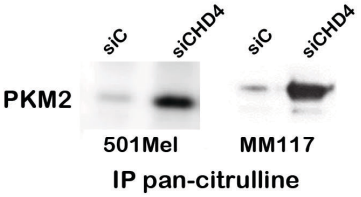

G

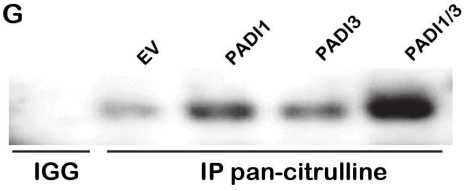

Coassolo et al., Figure S4

Supplementary Figure 4. CHD4 silencing increases citrullination in 501Mel cells. **A.** Increases in number of total and citrullinated PSMs in CHD4 silenced cells following immunoprecipitation (IP) with pan-citrulline antibody. Lower table shows PKM2 peptides with increased citrullination after pan-citrulline IP. **B**. Volcano plot showing proteins with increased or decreased total PSMs after pan-citrulline IP. **C**. Increased recovery of glycolytic enzymes following pan-citrulline IP. **D.** Immunoblot showing expression of recombinant PADI1 and PADI3 in cells transfected with the corresponding expression vectors of the empty vector (EV). **E.** Immunoblot showing expression of PKM2 in cells after CHD4 silencing or transfection with the PADI1 and PADI3 vectors in the cell extracts used for immunoprecipitation with pan-citrulline antibody. **F.** PKM2 in the pan-citrulline IPs from 501Mel or MM117 cells. **G.** Immunoblot showing PKM2 in the pan-citrulline IP after transfection with the PADI1 and/or PADI3 expression vectors.

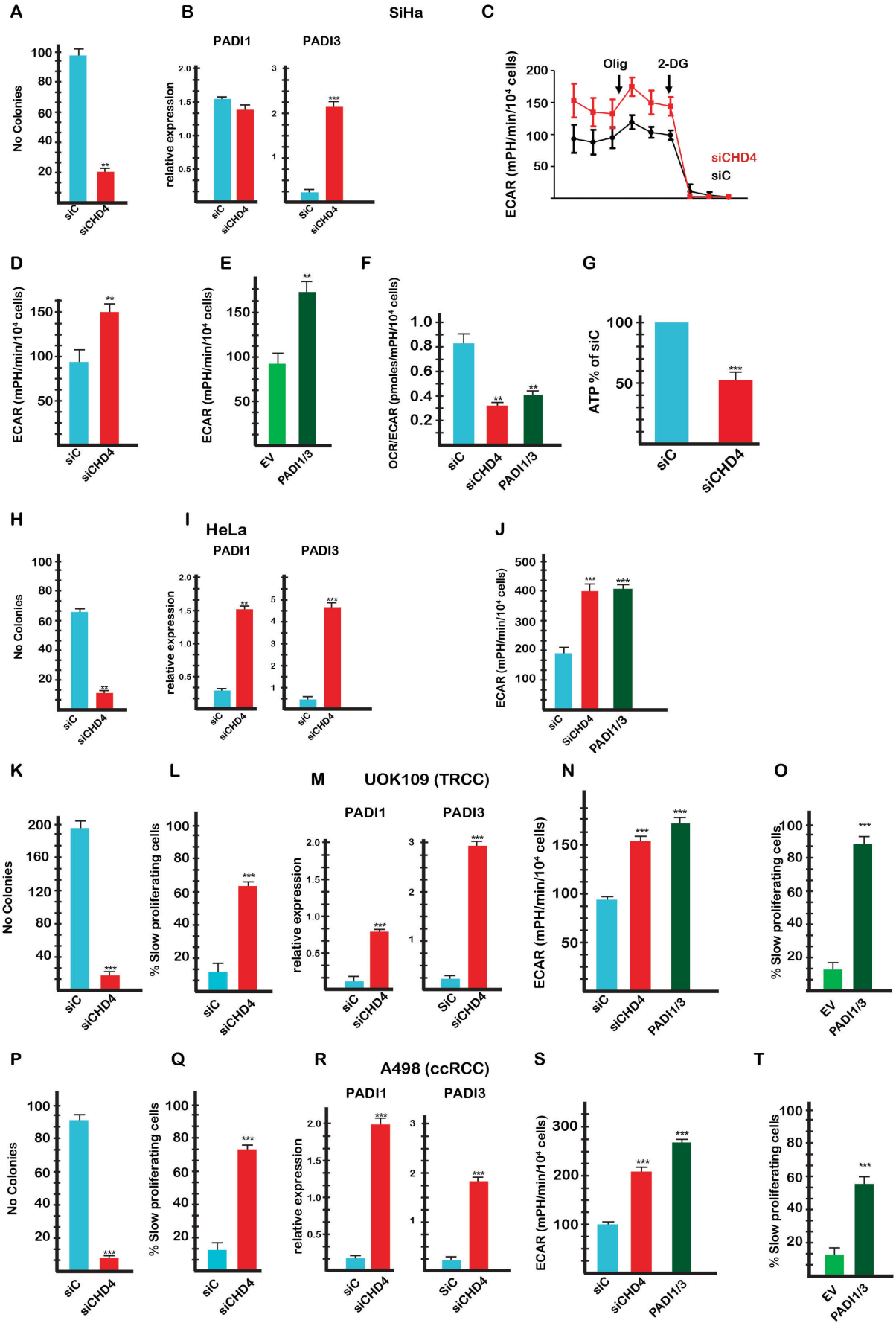

Coassolo et al., Figure S5

Supplementary Figure 5. Citrullination regulates glycolysis and proliferation in multiple types of cancer cells. **A**. Diminished clonogenicity of SiHA cells following CHD4 silencing. **B**. PADI1 and PADI3 expression in SiHA cells following CHD4 silencing. **C-D**. Basal and maximal glycolysis in SiHA cells following CHD4 silencing. **E.** Glycolysis in SiHA cells following PADI1/3 expression. **F.** OCR/ECAR ratio in SiHA cells following CHD4 silencing or PADI1/3 expression. **G.** Intracellular ATP levels in SiHA cells following CHD4 silencing. **H-J**. Clonogenicity, PADI1, PADI3 expression and glycolysis in HeLa cells following CHD4 silencing or PADI1/3 expression as indicated. **K-O**. Clonogenicity, PADI1, PADI3 expression and glycolysis and proliferation in UOK-109 translocation renal cell carcinoma cells following CHD4 silencing or PADI1/3 expression as indicated. **P-T**. Clonogenicity, PADI1, PADI3 expression and glycolysis and proliferation of A498 clear cell renal carcinoma cells following CHD4 silencing or PADI1/3 expression as indicated. In A,B,H,I,K,L,M,O,P,Q,R,T: N=3 and statistical unpaired t-tests analyses were performed by Prism 5 P-values: as above. In D,E,F,G,J,N,S: N=3 with 6 technical replicates for each N. P-values: as above.

Supplementary Dataset 1. Summary of RNA-seq results following CHD3 or CHD4 silencing in 501Mel cells. Shown are gene names, description, fold change, p-value and adjusted p-value. As indicated, other pages on the spreadsheet show the ontology analyses of each gene set.

Supplementary Dataset 2. Proteins enriched after pan-citrulline immunoprecipitation from CHD4 silenced cells. Shown are accessions, gene names, gene descriptions, -Log P-values, differences (siCHD4-siCTRL), sum peptides scores, percentage of coverage, peptide number, PSM number, NSAF values (PSMs/protein length), unique peptide numbers, amino acid number and molecular mass.

PUBLICATIONS

1) **MITF-high and chromatin-remodelling complex NURF is essential for differentiation of adult melanocyte stem cells.** Koludrovic D, Laurette P, Strub T, Keime C, Le Coz M, **Coassolo S**, Mengus G, Larue L, Davidson I. PLoS Genetics. 2015.
2) **MITF-low cells and a novel subpopulation expressing genes of both cell states contribute to intra and inter-tumoral heterogeneity of primary melanoma.** Ennen M, Keime C, Gambi G, Kieny A, **Coassolo S**, Thibault-Carpentier C, Margerin-Schaller F, Davidson G, Vagne C, Lipsker D and Davidson I. Clinical Cancer Research. 2017.
3) **Epigenetic regulation of gene expression in malignant melanoma.** Laurette P, Koludrovic D, **Coassolo S,** and Davidson I. Biologie Aujourd'hui. 210 (4) 283-295. 2017.
4) **Chromatin remodellers Brg1 and Bptf are required for normal gene expression and progression of oncogenic Braf-driven mouse melanoma.** Laurette P*, **Coassolo S*,** Davidson G, Michel I, Gambi G, Yao W, Sohier P, Li M, Mengus G, Larue L and Davidson I. Cell Death & Differentiation. 2019.
5) **Dynamic Evolution of Clonal Composition and Neoantigen Landscape in Recurrent Metastatic Melanoma with a Rare Combination of Driver Mutations.** Davidson G, **Coassolo S**, Kieny A, Ennen M, Pancreach E, Malouf G, Lipsker D and Davidson I. Journal of Investigative Dermatology. 2019.
6) **CHD4 regulates PADI1 and PADI3 expression linking pyruvate kinase M2 citrullination to glycolysis and proliferation. Sebastien Coassolo**, Guillaume Davidson, Luc Negroni, Giovanni Gambi, Sylvain Daujat, Christophe Romier and Irwin Davidson. Submitted to Science, August 2019. Available on bioRχiv: https://www.biorxiv.org/content/10.1101/718486v1

CONFERENCES

- **2016:** 2Nd Danube Conference on Epigenetics, Research Center for Natural Sciences, Budapest, Hungary.
- **2017:** VIII International Melanoma, Workshop, Sestri Levante, Liguria Italy.
- **2018:** European Society for Pigment Cell Research (ESPCR) annual meeting, Rennes, France.
- **2018:** TriRhena Transcription and Chromatin Club, Freiburg, Germany.
- **2019:** The American Society for Biochemistery and Molecular Biology (ASBMB), Annual Meeting, Orlando, Florida, USA.
- **2019:** Mechanism of Eukaryotic transcription, Cold Spring Harbor, New-York, USA

BIBLIOGRAPHY

Aalfs, J. D., & Kingston, R. E. (2000). What does 'chromatin remodeling' mean? *Trends in Biochemical Sciences*, *25*(11), 548–555. https://doi.org/10.1016/S0968-0004(00)01689-3

Abdel-Malek, Z., Swope, V. B., Suzuki, I., Akcali, C., Harriger, M. D., Boyce, S. T., … Hearing, V. J. (1995). Mitogenic and melanogenic stimulation of normal human melanocytes by melanotropic peptides. *Proceedings of the National Academy of Sciences of the United States of America*, *92*(5), 1789–1793. https://doi.org/10.1073/pnas.92.5.1789

Adameyko, I., Lallemend, F., Aquino, J. B., Pereira, J. A., Topilko, P., Müller, T., … Ernfors, P. (2009). Schwann Cell Precursors from Nerve Innervation Are a Cellular Origin of Melanocytes in Skin. *Cell*, *139*(2), 366–379. https://doi.org/10.1016/j.cell.2009.07.049

Akbani, R., Akdemir, K. C., Aksoy, B. A., Albert, M., Ally, A., Amin, S. B., … Zou, L. (2015). Genomic Classification of Cutaneous Melanoma. *Cell*, *161*(7), 1681–1696. https://doi.org/10.1016/j.cell.2015.05.044

Alhazmi, A. S., Mack, M., Petencin, A., Nelson, H., Rolle, T., Hiegel, J., … Landry, J. W. (2018). WITHDRAWN: The chromatin remodeling complex NURF localizes to gene bodies and is required for mRNA processing. *Journal of Biological Chemistry*, jbc.RA118.004382. https://doi.org/10.1074/JBC.RA118.004382

Alkhatib, S. G., & Landry, J. W. (2011). The Nucleosome Remodeling Factor. *FEBS Letters*, *585*(20), 3197–3207. https://doi.org/10.1016/j.febslet.2011.09.003

Almuhaideb, A., Papathanasiou, N., & Bomanji, J. (2011). 18F-FDG PET/CT imaging in oncology. *Annals of Saudi Medicine*, *31*(1), 3–13. https://doi.org/10.4103/0256-4947.75771

Amelio, I., Cutruzzolá, F., Antonov, A., Agostini, M., & Melino, G. (2014). Serine and glycine metabolism in cancer. *Trends in Biochemical Sciences*, *39*(4), 191–198. https://doi.org/10.1016/j.tibs.2014.02.004

Anastasiou, D., Poulogiannis, G., Asara, J. M., Boxer, M. B., Jiang, J., Shen, M., … Cantley, L. C. (2011). Inhibition of pyruvate kinase M2 by reactive oxygen species contributes to cellular antioxidant responses. *Science (New York, N.Y.)*, *334*(6060), 1278–1283. https://doi.org/10.1126/science.1211485

Anastasiou, D., Yu, Y., Israelsen, W. J., Jiang, J.-K., Boxer, M. B., Hong, B. S., … Vander Heiden, M. G. (2012). Pyruvate kinase M2 activators promote tetramer formation and suppress tumorigenesis. *Nature Chemical Biology*, *8*(10), 839–847. https://doi.org/10.1038/nchembio.1060

Ando, H., Niki, Y., Ito, M., Akiyama, K., Matsui, M. S., Yarosh, D. B., & Ichihashi, M. (2012). Melanosomes Are Transferred from Melanocytes to Keratinocytes through the Processes of Packaging, Release, Uptake, and Dispersion. *Journal of Investigative Dermatology*, *132*(4), 1222–1229. https://doi.org/10.1038/jid.2011.413

Ando, H., Niki, Y., Yoshida, M., Ito, M., Akiyama, K., Kim, J.-H., … Ichihashi, M. (2011). Involvement of pigment globules containing multiple melanosomes in the transfer of melanosomes from melanocytes to keratinocytes. *Cellular Logistics*, *1*(1), 12–20. https://doi.org/10.4161/cl.1.1.13638

Andrade, F., Darrah, E., Gucek, M., Cole, R. N., Rosen, A., & Zhu, X. (2010). Autocitrullination of human peptidyl arginine deiminase type 4 regulates protein citrullination during cell activation. *Arthritis & Rheumatism*, *62*(6), 1630–1640. https://doi.org/10.1002/art.27439

Ardlie, K. G., Deluca, D. S., Segre, A. V., Sullivan, T. J., Young, T. R., Gelfand, E. T., … Dermitzakis, E. T. (2015). The Genotype-Tissue Expression (GTEx) pilot analysis: Multitissue gene regulation in humans. *Science*, *348*(6235), 648–660. https://doi.org/10.1126/science.1262110

Arents, G., Burlingame, R. W., Wang, B. C., Love, W. E., & Moudrianakis, E. N. (1991). The nucleosomal core histone octamer at 3.1 A resolution: a tripartite protein assembly and a left-handed superhelix. *Proceedings of the National Academy of Sciences*, *88*(22), 10148–10152. https://doi.org/10.1073/pnas.88.22.10148

Arita, K., Hashimoto, H., Shimizu, T., Nakashima, K., Yamada, M., & Sato, M. (2004). Structural basis for Ca2+-induced activation of human PAD4. *Nature Structural & Molecular Biology*, *11*(8), 777–783. https://doi.org/10.1038/nsmb799

Armstrong, B. K. (1988). Epidemiology of Malignant Melanoma: Intermittent or Total Accumulated Exposure to the Sun? *The Journal of Dermatologic Surgery and Oncology*, *14*(8), 835–849. https://doi.org/10.1111/j.1524-4725.1988.tb03588.x

Aydin, Ö. Z., Vermeulen, W., & Lans, H. (2014). ISWI chromatin remodeling complexes in the DNA damage response. *Cell Cycle*, *13*(19), 3016–3025. https://doi.org/10.4161/15384101.2014.956551

Baade, P., Meng, X., Youlden, D., Aitken, J., & Youl, P. (2012). Time trends and latitudinal differences in melanoma thickness distribution in Australia, 1990-2006. *International Journal of Cancer*, *130*(1), 170–178. https://doi.org/10.1002/ijc.25996

Badal, B., Solovyov, A., Cecilia, S. Di, Chan, J. M., Chang, L.-W., Iqbal, R., … Celebi, J. T. (2017). *Transcriptional dissection of melanoma identifies a high-risk subtype underlying TP53 family genes and epigenome deregulation*. https://doi.org/10.1172/jci.insight.92102

Bagchi, A., Papazoglu, C., Wu, Y., Capurso, D., Brodt, M., Francis, D., … Mills, A. A. (2007). CHD5 Is a Tumor Suppressor at Human 1p36. *Cell*, *128*(3), 459–475. https://doi.org/10.1016/j.cell.2006.11.052

Balkwill, F., & Mantovani, A. (2001). Inflammation and cancer: back to Virchow? *The Lancet*, *357*(9255), 539–545. https://doi.org/10.1016/S0140-6736(00)04046-0

Ballantine, K. R., Watson, H., Macfarlane, S., Winstanley, M., Corbett, R. P., Spearing, R., … Sullivan, M. J. (2017). Small Numbers, Big Challenges: Adolescent and Young Adult Cancer Incidence and Survival in New Zealand. *Journal of Adolescent and Young Adult Oncology*, *6*(2), 277–285. https://doi.org/10.1089/jayao.2016.0074

Ballotti, R., & Bertolotto, C. (2017). Deregulated MITF sumoylation: A route to melanoma. *Molecular & Cellular Oncology*, *4*(4). https://doi.org/10.1080/23723556.2017.1331154

Bannister, A. J., & Kouzarides, T. (2011). Regulation of chromatin by histone modifications. *Cell Research*, *21*(3), 381–395. https://doi.org/10.1038/cr.2011.22

Bar-Sagi, D., & Feramisco, J. R. (1986). Induction of membrane ruffling and fluid-phase pinocytosis in quiescent fibroblasts by ras proteins. *Science (New York, N.Y.)*, *233*(4768), 1061–1068. Retrieved from http://www.ncbi.nlm.nih.gov/pubmed/3090687

Bartke, T., Vermeulen, M., Xhemalce, B., Robson, S. C., Mann, M., & Kouzarides, T. (2010). Nucleosome-Interacting Proteins Regulated by DNA and Histone Methylation. *Cell*, *143*(3), 470–484. https://doi.org/10.1016/j.cell.2010.10.012

Bartrons, R., Simon-Molas, H., Rodríguez-García, A., Castaño, E., Navarro-Sabaté, À., Manzano, A., & Martinez-Outschoorn, U. E. (2018). Fructose 2,6-Bisphosphate in Cancer Cell Metabolism. *Frontiers in Oncology*, *8*, 331. https://doi.org/10.3389/fonc.2018.00331

Batus, M., Waheed, S., Ruby, C., Petersen, L., Bines, S. D., & Kaufman, H. L. (2013). Optimal Management of Metastatic Melanoma: Current Strategies and Future Directions. *American Journal of Clinical Dermatology*, *14*(3), 179–194. https://doi.org/10.1007/s40257-013-0025-9

Beadling, C., Jacobson-Dunlop, E., Hodi, F. S., Le, C., Warrick, A., Patterson, J., … Corless, C. L. (2008). KIT Gene Mutations and Copy Number in Melanoma Subtypes. *Clinical Cancer Research*, *14*(21), 6821–6828. https://doi.org/10.1158/1078-0432.CCR-08-0575

Becker, P. B., & Workman, J. L. (2013). Nucleosome Remodeling and Epigenetics. *Cold Spring Harbor Perspectives in Biology*, *5*(9), a017905–a017905. https://doi.org/10.1101/cshperspect.a017905

Becker, T. M., Haferkamp, S., Dijkstra, M. K., Scurr, L. L., Frausto, M., Diefenbach, E., … Rizos, H. (2009). The chromatin remodelling factor BRG1 is a novel binding partner of the tumor suppressor p16INK4a. *Molecular Cancer*, *8*, 4. https://doi.org/10.1186/1476-4598-8-4

Belandia, B., Orford, R. L., Hurst, H. C., & Parker, M. G. (2002). Targeting of SWI/SNF chromatin remodelling complexes to estrogen-responsive genes. *The EMBO Journal*, *21*(15), 4094–4103. https://doi.org/10.1093/emboj/cdf412

Bennett, D. C. (2003). Human melanocyte senescence and melanoma susceptibility genes. *Oncogene*, *22*(20), 3063–3069. https://doi.org/10.1038/sj.onc.1206446

Berg, J. M. (Jeremy M., Tymoczko, J. L., Stryer, L., & Stryer, L. (2002). *Biochemistry*. W.H. Freeman.

Berger, S. L. (2007). The complex language of chromatin regulation during transcription. *Nature*, *447*(7143), 407–412. https://doi.org/10.1038/nature05915

Beroukhim, R., Mermel, C. H., Porter, D., Wei, G., Raychaudhuri, S., Donovan, J., … Meyerson, M. (2010). The landscape of somatic copy-number alteration across human cancers. *Nature*, *463*(7283), 899–905. https://doi.org/10.1038/nature08822

Bertolotto, C., Abbe, P., Hemesath, T. J., Bille, K., Fisher, D. E., Ortonne, J.-P., & Ballotti, R. (1998). Microphthalmia Gene Product as a Signal Transducer in cAMP-Induced Differentiation of Melanocytes. *The Journal of Cell Biology*, *142*(3), 827–835. https://doi.org/10.1083/jcb.142.3.827

Bertolotto, C., Lesueur, F., Giuliano, S., Strub, T., de Lichy, M., Bille, K., … Bressac-de Paillerets, B. (2011). A SUMOylation-defective MITF germline mutation predisposes to melanoma and renal carcinoma. *Nature*, *480*(7375), 94–98.

https://doi.org/10.1038/nature10539

Betters, E., Liu, Y., Kjaeldgaard, A., Sundström, E., & García-Castro, M. I. (2010). Analysis of early human neural crest development. *Developmental Biology*, *344*(2), 578–592. https://doi.org/10.1016/j.ydbio.2010.05.012

Beuret, L., Flori, E., Denoyelle, C., Bille, K., Busca, R., Picardo, M., … Ballotti, R. (2007). Up-regulation of MET Expression by α-Melanocyte-stimulating Hormone and MITF Allows Hepatocyte Growth Factor to Protect Melanocytes and Melanoma Cells from Apoptosis. *Journal of Biological Chemistry*, *282*(19), 14140–14147. https://doi.org/10.1074/jbc.M611563200

Bhutia, Y. D., Babu, E., Ramachandran, S., & Ganapathy, V. (2015a). Amino Acid Transporters in Cancer and Their Relevance to Glutamine Addiction. Novel Targets for the Design of a New Class of Anticancer Drugs. *Cancer Research*, *75*(9), 1782–1788. https://doi.org/10.1158/0008-5472.CAN-14-3745

Bicker, K. L., & Thompson, P. R. (2013). The protein arginine deiminases: Structure, function, inhibition, and disease. *Biopolymers*, *99*(2), 155–163. https://doi.org/10.1002/bip.22127

Birkeland, E., Zhang, S., Poduval, D., Geisler, J., Nakken, S., Vodak, D., … Lønning, P. E. (2018). *Patterns of genomic evolution in advanced melanoma*. https://doi.org/10.1038/s41467-018-05063-1

Biswas, S., & Rao, C. M. (2018). Epigenetic tools (The Writers, The Readers and The Erasers) and their implications in cancer therapy. *European Journal of Pharmacology*, *837*, 8–24. https://doi.org/10.1016/J.EJPHAR.2018.08.021

Bluemlein, K., Grüning, N.-M., Feichtinger, R. G., Lehrach, H., Kofler, B., Ralser, M., … Ralser, M. (2011). No evidence for a shift in pyruvate kinase PKM1 to PKM2 expression during tumorigenesis. *Oncotarget*, *2*(5), 393–400. https://doi.org/10.18632/oncotarget.278

Bond, A. M., Bhalala, O. G., & Kessler, J. A. (2012). The dynamic role of bone morphogenetic proteins in neural stem cell fate and maturation. *Developmental Neurobiology*, *72*(7), 1068–1084. https://doi.org/10.1002/dneu.22022

Bonet, C., Luciani, F., Ottavi, J.-F., Leclerc, J., Jouenne, F.-M., Boncompagni, M., … Bertolotto, C. (2017). Deciphering the Role of Oncogenic MITFE318K in Senescence Delay and Melanoma Progression. *JNCI: Journal of the National Cancer Institute*, *109*(8). https://doi.org/10.1093/jnci/djw340

Bornelö, S., Reynolds, N., Xenophontos, M., Dietmann, S., Bertone, P., & Correspondence, B. H. (2018). The Nucleosome Remodeling and Deacetylation Complex Modulates Chromatin Structure at Sites of Active Transcription to Fine-Tune Gene Expression. *Molecular Cell*, *71*, 56–72. https://doi.org/10.1016/j.molcel.2018.06.003

Bossi, D., Cicalese, A., Dellino, G. I., Luzi, L., Riva, L., D'Alesio, C., … Lanfrancone, L. (2016). In Vivo Genetic Screens of Patient-Derived Tumors Revealed Unexpected Frailty of the Transformed Phenotype. *Cancer Discovery*, *6*(6), 650–663. https://doi.org/10.1158/2159-8290.CD-15-1200

Bowen, N. J., Fujita, N., Kajita, M., & Wade, P. A. (2004). Mi-2/NuRD: multiple complexes for many purposes. *Biochimica et Biophysica Acta (BBA) - Gene Structure and Expression*, *1677*(1–3), 52–57. https://doi.org/10.1016/j.bbaexp.2003.10.010

Bowker-Kinley, M. M., Davis, W. I., Wu, P., Harris, R. A., & Popov, K. M. (1998). Evidence for existence of tissue-specific regulation of the mammalian pyruvate dehydrogenase complex. *The Biochemical Journal*, *329 (Pt 1)*(Pt 1), 191–196. https://doi.org/10.1042/bj3290191

Bowman, G. D. (2010). Mechanisms of ATP-dependent nucleosome sliding. *Current Opinion in Structural Biology*, *20*(1), 73–81. https://doi.org/10.1016/J.SBI.2009.12.002

Boyer, L. A., Latek, R. R., & Peterson, C. L. (2004). The SANT domain: a unique histone-tail-binding module? *Nature Reviews Molecular Cell Biology*, *5*(2), 158–163. https://doi.org/10.1038/nrm1314

Bracken, A. P., Brien, G. L., & Verrijzer, C. P. (2019a). Dangerous liaisons: interplay between SWI/SNF, NuRD, and Polycomb in chromatin regulation and cancer. *Genes & Development*. https://doi.org/10.1101/gad.326066.119

Breeden L, N. K. (1987). *Cell cycle control of the yeast HO gene: cis- and trans-acting regulators*. Retrieved from https://www.ncbi.nlm.nih.gov/pubmed/3542227

Breitzig, M., Bhimineni, C., Lockey, R., & Kolliputi, N. (2016). 4-Hydroxy-2-nonenal: a critical target in oxidative stress? *Am J Physiol Cell Physiol*, *311*, 537–543. https://doi.org/10.1152/ajpcell.00101.2016.-In

Brenner, M., & Hearing, V. J. (2008). The Protective Role of Melanin Against UV Damage in Human Skin†. *Photochemistry and*

Photobiology, *84*(3), 539–549. https://doi.org/10.1111/j.1751-1097.2007.00226.x

Bronner, M. E. (2012). *Formation and migration of neural crest cells in the vertebrate embryo*. https://doi.org/10.1007/s00418-012-0999-z

Brown, N. J., Higham, S. E., Perunovic, B., Arafa, M., Balasubramanian, S., & Rehman, I. (2013). Lactate Dehydrogenase-B Is Silenced by Promoter Methylation in a High Frequency of Human Breast Cancers. *PLoS ONE*, *8*(2), e57697. https://doi.org/10.1371/journal.pone.0057697

Bührens, R. I., Amelung, J. T., Reymond, M. A., & Beshay, M. (2009). Protein Expression in Human Non-Small Cell Lung Cancer: A Systematic Database. *Pathobiology*, *76*(6), 277–285. https://doi.org/10.1159/000245893

Buscà, R., Berra, E., Gaggioli, C., Khaled, M., Bille, K., Marchetti, B., … Ballotti, R. (2005). Hypoxia-inducible factor 1{alpha} is a new target of microphthalmia-associated transcription factor (MITF) in melanoma cells. *The Journal of Cell Biology*, *170*(1), 49–59. https://doi.org/10.1083/jcb.200501067

Buschbeck, M., & Hake, S. B. (2017). *Variants of core histones and their roles in cell fate decisions, development and cancer*. https://doi.org/10.1038/nrm.2016.166

Bush, W. D., & Simon, J. D. (2007). Quantification of Ca^{2+} binding to melanin supports the hypothesis that melanosomes serve a functional role in regulating calcium homeostasis. *Pigment Cell Research*, *20*(2), 134–139. https://doi.org/10.1111/j.1600-0749.2007.00362.x

Cai, Y., Geutjes, E.-J., de Lint, K., Roepman, P., Bruurs, L., Yu, L.-R., … Baylin, S. B. (2014). The NuRD complex cooperates with DNMTs to maintain silencing of key colorectal tumor suppressor genes. *Oncogene*, *33*(17), 2157–2168. https://doi.org/10.1038/onc.2013.178

Cairns, R. A., Harris, I. S., & Mak, T. W. (2011). Regulation of cancer cell metabolism. *Nature Publishing Group*, *11*. https://doi.org/10.1038/nrc2981

Campagne, C., Reyes-Gomez, E., Picco, M. E., Loiodice, S., Salaun, P., Ezagal, J., … Egidy, G. (2017). RACK1 cooperates with NRAS Q61K to promote melanoma in vivo. *Cellular Signaling*, *36*, 255–266. https://doi.org/10.1016/j.cellsig.2017.03.015

Cantó, C., Menzies, K. J., & Auwerx, J. (2015). NAD+ Metabolism and the Control of Energy Homeostasis: A Balancing Act between Mitochondria and the Nucleus. *Cell Metabolism*, *22*(1), 31–53. https://doi.org/10.1016/j.cmet.2015.05.023

Capello, M., Ferri-Borgogno, S., Cappello, P., & Novelli, F. (2011). α-enolase: a promising therapeutic and diagnostic tumor target. *FEBS Journal*, *278*(7), 1064–1074. https://doi.org/10.1111/j.1742-4658.2011.08025.x

Capello, M., Ferri-Borgogno, S., Riganti, C., Chattaragada, M. S., Principe, M., Roux, C., … Novelli, F. (2016). Targeting the Warburg effect in cancer cells through ENO1 knockdown rescues oxidative phosphorylation and induces growth arrest. *Oncotarget*, *7*(5), 5598–5612. https://doi.org/10.18632/oncotarget.6798

Carey, B. W., Finley, L. W. S., Cross, J. R., Allis, C. D., & Thompson, C. B. (2015). Intracellular α-ketoglutarate maintains the pluripotency of embryonic stem cells. *Nature*, *518*(7539), 413–416. https://doi.org/10.1038/nature13981

Carreira, S., Goodall, J., Denat, L., Rodriguez, M., Nuciforo, P., Hoek, K. S., … Goding, C. R. (2006). Mitf regulation of Dia1 controls melanoma proliferation and invasiveness. *Genes & Development*, *20*(24), 3426–3439. https://doi.org/10.1101/gad.406406

Ceruti, P., Principe, M., Capello, M., Cappello, P., & Novelli, F. (2013). Three are better than one: plasminogen receptors as cancer theranostic targets. *Experimental Hematology & Oncology*, *2*(1), 12. https://doi.org/10.1186/2162-3619-2-12

Cesi, G., Walbrecq, G., Zimmer, A., Kreis, S., & Haan, C. (2017). ROS production induced by BRAF inhibitor treatment rewires metabolic processes affecting cell growth of melanoma cells. *Molecular Cancer*, *16*(1), 102. https://doi.org/10.1186/s12943-017-0667-y

Chai, Y. J., Yi, J. W., Oh, S. W., Kim, Y. A., Yi, K. H., Kim, J. H., & Lee, K. E. (2017). Upregulation of SLC2 (GLUT) family genes is related to poor survival outcomes in papillary thyroid carcinoma: Analysis of data from The Cancer Genome Atlas. *Surgery (United States)*, *161*(1), 188–194. https://doi.org/10.1016/j.surg.2016.04.050

Chaneton, B., Hillmann, P., Zheng, L., Martin, A. C. L., Maddocks, O. D. K., Chokkathukalam, A., … Gottlieb, E. (2012). Serine is a natural ligand and allosteric activator of pyruvate kinase M2. *Nature*, *491*(7424), 458–462. https://doi.org/10.1038/nature11540

Chang, Y.-C., Chan, Y.-C., Chang, W.-M., Lin, Y.-F., Yang, C.-J., Su, C.-Y., … Hsiao, M. (2017). Feedback regulation of ALDOA activates the HIF-1α/MMP9 axis to promote lung cancer progression. *Cancer Letters*, *403*, 28–36. https://doi.org/10.1016/J.CANLET.2017.06.001

Chao, L. X., Patterson, S. S. L., Rademaker, A. W., Liu, D., & Kundu, R. V. (2017). Melanoma Perception in People of Color: A

Targeted Educational Intervention. *American Journal of Clinical Dermatology*, *18*(3), 419–427. https://doi.org/10.1007/s40257-016-0244-y

Chaoui, A., Kavo, A., Baral, V., Watanabe, Y., Lecerf, L., Colley, A., … Bondurand, N. (2015). Subnuclear re-localization of SOX10 and p54NRB correlates with a unique neurological phenotype associated with SOX10 missense mutations. *Human Molecular Genetics*, *24*(17), 4933–4947. https://doi.org/10.1093/hmg/ddv215

Chapman, P. B., Hauschild, A., Robert, C., Haanen, J. B., Ascierto, P., Larkin, J., … BRIM-3 Study Group. (2011). Improved Survival with Vemurafenib in Melanoma with BRAF V600E Mutation. *New England Journal of Medicine*, *364*(26), 2507–2516. https://doi.org/10.1056/NEJMoa1103782

Chappell, W. H., Steelman, L. S., Long, J. M., Kempf, R. C., Abrams, S. L., Franklin, R. A., … McCubrey, J. A. (2011). Ras/Raf/MEK/ERK and PI3K/PTEN/Akt/mTOR Inhibitors: Rationale and Importance to Inhibiting These Pathways in Human Health. *Oncotarget*, *2*(3), 135–164. https://doi.org/10.18632/oncotarget.240

Chavanas, S., Méchin, M.-C., Takahara, H., Kawada, A., Nachat, R., Serre, G., & Simon, M. (2004). Comparative analysis of the mouse and human peptidylarginine deiminase gene clusters reveals highly conserved non-coding segments and a new human gene, PADI6. *Gene*, *330*, 19–27. https://doi.org/10.1016/j.gene.2003.12.038

Cheli, Y., Guiliano, S., Botton, T., Rocchi, S., Hofman, V., Hofman, P., … Ballotti, R. (2011). Mitf is the key molecular switch between mouse or human melanoma initiating cells and their differentiated progeny. *Oncogene*, *30*(20), 2307–2318. https://doi.org/10.1038/onc.2010.598

Cheli, Yann, Ohanna, M., Ballotti, R., & Bertolotto, C. (2010). Fifteen-year quest for microphthalmia-associated transcription factor target genes. *Pigment Cell & Melanoma Research*, *23*(1), 27–40. https://doi.org/10.1111/j.1755-148X.2009.00653.x

Chen, G., Wang, L., Liu, S., Chuang, C., & Roche, T. E. (1996). Activated Function of the Pyruvate Dehydrogenase Phosphatase through Ca^{2+} -facilitated Binding to the Inner Lipoyl Domain of the Dihydrolipoyl Acetyltransferase. *Journal of Biological Chemistry*, *271*(45), 28064–28070. https://doi.org/10.1074/jbc.271.45.28064

Chen, T., Huang, Z., Tian, Y., Lin, B., He, R., Wang, H., … Wu, L. (2017). Clinical significance and prognostic value of Triosephosphate isomerase expression in gastric cancer. *Medicine*, *96*(19), e6865. https://doi.org/10.1097/MD.0000000000006865

Chen, T., Huang, Z., Tian, Y., Wang, H., Ouyang, P., Chen, H., … He, R. (2017). Role of triosephosphate isomerase and downstream functional genes on gastric cancer. *Oncology Reports*, *38*(3), 1822–1832. https://doi.org/10.3892/or.2017.5846

Chen, W.-Z., Pang, B., Yang, B., Zhou, J.-G., & Sun, Y.-H. (2011). Differential proteome analysis of conditioned medium of BPH-1 and LNCaP cells. *Chinese Medical Journal*, *124*(22), 3806–3809. Retrieved from http://www.ncbi.nlm.nih.gov/pubmed/22340245

Chen, X., Yang, T.-T., Zhou, Y., Wang, W., Qiu, X.-C., Gao, J., … Fan, Q.-Y. (2014). Proteomic profiling of osteosarcoma cells identifies ALDOA and SULT1A3 as negative survival markers of human osteosarcoma. *Molecular Carcinogenesis*, *53*(2), 138–144. https://doi.org/10.1002/mc.21957

Chen, Y.-J., Huang, X., Mahieu, N. G., Cho, K., Schaefer, J., & Patti, G. J. (2014). Differential Incorporation of Glucose into Biomass during Warburg Metabolism. *Biochemistry*, *53*(29), 4755–4757. https://doi.org/10.1021/bi500763u

Cheng, X. (2014). Structural and Functional Coordination of DNA and Histone Methylation. *Cold Spring Harbor Perspectives in Biology*, *6*(8), a018747–a018747. https://doi.org/10.1101/cshperspect.a018747

Cherrington, B. D., Morency, E., Struble, A. M., Coonrod, S. A., & Wakshlag, J. J. (2010). Potential Role for Peptidylarginine Deiminase 2 (PAD2) in Citrullination of Canine Mammary Epithelial Cell Histones. *PLoS ONE*, *5*(7), e11768. https://doi.org/10.1371/journal.pone.0011768

Cho, E., Rosner, B. A., & Colditz, G. A. (2005). Risk Factors for Melanoma by Body Site. *Cancer Epidemiology Biomarkers & Prevention*, *14*(5), 1241–1244. https://doi.org/10.1158/1055-9965.EPI-04-0632

Christofk, H. R., Vander Heiden, M. G., Harris, M. H., Ramanathan, A., Gerszten, R. E., Wei, R., … Cantley, L. C. (2008). The M2 splice isoform of pyruvate kinase is important for cancer metabolism and tumour growth. *Nature*, *452*(7184), 230–233. https://doi.org/10.1038/nature06734

Christofk, H. R., Vander Heiden, M. G., Wu, N., Asara, J. M., & Cantley, L. C. (2008a). Pyruvate kinase M2 is a

phosphotyrosine-binding protein. *Nature*, *452*(7184), 181–186. https://doi.org/10.1038/nature06667

Christophorou, M. A., Castelo-Branco, G., Halley-Stott, R. P., Oliveira, C. S., Loos, R., Radzisheuskaya, A., … Kouzarides, T. (2014). Citrullination regulates pluripotency and histone H1 binding to chromatin. *Nature*, *507*(7490), 104–108. https://doi.org/10.1038/nature12942

Chudnovsky, Y., Kim, D., Zheng, S., Whyte, W. A., Bansal, M., Bray, M.-A., … Chheda, M. G. (2014). ZFHX4 Interacts with the NuRD Core Member CHD4 and Regulates the Glioblastoma Tumor-Initiating Cell State. *Cell Reports*, *6*(2), 313–324. https://doi.org/10.1016/j.celrep.2013.12.032

Clapier, C. R., & Cairns, B. R. (2009b). The Biology of Chromatin Remodeling Complexes. *Annual Review of Biochemistry*, *78*(1), 273–304. https://doi.org/10.1146/annurev.biochem.77.062706.153223

Clapier, C. R., Iwasa, J., Cairns, B. R., & Peterson, C. L. (2017). Mechanisms of action and regulation of ATP-dependent chromatin-remodelling complexes. *Nature Reviews Molecular Cell Biology*, *18*(7), 407–422. https://doi.org/10.1038/nrm.2017.26

Clark, W. H., Elder, D. E., Guerry, D., Epstein, M. N., Greene, M. H., & Van Horn, M. (1984). A study of tumor progression: the precursor lesions of superficial spreading and nodular melanoma. *Human Pathology*, *15*(12), 1147–1165. Retrieved from http://www.ncbi.nlm.nih.gov/pubmed/6500548

Clark, W. H., From, L., Bernardino, E. A., & Mihm, M. C. (1969a). The histogenesis and biologic behavior of primary human malignant melanomas of the skin. *Cancer Research*, *29*(3), 705–727. Retrieved from http://www.ncbi.nlm.nih.gov/pubmed/5773814

Clarke, S. D. (1993). Regulation of fatty acid synthase gene expression: an approach for reducing fat accumulation. *Journal of Animal Science*, *71*(7), 1957–1965. https://doi.org/10.2527/1993.7171957x

Clayton, E., Doupé, D. P., Klein, A. M., Winton, D. J., Simons, B. D., & Jones, P. H. (2007). A single type of progenitor cell maintains normal epidermis. *Nature*, *446*(7132), 185–189. https://doi.org/10.1038/nature05574

Colantonio, S., Bracken, M. B., & Beecker, J. (2014). The association of indoor tanning and melanoma in adults: Systematic review and meta-analysis. *Journal of the American Academy of Dermatology*, *70*(5), 847-857.e18. https://doi.org/10.1016/j.jaad.2013.11.050

Colombo, S. L., Palacios-Callender, M., Frakich, N., Carcamo, S., Kovacs, I., Tudzarova, S., & Moncada, S. (2011). Molecular basis for the differential use of glucose and glutamine in cell proliferation as revealed by synchronized HeLa cells. *Proceedings of the National Academy of Sciences*, *108*(52), 21069–21074. https://doi.org/10.1073/pnas.1117500108

Colombo, S. L., Palacios-Callender, M., Frakich, N., De Leon, J., Schmitt, C. A., Boorn, L., … Moncada, S. (2010). Anaphase-promoting complex/cyclosome-Cdh1 coordinates glycolysis and glutaminolysis with transition to S phase in human T lymphocytes. *Proceedings of the National Academy of Sciences*, *107*(44), 18868–18873. https://doi.org/10.1073/pnas.1012362107

Colomer, D., Vives-Corrons, J. L., Pujades, A., & Bartrons, R. (1987). Control of phosphofructokinase by fructose 2,6-bisphosphate in B-lymphocytes and B-chronic lymphocytic leukemia cells. *Cancer Research*, *47*(7), 1859–1862. Retrieved from http://www.ncbi.nlm.nih.gov/pubmed/2949829

Commisso, C., Davidson, S. M., Soydaner-Azeloglu, R. G., Parker, S. J., Kamphorst, J. J., Hackett, S., … Bar-Sagi, D. (2013). Macropinocytosis of protein is an amino acid supply route in Ras-transformed cells. *Nature*, *497*(7451), 633–637. https://doi.org/10.1038/nature12138

Connor, H., Woods, H. F., & Ledingham, J. G. G. (1983). Comparison of the Kinetics and Utilisation of <i>D</i>(-)- and <i>L</i>(+)-Sodium Lactate in Normal Man. *Annals of Nutrition and Metabolism*, *27*(6), 481–487. https://doi.org/10.1159/000176723

Cortesi, L., Barchetti, A., De Matteis, E., Rossi, E., Della Casa, L., Marcheselli, L., … Iannone, A. (2009). Identification of Protein Clusters Predictive of Response to Chemotherapy in Breast Cancer Patients. *Journal of Proteome Research*, *8*(11), 4916–4933. https://doi.org/10.1021/pr900239h

Cosgrove, M. S., Boeke, J. D., & Wolberger, C. (2004). Regulated nucleosome mobility and the histone code. *Nature Structural & Molecular Biology*, *11*(11), 1037–1043. https://doi.org/10.1038/nsmb851

Costa Leite, T., Da Silva, D., Guimarães Coelho, R., Zancan, P., & Sola-Penna, M. (2007). Lactate favours the dissociation of skeletal muscle 6-phosphofructo-1-kinase tetramers down-regulating the enzyme and muscle glycolysis. *Biochemical Journal*, *408*(1), 123–130. https://doi.org/10.1042/BJ20070687

Costin, G.-E., & Hearing, V. J. (2007). Human skin pigmentation: melanocytes modulate skin color in response to stress. *The FASEB Journal*, *21*(4), 976–994. https://doi.org/10.1096/fj.06-6649rev

Cotsarelis, G., Sun, T.-T., & Lavker, R. M. (1990). Label-retaining cells reside in the bulge area of pilosebaceous unit: Implications for follicular stem cells, hair cycle, and skin carcinogenesis. *Cell*, *61*(7), 1329–1337. https://doi.org/10.1016/0092-8674(90)90696-C

Counihan, J. L., Grossman, E. A., & Nomura, D. K. (2018). Cancer Metabolism: Current Understanding and Therapies. *Chemical Reviews*, *118*(14), 6893–6923. https://doi.org/10.1021/acs.chemrev.7b00775

Cramer, S. F. (1984). The histogenesis of acquired melanocytic nevi. Based on a new concept of melanocytic differentiation. *The American Journal of Dermatopathology*, *6 Suppl*, 289–298. Retrieved from http://www.ncbi.nlm.nih.gov/pubmed/6528932

Crombie, I. K. (1979). Variation of melanoma incidence with latitude in North America and Europe. *British Journal of Cancer*, *40*(5), 774–781. https://doi.org/10.1038/bjc.1979.260

Cronin, J. C., Watkins-Chow, D. E., Incao, A., Hasskamp, J. H., Schonewolf, N., Aoude, L. G., … Pavan, W. J. (2013). SOX10 Ablation Arrests Cell Cycle, Induces Senescence, and Suppresses Melanomagenesis. *Cancer Research*, *73*(18), 5709–5718. https://doi.org/10.1158/0008-5472.CAN-12-4620

Cronin, Julia C., Wunderlich, J., Loftus, S. K., Prickett, T. D., Wei, X., Ridd, K., … Samuels, Y. (2009). Frequent mutations in the MITF pathway in melanoma. *Pigment Cell & Melanoma Research*, *22*(4), 435–444. https://doi.org/10.1111/j.1755-148X.2009.00578.x

Csibi, A., Fendt, S.-M., Li, C., Poulogiannis, G., Choo, A. Y., Chapski, D. J., … Blenis, J. (2013). The mTORC1 Pathway Stimulates Glutamine Metabolism and Cell Proliferation by Repressing SIRT4. *Cell*, *153*(4), 840–854. https://doi.org/10.1016/j.cell.2013.04.023

Cunha De Padua, M., Delodi, G., Vučetić, M., Durivault, J., Vial, V., Bayer, P., … Pouysségur, J. (2017). *Disrupting glucose-6-phosphate isomerase fully suppresses the "Warburg effect" and activates OXPHOS with minimal impact on tumor growth except in hypoxia*. Retrieved from www.impactjournals.com/oncotarget

Curthoys, N. P., & Watford, M. (1995). Regulation of Glutaminase Activity and Glutamine Metabolism. *Annual Review of Nutrition*, *15*(1), 133–159. https://doi.org/10.1146/annurev.nu.15.070195.001025

Curtin, J. A., Fridlyand, J., Kageshita, T., Patel, H. N., Busam, K. J., Kutzner, H., … Bastian, B. C. (2005). Distinct Sets of Genetic Alterations in Melanoma. *New England Journal of Medicine*, *353*(20), 2135–2147. https://doi.org/10.1056/NEJMoa050092

Cuthbert, G. L., Daujat, S., Snowden, A. W., Erdjument-Bromage, H., Hagiwara, T., Yamada, M., … Kouzarides, T. (2004). Histone Deimination Antagonizes Arginine Methylation. *Cell*, *118*(5), 545–553. https://doi.org/10.1016/j.cell.2004.08.020

Czarnecka, A. M., Klemba, A., Krawczyk, T., Zdrozny, M., Arnold, R. S., Bartnik, E., & Petros, J. A. (2010). Mitochondrial NADH-dehydrogenase polymorphisms as sporadic breast cancer risk factor. *Oncology Reports*, *23*(2), 531–535. Retrieved from http://www.ncbi.nlm.nih.gov/pubmed/20043118

D'alesio, C., Bellese, G., Gagliani, M. C., Lechiara, A., Dameri, M., Grasselli, E., … Castagnola, P. (2019). *The chromodomain helicase CHD4 regulates ERBB2 signaling pathway and autophagy in ERBB2 + breast cancer cells*. https://doi.org/10.1242/bio.038323

da Silva-Diz, V., Solé-Sánchez, S., Valdés-Gutiérrez, A., Urpí, M., Riba-Artés, D., Penin, R. M., … Muñoz, P. (2013). Progeny of Lgr5-expressing hair follicle stem cell contributes to papillomavirus-induced tumor development in epidermis. *Oncogene*, *32*(32), 3732–3743. https://doi.org/10.1038/onc.2012.375

Dai, J., Ji, Y., Wang, W., Kim, D., Fai, L. Y., Wang, L., … Zhang, Z. (2017). Loss of fructose-1,6-bisphosphatase induces glycolysis and promotes apoptosis resistance of cancer stem-like cells: an important role in hexavalent chromium-induced carcinogenesis. *Toxicology and Applied Pharmacology*, *331*, 164–173. https://doi.org/10.1016/j.taap.2017.06.014

Dang, C. V., Kim, J., Gao, P., & Yustein, J. (2008). The interplay between MYC and HIF in cancer. *Nature Reviews Cancer*, *8*(1), 51–56. https://doi.org/10.1038/nrc2274

Dar, A. A., Majid, S., Bezrookove, V., Phan, B., Ursu, S., Nosrati, M., … Kashani-Sabet, M. (2016). BPTF transduces MITF-driven prosurvival signals in melanoma cells. *Proceedings of the National Academy of Sciences*, *113*(22), 6254–6258. https://doi.org/10.1073/pnas.1606027113

Dar, A. A., Nosrati, M., Bezrookove, V., de Semir, D., Majid, S., Thummala, S., … Kashani-Sabet, M. (2015). The role of BPTF in melanoma progression and in response to BRAF-targeted therapy. *Journal of the National Cancer Institute*, *107*(5). https://doi.org/10.1093/jnci/djv034

Das, C., Tyler, J. K., & Churchill, M. E. A. (2010). The histone shuffle: histone chaperones in an energetic dance. *Trends in Biochemical Sciences*, *35*(9), 476–489. https://doi.org/10.1016/j.tibs.2010.04.001

Dasgupta, S., Rajapakshe, K., Zhu, B., Nikolai, B. C., Yi, P., Putluri, N., … O'Malley, B. W. (2018). Metabolic enzyme PFKFB4 activates transcriptional coactivator SRC-3 to drive breast cancer. *Nature*, *556*(7700), 249–254. https://doi.org/10.1038/s41586-018-0018-1

David, C. J., Chen, M., Assanah, M., Canoll, P., & Manley, J. L. (2010). HnRNP proteins controlled by c-Myc deregulate pyruvate kinase mRNA splicing in cancer. *Nature*, *463*(7279), 364–368. https://doi.org/10.1038/nature08697

Davies, H., Bignell, G. R., Cox, C., Stephens, P., Edkins, S., Clegg, S., … Futreal, P. A. (2002). Mutations of the BRAF gene in human cancer. *Nature*, *417*(6892), 949–954. https://doi.org/10.1038/nature00766

Davies, M. A., Stemke-Hale, K., Tellez, C., Calderone, T. L., Deng, W., Prieto, V. G., … Mills, G. B. (2008). A novel AKT3 mutation in melanoma tumours and cell lines. *British Journal of Cancer*, *99*(8), 1265–1268. https://doi.org/10.1038/sj.bjc.6604637

Dawson, M. A., & Kouzarides, T. (2012). Cancer Epigenetics: From Mechanism to Therapy. *Cell*, *150*(1), 12–27. https://doi.org/10.1016/j.cell.2012.06.013

Dayton, T. L., Jacks, T., & Vander Heiden, M. G. (2016). PKM2, cancer metabolism, and the road ahead. *EMBO Reports*, *17*(12), 1721–1730. https://doi.org/10.15252/embr.201643300

de Dieuleveult, M., Yen, K., Hmitou, I., Depaux, A., Boussouar, F., Dargham, D. B., … Gérard, M. (2016). Genome-wide nucleosome specificity and function of chromatin remodellers in ES cells. *Nature*, *530*(7588), 113–116. https://doi.org/10.1038/nature16505

De Dieuleveult, M., Yen, K., Hmitou, I., Depaux, A., Boussouar, F., Dargham, D. B., … Gérard, M. (2016). Genome-wide nucleosome specificity and function of chromatin remodellers in ES cells. *Nature*, *530*(7588), 113–116. https://doi.org/10.1038/nature16505

De Koning, L., Corpet, A., Haber, J. E., & Almouzni, G. (2007). Histone chaperones: an escort network regulating histone traffic. *Nature Structural & Molecular Biology*, *14*(11), 997–1007. https://doi.org/10.1038/nsmb1318

de la Serna, I. L., Ohkawa, Y., Higashi, C., Dutta, C., Osias, J., Kommajosyula, N., … Imbalzano, A. N. (2006). The Microphthalmia-associated Transcription Factor Requires SWI/SNF Enzymes to Activate Melanocyte-specific Genes. *Journal of Biological Chemistry*, *281*(29), 20233–20241. https://doi.org/10.1074/jbc.M512052200

Dean NELSON, B., Kabir, F., Nelson, B., & Kabir, F. (1986). *The role of the mitochondrial outer membrane in energy metabolism of tumor cells* (Vol. 68).

Deaton, A. M., & Bird, A. (2011). CpG islands and the regulation of transcription. *Genes & Development*, *25*(10), 1010–1022. https://doi.org/10.1101/gad.2037511

DeBerardinis, R. J., & Chandel, N. S. (2016). Fundamentals of cancer metabolism. *Science Advances*, *2*(5), e1600200.

https://doi.org/10.1126/sciadv.1600200

Dell'Angelica, E. C. (2003). Melanosome biogenesis: shedding light on the origin of an obscure organelle. *Trends in Cell Biology*, *13*(10), 503–506. Retrieved from http://www.ncbi.nlm.nih.gov/pubmed/14507476

Delmas, V., Stokes, D. G., & Perry, R. P. (1993). A mammalian DNA-binding protein that contains a chromodomain and an SNF2/SWI2-like helicase domain. *Proceedings of the National Academy of Sciences*, *90*(6), 2414–2418. https://doi.org/10.1073/pnas.90.6.2414

Dillon, B. J., Prieto, V. G., Curley, S. A., Ensor, C. M., Holtsberg, F. W., Bomalaski, J. S., & Clark, M. A. (2004). Incidence and distribution of argininosuccinate synthetase deficiency in human cancers: a method for identifying cancers sensitive to arginine deprivation. *Cancer*, *100*(4), 826–833. https://doi.org/10.1002/cncr.20057

Dombrauckas, J. D., Santarsiero, B. D., & Mesecar, A. D. (2005). Structural Basis for Tumor Pyruvate Kinase M2 Allosteric Regulation and Catalysis. *Biochemistry*, *44*(27), 9417–9429. https://doi.org/10.1021/bi0474923

Domingues, B., Lopes, J. M., Soares, P., & Pópulo, H. (2018). *Melanoma treatment in review*. 7–35. https://doi.org/10.2147/ITT.S134842

Dong, T., Liu, Z., Xuan, Q., Wang, Z., Ma, W., & Zhang, Q. (2017). Tumor LDH-A expression and serum LDH status are two metabolic predictors for triple negative breast cancer brain metastasis. *Scientific Reports*, *7*(1), 6069. https://doi.org/10.1038/s41598-017-06378-7

Du, J., Miller, A. J., Widlund, H. R., Horstmann, M. A., Ramaswamy, S., & Fisher, D. E. (2003). MLANA/MART1 and SILV/PMEL17/GP100 Are Transcriptionally Regulated by MITF in Melanocytes and Melanoma. *The American Journal of Pathology*, *163*(1), 333–343. https://doi.org/10.1016/S0002-9440(10)63657-7

Du, J., Widlund, H. R., Horstmann, M. A., Ramaswamy, S., Ross, K., Huber, W. E., … Fisher, D. E. (2004). Critical role of CDK2 for melanoma growth linked to its melanocyte-specific transcriptional regulation by MITF. *Cancer Cell*, *6*(6), 565–576. https://doi.org/10.1016/j.ccr.2004.10.014

Du, X., Wu, T., Lu, J., Zang, L., Song, N., Yang, T., … Wang, S. (2013). Decreased expression of chromodomain helicase DNA-binding protein 5 is an unfavorable prognostic marker in patients with primary gallbladder carcinoma. *Clinical and Translational Oncology*, *15*(3), 198–204. https://doi.org/10.1007/s12094-012-0903-2

Dunaway, G. A., & Kasten, T. P. (1987). Nature of the subunits of the 6-phosphofructo-1-kinase isoenzymes from rat tissues. *The Biochemical Journal*, *242*(3), 667–671. https://doi.org/10.1042/bj2420667

Dunaway, G. A., Kasten, T. P., Sebo, T., & Trapp, R. (1988). Analysis of the phosphofructokinase subunits and isoenzymes in human tissues. *Biochemical Journal*, *251*(3), 677–683. https://doi.org/10.1042/bj2510677

Dupin, E., Creuzet, S., & Le Douarin, N. M. (2006). The Contribution of the Neural Crest to the Vertebrate Body. In *Advances in experimental medicine and biology* (Vol. 589, pp. 96–119). https://doi.org/10.1007/978-0-387-46954-6_6

Důra, M., Němejcová, K., Jakša, R., Bártů, M., Kodet, O., Tichá, I., … Dundr, P. (2019). Expression of Glut-1 in Malignant Melanoma and Melanocytic Nevi: an Immunohistochemical Study of 400 Cases. *Pathology & Oncology Research*, *25*(1), 361–368. https://doi.org/10.1007/s12253-017-0363-7

Dynek, J. N., Chan, S. M., Liu, J., Zha, J., Fairbrother, W. J., & Vucic, D. (2008). Microphthalmia-Associated Transcription Factor Is a Critical Transcriptional Regulator of Melanoma Inhibitor of Apoptosis in Melanomas. *Cancer Research*, *68*(9), 3124–3132. https://doi.org/10.1158/0008-5472.CAN-07-6622

Eagle, H. (1955). Nutrition needs of mammalian cells in tissue culture. *Science (New York, N.Y.)*, *122*(3168), 501–514. Retrieved from http://www.ncbi.nlm.nih.gov/pubmed/13255879

Eberharter, A., & Becker, P. B. (2004). ATP-dependent nucleosome remodelling: factors and functions. *Journal of Cell Science*, *117*(17), 3707 LP – 3711. https://doi.org/10.1242/jcs.01175

Edward J. Land, ‡, Christopher A. Ramsden, *,‡ and, & Riley§, P. A. (2003). *Tyrosinase Autoactivation and the Chemistry of ortho-Quinone Amines†*. https://doi.org/10.1021/AR020062P

Elder, D. E. (1989). Human Melanocytic Neoplasms and Their Etiologic Relationship with Sunlight. *Journal of Investigative Dermatology*, *92*(5), S297–S303. https://doi.org/10.1038/JID.1989.86

Eller, M. S., Yaar, M., & Gilchrest, B. A. (1994). DNA damage and melanogenesis. *Nature*, *372*(6505), 413–414. https://doi.org/10.1038/372413a0

Elwood, J. M., Lee, J. A. H., Walter, S. D., Mo, T., & Green, A. E. S. (1974). Relationship of Melanoma and other Skin Cancer Mortality to Latitude and Ultraviolet Radiation in the United States and Canada. *International Journal of Epidemiology*, *3*(4), 325–332. https://doi.org/10.1093/ije/3.4.325

Ennen, M, Keime, C., Kobi, D., Mengus, G., Lipsker, D., Thibault-Carpentier, C., & Davidson, I. (2015). Single-cell gene

expression signatures reveal melanoma cell heterogeneity. *Oncogene*, *34*(25), 3251–3263. https://doi.org/10.1038/onc.2014.262

Ennen, Marie, Keime, C., Gambi, G., Kieny, A., Coassolo, S., Thibault-Carpentier, C., … Davidson, I. (2017). MITF-high and MITF-low cells and a novel subpopulation expressing genes of both cell states contribute to intra- and intertumoral heterogeneity of primary melanoma. *Clinical Cancer Research*, *23*(22), 7097–7107. https://doi.org/10.1158/1078-0432.CCR-17-0010

Enzo, E., Santinon, G., Pocaterra, A., Aragona, M., Bresolin, S., Forcato, M., … Dupont, S. (2015). Aerobic glycolysis tunes YAP/TAZ transcriptional activity. *The EMBO Journal*, *34*(10), 1349–1370. https://doi.org/10.15252/embj.201490379

Epstein, T., Xu, L., Gillies, R. J., & Gatenby, R. A. (2014). Separation of metabolic supply and demand: aerobic glycolysis as a normal physiological response to fluctuating energetic demands in the membrane. *Cancer & Metabolism*, *2*(1), 7. https://doi.org/10.1186/2049-3002-2-7

Erdmann, F., Lortet-Tieulent, J., Schüz, J., Zeeb, H., Greinert, R., Breitbart, E. W., & Bray, F. (2013). International trends in the incidence of malignant melanoma 1953-2008-are recent generations at higher or lower risk? *International Journal of Cancer*, *132*(2), 385–400. https://doi.org/10.1002/ijc.27616

Erecińska, M., & Nelson, D. (1990). Activation of glutamate dehydrogenase by leucine and its nonmetabolizable analogue in rat brain synaptosomes. *Journal of Neurochemistry*, *54*(4), 1335–1343. Retrieved from http://www.ncbi.nlm.nih.gov/pubmed/1968960

Ernfors, P. (2010). Cellular origin and developmental mechanisms during the formation of skin melanocytes. *Experimental Cell Research*, *316*(8), 1397–1407. https://doi.org/10.1016/j.yexcr.2010.02.042

Etchegaray, J.-P., & Mostoslavsky, R. (2016). Interplay between metabolism and epigenetics: a nuclear adaptation to environmental changes. *Molecular Cell*, *62*(5), 695. https://doi.org/10.1016/J.MOLCEL.2016.05.029

Everett, M. A., Yeargers, E., Sayre, R. M., & Olson, R. L. (1966). PENETRATION OF EPIDERMIS BY ULTRAVIOLET RAYS. *Photochemistry and Photobiology*, *5*(7), 533–542. https://doi.org/10.1111/j.1751-1097.1966.tb09843.x

Fahien, L. A., & Kmiotek, E. (1981). Regulation of glutamate dehydrogenase by palmitoyl-coenzyme A. *Archives of Biochemistry and Biophysics*, *212*(1), 247–253. https://doi.org/10.1016/0003-9861(81)90364-7

Fanis, P., Gillemans, N., Aghajanirefah, A., Pourfarzad, F., Demmers, J., Esteghamat, F., … van Dijk, T. B. (2012). Five Friends of Methylated Chromatin Target of Protein-Arginine-Methyltransferase[Prmt]-1 (Chtop), a Complex Linking Arginine Methylation to Desumoylation. *Molecular & Cellular Proteomics*, *11*(11), 1263–1273. https://doi.org/10.1074/mcp.M112.017194

Fedorenko, I. V, Gibney, G. T., & Smalley, K. S. M. (2013). NRAS mutant melanoma: biological behavior and future strategies for therapeutic management. *Oncogene*, *32*(25), 3009–3018. https://doi.org/10.1038/onc.2012.453

Feng, C., Gao, Y., Wang, C., Yu, X., Zhang, W., Guan, H., … Teng, W. (2013). Aberrant Overexpression of Pyruvate Kinase M2 Is Associated With Aggressive Tumor Features and the *BRAF* Mutation in Papillary Thyroid Cancer. *The Journal of Clinical Endocrinology & Metabolism*, *98*(9), E1524–E1533. https://doi.org/10.1210/jc.2012-4258

Feng, Y., & Wu, L. (2017). mTOR up-regulation of PFKFB3 is essential for acute myeloid leukemia cell survival. *Biochemical and Biophysical Research Communications*, *483*(2), 897–903. https://doi.org/10.1016/j.bbrc.2017.01.031

Feo, S., Oliva, D., Barbieri, G., Xu, W. M., Fried, M., & Giallongo, A. (1990). The gene for the muscle-specific enolase is on the short arm of human chromosome 17. *Genomics*, *6*(1), 192–194. Retrieved from http://www.ncbi.nlm.nih.gov/pubmed/2303260

Ferrara, G., & De Vanna, A. C. (2016). Fluorescence In Situ Hybridization for Melanoma Diagnosis. *The American Journal of Dermatopathology*, *38*(4), 253–269. https://doi.org/10.1097/DAD.0000000000000380

Ferreras, C., Hernández, E. D., Martínez-Costa, O. H., & Aragón, J. J. (2009). Subunit Interactions and Composition of the Fructose 6-Phosphate Catalytic Site and the Fructose 2,6-Bisphosphate Allosteric Site of Mammalian Phosphofructokinase. *Journal of Biological Chemistry*, *284*(14), 9124–9131. https://doi.org/10.1074/jbc.M807737200

Fert-Bober, J., Venkatraman, V., Hunter, C. L., Liu, R., Crowgey, E. L., Pandey, R., … Van Eyk, J. E. (2019). Mapping Citrullinated Sites in Multiple Organs of Mice Using Hypercitrullinated Library. *Journal of Proteome Research*, *18*(5), 2270–2278. https://doi.org/10.1021/acs.jproteome.9b00118

Feun, L. G., Marini, A., Walker, G., Elgart, G., Moffat, F., Rodgers, S. E., … Savaraj, N. (2012). Negative argininosuccinate synthetase expression in melanoma tumours may predict clinical benefit from arginine-depleting therapy with pegylated arginine deiminase. *British Journal of Cancer*, *106*(9), 1481–1485. https://doi.org/10.1038/bjc.2012.106

Fife, B. T., & Bluestone, J. A. (2008). Control of peripheral T-cell tolerance and autoimmunity via the CTLA-4 and PD-1

pathways. *Immunological Reviews*, *224*(1), 166–182. https://doi.org/10.1111/j.1600-065X.2008.00662.x

Fischer, G. M., Vashisht Gopal, Y. N., McQuade, J. L., Peng, W., DeBerardinis, R. J., & Davies, M. A. (2018). Metabolic strategies of melanoma cells: Mechanisms, interactions with the tumor microenvironment, and therapeutic implications. *Pigment Cell & Melanoma Research*, *31*(1), 11–30. https://doi.org/10.1111/pcmr.12661

Fitzpatrick, T. B. (1988). The validity and practicality of sun-reactive skin types I through VI. *Archives of Dermatology*, *124*(6), 869–871. Retrieved from http://www.ncbi.nlm.nih.gov/pubmed/3377516

Flaherty, K. T., Infante, J. R., Daud, A., Gonzalez, R., Kefford, R. F., Sosman, J., … Weber, J. (2012). Combined BRAF and MEK Inhibition in Melanoma with BRAF V600 Mutations. *New England Journal of Medicine*, *367*(18), 1694–1703. https://doi.org/10.1056/NEJMoa1210093

Flajollet, S., Poras, I., Carosella, E. D., & Moreau, P. (2009). RREB-1 is a transcriptional repressor of HLA-G. *Journal of Immunology (Baltimore, Md. : 1950)*, *183*(11), 6948–6959. https://doi.org/10.4049/jimmunol.0902053

Flavahan, W. A., Wu, Q., Hitomi, M., Rahim, N., Kim, Y., Sloan, A. E., … Hjelmeland, A. B. (2013). Brain tumor initiating cells adapt to restricted nutrition through preferential glucose uptake. *Nature Neuroscience*, *16*(10), 1373–1382. https://doi.org/10.1038/nn.3510

Fletcher L, Rider CC, T. C. (1976). Enolase isoenzymes. III. Chromatographic and immunological characteristics of rat brain enolase. - PubMed - NCBI. Retrieved May 17, 2019, from Biochim Biophys Acta website: https://www.ncbi.nlm.nih.gov/pubmed/990313

Freeman, G. J., Long, A. J., Iwai, Y., Bourque, K., Chernova, T., Nishimura, H., … Honjo, T. (2000). Engagement of the Pd-1 Immunoinhibitory Receptor by a Novel B7 Family Member Leads to Negative Regulation of Lymphocyte Activation. *Journal of Experimental Medicine*, *192*(7), 1027–1034. https://doi.org/10.1084/JEM.192.7.1027

Fu, J., Qin, L., He, T., Qin, J., Hong, J., Wong, J., … Xu, J. (2011). The TWIST/Mi2/NuRD protein complex and its essential role in cancer metastasis. *Cell Research*, *21*(2), 275–289. https://doi.org/10.1038/cr.2010.118

Fu, Q.-F., Liu, Y., Fan, Y., Hua, S.-N., Qu, H.-Y., Dong, S.-W., … Song, X. (2015). Alpha-enolase promotes cell glycolysis, growth, migration, and invasion in non-small cell lung cancer through FAK-mediated PI3K/AKT pathway. *Journal of Hematology & Oncology*, *8*(1), 22. https://doi.org/10.1186/s13045-015-0117-5

Fuchs, E., & Horsley, V. (2008). More than one way to skin . . . *Genes & Development*, *22*(8), 976–985. https://doi.org/10.1101/gad.1645908

Fuhrmann, J., Clancy, K. W., & Thompson, P. R. (2015). *Chemical Biology of Protein Arginine Modifications in Epigenetic Regulation*. https://doi.org/10.1021/acs.chemrev.5b00003

FUJISAKI, M., & SUGAWARA, K. (1981). Properties of Peptidylarginine Deiminase from the Epidermis of Newborn Rats1. *The Journal of Biochemistry*, *89*(1), 257–263. https://doi.org/10.1093/oxfordjournals.jbchem.a133189

Fujita, N., Jaye, D. L., Kajita, M., Geigerman, C., Moreno, C. S., & Wade, P. A. (2003). MTA3, a Mi-2/NuRD complex subunit, regulates an invasive growth pathway in breast cancer. *Cell*, *113*(2), 207–219. Retrieved from http://www.ncbi.nlm.nih.gov/pubmed/12705869

Fujita, T., Igarashi, J., Okawa, E. R., Gotoh, T., Manne, J., Kolla, V., … Brodeur, G. M. (2008). CHD5 , a Tumor Suppressor Gene Deleted From 1p36.31 in Neuroblastomas. *JNCI: Journal of the National Cancer Institute*, *100*(13), 940–949. https://doi.org/10.1093/jnci/djn176

Gao, P., Tchernyshyov, I., Chang, T.-C., Lee, Y.-S., Kita, K., Ochi, T., … Dang, C. V. (2009). c-Myc suppression of miR-23a/b enhances mitochondrial glutaminase expression and glutamine metabolism. *Nature*, *458*(7239), 762–765. https://doi.org/10.1038/nature07823

Gao, X., Wang, H., Yang, J. J., Liu, X., & Liu, Z.-R. (2012). Pyruvate Kinase M2 Regulates Gene Transcription by Acting as a Protein Kinase. *Molecular Cell*, *45*(5), 598–609. https://doi.org/10.1016/j.molcel.2012.01.001

Garbe, C., & Leiter, U. (2009). Melanoma epidemiology and trends. *Clinics in Dermatology*, *27*(1), 3–9. https://doi.org/10.1016/J.CLINDERMATOL.2008.09.001

Garbe, C., Peris, K., Hauschild, A., Saiag, P., Middleton, M., Bastholt, L., … European Organisation for Research and Treatment of Cancer (EORTC). (2016). Diagnosis and treatment of melanoma. European consensus-based interdisciplinary guideline – Update 2016. *European Journal of Cancer*, *63*, 201–217. https://doi.org/10.1016/j.ejca.2016.05.005

Garcia, I., Mayol, G., Rodríguez, E., Suñol, M., Gershon, T. R., Ríos, J., … Lavarino, C. (2010a). Expression of the neuron-specific protein CHD5 is an independent marker of outcome in neuroblastoma. *Molecular Cancer*, *9*(1), 277. https://doi.org/10.1186/1476-4598-9-277

Garcia, I., Mayol, G., Rodríguez, E., Suñol, M., Gershon, T. R., Ríos, J., … Lavarino, C. (2010b). Expression of the neuron-specific protein CHD5 is an independent marker of outcome in neuroblastoma. *Molecular Cancer*, *9*(1), 277. https://doi.org/10.1186/1476-4598-9-277

Garraway, L. A., & Sellers, W. R. (2006). Lineage dependency and lineage-survival oncogenes in human cancer. *Nature Reviews Cancer*, *6*(8), 593–602. https://doi.org/10.1038/nrc1947

Garraway, L. A., Widlund, H. R., Rubin, M. A., Getz, G., Berger, A. J., Ramaswamy, S., … Sellers, W. R. (2005). Integrative genomic analyses identify MITF as a lineage survival oncogene amplified in malignant melanoma. *Nature*, *436*(7047), 117–122. https://doi.org/10.1038/nature03664

Gast, A., Scherer, D., Chen, B., Bloethner, S., Melchert, S., Sucker, A., … Kumar, R. (2010). Somatic alterations in the melanoma genome: A high-resolution array-based comparative genomic hybridization study. *Genes, Chromosomes and Cancer*, *49*(8), 733–745. https://doi.org/10.1002/gcc.20785

Ge, Q., Nilasena, D. S., O'Brien, C. A., Frank, M. B., & Targoff, I. N. (1995). Molecular analysis of a major antigenic region of the 240-kD protein of Mi-2 autoantigen. *Journal of Clinical Investigation*, *96*(4), 1730–1737. https://doi.org/10.1172/JCI118218

George, A., Zand, D. J., Hufnagel, R. B., Sharma, R., Sergeev, Y. V., Legare, J. M., … Brooks, B. P. (2016). Biallelic Mutations in MITF Cause Coloboma, Osteopetrosis, Microphthalmia, Macrocephaly, Albinism, and Deafness. *The American Journal of Human Genetics*, *99*(6), 1388–1394. https://doi.org/10.1016/j.ajhg.2016.11.004

Ghazizadeh, S., & Taichman, L. B. (2001). Multiple classes of stem cells in cutaneous epithelium: a lineage analysis of adult mouse skin. *The EMBO Journal*, *20*(6), 1215. https://doi.org/10.1093/EMBOJ/20.6.1215

Giallongo, A., Feo, S., Moore, R., Croce, C. M., & Showe, L. C. (1986). Molecular cloning and nucleotide sequence of a full-length cDNA for human alpha enolase. *Proceedings of the National Academy of Sciences*, *83*(18), 6741–6745. https://doi.org/10.1073/pnas.83.18.6741

Giehl, K. (2005). Oncogenic Ras in tumour progression and metastasis. *Biological Chemistry*, *386*(3), 193–205. https://doi.org/10.1515/BC.2005.025

Giles, K. A., Gould, C. M., Du, Q., Skvortsova, K., Song, J. Z., Maddugoda, M. P., … Taberlay, P. C. (2019). Integrated epigenomic analysis stratifies chromatin remodellers into distinct functional groups. *Epigenetics & Chromatin*, *12*(1), 12. https://doi.org/10.1186/s13072-019-0258-9

Gillette, T. G., & Hill, J. A. (2015). Readers, writers, and erasers: chromatin as the whiteboard of heart disease. *Circulation Research*, *116*(7), 1245–1253. https://doi.org/10.1161/CIRCRESAHA.116.303630

Giuliano, S., Cheli, Y., Ohanna, M., Bonet, C., Beuret, L., Bille, K., … Bertolotto, C. (2010). Microphthalmia-Associated Transcription Factor Controls the DNA Damage Response and a Lineage-Specific Senescence Program in Melanomas. *Cancer Research*, *70*(9), 3813–3822. https://doi.org/10.1158/0008-5472.CAN-09-2913

Glaser, P. E., & Gross, R. W. (1995). Rapid plasmenylethanolamine-selective fusion of membrane bilayers catalyzed by an isoform of glyceraldehyde-3-phosphate dehydrogenase: discrimination between glycolytic and fusogenic roles of individual isoforms. *Biochemistry*, *34*(38), 12193–12203. Retrieved from http://www.ncbi.nlm.nih.gov/pubmed/7547960

Global Cancer Observatory. (2017). Retrieved June 5, 2019, from http://gco.iarc.fr/

Glover, J. D., Knolle, S., Wells, K. L., Liu, D., Jackson, I. J., Mort, R. L., & Headon, D. J. (2015). Maintenance of distinct melanocyte populations in the interfollicular epidermis. *Pigment Cell and Melanoma Research*, *28*(4), 476–480. https://doi.org/10.1111/pcmr.12375

Goding, C R. (2011). A picture of Mitf in melanoma immortality. *Oncogene*, *30*, 2304–2306. https://doi.org/10.1038/onc.2010.641

Goding, Colin R, & Arnheiter, H. (2019). *MITF-the first 25 years*. https://doi.org/10.1101/gad.324657.119

Gómez-del Arco, P., Perdiguero, E., Yunes-Leites, P. S., Acín-Pérez, R., Zeini, M., Garcia-Gomez, A., … Redondo, J. M. (2016). The Chromatin Remodeling Complex Chd4/NuRD Controls Striated Muscle Identity and Metabolic Homeostasis. *Cell Metabolism*, *23*(5), 881–892. https://doi.org/10.1016/j.cmet.2016.04.008

Gopal, Y. N. V., Rizos, H., Chen, G., Deng, W., Frederick, D. T., Cooper, Z. A., … Davies, M. A. (2014). Inhibition of mTORC1/2 Overcomes Resistance to MAPK Pathway Inhibitors Mediated by PGC1 and Oxidative Phosphorylation in Melanoma. *Cancer Research*, *74*(23), 7037–7047. https://doi.org/10.1158/0008-5472.CAN-14-1392

Grichnik, J. M., Ali, W. N., Burch, J. A., Byers, J. D., Garcia, C. A., Clark, R. E., & Shea, C. R. (1996). KIT expression reveals a population of precursor melanocytes in human skin. *The Journal of Investigative Dermatology*, *106*(5), 967–971. Retrieved from http://www.ncbi.nlm.nih.gov/pubmed/8618059

Grillo, M. A., & Colombatto, S. (2008). S-adenosylmethionine and its products. *Amino Acids*, *34*(2), 187–193. https://doi.org/10.1007/s00726-007-0500-9

Guerrin, M., Ishigami, A., Méchin, M.-C., Nachat, R., Valmary, S., Sebbag, M., … Serre, G. (2003). cDNA cloning, gene organization and expression analysis of human peptidylarginine deiminase type I. *The Biochemical Journal*, *370*(Pt 1), 167–174. https://doi.org/10.1042/BJ20020870

Günther, K., Rust, M., Leers, J., Boettger, T., Scharfe, M., Jarek, M., … Renkawitz, R. (2013). Differential roles for MBD2 and MBD3 at methylated CpG islands, active promoters and binding to exon sequences. *Nucleic Acids Research*, *41*(5), 3010–3021. https://doi.org/10.1093/nar/gkt035

Gurard-Levin, Z. A., Quivy, J.-P., & Almouzni, G. (2014). Histone Chaperones: Assisting Histone Traffic and Nucleosome Dynamics. *Annual Review of Biochemistry*, *83*(1), 487–517. https://doi.org/10.1146/annurev-biochem-060713-035536

Guy, G. P., Zhang, Y., Ekwueme, D. U., Rim, S. H., & Watson, M. (2017). The potential impact of reducing indoor tanning on melanoma prevention and treatment costs in the United States: An economic analysis. *Journal of the American Academy of Dermatology*, *76*(2), 226–233. https://doi.org/10.1016/J.JAAD.2016.09.029

Hachiya, A., Kobayashi, A., Ohuchi, A., Takema, Y., & Imokawa, G. (2001). The Paracrine Role of Stem Cell Factor/c-kit Signaling in the Activation of Human Melanocytes in Ultraviolet-B-Induced Pigmentation. *Journal of Investigative Dermatology*, *116*(4), 578–586. https://doi.org/10.1046/J.1523-1747.2001.01290.X

Hachiya, A., Kobayashi, A., Yoshida, Y., Kitahara, T., Takema, Y., & Imokawa, G. (2004). Biphasic Expression of Two Paracrine Melanogenic Cytokines, Stem Cell Factor and Endothelin-1, in Ultraviolet B-Induced Human Melanogenesis. *The American Journal of Pathology*, *165*(6), 2099–2109. https://doi.org/10.1016/S0002-9440(10)63260-9

Hacker, H., Steinberg, P., & Bannasch, P. (1998). Pyruvate kinase isoenzyme shift from L-type to M2-type is a late event in hepatocarcinogenesis induced in rats by a choline-deficient/DL- ethionine-supplemented diet. *Carcinogenesis*, *19*(1), 99–107. https://doi.org/10.1093/carcin/19.1.99

Haigis, M. C., Mostoslavsky, R., Haigis, K. M., Fahie, K., Christodoulou, D. C., Murphy, A. J., … Guarente, L. (2006). SIRT4 Inhibits Glutamate Dehydrogenase and Opposes the Effects of Calorie Restriction in Pancreatic β Cells. *Cell*, *126*(5), 941–954. https://doi.org/10.1016/j.cell.2006.06.057

Hall, W. A., Petrova, A. V, Colbert, L. E., Hardy, C. W., Fisher, S. B., Saka, B., … Yu, D. S. (2014). Low CHD5 expression activates the DNA damage response and predicts poor outcome in patients undergoing adjuvant therapy for resected pancreatic cancer. *Oncogene*, *33*(47), 5450–5456. https://doi.org/10.1038/onc.2013.488

Hammond, C. M., Strømme, C. B., Huang, H., Patel, D. J., & Groth, A. (2017). Histone chaperone networks shaping chromatin function. *Nature Reviews Molecular Cell Biology*, *18*(3), 141–158. https://doi.org/10.1038/nrm.2016.159

Han, A. L., Veeneman, B. A., El-Sawy, L., Day, K. C., Day, M. L., Tomlins, S. A., & Keller, E. T. (2017). Fibulin-3 promotes muscle-invasive bladder cancer. *Oncogene*, *36*(37), 5243–5251. https://doi.org/10.1038/onc.2017.149

Handolias, D., Salemi, R., Murray, W., Tan, A., Liu, W., Viros, A., … McArthur, G. A. (2010). Mutations in KIT occur at low frequency in melanomas arising from anatomical sites associated with chronic and intermittent sun exposure. *Pigment Cell & Melanoma Research*, *23*(2), 210–215. https://doi.org/10.1111/j.1755-148X.2010.00671.x

Hansen, W. R., Barsic-Tress, N., Taylor, L., & Curthoys, N. P. (1996). The 3'-nontranslated region of rat renal glutaminase mRNA contains a pH-responsive stability element. *American Journal of Physiology-Renal Physiology*, *271*(1), F126–F131. https://doi.org/10.1152/ajprenal.1996.271.1.F126

Haq, R., Shoag, J., Andreu-Perez, P., Yokoyama, S., Edelman, H., Rowe, G. C., … Widlund, H. R. (2013a). Oncogenic BRAF Regulates Oxidative Metabolism via PGC1α and MITF. *Cancer Cell*, *23*(3), 302–315. https://doi.org/10.1016/j.ccr.2013.02.003

Hara, M. R., Agrawal, N., Kim, S. F., Cascio, M. B., Fujimuro, M., Ozeki, Y., … Sawa, A. (2005). S-nitrosylated GAPDH initiates apoptotic cell death by nuclear translocation following Siah1 binding. *Nature Cell Biology*, *7*(7), 665–674. https://doi.org/10.1038/ncb1268

Hardeman, K. N., Peng, C., Paudel, B. B., Meyer, C. T., Luong, T., Tyson, D. R., … Fessel, J. P. (2017). Dependence On Glycolysis Sensitizes BRAF-mutated Melanomas For Increased Response To Targeted BRAF Inhibition. *Nature Publishing Group*, (February), 1–9. https://doi.org/10.1038/srep42604

Harp, J. M., Hanson, B. L., Timm, D. E., & Bunick, G. J. (2000). Asymmetries in the nucleosome core particle at 2.5 A

resolution. *Acta Crystallographica. Section D, Biological Crystallography*, *56*(Pt 12), 1513–1534. https://doi.org/10.1107/s0907444900011847

Hauschild, A., Grob, J.-J., Demidov, L. V, Jouary, T., Gutzmer, R., Millward, M., … Chapman, P. B. (2012). Dabrafenib in BRAF-mutated metastatic melanoma: a multicentre, open-label, phase 3 randomised controlled trial. *Lancet (London, England)*, *380*(9839), 358–365. https://doi.org/10.1016/S0140-6736(12)60868-X

Hayes, J. J., & Wolffe, A. P. (1995). *Chromatin Structure and Transcription*. https://doi.org/10.1007/978-3-642-79488-9_2

Hayward, N. K., Wilmott, J. S., Waddell, N., Johansson, P. A., Field, M. A., Nones, K., … Mann, G. J. (2017). Whole-genome landscapes of major melanoma subtypes. *Nature*, *545*(7653), 175–180. https://doi.org/10.1038/nature22071

He, J., Jin, Y., Chen, Y., Yao, H.-B., Xia, Y.-J., Ma, Y.-Y., … Shao, Q.-S. (2016). Downregulation of ALDOB is associated with poor prognosis of patients with gastric cancer. *OncoTargets and Therapy*, *Volume 9*, 6099–6109. https://doi.org/10.2147/OTT.S110203

Hearing, V. J. (2011). Determination of Melanin Synthetic Pathways. *Journal of Investigative Dermatology*, *131*(E1), E8–E11. https://doi.org/10.1038/skinbio.2011.4

Hearing, V. J., & Jiménez, M. (1987). Mammalian tyrosinase—The critical regulatory control point in melanocyte pigmentation. *International Journal of Biochemistry*, *19*(12), 1141–1147. https://doi.org/10.1016/0020-711X(87)90095-4

Hemesath, T. J., Steingrimsson, E., McGill, G., Hansen, M. J., Vaught, J., Hodgkinson, C. A., … Fisher, D. E. (1994). microphthalmia, a critical factor in melanocyte development, defines a discrete transcription factor family. *Genes & Development*, *8*(22), 2770–2780. https://doi.org/10.1101/gad.8.22.2770

Hershey, C. L., & Fisher, D. E. (2005). Genomic analysis of the Microphthalmia locus and identification of the MITF-J/Mitf-J isoform. *Gene*, *347*(1), 73–82. https://doi.org/10.1016/j.gene.2004.12.002

Hidaka, Y., Hagiwara, T., & Yamada, M. (2005). Methylation of the guanidino group of arginine residues prevents citrullination by peptidylarginine deiminase IV. *FEBS Letters*, *579*(19), 4088–4092. https://doi.org/10.1016/j.febslet.2005.06.035

Hitosugi, T., Zhou, L., Elf, S., Fan, J., Kang, H.-B., Seo, J. H., … Chen, J. (2012). Phosphoglycerate Mutase 1 Coordinates Glycolysis and Biosynthesis to Promote Tumor Growth. *Cancer Cell*, *22*(5), 585–600. https://doi.org/10.1016/j.ccr.2012.09.020

Hodgkinson, C. a., Moore, K. J., Nakayama, A., Steingrímsson, E., Copeland, N. G., Jenkins, N. a., & Arnheiter, H. (1993). Mutations at the mouse microphthalmia locus are associated with defects in a gene encoding a novel basic-helix-loop-helix-zipper protein. *Cell*, *74*(2), 395–404. https://doi.org/10.1016/0092-8674(93)90429-T

Hodi, F. S., O'Day, S. J., McDermott, D. F., Weber, R. W., Sosman, J. A., Haanen, J. B., … Urba, W. J. (2010). Improved Survival with Ipilimumab in Patients with Metastatic Melanoma. *New England Journal of Medicine*, *363*(8), 711–723. https://doi.org/10.1056/NEJMoa1003466

Hodis, E., Watson, I. R., Kryukov, G. V., Arold, S. T., Imielinski, M., Theurillat, J.-P., … Chin, L. (2012a). A Landscape of Driver Mutations in Melanoma. *Cell*, *150*(2), 251–263. https://doi.org/10.1016/j.cell.2012.06.024

Hoek, K. S., & Goding, C. R. (2010). Cancer stem cells versus phenotype-switching in melanoma. *Pigment Cell & Melanoma Research*, *23*(6), 746–759. https://doi.org/10.1111/j.1755-148X.2010.00757.x

Hoek, K. S., Schlegel, N. C., Brafford, P., Sucker, A., Ugurel, S., Kumar, R., … Dummer, R. (2006). Metastatic potential of melanomas defined by specific gene expression profiles with no BRAF signature. *Pigment Cell Research*, *19*(4), 290–302. https://doi.org/10.1111/j.1600-0749.2006.00322.x

Hoffmeister, H., Fuchs, A., Erdel, F., Pinz, S., Gröbner-Ferreira, R., Bruckmann, A., … Längst, G. (2017). CHD3 and CHD4 form distinct NuRD complexes with different yet overlapping functionality. *Nucleic Acids Research*, *45*(18), 10534–10554. https://doi.org/10.1093/nar/gkx711

Horsley, V., O'Carroll, D., Tooze, R., Ohinata, Y., Saitou, M., Obukhanych, T., … Fuchs, E. (2006). Blimp1 Defines a Progenitor Population that Governs Cellular Input to the Sebaceous Gland. *Cell*, *126*(3), 597–609. https://doi.org/10.1016/j.cell.2006.06.048

Hosios, A. M., Hecht, V. C., Danai, L. V., Johnson, M. O., Rathmell, J. C., Steinhauser, M. L., … Vander Heiden, M. G. (2016). Amino Acids Rather than Glucose Account for the Majority of Cell Mass in Proliferating Mammalian Cells. *Developmental Cell*, *36*(5), 540–549. https://doi.org/10.1016/J.DEVCEL.2016.02.012

Hou, L., & Pavan, W. J. (2008). Transcriptional and signaling regulation in neural crest stem cell-derived melanocyte development: do all roads lead to Mitf? *Cell Research*, *18*(12), 1163–1176. https://doi.org/10.1038/cr.2008.303

Hsiao, P.-W., Fryer, C. J., Trotter, K. W., Wang, W., & Archer, T. K. (2003). BAF60a mediates critical interactions between nuclear receptors and the BRG1 chromatin-remodeling complex for transactivation. *Molecular and Cellular Biology*, *23*(17), 6210–6220. https://doi.org/10.1128/mcb.23.17.6210-6220.2003

Hsueh, E. C., & Gorantla, K. C. (2016). Novel melanoma therapy. *Experimental Hematology & Oncology*, *5*, 23. https://doi.org/10.1186/s40164-016-0054-1

Hwang, I.-Y., Kwak, S., Lee, S., Kim, H., Lee, S. E., Kim, J.-H., … Youn, H.-D. (2016). Psat1-Dependent Fluctuations in α-Ketoglutarate Affect the Timing of ESC Differentiation. *Cell Metabolism*, *24*(3), 494–501. https://doi.org/10.1016/j.cmet.2016.06.014

Icard, P., Fournel, L., Wu, Z., Alifano, M., & Lincet, H. (2019). Interconnection between Metabolism and Cell Cycle in Cancer. *Trends in Biochemical Sciences*, *44*(6), 490–501. https://doi.org/10.1016/j.tibs.2018.12.007

Ichii-Nakato, N., Takata, M., Takayanagi, S., Takashima, S., Lin, J., Murata, H., … Saida, T. (2006). High Frequency of BRAFV600E Mutation in Acquired Nevi and Small Congenital Nevi, but Low Frequency of Mutation in Medium-Sized Congenital Nevi. *Journal of Investigative Dermatology*, *126*(9), 2111–2118. https://doi.org/10.1038/sj.jid.5700366

Ikeya, M., Lee, S. M. K., Johnson, J. E., McMahon, A. P., & Takada, S. (1997). Wnt signaling required for expansion of neural crest and CNS progenitors. *Nature*, *389*(6654), 966–970. https://doi.org/10.1038/40146

Imokawa, G., Miyagishi, M., & Yada, Y. (1995). Endothelin-1 as a New Melanogen: Coordinated Expression of Its Gene and the Tyrosinase Gene in UVB-Exposed Human Epidermis. *Journal of Investigative Dermatology*, *105*(1), 32–37. https://doi.org/10.1111/1523-1747.EP12312500

Ince-Dunn, G., Okano, H. J., Jensen, K. B., Park, W.-Y., Zhong, R., Ule, J., … Darnell, R. B. (2012). Neuronal Elav-like (Hu) Proteins Regulate RNA Splicing and Abundance to Control Glutamate Levels and Neuronal Excitability. *Neuron*, *75*(6), 1067–1080. https://doi.org/10.1016/j.neuron.2012.07.009

Innocenzi, D., Alò, P. L., Balzani, A., Sebastiani, V., Silipo, V., La Torre, G., … Calvieri, S. (2003). Fatty acid synthase expression in melanoma. *Journal of Cutaneous Pathology*, *30*(1), 23–28. https://doi.org/10.1034/j.1600-0560.2003.300104.x

Iqbal, M. A., Gupta, V., Gopinath, P., Mazurek, S., & Bamezai, R. N. K. (2014). Pyruvate kinase M2 and cancer: an updated assessment. *FEBS Letters*, *588*(16), 2685–2692. https://doi.org/10.1016/j.febslet.2014.04.011

Ishigami, A., Ohsawa, T., Asaga, H., Akiyama, K., Kuramoto, M., & Maruyama, N. (2002). Human peptidylarginine deiminase type II: molecular cloning, gene organization, and expression in human skin. *Archives of Biochemistry and Biophysics*, *407*(1), 25–31. Retrieved from http://www.ncbi.nlm.nih.gov/pubmed/12392711

Ito, M., & Cotsarelis, G. (2008). Is the hair follicle necessary for normal wound healing? *Journal of Investigative Dermatology*, *128*(5), 1059–1061. https://doi.org/10.1038/jid.2008.86

Ito, M., Liu, Y., Yang, Z., Nguyen, J., Liang, F., Morris, R. J., & Cotsarelis, G. (2005a). Stem cells in the hair follicle bulge contribute to wound repair but not to homeostasis of the epidermis. *Nature Medicine*, *11*(12), 1351–1354. https://doi.org/10.1038/nm1328

Ito, T., Yamauchi, M., Nishina, M., Yamamichi, N., Mizutani, T., Ui, M., … Iba, H. (2001). Identification of SWI·SNF Complex Subunit BAF60a as a Determinant of the Transactivation Potential of Fos/Jun Dimers. *Journal of Biological Chemistry*, *276*(4), 2852–2857. https://doi.org/10.1074/jbc.M009633200

Jaks, V., Barker, N., Kasper, M., van Es, J. H., Snippert, H. J., Clevers, H., & Toftgård, R. (2008). Lgr5 marks cycling, yet long-lived, hair follicle stem cells. *Nature Genetics*, *40*(11), 1291–1299. https://doi.org/10.1038/ng.239

Jensen, K. B., Collins, C. A., Nascimento, E., Tan, D. W., Frye, M., Itami, S., & Watt, F. M. (2009). Lrig1 Expression Defines a Distinct Multipotent Stem Cell Population in Mammalian Epidermis. *Cell Stem Cell*, *4*(5), 427–439. https://doi.org/10.1016/j.stem.2009.04.014

Jensen, P. J., Taylor, G., Lavker, R. M., Lehrer, M. S., & Sun, T. T. (2000). Involvement of follicular stem cells in forming not only the follicle but also the epidermis. *Cell*, *102*(4), 451–461. Retrieved from http://www.ncbi.nlm.nih.gov/entrez/query.fcgi?cmd=Retrieve&db=PubMed&dopt=Citation&list_uids=10966107

Jensen, U. B., Yan, X., Triel, C., Woo, S.-H., Christensen, R., & Owens, D. M. (2008). A distinct population of clonogenic and multipotent murine follicular keratinocytes residing in the upper isthmus. *Journal of Cell Science*, *121*(5), 609–617. https://doi.org/10.1242/jcs.025502

Jenuwein, T., & Allis, C. D. (2001). Translating the Histone Code. *Science*, *293*(5532), 1074–1080. https://doi.org/10.1126/science.1063127

Ji, S., Zhang, B., Liu, J., Qin, Y., Liang, C., Shi, S., … Yu, X. (2016). ALDOA functions as an oncogene in the highly metastatic pancreatic cancer. *Cancer Letters*, *374*(1), 127–135. https://doi.org/10.1016/J.CANLET.2016.01.054

Jiang, H., Ma, N., Shang, Y., Zhou, W., Chen, T., Guan, D., … Wei, D. (2017). Triosephosphate isomerase 1 suppresses growth, migration and invasion of hepatocellular carcinoma cells. *Biochemical and Biophysical Research Communications*, *482*(4), 1048–1053. https://doi.org/10.1016/J.BBRC.2016.11.156

Jiang, Y., Li, X., Yang, W., Hawke, D. H., Zheng, Y., Xia, Y., … Lu, Z. (2014). PKM2 Regulates Chromosome Segregation and Mitosis Progression of Tumor Cells. *Molecular Cell*, *53*(1), 75–87. https://doi.org/10.1016/j.molcel.2013.11.001

Jiang, Y., Qian, X., Shen, J., Wang, Y., Li, X., Liu, R., … Lu, Z. (2015). Local generation of fumarate promotes DNA repair through inhibition of histone H3 demethylation. *Nature Cell Biology*, *17*(9), 1158–1168. https://doi.org/10.1038/ncb3209

Jiang, Y., Wang, Y., Wang, T., Hawke, D. H., Zheng, Y., Li, X., … Lu, Z. (2014). PKM2 phosphorylates MLC2 and regulates cytokinesis of tumour cells. *Nature Communications*, *5*, 5566. https://doi.org/10.1038/ncomms6566

Jitrapakdee, S., St Maurice, M., Rayment, I., Cleland, W. W., Wallace, J. C., & Attwood, P. V. (2008). Structure, mechanism and regulation of pyruvate carboxylase. *The Biochemical Journal*, *413*(3), 369–387. https://doi.org/10.1042/BJ20080709

John E. Wilson. (2003). *Isozymes of mammalian hexokinase: structure, subcellular localization and metabolic function*. https://doi.org/10.1242/jeb.00241

Jones, M. H., Hamana, N., & Shimane, M. (2000). Identification and Characterization of BPTF, a Novel Bromodomain Transcription Factor. *Genomics*, *63*(1), 35–39. https://doi.org/10.1006/geno.1999.6070

Joshi, P., Greco, T. M., Guise, A. J., Luo, Y., Yu, F., Nesvizhskii, A. I., & Cristea, I. M. (2014). The functional interactome landscape of the human histone deacetylase family. *Molecular Systems Biology*, *9*(1), 672–672. https://doi.org/10.1038/msb.2013.26

Joshi, S., Davidson, G., Le Gras, S., Watanabe, S., Braun, T., Mengus, G., & Davidson, I. (2017). TEAD transcription factors are required for normal primary myoblast differentiation in vitro and muscle regeneration in vivo. *PLOS Genetics*, *13*(2), e1006600. https://doi.org/10.1371/journal.pgen.1006600

Juan, L. J., Utley, R. T., Adams, C. C., Vettese-Dadey, M., & Workman, J. L. (1994). Differential repression of transcription factor binding by histone H1 is regulated by the core histone amino termini. *The EMBO Journal*, *13*(24), 6031–6040. Retrieved from http://www.ncbi.nlm.nih.gov/pubmed/7813441

Jurica, M. S., Mesecar, A., Heath, P. J., Shi, W., Nowak, T., & Stoddard, B. L. (1998). The allosteric regulation of pyruvate kinase by fructose-1,6-bisphosphate. *Structure (London, England : 1993)*, *6*(2), 195–210. Retrieved from http://www.ncbi.nlm.nih.gov/pubmed/9519410

Kahn, A., Meienhofer, M. C., Cottreau, D., Lagrange, J. L., & Dreyfus, J. C. (1979). Phosphofructokinase (PFK) isozymes in man. I. Studies of adult human tissues. *Human Genetics*, *48*(1), 93–108. Retrieved from http://www.ncbi.nlm.nih.gov/pubmed/156693

Kamphorst, J. J., Nofal, M., Commisso, C., Hackett, S. R., Lu, W., Grabocka, E., … Rabinowitz, J. D. (2015). Human pancreatic cancer tumors are nutrient poor and tumor cells actively scavenge extracellular protein. *Cancer Research*, *75*(3), 544–553. https://doi.org/10.1158/0008-5472.CAN-14-2211

Kanno, T., Shiraiwa, M., Takahara, H., Kawada, A., Tezuka, T., Yamanouchi, J., … Manabe, M. (2000). Human Peptidylarginine Deiminase Type III: Molecular Cloning and Nucleotide Sequence of the cDNA, Properties of the Recombinant Enzyme, and Immunohistochemical Localization in Human Skin. *Journal of Investigative Dermatology*, *115*(5), 813–823. https://doi.org/10.1046/j.1523-1747.2000.00131.x

Kaplon, J., Zheng, L., Meissl, K., Chaneton, B., Selivanov, V. A., Mackay, G., … Peeper, D. S. (2013). A key role for mitochondrial gatekeeper pyruvate dehydrogenase in oncogene-induced senescence. *Nature*, *498*. https://doi.org/10.1038/nature12154

Katherine R. Mattaini and Matthew G. Vander Heiden. (2012). Glycosylation to Adapt to Stress. *Science*, *337*, 925–926. https://doi.org/10.1038/mi.2012.81

Kato, K., Okagawa, Y., Suzuki, F., Shimizu, A., Mokuno, K., & Takahashi, Y. (1983). Immunoassay of human muscle enolase subunit in serum: a novel marker antigen for muscle diseases. *Clinica Chimica Acta; International Journal of Clinical Chemistry*, *131*(1–2), 75–85. Retrieved from http://www.ncbi.nlm.nih.gov/pubmed/6349861

Kaunitz, G. J., Cottrell, T. R., Lilo, M., Muthappan, V., Esandrio, J., Berry, S., … Taube, J. M. (2017). Melanoma subtypes demonstrate distinct PD-L1 expression profiles. *Laboratory Investigation; a Journal of Technical Methods and Pathology*,

97(9), 1063–1071. https://doi.org/10.1038/labinvest.2017.64

Kebede, A. F., Schneider, R., & Daujat, S. (2015). Novel types and sites of histone modifications emerge as players in the transcriptional regulation contest. *FEBS Journal*, *282*(9), 1658–1674. https://doi.org/10.1111/febs.13047

Keenen, B., Qi, H., Saladi, S. V, Yeung, M., & de la Serna, I. L. (2010). Heterogeneous SWI/SNF chromatin remodeling complexes promote expression of microphthalmia-associated transcription factor target genes in melanoma. *Oncogene*, *29*(1), 81–92. https://doi.org/10.1038/onc.2009.304

Keller, K. E., Doctor, Z. M., Dwyer, Z. W., & Lee, Y.-S. (2014a). SAICAR Induces Protein Kinase Activity of PKM2 that Is Necessary for Sustained Proliferative Signaling of Cancer Cells. *Molecular Cell*, *53*(5), 700–709. https://doi.org/10.1016/j.molcel.2014.02.015

Kent, O. A., Fox-Talbot, K., & Halushka, M. K. (2013). RREB1 repressed miR-143/145 modulates KRAS signaling through downregulation of multiple targets. *Oncogene*, *32*(20), 2576–2585. https://doi.org/10.1038/onc.2012.266

Kerr, M. C., & Teasdale, R. D. (2009). Defining Macropinocytosis. *Traffic*, *10*(4), 364–371. https://doi.org/10.1111/j.1600-0854.2009.00878.x

Khavari, P. A., Peterson, C. L., Tamkun, J. W., Mendel, D. B., & Crabtree, G. R. (1993). BRG1 contains a conserved domain of the SWI2/SNF2 family necessary for normal mitotic growth and transcription. *Nature*, *366*(6451), 170–174. https://doi.org/10.1038/366170a0

Khorasanizadeh, S. (2004). *The Nucleosome : From Genomic Organization to Genomic Regulation University of Virginia Health System*. *116*, 259–272.

Kim, C. J., Reintgen, D. S., Balch, C. M., & Lee, H. (n.d.). *The New Melanoma Staging System From the Departments of Surgery (CJK, DSR) and Cutaneous Oncology Program (DSR), at the*. Retrieved from https://moffitt.org/File Library/Main Nav/Research and Clinical Trials/Cancer Control Journal/v9n1/09.pdf

Kim, J.-H., Baddoo, M. C., Park, E. Y., Stone, J. K., Park, H., Butler, T. W., … Ahn, E.-Y. E. (2016). SON and Its Alternatively Spliced Isoforms Control MLL Complex-Mediated H3K4me3 and Transcription of Leukemia-Associated Genes. *Molecular Cell*, *61*(6), 859–873. https://doi.org/10.1016/j.molcel.2016.02.024

Kim, J. E., Koo, K. H., Kim, Y. H., Sohn, J., & Park, Y. G. (2008). Identification of potential lung cancer biomarkers using an in vitro carcinogenesis model. *Experimental and Molecular Medicine*, *40*(6), 709. https://doi.org/10.3858/emm.2008.40.6.709

Kim, J., Tchernyshyov, I., Semenza, G. L., & Dang, C. V. (2006). HIF-1-mediated expression of pyruvate dehydrogenase kinase: A metabolic switch required for cellular adaptation to hypoxia. *Cell Metabolism*, *3*(3), 177–185. https://doi.org/10.1016/J.CMET.2006.02.002

Kim, Y. H., Jeong, D. C., Pak, K., Han, M.-E., Kim, J.-Y., Liangwen, L., … Oh, S.-O. (2017). SLC2A2 (GLUT2) as a novel prognostic factor for hepatocellular carcinoma. *Oncotarget*, *8*(40), 68381–68392. https://doi.org/10.18632/oncotarget.20266

King, A. J., Arnone, M. R., Bleam, M. R., Moss, K. G., Yang, J., Fedorowicz, K. E., … Laquerre, S. G. (2013). Dabrafenib; Preclinical Characterization, Increased Efficacy when Combined with Trametinib, while BRAF/MEK Tool Combination Reduced Skin Lesions. *PLoS ONE*, *8*(7), e67583. https://doi.org/10.1371/journal.pone.0067583

Kirstie E. Keller. (2012). SAICAR Stimulates Pyruvate Kinase Isoform M2 and Promotes Cancer Cell Survival in Glucose-Limited Conditions. *Science*, *338*. https://doi.org/10.1126/science.1227833

Klement, K., Luijsterburg, M. S., Pinder, J. B., Cena, C. S., Del Nero, V., Wintersinger, C. M., … Goodarzi, A. A. (2014). Opposing ISWI- and CHD-class chromatin remodeling activities orchestrate heterochromatic DNA repair. *The Journal of Cell Biology*, *207*(6), 717–733. https://doi.org/10.1083/jcb.201405077

Kloet, S. L., Baymaz, H. I., Makowski, M., Groenewold, V., Jansen, P. W. T. C., Berendsen, M., … Vermeulen, M. (2015). Towards elucidating the stability, dynamics and architecture of the nucleosome remodeling and deacetylase complex by using quantitative interaction proteomics. *FEBS Journal*, *282*(9), 1774–1785. https://doi.org/10.1111/febs.12972

Klungland, A., & Robertson, A. B. (2017). Oxidized C5-methyl cytosine bases in DNA: 5-Hydroxymethylcytosine; 5-formylcytosine; and 5-carboxycytosine. *Free Radical Biology and Medicine*, *107*, 62–68. https://doi.org/10.1016/j.freeradbiomed.2016.11.038

Kolla, V., Zhuang, T., Higashi, M., Naraparaju, K., & Brodeur, G. M. (2014). Role of CHD5 in Human Cancers: 10 Years Later.

Cancer Research, *74*(3), 652–658. https://doi.org/10.1158/0008-5472.CAN-13-3056

Koludrovic, D., Laurette, P., Strub, T., Keime, C., Le Coz, M., Coassolo, S., … Dana Koludrovic, Patrick Laurette, Thomas Strub, Céline Keime, Madeleine Le Coz, Sebastien Coassolo, Gabrielle Mengus, Lionel Larue, and I. D. (2015). Chromatin-Remodelling Complex NURF Is Essential for Differentiation of Adult Melanocyte Stem Cells. *PLOS Genetics*, *11*(10), e1005555. https://doi.org/10.1371/journal.pgen.1005555

Kondo, T., & Hearing, V. J. (2011). Update on the regulation of mammalian melanocyte function and skin pigmentation. *Expert Review of Dermatology*, *6*(1), 97–108. https://doi.org/10.1586/edm.10.70

Kosova, A. A., Khodyreva, S. N., & Lavrik, O. I. (2017). Role of glyceraldehyde-3-phosphate dehydrogenase (GAPDH) in DNA repair. *Biochemistry (Moscow)*, *82*(6), 643–654. https://doi.org/10.1134/S0006297917060013

Kouzarides, T. (2007). Chromatin Modifications and Their Function. *Cell*, *128*(4), 693–705. https://doi.org/10.1016/j.cell.2007.02.005

Koyama, H., Zhuang, T., Light, J. E., Kolla, V., Higashi, M., McGrady, P. W., … Brodeur, G. M. (2012). Mechanisms of CHD5 Inactivation in neuroblastomas. *Clinical Cancer Research : An Official Journal of the American Association for Cancer Research*, *18*(6), 1588–1597. https://doi.org/10.1158/1078-0432.CCR-11-2644

Kraushaar, D. C., Chen, Z., Tang, Q., Cui, K., Zhang, J., & Zhao, K. (2018). The gene repressor complex NuRD interacts with the histone variant H3.3 at promoters of active genes. *Genome Research*, *28*(11), 1646–1655. https://doi.org/10.1101/gr.236224.118

Krauthammer, M., Kong, Y., Bacchiocchi, A., Evans, P., Pornputtapong, N., Wu, C., … Halaban, R. (2015). Exome sequencing identifies recurrent mutations in NF1 and RASopathy genes in sun-exposed melanomas. *Nature Genetics*, *47*(9), 996–1002. https://doi.org/10.1038/ng.3361

Krebs, H. A. (1935). Metabolism of amino-acids. *Biochemical Journal*, *29*(8), 1951–1969. https://doi.org/10.1042/bj0291951

Krummel, M. F., & Allison, J. P. (1995). CD28 and CTLA-4 have opposing effects on the response of T cells to stimulation. *The Journal of Experimental Medicine*, *182*(2), 459–465. https://doi.org/10.1084/jem.182.2.459

Kumagai, H., & Sakai, H. (1983). A porcine brain protein (35 K protein) which bundles microtubules and its identification as glyceraldehyde 3-phosphate dehydrogenase. *Journal of Biochemistry*, *93*(5), 1259–1269. https://doi.org/10.1093/oxfordjournals.jbchem.a134260

Kumar, S. M., Yu, H., Edwards, R., Chen, L., Kazianis, S., Brafford, P., … Xu, X. (2007). Mutant V600E BRAF Increases Hypoxia Inducible Factor-1α Expression in Melanoma. *Cancer Research*, *67*(7), 3177–3184. https://doi.org/10.1158/0008-5472.CAN-06-3312

Kung, C., Hixon, J., Choe, S., Marks, K., Gross, S., Murphy, E., … Dang, L. (2012). Small Molecule Activation of PKM2 in Cancer Cells Induces Serine Auxotrophy. *Chemistry & Biology*, *19*(9), 1187–1198. https://doi.org/10.1016/j.chembiol.2012.07.021

Kwee, S. A., Hernandez, B., Chan, O., & Wong, L. (2012). Choline Kinase Alpha and Hexokinase-2 Protein Expression in Hepatocellular Carcinoma: Association with Survival. *PLoS ONE*, *7*(10), 46591. https://doi.org/10.1371/journal.pone.0046591

Kwong, L. N., & Davies, M. A. (2013). Navigating the therapeutic complexity of PI3K pathway inhibition in melanoma. *Clinical Cancer Research : An Official Journal of the American Association for Cancer Research*, *19*(19), 5310–5319. https://doi.org/10.1158/1078-0432.CCR-13-0142

LaBonne, C., & Bronner-Fraser, M. (1998). Induction and patterning of the neural crest, a stem cell-like precursor population. *Journal of Neurobiology*, *36*(2), 175–189. https://doi.org/10.1002/(SICI)1097-4695(199808)36:2<175::AID-NEU6>3.0.CO;2-Z

Labuschagne, C. F., van den Broek, N. J. F., Mackay, G. M., Vousden, K. H., & Maddocks, O. D. K. (2014). Serine, but not glycine, supports one-carbon metabolism and proliferation of cancer cells. *Cell Reports*, *7*(4), 1248–1258. https://doi.org/10.1016/j.celrep.2014.04.045

Lachiewicz, A. M., Berwick, M., Wiggins, C. L., & Thomas, N. E. (2008). Epidemiologic Support for Melanoma Heterogeneity

Using the Surveillance, Epidemiology, and End Results Program. *Journal of Investigative Dermatology*, *128*(5), 1340–1342. https://doi.org/10.1038/JID.2008.18

Lai, A. Y., & Wade, P. A. (2011). Cancer biology and NuRD: a multifaceted chromatin remodelling complex. *Nat Rev Cancer*, *11*(8), 588–596. https://doi.org/10.1038/nrc3091

Lancaster, H. O. (1956). Some geographical aspects of the mortality from melanoma in Europeans. *The Medical Journal of Australia*, *43*(26), 1082–1087. Retrieved from http://www.ncbi.nlm.nih.gov/pubmed/13347440

Land, E. J., & Riley, P. A. (2000). Spontaneous redox reactions of dopaquinone and the balance between the eumelanic and phaeomelanic pathways. *Pigment Cell Research*, *13*(4), 273–277. Retrieved from http://www.ncbi.nlm.nih.gov/pubmed/10952395

Lang, J., Tobias, E. S., & MacKie, R. (2011). Preliminary evidence for involvement of the tumour suppressor gene CHD5 in a family with cutaneous melanoma. *British Journal of Dermatology*, *164*(5), 1010–1016. https://doi.org/10.1111/j.1365-2133.2011.10223.x

Längst, G., Bonte, E. J., Corona, D. F., & Becker, P. B. (1999). Nucleosome movement by CHRAC and ISWI without disruption or trans-displacement of the histone octamer. *Cell*, *97*(7), 843–852. Retrieved from http://www.ncbi.nlm.nih.gov/pubmed/10399913

Lapouge, G., Youssef, K. K., Vokaer, B., Achouri, Y., Michaux, C., Sotiropoulou, P. A., & Blanpain, C. (2011). Identifying the cellular origin of squamous skin tumors. *Proceedings of the National Academy of Sciences*, *108*(18), 7431–7436. https://doi.org/10.1073/pnas.1012720108

Laugesen, A., & Helin, K. (2014). Chromatin Repressive Complexes in Stem Cells, Development, and Cancer. *Cell Stem Cell*, *14*(6), 735–751. https://doi.org/10.1016/j.stem.2014.05.006

Laurette, P., Coassolo, S., Davidson, G., Michel, I., Gambi, G., Yao, W., … Davidson, I. (2019). Chromatin remodellers Brg1 and Bptf are required for normal gene expression and progression of oncogenic Braf-driven mouse melanoma. *Cell Death & Differentiation*. https://doi.org/10.1038/s41418-019-0333-6

Laurette, P., Strub, T., Koludrovic, D., Keime, C., Le Gras, S., Seberg, H., … Davidson, I. (2015). Transcription factor MITF and remodeller BRG1 define chromatin organisation at regulatory elements in melanoma cells. *ELife*, *4*, 1–27. https://doi.org/10.7554/eLife.06857

Lawrence, M., Daujat, S., & Schneider, R. (2016). Lateral Thinking: How Histone Modifications Regulate Gene Expression. *Trends in Genetics*, *32*, 42–56. https://doi.org/10.1016/j.tig.2015.10.007

Le Guezennec, X., Vermeulen, M., Brinkman, A. B., Hoeijmakers, W. A. M., Cohen, A., Lasonder, E., & Stunnenberg, H. G. (2006). MBD2/NuRD and MBD3/NuRD, Two Distinct Complexes with Different Biochemical and Functional Properties. *Molecular and Cellular Biology*, *26*(3), 843–851. https://doi.org/10.1128/MCB.26.3.843-851.2006

Lechler, T., & Fuchs, E. (2005). Asymmetric cell divisions promote stratification and differentiation of mammalian skin. *Nature*, *437*(7056), 275–280. https://doi.org/10.1038/nature03922

Lee, C.-Y., Wang, D., Wilhelm, M., Zolg, D. P., Schmidt, T., Schnatbaum, K., … Kuster, B. (2018a). Mining the Human Tissue Proteome for Protein Citrullination. *Molecular & Cellular Proteomics*, *17*(7), 1378–1391. https://doi.org/10.1074/mcp.RA118.000696

Leiblich, A., Cross, S. S., Catto, J. W. F., Phillips, J. T., Leung, H. Y., Hamdy, F. C., & Rehman, I. (2006). Lactate dehydrogenase-B is silenced by promoter hypermethylation in human prostate cancer. *Oncogene*, *25*(20), 2953–2960. https://doi.org/10.1038/sj.onc.1209262

Lemire, J., Mailloux, R. J., & Appanna, V. D. (2008). Mitochondrial Lactate Dehydrogenase Is Involved in Oxidative-Energy Metabolism in Human Astrocytoma Cells (CCF-STTG1). *PLoS ONE*, *3*(2), e1550. https://doi.org/10.1371/journal.pone.0001550

Lemon, B., Inouye, C., King, D. S., & Tjian, R. (2001). Selectivity of chromatin-remodelling cofactors for ligand-activated transcription. *Nature*, *414*(6866), 924–928. https://doi.org/10.1038/414924a

Levy, C., Khaled, M., & Fisher, D. E. (2006). MITF: master regulator of melanocyte development and melanoma oncogene. *Trends in Molecular Medicine*, *12*(9), 406–414. https://doi.org/10.1016/j.molmed.2006.07.008

Li, B., Qiu, B., Lee, D. S. M., Walton, Z. E., Ochocki, J. D., Mathew, L. K., … Simon, M. C. (2014). Fructose-1,6-bisphosphatase opposes renal carcinoma progression. *Nature*, *513*(7517), 251–255. https://doi.org/10.1038/nature13557

Li, C., Shu, F., Lei, B., Lv, D., Zhang, S., & Mao, X. (2015). Expression of PGAM1 in renal clear cell carcinoma and its clinical significance. *International Journal of Clinical and Experimental Pathology*, *8*(8), 9410–9415. Retrieved from http://www.ncbi.nlm.nih.gov/pubmed/26464696

LI, H., XU, W., HUANG, Y., HUANG, X., XU, L., & LV, Z. (2012). Genistein demethylates the promoter of CHD5 and inhibits neuroblastoma growth in vivo. *International Journal of Molecular Medicine*, *30*(5), 1081–1086. https://doi.org/10.3892/ijmm.2012.1118

Li, M., Li, C., Allen, A., Stanley, C. A., & Smith, T. J. (2012). The structure and allosteric regulation of mammalian glutamate dehydrogenase. *Archives of Biochemistry and Biophysics*, *519*(2), 69–80. https://doi.org/10.1016/j.abb.2011.10.015

Li, T., Han, J., Jia, L., Hu, X., Chen, L., & Wang, Y. (2019). PKM2 coordinates glycolysis with mitochondrial fusion and oxidative phosphorylation. *Protein & Cell*. https://doi.org/10.1007/s13238-019-0618-z

Li, W., & Mills, A. A. (2014). Packing for the journey. *Cell Cycle*, *13*(12), 1833–1834. https://doi.org/10.4161/cc.29378

Li, X., Egervari, G., Wang, Y., Berger, S. L., & Lu, Z. (2018). Regulation of chromatin and gene expression by metabolic enzymes and metabolites. *Nature Reviews Molecular Cell Biology*. https://doi.org/10.1038/s41580-018-0029-7

Li, X., Jiang, Y., Meisenhelder, J., Yang, W., Hawke, D. H., Zheng, Y., … Lu, Z. (2016). Mitochondria-Translocated PGK1 Functions as a Protein Kinase to Coordinate Glycolysis and the TCA Cycle in Tumorigenesis. *Molecular Cell*, *61*(5), 705–719. https://doi.org/10.1016/j.molcel.2016.02.009

Li, Y., Zhang, J., Yue, J., Gou, X., & Wu, X. (n.d.). COMPREHENSIVE INVITED REVIEW Epidermal Stem Cells in Skin Wound Healing. *ADVANCES IN WOUND CARE*, *6*(9). https://doi.org/10.1089/wound.2017.0728

Liang, J., Cao, R., Wang, X., Zhang, Y., Wang, P., Gao, H., … Yang, W. (2017). Mitochondrial PKM2 regulates oxidative stress-induced apoptosis by stabilizing Bcl2. *Cell Research*, *27*(3), 329–351. https://doi.org/10.1038/cr.2016.159

Liang, Z., Brown, K. E., Carroll, T., Taylor, B., Ferreiró S Vidal, I., Hendrich, B., … Merkenschlager, M. (2017). *A high-resolution map of transcriptional repression*. https://doi.org/10.7554/eLife.22767.001

Limpert, A. S., Bai, S., Narayan, M., Wu, J., Yoon, S. O., Carter, B. D., & Lu, Q. R. (2013). NF- B Forms a Complex with the Chromatin Remodeler BRG1 to Regulate Schwann Cell Differentiation. *Journal of Neuroscience*, *33*(6), 2388–2397. https://doi.org/10.1523/JNEUROSCI.3223-12.2013

Lin, H., Wong, R. P. C., Martinka, M., & Li, G. (2010). *BRG 1 expression is increased in human cutaneous melanoma*. 502–510. https://doi.org/10.1111/j.1365-2133.2010.09851.x

Lin, J., Takata, M., Murata, H., Goto, Y., Kido, K., Ferrone, S., & Saida, T. (2009). Polyclonality of BRAF Mutations in Acquired Melanocytic Nevi. *JNCI: Journal of the National Cancer Institute*, *101*(20), 1423–1427. https://doi.org/10.1093/jnci/djp309

Lin, J. Y., & Fisher, D. E. (2007). *Melanocyte biology and skin pigmentation*. https://doi.org/10.1038/nature05660

Linge, A., Kennedy, S., O'Flynn, D., Beatty, S., Moriarty, P., Henry, M., … Meleady, P. (2012). Differential Expression of Fourteen Proteins between Uveal Melanoma from Patients Who Subsequently Developed Distant Metastases versus Those Who Did Not. *Investigative Opthalmology & Visual Science*, *53*(8), 4634. https://doi.org/10.1167/iovs.11-9019

Linsley, P. S., Greene, J. L., Brady, W., Bajorath, J., Ledbetter, J. A., & Peach, R. (1994). Human B7-1 (CD80) and B7-2 (CD86) bind with similar avidities but distinct kinetics to CD28 and CTLA-4 receptors. *Immunity*, *1*(9), 793–801. https://doi.org/10.1016/S1074-7613(94)80021-9

Lister, R., Pelizzola, M., Dowen, R. H., Hawkins, R. D., Hon, G., Tonti-Filippini, J., … Ecker, J. R. (2009). Human DNA methylomes at base resolution show widespread epigenomic differences. *Nature*, *462*(7271), 315–322. https://doi.org/10.1038/nature08514

Liu, H., Hew, H. C., Lu, Z.-G., Yamaguchi, T., Miki, Y., & Yoshida, K. (2009). DNA damage signaling recruits RREB-1 to the p53 tumour suppressor promoter. *Biochemical Journal*, *422*(3), 543–551. https://doi.org/10.1042/BJ20090342

Liu, J., Zhang, C., Lin, M., Zhu, W., Liang, Y., Hong, X., … Feng, Z. (2014). Glutaminase 2 negatively regulates the PI3K/AKT signaling and shows tumor suppression activity in human hepatocellular carcinoma. *Oncotarget*, *5*(9), 2635–2647. https://doi.org/10.18632/oncotarget.1862

Liu, K.-J., Shih, N.-Y., Liu, K., Shih, N., Liu, K., & Shih, N. (2007, January 1). *The role of enolase in tissue invasion and metastasis of pathogens and tumor cells*. Retrieved from https://www.scienceopen.com/document?vid=5add4e06-bc15-4b7b-b3a3-74569f72a6cb

Liu, W.-S., Liu, Y.-D., Fu, Q., Zhang, W.-J., Xu, L., Chang, Y., & Xu, J.-J. (2016). Prognostic significance of ubiquinol-cytochrome c reductase hinge protein expression in patients with clear cell renal cell carcinoma. *American Journal of Cancer Research*, *6*(4), 797–805. Retrieved from http://www.ncbi.nlm.nih.gov/pubmed/27186431

Locasale, J. W. (2013). Serine, glycine and one-carbon units: cancer metabolism in full circle. *Nature Reviews Cancer*, *13*(8),

572–583. https://doi.org/10.1038/nrc3557

Louphrasitthiphol, P., Ledaki, I., Chauhan, J., Falletta, P., Siddaway, R., Buffa, F. M., … Goding, C. R. (2019). MITF controls the TCA cycle to modulate the melanoma hypoxia response. *Pigment Cell & Melanoma Research*. https://doi.org/10.1111/pcmr.12802

Low, J. K. K., Webb, S. R., Silva, A. P. G., Saathoff, H., Ryan, D. P., Torrado, M., … Mackay, J. P. (2016). CHD4 is a peripheral component of the nucleosome remodeling and deacetylase complex. *Journal of Biological Chemistry*, *291*(30), 15853–15866. https://doi.org/10.1074/jbc.M115.707018

Luger, K., Mäder, A. W., Richmond, R. K., Sargent, D. F., & Richmond, T. J. (1997). Crystal structure of the nucleosome core particle at 2.8 Å resolution. *Nature*, *389*(6648), 251–260. https://doi.org/10.1038/38444

Lv, L., Xu, Y.-P., Zhao, D., Li, F.-L., Wang, W., Sasaki, N., … Xiong, Y. (2013). Mitogenic and Oncogenic Stimulation of K433 Acetylation Promotes PKM2 Protein Kinase Activity and Nuclear Localization. *Molecular Cell*, *52*(3), 340–352. https://doi.org/10.1016/J.MOLCEL.2013.09.004

Mackenzie, I. C. (1997). Retroviral transduction of murine epidermal stem cells demonstrates clonal units of epidermal structure. *Journal of Investigative Dermatology*, *109*(3), 377–383. https://doi.org/10.1111/1523-1747.ep12336255

Macpherson, J. A., Theisen, A., Masino, L., Fets, L., Driscoll, P. C., Encheva, V., … Anastasiou, D. (2019). Functional cross-talk between allosteric effects of activating and inhibiting ligands underlies PKM2 regulation. *ELife*, *8*. https://doi.org/10.7554/eLife.45068

Magnus, K. (1981). Habits of sun exposure and risk of malignant melanoma: An analysis of incidence rates in Norway 1955–1977 by cohort, sex, age, and primary tumor site. *Cancer*, *48*(10), 2329–2335. https://doi.org/10.1002/1097-0142(19811115)48:10<2329::AID-CNCR2820481032>3.0.CO;2-O

Mamczur, P., & Dzugaj, A. (2008). *Aldolase A is present in smooth muscle cell nuclei*. Retrieved from www.actabp.pl

Marangos, P. J., Parma, A. M., & Goodwin, F. K. (1978). Functional properties of neuronal and glial isoenzymes of brain enolase. *Journal of Neurochemistry*, *31*(3), 727–732. Retrieved from http://www.ncbi.nlm.nih.gov/pubmed/681951

Marathe, H. G., Mehta, G., Zhang, X., Datar, I., Mehrotra, A., Yeung, K. C., & de la Serna, I. L. (2013). SWI/SNF Enzymes Promote SOX10- Mediated Activation of Myelin Gene Expression. *PLoS ONE*, *8*(7), e69037. https://doi.org/10.1371/journal.pone.0069037

Marathe, H. G., Watkins-Chow, D. E., Weider, M., Hoffmann, A., Mehta, G., Trivedi, A., … de la Serna, I. L. (2017). BRG1 interacts with SOX10 to establish the melanocyte lineage and to promote differentiation. *Nucleic Acids Research*, *45*(11), 6442–6458. https://doi.org/10.1093/nar/gkx259

Marchiq, I., & Pouysségur, J. (2016). Hypoxia, cancer metabolism and the therapeutic benefit of targeting lactate/H+ symporters. *Journal of Molecular Medicine*, *94*(2), 155–171. https://doi.org/10.1007/s00109-015-1307-x

Marfella, C. G. A., & Imbalzano, A. N. (2007). The Chd Family of Chromatin Remodelers. *Mutation Research*, *618*(1–2), 30. https://doi.org/10.1016/J.MRFMMM.2006.07.012

Marinho-Carvalho, M. M., Costa-Mattos, P. V., Spitz, G. A., Zancan, P., & Sola-Penna, M. (2009). Calmodulin upregulates skeletal muscle 6-phosphofructo-1-kinase reversing the inhibitory effects of allosteric modulators. *Biochimica et Biophysica Acta (BBA) - Proteins and Proteomics*, *1794*(8), 1175–1180. https://doi.org/10.1016/J.BBAPAP.2009.02.006

Masamha, C. P., Xia, Z., Yang, J., Albrecht, T. R., Li, M., Shyu, A.-B., … Wagner, E. J. (2014). CFIm25 links alternative polyadenylation to glioblastoma tumour suppression. *Nature*, *510*(7505), 412–416. https://doi.org/10.1038/nature13261

Mazurek, S. (2011). Pyruvate kinase type M2: A key regulator of the metabolic budget system in tumor cells. *The International Journal of Biochemistry & Cell Biology*, *43*(7), 969–980. https://doi.org/10.1016/J.BIOCEL.2010.02.005

McDonel, P., Costello, I., & Hendrich, B. (2009). Keeping things quiet: Roles of NuRD and Sin3 co-repressor complexes during mammalian development. *The International Journal of Biochemistry & Cell Biology*, *41*(1), 108–116. https://doi.org/10.1016/j.biocel.2008.07.022

McFate, T., Mohyeldin, A., Lu, H., Thakar, J., Henriques, J., Halim, N. D., … Verma, A. (2008). Pyruvate Dehydrogenase Complex Activity Controls Metabolic and Malignant Phenotype in Cancer Cells. *Journal of Biological Chemistry*, *283*(33), 22700–22708. https://doi.org/10.1074/jbc.M801765200

McGill, G. G., Horstmann, M., Widlund, H. R., Du, J., Motyckova, G., Nishimura, E. K., … Fisher, D. E. (2002). Bcl2 regulation by the melanocyte master regulator Mitf modulates lineage survival and melanoma cell viability. *Cell*, *109*(6), 707–718. Retrieved from http://www.ncbi.nlm.nih.gov/pubmed/12086670

Mcgilvery, R. W., & Mokrasch, L. C. (1956). Purification and properties of fructose-1, 6-diphosphatase. *The Journal of Biological Chemistry*, *221*(2), 909–917. Retrieved from http://www.ncbi.nlm.nih.gov/pubmed/13357486

McKenzie, L. D., LeClair, J. W., Miller, K. N., Strong, A. D., Chan, H. L., Oates, E. L., … Chheda, M. G. (2019a). CHD4 regulates the DNA damage response and RAD51 expression in glioblastoma. *Scientific Reports*, *9*(1), 4444. https://doi.org/10.1038/s41598-019-40327-w

McKenzie, L. D., LeClair, J. W., Miller, K. N., Strong, A. D., Chan, H. L., Oates, E. L., … Chheda, M. G. (2019b). CHD4 regulates the DNA damage response and RAD51 expression in glioblastoma. *Scientific Reports*, *9*(1), 4444. https://doi.org/10.1038/s41598-019-40327-w

Melani, M., Simpson, K. J., Brugge, J. S., & Montell, D. (2008). Regulation of cell adhesion and collective cell migration by hindsight and its human homolog RREB1. *Current Biology : CB*, *18*(7), 532–537. https://doi.org/10.1016/j.cub.2008.03.024

Melero, I., Grimaldi, A. M., Perez-Gracia, J. L., & Ascierto, P. A. (2013). Clinical Development of Immunostimulatory Monoclonal Antibodies and Opportunities for Combination. *Clinical Cancer Research*, *19*(5), 997–1008. https://doi.org/10.1158/1078-0432.CCR-12-2214

Menendez, J. A., & Lupu, R. (2007). Fatty acid synthase and the lipogenic phenotype in cancer pathogenesis. *Nature Reviews Cancer*, *7*(10), 763–777. https://doi.org/10.1038/nrc2222

Mentch, S. J., Mehrmohamadi, M., Huang, L., Liu, X., Gupta, D., Mattocks, D., … Locasale, J. W. (2015). Histone Methylation Dynamics and Gene Regulation Occur through the Sensing of One-Carbon Metabolism. *Cell Metabolism*, *22*(5), 861–873. https://doi.org/10.1016/j.cmet.2015.08.024

Meyer-Siegler, K., Mauro, D. J., Seal, G., Wurzer, J., deRiel, J. K., & Sirover, M. A. (1991). A human nuclear uracil DNA glycosylase is the 37-kDa subunit of glyceraldehyde-3-phosphate dehydrogenase. *Proceedings of the National Academy of Sciences*, *88*(19), 8460–8464. https://doi.org/10.1073/pnas.88.19.8460

Michaloglou, C., Vredeveld, L. C. W., Mooi, W. J., & Peeper, D. S. (2008). BRAFE600 in benign and malignant human tumours. *Oncogene*, *27*(7), 877–895. https://doi.org/10.1038/sj.onc.1210704

Migita, T., Narita, T., Nomura, K., Miyagi, E., Inazuka, F., Matsuura, M., … Ishikawa, Y. (2008). ATP Citrate Lyase: Activation and Therapeutic Implications in Non-Small Cell Lung Cancer. *Cancer Research*, *68*(20), 8547–8554. https://doi.org/10.1158/0008-5472.CAN-08-1235

Millard, C. J., Watson, P. J., Celardo, I., Gordiyenko, Y., Cowley, S. M., Robinson, C. V., … Schwabe, J. W. R. (2013). Class I HDACs Share a Common Mechanism of Regulation by Inositol Phosphates. *Molecular Cell*, *51*(1), 57–67. https://doi.org/10.1016/j.molcel.2013.05.020

Miller, A. J., Levy, C., Davis, I. J., Razin, E., & Fisher, D. E. (2005). Sumoylation of MITF and Its Related Family Members TFE3 and TFEB. *Journal of Biological Chemistry*, *280*(1), 146–155. https://doi.org/10.1074/jbc.M411757200

Miller, A. J., & Mihm, M. C. (2006). Melanoma. *New England Journal of Medicine*, *355*(1), 51–65. https://doi.org/10.1056/NEJMra052166

Miller, A., Ralser, M., Kloet, S. L., Loos, R., Nishinakamura, R., Bertone, P., … Hendrich, B. (2016). Sall4 controls differentiation of pluripotent cells independently of the Nucleosome Remodelling and Deacetylation (NuRD) complex. *Development (Cambridge, England)*, *143*(17), 3074–3084. https://doi.org/10.1242/dev.139113

Miller, T. C., & Costa, A. (2017). The architecture and function of the chromatin replication machinery. *Current Opinion in Structural Biology*, *47*, 9–16. https://doi.org/10.1016/j.sbi.2017.03.011

Moan, J., Grigalavicius, M., Baturaite, Z., Dahlback, A., & Juzeniene, A. (2015). The relationship between UV exposure and incidence of skin cancer. *Photodermatology, Photoimmunology & Photomedicine*, *31*(1), 26–35. https://doi.org/10.1111/phpp.12139

Mohd-Sarip, A., Teeuwssen, M., Bot, A. G., De Herdt, M. J., Willems, S. M., Baatenburg de Jong, R. J., … Verrijzer, C. P. (2017a). DOC1-Dependent Recruitment of NURD Reveals Antagonism with SWI/SNF during Epithelial-Mesenchymal Transition in Oral Cancer Cells. *Cell Reports*, *20*(1), 61–75. https://doi.org/10.1016/j.celrep.2017.06.020

Mohd-Sarip, A., Teeuwssen, M., Bot, A. G., De Herdt, M. J., Willems, S. M., Baatenburg de Jong, R. J., … Verrijzer, C. P. (2017b). DOC1-Dependent Recruitment of NURD Reveals Antagonism with SWI/SNF during Epithelial-Mesenchymal Transition in Oral Cancer Cells. *Cell Reports*, *20*(1), 61–75. https://doi.org/10.1016/J.CELREP.2017.06.020

Mohit Jain. (2012). Metabolite Profiling Identifies a Key Role for Glycine in Rapid Cancer Cell Proliferation. *Science Mag*. https://doi.org/10.1126/science.1221551

Moreadith, R. W., & Lehninger, A. L. (1984). The pathways of glutamate and glutamine oxidation by tumor cell mitochondria. Role of mitochondrial NAD(P)+-dependent malic enzyme. *The Journal of Biological Chemistry*, *259*(10), 6215–6221. Retrieved from http://www.ncbi.nlm.nih.gov/pubmed/6144677

Moreno-Sánchez, R., Rodríguez-Enríquez, S., Marín-Hernández, A., & Saavedra, E. (2007a). Energy metabolism in tumor cells. *FEBS Journal*, *274*(6), 1393–1418. https://doi.org/10.1111/j.1742-4658.2007.05686.x

Moreno-Sánchez, R., Rodríguez-Enríquez, S., Marín-Hernández, A., & Saavedra, E. (2007b). Energy metabolism in tumor cells. *FEBS Journal*, *274*(6), 1393–1418. https://doi.org/10.1111/j.1742-4658.2007.05686.x

Morey, L., Brenner, C., Fazi, F., Villa, R., Gutierrez, A., Buschbeck, M., … Di Croce, L. (2008). MBD3, a Component of the NuRD Complex, Facilitates Chromatin Alteration and Deposition of Epigenetic Marks. *Molecular and Cellular Biology*, *28*(19), 5912–5923. https://doi.org/10.1128/MCB.00467-08

Morfouace, M., Lalier, L., Oliver, L., Cheray, M., Pecqueur, C., Cartron, P.-F., & Vallette, F. M. (2014). Control of glioma cell death and differentiation by PKM2-Oct4 interaction. *Cell Death & Disease*, *5*(1), e1036. https://doi.org/10.1038/cddis.2013.561

Morgan, H. P., O'Reilly, F. J., Wear, M. A., O'Neill, J. R., Fothergill-Gilmore, L. A., Hupp, T., & Walkinshaw, M. D. (2013). M2 pyruvate kinase provides a mechanism for nutrient sensing and regulation of cell proliferation. *Proceedings of the National Academy of Sciences*, *110*(15), 5881–5886. https://doi.org/10.1073/pnas.1217157110

Morris, S. A., Baek, S., Sung, M.-H., John, S., Wiench, M., Johnson, T. A., … Hager, G. L. (2014a). Overlapping chromatin-remodeling systems collaborate genome wide at dynamic chromatin transitions. *Nature Structural & Molecular Biology*, *21*(1), 73–81. https://doi.org/10.1038/nsmb.2718

Mort, R. L., Jackson, I. J., & Patton, E. E. (2015). *The melanocyte lineage in development and disease*. *142*, 1387. https://doi.org/10.1242/dev.123729

Moshkin, Y. M., Chalkley, G. E., Kan, T. W., Reddy, B. A., Ozgur, Z., Ijcken, W. F. J. van, … Verrijzer, C. P. (2012). Remodelers Organize Cellular Chromatin by Counteracting Intrinsic Histone-DNA Sequence Preferences in a Class-Specific Manner. *Molecular and Cellular Biology*, *32*(3), 675–688. https://doi.org/10.1128/MCB.06365-11

Muchardt, C., & Yaniv, M. (1993). A human homologue of Saccharomyces cerevisiae SNF2/SWI2 and Drosophila brm genes potentiates transcriptional activation by the glucocorticoid receptor. *The EMBO Journal*, *12*(11), 4279–4290. Retrieved from http://www.ncbi.nlm.nih.gov/pubmed/8223438

Mukai, T., Joh, K., Arai, Y., Yatsuki, H., & Hori, K. (1986). Tissue-specific expression of rat aldolase A mRNAs. Three molecular species differing only in the 5'-terminal sequences. *The Journal of Biological Chemistry*, *261*(7), 3347–3354. Retrieved from http://www.ncbi.nlm.nih.gov/pubmed/3753977

Mulero-Navarro, S., & Esteller, M. (n.d.). Chromatin remodeling factor CHD5 is silenced by promoter CpG island hypermethylation in human cancer. *Epigenetics*, *3*(4), 210–215. https://doi.org/10.4161/epi.3.4.6610

Mulero-Navarro, S., & Esteller, M. (2008). Chromatin remodeling factor CHD5 is silenced by promoter CpG island hypermethylation in human cancer. *Epigenetics*, *3*(4), 210–215. https://doi.org/10.4161/epi.3.4.6610

Mullarky, E., Mattaini, K. R., Vander Heiden, M. G., Cantley, L. C., & Locasale, J. W. (2011). PHGDH amplification and altered glucose metabolism in human melanoma. *Pigment Cell & Melanoma Research*, *24*(6), 1112–1115. https://doi.org/10.1111/j.1755-148X.2011.00919.x

Müller, J., Krijgsman, O., Tsoi, J., Robert, L., Hugo, W., Song, C., … Peeper, D. S. (2014). Low MITF/AXL ratio predicts early resistance to multiple targeted drugs in melanoma. *Nature Communications*, *5*. https://doi.org/10.1038/ncomms6712

Murre, C, McCaw, P. S., Vaessin, H., Caudy, M., Jan, L. Y., Jan, Y. N., … Lassar, A. B. (1989). Interactions between heterologous helix-loop-helix proteins generate complexes that bind specifically to a common DNA sequence. *Cell*, *58*(3), 537–544. Retrieved from http://www.ncbi.nlm.nih.gov/pubmed/2503252

Murre, Cornelis, Bain, G., van Dijk, M. A., Engel, I., Furnari, B. A., Massari, M. E., … Stuiver, M. H. (1994). Structure and function of helix-loop-helix proteins. *Biochimica et Biophysica Acta (BBA) - Gene Structure and Expression*, *1218*(2), 129–135. https://doi.org/10.1016/0167-4781(94)90001-9

Musselman, C. A., Ramirez, J., Sims, J. K., Mansfield, R. E., Oliver, S. S., Denu, J. M., … Kutateladze, T. G. (2012). Bivalent recognition of nucleosomes by the tandem PHD fingers of the CHD4 ATPase is required for CHD4-mediated repression. *Proceedings of the National Academy of Sciences*, *109*(3), 787–792. https://doi.org/10.1073/pnas.1113655109

Musselman, Catherine A., Mansfield, R. E., Garske, A. L., Davrazou, F., Kwan, A. H., Oliver, S. S., … Kutateladze, T. G. (2009). Binding of the CHD4 PHD2 finger to histone H3 is modulated by covalent modifications. *Biochemical Journal*, *423*(2), 179–187. https://doi.org/10.1042/BJ20090870

Nakashima, K., Hagiwara, T., Ishigami, A., Nagata, S., Asaga, H., Kuramoto, M., … Yamada, M. (1999). Molecular Characterization of Peptidylarginine Deiminase in HL-60 Cells Induced by Retinoic Acid and 1α,25-Dihydroxyvitamin D 3. *Journal of Biological Chemistry*, *274*(39), 27786–27792. https://doi.org/10.1074/jbc.274.39.27786

Nakashima, K., Hagiwara, T., & Yamada, M. (2002). Nuclear Localization of Peptidylarginine Deiminase V and Histone Deimination in Granulocytes. *Journal of Biological Chemistry*, *277*(51), 49562–49568. https://doi.org/10.1074/jbc.M208795200

Neigeborn, L., & Carlson, M. (1984). Genes affecting the regulation of SUC2 gene expression by glucose repression in Saccharomyces cerevisiae. *Genetics*, *108*(4), 845–858. Retrieved from http://www.ncbi.nlm.nih.gov/pubmed/6392017

Newton Bishop, J. A., Wachsmuth, R. C., Harland, M., Bataille, V., Pinney, E., Mack, P., … Timothy Bishop, D. (2000). Genotype/Phenotype and Penetrance Studies in Melanoma Families with Germline CDKN2A Mutations. *Journal of Investigative Dermatology*, *114*(1), 28–33. https://doi.org/10.1046/j.1523-1747.2000.00823.x

Nie, Z., Xue, Y., Yang, D., Zhou, S., Deroo, B. J., Archer, T. K., & Wang, W. (2000). A specificity and targeting subunit of a human SWI/SNF family-related chromatin-remodeling complex. *Molecular and Cellular Biology*, *20*(23), 8879–8888. https://doi.org/10.1128/mcb.20.23.8879-8888.2000

Nijhof, J. G. W., Braun, K. M., Giangreco, A., van Pelt, C., Kawamoto, H., Boyd, R. L., … van Ewijk, W. (2006). The cell-surface marker MTS24 identifies a novel population of follicular keratinocytes with characteristics of progenitor cells. *Development*, *133*(15), 3027–3037. https://doi.org/10.1242/dev.02443

Nikolaev, S. I., Rimoldi, D., Iseli, C., Valsesia, A., Robyr, D., Gehrig, C., … Antonarakis, S. E. (2012). Exome sequencing identifies recurrent somatic MAP2K1 and MAP2K2 mutations in melanoma. *Nature Genetics*, *44*(2), 133–139. https://doi.org/10.1038/ng.1026

Nio, K., Yamashita, T., Okada, H., Kondo, M., Hayashi, T., Hara, Y., … Kaneko, S. (2015). Defeating EpCAM+ liver cancer stem cells by targeting chromatin remodeling enzyme CHD4 in human hepatocellular carcinoma. *Journal of Hepatology*, *63*(5), 1164–1172. https://doi.org/10.1016/j.jhep.2015.06.009

Nissan, M. H., Pratilas, C. A., Jones, A. M., Ramirez, R., Won, H., Liu, C., … Solit, D. B. (2014). Loss of NF1 in Cutaneous Melanoma Is Associated with RAS Activation and MEK Dependence. *Cancer Research*, *74*(8), 2340–2350. https://doi.org/10.1158/0008-5472.CAN-13-2625

Nitarska, J., Smith, J. G., Sherlock, W. T., Hillege, M. M. G., Nott, A., Barshop, W. D., … Riccio, A. (2016). A Functional Switch of NuRD Chromatin Remodeling Complex Subunits Regulates Mouse Cortical Development. *Cell Reports*, *17*(6), 1683–1698. https://doi.org/10.1016/j.celrep.2016.10.022

Noguchi, T., Ward, J. P., Gubin, M. M., Arthur, C. D., Lee, S. H., Hundal, J., … Schreiber, R. D. (2017). Temporally Distinct PD-L1 Expression by Tumor and Host Cells Contributes to Immune Escape. *Cancer Immunology Research*, *5*(2), 106–117. https://doi.org/10.1158/2326-6066.CIR-16-0391

Nordlund, J. J., Collins, C. E., & Rheins, L. A. (1986). Prostaglandin E2 and D2 but Not MSH Stimulate the Proliferation of Pigment Cells in the Pinnal Epidermis of the DBA/2 Mouse. *Journal of Investigative Dermatology*, *86*(4), 433–437. https://doi.org/10.1111/1523-1747.EP12285717

O'Neill, J. R., Walkinshaw, M. D., Hupp, T., Fothergill-Gilmore, L. A., Morgan, H. P., Wear, M. A., & O'Reilly, F. J. (2013). M2 pyruvate kinase provides a mechanism for nutrient sensing and regulation of cell proliferation. *Proceedings of the National Academy of Sciences*, *110*(15), 5881–5886. https://doi.org/10.1073/pnas.1217157110

O'Shaughnessy-Kirwan, A., Signolet, J., Costello, I., Gharbi, S., & Hendrich, B. (2015). Constraint of gene expression by the chromatin remodelling protein CHD4 facilitates lineage specification. *Development (Cambridge, England)*, *142*(15), 2586–2597. https://doi.org/10.1242/dev.125450

O'Shaughnessy, A., & Hendrich, B. (2013). CHD4 in the DNA-damage response and cell cycle progression: not so NuRDy now. *Biochemical Society Transactions*, *41*(3), 777–782. https://doi.org/10.1042/BST20130027

Ohanna, M., Bonet, C., Bille, K., Allegra, M., Davidson, I., Bahadoran, P., … Bertolotto, C. (2014). SIRT1 promotes proliferation and inhibits the senescence-like phenotype in human melanoma cells. In *Oncotarget* (Vol. 5). Retrieved from www.impactjournals.com/oncotarget/

Okamoto, N., Aoto, T., Uhara, H., Yamazaki, S., Akutsu, H., Umezawa, A., … Nishimura, E. K. (2014). A melanocyte-melanoma precursor niche in sweat glands of volar skin. *Pigment Cell & Melanoma Research*, *27*(6), 1039–1050. https://doi.org/10.1111/pcmr.12297

Okar, D. A., & Lange, A. J. (1999). Fructose-2,6-bisphosphate and control of carbohydrate metabolism in eukaryotes. *BioFactors (Oxford, England)*, *10*(1), 1–14. Retrieved from http://www.ncbi.nlm.nih.gov/pubmed/10475585

Oliveria, S. A., Saraiya, M., Geller, A. C., Heneghan, M. K., & Jorgensen, C. (2006). Sun exposure and risk of melanoma. *Archives of Disease in Childhood*, *91*(2), 131–138. https://doi.org/10.1136/adc.2005.086918

Omholt, K., Kröckel, D., Ringborg, U., & Hansson, J. (2006). Mutations of PIK3CA are rare in cutaneous melanoma. *Melanoma Research*, *16*(2), 197–200. https://doi.org/10.1097/01.cmr.0000200488.77970.e3

Ondrušová, L., Vachtenheim, J., Réda, J., Žáková, P., & Benková, K. (2013). MITF-Independent Pro-Survival Role of BRG1-Containing SWI/SNF Complex in Melanoma Cells. *PLoS ONE*, *8*(1), e54110. https://doi.org/10.1371/journal.pone.0054110

Oshima, H., Rochat, A., Kedzia, C., Kobayashi, K., & Barrandon, Y. (2001). Morphogenesis and Renewal of Hair Follicles from Adult Multipotent Stem Cells. *Cell*, *104*(2), 233–245. https://doi.org/10.1016/S0092-8674(01)00208-2

Ostapcuk, V., Mohn, F., Carl, S. H., Basters, A., Hess, D., Iesmantavicius, V., … Bühler, M. (2018). Activity-dependent neuroprotective protein recruits HP1 and CHD4 to control lineage-specifying genes. *Nature*, *557*(7707), 739–743. https://doi.org/10.1038/s41586-018-0153-8

Østerlind, A., Hou-Jensen, K., & Møller Jensen, O. (1988). Incidence of cutaneous malignant melanoma in Denmark 1978-1982. Anatomic site distribution, histologic types, and comparison with non-melanoma skin cancer. *British Journal of Cancer*, *58*(3), 385–391. https://doi.org/10.1038/bjc.1988.225

Ott, P. A., Carvajal, R. D., Pandit-Taskar, N., Jungbluth, A. A., Hoffman, E. W., Wu, B.-W., … Wolchok, J. D. (2013). Phase I/II study of pegylated arginine deiminase (ADI-PEG 20) in patients with advanced melanoma. *Investigational New Drugs*, *31*(2), 425–434. https://doi.org/10.1007/s10637-012-9862-2

Padovese, V., Franco, G., Valenzano, M., Pecoraro, L., Cammilli, M., & Petrelli, A. (2018). Skin cancer risk assessment in dark skinned immigrants: the role of social determinants and ethnicity. *Ethnicity & Health*, *23*(6), 649–658. https://doi.org/10.1080/13557858.2017.1294657

Pal, S., Yun, R., Datta, A., Lacomis, L., Erdjument-Bromage, H., Kumar, J., … Sif, S. (2003). mSin3A/histone deacetylase 2- and PRMT5-containing Brg1 complex is involved in transcriptional repression of the Myc target gene cad. *Molecular and Cellular Biology*, *23*(21), 7475–7487. https://doi.org/10.1128/mcb.23.21.7475-7487.2003

Palmieri, D., Fitzgerald, D., Shreeve, S. M., Hua, E., Bronder, J. L., Weil, R. J., … Steeg, P. S. (2009). Analyses of resected human brain metastases of breast cancer reveal the association between up-regulation of hexokinase 2 and poor prognosis. *Molecular Cancer Research : MCR*, *7*(9), 1438–1445. https://doi.org/10.1158/1541-7786.MCR-09-0234

Pancholi, V. (2001). Multifunctional alpha-enolase: its role in diseases. *Cellular and Molecular Life Sciences : CMLS*, *58*(7), 902–920. Retrieved from http://www.ncbi.nlm.nih.gov/pubmed/11497239

Park, S.-H., Ozden, O., Liu, G., Song, H. Y., Zhu, Y., Yan, Y., … Gius, D. (2016). SIRT2-Mediated Deacetylation and Tetramerization of Pyruvate Kinase Directs Glycolysis and Tumor Growth. *Cancer Research*, *76*(13), 3802–3812. https://doi.org/10.1158/0008-5472.CAN-15-2498

Parmenter, T. J., Kleinschmidt, M., Kinross, K. M., Bond, S. T., Li, J., Kaadige, M. R., … McArthur, G. A. (2014). Response of BRAF-Mutant Melanoma to BRAF Inhibition Is Mediated by a Network of Transcriptional Regulators of Glycolysis. *Cancer Discovery*, *4*(4), 423–433. https://doi.org/10.1158/2159-8290.CD-13-0440

Paterson, & Christie. (1974). *T e epidermal proliferative unit : The possible role of the central basal cells. 77-88.*

Pavlick, A. C., Ribas, A., Gonzalez, R., Hamid, O., Gajewski, T., Daud, A., … McArthur, G. A. (2015). Extended follow-up
resultsof phase Ib study (BRIM7) of vemurafenib (VEM) with cobimetinib (COBI) in *BRAF* -mutant melanoma. *Journal of Clinical Oncology*, *33*(15_suppl), 9020–9020. https://doi.org/10.1200/jco.2015.33.15_suppl.9020

Pegoraro, G., & Misteli, T. (2009). The central role of chromatin maintenance in aging. *Aging*, *1*(12), 1017–1022. https://doi.org/10.18632/aging.100106

Peng, S.-Y., Lai, P.-L., Pan, H.-W., Hsiao, L.-P., & Hsu, H.-C. (2008). Aberrant expression of the glycolytic enzymes aldolase B and type II hexokinase in hepatocellular carcinoma are predictive markers for advanced stage, early recurrence and poor prognosis. *Oncology Reports*, *19*(4), 1045–1053. Retrieved from http://www.ncbi.nlm.nih.gov/pubmed/18357395

Pérez-Gómez, B., Aragonés, N., Gustavsson, P., Lope, V., López-Abente, G., & Pollán, M. (2008). Do sex and site matter? Different age distribution in melanoma of the trunk among Swedish men and women. *British Journal of Dermatology*, *158*(4), 766–772. https://doi.org/10.1111/j.1365-2133.2007.08429.x

Perriello, G., Jorde, R., Nurjhan, N., Stumvoll, M., Dailey, G., Jenssen, T., … Gerich, J. E. (1995). Estimation of glucose-alanine-lactate-glutamine cycles in postabsorptive humans: role of skeletal muscle. *The American Journal of Physiology*, *269*(3 Pt 1), E443-50. https://doi.org/10.1152/ajpendo.1995.269.3.E443

Phelan, M. L., Sif, S., Narlikar, G. J., & Kingston, R. E. (1999). Reconstitution of a core chromatin remodeling complex from SWI/SNF subunits. *Molecular Cell*, *3*(2), 247–253. Retrieved from http://www.ncbi.nlm.nih.gov/pubmed/10078207

Pilkis, S. J., Claus, T. H., Kurland, I. J., & Lange, A. J. (1995). 6-Phosphofructo-2-Kinase/Fructose-2,6-Bisphosphatase: A Metabolic Signaling Enzyme. *Annual Review of Biochemistry*, *64*(1), 799–835. https://doi.org/10.1146/annurev.bi.64.070195.004055

Pillaiyar, T., Manickam, M., & Jung, S.-H. (2017). Downregulation of melanogenesis: drug discovery and therapeutic options. *Drug Discovery Today*, *22*(2), 282–298. https://doi.org/10.1016/j.drudis.2016.09.016

Pogenberg, V., Ogmundsdottir, M. H., Bergsteinsdottir, K., Schepsky, A., Phung, B., Deineko, V., … Wilmanns, M. (2012). Restricted leucine zipper dimerization and specificity of DNA recognition of the melanocyte master regulator MITF. *Genes & Development*, *26*(23), 2647–2658. https://doi.org/10.1101/gad.198192.112

Pollock, P. M., Harper, U. L., Hansen, K. S., Yudt, L. M., Stark, M., Robbins, C. M., … Meltzer, P. S. (2003). High frequency of BRAF mutations in nevi. *Nature Genetics*, *33*(1), 19–20. https://doi.org/10.1038/ng1054

POPESCU, N. A., BEARD, C. M., TREACY, P. J., WINKELMANN, R. K., O'BRIEN, P. C., & KURLAND, L. T. (1990). Cutaneous Malignant Melanoma in Rochester, Minnesota: Trends in Incidence and Survivorship, 1950 Through 1985. *Mayo Clinic Proceedings*, *65*(10), 1293–1302. https://doi.org/10.1016/S0025-6196(12)62140-5

Pópulo, H., Caldas, R., Lopes, J. M., Pardal, J., Máximo, V., & Soares, P. (2015). Overexpression of pyruvate dehydrogenase kinase supports dichloroacetate as a candidate for cutaneous melanoma therapy. *Expert Opinion on Therapeutic Targets*, *19*(6), 733–745. https://doi.org/10.1517/14728222.2015.1045416

Porporato, P. E., Dhup, S., Dadhich, R. K., Copetti, T., & Sonveaux, P. (2011). Anticancer targets in the glycolytic metabolism of tumors: a comprehensive review. *Frontiers in Pharmacology*, *2*, 49. https://doi.org/10.3389/fphar.2011.00049

Poulain, L., Sujobert, P., Zylbersztejn, F., Barreau, S., Stuani, L., Lambert, M., … Chesnais, V. (2017). *High mTORC1 activity drives glycolysis addiction and sensitivity to G6PD inhibition in acute myeloid leukemia cells*. (August 2016), 2326–2335. https://doi.org/10.1038/leu.2017.81

Prickett, T. D., Agrawal, N. S., Wei, X., Yates, K. E., Lin, J. C., Wunderlich, J. R., … Samuels, Y. (2009). Analysis of the tyrosine kinome in melanoma reveals recurrent mutations in ERBB4. *Nature Genetics*, *41*(10), 1127–1132. https://doi.org/10.1038/ng.438

Prince, S., Carreira, S., Vance, K. W., Abrahams, A., & Goding, C. R. (2004). Tbx2 Directly Represses the Expression of the p21WAF1 Cyclin-Dependent Kinase Inhibitor. *Cancer Research*, *64*(5), 1669–1674. https://doi.org/10.1158/0008-5472.CAN-03-3286

Proost, P., Loos, T., Mortier, A., Schutyser, E., Gouwy, M., Noppen, S., … Van Damme, J. (2008). Citrullination of CXCL8 by peptidylarginine deiminase alters receptor usage, prevents proteolysis, and dampens tissue inflammation. *The Journal of Experimental Medicine*, *205*(9), 2085–2097. https://doi.org/10.1084/jem.20080305

Puigserver, P., & Spiegelman, B. M. (2003). Peroxisome Proliferator-Activated Receptor-γ Coactivator 1α (PGC-1α): Transcriptional Coactivator and Metabolic Regulator. *Endocrine Reviews*, *24*(1), 78–90. https://doi.org/10.1210/er.2002-0012

Qi, W., Chen, H., Xiao, T., Wang, R., Li, T., Han, L., & Zeng, X. (2016). Acetyltransferase p300 collaborates with chromodomain helicase DNA-binding protein 4 (CHD4) to facilitate DNA double-strand break repair. *Mutagenesis*, *31*(2), 193–203. https://doi.org/10.1093/mutage/gev075

Qi, Y.-J., He, Q.-Y., Ma, Y.-F., Du, Y.-W., Liu, G.-C., Li, Y.-J., … Chiu, J.-F. (2008). Proteomic identification of malignant transformation-related proteins in esophageal squamous cell carcinoma. *Journal of Cellular Biochemistry*, *104*(5), 1625–1635. https://doi.org/10.1002/jcb.21727

Quan, J., & Yusufzai, T. (2014). The Tumor Suppressor Chromodomain Helicase DNA-binding Protein 5 (CHD5) Remodels Nucleosomes by Unwrapping. *Journal of Biological Chemistry*, *289*(30), 20717–20726. https://doi.org/10.1074/jbc.M114.568568

Quintana, E., Shackleton, M., Foster, H. R., Fullen, D. R., Sabel, M. S., Johnson, T. M., & Morrison, S. J. (2010). Phenotypic Heterogeneity among Tumorigenic Melanoma Cells from Patients that Is Reversible and Not Hierarchically Organized. *Cancer Cell*, *18*(5), 510–523. https://doi.org/10.1016/j.ccr.2010.10.012

Raijmakers, R., Zendman, A. J. W., Egberts, W. V., Vossenaar, E. R., Raats, J., Soede-Huijbregts, C., … Pruijn, G. J. M. (2007). Methylation of Arginine Residues Interferes with Citrullination by Peptidylarginine Deiminases in vitro. *Journal of Molecular Biology*, *367*(4), 1118–1129. https://doi.org/10.1016/j.jmb.2007.01.054

Rambow, F., Rogiers, A., Marin-Bejar, O., Aibar, S., Femel, J., Dewaele, M., … Marine, J. C. (2018). Toward Minimal Residual

Disease-Directed Therapy in Melanoma. *Cell*, *174*(4), 843-855.e19. https://doi.org/10.1016/j.cell.2018.06.025

Randazzo, F. M., Khavari, P., Crabtree, G., Tamkun, J., & Rossant, J. (1994). brg1: A Putative Murine Homologue of the Drosophila brahma Gene, a Homeotic Gene Regulator. *Developmental Biology*, *161*(1), 229–242. https://doi.org/10.1006/dbio.1994.1023

Redis, R. S., Vela, L. E., Lu, W., Ferreira de Oliveira, J., Ivan, C., Rodriguez-Aguayo, C., … Calin, G. A. (2016). Allele-Specific Reprogramming of Cancer Metabolism by the Long Non-coding RNA CCAT2. *Molecular Cell*, *61*(4), 520–534. https://doi.org/10.1016/j.molcel.2016.01.015

Reik, W. (2007). Stability and flexibility of epigenetic gene regulation in mammalian development. *Nature*, *447*(7143), 425–432. https://doi.org/10.1038/nature05918

Ren, F., Wu, H., Lei, Y., Zhang, H., Liu, R., Zhao, Y., … Huang, C. (2010). Quantitative proteomics identification of phosphoglycerate mutase 1 as a novel therapeutic target in hepatocellular carcinoma. *Molecular Cancer*, *9*(1), 81. https://doi.org/10.1186/1476-4598-9-81

Révillion, F., Pawlowski, V., Hornez, L., & Peyrat, J. P. (2000). Glyceraldehyde-3-phosphate dehydrogenase gene expression in human breast cancer. *European Journal of Cancer (Oxford, England : 1990)*, *36*(8), 1038–1042. Retrieved from http://www.ncbi.nlm.nih.gov/pubmed/10885609

Reynolds, N., Salmon-Divon, M., Dvinge, H., Hynes-Allen, A., Balasooriya, G., Leaford, D., … Hendrich, B. (2012). NuRD-mediated deacetylation of H3K27 facilitates recruitment of Polycomb Repressive Complex 2 to direct gene repression. *The EMBO Journal*, *31*(3), 593–605. https://doi.org/10.1038/emboj.2011.431

Ribas, A., Puzanov, I., Dummer, R., Schadendorf, D., Hamid, O., Robert, C., … Daud, A. (2015). Pembrolizumab versus investigator-choice chemotherapy for ipilimumab-refractory melanoma (KEYNOTE-002): a randomised, controlled, phase 2 trial. *The Lancet. Oncology*, *16*(8), 908–918. https://doi.org/10.1016/S1470-2045(15)00083-2

Richtig, G., Hoeller, C., Kashofer, K., Aigelsreiter, A., Heinemann, A., Kwong, L. N., … Richtig, E. (2017). Beyond the BRAFV600E hotspot: biology and clinical implications of rare *BRAF* gene mutations in melanoma patients. *British Journal of Dermatology*, *177*(4), 936–944. https://doi.org/10.1111/bjd.15436

Rider, M. H., Bertrand, L., Vertommen, D., Michels, P. A., Rousseau, G. G., & Hue, L. (2004). 6-Phosphofructo-2-kinase/fructose-2,6-bisphosphatase: head-to-head with a bifunctional enzyme that controls glycolysis. *Biochemical Journal*, *381*(3), 561–579. https://doi.org/10.1042/BJ20040752

Riera, L., Manzano, A., Navarro-Sabaté, A., Perales, J. C., & Bartrons, R. (2002). Insulin induces PFKFB3 gene expression in HT29 human colon adenocarcinoma cells. *Biochimica et Biophysica Acta*, *1589*(2), 89–92. https://doi.org/10.1016/s0167-4889(02)00169-6

Rivers, J. K. (2004). Is there more than one road to melanoma? *The Lancet*, *363*(9410), 728–730. https://doi.org/10.1016/S0140-6736(04)15649-3

Robbins, C. M., Tembe, W. A., Baker, A., Sinari, S., Moses, T. Y., Beckstrom-Sternberg, S., … Carpten, J. D. (2011). Copy number and targeted mutational analysis reveals novel somatic events in metastatic prostate tumors. *Genome Research*, *21*(1), 47–55. https://doi.org/10.1101/gr.107961.110

Robert, C., Schachter, J., Long, G. V., Arance, A., Grob, J. J., Mortier, L., … KEYNOTE-006 investigators. (2015). Pembrolizumab versus Ipilimumab in Advanced Melanoma. *New England Journal of Medicine*, *372*(26), 2521–2532. https://doi.org/10.1056/NEJMoa1503093

Robey, R. B., & Hay, N. (2006). Mitochondrial hexokinases, novel mediators of the antiapoptotic effects of growth factors and Akt. *Oncogene*, *25*(34), 4683–4696. https://doi.org/10.1038/sj.onc.1209595

Roesch, A., Fukunaga-Kalabis, M., Schmidt, E. C., Zabierowski, S. E., Brafford, P. A., Vultur, A., … Herlyn, M. (2010). A Temporarily Distinct Subpopulation of Slow-Cycling Melanoma Cells Is Required for Continuous Tumor Growth. *Cell*, *141*(4), 583–594. https://doi.org/10.1016/j.cell.2010.04.020

Rogers, G. E., Harding, H. W. J., & Llewellyn-Smith, I. J. (1977). The origin of citrulline-containing proteins in the hair follicle and the chemical nature of trichohyalin, an intracellular precursor. *Biochimica et Biophysica Acta (BBA) - Protein Structure*, *495*(1), 159–175. https://doi.org/10.1016/0005-2795(77)90250-1

Rogers, G. E., & Simmonds, D. H. (1958). Content of Citrulline and Other Amino-Acids in a Protein of Hair Follicles. *Nature*, *182*(4629), 186–187. https://doi.org/10.1038/182186a0

Rogers Ge. (1962). *Occurrence of citrulline in proteins.* Retrieved from https://www.ncbi.nlm.nih.gov/pubmed/14493344

Rong, Y., Wu, W., Ni, X., Kuang, T., Jin, D., Wang, D., & Lou, W. (2013). Lactate dehydrogenase A is overexpressed in pancreatic cancer and promotes the growth of pancreatic cancer cells. *Tumor Biology*, *34*(3), 1523–1530.

https://doi.org/10.1007/s13277-013-0679-1

Rose, I. A., & Warms, J. V. (1967). Mitochondrial hexokinase. Release, rebinding, and location. *The Journal of Biological Chemistry*, *242*(7), 1635–1645. Retrieved from http://www.ncbi.nlm.nih.gov/pubmed/4225734

Ross, M. I., & Gershenwald, J. E. (2011). Evidence-based treatment of early-stage melanoma. *Journal of Surgical Oncology*, *104*(4), 341–353. https://doi.org/10.1002/jso.21962

Ruthenburg, A. J., Li, H., Milne, T. A., Dewell, S., McGinty, R. K., Yuen, M., … Allis, C. D. (2011). Recognition of a Mononucleosomal Histone Modification Pattern by BPTF via Multivalent Interactions. *Cell*, *145*(5), 692–706. https://doi.org/10.1016/j.cell.2011.03.053

Saladi, S., Keenen, B., Marathe, H. G., Qi, H., Chin, K.-V., & de la Serna, I. L. (2010). Modulation of extracellular matrix/adhesion molecule expression by BRG1 is associated with increased melanoma invasiveness. *Molecular Cancer*, *9*(1), 280. https://doi.org/10.1186/1476-4598-9-280

Sanborn, J. Z., Chung, J., Purdom, E., Wang, N. J., Kakavand, H., Wilmott, J. S., … Cho, R. J. (2015). Phylogenetic analyses of melanoma reveal complex patterns of metastatic dissemination. *Proceedings of the National Academy of Sciences of the United States of America*, *112*(35), 10995–11000. https://doi.org/10.1073/pnas.1508074112

Sarkar, D., Leung, E. Y., Baguley, B. C., Finlay, G. J., & Askarian-Amiri, M. E. (2015). *Epigenetic regulation in human melanoma: past and future*. https://doi.org/10.1080/15592294.2014.1003746

Sato-Jin, K., Nishimura, E. K., Akasaka, E., Huber, W., Nakano, H., Miller, A., … Imokawa, G. (2008). Epistatic connections between microphthalmia-associated transcription factor and endothelin signaling in Waardenburg syndrome and other pigmentary disorders. *FASEB Journal : Official Publication of the Federation of American Societies for Experimental Biology*, *22*(4), 1155–1168. https://doi.org/10.1096/fj.07-9080com

Schauer, E., Trautinger, F., Köck, A., Schwarz, A., Bhardwaj, R., Simon, M., … Luger, T. A. (1994). Proopiomelanocortin-derived peptides are synthesized and released by human keratinocytes. *The Journal of Clinical Investigation*, *93*(5), 2258–2262. https://doi.org/10.1172/JCI117224

Schek, N., Hall, B. L., & Finn, O. J. (1988). Increased glyceraldehyde-3-phosphate dehydrogenase gene expression in human pancreatic adenocarcinoma. *Cancer Research*, *48*(22), 6354–6359. Retrieved from http://www.ncbi.nlm.nih.gov/pubmed/3180054

Schellekens, G. A., de Jong, B. A., van den Hoogen, F. H., van de Putte, L. B., & van Venrooij, W. J. (1998). Citrulline is an essential constituent of antigenic determinants recognized by rheumatoid arthritis-specific autoantibodies. *The Journal of Clinical Investigation*, *101*(1), 273–281. https://doi.org/10.1172/JCI1316

Schepeler, T., Page, M. E., & Jensen, K. B. (2014). *Heterogeneity and plasticity of epidermal stem cells*. https://doi.org/10.1242/dev.104588

Schepsky, A., Bruser, K., Gunnarsson, G. J., Goodall, J., Hallsson, J. H., Goding, C. R., … Hecht, A. (2006). The Microphthalmia-Associated Transcription Factor Mitf Interacts with -Catenin To Determine Target Gene Expression. *Molecular and Cellular Biology*, *26*(23), 8914–8927. https://doi.org/10.1128/MCB.02299-05

Schepsky, Alexander, Bruser, K., Gunnarsson, G. J., Goodall, J., Hallsson, J. H., Goding, C. R., … Hecht, A. (2006). The microphthalmia-associated transcription factor Mitf interacts with beta-catenin to determine target gene expression. *Molecular and Cellular Biology*, *26*(23), 8914–8927. https://doi.org/10.1128/MCB.02299-05

Schiaffino, M. V. (2010). Signaling pathways in melanosome biogenesis and pathology. *The International Journal of Biochemistry & Cell Biology*, *42*(7), 1094–1104. https://doi.org/10.1016/j.biocel.2010.03.023

Scott, D. A., Richardson, A. D., Filipp, F. V, Knutzen, C. A., Chiang, G. G., Ronai, E. A., … Smith, J. W. (2011). *Comparative Metabolic Flux Profiling of Melanoma Cell Lines BEYOND THE WARBURG EFFECT * □ S*. https://doi.org/10.1074/jbc.M111.282046

Seelig, H. P., Moosbrugger, I., Ehrfeld, H., Fink, T., Renz, M., & Genth, E. (1995). The major dermatomyositis-specific Mi-2 autoantigen is a presumed helicase involved in transcriptional activation. *Arthritis and Rheumatism*, *38*(10), 1389–1399. Retrieved from http://www.ncbi.nlm.nih.gov/pubmed/7575689

Seleit, I., Bakry, O. A., Abdou, A. G., & Dawoud, N. M. (2014). Immunohistochemical study of melanocyte-melanocyte stem cell lineage in vitiligo; A clue to interfollicular melanocyte stem cell reservoir. *Ultrastructural Pathology*, *38*(3), 186–198. https://doi.org/10.3109/01913123.2013.870274

Semenza, G. L., Jiang, B. H., Leung, S. W., Passantino, R., Concordet, J. P., Maire, P., & Giallongo, A. (1996). Hypoxia response elements in the aldolase A, enolase 1, and lactate dehydrogenase A gene promoters contain essential binding sites for hypoxia-inducible factor 1. *The Journal of Biological Chemistry*, *271*(51), 32529–32537.

https://doi.org/10.1074/jbc.271.51.32529

Serganova, I., Cohen, I. J., Vemuri, K., Shindo, M., Maeda, M., Mane, M., … Blasberg, R. (2018). LDH-A regulates the tumor microenvironment via HIF-signaling and modulates the immune response. *PLOS ONE*, *13*(9), e0203965. https://doi.org/10.1371/journal.pone.0203965

Shain, A. H., & Bastian, B. C. (2016). From melanocytes to melanomas. *Nature Reviews Cancer*, *16*(6), 345–358. https://doi.org/10.1038/nrc.2016.37

Shain, A. H., Joseph, N. M., Yu, R., Benhamida, J., Liu, S., Prow, T., … Bastian, B. C. (2018a). Genomic and Transcriptomic Analysis Reveals Incremental Disruption of Key Signaling Pathways during Melanoma Evolution. *Cancer Cell*, *34*(1), 45-55.e4. https://doi.org/10.1016/j.ccell.2018.06.005

Shain, A. H., Yeh, I., Kovalyshyn, I., Sriharan, A., Talevich, E., Gagnon, A., … Bastian, B. C. (2015). The Genetic Evolution of Melanoma from Precursor Lesions. *New England Journal of Medicine*, *373*(20), 1926–1936. https://doi.org/10.1056/NEJMoa1502583

Shakhova, O., Zingg, D., Schaefer, S. M., Hari, L., Civenni, G., Blunschi, J., … Sommer, L. (2012). Sox10 promotes the formation and maintenance of giant congenital naevi and melanoma. *Nature Cell Biology*, *14*(8), 882–890. https://doi.org/10.1038/ncb2535

Shen, W., Sakamoto, N., & Yang, L. (2016). Melanoma-specific mortality and competing mortality in patients with non-metastatic malignant melanoma: a population-based analysis. *BMC Cancer*, *16*(1), 413. https://doi.org/10.1186/s12885-016-2438-3

Sheng, S. L., Liu, J. J., Dai, Y. H., Sun, X. G., Xiong, X. P., & Huang, G. (2012). Knockdown of lactate dehydrogenase A suppresses tumor growth and metastasis of human hepatocellular carcinoma. *FEBS Journal*, *279*(20), 3898–3910. https://doi.org/10.1111/j.1742-4658.2012.08748.x

Shimazu, T., Hirschey, M. D., Newman, J., He, W., Shirakawa, K., Le Moan, N., … Verdin, E. (2013). Suppression of Oxidative Stress by -Hydroxybutyrate, an Endogenous Histone Deacetylase Inhibitor. *Science*, *339*(6116), 211–214. https://doi.org/10.1126/science.1227166

Shimbo, T., Du, Y., Grimm, S. A., Dhasarathy, A., Mav, D., Shah, R. R., … Wade, P. A. (2013). MBD3 Localizes at Promoters, Gene Bodies and Enhancers of Active Genes. *PLoS Genetics*, *9*(12), e1004028. https://doi.org/10.1371/journal.pgen.1004028

Shirai, H., Mokrab, Y., & Mizuguchi, K. (2006). The guanidino-group modifying enzymes: Structural basis for their diversity and commonality. *Proteins: Structure, Function, and Bioinformatics*, *64*(4), 1010–1023. https://doi.org/10.1002/prot.20863

Sif, S. (2004). ATP-dependent nucleosome remodeling complexes: Enzymes tailored to deal with chromatin. *Journal of Cellular Biochemistry*, *91*(6), 1087–1098. https://doi.org/10.1002/jcb.20005

Singh, R., & Green, M. R. (1993). Sequence-specific binding of transfer RNA by glyceraldehyde-3-phosphate dehydrogenase. *Science (New York, N.Y.)*, *259*(5093), 365–368. Retrieved from http://www.ncbi.nlm.nih.gov/pubmed/8420004

Slipicevic, A., & Herlyn, M. (2015). KIT in melanoma: many shades of gray. *The Journal of Investigative Dermatology*, *135*(2), 337–338. https://doi.org/10.1038/jid.2014.417

Slominski, A., Tobin, D. J., Shibahara, S., & Wortsman, J. (2004). Melanin Pigmentation in Mammalian Skin and Its Hormonal Regulation. *Physiological Reviews*, *84*(4), 1155–1228. https://doi.org/10.1152/physrev.00044.2003

Smith, S., & Stillman, B. (1991). Stepwise assembly of chromatin during DNA replication in vitro. *The EMBO Journal*, *10*(4), 971–980. Retrieved from http://www.ncbi.nlm.nih.gov/pubmed/1849080

Smits, A. H., Jansen, P. W. T. C., Poser, I., Hyman, A. A., & Vermeulen, M. (2013). Stoichiometry of chromatin-associated protein complexes revealed by label-free quantitative mass spectrometry-based proteomics. *Nucleic Acids Research*, *41*(1), e28–e28. https://doi.org/10.1093/nar/gks941

Snippert, H. J., Haegebarth, A., Kasper, M., Jaks, V., van Es, J. H., Barker, N., … Clevers, H. (2010). Lgr6 Marks Stem Cells in the Hair Follicle That Generate All Cell Lineages of the Skin. *Science*, *327*(5971), 1385–1389. https://doi.org/10.1126/science.1184733

Som, P., Atkins, H. L., Bandoypadhyay, D., Fowler, J. S., MacGregor, R. R., Matsui, K., … Zabinski, S. V. (1980). A fluorinated glucose analog, 2-fluoro-2-deoxy-D-glucose (F-18): nontoxic tracer for rapid tumor detection. *Journal of Nuclear Medicine : Official Publication, Society of Nuclear Medicine*, *21*(7), 670–675. Retrieved from http://www.ncbi.nlm.nih.gov/pubmed/7391842

Sommer, L. (2011). Generation of melanocytes from neural crest cells. *Pigment Cell & Melanoma Research*, *24*(3), 411–421. https://doi.org/10.1111/j.1755-148X.2011.00834.x

Son, J., Lyssiotis, C. A., Ying, H., Wang, X., Hua, S., Ligorio, M., … Kimmelman, A. C. (2013). Glutamine supports pancreatic cancer growth through a KRAS-regulated metabolic pathway. *Nature*, *496*(7443), 101–105. https://doi.org/10.1038/nature12040

Specenier, P. (2016). Nivolumab in melanoma. *Expert Review of Anticancer Therapy*, *16*(12), 1247–1261. https://doi.org/10.1080/14737140.2016.1249856

Srinivasan, S., Guha, M., Dong, D. W., Whelan, K. A., Ruthel, G., Uchikado, Y., … Avadhani, N. G. (2016). Disruption of cytochrome c oxidase function induces the Warburg effect and metabolic reprogramming. *Oncogene*, *35*(12), 1585–1595. https://doi.org/10.1038/onc.2015.227

Staal, G. E., Kalff, A., Heesbeen, E. C., van Veelen, C. W., & Rijksen, G. (1987). Subunit composition, regulatory properties, and phosphorylation of phosphofructokinase from human gliomas. *Cancer Research*, *47*(19), 5047–5051. Retrieved from http://www.ncbi.nlm.nih.gov/pubmed/2957049

Stang, A., Stabenow, R., Eisinger, B., & Jöckel, K.-H. (2003). Site- and gender-specific time trend analyses of the incidence of skin melanomas in the former German Democratic Republic (GDR) including 19 351 cases. *European Journal of Cancer*, *39*(11), 1610–1618. https://doi.org/10.1016/S0959-8049(03)00359-9

Stanley, F. K. T., Moore, S., & Goodarzi, A. A. (2013a). CHD chromatin remodelling enzymes and the DNA damage response. *Mutation Research/Fundamental and Molecular Mechanisms of Mutagenesis*, *750*(1–2), 31–44. https://doi.org/10.1016/j.mrfmmm.2013.07.008

Stanley, F. K. T., Moore, S., & Goodarzi, A. A. (2013b). CHD chromatin remodelling enzymes and the DNA damage response. *Mutation Research/Fundamental and Molecular Mechanisms of Mutagenesis*, *750*(1–2), 31–44. https://doi.org/10.1016/j.mrfmmm.2013.07.008

Stark, M. S., Woods, S. L., Gartside, M. G., Bonazzi, V. F., Dutton-Regester, K., Aoude, L. G., … Hayward, N. K. (2012). Frequent somatic mutations in MAP3K5 and MAP3K9 in metastatic melanoma identified by exome sequencing. *Nature Genetics*, *44*(2), 165–169. https://doi.org/10.1038/ng.1041

Steingrímsson, E., Copeland, N. G., & Jenkins, N. a. (2004). Melanocytes and the microphthalmia transcription factor network. *Annual Review of Genetics*, *38*, 365–411. https://doi.org/10.1146/annurev.genet.38.072902.092717

Steingrmsson, E. (2008). All for one, one for all: alternative promoters and Mitf. *Pigment Cell & Melanoma Research*, *21*(4), 412–414. https://doi.org/10.1111/j.1755-148X.2008.00473.x

Stern, M., Jensen, R., & Herskowitz, I. (1984). Five SWI genes are required for expression of the HO gene in yeast. *Journal of Molecular Biology*, *178*(4), 853–868. Retrieved from http://www.ncbi.nlm.nih.gov/pubmed/6436497

Stevens, T. J., Lando, D., Basu, S., Atkinson, L. P., Cao, Y., Lee, S. F., … Laue, E. D. (2017). 3D structures of individual mammalian genomes studied by single-cell Hi-C. *Nature*, *544*(7648), 59–64. https://doi.org/10.1038/nature21429

Steventon, B., Araya, C., Linker, C., Kuriyama, S., & Mayor, R. (2009). Differential requirements of BMP and Wnt signaling during gastrulation and neurulation define two steps in neural crest induction. *Development*, *136*(5), 771–779. https://doi.org/10.1242/dev.029017

Stierner, U., Augustsson, A., Rosdahl, I., & Suurküla, M. (1992). Regional distribution of common and dysplastic naevi in relation to melanoma site and sun exposure. A case-control study. *Melanoma Research*, *1*(5–6), 367–375. Retrieved from http://www.ncbi.nlm.nih.gov/pubmed/1422192

Stine, Z. E., Walton, Z. E., Altman, B. J., Hsieh, A. L., & Dang, C. V. (2015). MYC, Metabolism, and Cancer. *Cancer Discovery*, *5*(10), 1024–1039. https://doi.org/10.1158/2159-8290.CD-15-0507

Strub, T., Giuliano, S., Ye, T., Bonet, C., Keime, C., Kobi, D., … Davidson, I. (2011). Essential role of microphthalmia transcription factor for DNA replication, mitosis and genomic stability in melanoma. *Oncogene*, *30*(20), 2319–2332. https://doi.org/10.1038/onc.2010.612

Su, F., Viros, A., Milagre, C., Trunzer, K., Bollag, G., Spleiss, O., … Marais, R. (2012). *RAS* Mutations in Cutaneous Squamous-Cell Carcinomas in Patients Treated with BRAF Inhibitors. *New England Journal of Medicine*, *366*(3), 207–215. https://doi.org/10.1056/NEJMoa1105358

Suganuma, T., & Workman, J. L. (2011). Signals and Combinatorial Functions of Histone Modifications. *Annual Review of Biochemistry*, *80*(1), 473–499. https://doi.org/10.1146/annurev-biochem-061809-175347

Sui, D., & Wilson, J. E. (1997). Structural Determinants for the Intracellular Localization of the Isozymes of Mammalian Hexokinase: Intracellular Localization of Fusion Constructs Incorporating Structural Elements from the Hexokinase

Isozymes and the Green Fluorescent Protein. *Archives of Biochemistry and Biophysics*, *345*(1), 111–125. https://doi.org/10.1006/abbi.1997.0241

Sullivan, R. J., Weber, J. S., Patel, S. P., Dummer, R., Miller, W. H., Cosgrove, D., … Ascierto, P. A. (2015). A phase Ib/II study of BRAF inhibitor (BRAFi) encorafenib (ENCO) plus MEK inhibitor (MEKi) binimetinib (BINI) in cutaneous melanoma patients naive to BRAFi treatment. *Journal of Clinical Oncology*, *33*(15_suppl), 9007–9007. https://doi.org/10.1200/jco.2015.33.15_suppl.9007

Sun, L., Liu, X., Fu, H., Zhou, W., & Zhong, D. (2016). 2-Deoxyglucose Suppresses ERK Phosphorylation in LKB1 and Ras Wild-Type Non-Small Cell Lung Cancer Cells. *PLOS ONE*, *11*(12), e0168793. https://doi.org/10.1371/journal.pone.0168793

Sun, Q., Chen, X., Ma, J., Peng, H., Wang, F., Zha, X., … Zhang, H. (2011). Mammalian target of rapamycin up-regulation of pyruvate kinase isoenzyme type M2 is critical for aerobic glycolysis and tumor growth. *Proceedings of the National Academy of Sciences*, *108*(10), 4129–4134. https://doi.org/10.1073/pnas.1014769108

Sun, S., Li, H., Chen, J., Qian, Q., Sun, * S, & Li, H. (2017). *Lactic Acid: No Longer an Inert and End-Product of Glycolysis*. https://doi.org/10.1152/physiol.00016.2017

Suzuki, I., Cone, R. D., Im, S., Nordlund, J., & Abdel-Malek, Z. A. (1996). Binding of melanotropic hormones to the melanocortin receptor MC1R on human melanocytes stimulates proliferation and melanogenesis. *Endocrinology*, *137*(5), 1627–1633. https://doi.org/10.1210/en.137.5.1627

Suzuki, S., Tanaka, T., Poyurovsky, M. V., Nagano, H., Mayama, T., Ohkubo, S., … Prives, C. (2010). Phosphate-activated glutaminase (GLS2), a p53-inducible regulator of glutamine metabolism and reactive oxygen species. *Proceedings of the National Academy of Sciences*, *107*(16), 7461–7466. https://doi.org/10.1073/pnas.1002459107

Sviderskaya, E. V., Gray-Schopfer, V. C., Hill, S. P., Smit, N. P., Evans-Whipp, T. J., Bond, J., … Bennett, D. C. (2003). p16/Cyclin-Dependent Kinase Inhibitor 2A Deficiency in Human Melanocyte Senescence, Apoptosis, and Immortalization: Possible Implications for Melanoma Progression. *JNCI Journal of the National Cancer Institute*, *95*(10), 723–732. https://doi.org/10.1093/jnci/95.10.723

Swinstead, E. E., Paakinaho, V., Presman, D. M., & Hager, G. L. (2016). Pioneer factors and ATP-dependent chromatin remodeling factors interact dynamically: A new perspective. *BioEssays*, *38*(11), 1150–1157. https://doi.org/10.1002/bies.201600137

Szeliga, M., Bogacińska-Karaś, M., Kuźmicz, K., Rola, R., & Albrecht, J. (2016). Downregulation of *GLS2* in glioblastoma cells is related to DNA hypermethylation but not to the p53 status. *Molecular Carcinogenesis*, *55*(9), 1309–1316. https://doi.org/10.1002/mc.22372

Takenaka, M., Noguchi, T., Sadahiro, S., Hirai, H., Yamada, K., Matsuda, T., … Tanaka, T. (1991). Isolation and characterization of the human pyruvate kinase M gene. *European Journal of Biochemistry*, *198*(1), 101–106. https://doi.org/10.1111/j.1432-1033.1991.tb15991.x

Talasniemi, J. P., Pennanen, S., Savolainen, H., Niskanen, L., & Liesivuori, J. (2008). Analytical investigation: Assay of d-lactate in diabetic plasma and urine. *Clinical Biochemistry*, *41*(13), 1099–1103. https://doi.org/10.1016/J.CLINBIOCHEM.2008.06.011

Tarrado-Castellarnau, M., Diaz-Moralli, S., Polat, I. H., Sanz-Pamplona, R., Alenda, C., Moreno, V., … Cascante, M. (2017). Glyceraldehyde-3-phosphate dehydrogenase is overexpressed in colorectal cancer onset. *Translational Medicine Communications*, *2*(1), 6. https://doi.org/10.1186/s41231-017-0015-7

Tarze, A., Deniaud, A., Le Bras, M., Maillier, E., Molle, D., Larochette, N., … Brenner, C. (2007). GAPDH, a novel regulator of the pro-apoptotic mitochondrial membrane permeabilization. *Oncogene*, *26*(18), 2606–2620. https://doi.org/10.1038/sj.onc.1210074

Tencer, A. H., Cox, K. L., Di, L., Poirier, M. G., Musselman, C. A., & Kutateladze, T. G. (2017). Covalent Modifications of Histone H3K9 Promote Binding of CHD3. *Cell Reports*, *21*, 455–466. https://doi.org/10.1016/j.celrep.2017.09.054

Thiagalingam, A., De Bustros, A., Borges, M., Jasti, R., Compton, D., Diamond, L., … Nelkin, B. D. (1996). RREB-1, a novel zinc finger protein, is involved in the differentiation response to Ras in human medullary thyroid carcinomas. *Molecular and Cellular Biology*, *16*(10), 5335–5345. https://doi.org/10.1128/MCB.16.10.5335

Thody, A. J., & Graham, A. (1998). Does α-MSH Have a Role in Regulating Skin Pigmentation in Humans? *Pigment Cell Research*, *11*(5), 265–274. https://doi.org/10.1111/j.1600-0749.1998.tb00735.x

Tilvawala, R., Nguyen, S. H., Maurais, A. J., Nemmara, V. V., Nagar, M., Salinger, A. J., … Thompson, P. R. (2018). The Rheumatoid Arthritis-Associated Citrullinome. *Cell Chemical Biology*, *25*(6), 691-704.e6.

https://doi.org/10.1016/j.chembiol.2018.03.002

Timmerman, L. A., Holton, T., Yuneva, M., Louie, R. J., Padró, M., Daemen, A., … Gray, J. W. (2013). Glutamine Sensitivity Analysis Identifies the xCT Antiporter as a Common Triple-Negative Breast Tumor Therapeutic Target. *Cancer Cell*, *24*(4), 450–465. https://doi.org/10.1016/J.CCR.2013.08.020

Tirosh, I., Izar, B., Prakadan, S. M., Wadsworth, M. H., Treacy, D., Trombetta, J. J., … Garraway, L. A. (2016a). Dissecting the multicellular ecosystem of metastatic melanoma by single-cell RNA-seq. *Science (New York, N.Y.)*, *352*(6282), 189–196. https://doi.org/10.1126/science.aad0501

Tirosh, I., Izar, B., Prakadan, S. M., Wadsworth, M. H., Treacy, D., Trombetta, J. J., … Garraway, L. A. (2016b). Dissecting the multicellular ecosystem of metastatic melanoma by single-cell RNA-seq. *Science (New York, N.Y.)*, *352*(6282), 189–196. https://doi.org/10.1126/science.aad0501

Tisdale, E. J. (2001). Glyceraldehyde-3-phosphate dehydrogenase is required for vesicular transport in the early secretory pathway. *The Journal of Biological Chemistry*, *276*(4), 2480–2486. https://doi.org/10.1074/jbc.M007567200

Tokunaga, K., Nakamura, Y., Sakata, K., Fujimori, K., Ohkubo, M., Sawada, K., & Sakiyama, S. (1987). Enhanced expression of a glyceraldehyde-3-phosphate dehydrogenase gene in human lung cancers. *Cancer Research*, *47*(21), 5616–5619. Retrieved from http://www.ncbi.nlm.nih.gov/pubmed/3664468

Tong, J. K., Hassig, C. A., Schnitzler, G. R., Kingston, R. E., & Schreiber, S. L. (1998). Chromatin deacetylation by an ATP-dependent nucleosome remodelling complex. *Nature*, *395*(6705), 917–921. https://doi.org/10.1038/27699

Torchy, M. P., Hamiche, A., & Klaholz, B. P. (2015). Structure and function insights into the NuRD chromatin remodeling complex. *Cellular and Molecular Life Sciences*, *72*(13), 2491–2507. https://doi.org/10.1007/s00018-015-1880-8

Torrado, M., Low, J. K. K., Silva, A. P. G., Schmidberger, J. W., Sana, M., Tabar, M. S., … Mackay, J. P. (2017). Refinement of the subunit interaction network within the nucleosome remodelling and deacetylase (NuRD) complex. *The FEBS Journal*, *284*(24), 4216–4232. https://doi.org/10.1111/febs.14301

Tropberger, P., & Schneider, R. (2013). Scratching the (lateral) surface of chromatin regulation by histone modifications. *Nature Structural & Molecular Biology*, *20*(6), 657–661. https://doi.org/10.1038/nsmb.2581

Tseng, P.-L., Chen, C.-W., Hu, K.-H., Cheng, H.-C., Lin, Y.-H., Tsai, W.-H., … Chang, W.-T. (2018). The decrease of glycolytic enzyme hexokinase 1 accelerates tumor malignancy via deregulating energy metabolism but sensitizes cancer cells to 2-deoxyglucose inhibition. *Oncotarget*, *9*(27), 18949–18969. https://doi.org/10.18632/oncotarget.24855

Tsoi, J., Robert, L., Paraiso, K., Galvan, C., Sheu, K. M., Lay, J., … Graeber, T. G. (2018). Multi-stage Differentiation Defines Melanoma Subtypes with Differential Vulnerability to Drug-Induced Iron-Dependent Oxidative Stress. *Cancer Cell*, *33*(5), 890-904.e5. https://doi.org/10.1016/j.ccell.2018.03.017

Tsukiyama, T., Daniel, C., Tamkun, J., & Wu, C. (1995). ISWI, a member of the SWI2/SNF2 ATPase family, encodes the 140 kDa subunit of the nucleosome remodeling factor. *Cell*, *83*(6), 1021–1026. Retrieved from http://www.ncbi.nlm.nih.gov/pubmed/8521502

Tsukiyama, T., & Wu, C. (1995). Purification and properties of an ATP-dependent nucleosome remodeling factor. *Cell*, *83*(6), 1011–1020. Retrieved from http://www.ncbi.nlm.nih.gov/pubmed/8521501

Tyanova, S., Temu, T., Sinitcyn, P., Carlson, A., Hein, M. Y., Geiger, T., … Cox, J. (2016). The Perseus computational platform for comprehensive analysis of (prote)omics data. *Nature Methods*, *13*(9), 731–740. https://doi.org/10.1038/nmeth.3901

Udono, T., Yasumoto, K., Takeda, K., Amae, S., Watanabe, K., Saito, H., … Shibahara, S. (2000). Structural organization of the human microphthalmia-associated transcription factor gene containing four alternative promoters. *Biochimica et Biophysica Acta*, *1491*(1–3), 205–219. https://doi.org/10.1016/s0167-4781(00)00051-8

Vachtenheim, J., & Borovanský, J. (2010a). “Transcription physiology” of pigment formation in melanocytes: central role of MITF. *Experimental Dermatology*, *19*(7), 617–627. https://doi.org/10.1111/j.1600-0625.2009.01053.x

Vachtenheim, J., & Borovanský, J. (2010b). “Transcription physiology” of pigment formation in melanocytes: central role of MITF. *Experimental Dermatology*, *19*(7), 617–627. https://doi.org/10.1111/j.1600-0625.2009.01053.x

Vachtenheim, J., Ondrušová, L., & Borovanský, J. (2010). SWI/SNF chromatin remodeling complex is critical for the expression of microphthalmia-associated transcription factor in melanoma cells. *Biochemical and Biophysical Research Communications*, *392*(3), 454–459. https://doi.org/10.1016/j.bbrc.2010.01.048

Vander Heiden, M. G., Cantley, L. C., & Thompson, C. B. (2009). Understanding the Warburg Effect: The Metabolic Requirements of Cell Proliferation. *Science*, *324*(5930), 1029–1033. https://doi.org/10.1126/science.1160809

Vazquez, A., Markert, E. K., & Oltvai, Z. N. (2011). Serine Biosynthesis with One Carbon Catabolism and the Glycine Cleavage System Represents a Novel Pathway for ATP Generation. *PLoS ONE*, *6*(11), e25881.

https://doi.org/10.1371/journal.pone.0025881

Verfaillie, A., Imrichova, H., Atak, Z. K., Dewaele, M., Rambow, F., Hulselmans, G., … Aerts, S. (2015). Decoding the regulatory landscape of melanoma reveals TEADS as regulators of the invasive cell state. *Nature Communications*, *6*, 6683. https://doi.org/10.1038/ncomms7683

Vettese-Dadey, M., Grant, P. A., Hebbes, T. R., Crane- Robinson, C., Allis, C. D., & Workman, J. L. (1996). Acetylation of histone H4 plays a primary role in enhancing transcription factor binding to nucleosomal DNA in vitro. *The EMBO Journal*, *15*(10), 2508–2518. Retrieved from http://www.ncbi.nlm.nih.gov/pubmed/8665858

Vomastek, T., Iwanicki, M. P., Schaeffer, H.-J., Tarcsafalvi, A., Parsons, J. T., & Weber, M. J. (2007). RACK1 Targets the Extracellular Signal-Regulated Kinase/Mitogen-Activated Protein Kinase Pathway To Link Integrin Engagement with Focal Adhesion Disassembly and Cell Motility. *Molecular and Cellular Biology*, *27*(23), 8296–8305. https://doi.org/10.1128/MCB.00598-07

Vossenaar, E. R., Zendman, A. J. W., van Venrooij, W. J., & Pruijn, G. J. M. (2003). PAD, a growing family of citrullinating enzymes: genes, features and involvement in disease. *BioEssays*, *25*(11), 1106–1118. https://doi.org/10.1002/bies.10357

Vousden, K. H., Holding, F. P., Zheng, L., Gottlieb, E., Chokkathukalam, A., Hillmann, P., … O'Reilly, M. (2012). Serine is a natural ligand and allosteric activator of pyruvate kinase M2. *Nature*, *491*(7424), 458–462. https://doi.org/10.1038/nature11540

Waddington, C. H. (1942). The Epigenotype. *International Journal of Epidemiology*, *41*(1), 10–13. https://doi.org/10.1093/ije/dyr184

Wade, P. A., Jones, P. L., Vermaak, D., & Wolffe, A. P. (1998). A multiple subunit Mi-2 histone deacetylase from Xenopus laevis cofractionates with an associated Snf2 superfamily ATPase. *Current Biology : CB*, *8*(14), 843–846. Retrieved from http://www.ncbi.nlm.nih.gov/pubmed/9663395

Walsh, J. L., Keith, T. J., & Knull, H. R. (1989). Glycolytic enzyme interactions with tubulin and microtubules. *Biochimica et Biophysica Acta*, *999*(1), 64–70. Retrieved from http://www.ncbi.nlm.nih.gov/pubmed/2553125

Walunas, T. L., Lenschow, D. J., Bakker, C. Y., Linsley, P. S., Freeman, G. J., Green, J. M., … Bluestone, J. A. (1994). CTLA-4 can function as a negative regulator of T cell activation. *Immunity*, *1*(5), 405–413. https://doi.org/10.1016/1074-7613(94)90071-X

Wan, P. T. ., Garnett, M. J., Roe, S. M., Lee, S., Niculescu-Duvaz, D., Good, V. M., … Marais, R. (2004). Mechanism of Activation of the RAF-ERK Signaling Pathway by Oncogenic Mutations of B-RAF. *Cell*, *116*(6), 855–867. https://doi.org/10.1016/S0092-8674(04)00215-6

Wang, D., Yin, L., Wei, J., Yang, Z., & Jiang, G. (2017). ATP citrate lyase is increased in human breast cancer, depletion of which promotes apoptosis. *Tumor Biology*, *39*(4), 101042831769833. https://doi.org/10.1177/1010428317698338

Wang, J., Chen, H., Fu, S., Xu, Z.-M., Sun, K.-L., & Fu, W.-N. (2011). The involvement of CHD5 hypermethylation in laryngeal squamous cell carcinoma. *Oral Oncology*, *47*(7), 601–608. https://doi.org/10.1016/j.oraloncology.2011.05.003

Wang, L., He, S., TU, Y., Ji, P., Zong, J., Zhang, J., … Zhang, Y. (2013a). Downregulation of chromatin remodeling factor CHD5 is associated with a poor prognosis in human glioma. *Journal of Clinical Neuroscience*, *20*(7), 958–963. https://doi.org/10.1016/j.jocn.2012.07.021

Wang, L., He, S., TU, Y., Ji, P., Zong, J., Zhang, J., … Zhang, Y. (2013b). Downregulation of chromatin remodeling factor CHD5 is associated with a poor prognosis in human glioma. *Journal of Clinical Neuroscience*, *20*(7), 958–963. https://doi.org/10.1016/j.jocn.2012.07.021

Wang, P., Sun, C., Zhu, T., & Xu, Y. (2015). Structural insight into mechanisms for dynamic regulation of PKM2. *Protein and Cell*, *6*(4), 275–287. https://doi.org/10.1007/s13238-015-0132-x

Wang, T., Yu, Q., Li, J., Hu, B., Zhao, Q., Ma, C., … Jiang, Y. (2017). O-GlcNAcylation of fumarase maintains tumour growth under glucose deficiency. *Nature Cell Biology*, *19*(7), 833–843. https://doi.org/10.1038/ncb3562

Wang, W., Xue, Y., Zhou, S., Kuo, A., Cairns, B. R., & Crabtree, G. R. (1996). Diversity and specialization of mammalian SWI/SNF complexes. *Genes & Development*, *10*(17), 2117–2130. https://doi.org/10.1101/gad.10.17.2117

Wang, Yan, Zhang, H., Chen, Y., Sun, Y., Yang, F., Yu, W., … Shang, Y. (2009). LSD1 Is a Subunit of the NuRD Complex and Targets the Metastasis Programs in Breast Cancer. *Cell*, *138*(4), 660–672. https://doi.org/10.1016/j.cell.2009.05.050

Wang, Yugang, Guo, Y. R., Liu, K., Yin, Z., Liu, R., Xia, Y., … Lu, Z. (2017). KAT2A coupled with the α-KGDH complex acts as a histone H3 succinyltransferase. *Nature*, *552*(7684), 273–277. https://doi.org/10.1038/nature25003

Wang, Z.-Y., Loo, T. Y., Shen, J.-G., Wang, N., Wang, D.-M., Yang, D.-P., … Chen, J.-P. (2012). LDH-A silencing suppresses breast cancer tumorigenicity through induction of oxidative stress mediated mitochondrial pathway apoptosis. *Breast*

Cancer Research and Treatment, *131*(3), 791–800. https://doi.org/10.1007/s10549-011-1466-6

Warburg, O, Wind, F., & Negelein, E. (1927). The metabolism of tumors in the body. *The Journal of General Physiology*, *8*(6), 519–530. https://doi.org/10.1085/jgp.8.6.519

Warburg, Otto. (1924). Uber den Stoffwechsel der Carcinomzelle. *Die Naturwissenschaften*, *12*(50), 1131–1137. https://doi.org/10.1007/BF01504608

Ward, P. S., Patel, J., Wise, D. R., Abdel-Wahab, O., Bennett, B. D., Coller, H. A., … Thompson, C. B. (2010). The Common Feature of Leukemia-Associated IDH1 and IDH2 Mutations Is a Neomorphic Enzyme Activity Converting α-Ketoglutarate to 2-Hydroxyglutarate. *Cancer Cell*, *17*(3), 225–234. https://doi.org/10.1016/j.ccr.2010.01.020

Ward, W. H., & Farma, J. M. (2017). *CUTANEOUS MELANOMA Etiology and Therapy*. Retrieved from https://www.ncbi.nlm.nih.gov/books/NBK481860/pdf/Bookshelf_NBK481860.pdf

Wasmeier, C., Hume, A. N., Bolasco, G., & Seabra, M. C. (2008). Melanosomes at a glance. *Journal of Cell Science*, *121*(Pt 24), 3995–3999. https://doi.org/10.1242/jcs.040667

Watson, M., Geller, A. C., Tucker, M. A., Guy, G. P., & Weinstock, M. A. (2016). Melanoma burden and recent trends among non-Hispanic whites aged 15–49 years, United States. *Preventive Medicine*, *91*, 294–298. https://doi.org/10.1016/J.YPMED.2016.08.032

Webb, B. A., Forouhar, F., Szu, F.-E., Seetharaman, J., Tong, L., & Barber, D. L. (2015). Structures of human phosphofructokinase-1 and atomic basis of cancer-associated mutations. *Nature*, *523*(7558), 111–114. https://doi.org/10.1038/nature14405

Wei Chin Chou, 2, Makoto Takeo1, 2, Piul Rabbani1, 2, Hai Hu1, 2, Wendy Lee1, 2, Young Rock Chung1, 2, John Carucci1, Paul Overbeek3, and M. I. (2013). *Direct migration of follicular melanocyte stem cells to the epidermis after wounding or UVB irradiation is dependent on Mc1r signaling*. *14*(4), 220–227. https://doi.org/10.1177/1098300712437042.Improving

Wei, M. L. (2006). Hermansky-Pudlak syndrome: a disease of protein trafficking and organelle function. *Pigment Cell Research*, *19*(1), 19–42. https://doi.org/10.1111/j.1600-0749.2005.00289.x

Wellbrock, C., & Arozarena, I. (2015). Microphthalmia-associated transcription factor in melanoma development and MAP-kinase pathway targeted therapy. *Pigment Cell & Melanoma Research*, *28*(4), 390–406. https://doi.org/10.1111/pcmr.12370

Wellbrock, C., Karasarides, M., & Marais, R. (2004). The RAF proteins take centre stage. *Nature Reviews Molecular Cell Biology*, *5*(11), 875–885. https://doi.org/10.1038/nrm1498

Wellbrock, C., & Marais, R. (2005). Elevated expression of MITF counteracts B-RAF–stimulated melanocyte and melanoma cell proliferation. *The Journal of Cell Biology*, *170*(5), 703–708. https://doi.org/10.1083/jcb.200505059

Wellbrock, C., Rana, S., Paterson, H., Pickersgill, H., Brummelkamp, T., & Marais, R. (2008). Oncogenic BRAF Regulates Melanoma Proliferation through the Lineage Specific Factor MITF. *PLoS ONE*, *3*(7), e2734. https://doi.org/10.1371/journal.pone.0002734

Wellen, K. E., Lu, C., Mancuso, A., Lemons, J. M. S., Ryczko, M., Dennis, J. W., … Thompson, C. B. (2010). The hexosamine biosynthetic pathway couples growth factor-induced glutamine uptake to glucose metabolism. *Genes & Development*, *24*(24), 2784–2799. https://doi.org/10.1101/gad.1985910

Wen, Y.-A., Zhou, B.-W., Lv, D.-J., Shu, F.-P., Song, X.-L., Huang, B., … Zhao, S.-C. (2018). Phosphoglycerate mutase 1 knockdown inhibits prostate cancer cell growth, migration, and invasion. *Asian Journal of Andrology*, *20*(2), 178–183. https://doi.org/10.4103/aja.aja_57_17

White, A. C., Tran, K., Khuu, J., Dang, C., Cui, Y., Binder, S. W., & Lowry, W. E. (2011). Defining the origins of Ras/p53-mediated squamous cell carcinoma. *Proceedings of the National Academy of Sciences*, *108*(18), 7425–7430. https://doi.org/10.1073/pnas.1012670108

Whiteman, D. C., Green, A. C., & Olsen, C. M. (2016). The Growing Burden of Invasive Melanoma: Projections of Incidence Rates and Numbers of New Cases in Six Susceptible Populations through 2031. *Journal of Investigative Dermatology*, *136*(6), 1161–1171. https://doi.org/10.1016/J.JID.2016.01.035

Widakowich, C., de Castro, G., de Azambuja, E., Dinh, P., & Awada, A. (2007). Review: Side Effects of Approved Molecular Targeted Therapies in Solid Cancers. *The Oncologist*, *12*(12), 1443–1455. https://doi.org/10.1634/theoncologist.12-12-1443

Wierenga, R. K., Kapetaniou, • E G, & Venkatesan, • R. (n.d.). *Triosephosphate isomerase: a highly evolved biocatalyst DHAP Dihydroxyacetone phosphate IPP 2-(N-formyl-N-hydroxy)-amino-ethylphosphonate PGH Phosphoglycolohydroxamate PGI Phosphoglucose isomerase RPI D-Ribose-5-phosphate isomerase TIM Triosephosphate isomerase 2PG 2-*

Phosphoglycollate. https://doi.org/10.1007/s00018-010-0473-9

Wilczewski, C. M., Hepperla, A. J., Shimbo, T., Wasson, L., Robbe, Z. L., Davis, I. J., … Conlon, F. L. (2018). CHD4 and the NuRD complex directly control cardiac sarcomere formation. *Proceedings of the National Academy of Sciences of the United States of America*, *115*(26), 6727–6732. https://doi.org/10.1073/pnas.1722219115

Wilson, B. G., Wang, X., Shen, X., McKenna, E. S., Lemieux, M. E., Cho, Y.-J., … Roberts, C. W. M. (2010). Epigenetic Antagonism between Polycomb and SWI/SNF Complexes during Oncogenic Transformation. *Cancer Cell*, *18*(4), 316–328. https://doi.org/10.1016/j.ccr.2010.09.006

Wise, D. R., & Thompson, C. B. (2010). Glutamine addiction: a new therapeutic target in cancer. *Trends in Biochemical Sciences*, *35*(8), 427–433. https://doi.org/10.1016/j.tibs.2010.05.003

Witalison, E. E., Thompson, P. R., & Hofseth, L. J. (2015). Protein Arginine Deiminases and Associated Citrullination: Physiological Functions and Diseases Associated with Dysregulation. *Current Drug Targets*, *16*(7), 700–710. Retrieved from http://www.ncbi.nlm.nih.gov/pubmed/25642720

Wolf, A., Agnihotri, S., Micallef, J., Mukherjee, J., Sabha, N., Cairns, R., … Guha, A. (2011). Hexokinase 2 is a key mediator of aerobic glycolysis and promotes tumor growth in human glioblastoma multiforme. *The Journal of Experimental Medicine*, *208*(2), 313–326. https://doi.org/10.1084/jem.20101470

Wong, R. R. Y., Chan, L. K. Y., Tsang, T. P. T., Lee, C. W. S., Cheung, T. H., Yim, S. F., … Chung, T. K. H. (2011). CHD5 Downregulation Associated with Poor Prognosis in Epithelial Ovarian Cancer. *Gynecologic and Obstetric Investigation*, *72*(3), 203–207. https://doi.org/10.1159/000323883

Wood, K., & Luke, J. (2017). *The Biology and Therapeutic Approach to BRAF-Mutant Cutaneous Melanoma*. Retrieved from http://gotoper-com.s3.amazonaws.com/_media/_pdf/AJHO_JAN_melanoma.pdf

Workman, J. L., & Kingston, R. E. (n.d.). Nucleosome Core Displacement in Vitro via a Metastable Transcription Factor-Nucleosome Complex. *Science*, Vol. 258, pp. 1780–1784. https://doi.org/10.2307/2880380

Wu, C., Khan, S. A., Peng, L.-J., & Lange, A. J. (2006). Roles for fructose-2,6-bisphosphate in the control of fuel metabolism: Beyond its allosteric effects on glycolytic and gluconeogenic enzymes. *Advances in Enzyme Regulation*, *46*(1), 72–88. https://doi.org/10.1016/j.advenzreg.2006.01.010

Wu, Xiao, Zhu, Z., Li, W., Fu, X., Su, D., Fu, L., … Dong, J.-T. (2012). Chromodomain helicase DNA binding protein 5 plays a tumor suppressor role in human breast cancer. *Breast Cancer Research*, *14*(3), R73. https://doi.org/10.1186/bcr3182

Wu, Xufeng, Bowers, B., Rao, K., Wei, Q., & Hammer, J. A. (1998). Visualization of Melanosome Dynamics within Wild-Type and Dilute Melanocytes Suggests a Paradigm for Myosin V Function In Vivo. *The Journal of Cell Biology*, *143*(7), 1899–1918. https://doi.org/10.1083/jcb.143.7.1899

Wysocka, J., Swigut, T., Xiao, H., Milne, T. A., Kwon, S. Y., Landry, J., … Allis, C. D. (2006). A PHD finger of NURF couples histone H3 lysine 4 trimethylation with chromatin remodelling. *Nature*, *442*(7098), 86–90. https://doi.org/10.1038/nature04815

Xia, Z., Donehower, L. A., Cooper, T. A., Neilson, J. R., Wheeler, D. A., Wagner, E. J., & Li, W. (2014). Dynamic analyses of alternative polyadenylation from RNA-seq reveal a 3′-UTR landscape across seven tumour types. *Nature Communications*, *5*(1), 5274. https://doi.org/10.1038/ncomms6274

Xiangyun, Y., Xiaomin, N., linping, G., Yunhua, X., Ziming, L., Yongfeng, Y., … Shun, L. (2017). Desuccinylation of pyruvate kinase M2 by SIRT5 contributes to antioxidant response and tumor growth. *Oncotarget*, *8*(4). https://doi.org/10.18632/oncotarget.14346

Xiao, H, Sandaltzopoulos, R., Wang, H. M., Hamiche, A., Ranallo, R., Lee, K. M., … Wu, C. (2001). Dual functions of largest NURF subunit NURF301 in nucleosome sliding and transcription factor interactions. *Molecular Cell*, *8*(3), 531–543. Retrieved from http://www.ncbi.nlm.nih.gov/pubmed/11583616

Xiao, Hua, Sandaltzopoulos, R., Wang, H.-M., Hamiche, A., Ranallo, R., Lee, K.-M., … Wu, C. (2001). Dual Functions of Largest NURF Subunit NURF301 in Nucleosome Sliding and Transcription Factor Interactions. *Molecular Cell*, *8*(3), 531–543. https://doi.org/10.1016/S1097-2765(01)00345-8

Xiaoyu, H., Yiru, Y., Shuisheng, S., Keyan, C., Zixing, Y., Shanglin, C., … Jie, M. (2018). The mTOR Pathway Regulates PKM2 to Affect Glycolysis in Esophageal Squamous Cell Carcinoma. *Technology in Cancer Research & Treatment*, *17*(382), 1–10. https://doi.org/10.1177/1533033818780063

Xie, C.-R., Li, Z., Sun, H.-G., Wang, F.-Q., Sun, Y., Zhao, W.-X., … Yin, Z.-Y. (2015a). Mutual regulation between CHD5 and EZH2 in hepatocellular carcinoma. *Oncotarget*, *6*(38), 40940. https://doi.org/10.18632/ONCOTARGET.5724

Xie, C.-R., Li, Z., Sun, H.-G., Wang, F.-Q., Sun, Y., Zhao, W.-X., … Yin, Z.-Y. (2015b). Mutual regulation between CHD5 and

EZH2 in hepatocellular carcinoma. *Oncotarget*, *6*(38), 40940. https://doi.org/10.18632/ONCOTARGET.5724

Xie, H., Hanai, J., Ren, J.-G., Kats, L., Burgess, K., Bhargava, P., … Seth, P. (2014). Targeting lactate dehydrogenase-A inhibits tumorigenesis and tumor progression in mouse models of lung cancer and impacts tumor initiating cells. *Cell Metabolism*, *19*(5), 795. https://doi.org/10.1016/J.CMET.2014.03.003

Xin, M., Qiao, Z., Li, J., Liu, J., Song, S., Zhao, X., … Huang, G. (2016). miR-22 inhibits tumor growth and metastasis by targeting ATP citrate lyase: evidence in osteosarcoma, prostate cancer, cervical cancer and lung cancer. *Oncotarget*, *7*(28), 44252–44265. https://doi.org/10.18632/oncotarget.10020

Xu, S., Ao, J., Gu, H., Wang, X., Xie, C., Meng, D., … Liu, M. (2017). IL-22 Impedes the Proliferation of Schwann cells: Transcriptome Sequencing and Bioinformatics Analysis. *Molecular Neurobiology*, *54*(4), 2395–2405. https://doi.org/10.1007/s12035-016-9699-3

Xue, Y., Wong, J., Moreno, G. T., Young, M. K., Côté, J., & Wang, W. (1998). NURD, a novel complex with both ATP-dependent chromatin-remodeling and histone deacetylase activities. *Molecular Cell*, *2*(6), 851–861. Retrieved from http://www.ncbi.nlm.nih.gov/pubmed/9885572

Yadav, T., & Whitehouse, I. (2016). Replication-Coupled Nucleosome Assembly and Positioning by ATP-Dependent Chromatin-Remodeling Enzymes. *Cell Reports*, *15*(4), 715–723. https://doi.org/10.1016/j.celrep.2016.03.059

Yamaguchi, Y., & Hearing, V. J. (2009). Physiological factors that regulate skin pigmentation. *BioFactors (Oxford, England)*, *35*(2), 193–199. https://doi.org/10.1002/biof.29

Yamamoto, T., Kudo, M., Peng, W.-X., Takata, H., Takakura, H., Teduka, K., … Naito, Z. (2016). Identification of aldolase A as a potential diagnostic biomarker for colorectal cancer based on proteomic analysis using formalin-fixed paraffin-embedded tissue. *Tumor Biology*, *37*(10), 13595–13606. https://doi.org/10.1007/s13277-016-5275-8

Yan, Z., Cui, K., Murray, D. M., Ling, C., Xue, Y., Gerstein, A., … Wang, W. (2005). PBAF chromatin-remodeling complex requires a novel specificity subunit, BAF200, to regulate expression of selective interferon-responsive genes. *Genes & Development*, *19*(14), 1662–1667. https://doi.org/10.1101/gad.1323805

Yang, J., Liu, H., Liu, X., Gu, C., Luo, R., & Chen, H.-F. (2016). Synergistic Allosteric Mechanism of Fructose-1,6-bisphosphate and Serine for Pyruvate Kinase M2 via Dynamics Fluctuation Network Analysis. *Journal of Chemical Information and Modeling*, *56*(6), 1184–1192. https://doi.org/10.1021/acs.jcim.6b00115

Yang, W., Xia, Y., Hawke, D., Li, X., Liang, J., Xing, D., … Lu, Z. (2012). *PKM2 Phosphorylates Histone H3 and Promotes Gene Transcription and Tumorigenesis*. https://doi.org/10.1016/j.cell.2012.07.018

Yang, W., Xia, Y., Ji, H., Zheng, Y., Liang, J., Huang, W., … Lu, Z. (2011). Nuclear PKM2 regulates β-catenin transactivation upon EGFR activation. *Nature*, *480*(7375), 118–122. https://doi.org/10.1038/nature10598

Yang, W., Zheng, Y., Xia, Y., Ji, H., Chen, X., Guo, F., … Lu, Z. (2012). ERK1/2-dependent phosphorylation and nuclear translocation of PKM2 promotes the Warburg effect. *Nature Cell Biology*, *14*(12), 1295–1304. https://doi.org/10.1038/ncb2629

Yanming Wang; Joanna Wysocka. (2004). *Human PAD4 Regulates Histone Arginine Methylation Levels via Demethylimination*. Retrieved from http://science.sciencemag.org/

Yao, D. C., Tolan, D. R., Murray, M. F., Harris, D. J., Darras, B. T., Geva, A., & Neufeld, E. J. (2004). Hemolytic anemia and severe rhabdomyolysis caused by compound heterozygous mutations of the gene for erythrocyte/muscle isozyme of aldolase, ALDOA(Arg303X/Cys338Tyr). *Blood*, *103*(6), 2401–2403. https://doi.org/10.1182/blood-2003-09-3160

Yao, F., Zhao, T., Zhong, C., Zhu, J., & Zhao, H. (2013). LDHA is necessary for the tumorigenicity of esophageal squamous cell carcinoma. *Tumor Biology*, *34*(1), 25–31. https://doi.org/10.1007/s13277-012-0506-0

Ye, F., Chen, Y., Xia, L., Lian, J., & Yang, S. (2018). Aldolase A overexpression is associated with poor prognosis and promotes tumor progression by the epithelial-mesenchymal transition in colon cancer. *Biochemical and Biophysical Research Communications*, *497*(2), 639–645. https://doi.org/10.1016/j.bbrc.2018.02.123

Ye, J., Fan, J., Venneti, S., Wan, Y.-W., Pawel, B. R., Zhang, J., … Thompson, C. B. (2014). Serine Catabolism Regulates Mitochondrial Redox Control during Hypoxia. *Cancer Discovery*, *4*(12), 1406–1417. https://doi.org/10.1158/2159-8290.CD-14-0250

Yogev, O., Yogev, O., Singer, E., Shaulian, E., Goldberg, M., Fox, T. D., & Pines, O. (2010). Fumarase: A Mitochondrial Metabolic Enzyme and a Cytosolic/Nuclear Component of the DNA Damage Response. *PLoS Biology*, *8*(3), e1000328. https://doi.org/10.1371/journal.pbio.1000328

Yokoyama, S., Woods, S. L., Boyle, G. M., Aoude, L. G., MacGregor, S., Zismann, V., … Brown, K. M. (2011). A novel recurrent mutation in MITF predisposes to familial and sporadic melanoma. *Nature*, *480*(7375), 99–103.

https://doi.org/10.1038/nature10630

Yoshida, M., Takahashi, Y., & Inoue, S. (2000). Histamine Induces Melanogenesis and Morphologic Changes by Protein Kinase A Activation via H2 Receptors in Human Normal Melanocytes. *Journal of Investigative Dermatology*, *114*(2), 334–342. https://doi.org/10.1046/J.1523-1747.2000.00874.X

Yuan, M., Mcnae, I. W., Chen, Y., Blackburn, E. A., Wear, M. A., Michels, P. A. M., … Walkinshaw, M. D. (2018). *An allostatic mechanism for M2 pyruvate kinase as an amino-acid sensor*. https://doi.org/10.1042/BCJ20180171

Zancan, P., Almeida, F. V. R., Faber-Barata, J., Dellias, J. M., & Sola-Penna, M. (2007a). Fructose-2,6-bisphosphate counteracts guanidinium chloride-, thermal-, and ATP-induced dissociation of skeletal muscle key glycolytic enzyme 6-phosphofructo-1-kinase: A structural mechanism for PFK allosteric regulation. *Archives of Biochemistry and Biophysics*, *467*(2), 275–282. https://doi.org/10.1016/j.abb.2007.08.032

Zancan, P., Almeida, F. V. R., Faber-Barata, J., Dellias, M., & Sola-Penna, M. (2007b). *Fructose-2,6-bisphosphate counteracts guanidinium chloride-, thermal-, and ATP-induced dissociation of skeletal muscle key glycolytic enzyme 6-phosphofructo-1-kinase: A structural mechanism for PFK allosteric regulation*. https://doi.org/10.1016/j.abb.2007.08.032

Zancan, P., Marinho-Carvalho, M. M., Faber-Barata, J., Dellias, J. M. M., & Sola-Penna, M. (2008). ATP and fructose-2,6-bisphosphate regulate skeletal muscle 6-phosphofructo-1-kinase by altering its quaternary structure. *IUBMB Life*, *60*(8), 526–533. https://doi.org/10.1002/iub.58

Zecchin, K. G., Rossato, F. A., Raposo, H. F., Melo, D. R., Alberici, L. C., Oliveira, H. C., … Graner, E. (2011). Inhibition of fatty acid synthase in melanoma cells activates the intrinsic pathway of apoptosis. *Laboratory Investigation*, *91*(2), 232–240. https://doi.org/10.1038/labinvest.2010.157

Zeller, K. I., Jegga, A. G., Aronow, B. J., O'Donnell, K. A., & Dang, C. V. (2003). An integrated database of genes responsive to the Myc oncogenic transcription factor: identification of direct genomic targets. *Genome Biology*, *4*(10), R69. https://doi.org/10.1186/gb-2003-4-10-r69

Zhang, G., Frederick, D. T., Wu, L., Wei, Z., Krepler, C., Srinivasan, S., … Herlyn, M. (2016). Targeting mitochondrial biogenesis to overcome drug resistance to MAPK inhibitors. *The Journal of Clinical Investigation*, *126*(5), 1834–1856. https://doi.org/10.1172/JCI82661

Zhang, J.-Y., Zhang, F., Hong, C.-Q., Giuliano, A. E., Cui, X.-J., Zhou, G.-J., … Cui, Y.-K. (2015). Critical protein GAPDH and its regulatory mechanisms in cancer cells. *Cancer Biology & Medicine*, *12*(1), 10–22. https://doi.org/10.7497/j.issn.2095-3941.2014.0019

Zhang, Jiayi, Dai, J., Zhao, E., Lin, Y., Zeng, L., Chen, J., … Mao, Y. (2004). cDNA cloning, gene organization and expression analysis of human peptidylarginine deiminase type VI. *Acta Biochimica Polonica*, *51*(4), 1051–1058. https://doi.org/0451041051

Zhang, Juan, Wang, J., Xing, H., Li, Q., Zhao, Q., & Li, J. (2016). Down-regulation of FBP1 by ZEB1-mediated repression confers to growth and invasion in lung cancer cells. *Molecular and Cellular Biochemistry*, *411*(1–2), 331–340. https://doi.org/10.1007/s11010-015-2595-8

Zhang, M., Qureshi, A. A., Geller, A. C., Frazier, L., Hunter, D. J., & Han, J. (2012). Use of Tanning Beds and Incidence of Skin Cancer. *Journal of Clinical Oncology*, *30*(14), 1588–1593. https://doi.org/10.1200/JCO.2011.39.3652

Zhang, Xiaoqian, Liu, X., Zhang, M., Li, T., Muth, A., Thompson, P. R., … Zhang, X. (2016). Peptidylarginine deiminase 1-catalyzed histone citrullination is essential for early embryo development. *Scientific Reports*, *6*(1), 38727. https://doi.org/10.1038/srep38727

Zhang, Xuesen, Gamble, M. J., Stadler, S., Cherrington, B. D., Causey, C. P., Thompson, P. R., … Coonrod, S. A. (2011). Genome-Wide Analysis Reveals PADI4 Cooperates with Elk-1 to Activate c-Fos Expression in Breast Cancer Cells. *PLoS Genetics*, *7*(6), e1002112. https://doi.org/10.1371/journal.pgen.1002112

Zhang, Y, LeRoy, G., Seelig, H. P., Lane, W. S., & Reinberg, D. (1998). The dermatomyositis-specific autoantigen Mi2 is a component of a complex containing histone deacetylase and nucleosome remodeling activities. *Cell*, *95*(2), 279–289. Retrieved from http://www.ncbi.nlm.nih.gov/pubmed/9790534

Zhang, Yong, Liu, T., Meyer, C. A., Eeckhoute, J., Johnson, D. S., Bernstein, B. E., … Liu, X. S. (2008). Model-based Analysis of ChIP-Seq (MACS). *Genome Biology*, *9*(9), R137. https://doi.org/10.1186/gb-2008-9-9-r137

Zhang, Z., Wippo, C. J., Wal, M., Ward, E., Korber, P., & Pugh, B. F. (2011). A Packing Mechanism for Nucleosome Organization Reconstituted Across a Eukaryotic Genome. *Science*, *332*(6032), 977 LP – 980. https://doi.org/10.1126/science.1200508

Zhao, L., Huang, Y., & Zheng, J. (2013). STAT1 Regulates Human Glutaminase 1 Promoter Activity through Multiple Binding

Sites in HIV-1 Infected Macrophages. *PLoS ONE*, *8*(9), e76581. https://doi.org/10.1371/journal.pone.0076581

Zhao, M., Fang, W., Wang, Y., Guo, S., Shu, L., Wang, L., … Liu, Z. (2015). Enolase-1 is a therapeutic target in endometrial carcinoma. *Oncotarget*, *6*(17), 15610–15627. https://doi.org/10.18632/oncotarget.3639

Zhao, R., Yan, Q., Lv, J., Huang, H., Zheng, W., Zhang, B., & Ma, W. (2012). CHD5, a tumor suppressor that is epigenetically silenced in lung cancer. *Lung Cancer*, *76*(3), 324–331. https://doi.org/10.1016/j.lungcan.2011.11.019

Zheng, J. (2012). Energy metabolism of cancer: Glycolysis versus oxidative phosphorylation (Review). *Oncology Letters*, *4*(6), 1151–1157. https://doi.org/10.3892/ol.2012.928

Zheng, L., Roeder, R. G., & Luo, Y. (2003). S phase activation of the histone H2B promoter by OCA-S, a coactivator complex that contains GAPDH as a key component. *Cell*, *114*(2), 255–266. Retrieved from http://www.ncbi.nlm.nih.gov/pubmed/12887926

Zhou, D., Bai, F., Zhang, X., Hu, M., Zhao, G., Zhao, Z., & Liu, R. (2014). SOX10 is a novel oncogene in hepatocellular carcinoma through Wnt/β-catenin/TCF4 cascade. *Tumor Biology*, *35*(10), 9935–9940. https://doi.org/10.1007/s13277-014-1893-1

Zhuang, T., Hess, R. A., Kolla, V., Higashi, M., Raabe, T. D., & Brodeur, G. M. (2014). CHD5 is required for spermiogenesis and chromatin condensation. *Mechanisms of Development*, *131*, 35–46. https://doi.org/10.1016/j.mod.2013.10.005

Zlatanova, J., Bishop, T. C., Victor, J.-M., Jackson, V., & van Holde, K. (2009). The Nucleosome Family: Dynamic and Growing. *Structure*, *17*(2), 160–171. https://doi.org/10.1016/j.str.2008.12.016

UNIVERSITÉ DE STRASBOURG

Sébastien COASSOLO

LA LIGUE CONTRE LE CANCER

The CHD4 NuRD complex links epigenetics to glycolytic flux and proliferation of melanoma and a variety of cancer cells

Abstract in ENGLISH

The Nucleosome Remodelling and Deacetylation (NuRD) complex is an epigenetic regulator of gene expression that includes two mutually exclusive ATPase subunits CHD3 and CHD4. Our results show that NuRD associates with essential melanoma cell transcription factors namely MITF and SOX10.

However, despite their physical association and genomic co-localization, CHD4-NuRD does not appear to act as a cofactor for MITF or SOX10 regulated gene expression. Nevertheless, CHD4 silencing leads to a slow growth phenotype and de-represses the expression of PADI1 (Protein Arginine DeIminase 1) and PADI3, two enzymes involved in converting arginines to citrullines in melanoma and multiple types of cancer cells. Increased expression of PADI1 and PADI3 enhances citrullination of arginines within the key glycolytic regulatory enzyme PKM2 then promoting excessive glycolysis, lowering ATP levels and slowing down proliferation. PKM2 citrullination lowers its sensitivity to allosteric inhibitors thus shifting equilibrium towards allosteric activators thereby bypassing the normal physiological regulation of glycolysis.

Overall, our results lead to describe a novel pathway linking, epigenetic regulation of PADI1 and PADI3 expression by CHD4/NuRD and reprogramming of PKM2 allosteric regulation through arginines citrullination, to glycolytic flux and cancer cell proliferation.

Key words: NuRD, chromatin remodelling, citrullination, epigenetics, glycolysis, cancer

Abstract in FRENCH

Le complexe de remodelage de la chromatine NuRD, composé des sous-unités catalytiques CHD3 et CHD4, est un régulateur épigénétique de l'expression génique. Nos résultats montrent que NuRD s'associe avec les facteurs de transcription essentiels du mélanome que sont MITF et SOX10. Cependant, malgré une association physique et une co-localisation génomique, CHD4/NuRD ne semble pas agir comme un cofacteur important pour MITF ou SOX10.

Néanmoins, la répression de CHD4 conduit à un ralentissement de la prolifération et dé-réprime l'expression des enzymes PADI1 et PADI3 dans les cellules de mélanome ainsi que dans de nombreux types de cellules cancéreuses. Ainsi, l'induction de ces enzymes, responsables de la conversion des arginines en citrullines, entraîne la citrullination spécifique de PKM2, une enzyme glycolytique essentielle, diminuant ainsi sa sensibilité aux inhibiteurs allostériques, et donc altérant l'équilibre physiologique entre activateurs et inhibiteurs de l'enzyme.

L'ensemble de ce travail de thèse a permis de mettre en évidence une nouvelle voie reliant, d'une part la régulation épigénétique de l'expression de PADI1 et PADI3 par CHD4/NuRD ainsi que la reprogrammation de la régulation allostérique de PKM2 via la citrullination d'arginines, au flux glycolytique et au contrôle de la prolifération des cellules cancéreuses d'autre part.

Mots clés: NuRD, remodelage de la chromatine, citrullination, épigénétique, glycolyse, cancer